Synthetic and Mechanistic Investigations of Iridium-Catalysed Imine Hydrogenation

Inauguraldissertation

zur
Erlangung der Würde eines Doktors der Philosophie
vorgelegt der
Philosophisch-Naturwissenschaftlichen Fakultät
der Universität Basel

von

York Schramm

aus

Baden AG

Basel, 2013

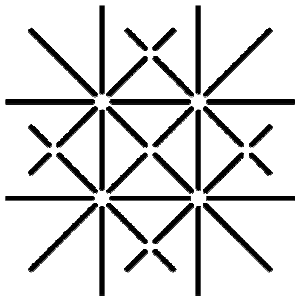

UNI
BASEL

Genehmigt von der Philosophisch-Naturwissenschaftlichen Fakultät
auf Antrag von

Prof. Dr. Andreas Pfaltz

Prof. Dr. Thomas Ward

Basel, den 26. März 2013

Prof. Dr. Jörg Schibler
Dekan

creative commons

Namensnennung-Keine kommerzielle Nutzung-Keine Bearbeitung 2.5 Schweiz

---

Sie dürfen:

das Werk vervielfältigen, verbreiten und öffentlich zugänglich machen

Zu den folgenden Bedingungen:

Namensnennung. Sie müssen den Namen des Autors/Rechteinhabers in der von ihm festgelegten Weise nennen (wodurch aber nicht der Eindruck entstehen darf, Sie oder die Nutzung des Werkes durch Sie würden entlohnt).

Keine kommerzielle Nutzung. Dieses Werk darf nicht für kommerzielle Zwecke verwendet werden.

Keine Bearbeitung. Dieses Werk darf nicht bearbeitet oder in anderer Weise verändert werden.

- Im Falle einer Verbreitung müssen Sie anderen die Lizenzbedingungen, unter welche dieses Werk fällt, mitteilen. Am Einfachsten ist es, einen Link auf diese Seite einzubinden.
- Jede der vorgenannten Bedingungen kann aufgehoben werden, sofern Sie die Einwilligung des Rechteinhabers dazu erhalten.
- Diese Lizenz lässt die Urheberpersönlichkeitsrechte unberührt.

Quelle: http://creativecommons.org/licenses/by-nc-nd/2.5/ch/ Datum: 3.4.2009

Für meine Familie

This thesis was supervised by Prof. Dr. Andreas Pfaltz from March 2009 to March 2013 at the University of Basel, Department of Chemistry.

Parts of this work has been published previously:

"Discovery of an iridacycle catalyst with improved reactivity and enantioselectivity in the hydrogenatioin of dialkyl ketimines"
Y. Schramm, F. Barrios-Landeros, A. Pfaltz, *Chem. Sci.* **2013**, *4*, 2760-2766.

Acknowledgements

I wish to express my deep gratitude to my supervisor *Prof. Dr. Andreas Pfaltz* for the opportunity to conduct my doctoral studies in his research group, for giving me such an interesting and challenging project and for providing an excellent working environment. The support, confidence and freedom in developing the project as well as the fruitful discussions throughout my PhD are gratefully acknowledged.

I am very thankful to *Prof. Dr. Thomas Ward* for accepting the co-examination of this thesis as well as the many scientific discussions throughout my doctoral studies.

I am also thankful to *Prof. Dr. Markus Meuwly* for chairing the defence.

Dr. Ali Lennox, *Tom Eaton*, *Marc Müller*, *Florian Bächle, Maurizio Bernasconi, Christophe Daeppen and Leo Betschart* invested a lot of time proof-reading and correcting this written thesis. Many thanks for that, guys!

Robin Wehlauch and *Silvan Wirthensohn* are thanked for their synthetic contributions in their Wahlpraktikum and student courses.

I am very thankful to *Dr. Adnan Ganic*, *Dr. Ivana Fleischer*, *Dr. Michael Parmentier*, *Dr. René Tannert* and *Dr. Anthony Weatherwax* for the many discussions during my PhD. I would especially like to thank *Adnan* for all the late-night lab discussions which saved me from conducting a series of pointless experiments. Furthermore, I thank *Dr. Eileen Jackson* for organising the CCROS workshop with me and making it an absolutely smooth conference!

I would like to thank *Dr. Christian Ebner*, *Florian Bächle* and *Patrick Isenegger* for measuring numerous ESI mass spectra. Furthermore, I would like to thank *Dr. Markus Neuburger* for X-Ray crystallography measurements and structure refinement. *Dr. Heinz Nadig* and *Dr. Xiangyang Zhang* (ETH Zürich) are thanked for recording EI and FAB as well as high resolution ESI mass spectra. *Werner Kirsch* and *Dr. Sylvie Mittleheisser* are acknowledged for performing elemental analyses.

I would also like to thank all former and present members of the *Pfaltz* group and especially Lab 204 for the good working atmosphere as well as the colleagues from the department for the fun we had outside work. I would also like to thank *Marina Mambelli* for all the organisational work and all matters not related to chemistry.

Ich möchte mich bei meiner Freundin *Xiang*, sowie meiner Familie, *Kai* und *Karin* für die stete Unterstützung äusserst herzlich bedanken.

Financial support by the *KTI* and the *SNF* is gratefully acknowledged.

Table of contents

Objetives of the thesis

Chiral amines occur as structural elements in many biologically active natural and unnatural products. In addition, they find applications as chiral auxiliaries, catalysts, and resolving agents. Consequently, the asymmetric hydrogenation of imines has received much attention as a direct, atom-economical route to optically active amines. The *Pfaltz* group has developed chiral iridium catalysts enabling the reduction of imines, bearing at least one aryl substituent, in excellent enantioselectivities (up to 96% *ee*). However, purely aliphatic imines gave only low conversions and enantioselectivities. Therefore, the development of an efficient protocol for the hydrogenation of purely aliphatic imines remained of great interest.

The goal of this doctoral thesis was to continue the studies initiated by *F. Barrios* to gain a better understanding of the reaction course in imine hydrogenation as well as to develop an efficient protocol for the iridium-catalysed asymmetric hydrogenation of aliphatic imines.

In the first chapter, the aim was to identify and further investigate the active catalyst in solution. By using an achiral iridium complex (with an achiral ligand) and a chiral imine additive, the preparation of a chiral catalyst under reaction conditions would demonstrate that cyclometalation of the imine additive by the iridium complex generated a more reactive and selective catalyst prior to commencing the catalytic cycle of hydrogenation.

The goal of second chapter was to prepare a chiral imine ligand, which would be used as an additional ligand for the generation of the chiral catalyst in solution. Three different ligand scaffolds were designed with different steric and electronic properties.

The aim of the third project was to optimize the synthetic protocol for asymmetric hydrogenation of purely aliphatic imines. An extended catalyst and additive screening as well as optimisation of the reaction conditions would result in a highly selective hydrogenation methodology for these substrates.

Chapter 1 – Introduction

Chirality

The left and the right human hand, converse twisting snake houses or corkstrew stairs appear to be similar to the general audience. But when attempting to superimpose such objects, they cannot be brought into congruence. They are called chiral, an expression that stems from the greek word "χέιρ" (cheir) = hand. The same principle applies in chemistry. Molecules which look the same but are mirror images of each other are called enantiomers (greek: "ενάντιος" (enantios) = opposite). Enantiomers exhibit the same physical properties except their optical rotation which is of opposite orientation. Furthermore, they operate in different ways in a chiral environment, such as the human body and thus exhibit different physiological properties. Many examples of enantiomers with different physiological properties are known and some are shown in Figure 1. An every-day example is the monoterpene carvone (**1**) found in many essential oils. While the (*S*)-enantiomer smells like caraway, the (*R*)-enantiomer tastes like spearmint. Another example is aspargine (**2**), a common amino acid. Whereas the (*S*)-enantiomer tastes bitter, the (*R*)-enantiomer is tastes sweet.[1] More dramatic examples can be found in medicine. The first incident that emphazised the importance of enantiomerically pure drugs was Contergan (Thalidomid) (**3**), where the (*R*)-enantiomer acts as a sedative but the (*S*)-enantiomer is highly teratogenic.

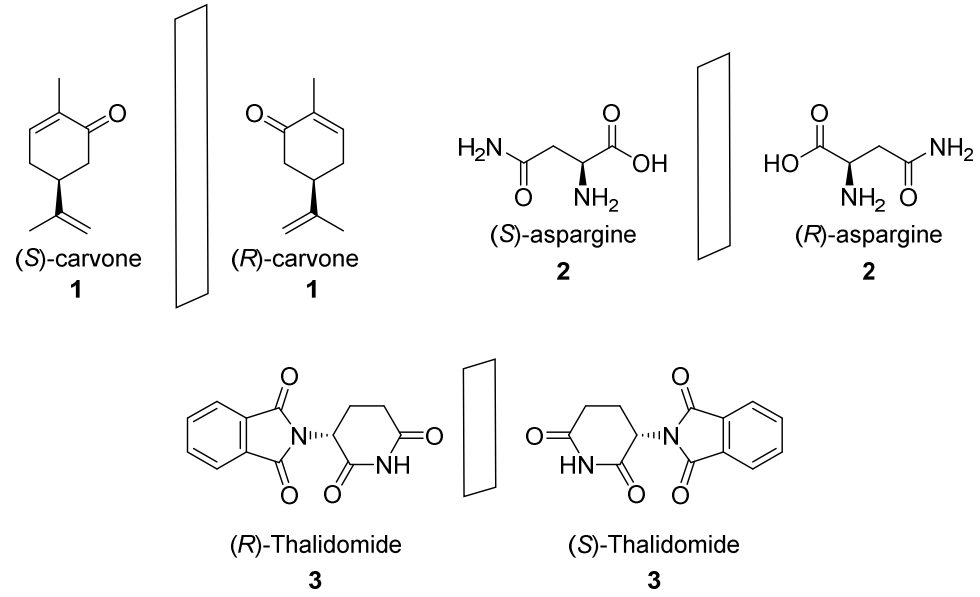

Figure 1: Enantiomers of commonly encountered every-day chemicals

These examples highlight the need for selective preparation of drugs. Therefore chemists have a strong and long-standing interest in the stereoselective synthesis of drugs. Several methods can be used to obtain enantiomerically pure material. Four different approaches have been developed to date:

First of all, application of enantiomerically pure substances isolated from natural resources, which are summarized as the "chiral pool". Examples include amino acids, monosaccharides, terpenes or alkaloids;

Secondly, resolution (racemate separation), which is achieved by addition of an enantiomerically enriched material to afford crystallisation of diastereomerically pure salts or applying separation techniques such as chromatography with chiral stationary phase to afford enantiomer separation. This method can only deliver a maximum of 50% yield.

Thirdly, to overcome the loss of 50% of the material, variations of resolution such as dynamic kinetic resolution, where interconversion of the racemic starting materials is faster than subsequent separation by derivatisation of the material, have been developed. Such procedures are also called DYKAT (dynamic kinetic asymmetric transformation);

Fourthly, enzymatic or microbiological transformations; these are highly selective and efficient processes but often display limited substrate scope. A famous example is the lipase *Candida antarctica* which has been applied in numerous industrial processes;[2]

Ultimately, asymmetric synthesis and catalysis; while a reagent based approach has been the main focus in the early days of investigating stereoselective synthesis, in the last three to four decades the use of chiral catalysts has emerged as a very powerful tool for the preparation of enantiomerically pure building blocks.[3]

Asymmetric Synthesis and Catalysis

Asymmetric catalysis can often out-compete other approaches by a number of factors. Artificial catalysts offer a large substrate scope and can also be used in organic solvents in contrary to enzymatic or microbiological catalytic processes. In asymmetric synthesis, auxiliaries need to be removed and disposed of and therefore often require elaborate or cumbersome purification processes. Furthermore, the generation of large amounts of waste displays a major drawback. On the other hand, artificial catalysts can circumvent these issues both in economic as well as ecological terms. As an example, asymmetric hydrogenation offers a number of highly desirable advantages. Perfect atom economy, in that all the atoms the molecules applied in the reaction (hydrogen gas and substrate) are incorporated in the product. Usually, high conversions and high selectivities are obtained with low catalyst loadings, while reactions are conducted under mild conditions, thus offering a large functional group tolerance.

The importance of asymmetric hydrogenation had been rewarded, together with asymmetric oxidation of organic molecules, with the Nobel prize in chemistry in 2001 given to *Knowles*, *Noyori* and *Sharpless*.[1]

Famous examples of industrial asymmetric hydrogenation processes include L-DOPA (**7**) which has been produced on a one ton scale per year (Scheme 1).[4],[5]

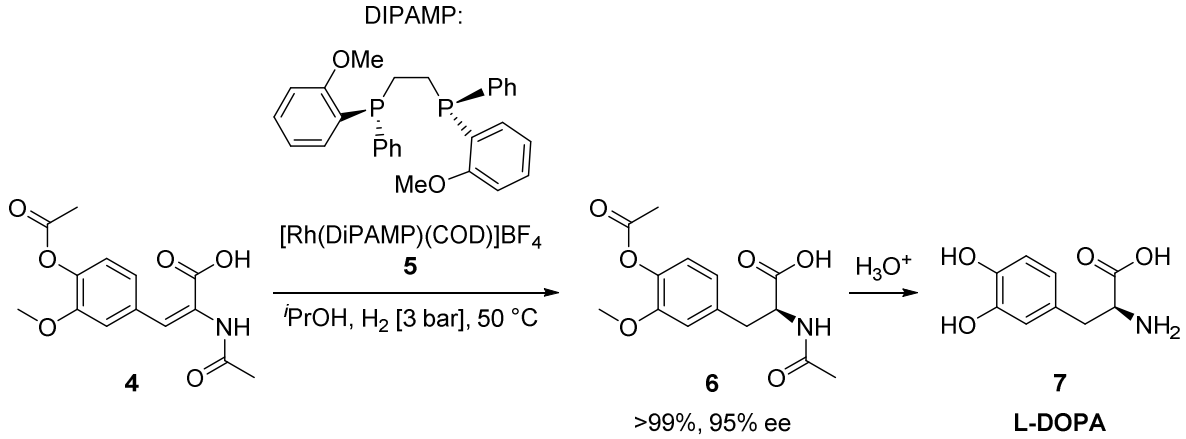

Scheme 1: Industrial rhodium-catalysed asymmetric hydrogenation of enamine **4** in the L-DOPA process

Vitamin E (**11**) (Scheme 2)[6] and Metolachlor (**15**) (Scheme 3)[7] are produced on much larger scale (300 to >10'000 tons per year) and highlight the importance of asymmetric hydrogenation for the chemical industry.

[1] http://www.nobelprize.org/nobel_prizes/chemistry/laureates/2001/press.html

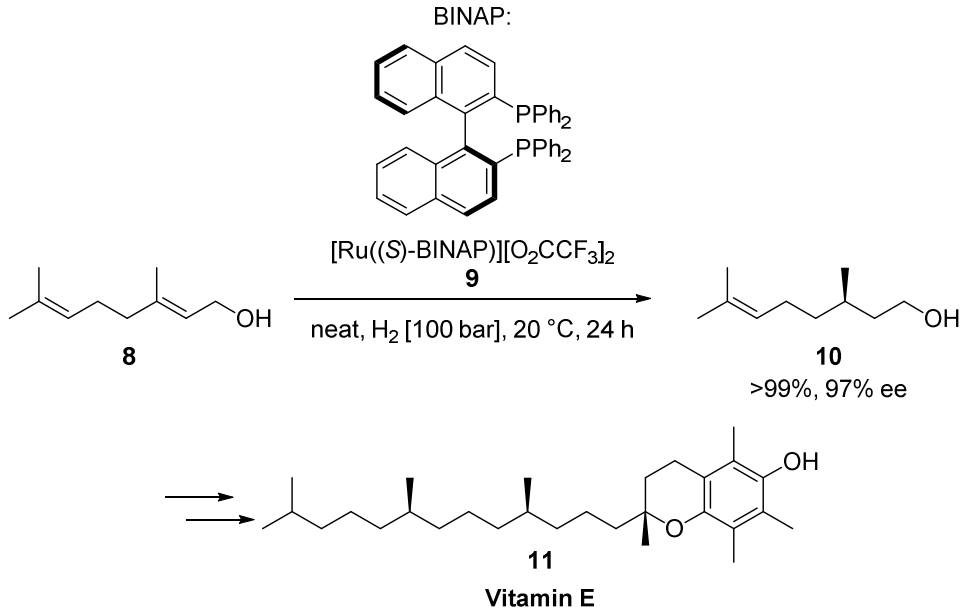

Scheme 2: Industrial ruthenium-catalysed asymmetric hydrogenation of allylic alcohol **8** by *BASF*

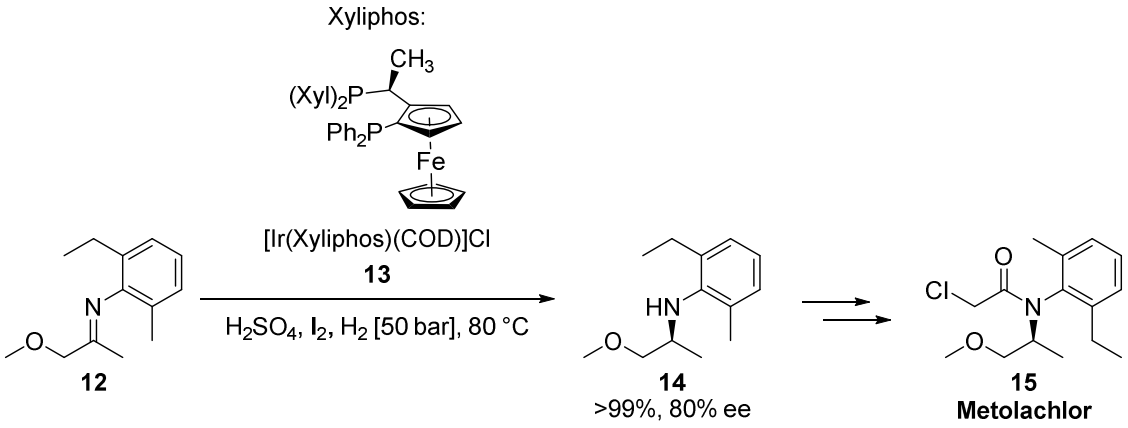

Scheme 3: Industrial iridium-cataysed asymmetric hydrogenation of imine **12** by *Syngenta*

Large scale test reactions have also been conducted in the pharmaceutical industry, such as on levofloxacin[8] (**19**) (Scheme 4) or dextrometorphan[9] (Scheme 5).

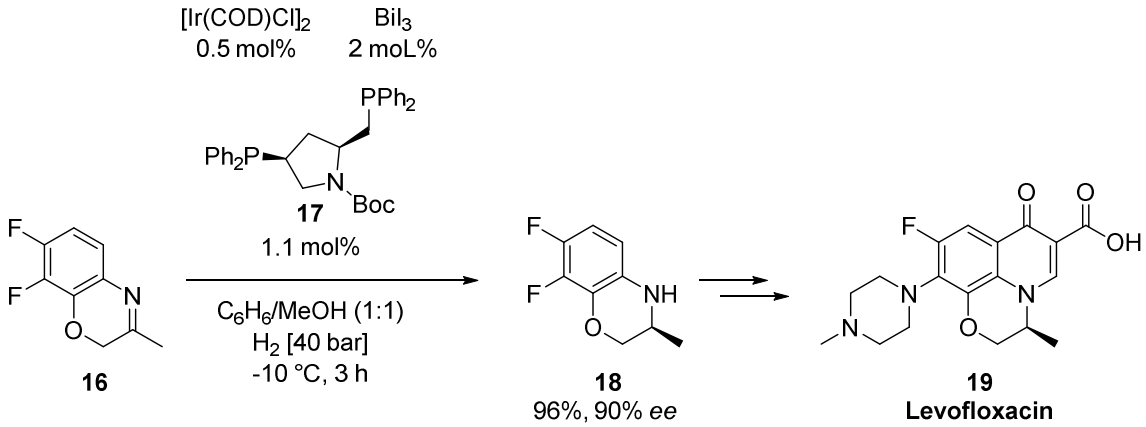

Scheme 4: Industrial iridium-catalysed asymmetric hydrogenation of imine **16** by *Daichi Pharmaceuticals*

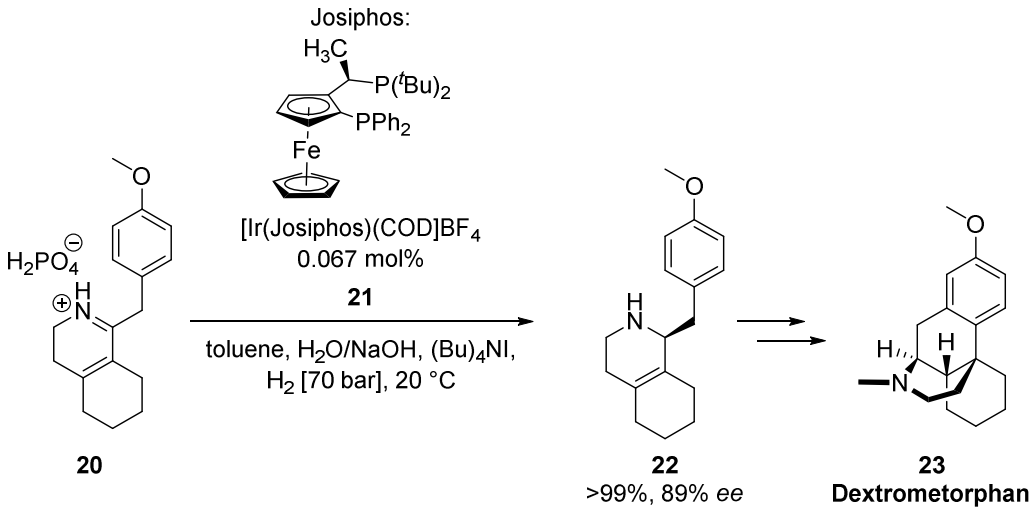

Scheme 5: Industrial iridium-catalysed asymmetric hydrogenation of imine **20** by *Lonza*

Chiral amines

Chiral amines are ubiquitous in nature. They are found in many natural products as well as in synthetic targets, both drug candidates and agrochemical agents. A selection is given in Figure 2 and Figure 3. Chiral amines can be prepared by plethora of synthetic methods. Before the development of stereoselective synthesis, the only method to isolate enantiomerically pure amines was by recrystallisation with enantiopure carboxylic acids such as tartaric acid or malic acid. A representative example for an industrial synthesis evolving from resolution to asymmetric synthesis is given in the case of Tamsulosin (**27**).[10],[11]

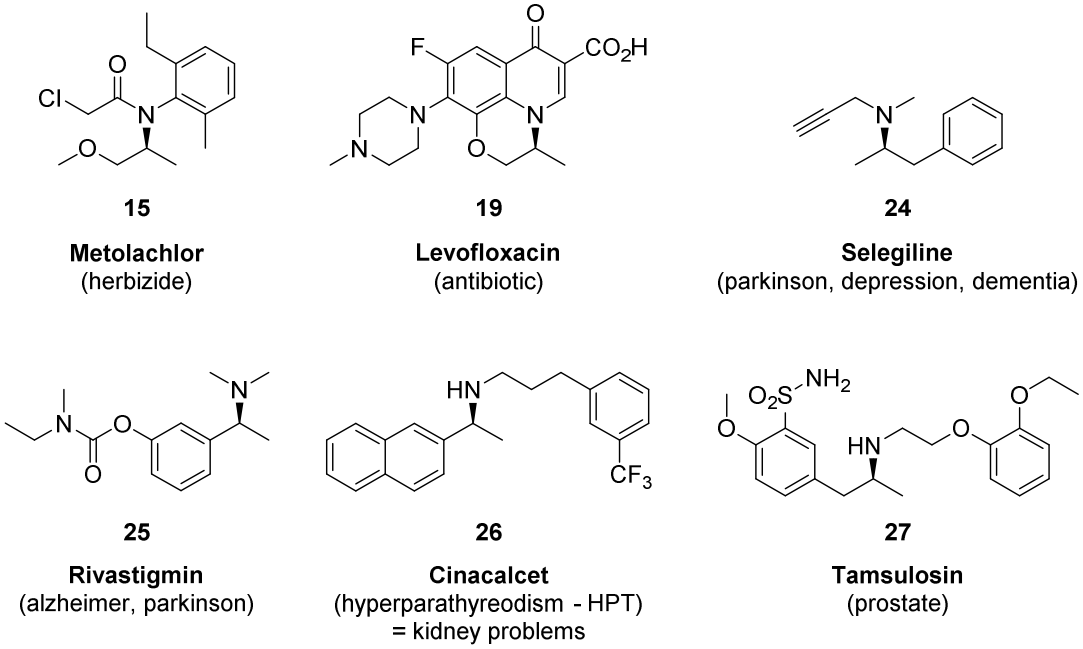

Figure 2: Pharmaceuticals, drug candidates and agrochemicals containing chiral amines

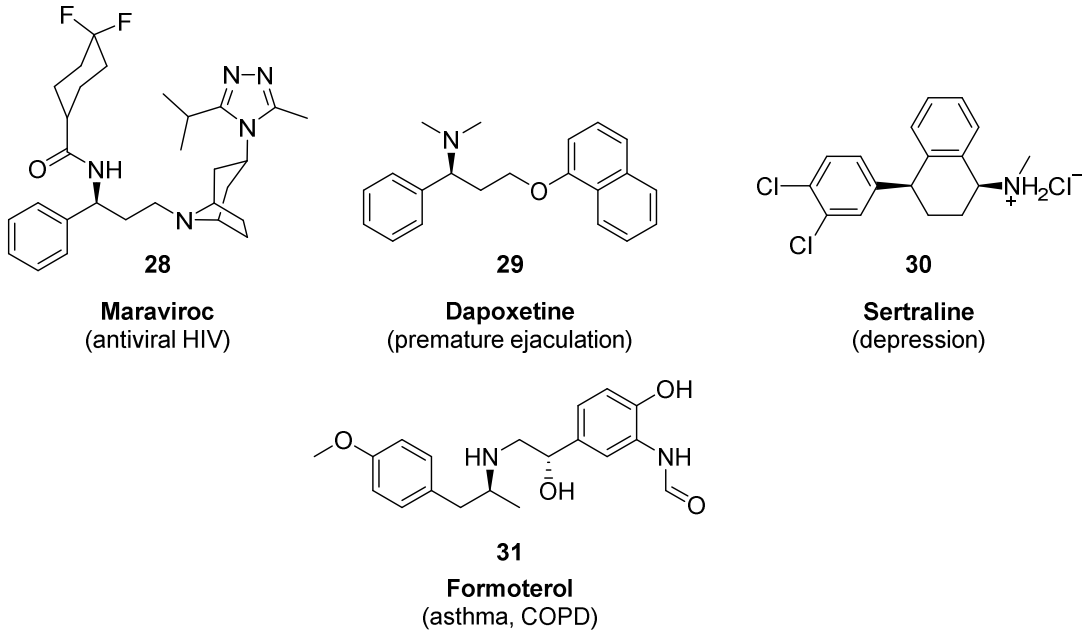

Figure 3: Pharmaceuticals, drug candidates and agrochemicals containing chiral amines

Over the years three main synthetic approaches for the preparation of chiral amines have evolved (Scheme 6). (1) Formation of a carbon-carbon bond by nucleophilic addition of an organometallic reagent to an aldimine or ketimine. (2) Reduction of prochiral imines with a chiral catalyst and a hydrogen source. (3) carbon-nitrogen bond formation by carbene insertion into a N-H bond.

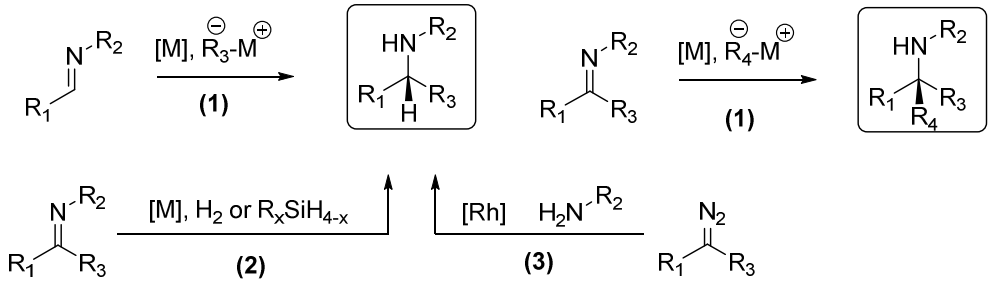

Scheme 6: Synthetic procedures to prepare chiral amines

Enantioselective hydrogenation of imines represents the most efficient method out of the three to prepare enantiomerically enriched chiral amines (except for the preparation of quaternary stereogenic centres alpha to an amine). Nevertheless, imine hydrogenation bears a number of challenges:

- C=N double bonds are intrinsically not very reactive and require a Lewis acid to promote nucleophilic attack.
- C=N double bonds are sensitive to hydrolysis, especially under Lewis acidic conditions.
- They exist as anti/syn isomers, as aminals in the presence of amines and as hemiaminals in the presence of alcohols. Imines with an alkyl substituent at the iminoyl carbon can also undergo imine-enamine tautomerisation. Such species interconvert under the reaction conditons.
- The reactivity of a C=N double bond is highly dependent on the nitrogen substituent and thus sometimes limits the substrate scope.
- The product amines are strong ligands and thus may poison and deactivate the catalyst.

The C=N double bond – isomerisation and other phenomena

Many difficulties with reducing imine double bonds are associated with their existence as *E*/*Z* isomers, imine/enamine tautomerism as well as *E*/*Z* interconversion in solution.

McCarthy and co-workers have investigated the uncatalysed *syn-anti* interconversion of *N*-aryl and *N*-alkyl imines (Scheme 7).[12] For aldimines, energy barriers between 14-20 kcal mol^{-1} were determined for uncatalysed isomerisation in solution (CCl_4). The low barriers were explained by the "lateral shift mechanism", also described as in-plane inversion. This isomerisation mechanism involves a linear transition state, where the nitrogen is adopting an sp-configuration. All the π-bonds in the aromatic system remain intact and the unshared electron pair is occupying the *p*-orbital of the nitrogen in the transition state.

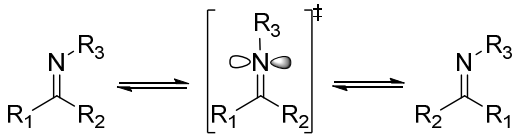

Scheme 7: "Lateral shift mechanism" in the *E*/*Z* isomerisation of imines

Kessler and co-workers have studied the influence of substituents at the *N*-aryl ring in the thermal isomerisation of chinonaniles **32** (Scheme 8).[13] By determining the coalescence temperature of the proton in capital letter by NMR studies, a clear trend towards facilitated isomerisation by electron-poor chinonaniles was observed (

Table 1). However, the substituent in *para*-position (*e.g.* methoxy) facilitates a rotational mechanism by electron pair migration to a phenoxide zwitterionic structure.

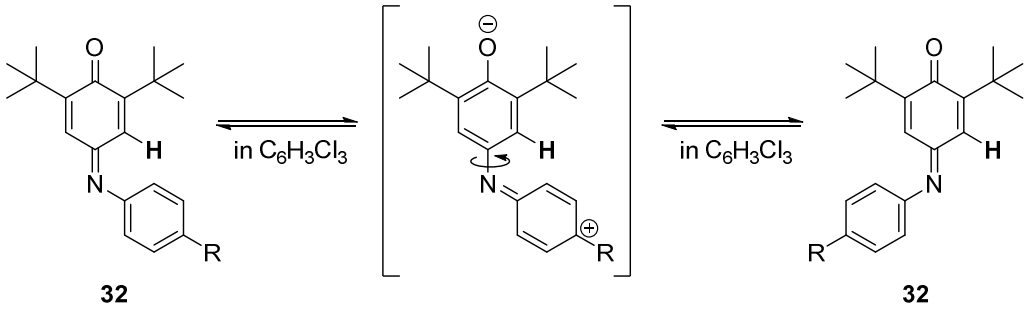

32 **32**

Scheme 8: Thermic isomerisation of chinonaniles **32**

Table 1: Coalescence temperatures of different chinonaniles **32** with electron-withdrawing and –donating substituents

Coalescence T [°C]	152	146	144	144	140	134	125	125	96	90	68
R	OMe	^{t}Bu	$N(Me)_2$	F	H	SMe	Br	I	CO_2Et	C(=O)Me	NO_2

Clark and *Parker* reported on a thermodynamic study of imine-enamine tautomerisation in different solvents (Scheme 9).[14] A clear trend of polar solvents favouring enamine **34** and **35** formation was observed. However, only poor solvent dependence on the *cis*-/*trans*-isomerisation of the enamine tautomers **34** and **35** was observed. This suggested that isomerisation would predominantly proceed *via* the imine tautomer **33**. Studies were conducted in d_6-DMSO, where imine-enamine tautomerisation is clearly favoured over *E*/*Z* interconversion.

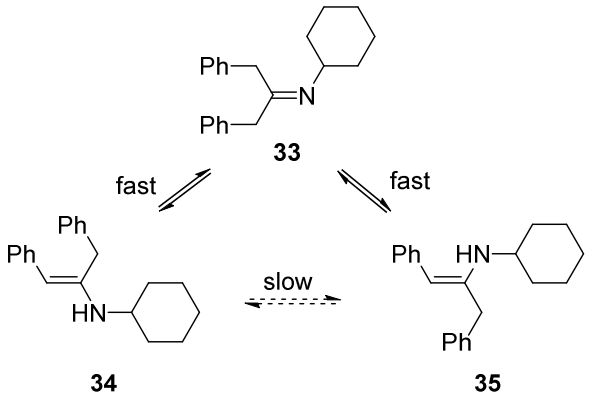

Scheme 9: Enamine interconversion of **34** and **35** *via* **33**

Jennings and *Boyd* investigated thermal interconversion on a series of *N*-alkyl ketimines by ^{1}H-NMR coalescence experiments in apolar solution (biphenyl, m.p. 69 °C) (Scheme 10).[15] The ΔG values observed were insensitive to the nature of the iminoyl carbon substituents (e.g. aryl, alkyl or hydrogen). They concluded that thermal *E*/*Z* interconversion occurred by a mechanism close to pure nitrogen inversion. For an *N*-aryl substituent, the energy of the dipolar (or diradical) transition state to result in rotation around the C=N double bond, would be considerably lowered. This interconversion mechanism was called out-of-plane rotation.

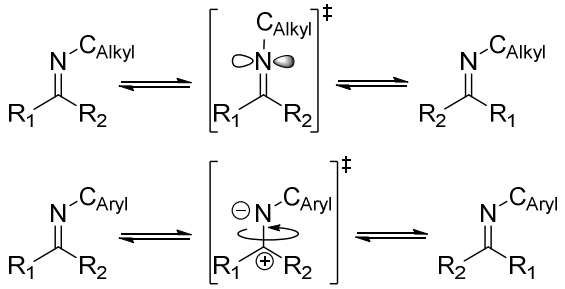

Scheme 10: Imine interconversion processes of nitrogen inversion (C_{Alkyl}) and out-of-plane rotation (C_{Aryl})

Furthermore, a strong solvent dependence on the interconversion mechanism was observed. While *E*/*Z* interconversion of **36** in diphenyl solution was fast at 200 °C, imine-enamine tautomerisation was slow. However, when **36** was dissolved in trichlorobenzene, *E*/*Z* interconversion was observed already at 140 °C by coalescence. Additionally the imine and enamine signals collapsed at 200 °C consistent with rapid imine-enamine tautomerisation. A more illustrative example is the rapid imine-enamine tautomerisation of **37** in deuterated methanol. Imine **37** can be crystallized in pure *Z* isomeric form. Once dissolved, the *C*-methyl protons rapidly show concomitant deuterium incorporation. This example demonstrated the dominance of imine/enamine tautomerism over *E*/*Z* isomerisation in methanol.

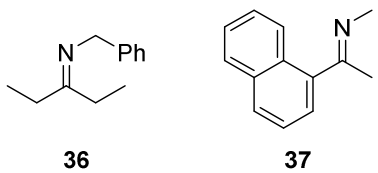

Figure 4: Imines **36** and **37**

Fischer and *Albrecht* investigated *E*/*Z* imine-enamine equilibria of several *N*-aryl propiophenone-derived imines **38** by NMR spectroscopy with regards to *N*-aryl substituent effects (Scheme 11, Table 2).[16] Only substituents in the *meta*-position of the *N*-aryl ring displayed a clear Hammet dependence. Substituents in the *para*-position of the *N*-aryl ring result in additional stabilizing and destabilizing effects which could not be correlated or described with Hammet coefficients.

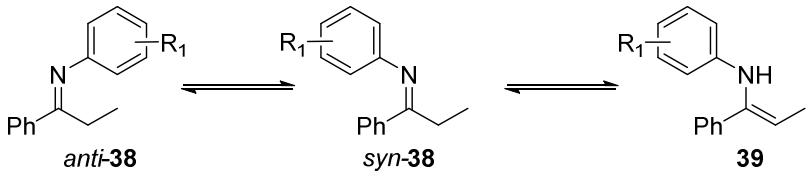

Scheme 11: Imine-enamine tautomerism of **38** to **39**

Table 2: Percentage of enamine **39** observed by ^{1}H-NMR with different substituents at the *N*-Aryl ring on **38**

R_1	% enamine
4-NMe_2	0
4-OPh	2.2
4-OMe	1.6
4-Me	3.0
4-F	2.4
4-Br	5.3
4-Cl	5.7
4-CN	27.5
4-NO_2	38.9
3-Me	4.0
3-OMe	4.1
3-F	7.4
3-Br	7.0
3-NO_2	10.7
H	3.9

The studies on *E/Z* ketimine isomers by *Jennings* and *Boyd* were extended to investigations of the equilibrium distribution of acyclic *N*-alkyl imines **40** to **45** (Figure 5).[17] Steric factors were investigated by increasing the size of the C_{Alkyl}-substituent and it appeared that the larger the C_{Alkyl}-substituent, the *E*-isomer became more destabilized due to steric repulsion. This also concluded that the steric bulk exhibited by a phenyl group lies in the range of a *n*-propyl and *iso*-propyl group.

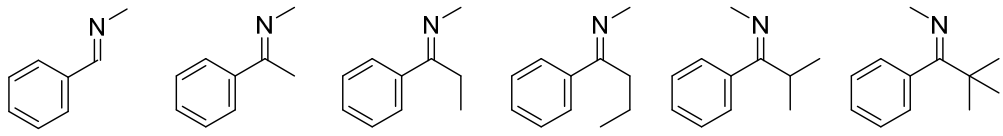

40	**41**	**42**	**43**	**44**	**45**
E/Z	*E/Z*	*E/Z*	*E/Z*	*E/Z*	*E/Z*
100:0	93:7	74:26	70:30	5:95	0:100

Figure 5: Investigation of imine-enamine ratio with regards to the C_{Alkyl}-substituent at the iminoyl carbon in **40** to **45**

On the other hand, electronic effects appeared to overrule steric repulsion. Three examples of increasing steric bulk around the *N*-alkyl substituent in **46** to **48** did not change the ratio of *E/Z* isomers significantly (Figure 6). The ratio of *E/Z* isomers did not change significantly over a large solvent range either: $CDCl_3$, CCl_4, C_6D_6, $C_6H_3Cl_3$, CD_3CN, $(CD_3)_2CO$ and ^{t}BuOH.

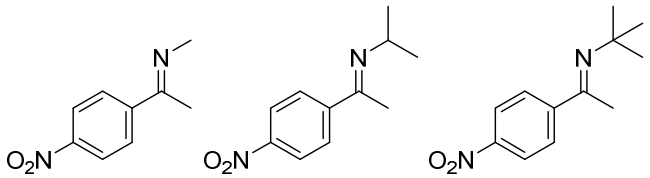

46	**47**	**48**
E/*Z*	*E*/*Z*	*E*/*Z*
97:3	95:5	98:2

Figure 6: Unaffected *E*/*Z* ratio of imines **46** to **48** with increasing size of the *N*-substituent

Steric repulsion between *ortho*-substituents of imine **49** resulted in formation of the of the *Z* isomer. While steric clash could be prevented by a rotation of the phenyl substitent out of the plane of delocalization, also a destabilizing repulsive interaction between the nitrogen lone pair and the aromatic π-electrons was discussed (Scheme 12).

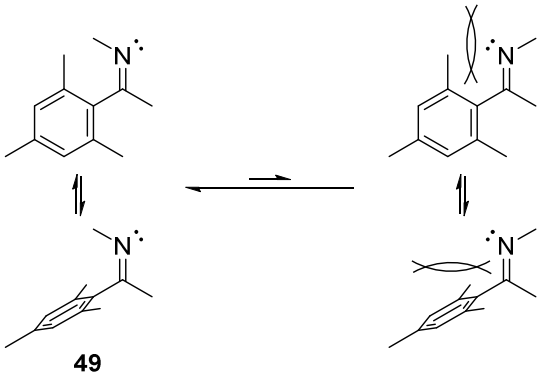

49

Scheme 12: Favoured formation of the *Z* isomer in **49** due to electronic repulsion of the aryl ring and the nitrogen atom lone pair

James and co-workers investigated the rate of isomerisation of **50** in benzene/MeOH 1:1 at ambient temperature (Figure 7).[18] Isomerisation rates of *Z*=>*E* of 155 h^{-1} and *E*=>*Z* of 11 h^{-1} were determined by EXSY NMR experiments. These values have been obtained with large mixing times of 1.8 seconds. Thus, they need to be considered with care, since accurate numbers can only be obtained with much shorter mixing times. They also investigated the asymmetric hydrogenation of imine **50**. The TOF of their catalyst was determined to be between 14 to 66 h^{-1}. Since the *E*/*Z* isomer ratio and the rate of isomerisation did not affect the *ee*, it was concluded that the rate of the reaction entirely depended on the diffusion of hydrogen into the solution and not isomerisation. Isomerisation processes catalysed or promoted by the transition metal have not been discussed but may well be considered in such an example.

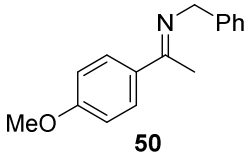

50

Figure 7: Imine **50**

Kocovsky and co-workers have analysed a number of *N*-aryl imines with aromatic, heteroaromatic and alkyl substituents at both carbons adjacent to iminoyl funtionality (Figure 8). The main configuration of the imine double bond was observed to be *E* with *E*/*Z* ratios between 10:1 and 7:1. This only holds true as long as one substituent is large (e.g. aryl) and one is small (e.g. methyl) as in **51**. Mixtures are observed when both substituents are sterically demanding, especially in the case of an aryl and a large alkyl substituent as in **52**. Enamines have been observed predominantly in substrates bearing electron withdrawing substituents such CH_2COOEt as in **53**. They postulated the enamine form to be more stable due to a stabilizing hydrogen-

bonding between the N-H proton and the electron-withdrawing group. Equilibration of imines was observed in $CDCl_3$ solution in the case of β-enamino nitriles as **54**. Also, traces of Brønsted acids were shown to facilitate isomerisation.

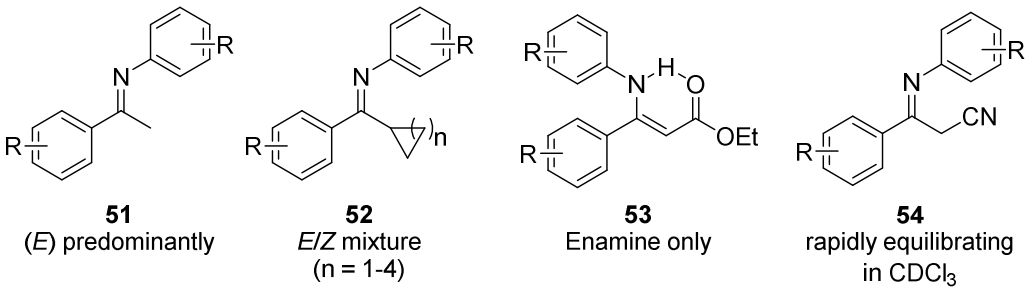

Figure 8: Predominant imine or enamine tautomer of **51** to **54** observed in solution, depending on the substrate structure and substituent

Facilitated isomerisation by Brønsted acids is particularly interesting since iridium hydride species have been demonstrated to be Brønsted acidic. Therefore, *E*/*Z* ratio of *N*-aryl imines in solution can possibly be ignored due to rapid interconversion in case where *E*/*Z* isomerisation is faster than hydrogenation, e.g. catalysed by metal coordination or Brønsted acidic hydrides.

Asymmetric Imine Hydrogenation

The first approach for the preparation of enantiomerically enriched chiral amines was reported by *Kagan* and co-workers. They developed a hydrosilylation reaction catalysed by rhodium catalyst **56** with ligand **57** and subsequent hydrolysis to afford the chiral amines **58** and **60** (Scheme 13).[19] Rhodium-catalysed hydrosilylation had been developed independently by *Ojima* and co-workers[20] using *Wilkinson's* catalyst and Ph_2SiH_2.[2]

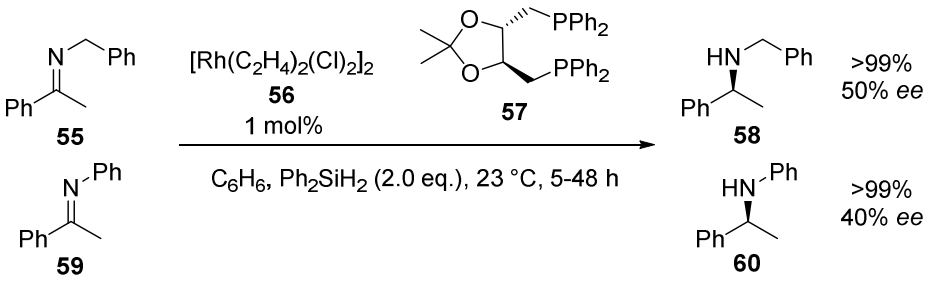

Scheme 13: Asymmetric rhodium-catalysed imine hydrosilylation of **55** and **59**

This newly developed protocol for imine hydrosilylation also paved the way for the development of enantioselective hydrogenation of imines. While homogeneous hydrogenation of imines had already been reported by *McQuillin* and co-workers employing a rhodium catalyst $[(Py)_3RhCl_3]$ and sodium borohydride in the presence of hydrogen gas,[21] *Scorrano* and co-workers reported the first example of an asymmetric hydrogenation of an imine (Scheme 14).[22] They generated a rhodium catalyst **61** very similar to the one *Kagan* used in the hydrosilylation of imines.

[2] *Kagan* and co-workers were not aware of this discovery when submitting their work.

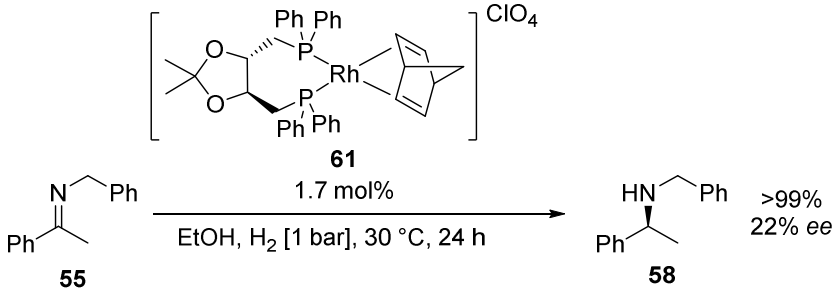

Scheme 14: Asymmetric rhodium-catalysed imine hydrogenation of **55** using **61**

During the next decade, with the development of new chiral phopshorus ligands such as **63**, higher enantioselectivities were achieved. Furthermore, a temperature dependence was noted. Conducting reactions at lower temperature provided higher enantioselectivities while maintaining reactivity. A selected example is given in Scheme 15.[23],[24]

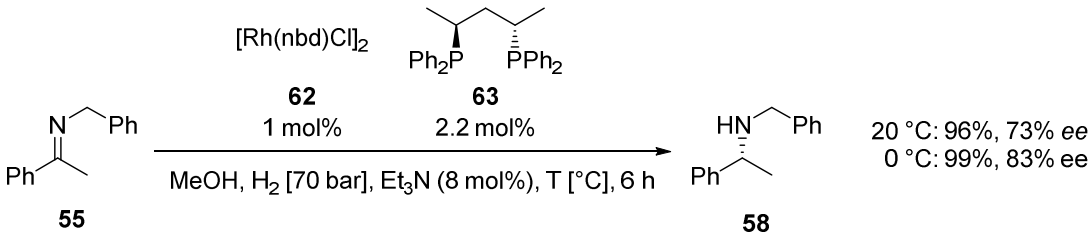

Scheme 15: Improved *ee* in the asymmetric rhodium-catalysed hydrogenation of imine **55** at lower temperature

By the time of the late 1980's, asymmetric hydrogenation had been established on C=C, C=O and C=N double bonds with rhodium and ruthenium catalysts. Industrial asymmetric hydrogenations were dominated by rhodium and ruthenium catalysts due to their high efficiencies and extensive studies in the literature. This drastically changed in 1990 when an industrial team of researchers led by *Blaser* and co-workers reported on the first enantioselective hydrogenation of imines using iridium complexes generated from **64** and chiral phosphorus ligands such as **63**. Efforts were devoted to structural analogues **65** and **66** of the potent herbicide Metolachlor (Scheme 16).[25] Further studies led to the currently applied protocol using Xyliphos ligands (Scheme 3).

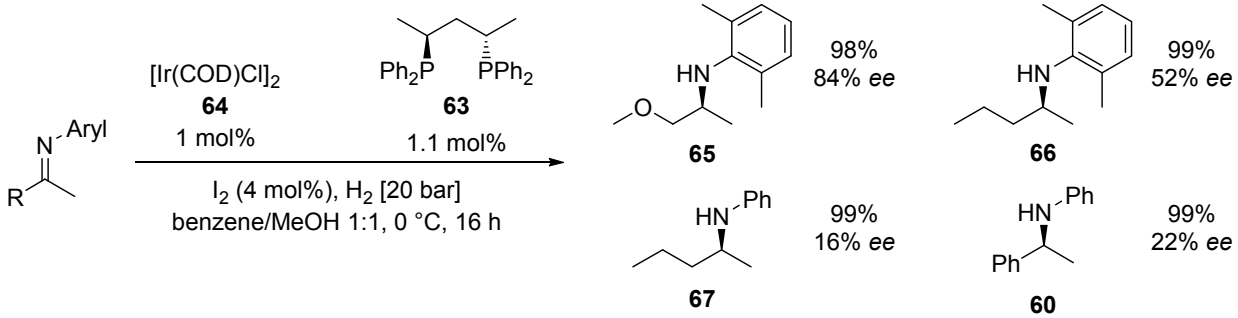

Scheme 16: First example of iridium-catalysed asymmetric imine hydrogenation

Shortly after the discovery of *Blaser*, *Osborn* and co-workers reported similar results on the asymmetric hydrogenation of imines by iridium(III) hydride complexes such as **69** or **70**. Very low catalyst loadings up to 0.1 mol% showed highly efficient asymmetric reduction of imine **68** (Scheme 17) and **59** (Scheme 18) albeit with low to moderate enantioselectivities. The catalyst was optimized for each substrate. The role of iodine was demonstrated to be of critical importance. The complexes were prepared by refluxing $[Ir(I)(P'P)(COD)]BF_4$ in the presence of LiI. The oxidation was postulated to occur due to the presence of

water by an unknown mechanism.[26] Such an oxidation thus probably also occurs *in situ* in the system reported by *Blaser*.[3,27]

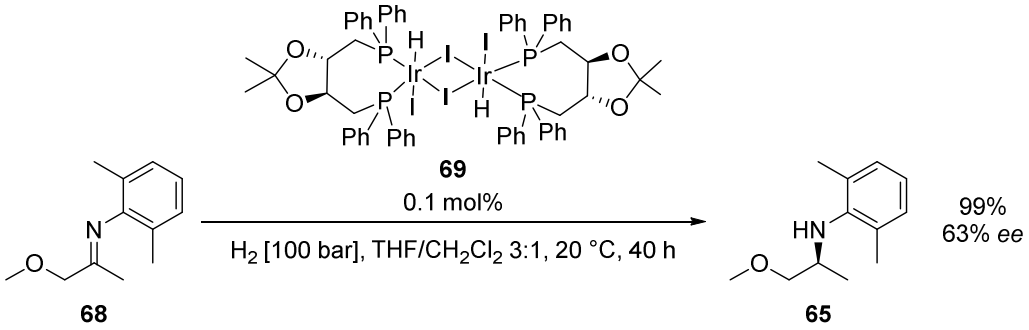

Scheme 17: Asymmetric hydrogenation of imine **68** by iridium(III) hydride iodo-bridged trimer **69**

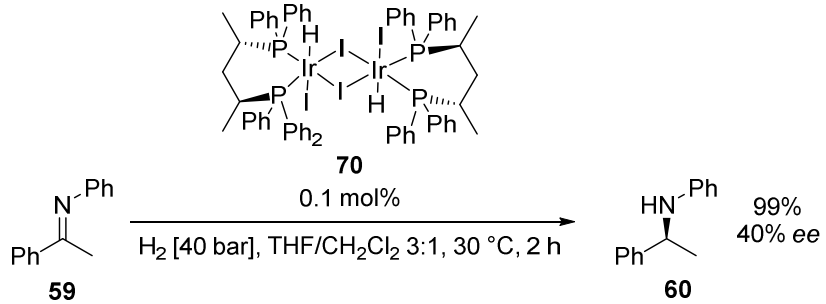

Scheme 18: Asymmetric hydrogenation of imine **70** by iridium(III) hydride iodo-bridged trimer **70**

In 1992, *Buchwald* and co-workers developed a titanocene complex **72** and employed it in asymmetric hydrogenation of imines. While excellent enantioselectivites were obtained for cyclic amines such as **73**, moderate to high enantioselectivities were observed with acyclic imines such as **55** (Scheme 19). Very high hydrogen gas pressure, elevated reaction temperature, long reaction times and an impractical preparation of the catalyst from complex **71** with *n*-butyl lithium represented major drawbacks of this methodology. Furthermore, the *E*/*Z* ratio of the imine could be well correlated to the enantiomeric excess observed for each substrate and therefore limited the possibilities towards optimisation.[28]

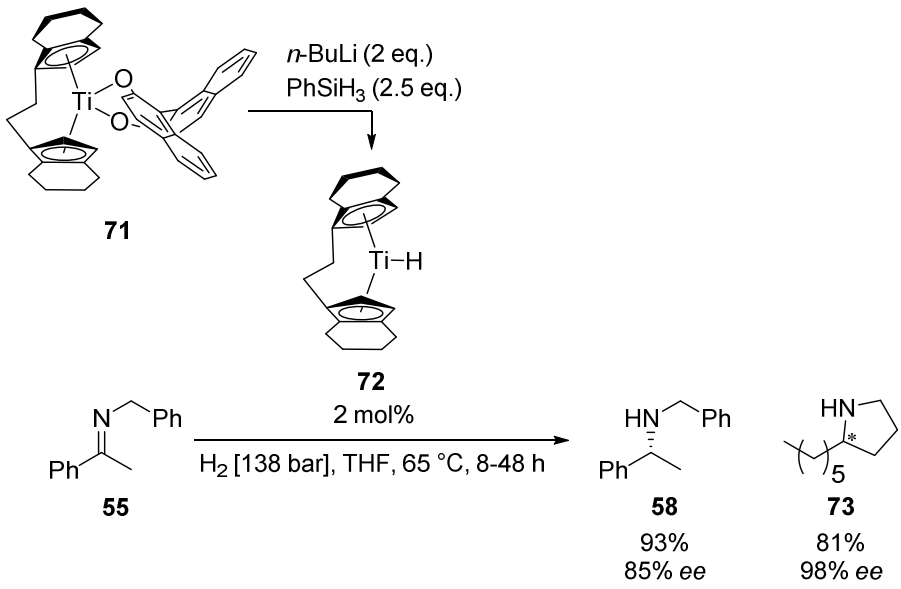

Scheme 19: Titanocene **72** catalysed asymmetric hydrogenation of imine **55**

[3] details are given in the mechanistic section

In 1996, *Noyori* and co-workers showed high *ee*'s in the asymmetric transfer hydrogenation of imines employing a ruthenium-diamine complex **74** and **75**. While excellent enantioselectivities and very fast reactions were obtained for cyclic substrates such as tetrahydroquinoline **75** (Scheme 21), moderate to good enantioselectivities with very long reaction times were observed for acyclic imine **55** (Scheme 20).[29]

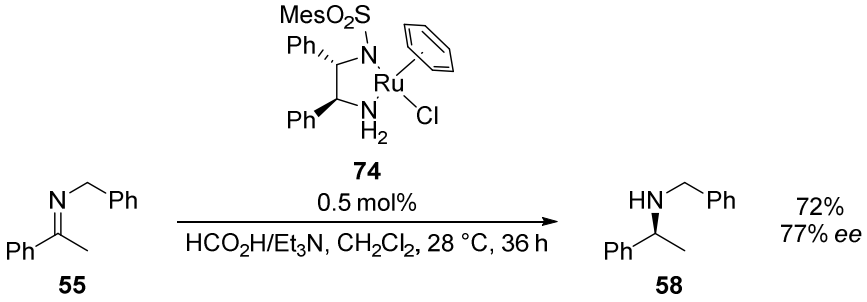

Scheme 20: Asymmetric hydrogenation of imine **55** by ruthenium catalyst **74**

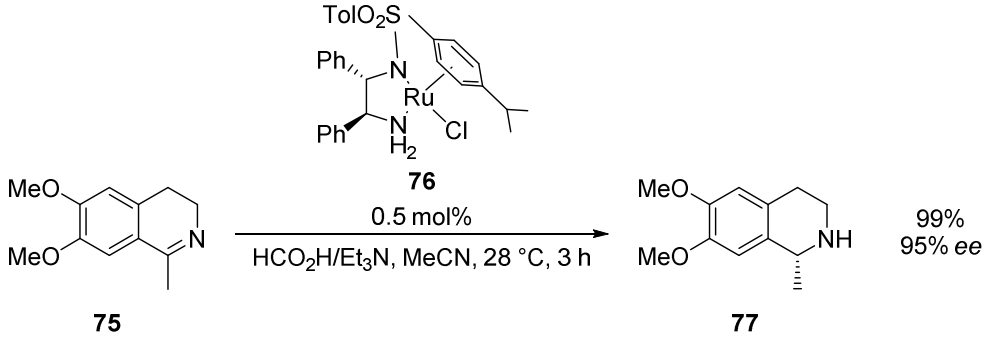

Scheme 21: Asymmetric hydrogenation of tetrahydroquinoline **75** by ruthenium catalyst **76**

In 1997, *Pfaltz* and co-workers[30] developed iridium catalyst **78** with a phosphine-oxazoline ligand and used it in the asymmetric hydrogenation of imines (Scheme 22). The isopropyl substituent on the oxazoline was demonstrated to be optimal for imine hydrogenation. Full conversion with moderate to high enantioselectivities was observed for a number of substrates. A remarkable concentration effect was observed in the case of imine **59**: decreasing the substrate and catalyst concentration improved the enantioselectivity of the hydrogenation significantly. Such high enantioselectivites marked a significant improvement of iridium catalysts in asymmetric imine hydrogenation.

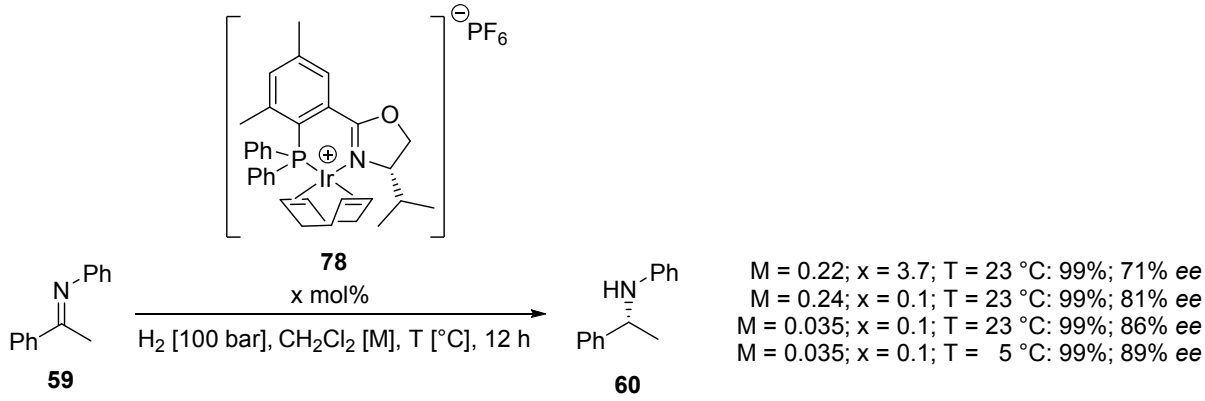

Scheme 22: Asymmetric hydrogenation of imine **59** with iridium-PHOX catalyst **78**

A careful study of the different substituents at the imine was conducted (Scheme 23).

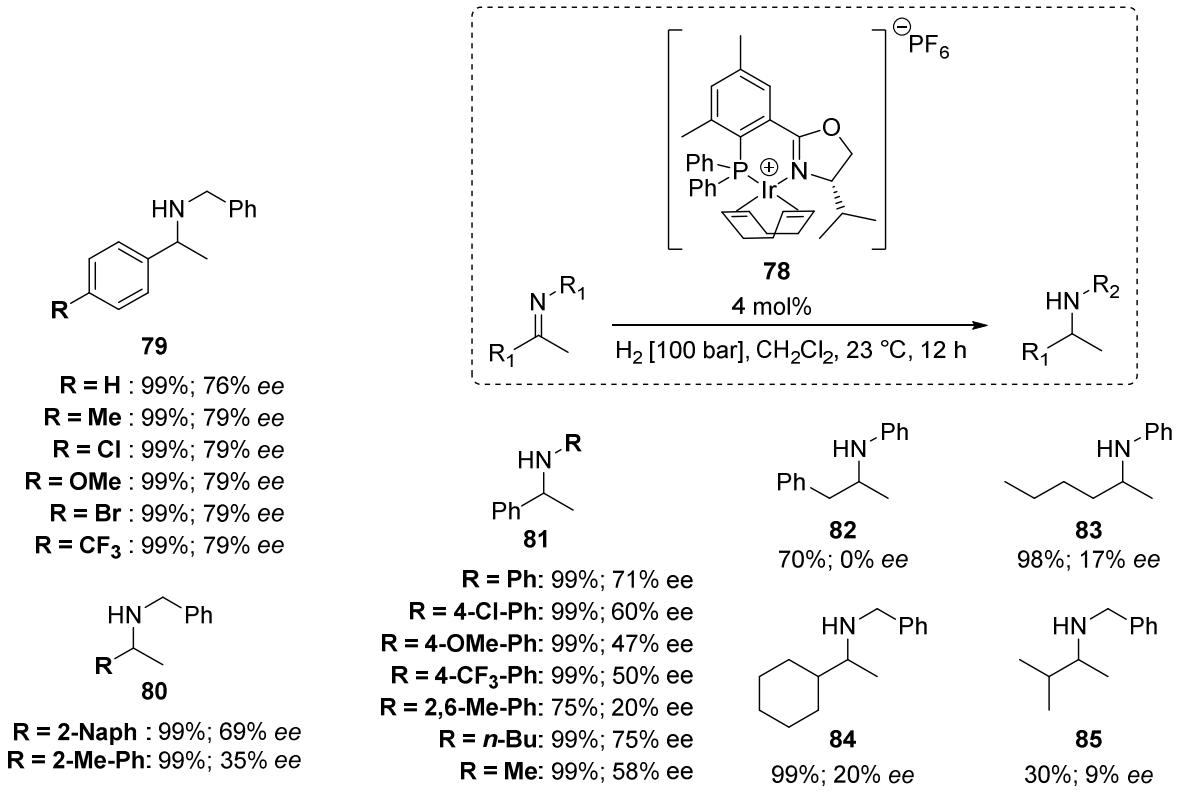

Scheme 23: Substrate scope evaluated in asymmetric hydrogenation of imines catalysed by iridium-PHOX complexes

While acetophenone *N*-benzyl derived imines like **79** showed high reactivity and selectivity irrespective of their substituents, increasing the steric bulk at the acetophenone ring as in **80** decreased the *ee* while maintaining reactivity. Aryl-alkyl imines with different *N*-substituents **81** provided the corresponding amines in high yields and varying enantioselectivities. The steric bulk and electronic effect of the *N*-substituent appeared to influence both reactivity and selectivity. Quite drastically, both *ee* and conversion were low in the case of dialkyl-derived *N*-benzyl and *N*-phenyl imines **82** to **85**. Electronically activated imines such as oximes, oxime ethers, hydrazones and imines derived from trifluoromethylphenyl ketone showed no reactivity. Cyclic imines were reduced with moderate enantioselectivities. No correlation between the *E*/*Z* ratio of the imine and the enantioselectivity was observed. Furthermore, higher enantioselectivity was obtained with interconverting acyclic *E*/*Z* imines compared to cyclic imines with fixed geometry. Additives such as iodide, phthalimide and amines were evaluated. While iodide resulted in significantly lower enantioselectivity and opposed optical rotation of the product amine, sodium acetate or 1,2-diaminoethane completely inhibited the reaction.

The discovery by *Pfaltz* and co-workers marked the beginning of a plethora of chiral iridium complexes employed as catalysts for asymmetric imine hydrogenation. A summary of the progress over the last 15 years is given on the following pages.

A detailed reinvestigation of modified phosphine-oxazoline complexes developed in the *Pfaltz* laboratory depicted highly effective and selective catalysts for asymmetric imine hydrogenation.[31] Iridium complexes with a SimplePHOX ligand as **87** showed enhanced reactivity and selectivity when comparing to previously employed PHOX catalyst **86**. Reaction temperatures could be lowered to -20 °C maintaining reactivity with the SimplePHOX catalysts (Scheme 24). While hydrogen pressure did not influence the outcome of the reaction, lowering the catalyst loading to 0.1 mol% resulted in reduced conversion. It stated in the paper, that "imines derived from dialkylketones gave only low conversion and enantioselectivity, whereas cyclic imines with a C=N bond in a five or six-membered ring showed no reactivity." No further details on such experiments were provided.

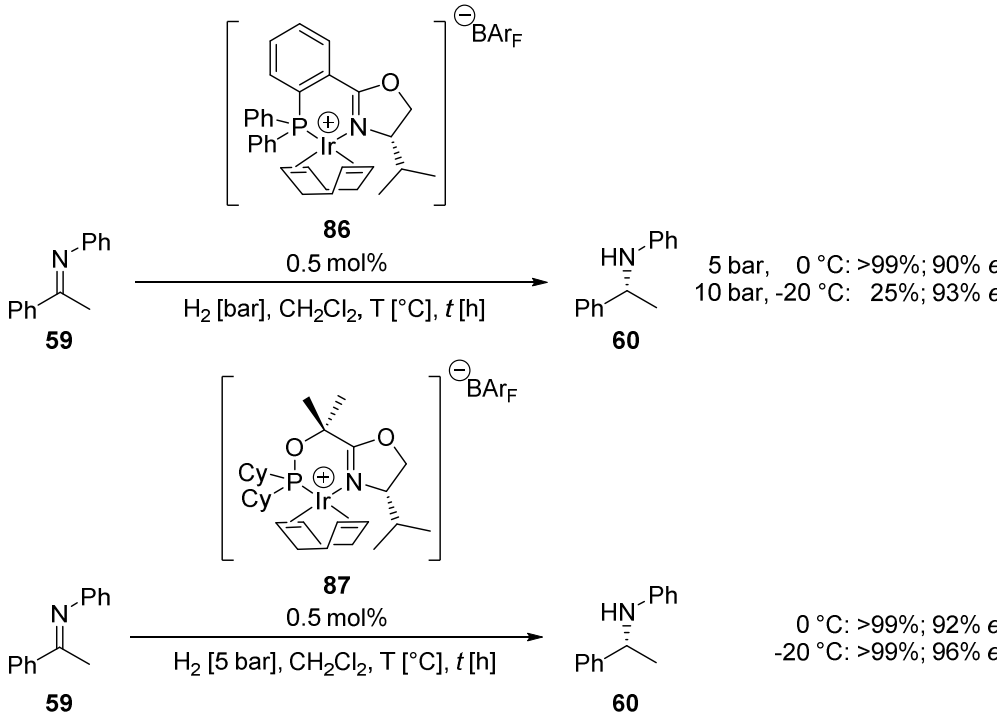

Scheme 24: Asymmetric hydrogenation of imine **59** with complexes **86** or **87**

Zhang and co-workers reported on highly selective imine hydrogenation employing iridium-ferrocene-binaphane ligand **88**.[32] While high to excellent enantioselectivities were observed in the case of **89** and **60**, dialkyl imines showed significantly reduced reactivity and selectivity as seen for amines **90**, **91** and **92** (Scheme 25). Many additives such as phthalimide, TBAI or benzylamine did not give any improvement. Iodine on the other hand depicted opposite effects. In one example, the *ee* could be improved to 94% but with a similar substrate, it eroded from 99% to 69%. The cause was not further investigated. An iridium(III)-species was postulated to be the active catalyst during hydrogenation, and the catalyst was suggested to maintain its oxidation state under reaction conditions.[4]

[4] in relation to the findings by *Spindler* and *Osborn*

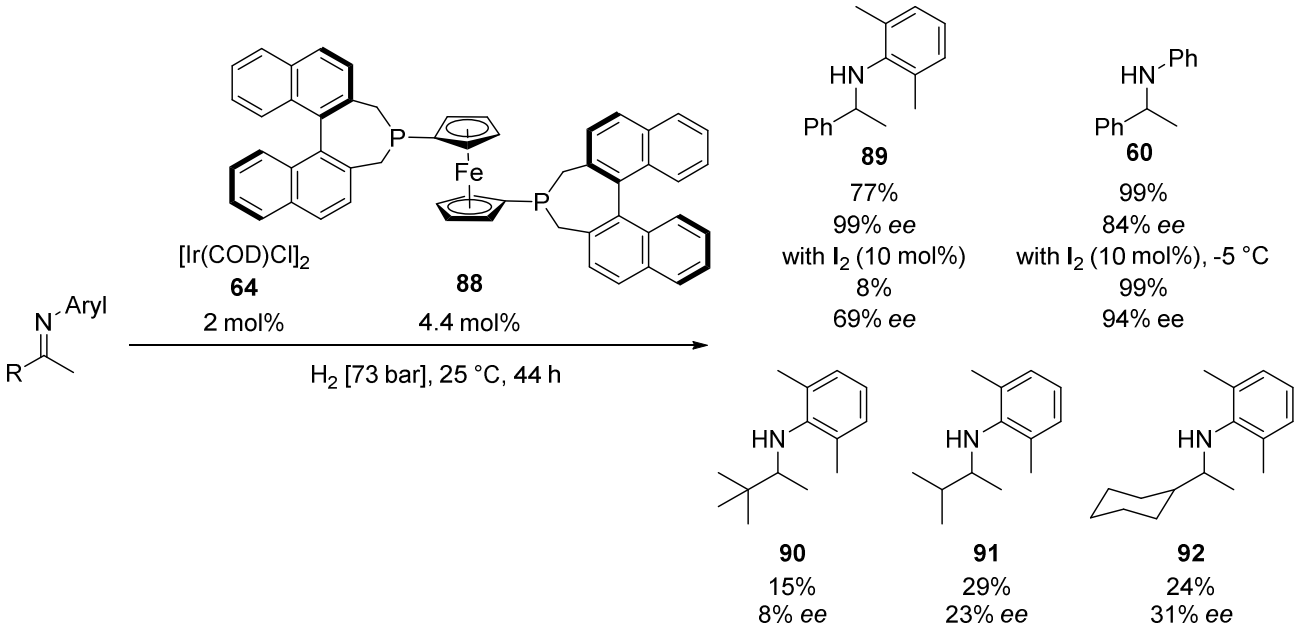

Scheme 25: Asymmetric hydrogenation of N-Aryl imines using **64** and **88**[5]

The same system has also been applied to NH imines in 2009.[33] The hydrochloric salts of NH imines were directly subjected to hydrogenation conditions. While excellent results were obtained with acetophenone-derived imines, only two dialkyl imines displayed high conversion with reduced enantioselectivity (Scheme 26). Preliminary mechanistic information was obtained with deuterium hydrogenation and deuterium incorporation was only observed at the α-position of the amine to about 60%.

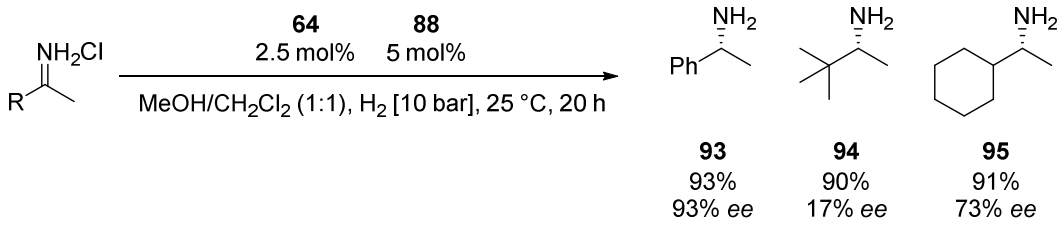

Scheme 26: Asymmetric hydrogenation of NH imines using **64** and **88**

In 2004, *Andersson* and co-workers introduced new Ir(P'N) complexes such as **96**, analogous to the phosphineoxazolines by *Pfaltz*, for asymmetric imine hydrogenation.[34] Only acetophenone-derived *N*-aryl imines were tested, giving results similar to *Pfaltz'* phosphineoxazoline catalysts. In 2006, Andersson and co-workers reported on a more detailed study of imine hydrogenation using their previously introduced iridium(P´N) catalysts.[35] While imine **59** afforded amine **60** in full conversion and high *ee*, dialkyl derived imines gave the corresponding amines as **97** in low yield. Amine **98** was not obtained (Scheme 27), neither were cyclic amines.

[5] The authors did not determine absolute configuration, no supporting information is available.

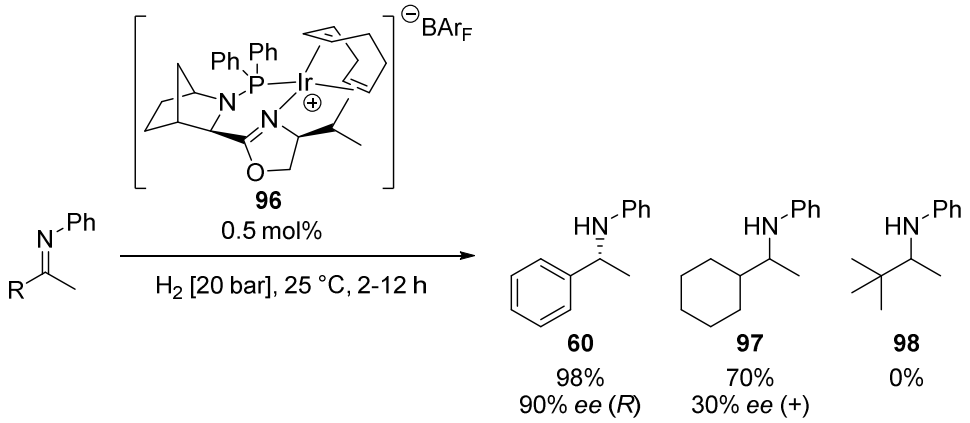

Scheme 27: Asymmetric hydrogenation of imines using **96**

Bolm and co-workers introduced chiral sulfoxime ligands such as **100** for enantioselective imine hydrogenation.[36] Iodine was required to oxidize the catalyst since the absence of iodine resulted in no catalytic activity. Only acetophenone-derived *N*-aryl imines were evaluated. Within 4 to 12 hours, full conversion was achieved with high enantioselectivity in the case of imine **99** (Scheme 28).

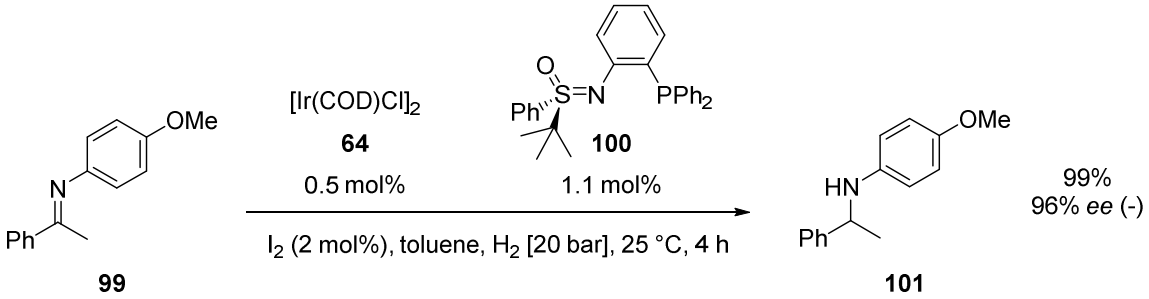

Scheme 28: Asymmetric imine hydrogenation with iridium-sulfoxime catalyts generated from **64** and **100**

Imamoto and co-workers reported on highly active iridium catalysts such as **102** for enantioselective imine hydrogenation. Different acetophenone-derived *N*-aryl amines such as **103** were prepared with up to 99% enantioselectivity (Scheme 29). Only the complex with a BAr_F counterion showed catalytic activity. The only example of a dialkyl amine **98** did not show any conversion.[37]

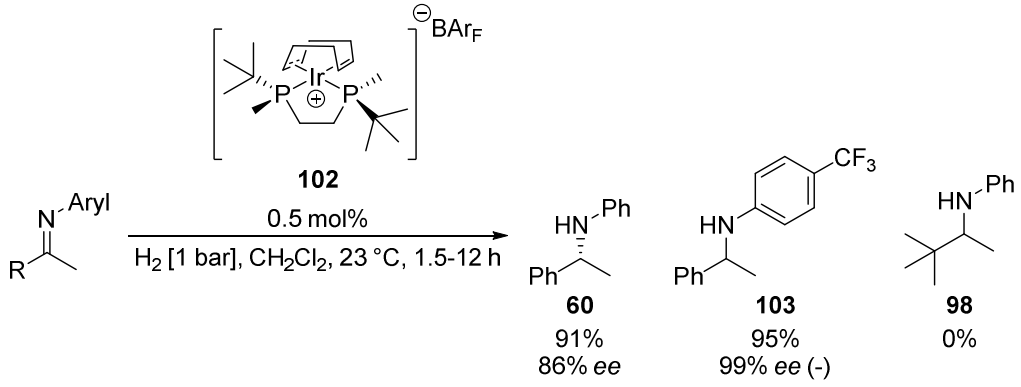

Scheme 29: Asymmetric hydrogenation of imines using **102**

Zhou and co-workers introduced highly elaborate spiro phosphinooxazoline iridium complexes such as **104** as catalysts for asymmetric imine hydrogenation.[38] Only acetophenone-derived *N*-aryl imines were evaluated providing the corresponding amines **60** or **105** in full conversion and high enantioselectivities (Scheme 30). As shown, electron-withdrawing substituents at the *N*-aryl ring in amine **105** resulted in slightly increased enantioselectivity.

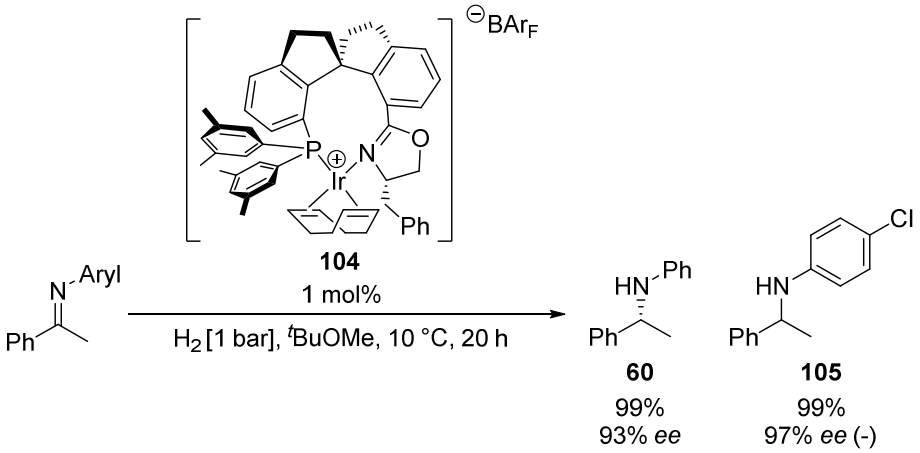

Scheme 30: Asymmetric hydrogenation of imines using **104**

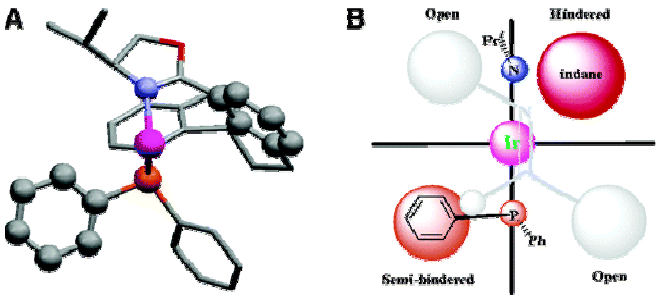

Figure 9: Cartoon model of complex **104** attempting to explain its enantioinduction

The origin of enantioselectivity was explained in a cartoon model (Figure 9). The space around the metal centre was divided into quadrants. In the upper right the steric repulsion of the ligand backbone structure was postulated to hinder the substrate placing any bulky substituent into that quadrant. On the other hand, the lower left quadrant is experiencing less steric bulk by only one of the phosphorus substituents. This might allow the second least sterically demanding methyl group of the substrate being placed in that quadrant. Ultimately, the upper left as well as the lower right were believed to be the least sterically demanding. Therefore, the two large phenyl substituents of the substrate could be placed in these quadrants. According to this model, hydrogen would be added to the substrate from its *Si* face to furnish the (*R*)-amine, the same enantiomer that is also observed in the catalytic reaction.

Knochel introduced ferrocenyl P'N iridium complex **106** as a catalyst for asymmetric imine hydrogenation. Only acetophenone-derived *N*-aryl imines were evaluated.[39] Increasing the steric bulk at the *N*-aryl ring improved the enantioselectivity significantly as demonstrated on amine **107** (Scheme 31).

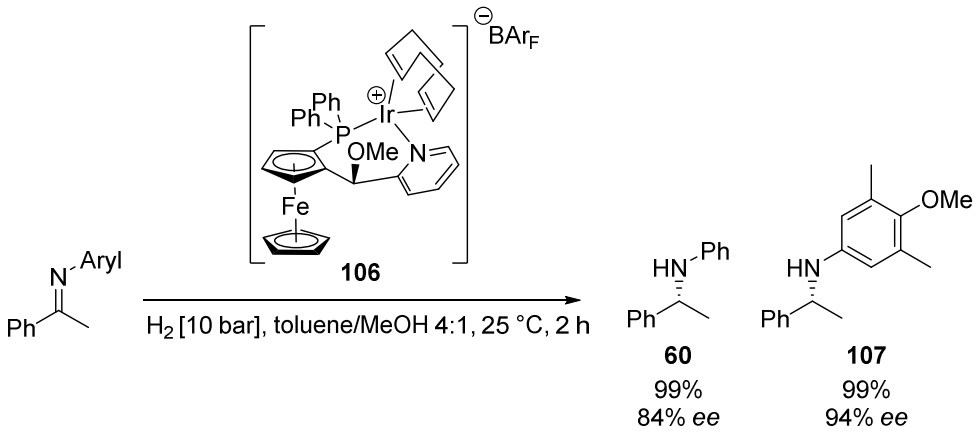

Scheme 31: Asymmetric hydrogenation of imines using **106**

In 2009, *Feringa* and co-workers reported on monodentate phosphoramidite ligands like **108** employed in iridium catalysed asymmetric imine hydrogenation.[40] Similar to the findings by Knochel, increasing the steric bulk at the *N*-aryl substituent resulted in significantly improved enantioselectivity (Scheme 32). A clear trend towards increased reactivity with less coordinating counterions was observed. While BAr$_F$ and

PF_6 provided the corresponding amines at atmospheric hydrogen pressure, 50 bar hydrogen gas pressure was required when using the chloride precursor. The only dialkyl *N*-phenyl imine evaluated gave poor enantioselectivity as seen with amine **83**.

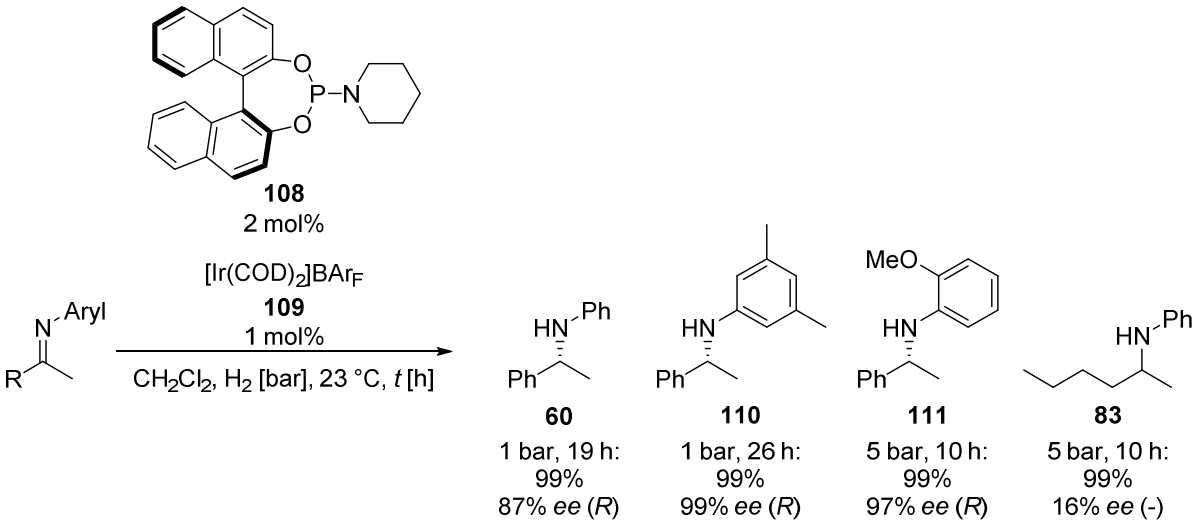

Scheme 32: Asymmetric imine hydrogenation with iridium-phosphoramidite catalyts generated from **108** and **109**

In 2008, *Xiao* and co-workers reported on chiral counterion-aided asymmetric imine hydrogenation. Iridium diamine complexes such as **112** were tested in combination with chiral phosphoric Brønsted acids such as **113**.[41]

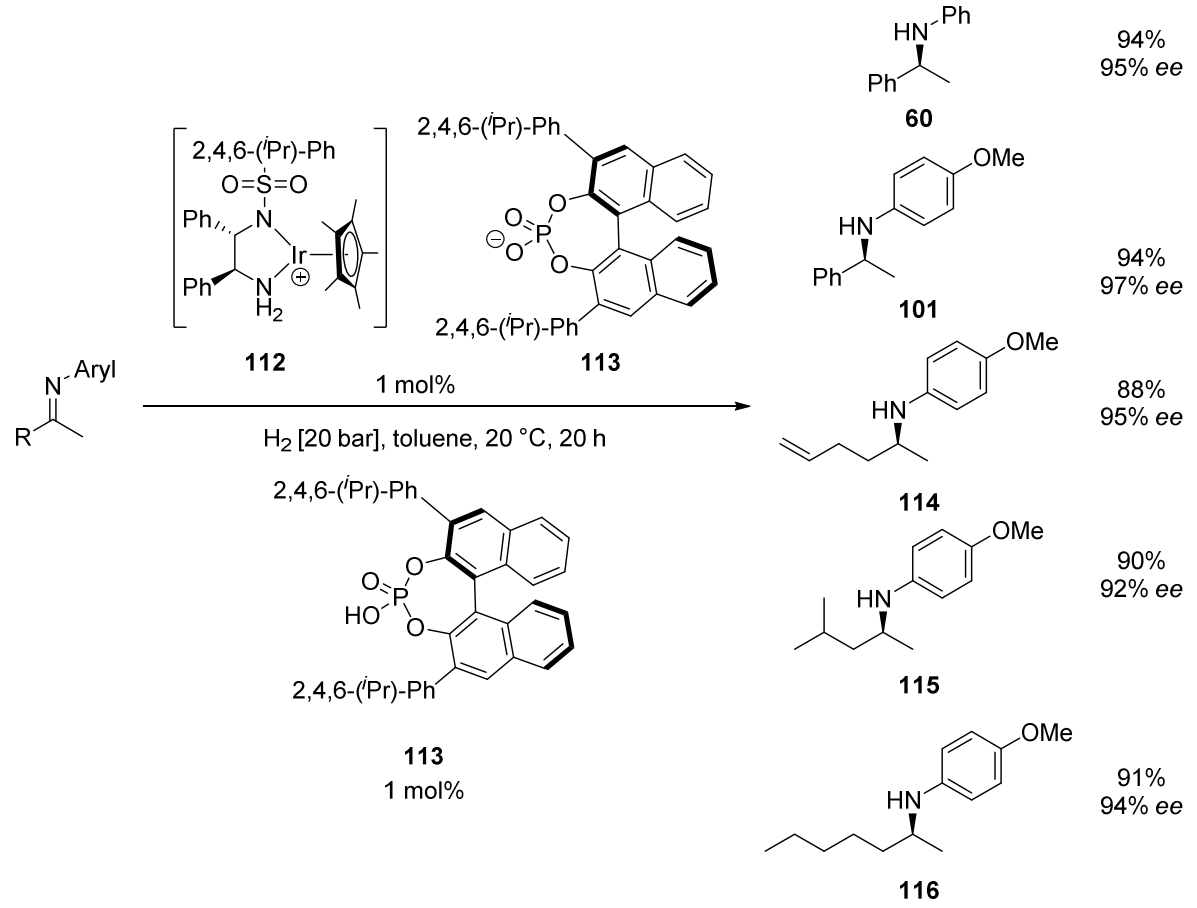

Scheme 33: Asymmetric imine hydrogenation with complex **112**-**113**

While no conversion was observed when using the iridium(III) complex **112** alone, addition of phosphoric acid **113** resulted in high conversion with up to 97% *ee* (Scheme 33). The protonated complex, generated by

protonation of the neutral complex with the phosphoric acid furnished a significantly more reactive catalyst. Addition of yet another equivalent of phosphoric acid **113** with regards to the catalyst resulted in high conversion while maintaining the excellent enantioselectivity. Acetophenone-derived, as well as dialkyl *N*-aryl imines, were hydrogenated with high conversion and excellent enantioselectivities. However, the enormous molecular weight of the catalyst, its elaborate synthesis and incomplete conversion represent major disadvantages of this methodology.

The same catalyst was also evaluated in reductive amination of **117** and **118**.[42] While no imine condensation and isolation is required prior to reduction, chemoselectivity issues arise due to competitive ketone reduction (Scheme 34). Similar enantioselectivities to the one's in imine hydrogenation are obtained. Again, excellent results with acetophenone-derived, as well as dialkyl *N*-aryl imines, have been obtained. Despite being conceptually interesting, 5 mol% catalyst loading with such a large catalyst remains intolerable compared to state-of-the-art methodology. Furthermore, higher yields are obtained over two steps when reactions are carried out separately.

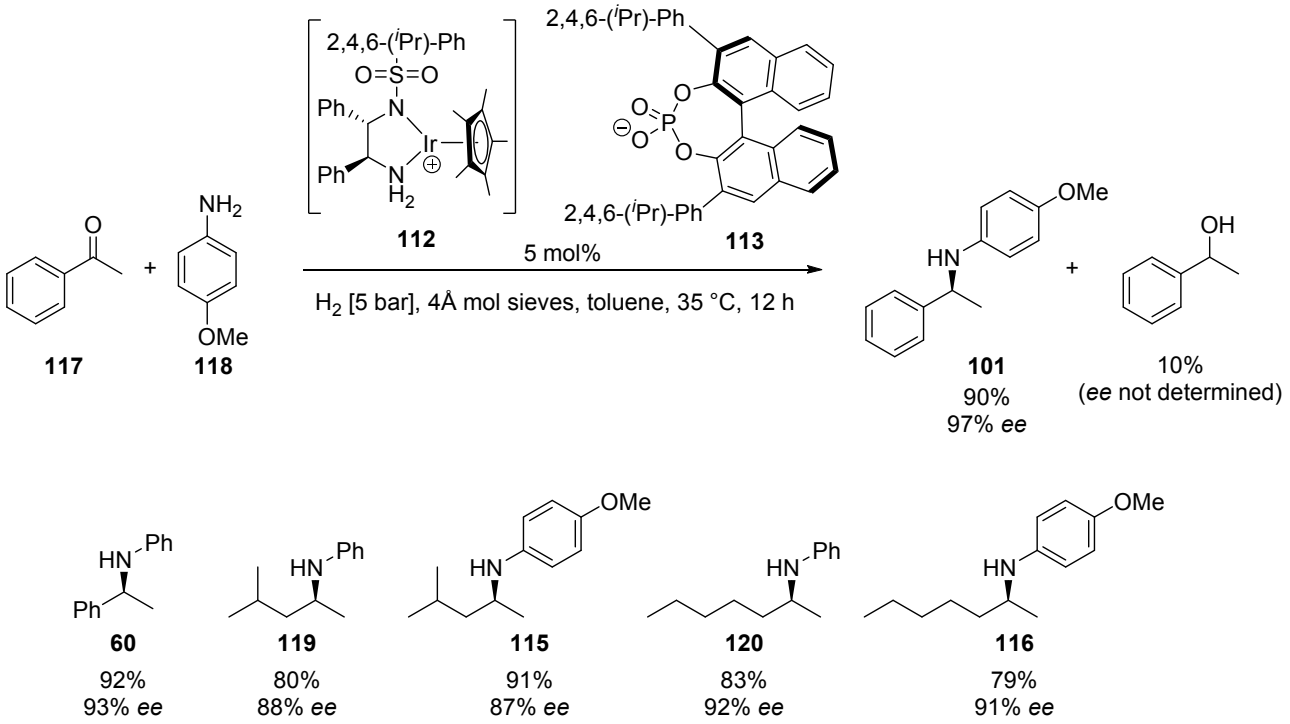

Scheme 34: Asymmetric reductive amination using complex **112**-**113**

A very interesting catalyst structure was reported also by *Xiao* and co-workers.[43] While investigating Ir(Cp*)Cl dimer complexes as catalysts for reductive amination of **121** and **118**, formation of a cyclometalated complex **122** was observed. These complexes proved to be highly versatile and effective catalysts for reductive amination employing an azeotropic mixture of formic acid and triethylamine (Scheme 35). No example of an enantioselective reaction was reported. Complexes with electron-withdrawing substituents displayed higher reactivity.

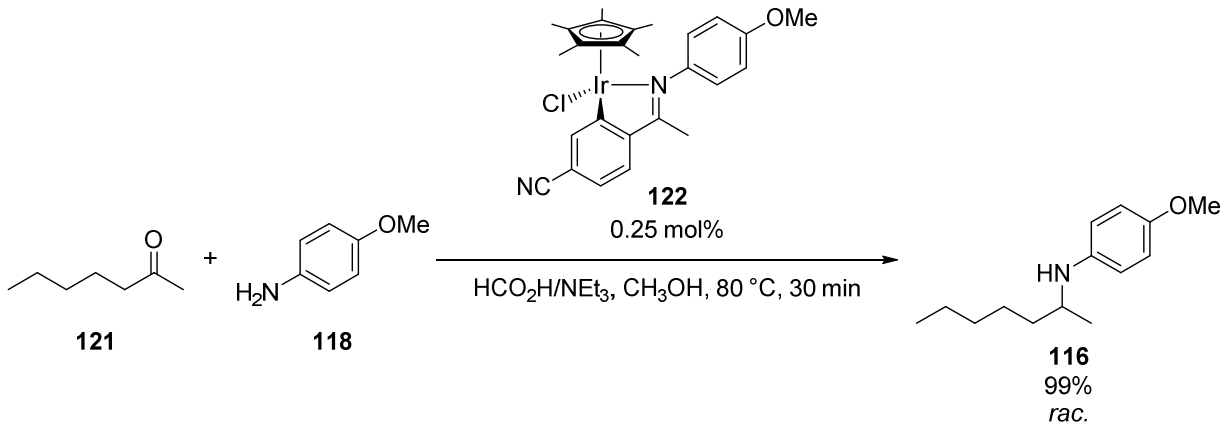

Scheme 35: Reductive amination with iridacycles such as **122**

Asymmetric hydrogenation of imines has also been achieved with iron catalysts. *Beller* and co-workers reported on a iron(II)-PNNP catalyst prepared *in situ* from **124** and **125** for asymmetric imine transfer hydrogenation.[44] While *N*-phenyl and *N*-tosyl imines gave no conversion, *N*-phosphinyl imines such as **123** gave excellent results (Scheme 36). A catalytic amount of base is required for high enantioselectivity. Side reactions such as aldol condensations as well as hydrolysis are observed. Especially substrates with large sterically demanding substituents decomposed prior to reduction. With dialkyl imines lower conversions with poor enantioselectivities were obtained.

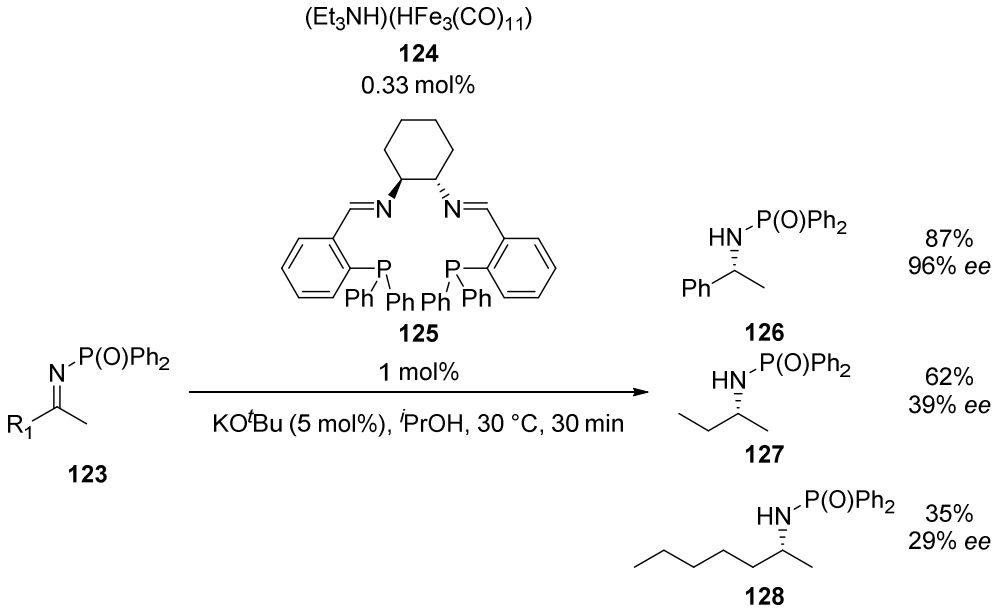

Scheme 36: Asymmetric hydrogenation of *N*-phosphinyl imines as **123** with an Fe-catalyst

Beller and co-workers also reported on asymmetric imine hydrogenation using a combination of an achiral organometallic catalyst with a chiral organic Brønsted acid.[45] With iron(III)-complex **129** and chiral phosphoric acid **113**, high enantioselectivities were obtained with both acetophenone-derived and dialkyl imines (Scheme 37). Side reactions such as aldol condensations and hydrolysis could be minimized when conducting reactions under anhydrous conditions.

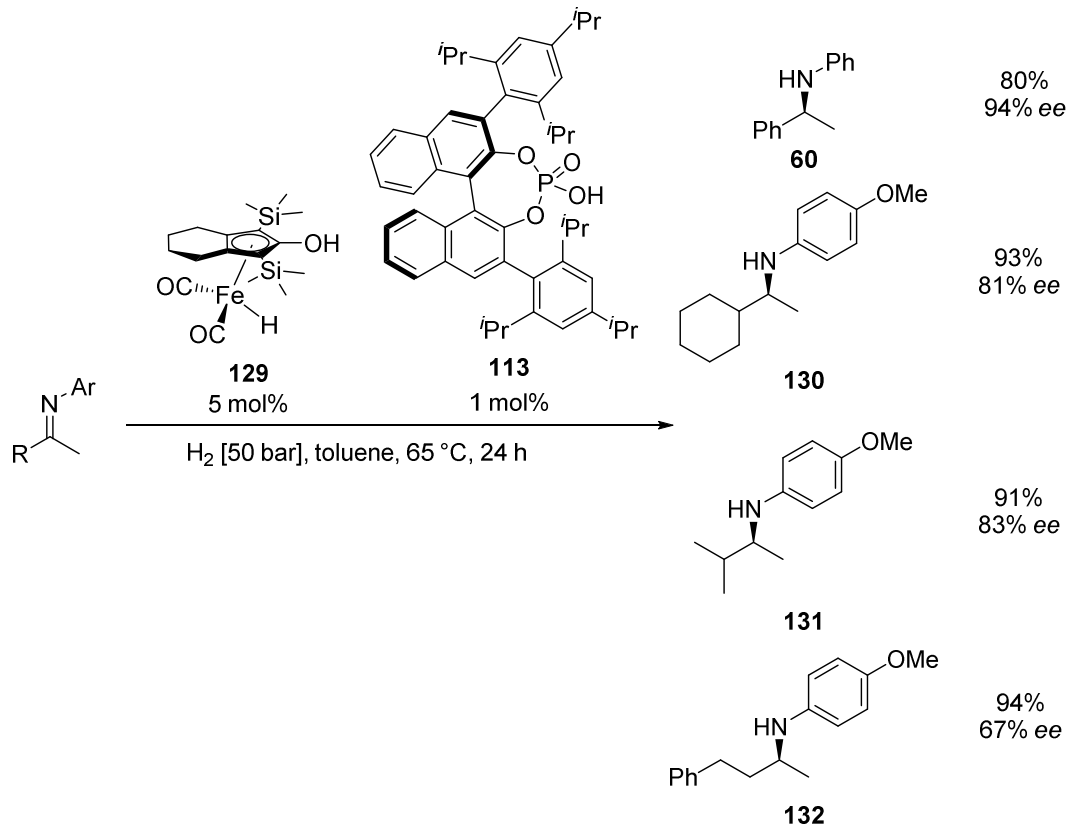

Scheme 37: Asymmetric hydrogenation of imines using an iron(III) complex **129** in combination with chiral phosphoric acid **113**

Other catalytic protocols for the preparation of chiral amines

Apart from metal-catalysed asymmetric hydrogenation, a number of catalytic methods for the preparation of chiral amines have been developed. Hydrosilylation has been extensively studied since its discovery by *Kagan* in 1973. A very versatile organocatalyst **133** (Sigamide) has emerged which is able to convert a plethora of imines with both aromatic and aliphatic groups at the prochiral carbon (Scheme 38). The nitrogen is generally protected with *para*-methoxy-phenyl to ease preparation of primary amines by oxidative deprotection.[46]

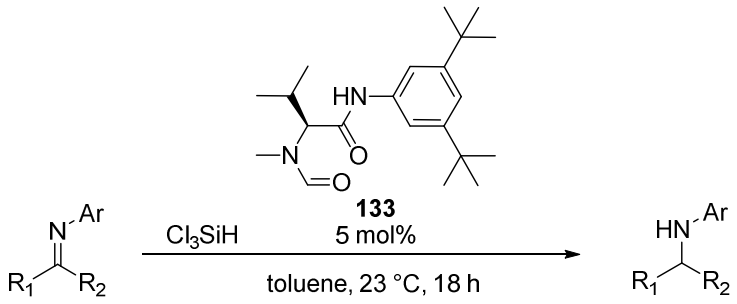

Scheme 38: Organocatalytic hydrosilylation employing *Sigamide*

Similar to hydrosilylation, asymmetric reduction employing chiral oxazaborolidine **135** and using borane as the hydrogen source was developed by *Itsuno* and co-workers (Scheme 39).[47]

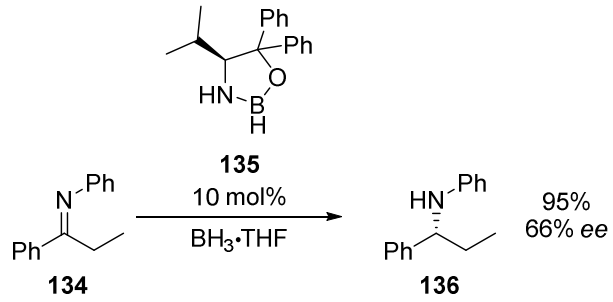

Scheme 39: Asymmetric reduction with chiral oxazaborolidine **135**

Mukaiyama and co-workers reported a chiral cobalt catalyst **138** using boronate **139** as a hydrogen source for the asymmetric reduction of imine **137** (Scheme 40).[48]

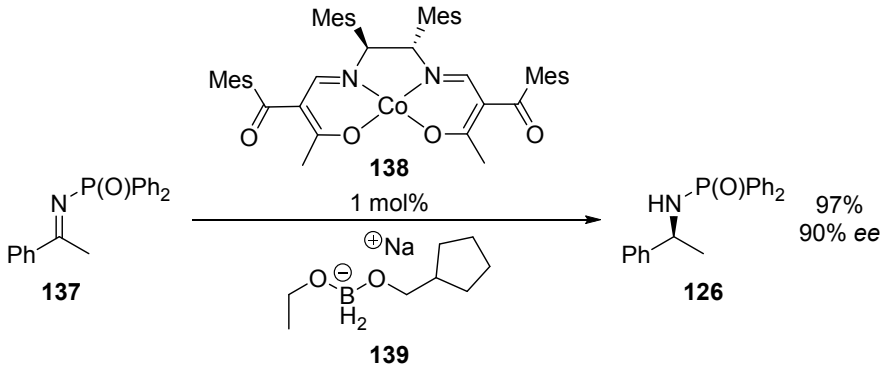

Scheme 40: Asymmetric reduction with cobalt catalyst **138**

Organocatalytic asymmetric imine reduction has been independently discovered by *Rueping* and *List* in 2005. Both reported asymmetric reductions using a chiral phopshoric acid and Hantzsch ester **140** as the hydrogen source (Scheme 41). The work of *Rueping* only reported on acetophenone-derived *N*-aryl imines with moderate to high enantioselectivities.[49] On the other hand, *List* and co-workers reported one dialkyl imine with high enantioselectivity of 90%.[50] Long reaction times and stoichiometric waste products represent two main disadvantages of such organocatalysed imine reduction over metal-catalysed imine hydrogenation.

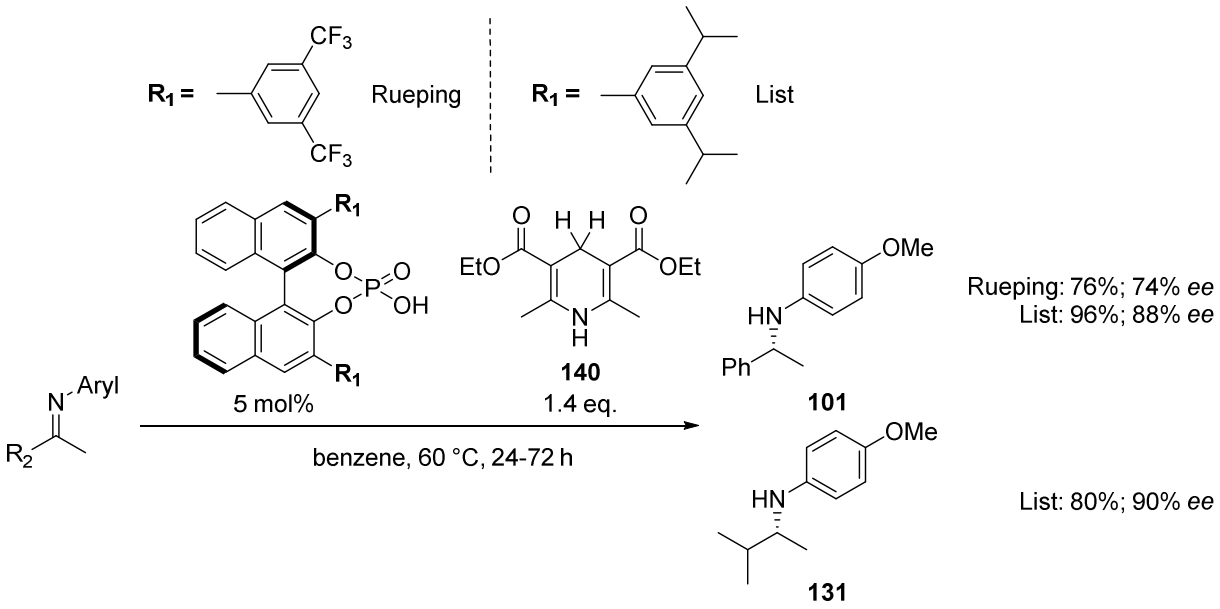

Scheme 41: Asymmetric organocatalytic reduction of imines with chiral phosphoric acids and **140**

Other hydrogen sources for organocatalysed imine reduction are benzothiazolines. An efficient synthetic method has been developed by *Akiyama* (Scheme 42).[51] Interestingly, the hydride source bears a stereogenic carbon. The influence thereof has not been investigated yet.

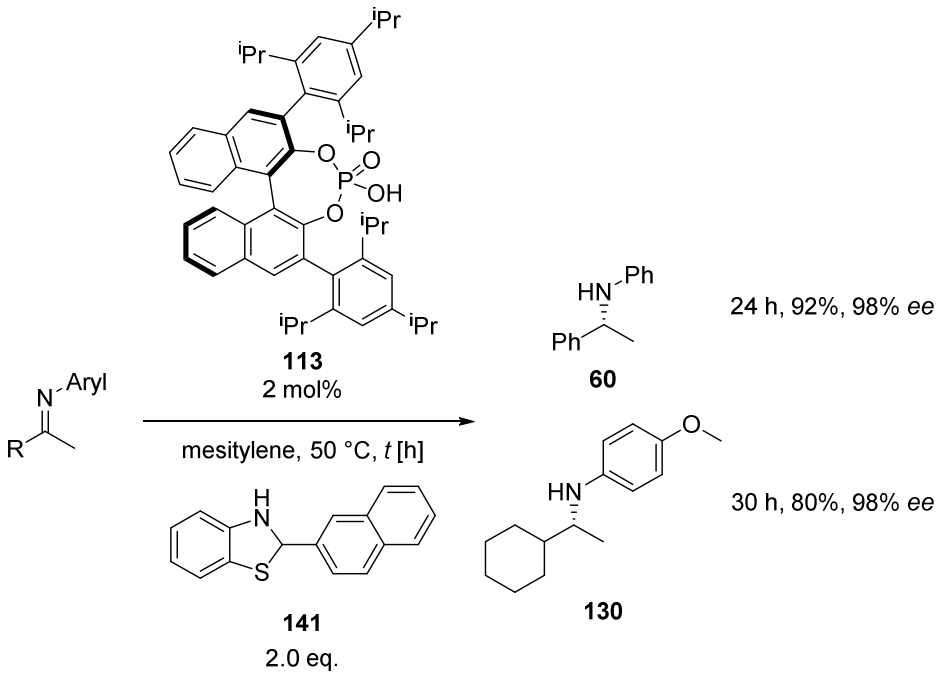

Scheme 42: Asymmetric organocatalytic reduction of imines with **113** and **141**

The concept of organocatalytic imine reduction employing stochiometric hydrogen sources has also been merged with alkyne hydroamination.[52] In a primary step of the catalytic cycle, a gold complex **144** affords the corresponding enamine which is – after imine/enamine tautomerisation - reduced *in situ* to afford the desired chiral amine **60** (Scheme 43). While nitrogen substituents are limited to aniline derivatives (**142**), both aromatic and aliphatic substituents at the alkyne (**143**) were used. Generally, high enantioselectivities are obtained, albeit with the drawback of very long reaction times and incomplete conversions. If the reaction sequence was conducted in a stepwise manner, similar results as in the overall reaction were obtained.

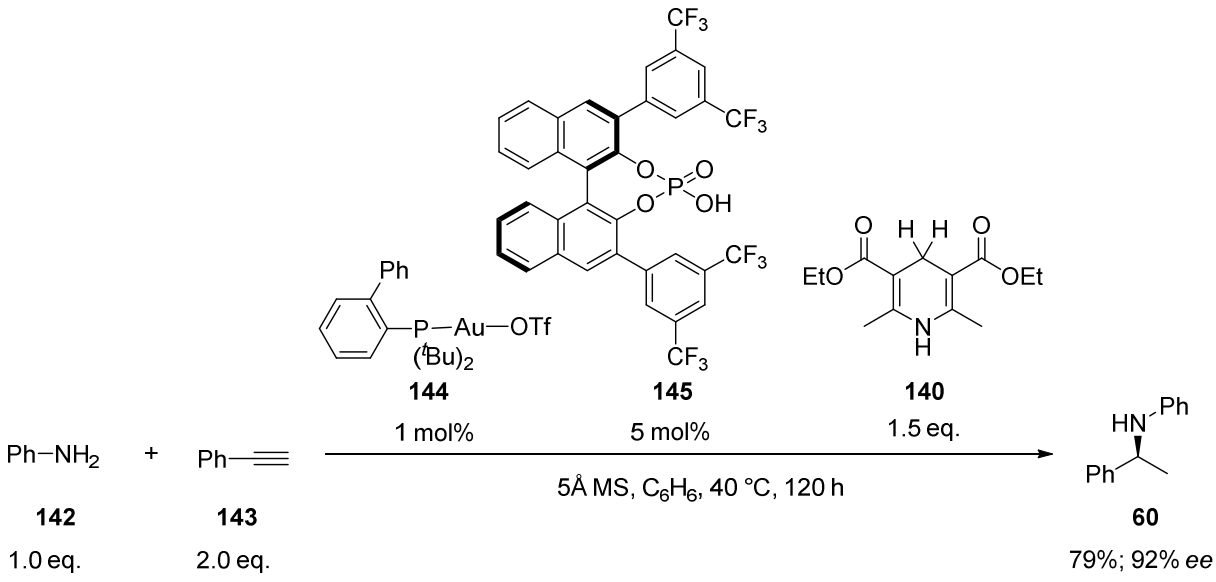

Scheme 43: One-pot hydroamination and imine reduction

Mechanistic studies of iridium-catalysed imine hydrogenations

Togni and co-workers have postulated a general mechanistic picture for the catalytic cycle of imine hydrogenation (Scheme 44).[53] The initial step of the catalytic cycle is the formation of an iridium hydride complex. The imine **146** can then coordinate onto (**148**). Subsequent hydride transfer generates an iridium amide complex **149**. Heterolytic hydrogen cleavage and amide protonation regenerates the iridium hydride complex **150** and frees the product amine **147**.

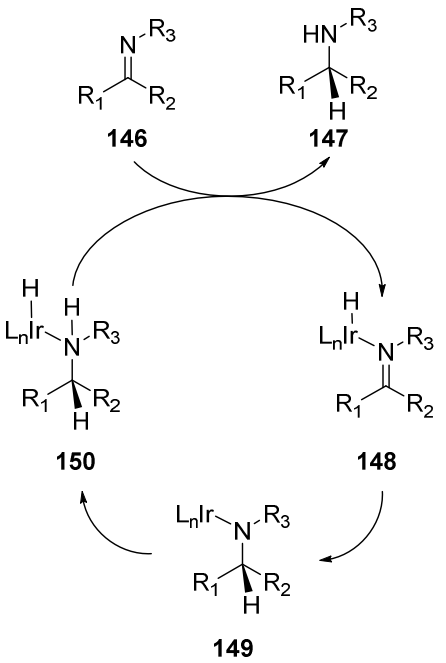

Scheme 44: General catalytic cycle for imine hydrogenation postulated by *Togni*

Oxidative addition of hydrogen to metal complexes has been postulated as the primary step in iridium catalysed hydrogenation reactions. Indeed, Crabtree and Morris identified iridium hydride complexes **152**, **154**, **155** and **156** when subjecting iridium complexes **151** or **153** to an atmosphere of hydrogen at low temperature (Scheme 45).[54],[55]

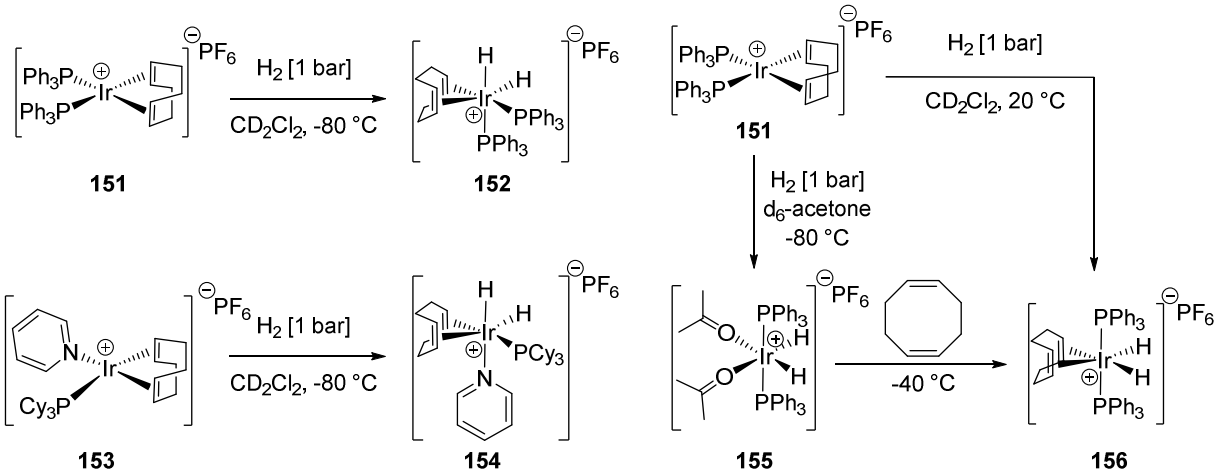

Scheme 45: Preparation of several iridium hydride complexes by *Crabtree* and *Morris*

Landis and co-workers conducted a detailed study on oxidative addition of hydrogen onto iridium diphosphine complex **157**. Similar to *Crabtree's* findings, heterolytic cleavage occurred at -80 °C under kinetic control, but at temperatures around -45 °C dihydride complexes underwent isomerisation reactions to form the thermodynamic products **158** and **159** (Scheme 46).[56] Isotope studies with deuterium gas revealed

scrambling through COD-allyl species even at very low temperatures. Such scrambling processes did not involve reductive elimination of hydrogen and formation of iridium(I) complexes.

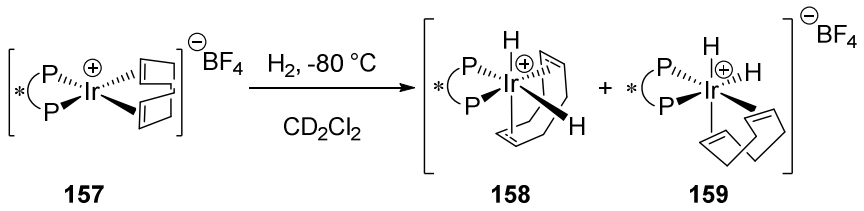

Scheme 46: Oxidative addition and subsequent isomerisation of iridium hydride complex **157** to **158** and **159**

Similar results have also been observed by *Pfaltz* and co-workers when investigating oxidative addition of hydrogen with iridium phosphineoxazoline complex **86** (Scheme 47). The observed dihydride intermediates **160**, **161** and **162** were postulated to be present during the early stage of the catalytic cycle in enantioselective hydrogenation. In a combined experimental and computational study the corresponding isomers were characterised.[57]

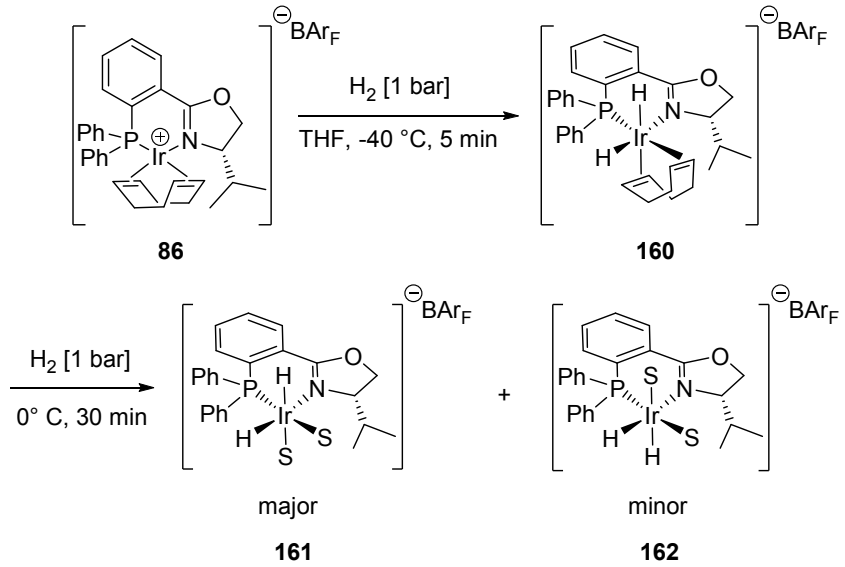

Scheme 47: Observation of dihydride complexes **160**, **161** and **162** upon subjection of **86** to hydrogen at low temperature

The observation of only one (out of four possible) diastereomers with cyclooctadiene in the coordination sphere of the iridium centre is in accordance with the findings by *Crabtree*. He demonstrated that iridium complexes of the type $((PR_3)(Py)Ir(COD))PF_6$ form hydride complex **154** (Scheme 45) where one hydride is situated *trans* to the nitrogen.[58] Furthermore, the steric repulsion of the cyclohexyl rings at the phosphorus direct the position of the cyclooctadiene. With regard to the dihydride disolvent complexes, different ratios of isomers were obtained. As observed by *Landis*, the reaction is occurring under kinetic control. Similar to the cyclooctadiene complex **154**, coordination of the hydride to a weak *trans*-donor such as nitrogen or a solvent molecule is favoured. In order to explain the driving force of oxidative addition at such low temperatures, a study of the binding strength to iridium centres can be considered.[59] The binding strength of several ligands has been investigated on a 14-electron iridium(III) d^6-complex **163** (Figure 10). The complex can be generated by counterion abstraction using $NaBAr_F$. The "naked" 14-electron complex **163** was then tested in competitive binding. In this study the order of bonding strength was determined to be $H_2 > CH_2Cl_2 >$ agostic C-H.

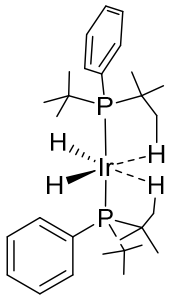

163

Figure 10: Agostic C-H—Ir interaction in **163**

The behaviour of iridium complexes with cyclooctadiene as a ligand has also been studied with cyclometalated complex **164** by *van Koten* and co-workers.[60] The isomerisation of such iridium complexes with cyclooctadiene within the coordination sphere was studied with cyclometalated benzylic amines (Scheme 48). This amine bore a substituent in the *meta* position. Thus isomerisation of the cyclooctadiene ligand would be observed by the formation of a new complex **171** where the substituent changed from R_{ortho} to R_{para}. Once the substituent was in the *para*-position, no fluxional behaviour between -80 and +105 °C could be observed by NMR. In deuterium labelling studies, no exchange with the solvent (benzene or toluene) was observed. First order kinetics indicated that an intra- rather than an intermolecular process is operating. Deuterium incorporation was observed at one of the *N*-methyl groups. The conversion of the cyclometalated complex can therefore be explained by the mechanism via **165** to **170** outlined below involving reversible C-H activation of both a sp^2 (**165**<->**169**) and a sp^3-hybridized carbon centre (**164**<->**165** and **170**<->**171**).

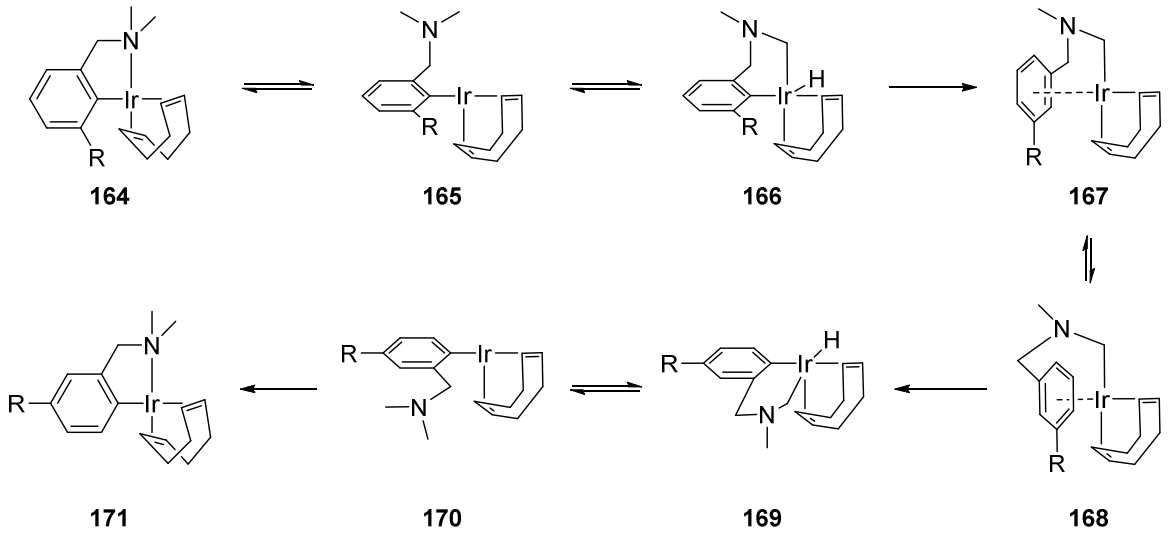

Scheme 48: Isomerisation of iridacycle **164** to **171** by reversible sp^2- and sp^3-C-H activation

The last step of the catalytic cycle is postulated to be the reductive elimination of an iridium-coordinated amide. Simultaneous heterolytic cleavage of hydrogen gas regenerates the hydride and dissociates the amide by protonation. *Rettig* and co-workers demonstrated that iridium-amide complexes such as **172** cleave hydrogen heterolytically (Scheme 49).[61] Interestingly, an opposite *syn* orientation between the NH proton and the halide was observed in **173**. It was explained by intramolecular hydrogen bonding between the NH and the halide. The controlling factor of the observed stereochemistry is thus the hydrogen bonding. This interaction is also stabilising the otherwise unstable metal hydrides, as no loss of hydrogen was observed even when complex **173** was heated to 80 °C *in vacuo*. On the other hand, heating **173** to 80 °C under an atmosphere of hydrogen generated dihydride complex **174** along with methane elimination.

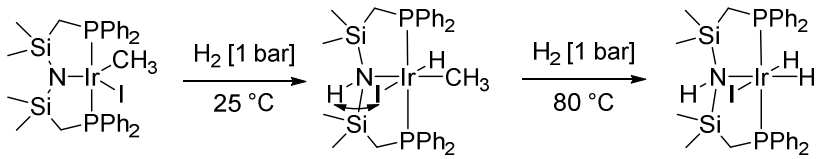

Scheme 49: Preparation of complex **173** mimicing reductive elimination in imine hydrogenation

Even more surprising is the oxidative addition of hydrogen to olefin-coordinated iridium amide complex **175**. At atmospheric hydrogen pressure in the presence of excess methylene dihalide, e.g. dichloromethane,

formation of halide complex **176** is observed (Scheme 50). The transformation was postulated to proceed via a *mer*-amine-trihydride IrH_3[P'NH'P] intermediate.

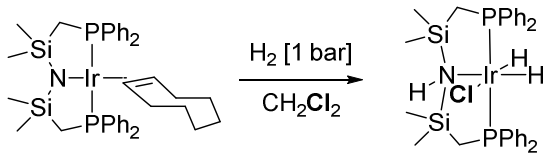

175 **176**

Scheme 50: Activation of CH_2Cl_2 under hydrogenation conditions by iridium-amide complex **175** to afford **176**

For all steps in the catalytic cycle that occur between heterolytic hydrogen cleavage and reduced amide dissociation, no exact experimentally derived picture exists to date. Several groups have conducted detailed investigations of iridium catalysed imine hydrogenation.

Spindler and co-workers detected benficial effects with iodine as the counterion (Scheme 16).[25] Addition of iodine resulted in increased reaction rates as well as higher enantioselectivities. Iodine was suggested to serve as the oxidant for the iridium(I) complex **64** to form the active iridium(III) catalyst. Detailed mechanistic investigations by *Togni* and co-workers later strengthened this hypothesis (explanation given later in this chapter). Furthermore, when investigating a range of *N*-aryl imines, the equilibrium of the *syn*- and *anti*-isomers, as well as imine-enamine tautomerisation, were demonstrated to proceed faster than hydrogenation by H/D exchange experiments in d_4-MeOD. This concluded that the *anti*/*syn* ratio was not selectivity-determining in this case.

Deuterium labelling experiments were conducted by *Osborn* and co-workers[27] on the very same substrate **68**-CD_3 as investigated by *Spindler* (Scheme 51). More than 95% Incorporation of hydrogen across the C=N double bond was observed, which ruled out hydrogenation of the enamine tautomer. Kinetic experiments indicated a rate dependece of 0.5 on the catalyst loading. This suggested that the dimer **69** is in equilibrium with a small quantity of monomer and another monomer-imine complex. Those species were considered to be the active catalysts in the catalytic cycle. Furthermore, deuterium labelling experiments indicated no observable isotope effect. This was attributed to the fact that only small quantities of monomeric catalyst are active during catalysis.

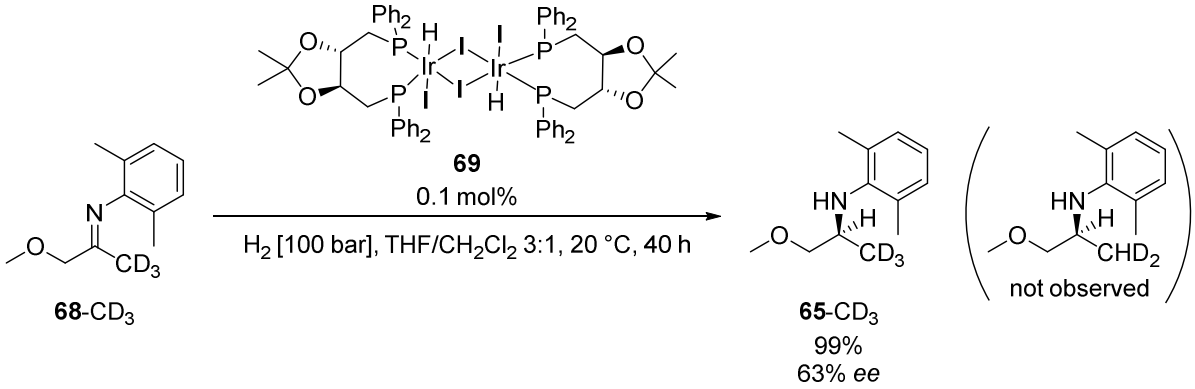

68-CD_3 **65**-CD_3
99%
63% *ee*

Scheme 51: Deuterium labelling experiments on imine **68**-CD_3 by *Osborn*

Similar results were observed by *James* and co-workers investigating related rhodium-catalysed imine hydrogenation by high-pressure NMR experiments.[18] With this specific setup, several aspects of the reaction were investigated. The starting imine was observed predominantly as the *E* isomer with an *E*/*Z* ratio of 14:1. The isomerisation rates for both isomers at 25 °C were determined to be 155 h^{-1} for *Z*->*E* and 11 h^{-1} for *E*->*Z*. As the TOF of the catalyst were determined to be between 14-66 h^{-1}, no conclusions regarding the hydrogenation selectivity with regards to the *E*/*Z* isomerisation could be drawn. Diffusion of hydrogen gas

into the solution was observed to be rate-determining since a zero-order kinetic behaviour was detected. In order to exclude the possibilty of the enamine being the reduced substrate, deuterium labelling experiments were conducted (Scheme 52). While concomitant deuterium incorporation at the methyl group in d_4-MeOD was observed due to imine-enamine tautomerism, no deuterium-hydrogen scrambling was observed in imine **55**-CD_3.

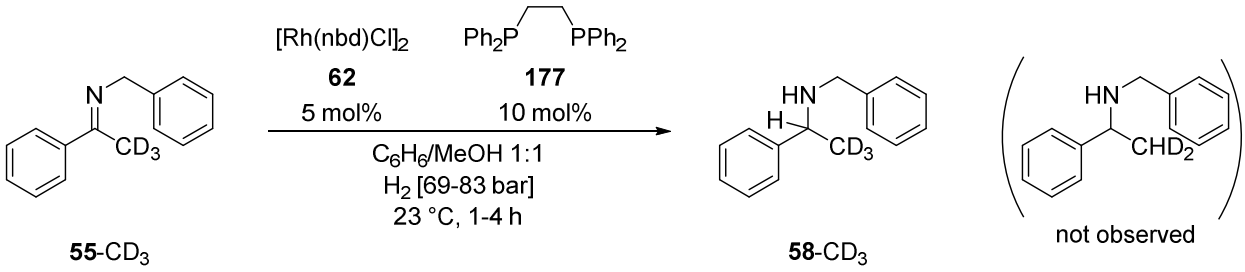

Scheme 52: Deuterium labelling experiments on **55**-CD_3 by James

Buchwald and *Willoughby* detected a strong dependence on the *E*/*Z* ratio of the imines and the observed enantiomeric excess of the product amine **84** (Scheme 53).[62],[63] While cyclic substrates gave the corresponding amines in very high *ee*'s, acyclic imines such as **178** were reduced with *ee*'s between 58% and 86%. The *E*/*Z* ratio of the imine **178** did not remain constant over the course of the reaction. It rose from 11:1 up to 30:1 in favour of the *E* isomer when conducting the reaction at 65 °C. With higher temperature (75 °C) it only rose to 18:1. Two conclusions were drawn from this observation. Primarily, the *Z*-isomer is more reactive and secondly, *E*/*Z* isomerisation is slower than hydrogenation at high pressure. Probably *E*/*Z* isomerisation is unaffected by the presence of the chiral catalyst. The enantiomeric excess of the product amine **84** can thus be correlated to *E*/*Z* ratio of the imine in solution (11:1 = 91.7:8.3 = 83% *ee*). Furthermore, a strong dependence on hydrogen pressure and *ee* was observed. It was explained by a slow hydrogenation, constant *E*/*Z*-isomerisation and thus overall lower enantioselectivity in the catalytic reaction. If the reaction was conducted stochiometrically, 83% *ee* was observed.

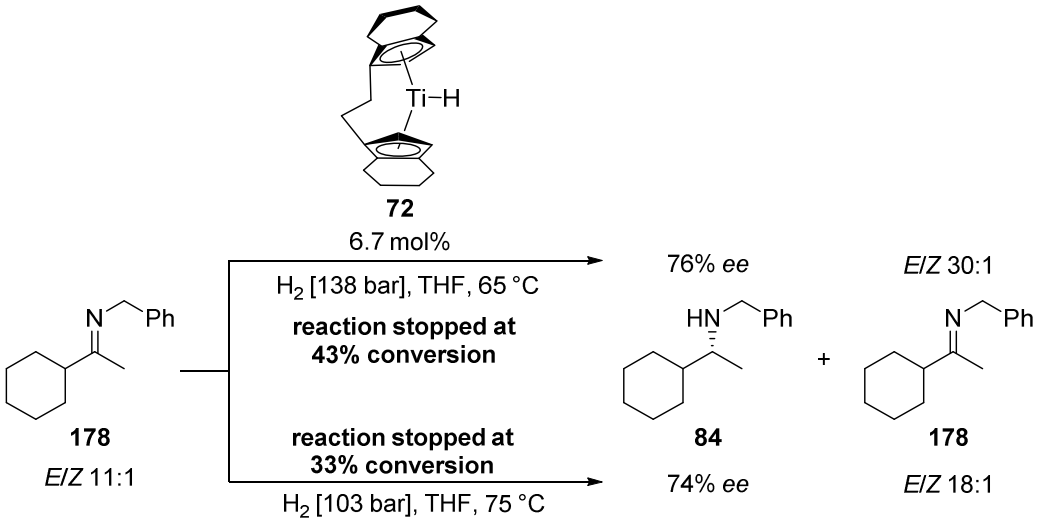

Scheme 53: Correlation of *E*/*Z* isomer ratio and *ee* in imine hydrogenation by **72**

Imine hydrolysis of coordinated substrates has been observed in rhodium-catalysed imine hydrogenation as a side reaction and possible origin of catalyst poisoning.[64] Even when preparing reactions under inert atmosphere, low residual amounts of water resulted in the formation of a rhodium(I) complex **184** with two inequivalent NH_2 protons. This complex could be isolated and characterized by X-Ray crystallography (Scheme 54).

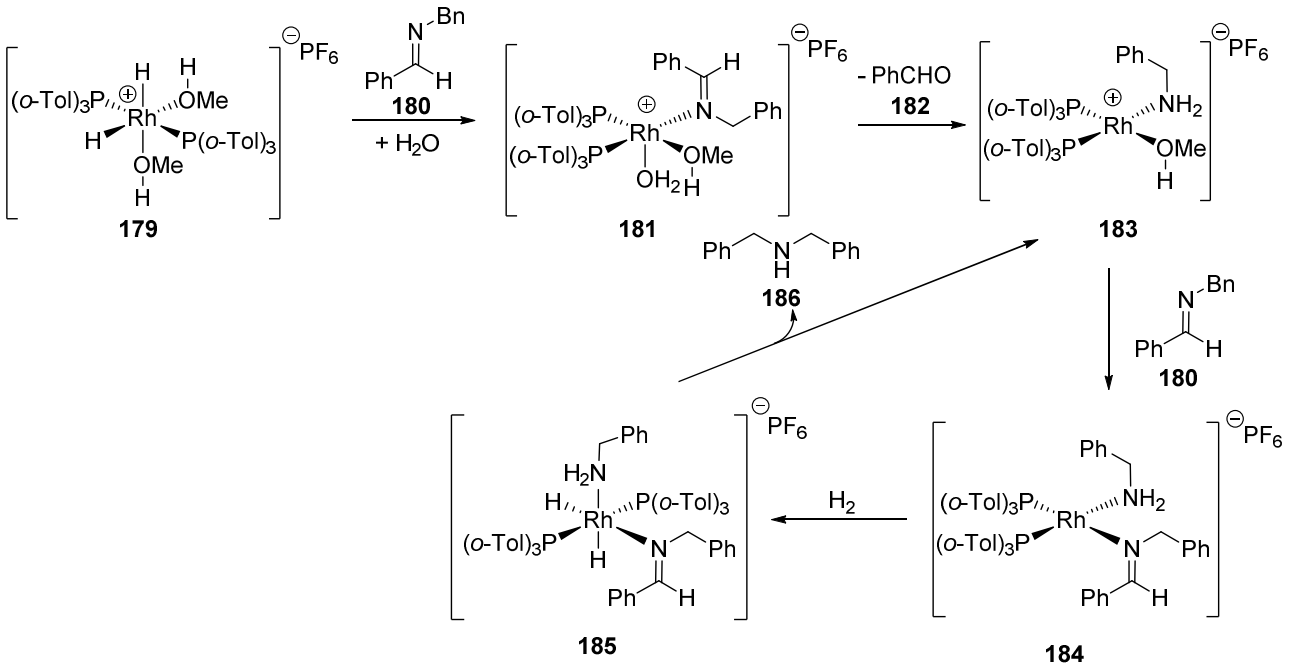

Scheme 54: Observation and identification of complex **184** bearing inequivalent amine protons

Togni and co-workers conducted a detailed study on iridium Xyliphos complexes used in the asymmetric hydrogenation of metolachlor.[65] Several intermediates were isolated in the course of the investigation (Scheme 55). When **64** and ligand **187** were mixed, clear formation of [Ir(P'P)(COD)]Cl complex **13** ensued. Counterion exchange with tetrafluoroborate afforded **188**. Interestingly, attempted counterion exchange with iodide furnished a neutral square pyramidal iridium(I) complex **189**. Treatment with tetrafluoroboric acid afforded iodo-hydride complex **190** which isomerised to **191**.

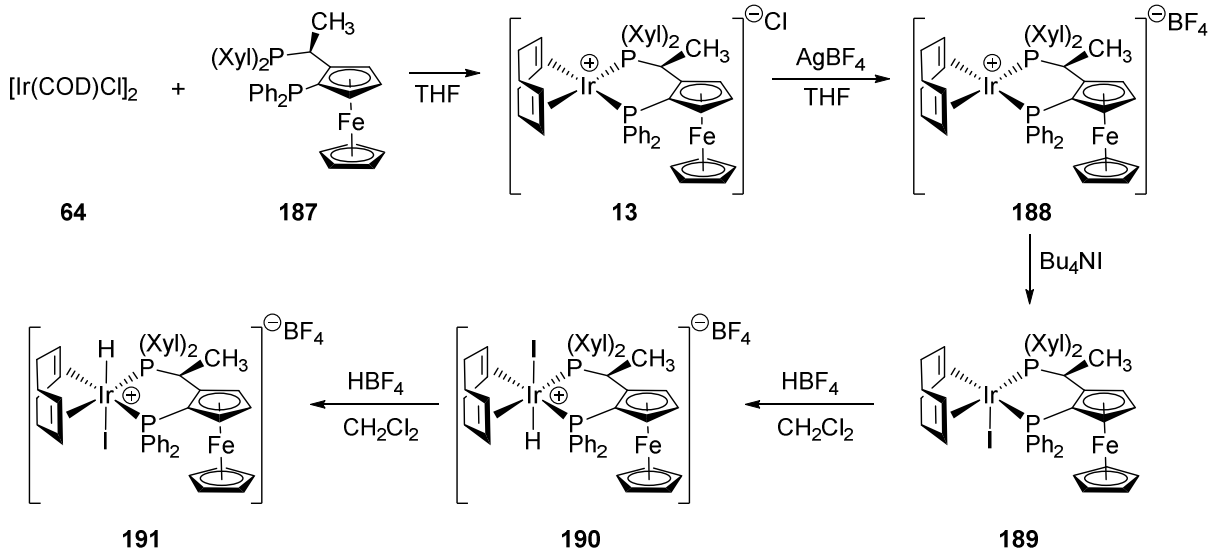

Scheme 55: Iridium complexes obtained from complex **13** in attempted counterion exchange

Upon addition of iodine it formed an iodo-bridged iridium(III) dimer **192** by oxidation of **189** (Scheme 56). Complex **192** was demonstrated to be the most active catalyst out of all structures **188** to **192** with similar values to the *in situ* generated catalyst. Halide-free complex **188** showed the poorest activity while complexes **190** and **191** depicted similar activity compared to **192**. It was concluded that under hydrogenation conditions a species such as **190** or **191** is present and closely related to the active catalyst. It also explained the crucial role of iodine as an additive. In order to generate the active catalyst, iodine aids oxidation of the iridium(I) precursor **64** *via* dissociation or hydrogenation of the cyclooctadiene ligand to form the iridium(III) dimer **192**.

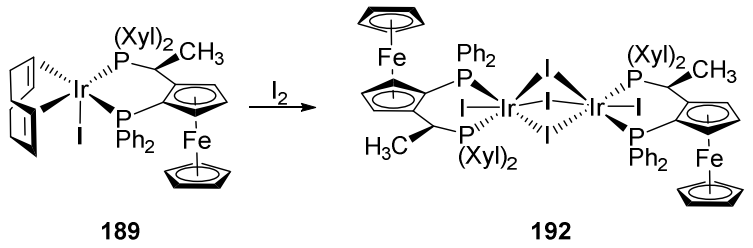

189 **192**

Scheme 56: Preparation of iodo-bridged trimer **192**

Several iridium(III) complexes were studied as catalyst-substrate adducts on the Metolachlor-related model substrate **68** (Scheme 57). Four different imine dihydride adducts **193** were observed with N,O-coordination. The C=N double bond was always situated *trans* to a phosphorus atom of the ligand in η^1-coordination. This configuration is consistent with the relative *trans* influence of the H, N, O and P donors. The iminoyl carbon is more electrophilic (if *trans* to the less basic phosphane), the hydride is more nucleophilic (if *trans* to the more basic phosphane). Chemical exchange between **193a** and **193c** is observed on the NMR time scale. Such an exchange is consistent with a mechanism of dissociation of the ether-tethered oxygen (which is observed always *trans* to a hydride) and occupation of this vacant position by one of the phosphorus atoms of the ligand.

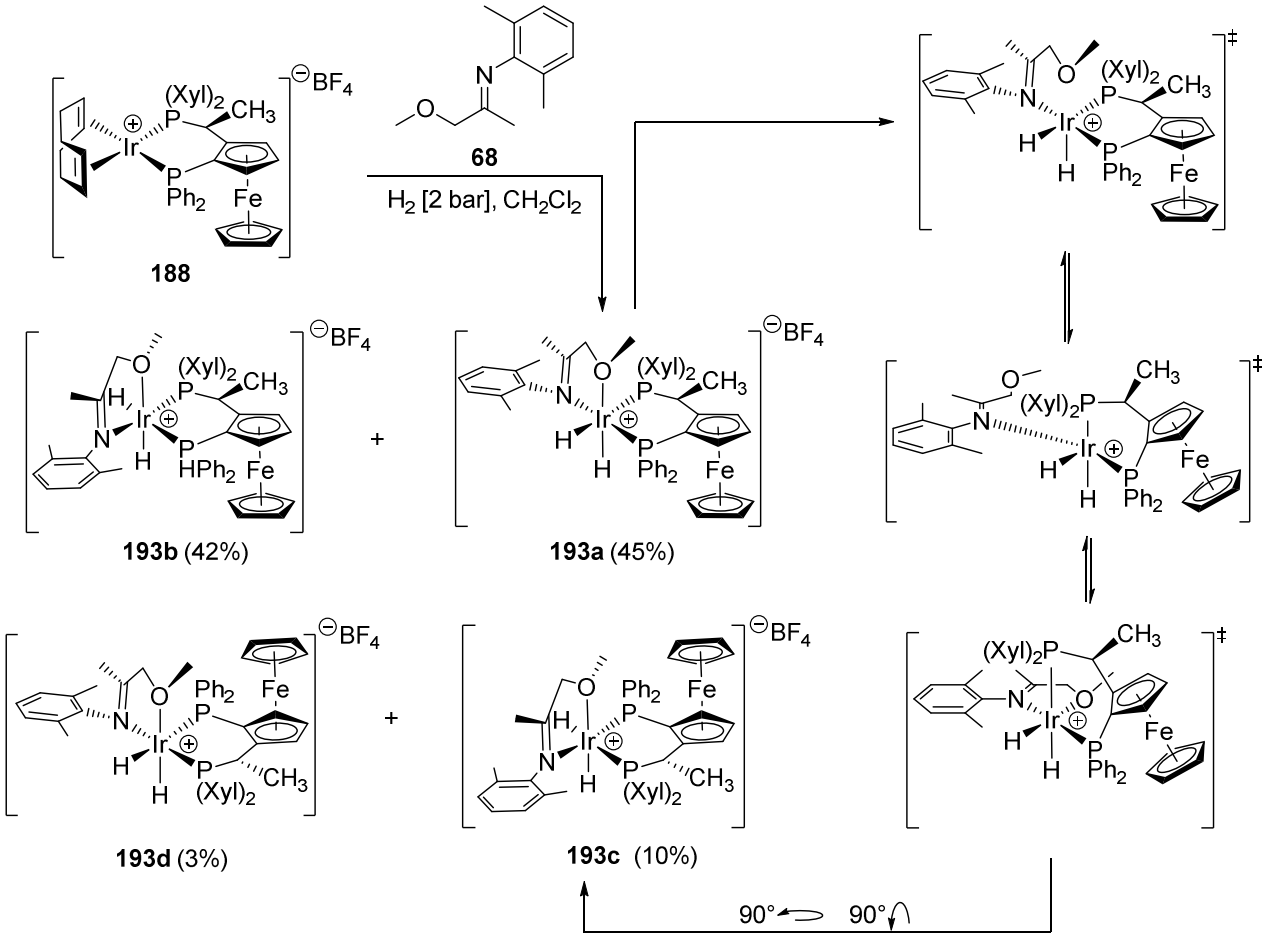

188 **68** **193b** (42%) **193a** (45%) **193d** (3%) **193c** (10%)

Scheme 57: Identification of several imine adduct complexes **193**

The mechanistic studies by *Togni* were extended with kinetic investigations. Analogous amine complexes such as **194** were observed at low temperature by NMR experiments (Scheme 58).[53] These complexes were unstable in CH_2Cl_2 solution and the amine was readily displaced by the imine **68** to afford **197**. If no imine was added, η^6-coordination of the aryl ring of the amine was observed at room temperature (**195**). This led to the conclusion that the imine is a much better ligand than the amine, as well as imine coordination is favoured over η^6-amine coordination. This is consistent with the industrial process where hydrogenation

proceeds rapidly to completion despite a very high concentration of product amine at the end of the reaction. Reversible C-H activation (β-hydride elimination) of the amine complex in THF was observed over the course of 12 hours at room temperature *via* **196**.[60]

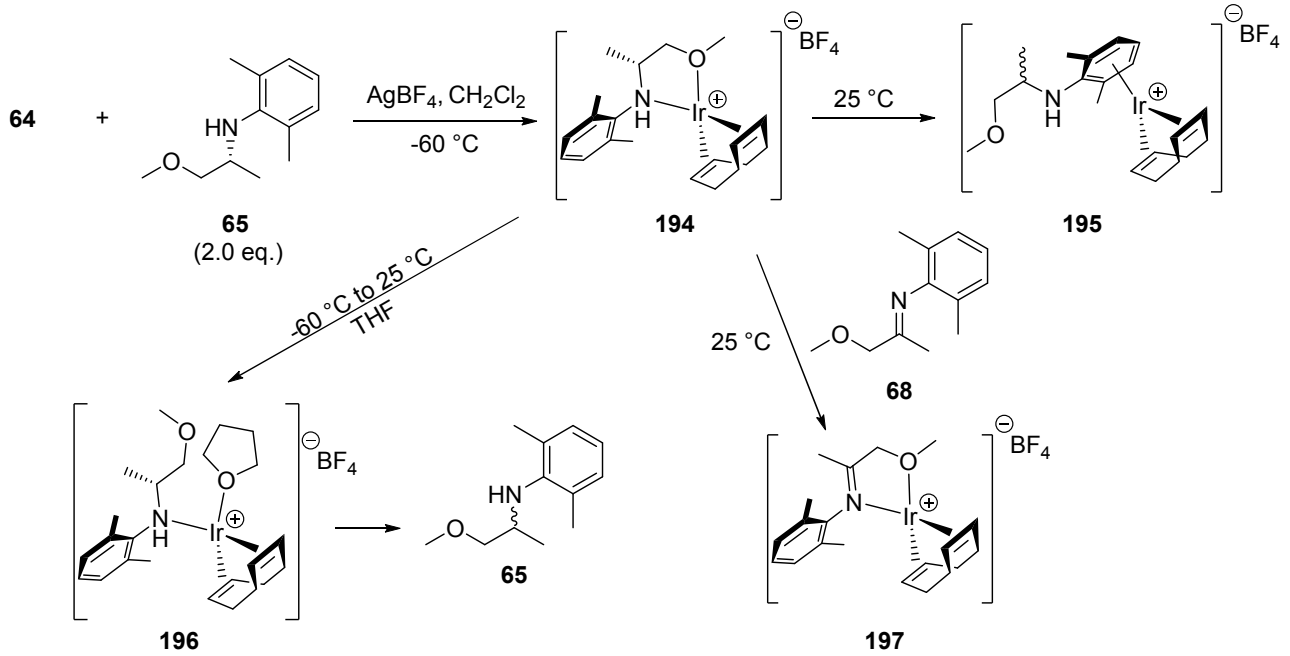

Scheme 58: Iridium amine adduct complexes **194**, **195** and **196**

*Shvo´*s diruthenium bridging hydride complex **198** is an efficient catalyst for aldehyde, ketone and imine transfer hydrogenation (Scheme 59).[66],[67],[68] Detailed mechanistic studies have been conducted with aldehydes and the two mononuclear ruthenium complexes **199** and **200** have been postulated to be in equilibrium with the dimer. The hydroxy-cyclopentadienyl ruthenium hydride **199** was proposed to be the active catalyst. Shvo's catalyst was used for experiments to understand the mechanism of Noyori-type half-sandwich complexes with ruthenium or iridium as the metal centre.

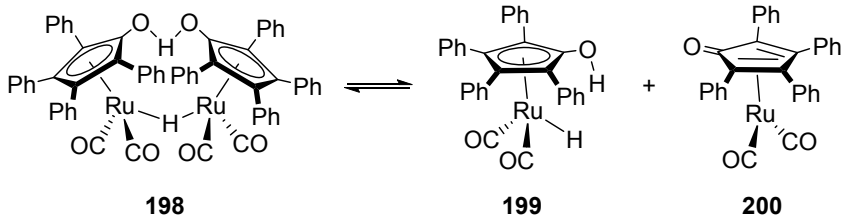

Scheme 59: *Shvo´*s diruthenium bridging hydride complex **198** and its monomers **199** and **200**

Two possible mechanisms for C=N double bond reduction have been postulated: An inner-sphere mechanism (Scheme 60),[69] where the nitrogen atom of the imine coordinates onto the metal centre, and an outer-sphere mechanism (Scheme 61),[70] where a proton and a hydride are transferred in a concerted fashion onto the imine without coordination to the metal centre.

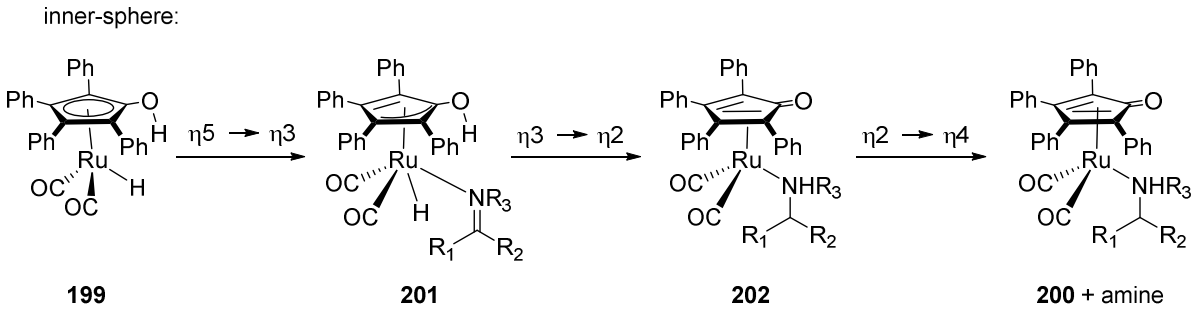

Scheme 60: Inner-sphere mechanism of an imine hydrogenation by *Shvo's* catalyst **199**

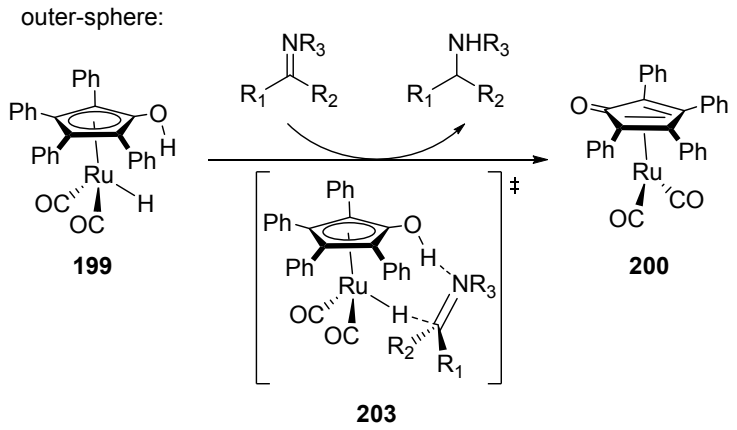

Scheme 61: Outer-sphere mechanism of an imine hydrogenation by *Shvo's* catalyst **199**

Casey and co-workers trapped a Ru-amine complex when mixing **199** with imine **204** (Scheme 62). They predominantly observed the trapped amine **206** derived from the imine nitrogen which supported a concerted outer-sphere mechanism.[70]

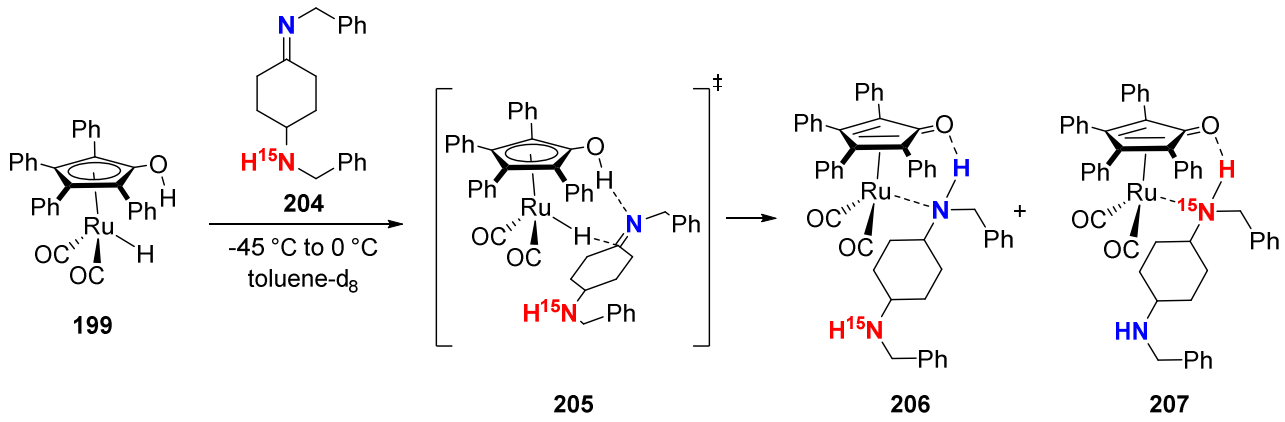

Scheme 62: Trapping of imine **204** by *Shvo's* catalyst **199** indicating an outer-sphere mechanism

A computational study by *Lledos* and co-workers supported such an outer-sphere mechanism quite clearly by the calculated energy profiles when compared to a possible inner-sphere mechanism.[71]

Oro and co-workers investigated complex $(Ir(C_6H_6)(P^iPr_3)(H)_2)BF_4$ **208** as a model catalyst for homogeneous imine hydrogenation.[72] Starting from arene half-sandwich complex **208** (Scheme 63), ligand displacement by excess nitrile solvent readily occurred. Both complexes **208** and **211** are active catalysts for imine hydrogenation but complex **208** was shown to be much more reactive than **211**.

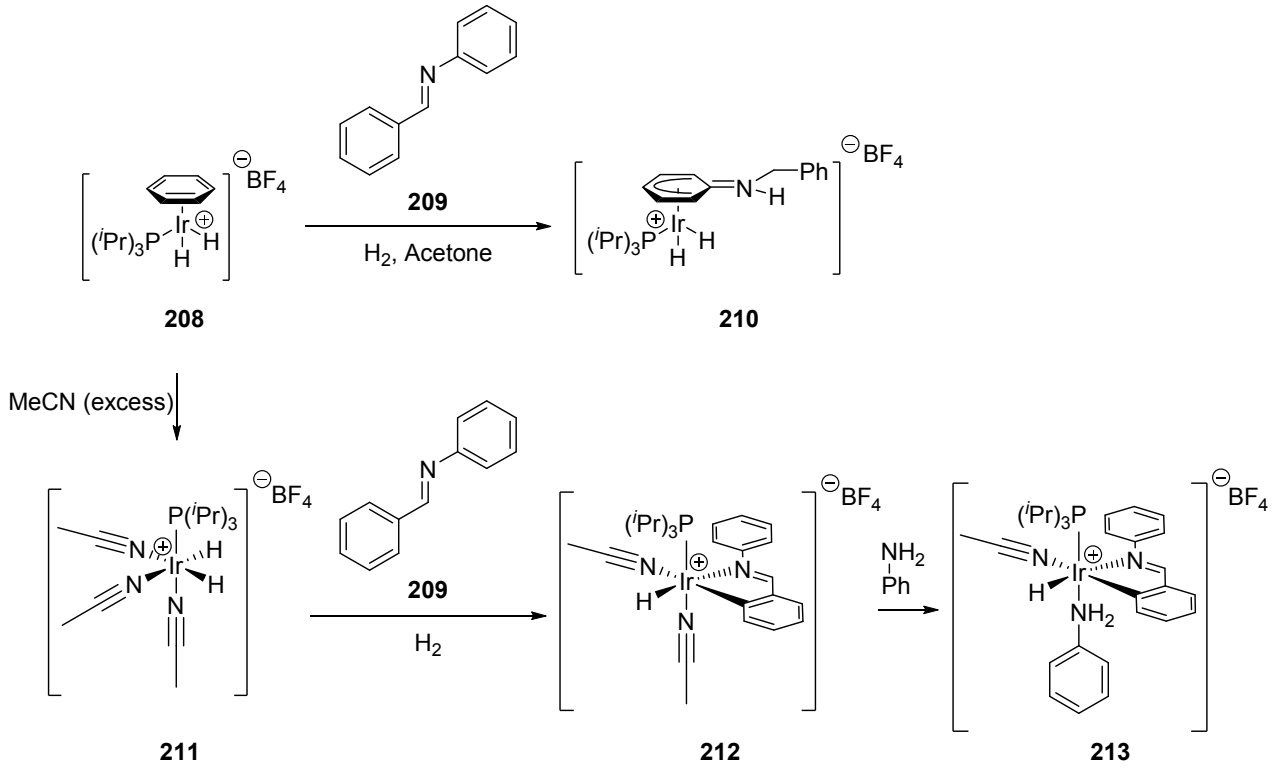

Scheme 63: Identification of iridacycles **212** and **213** in the course of investigating homogeneous imine hydrogenation catalysed by **208** or **211**

The poor performance of **211** was explained by NMR spectroscopic studies which revealed cyclometalation of the imine **209** to give **212**. The aniline complex **213** was observed due to imine hydrolysis if water was not strictly excluded. Furthermore, adding up to 5 equivalents of aniline did not disturb or influence the activity of catalyst **211**, **212** or **213** in imine hydrogenation.

The observation of a cyclometalated imine was also reported by *James* and co-workers as a common activation phenomena encountered in iridium catalysed imine hydrogenation.[73] In order to gain a better understanding and ease cyclometalation, *Oro* and co-workers investigated diphenyl NH imine **214** which clearly depicted a stronger tendency towards cyclometalation than imine **209** (Scheme 64). Both precursors **208** and **211** formed the same complex **215**, which did not display any catalytic activity for imine hydrogenation. Multiple substrate cyclometalation was therefore suggested as a pathway for catalyst deactivation.

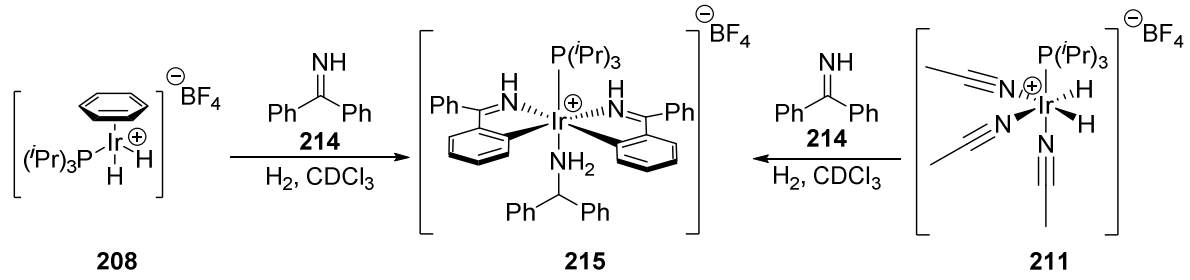

Scheme 64: Preparation of double iridacycle **215**

Cyclometalation was shown to be favoured in strongly coordinating solvents such as acetone or methanol (Scheme 65). However, under hydrogenation conditions, such cyclometalated structures are disfavoured and formation of the η^5-coordinated complexes like **210** was observed. Complex **210** was recognized to also be the sole catalyst resting state when **208** is used in other solvents such as 1,2-dichloroethane or THF. In kinetic experiments a first-order dependence on catalyst, imine and hydrogen concentration was observed. This result was deemed unhelpful since it is compatible with various sequences of elementary reactions.

Addition of aniline prior to commencing the catalysis significantly shortened induction periods. This undermined that η^5-coordination, as in the formation of **210**, was of critical importance.

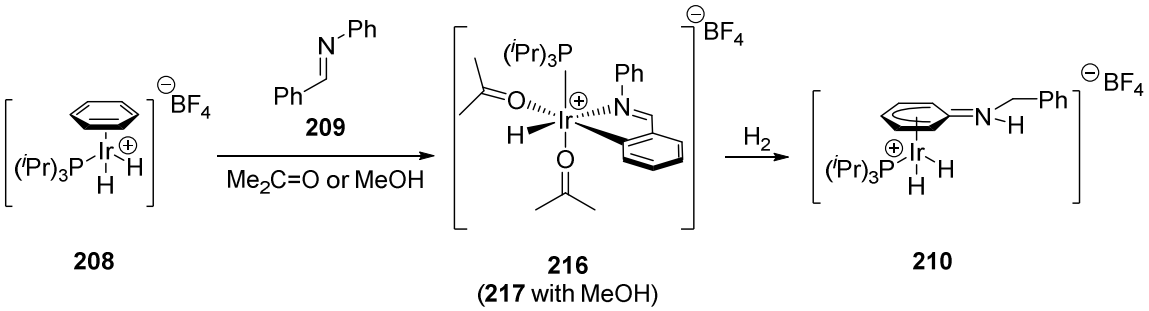

Scheme 65: Rearrangement of iridacycles as **216** or **217** under hydrogen atmosphere in acetone or methanol

When attempting to inactivate complexes **212**, **216** or **217** by addition of tetraphenyl borate[6,[74]] formation of **218** and >90% recovered imine **209** were detected (Scheme 66). The rearrangement of complexes such as **212** to **210** proceeds thus at a slower rate than deactivation by BPh_4 coordination. Furthermore, it was concluded that solvent-coordinated cyclometalated imine complexes **212**, **216** or **217** do not act as hydrogenation catalysts since they rather rearrange to complexes like **210** prior to catalysis.

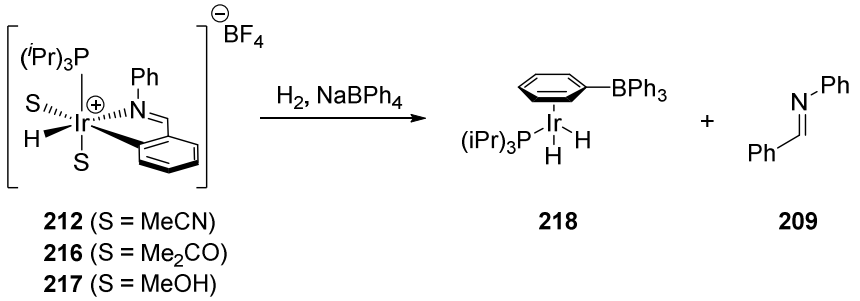

Scheme 66: Generation of η^6-arene complex **218** from hydride-disolvent complexes **212**, **216** and **217**

The η^5-coordinated dihydride complex **210** readily reacted with imine **209** to form the cyclometalated complexes **212**, **216** or **217** via the corresponding dihydride tri-solvent complex **216** (S = Acetone or MeOH, Scheme 67). This observation was not made in less coordinating solvents such as THF or CH_2Cl_2 where complex **210** remained unchanged. The latter two examples of **218** and **220** demonstrated cyclometalation to be reversible by rearrangement of the catalyst in solution. Therefore η^5-coordinated **210** and cyclometalated complexes **212**, **216** or **217** were believed to be in equilibrium under hydrogenation conditions.

[6] to form stable neutral dihydride complexes

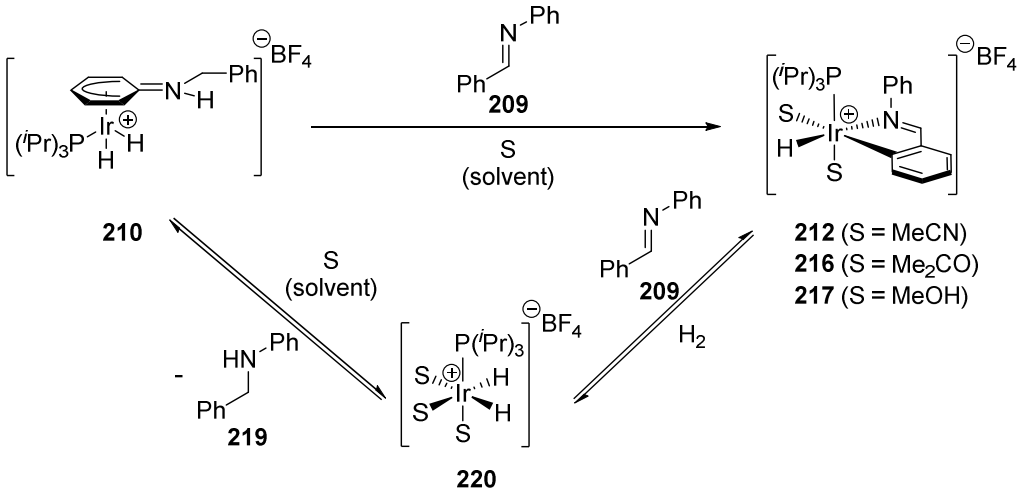

Scheme 67: Reversibility of iridacycle formation in complexes **212**, **216** and **217**

Furthermore, mixtures of complex **210** and imine **209** formed dimeric cyclometalated complex **221** (Scheme 68). When heated to 50°C for prolonged time, complex **222** is formed. The substitution of hydrides to chlorides is commonly observed for iridium(III) hydride complexes in chlorinated solvents as reported by Oro and co-workers.[75] These dimeric complexes **221** and **222** did not show any catalytic activity in imine hydrogenation and the formation of **222** during catalysis is unlikely due to the requirement of extensive heating periods of the reaction mixture in the presence of excess imine.

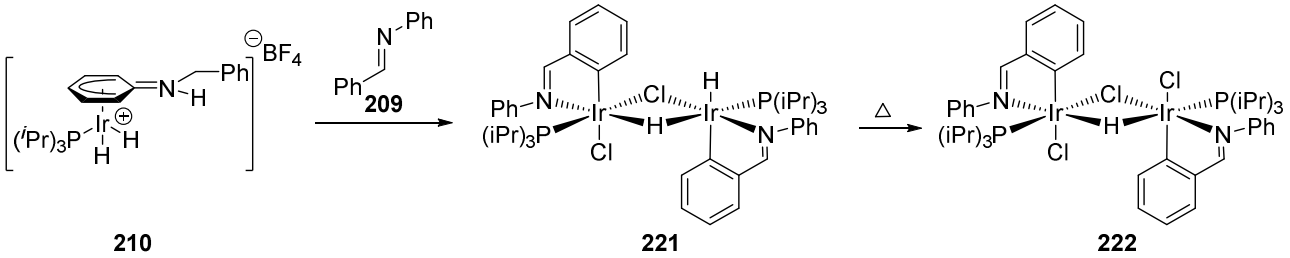

Scheme 68: Formation of hydrido-chloro dimer iridacycle complexes **221** and **222**

Concomitant hydrogen-deuterium exchange was observed when complex **210** was dissolved in CD_2Cl_2 and subjected to a deuterium atmosphere at room temperature for one hour (Scheme 69).

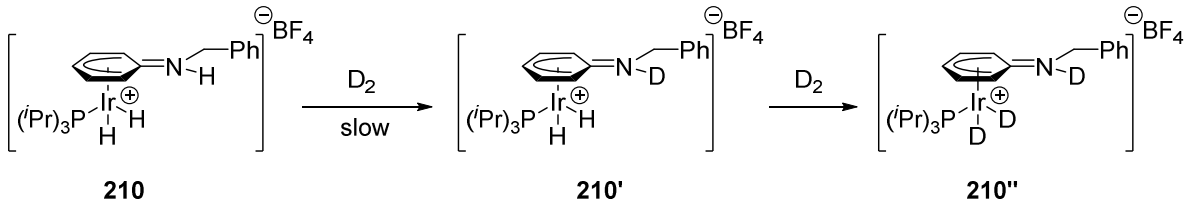

Scheme 69: Concomitant incorporation of deuterium into complex **210** under D_2 atmosphere

NH-ND exchange was observed in d_4-MeOD (Scheme 70).

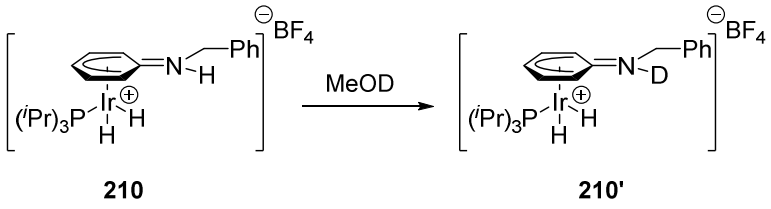

Scheme 70: Proton-Deuterium exchange in deuterated methanol

In conclusion, a mechanism which strongly depended on hydrogen bonding was postulated: Reduction of the C=N double bond takes place in an ionic outer-sphere mechanism of a catalyst formed *in situ* with direct involvement of the product amine (Scheme 71). The product amine is deprotonating the dihydride complex **223** to facilitate oxidative addition of hydrogen gas giving **224**. The coordinative versatility of a benzene ring to undergo either η^6- (**223**) or η^4-coordination (**224** and **225**) renders this process feasible. Amine to imine exchange was calculated to be the most endothermic process in the catalytic cycle.

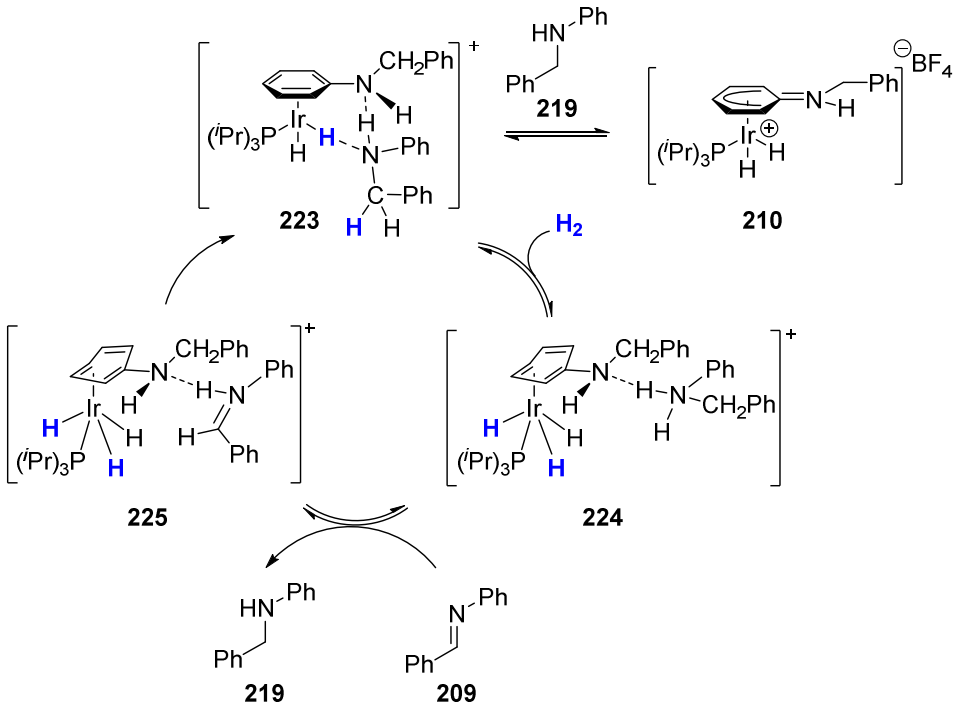

Scheme 71: Postulated catalytic cycle by *Oro* for imine hydrogenation of **209** employing **208**

Sanchez-Delgado and co-workers have investigated the kinetics of $[Ir(PBn_3)(Py)COD]PF_6$ complex **226**, an analogous complex to the Crabtree catalyst.[76] The P'N complex showed higher activity than the corresponding P'P complex (Scheme 72).

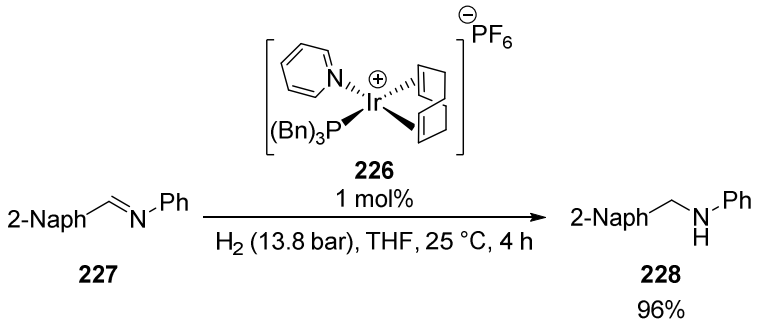

Scheme 72: Hydrogenation of imine **227** by *Crabtree* analogous complex **226**

At low temperature, the unstable dihydride di-solvent complex **229** was formed (Scheme 73). When the dihydride complex **229** was subjected to imine substrate, fast displacement of the solvent molecules with formation of two new species **230** and **231** was observed. The greater the excess of imine added, **231** was favoured. It was therefore suggested, that a mono-coordinated **230** and a di-coordinated imine-iridium complex **231** exist in solution. The rate determining step of the reaction was determined to be the dissociation of the reduced amine in **232** and re-coordination of a hydrogen molecule to the iridium centre to afford **230**. The major species in solution was determined to be the THF-dihydride **230**, which had also been observed by NMR spectroscopy. Therefore, the rate law was determined to be of third order and dependent

on Ir, imine and hydrogen. The solubilty of hydrogen in THF was pointed out to be temperature-independent and the activation energy was determined to be around 16 kcal/mol for this transformation.

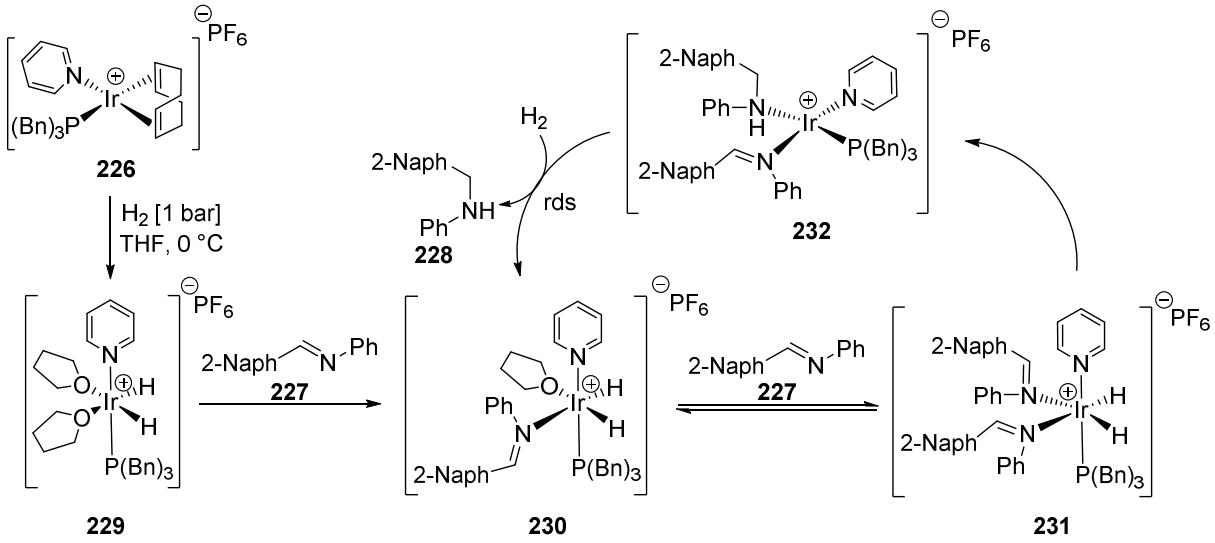

Scheme 73: Proposed catalytic cycle by *Sanchez-Delgado* for imine hydrogenation of **227** by **226**

In a theoretical study on asymmetric imine hydrogenation with iridium phosphineoxazoline complexes, calculations on nine different possible mechanisms were calculated by *Hopmann* and *Bayer*.[77]

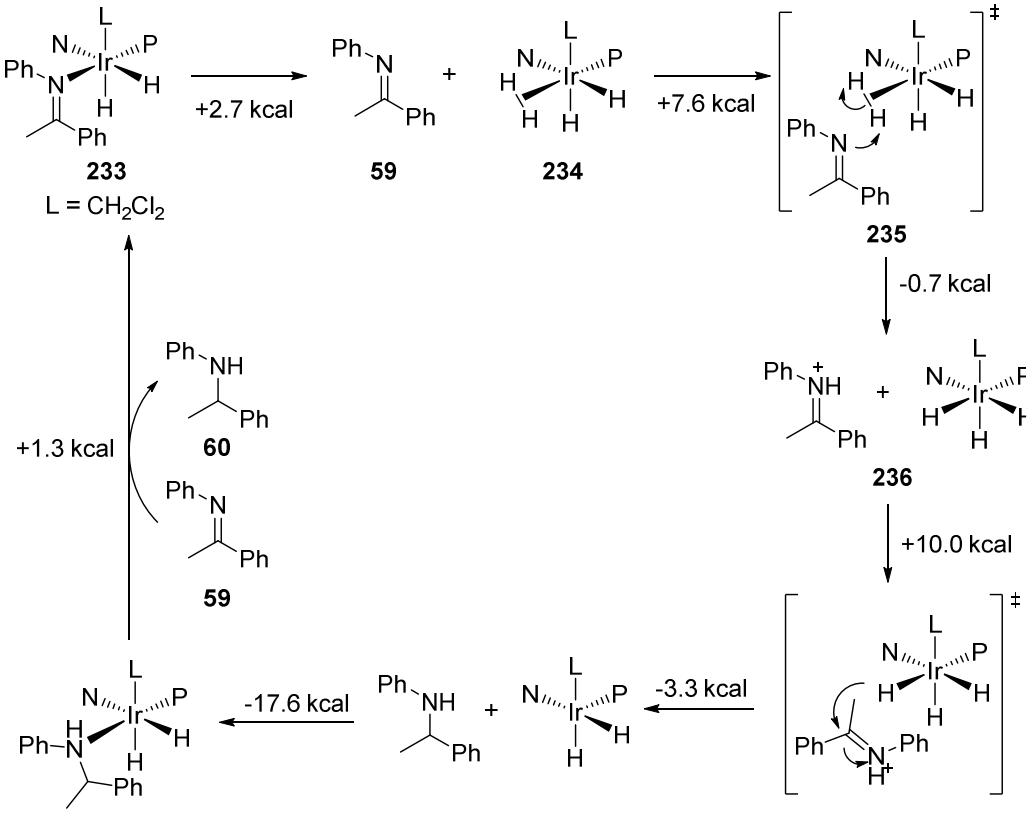

Scheme 74: Postulated catalytic cycle by *Hopmann* and *Bayer*, numbers indicating energy differences between computed energies of structures

All calculations were started from dihydride imine complex **233**. Relatively high overall energy barriers of 43.5 to 57.5 kcal mol^{-1} were computed for mechanisms involving coordination of the substrate to the iridium centre. Therefore, several outer-sphere mechanisms, involving a dissociated imine, were computed. Overall energy barriers between 32.8 to 17.7 kcal mol^{-1} clearly indicated that such a mechanism is favoured. The

calculated mechanism with the lowest overall barrier is depicted in Scheme 74. While η^2-coordination was unfavoured, a stepwise protonation affording **236** – hydride transfer *via* **237** – sequence proved more viable. Ultimately, rearrangment of the hydride ligands and introduction of an additional labile ligand (H_2 or CH_2Cl_2) lowered the overall barrier significantly. The results indicated that the iridium centre adopts an iridium(III) oxidation state throughout the catalytic cycle. However, a dihydride intermediate **233** is in equilibrium with the dihydride-dihydrogen complex **234** species via dihydrogen coordination.

The calculated mechanism is partially similar to the one calculated and experimentally observed with dinuclear iridium complexes by *Oro* and co-workers.[78] In both examples, a stepwise protonation and a concerted dihydrogen coordination - hydride transfer sequence from an iridium(III) hydride complex to a free imine has been postulated. This suggested an outer-sphere mechanism. Nevertheless, the Brønsted acidic nature of iridium complexes might also result in protonation of the imine prior to hydrogenation. This has not been considered in the computational study.

Cyclometalation in imine hydrogenation

Cyclometalation of imine and azo-compounds onto an iridium centre was first reported by *Stufkens* and co-workers investigating insertion of labile iridium(I) complex **240** into sp^2-hybridized C-H bonds (Figure 11).[79]

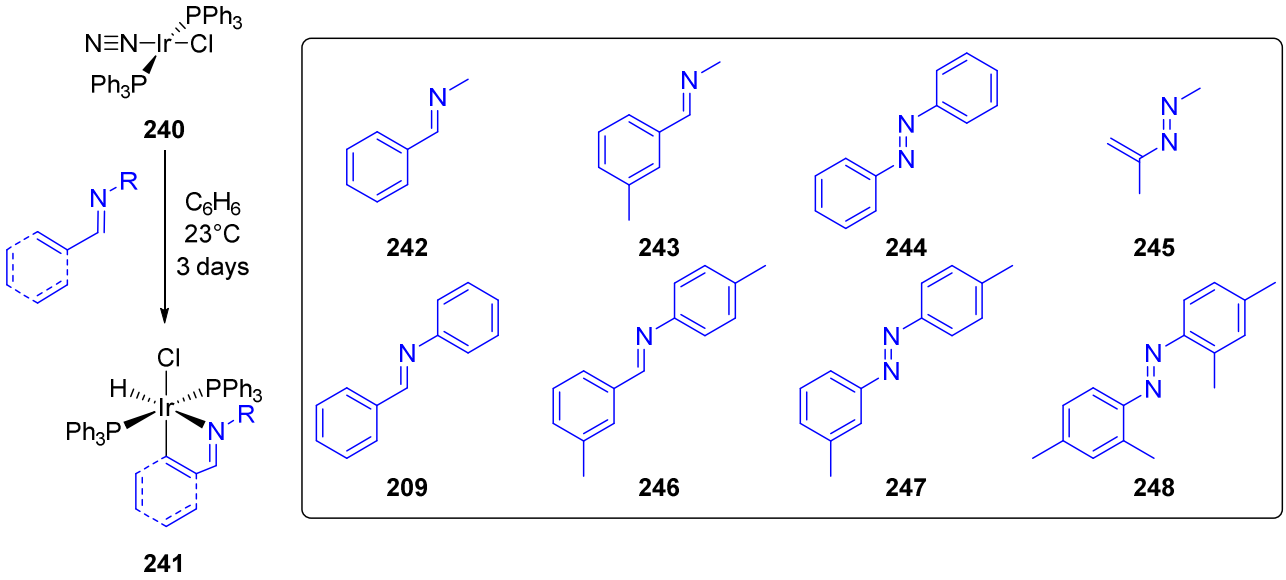

Figure 11: First reported cyclometalation of different imines and diazocompounds **209** and **242**-**248**

The iridium hydride complexes such as **241** were characterised by their specific IR frequency of the iridium-hydride bond in the range of 2000 to 2200 cm^{-1}. No exchange of the hydride to a deuteride was observed when the complexes were dissolved in deuterated solvents such as chloroform or benzene. The frequency of the C=N double bond is lowered upon complexation which corresponds to a slight elongation of the bond. The chemical NMR shifts of the hydrides indicate its position to be *trans* to the ligand with a low *trans* influence. In structurally comparable $[Pd(PR_3)_2(Imine)Cl]$ complexes only η^1-imine $\sigma(N)$-coordination was observed.[80]

The role of metal basicity was discussed comparing C-H activation abilities of palladium(II), iridium(I) and rhodium(I) complexes. It was concluded that the attack of C-H bonds of azo- and imine-ligands by Rh(I) and Ir(I) is strongly dependent on: a) the electronic (basic) properties of the metal atom; b) the type of C-H bond

with the preference of reactivity aromatic > olefinic > aliphatic. Cyclometalations are more feasible with electron-rich metal centres. This was demonstrated using basic tri-alkyl phosphines compared to electron-poor tri-aryl phosphines. On the other hand, with electron-accepting ligand such as CO, only σ-*N*-η^1-coordinated complexes were observed with Rh(I). These results led to the conclusion, that cyclometalation proceeds via prior η^1-imine coordination, followed by intramolecular addition of the C-H bond to the metal centre.

The reactivity of cyclometalated complexes such as **250** has been studied by treatment with halogens, silver perchlorate, nitriles and carbon monoxide (Scheme 75). The iridacylces were shown to be stable under a number of reaction conditions. While ligand exchange reactions proceeded with halogens giving **252** and **253**, the cationic complexes had to be generated prior to exchange with carbon monoxide (**251**) or nitriles (**252**). The neutral iridacycle **250** did not show any reactivity with a number of reagents such as acidic HCl, electrophilic carbon monoxide, basic phosphine or hydrogen.

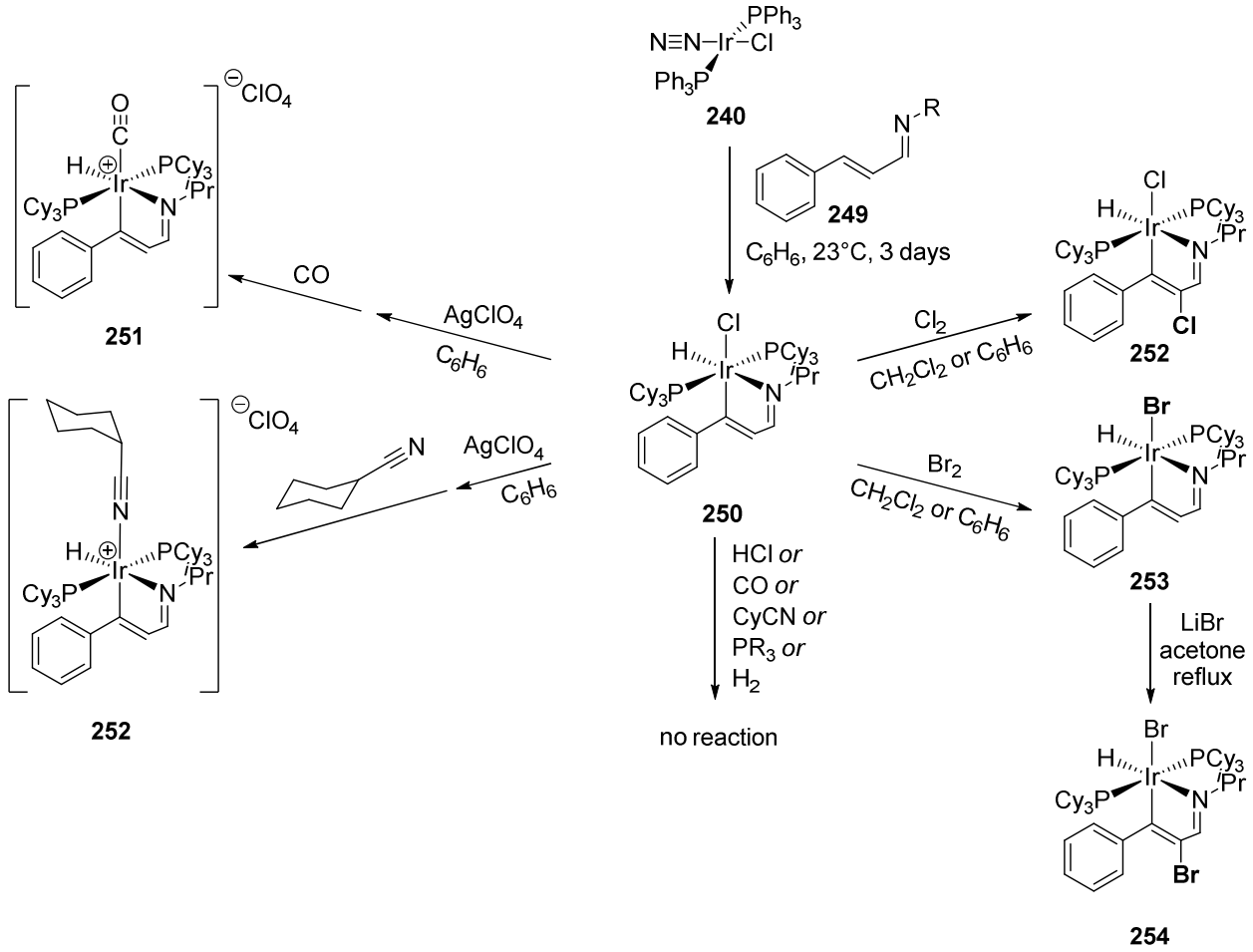

Scheme 75: Reactivity studies of iridacycle **250**

James and co-workers have studied imine hydrogenation with different metals (Rh, Ru and Ir) in great detail. In attempts to isolate intermediates in the course of rhodium-catalysed imine hydrogenation, an iridacycle **256** was observed (Scheme 76).[73] In **256**, a somewhat longer Ir-O bond distance was observed by X-Ray crystallography, which was attributed to the strong *trans*-influence of the *ortho*-C-ligand. The high-field NMR shift of the hydride (-16.35 ppm) is explained by the small *trans*-influence of the imine-*N*-ligand.

Coordination of the imine-nitrogen in η^1-fashion in **255** results in reductive elimination of hydrogen gas from **155**, which has been observed and evidenced by ^{1}H-NMR experiments. The metal centre is rendered basic and nucleophilic by two phosphine ligands. Hydrogen evolution formally results in reduction of Ir(III) to Ir(I) and re-oxidation to Ir(III) by cyclometalation.

Hydrolysis was only observed in methanol. It was suggested that competitive coordination between acetone and water is in favour of acetone. Since pre-coordination of water is necessary for imine hydrolysis, it is not observed in acetone. Imine hydrolysis under hydrogenation conditions has also been observed with a rhodium^{I} complex (Scheme 54).[64]

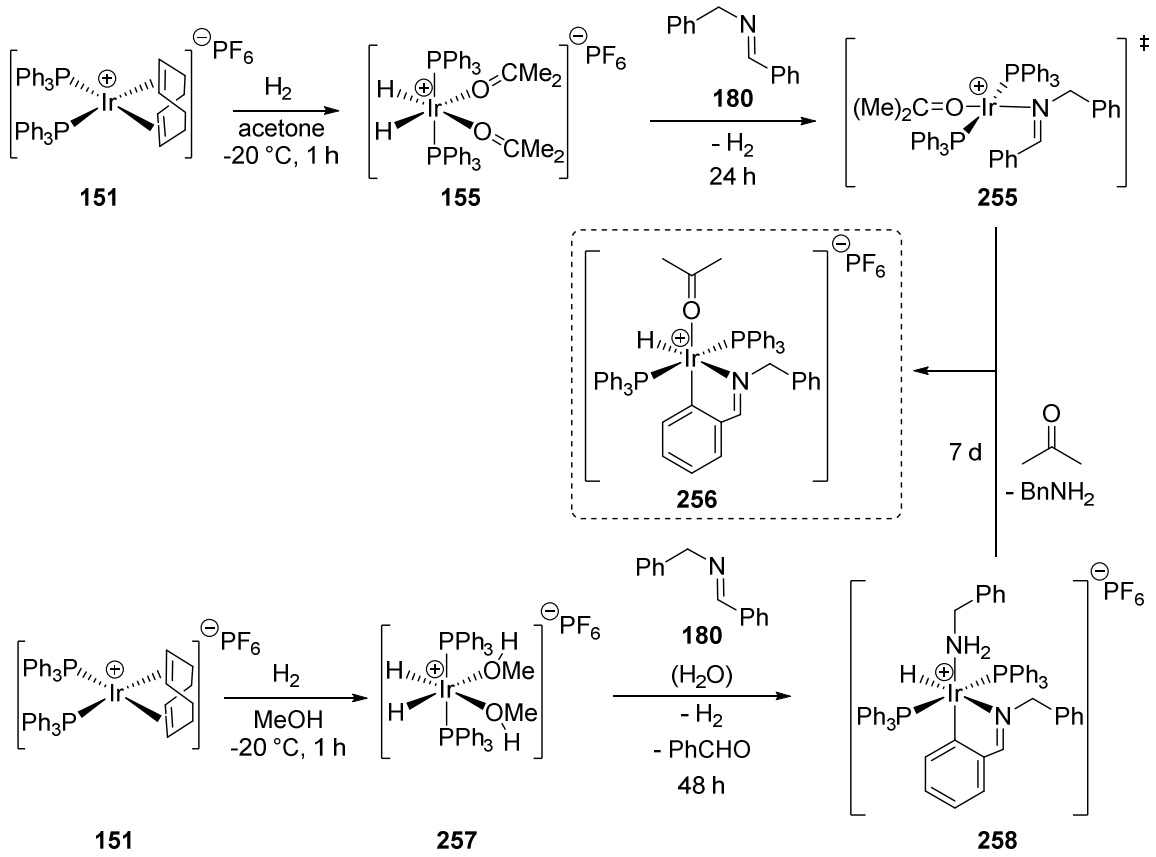

Scheme 76: Formation of iridacycle **256** under hydrogenation conditions

When the cyclometalated complex was subjected to hydrogenation conditions, precipitation of catalytically inactive neutral dihydride complex was observed (Scheme 77).

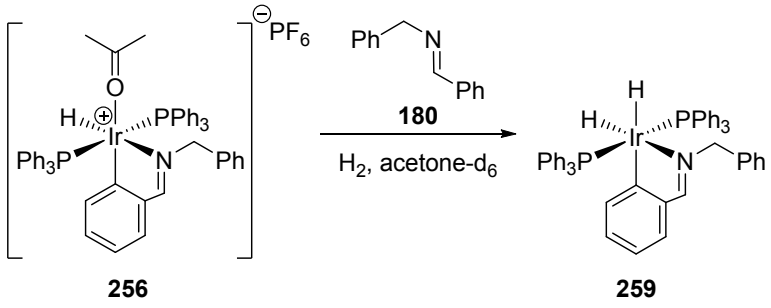

Scheme 77: Preparation of neutral dihydride complex **259**

Cyclometalation of Ir(III) dihydro-bis-solvent complexes was studied in further detail (Figure 12).[81] Stochiometric addition of imines to di-hydride complexes **155** or **257** (Scheme 76) readily ensued in iridacycle formation of **260**, **261** and **262** apart from *N*-perfluorophenyl which remained unaffected over the course of several hours. Surprisingly chelation *via* the phenol group in **261** was not observed but C-H activation instead. This is in contrast to Cu(II), Ru(II) and V(IV) complexes which all preferentially form *N,O* chelated complexes. All three complexes did not show any catalytic activity under hydrogenation conditions.

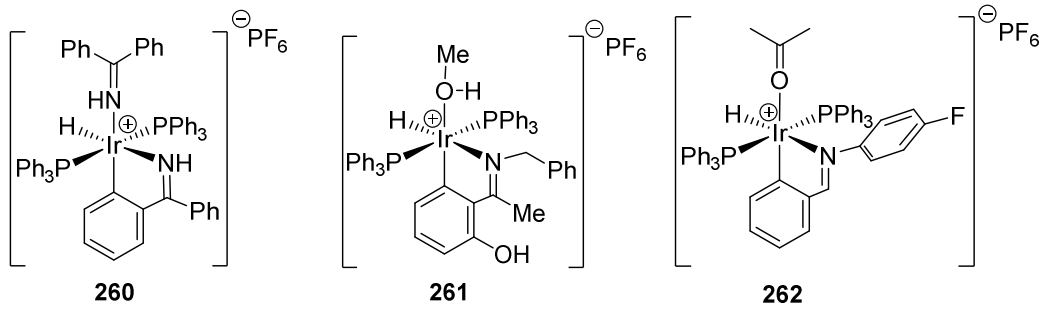

Figure 12: Iridacycles **260**, **261** and **262**

In order to understand the general lack of reactivity of such complexes under hydrogenation conditions, *James* and co-workers generated Ir(III) cyclometalated imine complexes *in situ* (Scheme 78).[82] In all cases precipitation of neutral di-hydride complexes and concomitant generation of HPF_6 was observed.

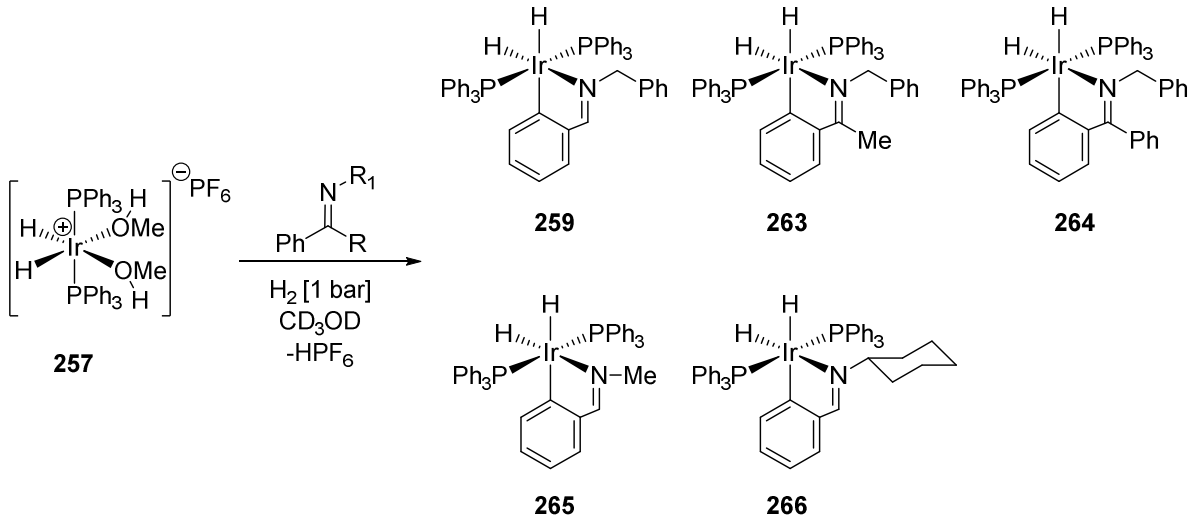

Scheme 78: Preparation of neutral dihydride iridacycles **259** and **263**-**266**

The supernatant of such reaction mixtures contained only imine and no trace of amine by GC analysis. The neutral di-hydride complexes are insoluble in MeOH, but soluble in CH_2Cl_2. No catalytic activity was observed under hydrogenation conditions in CH_2Cl_2 either. The formation of di-hydride complexes such as **270** by heterolytic cleavage of dihydrogen has also been observed by *Crabtree* (Scheme 79).[83]

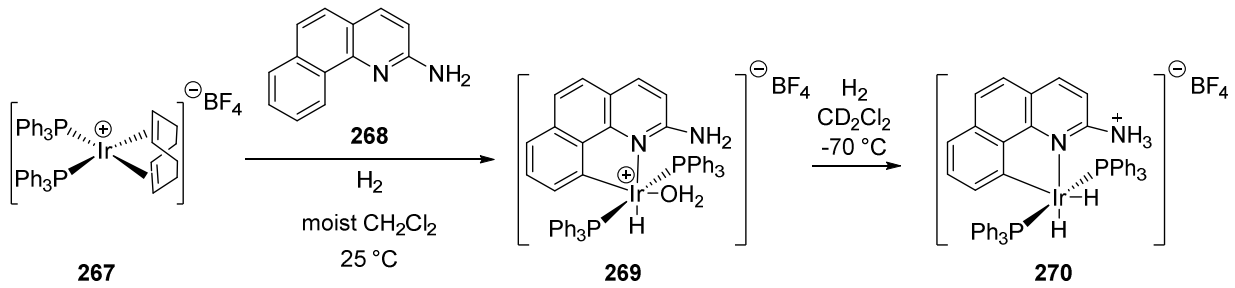

Scheme 79: Generation of cationic dihydride complex **270** by *Crabtree*

In order to understand the mechanism of cyclometalation, *James* and co-workers conducted deuterium experiments on **257**-D_4. Interestingly, even under exclusion of hydrogen gas and protic hydrogen sources, the di-hydride complex was observed. Not even trace amounts of the deuterated complex were observed by ^{1}H-NMR (Scheme 80).

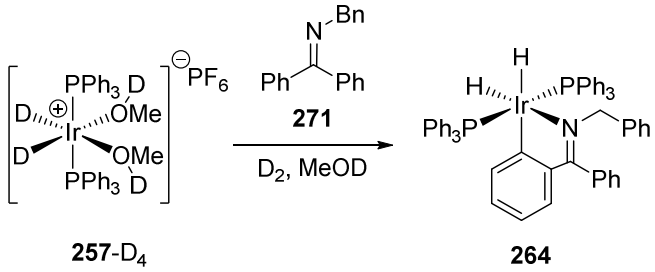

257-D_4 **264**

Scheme 80: Generation of **264** from deuterated **257**-D_4 under deuterium gas

The catalytic inactivity of the neutral dihydro complexes such as **264** was explained by their non-polar character. Ir- and Rh-cationic species are essential for effective imine hydrogenation. This can be explained by the fact that "Rh(III) cyclometalated complexes undergo reversible reductive elimination of the cyclometalated imine to furnish the Rh(I) complexes, which can then undergo the required oxidative addition of H_2".

However, out of all substrates studied in imine hydrogenation and substrate cyclometalation, a completely contrasting behaviour was observed with imine **209** (Scheme 81).[81] While the analogous Rh(III) complex **179** (Scheme 54) was deactivated by the amine product (η^4-coordination of the aniline) the iridium complex **151** afforded amine **219** *via* **257** and **272** quantitatively with 2 mol% catalyst at atmospheric hydrogen pressure within 1 hour.

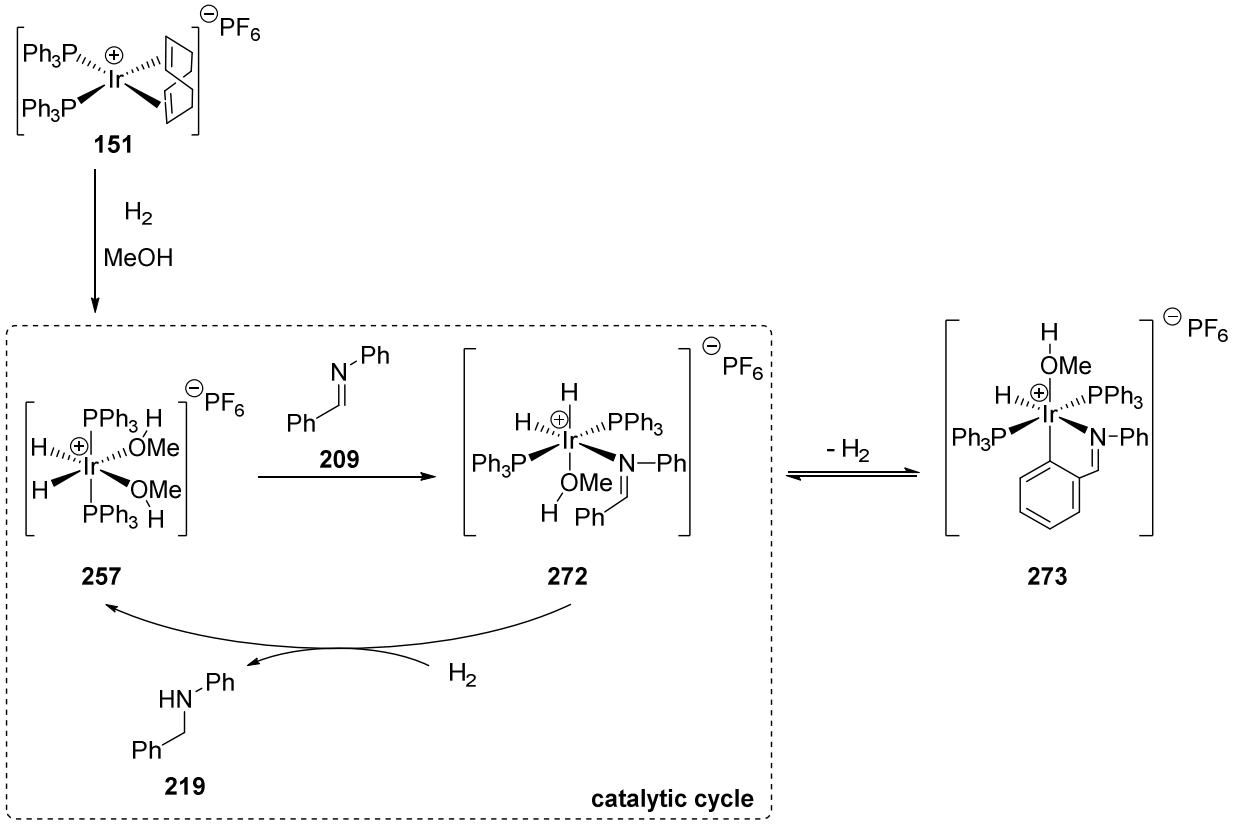

Scheme 81: Catalytic imine hydrogenation with iridacycle **258** as an out-of-cycle reservoir complex

Cyclometalation of imine **209** was explained to be less favoured due to the electron-poor C=N double bond, as well as the steric bulk exhibited by the close proximity of the *N*-aryl ring. Indeed, the stoichiometric reaction of the dihydro-bis-solvent complex **257** and imine **209** revealed only partial formation of the cyclometalated species **273** in MeOD solution. Furthermore, when excess imine was added and the argon atmosphere was replaced by a hydrogen atmosphere, the signals of the cyclometalated complex disappeared and the dihydrido-bis-solvent **257** complex was regenerated. This clearly demonstrated the reversibility of

the cyclometalation reaction under catalytic conditions. Thus, hydrogenation occurred *via* hydrogen transfer in the di-hydrido-η^1-imine intermediate **272**.

A more general picture of the reactivity of cyclometalation was reported by *Martinez*.[84] In a series of cyclopalladation reactions, selective formation of the endometallacycle was observed. Similar results were observed by *Barloy* when imines were subjected to $[Ir(Cp^*)(Cl_2)]_2$ complexes affording cationic iridacycles (Figure 13).[85] *Barloy* and coworkers noted another striking difference in diastereomer formation. Acyclic imines, contrary to cyclic ones, were unable to control the configuration at the metal so that a 1:1 mixture of **274** and **275** was obtained. Furthermore, epimerisation of the CH(Me)(Ph) phenyl ring was observed in *EXSY* NMR experiments as well as chemical exchange between both diastereomeric metal complexes. This demonstrated the many degrees of freedom cyclometalated acyclic ligands experience with Cp* ligands.

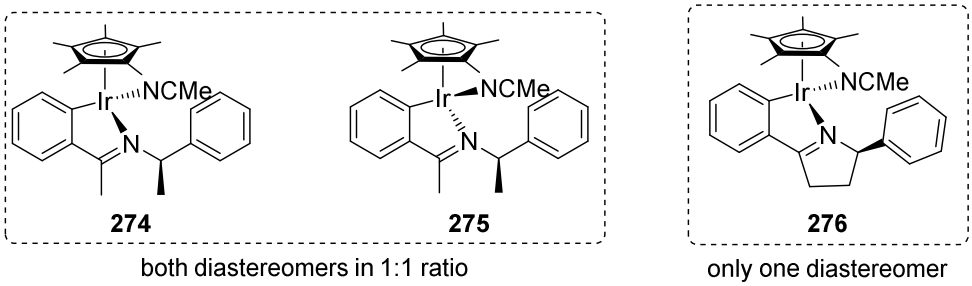

Figure 13: Iridacycles **274**, **275** and **276**

Cyclometalation of $[Ir(Cp^*)(Cl)_2]_2$ (**279**) with benzaldimines **277** and **278** has been studied by *Jones* and co-workers with regards to regioselectivity (substrates with *meta*-substituents), kinetics (substrates with *para*-substituents) and mechanism (electrophilic C-H activation).[86] Since cyclometalation reactions are about 10 times faster with **277** than with **278**, an electrophilic C-H activation mechanism was postulated (Scheme 82). In kinetic studies, a primary isotope effect was investigated with a fully deuterated benzaldimine. Since a KIE larger than 5 was detected, the consistency with an electrophilic C-H activation mechanism was strengthened.

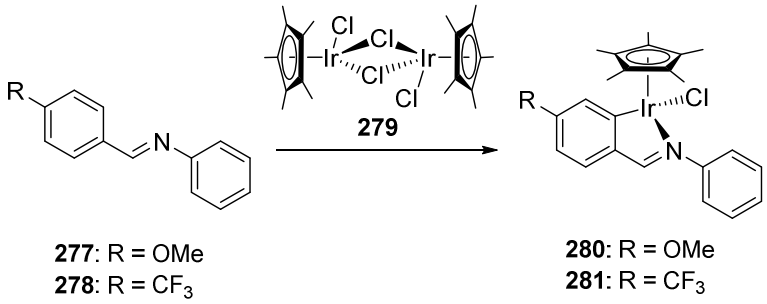

Scheme 82: Preparation of iridacycles **280** and **281**

Regioselectivity was found to be extremely sensitive to steric effects. With **283**, **285** and **286** only the first regioisomers **289**, **291** and **292** was isolated (Scheme 83). With **282**, **284** or **287** a mixture of both regioisomers **288**/**294**, **290**/**295** and **293**/**296** was observed. Fluorine (**290**/**295**) is an exception forming preferentially **295** due to the „*ortho* effect".

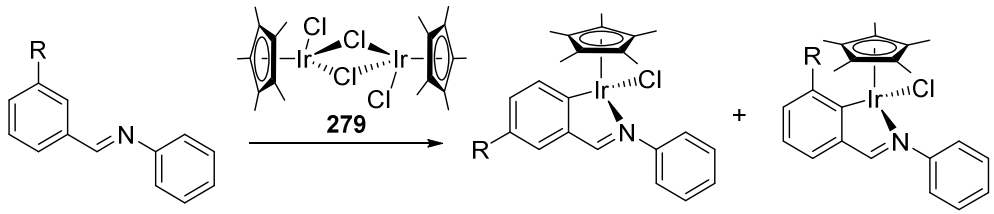

282: R = OMe
283: R = Me
284: R = F
285: R = COOMe
286: R = CF_3
287: R = CN

288: R = OMe
289: R = Me
290: R = F
291: R = COOMe
292: R = CF_3
293: R = CN

1.7 : 1.0 **294**: R = OMe
1.0 : 2.3 **295**: R = F
1.3 : 1.0 **296**: R = CN

Scheme 83: Generation of diastereomeric mixtures of iridacycles depending on the substituent

Steric effects also play an important role in the cyclometalation of meta-substituted aldimine **297**. Regioisomer **298** is strongly favoured compared to **299** (Scheme 84).

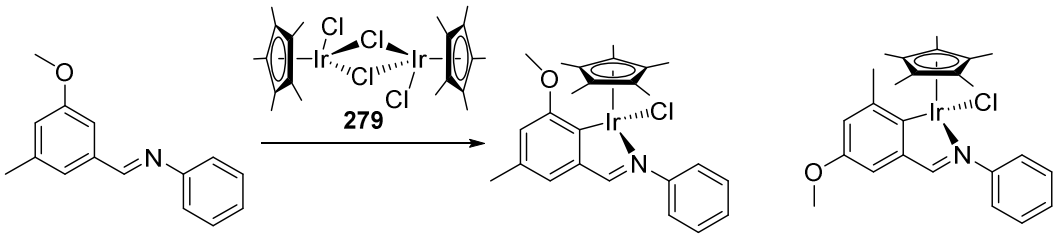

297 **298** 10:1 **299**

Scheme 84: Regioselective cyclometalation of imine **297** favouring iridacycle **298**

Cyclometalation was demonstrated to be reversible under acidic conditions. Addition of trifluoroacetic acid to **288** (**294**) in MeOH afforded equilibrium of both complexes within 2 hours (Scheme 85). This result is similar to those observed in acid-promoted rearrangements of palladacycles.

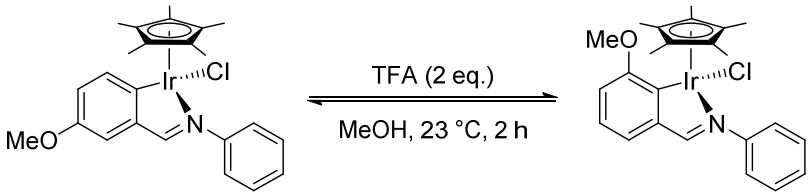

288 **294**

Scheme 85: Reversible cyclometalation of **288** in acidic methanol solution

Additive effects in imine hydrogenation

Tani and co-workers identified protic amines such as **301** as additives giving higher conversions in the asymmetric hydrogenation of imine **55** using iridium BINAP complexes generated from **64** and **300** (Scheme 86).[87] While a chiral amine additive did not influence the enantioselectivity of the catalyst in a positive or negative manner, both aromatic and aliphatic amines afforded higher enantioselectivities. The reaction was stopped at 60% conversion and the *E*/*Z* ratio of the acyclic imine **55** was similar to the beginning (92:8).

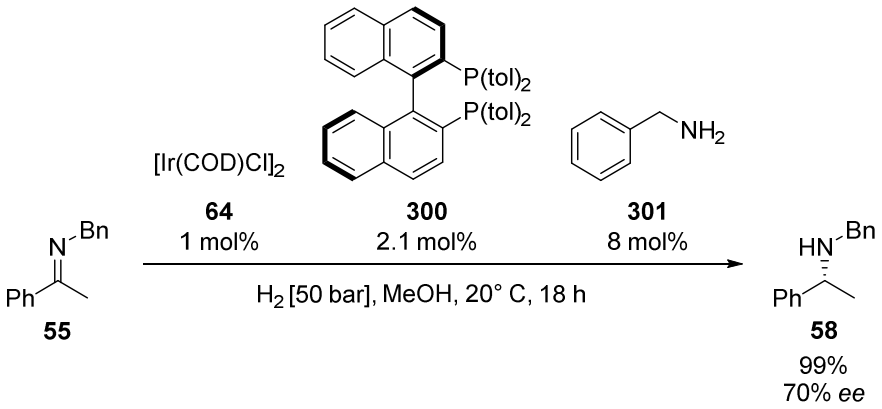

Scheme 86: Asymmetric hydrogenation of imine **55** using amine **301** as additive

Zhu and *Zhang* investigated iridium-catalysed imine hydrogenation of 2,3,3-trimethylindolenine (**302**) (Scheme 87).[88] While chiral amines or iodide sources resulted in low to no conversion, addition of phtalimide (**304**) resulted in full conversion and high enantioselectivity. Apolar solvents such as toluene or dichloromethane gave very high enantioselectivities whereas polar solvents such as DMF or MeOH gave very low enantioselectivities. The beneficial effect was primarily rationalized based on findings by *Colquhoun*.[89] He reported on imidato ligands which acted as pseudo-halogen ligands in terms of their σ-acceptor and π-donor properties. However, *N*-methylated phthalimide gave similar results and potassium phthalimide gave very low enantiomeric excess. Therefore, the direct influence of an Ir-*N* bond was questioned. Nevertheless, coordination via one oxygen atom is possible. Indeed, 1,3-indanedione forms a keto-enol species in solution and the presence of it as an additive increased the enantioselectivity of the hydrogenation. However, the improvement was not found with other imine substrates. Furthermore, addition of Brønsted acids gave better conversion but similar enantioselectivity.

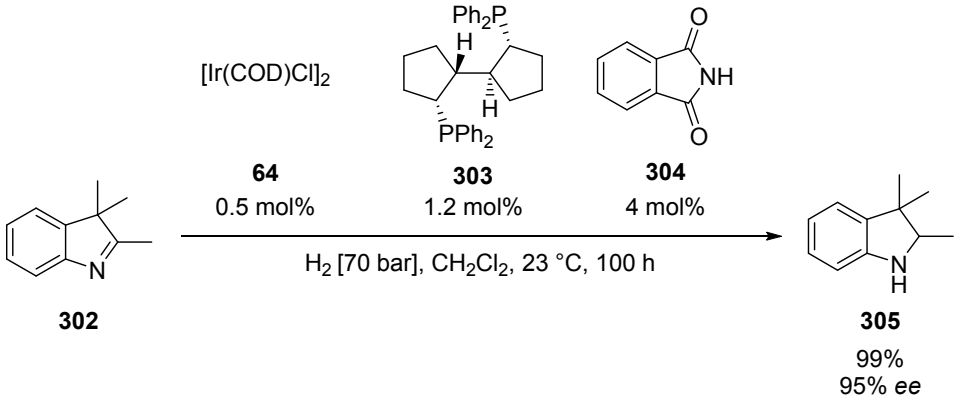

Scheme 87: Asymmetric hydrogenation of imine **302** using phtalimide (**304**) as additive

Chapter 2 – A Summary of Previous Results by *F. Barrios-Landeros*

The project of this doctoral thesis was based on results of *Dr. Fabiola Barrios-Landeros*. She conducted post-doctoral studies in the research group of *Prof. Andreas Pfaltz* from April 2007 to December 2008. Within that time, I worked along her as a project student for eight weeks. The results from the internship are included in this chapter of previous results.

This chapter is based on the progress report of *Dr. Fabiola Barrios-Landeros* of April 2008 and the leaving presentation of December 2008. The text has been modified but the main structure has been used. I, York Schramm, hereby clearly claim that this chapter is **not** out of my intellectual effort. It solely is added to aid the reader understand how the project developed.

Dihydride Iridium Intermediates

In the introduction chapter an overview of previous studies on oxidative hydrogen addition to iridium complexes was given. Among these studies, *Mazet* and co-workers had reported on dihydride species being formed under catalytic conditions (Scheme 88).[57] The iridium complex [Ir(COD)(PHOX)]BAr_F **86** was activated under atmospheric hydrogen pressure at low temperatures. Primarily, the dihydride species **160** with the cyclooctadiene still coordinated was observed. Prolongued exposure to hydrogen resulted in hydrogenation of the cyclooctadiene and formation of two dihydride disolvent complexes **161** and **162**. The exact geometrical identity of the different dihydride complexes was studied by *Mazet* (studied by ^{1}H nOe and ^{31}P NMR experiments) at only about 30% conversion of complex **86**.

F. Barrios subjected the reaction mixture to hydrogen gas until complex **86** was no longer detected and observed **160** as well as all isomers of the dihydride complexes **161**, **162**, **306** and **307**.

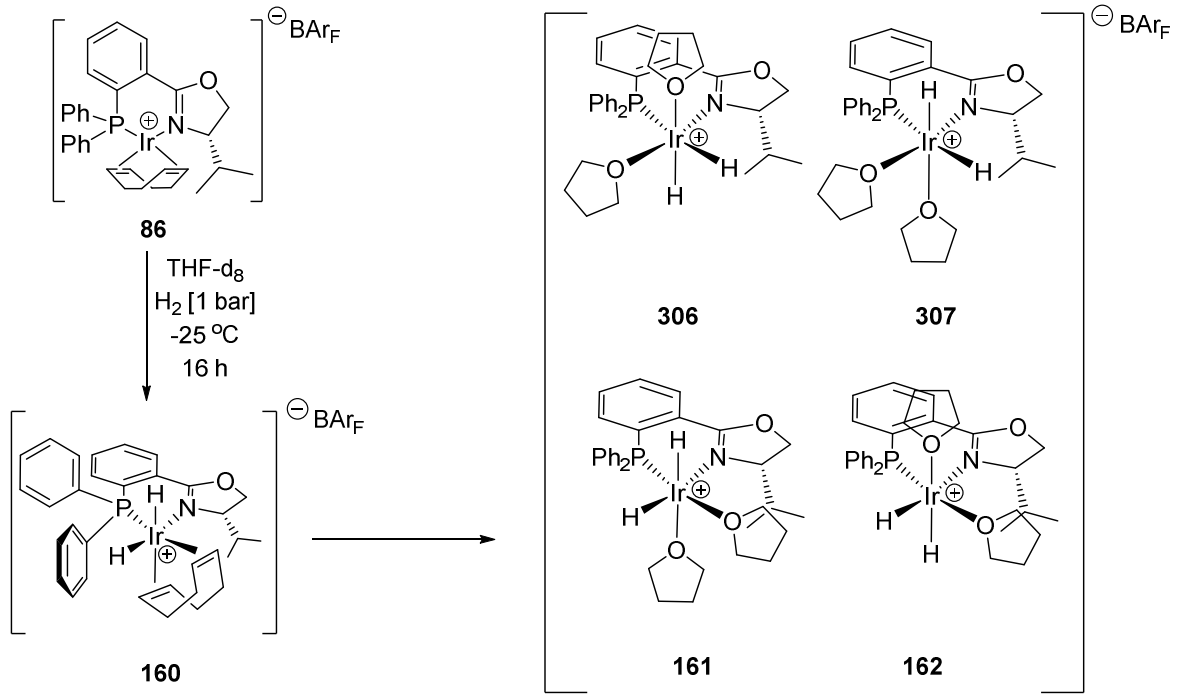

Scheme 88: Activation of complex **86** to afford dihydride complexes **160**, **161**, **162**, **306** and **307**

Overall a different ratio of the octahedral complex isomers was observed compared to the studies by *Mazet*. **161** and **162** are the major species and **306** and **307** the minor ones. Both complexes **161** and **162** are electronically favored due to the *trans* influences of their corresponding ligands. One hydride ligand is coordinated *trans* to the nitrogen and a solvent molecule *trans* to phosphorus of the phosphine oxazoline ligand. The second hydride ligand is coordinated *trans* to a second solvent molecule, exhibiting its characteristic high field NMR shift. The ^{1}H- (Spectrum 1) and ^{31}P{^{1}H}-NMR spectra (Spectrum 2) of these complexes were recorded at –73 °C to avoid signal overlapping.

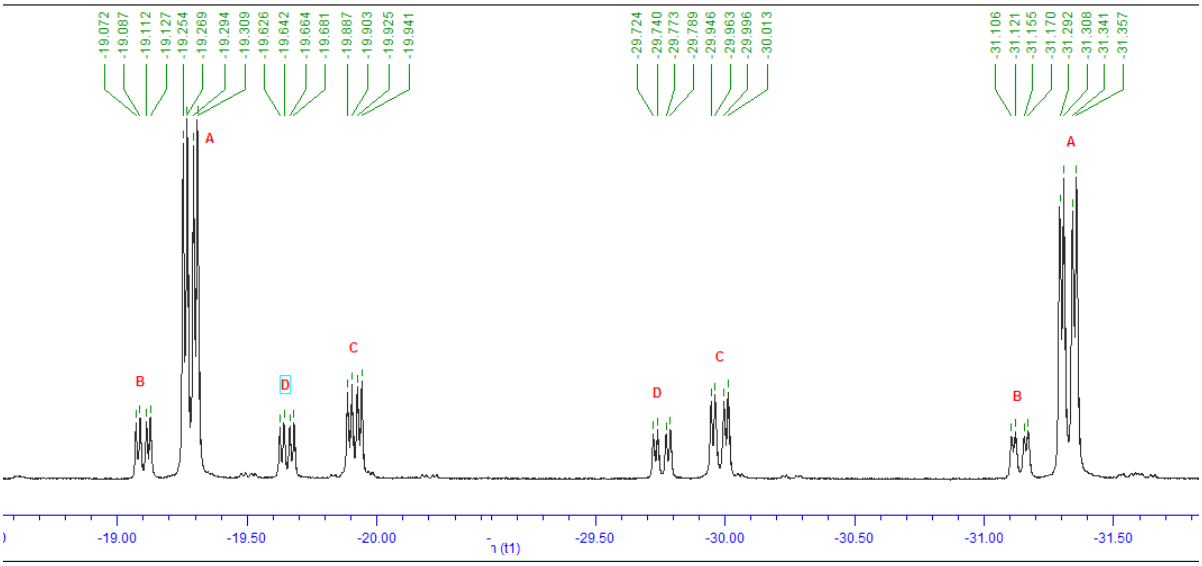

Spectrum 1: ^{1}H-NMR spectra of dihydride species **161**, **162**, **306** and **307** observed in solution at -73 °C in THF-d_8

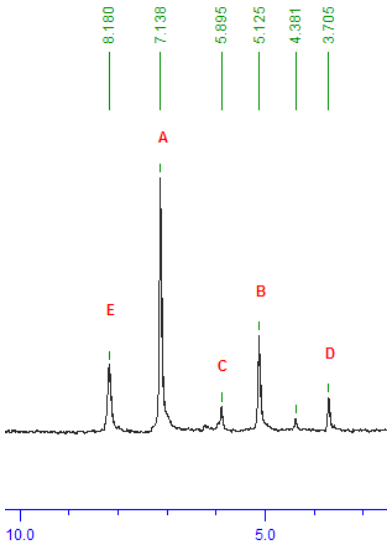

Spectrum 2: ^{31}P{^{1}H}-NMR spectra of dihydride species **161**, **162**, **306** and **307** observed in solution at -73 °C in THF-d_8

Since many studies on asymmetric (imine) hydrogenation, both experimental and computational one's, suggested involvement of iridium hydride species during the catalytic cycle at some stage,[7] the activated species for the hydrogenation of imines could be formed from the corresponding dihydride species **161**, **162**, **306** and **307**.

Therefore, the activation of complex **86** was monitored by NMR and the subsequent reaction with imine **59** afforded a species that contained a single hydride signal (Scheme 89). Upon complete activation of complex **86** to dihydride complexes **161**, **162**, **306** and **307** in THF, addition of imine **59** at 0 °C resulted in formation of a hydride-imine complex **308**. The signals in the ^{1}H-NMR spectra of the COD-bound complex **160** remained unchanged, whereas the signals of the COD-free dihydride unsaturated complexes **161**, **162**, **306** and **307** disappeared and a new monohydride species appeared. The postulated structure of the cyclometalated imine complex **308** was supported by ESI-MS analysis. Imine **59** was not reduced under these conditions as only imine **59** (and not the amine **60**) was detected by GC-MS analysis of the reaction mixture. Complex **308** was also prepared by directly mixing **86** and **59** at 0 °C.

[7] See chapter 1

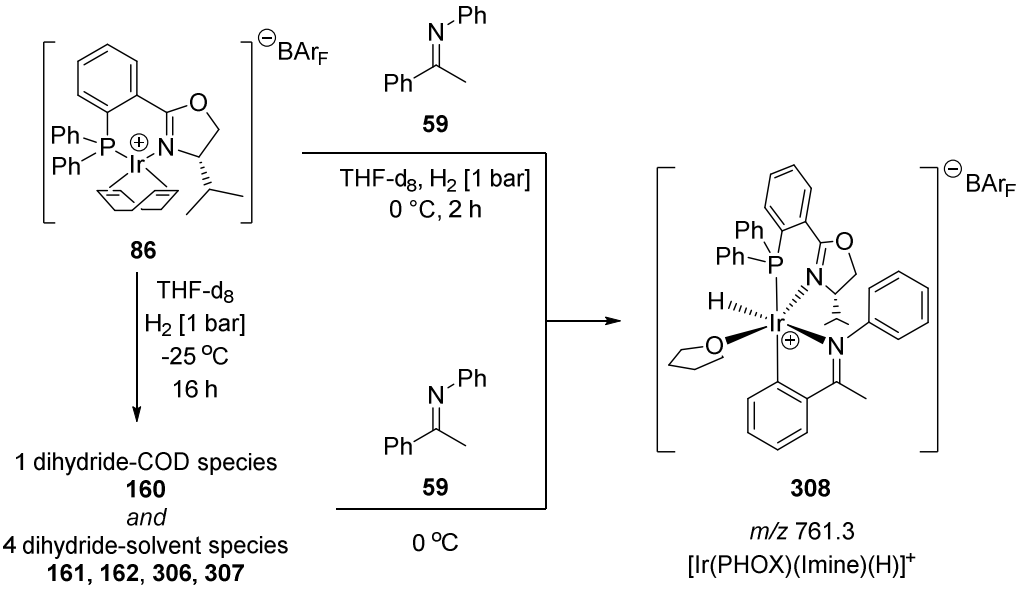

Scheme 89: Preparation of complex **308**

If the same reaction was performed in dichloromethane, a different species displaying a single ^{1}H-NMR hydride and one ^{31}P{^{1}H}-NMR signal was obtained (Scheme 90). However, imine **59** was hydrogenated under these conditions and amine **60** was observed by ^{1}H-NMR spectroscopy and detected by GC-MS analysis. ESI-MS measurements confirmed the corresponding cyclometalated amine complex **309**. Complex **309** was also prepared from **86** and racemic **60** (2 equivalents) under identical reaction conditions.

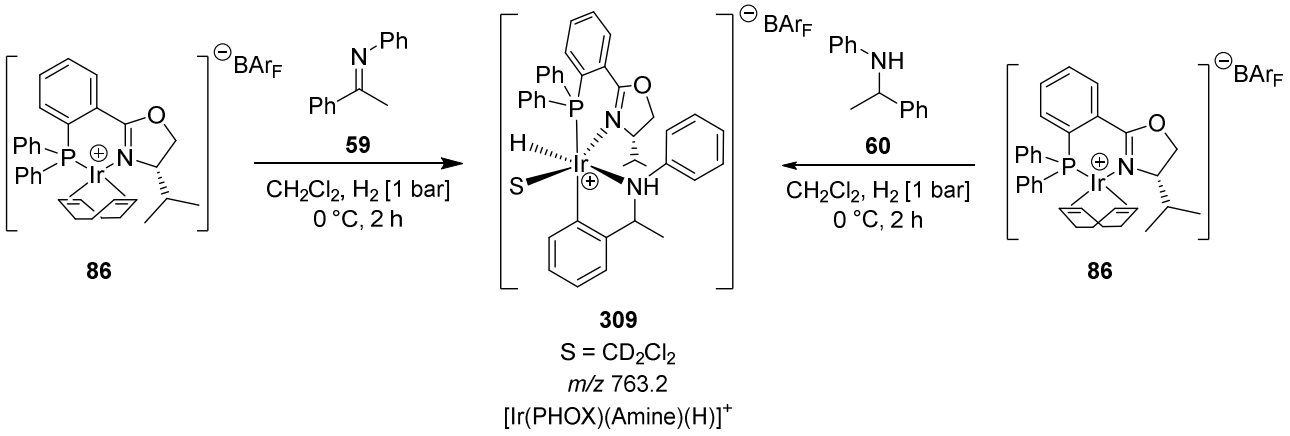

Scheme 90: Preparation of complex **309**

Characterization of cyclometalated intermediates

In order to verify cyclometalation had occurred at the *ortho*-position of the imine, complex **86** and imine **310** were reacted to form complex **311** (Scheme 91). Clear formation of a single hydride species with one ^{31}P-NMR signal was observed.

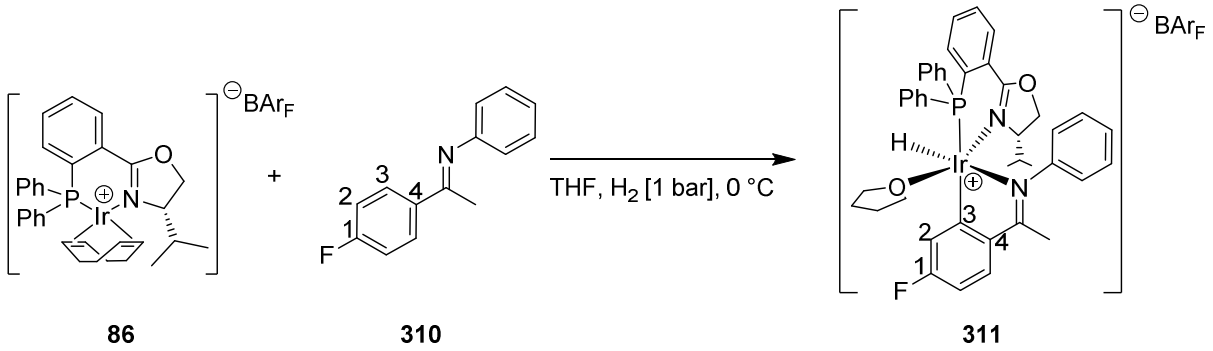

86 **310** **311**

Scheme 91: Preparation of iridacycle **311** with *p*-F-imine **310**

Since the intermediate is formed *in situ* in the presence of 2 to 3 equivalents of imine **310**, it was impossible to analyze the aromatic region in the ^{1}H-NMR. Therefore ^{13}C NMR analysis was used to identify C3 from all other aromatic carbon signals. Both the chemical shift and heteronuclear coupling of C3 were expected to change significantly upon binding to the iridium metal. The expected C3 carbon could be observed at 128.5 ppm as a doublet of doublets of doublets (J = 31.7, 5.4 and 2.8 Hz, Spectrum 3). The splitting of the signal arises from the heteronuclear coupling of the carbon atom to phosphorus, fluorine and the hydride. Two-dimensional HMBC analysis clearly depicted this signal to be C3 and therefore evidenced the *ortho*-cyclometalation of the imine.

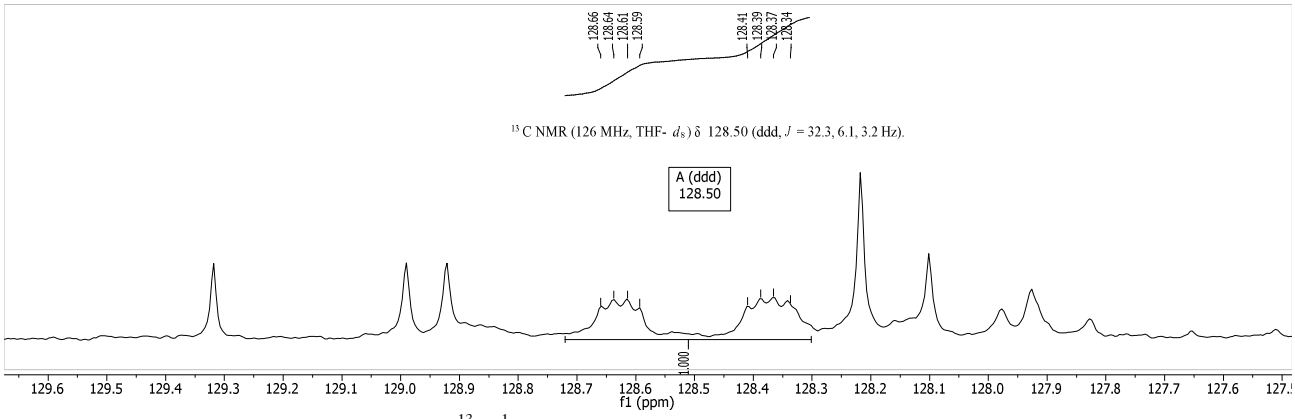

Spectrum 3: ^{13}C{^{1}H}-NMR in THF-d$_8$ at -33 °C of iridacycle **311**

Complexes **161**, **162**, **306** and **307** were mixed with imine **59** at -73 °C to evaluate the propensity of the cyclometalation (Spectrum 4 and Scheme 92). Within 5 minutes of addition, two new hydride signals were observed.

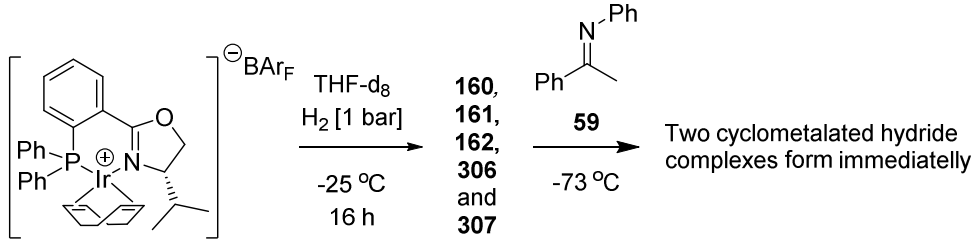

86

Scheme 92: Addition of imine **59** to dihydride complexes **161**, **162**, **306** and **307** at -73 °C

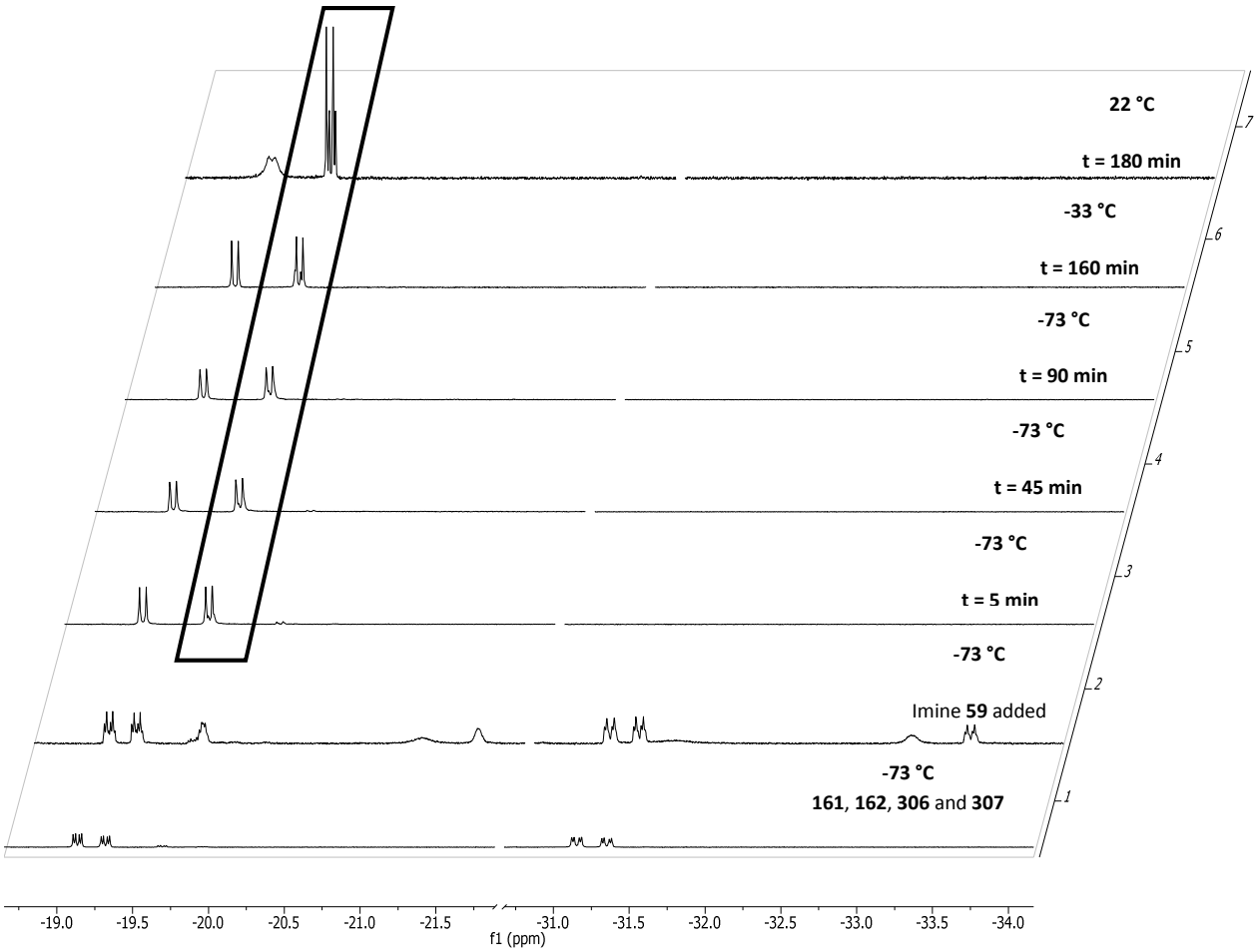

Spectrum 4: ^{1}H-NMR spectra following the formation of iridacycle **308** from -73 °C to 22 °C

The two signals corresponding to the dihydride complexes **161** and **162** disappeared almost completely while two new signals of iridacycle **308** and **308'** appeared (Scheme 93).

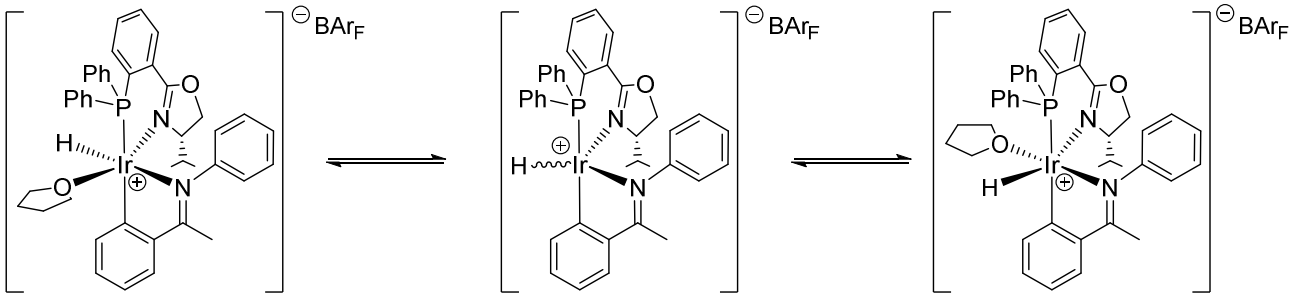

308 **308'**

Scheme 93: Interconversion of configurational isomers of **308** and **308'**

For comparison, allowing the dihydride complexes **161**, **162**, **306** and **307** warm up to room temperature for only 3 minutes resulted in decomposition. The two newly formed hydride complexes were assigned as interconverting configurational isomers, one being the thermodynamically and one the kinetically favoured product. Upon warming the complex mixture from -73 °C to -33 °C and then to room temperature (22 °C), one hydride species was transformed into the other (Spectrum 4). Judging from the similar chemical shifts as well as the coupling constants, the hydride is expected to be *cis* to the phosphorus. As it is a very strong *trans*-donor (strong σ-donor), it is expected to be situated *trans* to a weak donor (a π-acceptor). Thus, it should be opposite of either nitrogen. With the restriction of the hydride being *cis* to the phosphorus and *trans* to a nitrogen atom, an isomerisation pathway involving a trigonal planar intermediate can be postulated. Interconversion *via* dissociation of a THF molecule would become more feasible with increased

temperature to afford the thermodynamically favoured isomer **308**. This experiment clearly demonstrated that imine cyclometalation onto dihydride complexes **161** and 1**62** occurs within minutes even at –73 °C. This high reactivity of the imine with dihydride complexes suggests that the same process takes place under catalytic conditions at room temperature. While reduction of imine **59** is not observed in THF, experiments aiming at isolating complex **308** could not be performed in CH_2Cl_2 since imine **59** is directly reduced and hence complex **309** formed.

Attempts to crystallize the iridacycle **308** prepared from complex **86** with BAr_F as a counterion were unsuccessful. On the other hand, starting from the corresponding PF_6 complex **312**, single crystals of **313** were obtained (Scheme 94) and the structure was determined by X-ray crystallography (Figure 14).

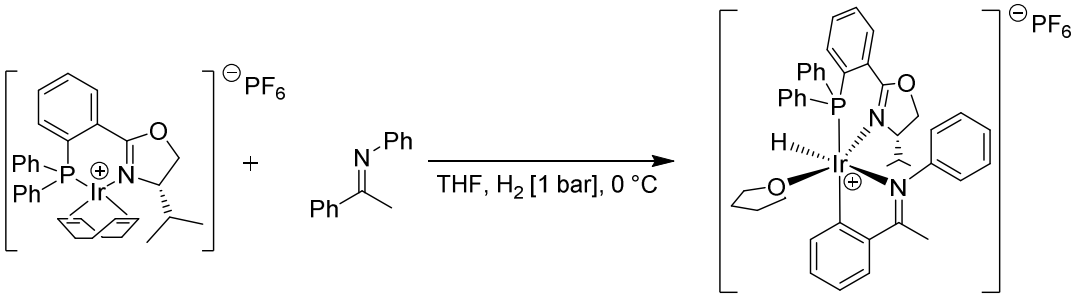

312 **59** **313**

Scheme 94: Preparation of complex **313** furnishing X-Ray quality crystals

The cyclometalated nature of the iridium(III)-complex was confirmed. The complex is octahedral with a PHOX ligand, a cyclometalated imine **59**, one molecule of THF and a hydride in the coordination sphere (Figure 14).

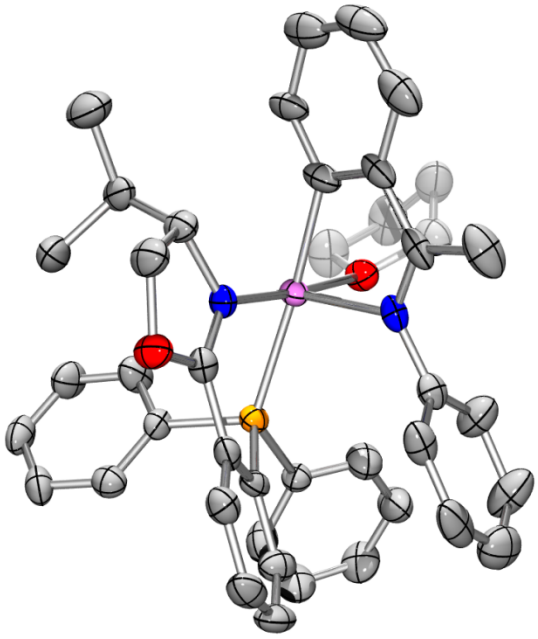

Figure 14: Crystal structure of complex **313**

The exact position of the hydride could not be determined by X-ray diffraction but the free coordination site can be well recognized. The hydride ligand is *cis* to the phosphorus atom which is consistent with the heteronuclear coupling constant of $J_{P\text{-}H} \approx 20$ Hz. Selected bond lengths and angles are depicted in Table 3. Six out of the eight angles formed around the metal are between 85 and 98 degrees consistent with the octahedral environment around the metal. The atoms in the cyclometal plane have distorted angles of 77.0 and 103.5 due to the 5-membered ring constraint.

Table 3: Selected bond lengths and angles of complex **313**

Atoms	Bond lenghts (Å)	Atoms	Angles (deg)
Ir1 O2	2.12	P1 Ir1 O2 (THF)	98.2
Ir1 C25	2.06	P1 Ir1 C25	173.4
Ir1 N2 (Imine)	2.20	P1 Ir1 N2 (Imine)	103.5
Ir1 P1	2.32	P1 Ir1 N1 (PHOX)	85.4
Ir1 N1 (PHOX)	2.04	N1 (PHOX) Ir1 O2	175.8
		N1 (PHOX) Ir1 C25	88.1
		N1 (PHOX) Ir1 N2 (Imine)	89.7
		N2 (Imine) Ir1 O2	91.6
		N2 (Imine) Ir1 C25	77.0
		O2 Ir1 C25	88.4

In order to better understand the stability of the iridacycle under hydrogenation conditions, iridacycle **308** was subjected to imine **314** under hydrogenation conditions and aliquot analysis by ESI-MS was performed every 15 minutes.

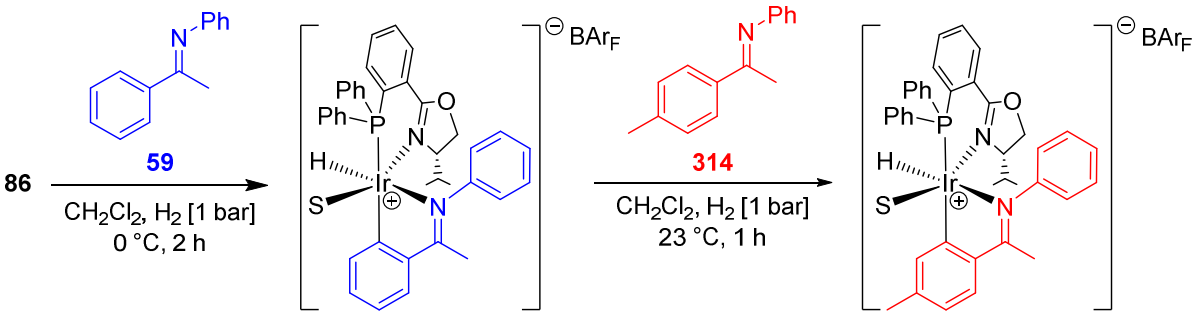

308
mass 761.3
$[Ir(PHOX)(\mathbf{59})(H)]^+$

315
mass 775.2
$[Ir(PHOX)(\mathbf{314})(H)]^+$

Scheme 95: Exchange of cyclometalated imine **59** in complex **308** for imine **314**

Spectrum 5 shows an aliquot of the reaction mixture at the beginning. No signal corresponding to iridacycle **315** was observed in earlier aliquots. At the end of the reaction, a small signal corresponding to iridacycle **315** can be observed (Spectrum 6). With regards to the reactivity of iridacycle **308**, exchange can be neglected. The appearance of the mass signals might originate from decomposition processes of **308** undergoing cyclometalation with imine **314**.

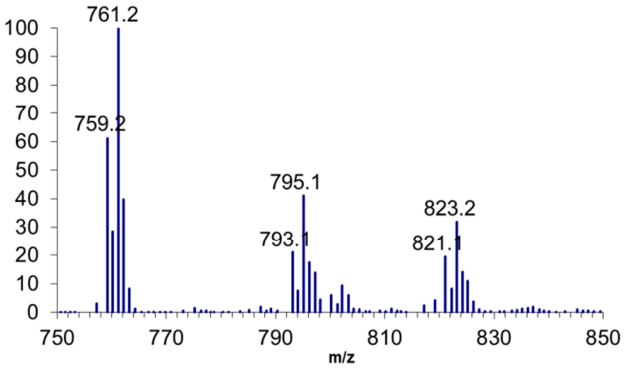

Spectrum 5: ESI-MS spectra of **308** at the beginning of the reaction

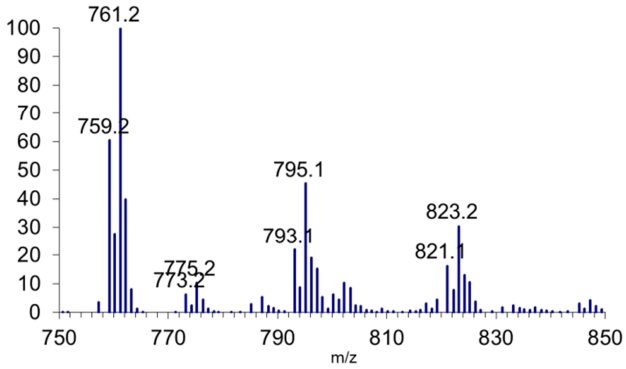

Spectrum 6: ESI-MS spectra of **308** (and **315**) at the end of the reaction

On the other hand, if amine **316** was cyclometalated to generate iridacycle **317** (Scheme 96 and Spectrum 7), addition of imine **59** under hydrogenation conditions resulted in complete exchange of the amine to the imine affording complex **308** was observed (Spectrum 8).

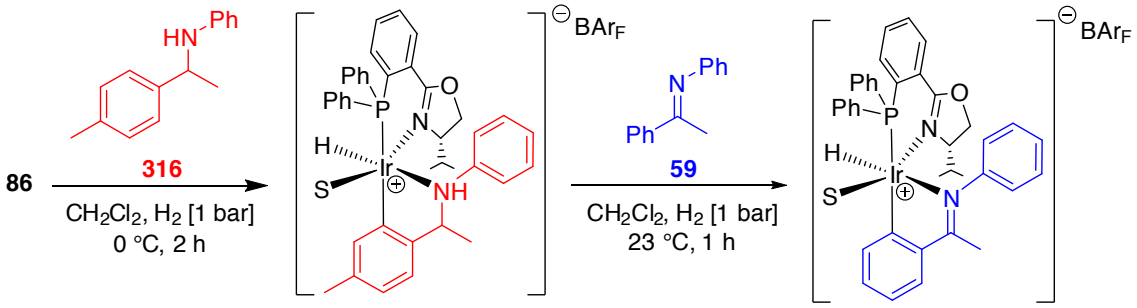

Scheme 96: Exchange of amine **316** by imine **59** on iridacycle **317**

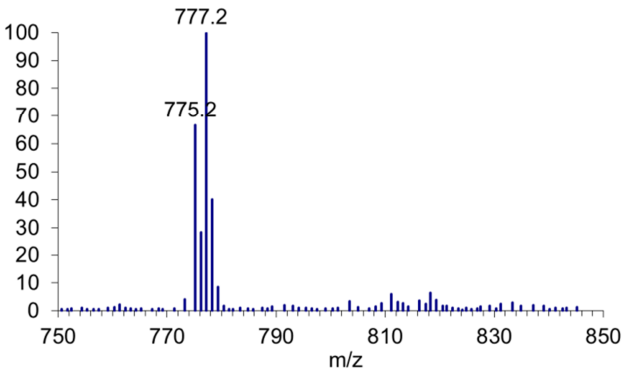

Spectrum 7: ESI-MS spectra of **317** at the beginning of the reaction

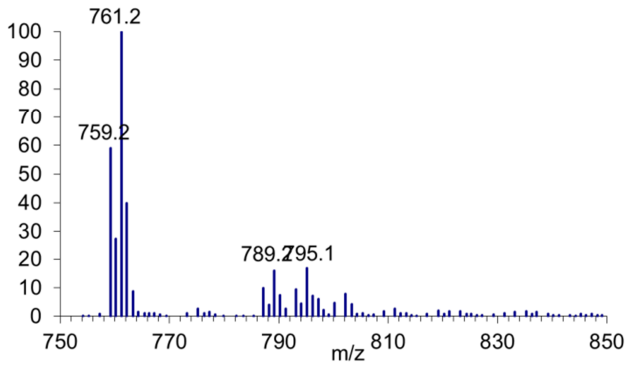

Spectrum 8: ESI-MS spectra of **308** at the end of the reaction

Under deuteration conditions, a gradual increase of the mass intensities can be observed (Scheme 97 and Spectrum 10). This suggests that under deuteration conditions, multiple isomerisation and scrambling processes are occurring at the cyclometalated complex **308**.

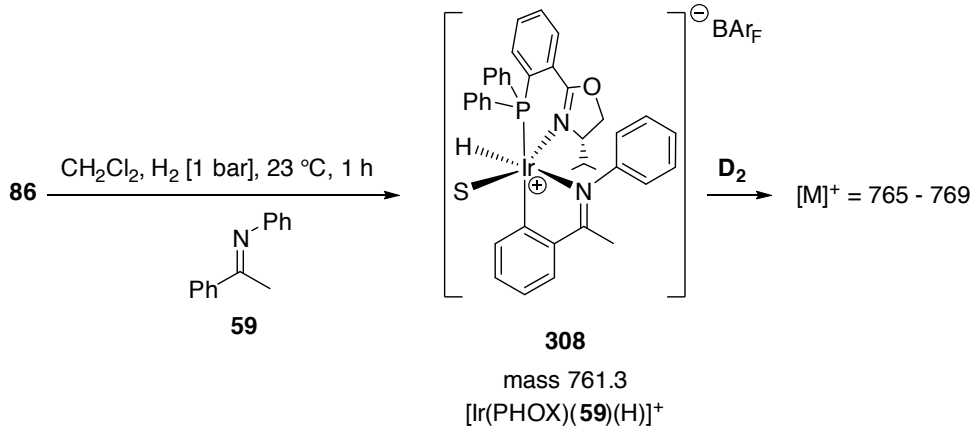

Scheme 97: Concomitant incorporation of deuterium into iridacycle **308**

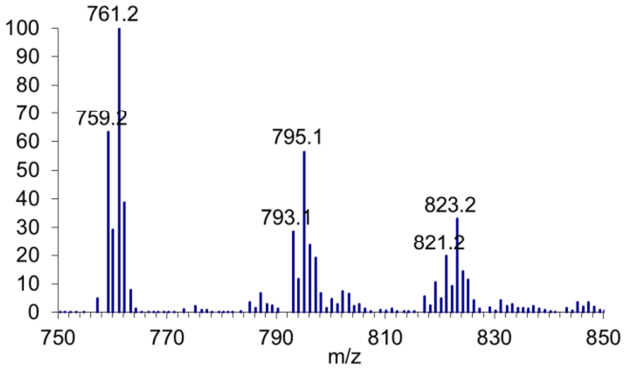

Spectrum 9: Initial ESI-MS spectra of iridacycle **308**

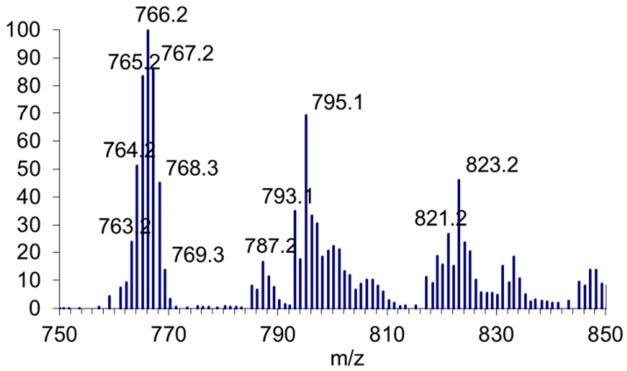

Spectrum 10: ESI-MS spectra after prolongued exposure of iridacycle **308** to deuteration conditions

In order to identify the resting state of the iridium complex under reaction conditions, ^{15}N-labelling was used to determine whether the cyclometalated substrate was reduced or not, judged by the chemical shift in the ^{15}N-NMR spectrum. Furthermore, imine cyclometalation was believed to be irreversible whereas amine cyclometalation was expected to be reversible. The corresponding iridacycles **308** (Scheme 98) and **309** (Scheme 99) were mixed with ^{15}N-labelled imine **59** or amine **60** and allowed to exchange overnight. With **308**, no scrambling of imine was observed by ^{15}N-NMR spectroscopy.

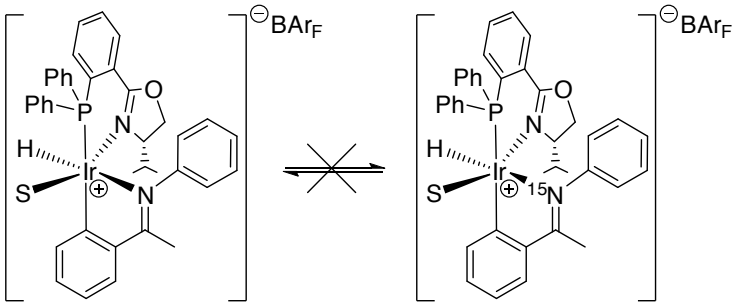

308 **^{15}N-308**

Scheme 98: Exchange of imine **59** investigated with labelled ^{15}N-**59**

On the other hand, subjecting complex **309** (Figure 15 and Spectrum 11) to ^{15}N-amine **60**, exchange to a thermodynamic equilibrium of **309** and ^{15}N-**309** could be detected by ^{1}H-NMR spectroscopy due to the specific coupling of the hydride (Scheme 99, Spectrum 12 and Spectrum 13).

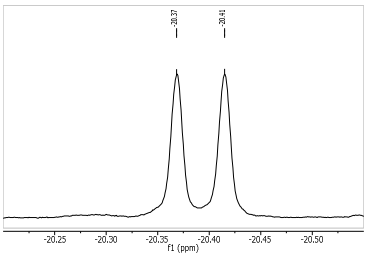

Spectrum 11: ^{1}H-NMR of **309** (^{14}N: doublet)

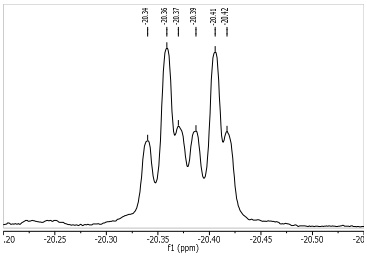

Spectrum 12: ^{1}H-NMR of ^{15}N-**309** (^{14}N: doublet & ^{15}N: dd)

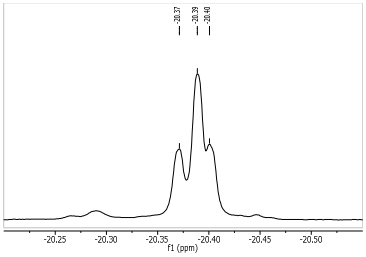

Spectrum 13: ^{1}H{^{31}P}-NMR of ^{15}N-**309** (^{14}N: singlet & ^{15}N:doublet)

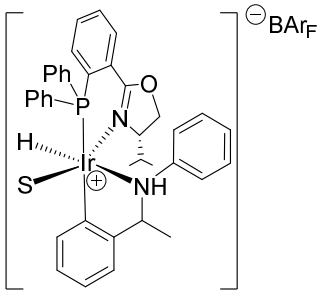

309

Figure 15: Complex **309**

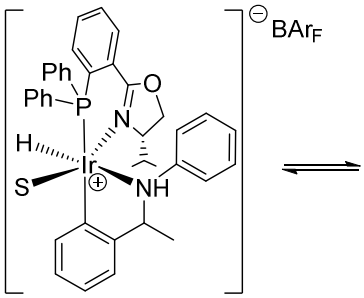

309

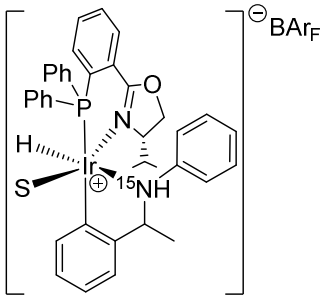

^{15}N-**309**

Scheme 99: Interconversion of complexes **309** and ^{15}N-**309**

Cyclometalated complexes as catalysts

Both NMR spectroscopic and ESI-MS analysis indicated that the cyclometalated complexes were stable in solution. To elucidate whether they are intermediates in the catalytic cycle or iridacycle formation is only a side reaction under reaction conditions, their role in the course of the reaction was investigated.

A previous study in our lab demonstrated that dialkyl imines were hydrogenated in low conversion and low enantiomeric excesses.[30],[31] Possibly due to prevention of *ortho*-metalation, the active catalyst cannot be formed. Therefore, reductions of imines with different substitution patterns at the *ortho* position of the aromatic ring were conducted to evaluate the difference in reactivity and enantioselectivity (Table 4). At atmospheric hydrogen pressure imine **59** (Entry 1) is hydrogenated in full conversion and 88% *ee*. Reactivity is lowered with a methyl- or fluoro-substituent at the *ortho*-position in imines **318**, **319** and **320** (Entries 2, 4 and 5). At higher pressure, imine **318** is reduced with 70% conversion (Entry 3), but imine **320** only in 11% conversion (Entry 6). Imines **310**, **314**, **322**, **323** and **324** (Entries 9 to 13) were tested to evaluate electronic effects at the aromatic ring. All substrates were fully reduced and 81% *ee* (electron-rich or –neutral) to 88% *ee* (electron-poor) was observed.

Substrates hindering or preventing *ortho*-C-H activation either by destabilizing a planar Aryl-(C=N) orientation (**318**), heteroatom substitution (**319**), absence of a sp^2-aromatic C-H bond in the *ortho*-position (**320**) or a methylene group (**321**) did not react under 1 bar hydrogen over the course of four hours. This suggests that *ortho*-metalation of the substrate is required to form an active catalyst. However, increased pressure did furnish the corresponding amines, which suggests that under forcing conditions alternative reaction pathways are possible.

Table 4: Hydrogenation of imines **59, 310, 314** and **318**-**324**

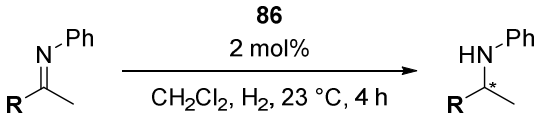

Entry	Imine	*p* [bar]	Conv. [%][a]	*ee* [%][b]
1	**59** (R = Ph)	1	>99	88
2	**318** (R = 2-Me-Ph)	1	0	-
3		50	70	67
4	**319** (R = 2-F-Ph)	1	95	-
5	**320** (R = 2,6-di-F-Ph)	1	0	-
6		50	11	-
7	**321** (R = Bn)	1	0	-
8		50	>99	n.d.[c]
9	**314** (R = 4-Me-Ph)	1	>99	81
10	**322** (R = 4-OMe-Ph)	1	>99	81
11	**310** (R = 4-F-Ph)	1	>99	86
12	**323** (R = 4-Cl-Ph)	1	>99	86
13	**324** (R = 4-CF_3-Ph)	1	>99	88

a) Determined by GC analysis; b) determined by HPLC on a chiral stationary phase; c) n.d. = not determined.

To test whether the *ortho*-metalated iridacycle was an active catalyst or the active catalyst was formed thereof, **86** was activated in the presence of **59** in THF to afford **308**, redissolved in CH_2Cl_2 and directly injected as a catalyst into the reaction mixture (Scheme 100).

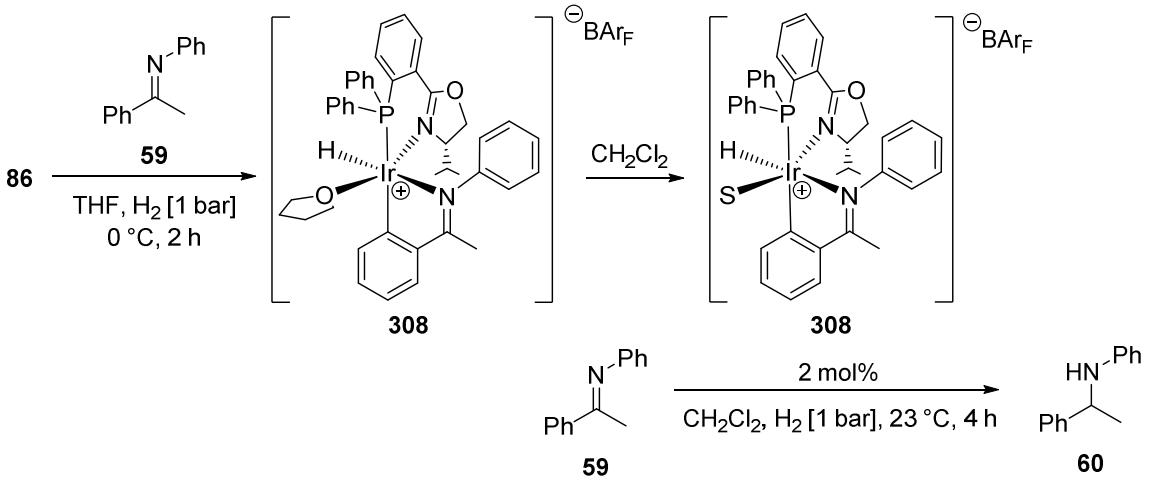

Scheme 100: Asymmetric hydrogenation of imine **59** using iridacycle **308** formed *in situ*

In the hydrogenation of imine **59**, full conversion with only 26% *ee* were obtained. Attempts to isolate and crystallize **308** remained unsuccessful. However, a yellow solid was obtained after elution on silica gel. The isolated complex displayed no BAr_F signals in the ^1H- and ^{19}F-NMR. It still had one hydride ^1H-NMR signal and one $^{31}P\{^1H\}$-NMR signal. The exact nature of complex **325** was not elucidated and the counterion was tentatively assigned as a chloride (Scheme 101).

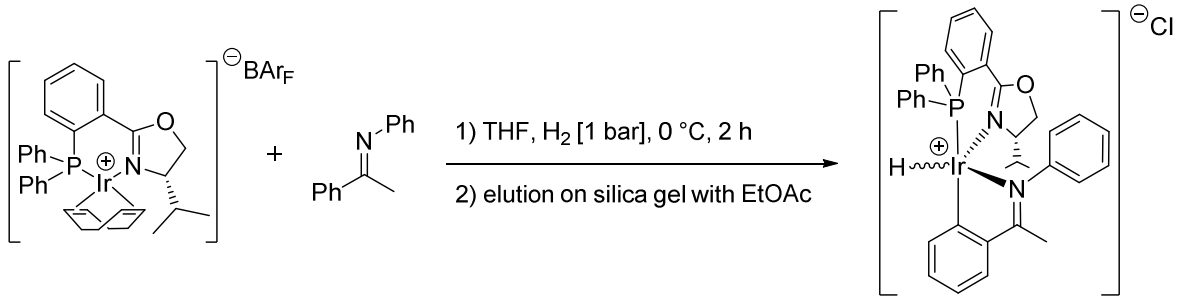

Scheme 101: Preparation and isolation of complex **325**

The catalytic activity of the isolated cyclometalated iridium complex **325** was tested. With 2 mol% of **325** no conversion of imine **59** was observed under hydrogenation conditions. This lack of reactivity can be attributed to the counterion. If the counterion was a chloride, it could as well serve as a ligand within the coordination sphere of the iridium centre and thus prevent coordination of an imine or hydrogen molecule. Therefore abstraction of the chloride with $NaBAr_F$ should result in a free coordination site to render the complex an active catalyst. Indeed, if **325** was mixed with an equimolar amount of $NaBAr_F$ and tested in catalysis, imine reduction proceeded in 80% conversion and 87% *ee* (Scheme 102). Under similar reaction conditions virtually identical enantiomeric excess and similar but lower conversion of 80% were observed when using **86** as the catalyst (>99%, 87% *ee*). This experiment clearly demonstrated that **325** generated an active catalyst upon addition of $NaBAr_F$. Both complex **86** with imine **59** as well as iridacycle **325** formed the same catalytically active species under hydrogenation conditions.

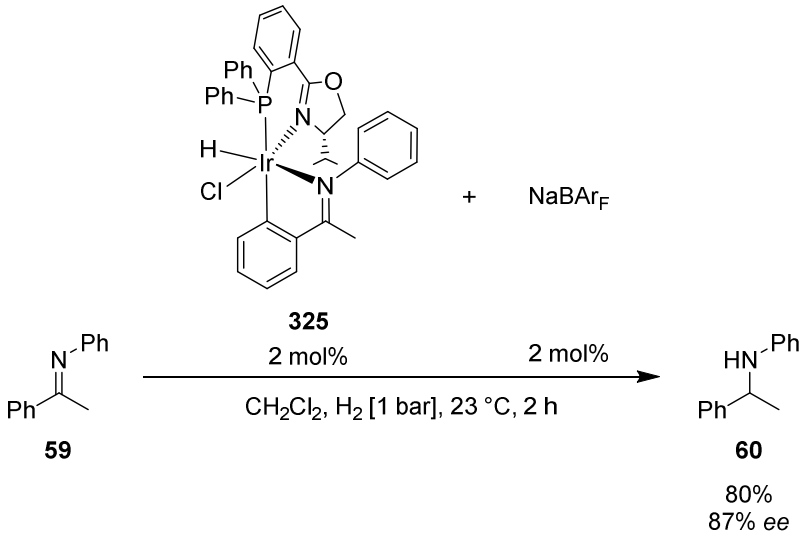

Scheme 102: Asymmetric hydrogenation of imine **59** using iridacycle **325** as a catalyst

Catalytic Deuteration

In the course of attempting to prepare the cyclometalated amine complex with a deuteride, the ^{1}H-NMR spectrum of the amine after the reaction revealed incorporation of deuterium at the *ortho*-position of the aromatic ring (Spectrum 14). The same result was obtained when amine **60** was subjected to deuteration conditions (Scheme 103). This demonstrated the lability and reversibility of amine cyclometalation.

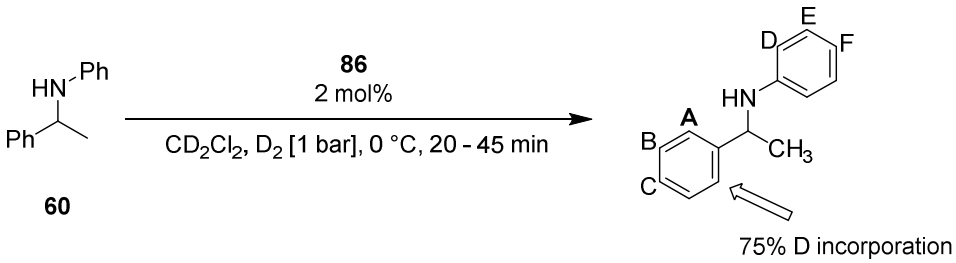

Scheme 103: Reversible cyclometalation of amine **7** and resulting deuterium incorporation at the *ortho*-position **A**

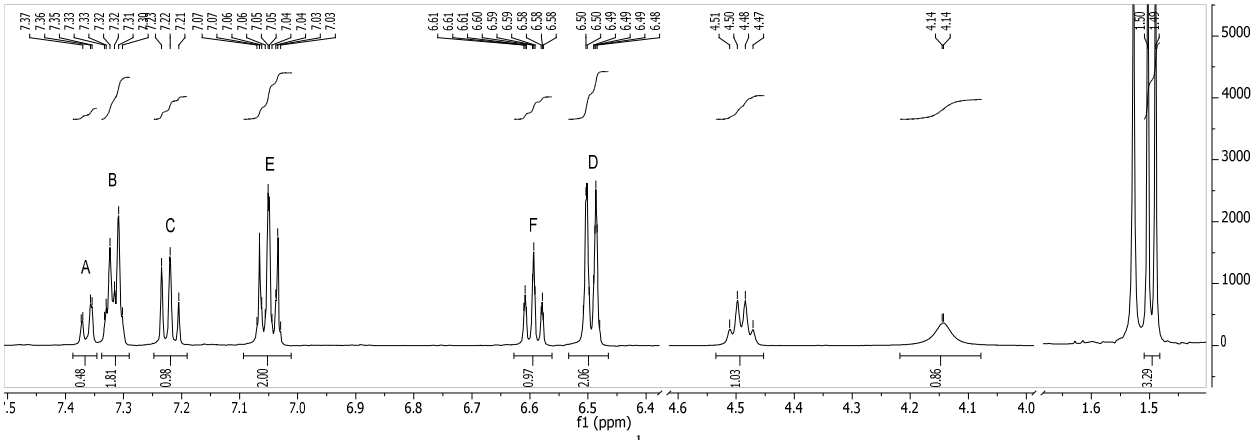

Spectrum 14: Aromatic region of the ^{1}H NMR spectra of deuterated amine **60**.
Signal A has an integral of only 0.5 instead of 2

While both the imine and amine substrate were shown to cyclometalate, it remained unclear whether deuterium incorporation would take place before or after the substrate had been reduced. In order to assess the extent of deuterium incorporation before reduction of the imine substrate, it was subjected to deuteration conditions in THF (Scheme 104). While hydrogenation of imine takes place at room temperature in CH_2Cl_2, the reaction in coordinating solvents like THF is slow. To inhibit reduction of the C=N double bond and solely study reversible cyclometalation of the imine under catalytic deuteration conditions, the imine was reduced with D_2 in THF at low temperature.

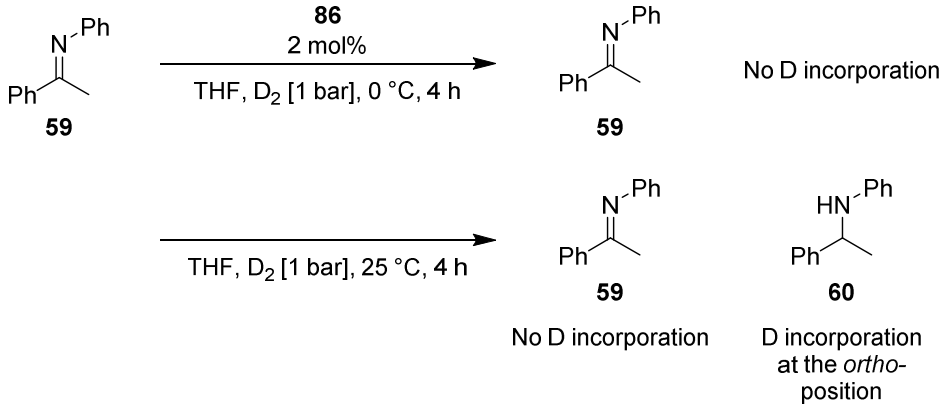

Scheme 104: Incorporation of deuterium in the imine **59** and amine **60**

At 0 °C the imine was recovered and had no deuterium incorporation at any position. While formation of the cyclometalated complex was demonstrated under these conditions, this suggested that upon generation of iridacycle **308**, addition of D_2 and elimination of C–D does not take place under these conditions. Furthermore, after cyclometalation, the resulting iridium catalyst is stable and no reversible cyclometalation of the imine occurs. At 23 °C 35% conversion to the amine **60** was observed after four hours. The imine and amine recovered were analyzed by ^{1}H- and ^{2}D-NMR spectroscopy and deuterium incorporation was only observed at the *ortho*-position of the amine. If the reduction of the imine occurs, it possibly also involves

formation of an aromatic C-D bond when the product amine is released. In other words, the imine is bound to the metal center via the *ortho*-carbon and this bond is broken after the C=N double bond has been reduced. Therefore a cyclometalated species is involved in the catalytic cycle at some stage.

From a simplified mechanistic perspective, one would expect hydrogen to add across the C=N double bond. While incorporation of deuterium into the *ortho*-position of the acetophenone ring can be explained by reversible cyclometalation, deuterium should also be incorporated at the α-position and the nitrogen atom of the product amine (Scheme 105).

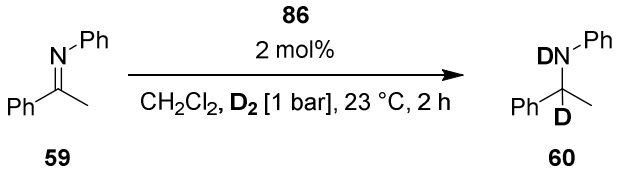

Scheme 105: Catalytic deuteration of imine **59**

In one experiment (batch 1), incorporation of deuterium at the α-position and at the methyl group was observed (Scheme 106) whereas a second experiment (batch 2) showed deuterium at the *ortho*-position as well. No deuterium label was detected at the nitrogen since the acidic *N*-deuterium was exchanged for a proton during workup. Incorporation of deuterium at the methyl group can occur by imine/enamine tautomerism. Moreover, deuterium incorporation in the α-position did only occur to a partial extent. Within the two batches of the identical reaction setup, significant differences in overall deuterium incorporation were observed. To test whether the proton or deuterium scrambling originated from adventitious water or the solvent, all solvents were degassed and distilled over CaH_2. The results were not significantly different between the reactions with crown cap solvent and dried solvents and neither when comparing reactions in CD_2Cl_2 instead of CH_2Cl_2. Therefore, the possible role of solvent or adventitious water as the source of scrambling was discarded.

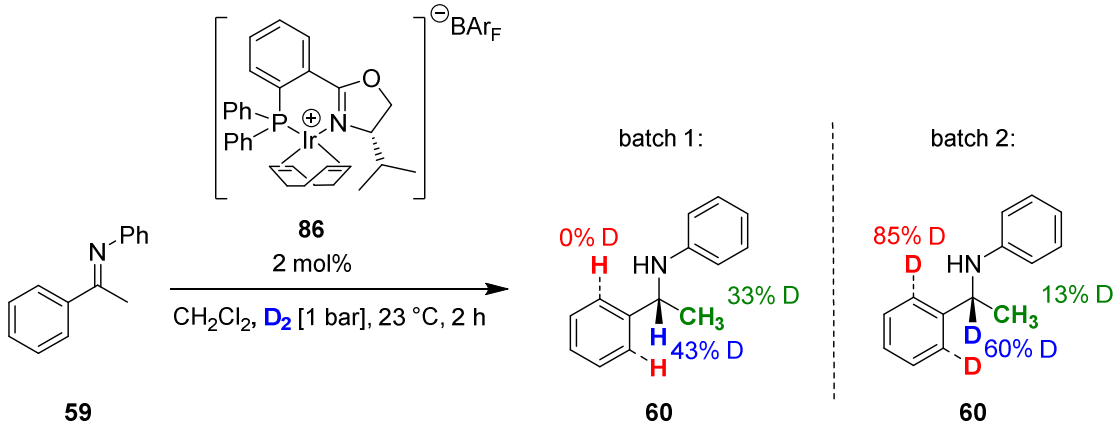

Scheme 106: Catalytic deuteration of unlabelled imine **59** with deuterium gas

To elucidate the origin of the protons in the α-position in the deuteration with D_2, differently ^{2}D-labeled imines of **59** were prepared *via* condensation of d_5- or d_7-aniline and CD_3-, C_6D_5- or d_8-acetophenone (Scheme 107). However, incomplete labelling of the methyl group was observed due to residual water in KO^{t}Bu during preparation of **59**-d_3 and **59**-d_{13}. Therefore, deuterium labelling was enriched *via* imine/enamine tautomerism with d_4-methanol.

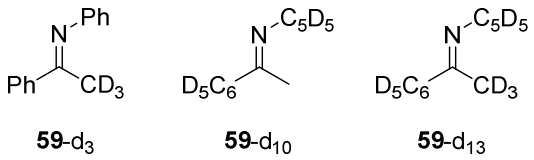

59-d_3 **59**-d_{10} **59**-d_{13}

Scheme 107: Differently labelled imine substrates of **59**

59-d_3 displayed high incorporation of hydrogen or deuterium along the C=N double bond with respect to the gas employed. While in the 1st batch significant incorporation of hydrogen at the methyl position was observed, only low ^{1}H-incorporation at the methyl-position was observed in the 2nd batch. Overall, these observations were in accordance with a mechanism of deuterium being added across the C=N double bond. Minor isomerisation processes as well as reversible post-hydrogenative deuterium incorporation at the *ortho*-position have occurred (Scheme 108).

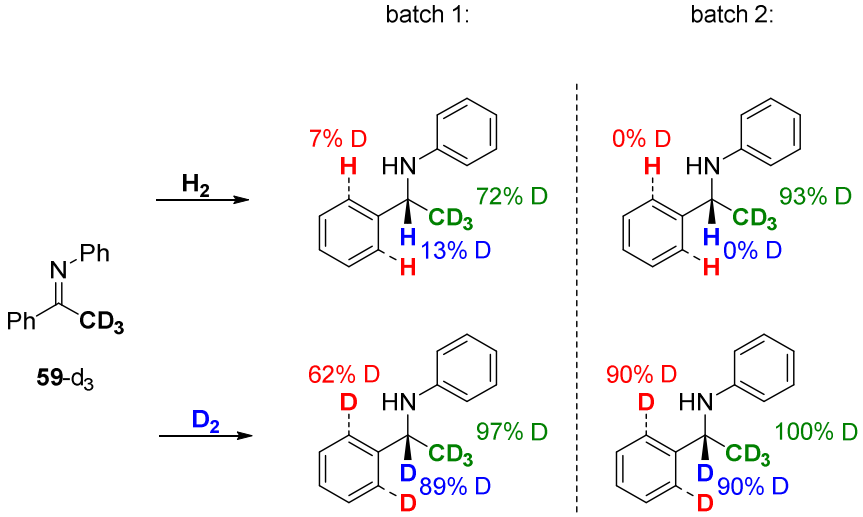

Scheme 108: Catalytic hydrogenation and deuteration of imine **59**-d_3

Imine **59**-d_{10} displayed inconsistent results. While complete hydrogen incorporation at the α-position was retained with hydrogen gas, the origin as well as the inconsistency between the two batches when using deuterium could not be explained. Furthermore, inconsistent incorporation of deuterium at the methyl position within the two batches was observed (Scheme 109).

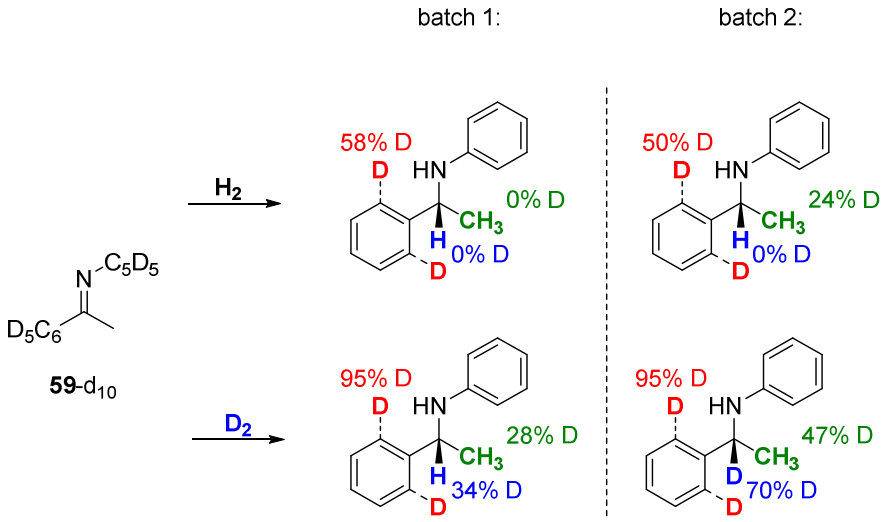

Scheme 109: Catalytic hydrogenation and deuteration of imine **59**-d_{10}

The picture became even more complicated with **59**-d_{13}. Incorporation of hydrogen at three positions under deuterium conditions with a fully deuterated substrate questioned the experimental setup (Scheme 110).

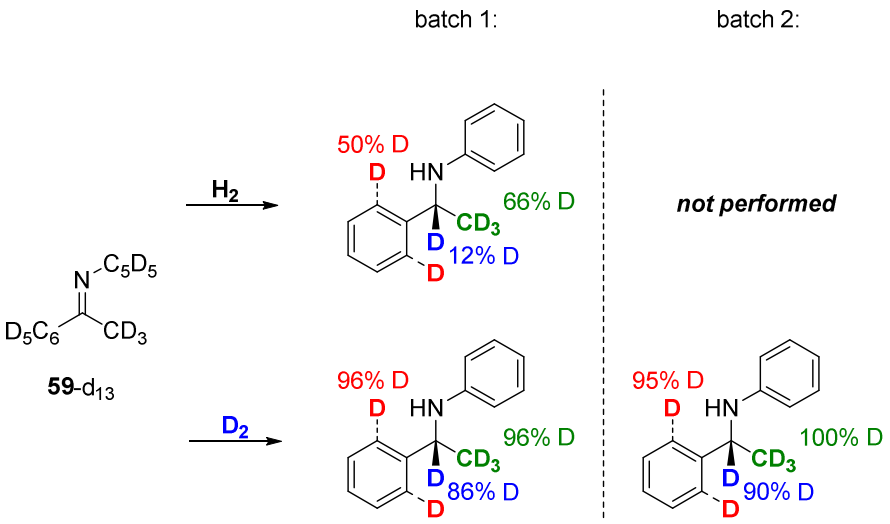

Scheme 110: Catalytic hydrogenation and deuteration of imine **59**-d_{13}

One possible explanation for incorporation of hydrogen at the α-carbon under deuteration conditions is the formation of an Ir–H bond by cyclometalation of the imine. This hydride would be transferred to the α-carbon of the imine substrate. If the hydrogen from the methyl group ends up at the α-carbon, a tautomerization process via imine/enamine interconversion occurs during catalysis which in turn can result in exchange between the methyl protons and the Ir-hydrides due to their acidity.

The deuterium labelling experiments gave rise to the speculation that an imine/enamine tautomerisation under hydrogenation conditions could be part of the catalytic cycle (Scheme 111). Such an imine/enamine tautomerisation could be catalysed by Brønsted acidic hydrides or the reduced amines.

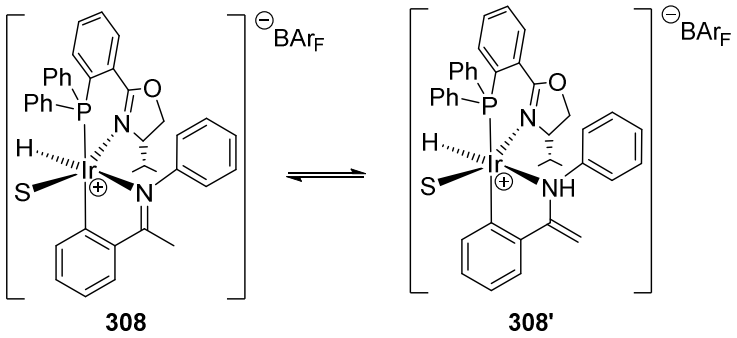

Scheme 111: Possible imine-enamine tautomerisation of imine **59** upon cyclometalation before undergoing hydrogenation

Therefore, substrates preventing imine/enamine tautomerism such as **326** and **327** were tested to assess whether or not the methyl group was the source of protons that incorporate at the α-carbon during deuteration. If the substrate does not undergo reduction when tautomerization is prevented, an alternate mechanism could be proposed, i.e. reduction of the C=C bond in the enamine tautomer.
Imine **326** was not reduced at 1 bar or even at 50 bar of H_2 pressure (Table 5). This result could be due to the change in electronic properties of the substrate or because tautomerization in this substrate is prevented. Imine **326** with a *tert*-butyl group could not be hydrogenated at 1 or 50 bar pressure. The experiment was not suitable to rule out an enamine mechanism. It was not possible to assess if the lack of reactivity is due to the increased steric hindrance or because the substrate cannot undergo tautomerization.

Table 5: Reduction of imines **326** and **327**

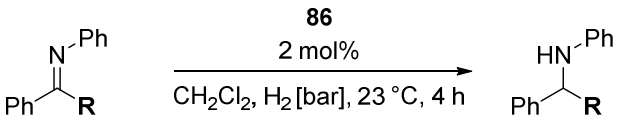

Entry	Imine	*p* [bar]	Conv. [%][a]	*ee* [%][b]
1	**326** (R = CF_3)	1	0	-
		50	<1	-
2	**327** (R = ^{t}Bu)	1	0	-
		50	0	-

a) Determined by GC analysis; b) determined by HPLC on a chiral stationary phase.

React-IR Studies

The catalytic hydrogenation of imine **59** was monitored by *in situ* infrared spectroscopy. The reactions were setup in a three neck flask with a H_2 inlet adaptor, pressure gauge and IR probe. The reaction was performed on a 0.5 mmol scale of imine **59** in 4 mL of CH_2Cl_2 with 2% catalyst and different hydrogen pressures. The substrate solution under H_2 atmosphere was equilibrated and the catalyst was added by syringe. The change in the concentration of imine and amine were monitored acquiring a spectrum every 2 min.
Initial experiments displayed a linear behavior, suggesting a zero order dependence of the reaction on the concentration of substrate. Alternatively the limited solubility of hydrogen gas could explain the observed linear behaviour. Therefore reaction conditions, under which hydrogenation is slower than hydrogen gas diffusion into the solution were investigated. While conducting the reaction at –78 °C failed due to insolubility of the imine, hydrogen pressure could only be varied between 1 and 2 bar. Lowering the catalyst loading from 3 mol% to 1 mol% depicted an exponential decay of the imine as well as an exponential growth of the amine concentration when monitored by React-IR. The different behaviour is depicted in Figure 17 comparing three different catalyst loadings.

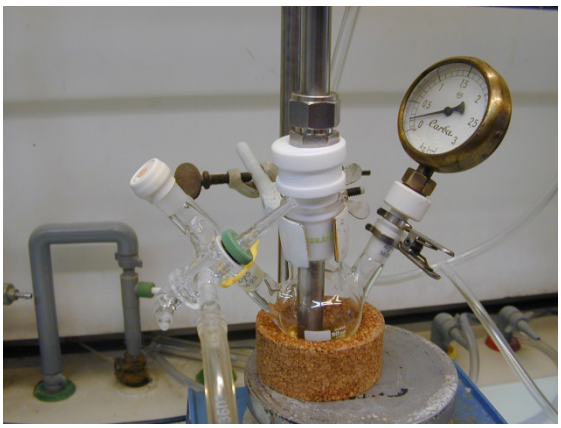

Figure 16: General setup of monitoring the reaction by ReactIR

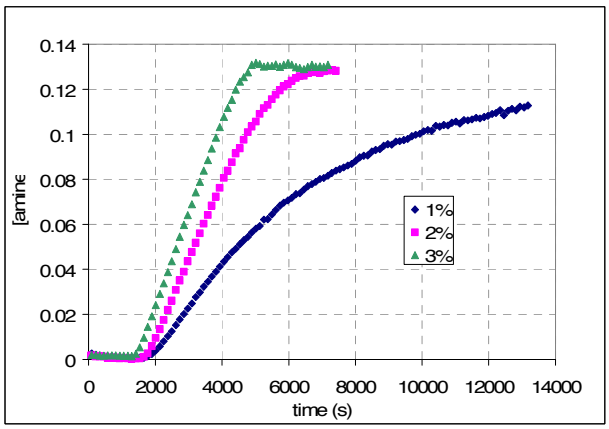

Figure 17: Profile of amine formation at different catalyst loadings.

Sufficiently different rates were observed with hydrogen gas pressure between 1.2 and 1.8 bar. A linear trend was observed, but rates were too low to determine the reaction order since the reaction could only be followed at low pressures.

Asymmetric Hydrogenation of Dialkyl Imines

Since cyclometalation was demonstrated to be a key element in the catalytic cycle, the low reactivity of aliphatic imines such as **328**, **329**, **330** and **331** could be explained by their inability to form the active catalyst for imine hydrogenation. Speculatively, iridacycle **308** formed under hydrogenation conditions could be a superior catalyst compared to **86**. Indeed, addition of **59** to generate complex **308** *in situ* resulted in higher conversion both at atmospheric as well as 50 bar hydrogen pressure (entries 5 vs. 6; 7 vs. 8; 9 vs. 10). Entries 11 and 12 also show a change in the enantioselectivity. No experiments have been conducted with the isolated complex **308**.

Table 6: Asymmetric hydrogenation of dialkyl imines **328** to **331**

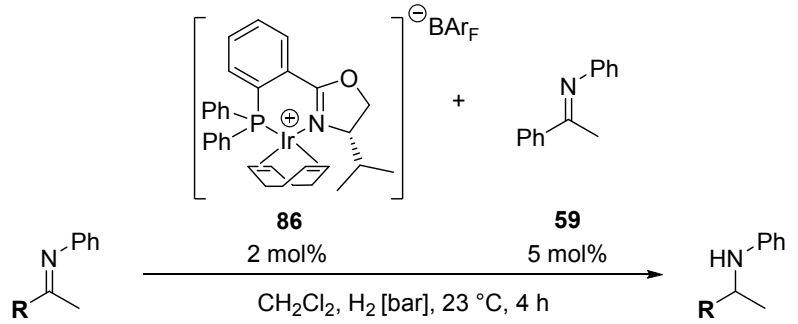

Entry	Imine	Additive	H_2 [bar]	Conv. [%][a]	*ee* [%][b]
1	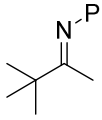	-	1	0	-
2	**328**	**2**	1	0	-
3	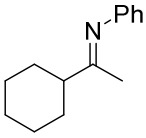	-	1	n.d.[c]	69
4	**329**	**2**	1	n.d.[c]	71
5	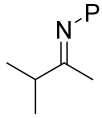	-	1	0	-
6		**2**	1	10	-
7		-	50	25	-
8	**330**	**2**	50	>99	60
9	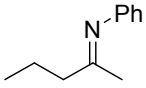	-	1	0	-
10		**2**	1	70	-
11		-	50	>99	31
12	**331**	**2**	50	>99	23

a) Determined by GC analysis; b) determined by HPLC on a chiral stationary phase; c) n.d. = not determined.

Chemoselective hydrogenation was observed when attempting to hydrogenate trisubstituted olefin **332** in the presence of imine **59**. While hydrogenation of **332** readily occurs within two hours at atmospheric hydrogen pressure, complete inhibition of olefin reduction was observed upon addition of imine **59** (Scheme 112).

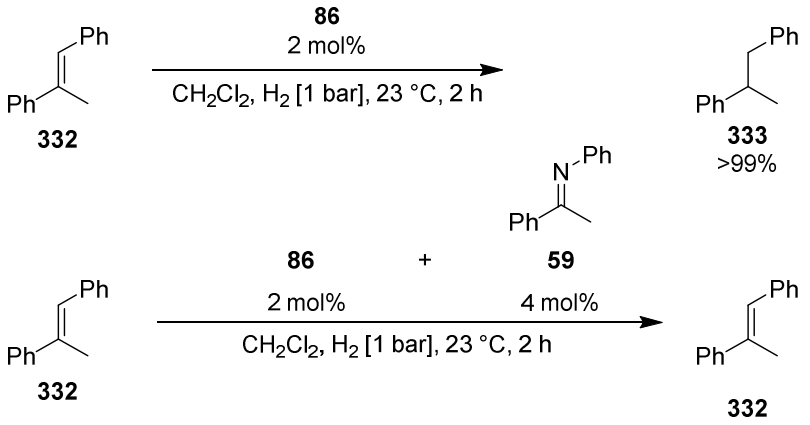

Scheme 112: Inhibition of olefin hydrogenation by catalyst **86** in the presence of imine **59**

Complete reduction of imine **59** to amine **60** was observed in stoichiometric presence of olefin **332** (Scheme 113). Similar to the 2nd experiment in Scheme 112, iridacycle **308** was formed *in situ* and appeared to be favoured over formation of other iridium complexes under hydrogenation conditions as well as olefin reduction. Addition of **60** resulted in generation of an iridium species which was not able to hydrogenate olefin **332** either.

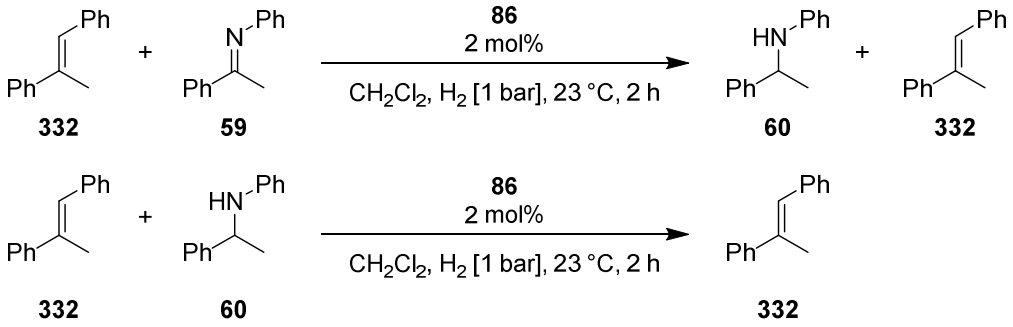

Scheme 113: Hydrogenation of olefin **332** inhibited both by imine **59** and amine **60**

Summary / Conclusions

C-H activation is not a side reaction that occurs under catalytic hydrogenation conditions. The formation of a cyclometalated complex seems to occur prior to hydrogenation. This is supported by the irreversibility of the cyclometalation of the imine. The cyclometalated complex represents a catalytically active species under hydrogenation conditions. The cyclometalated amine can be formed in CH_2Cl_2 under hydrogenation conditions.

The cyclometalated complex is therefore believed to be a key intermediate in the course of the reaction, possibly resembling the active complex to a very close extent. This is disclosed by the inability of the cyclometalated complex to undergo exchange of the coordinated imine.

Furthermore, activation of the Ir-PHOX complex **86** with H_2 was shown to result in complete conversion to unsaturated dihydride intermediates which are stable at low temperature in THF (^{1}H- and ^{31}P{^{1}H}-NMR). These dihydride complexes are very reactive and cyclometalate imines at –78 °C within a few minutes. The identity of the cyclometalated complex was established by ESI-MS analysis, NMR studies and a X-Ray crystal structure of the related PF_6 complex **313**.

The cyclometalated complex **325** was used as a precatalyst and turned into an active species that catalysed imine hydrogenation upon addition of an equimolar amount of $NaBAr_F$. Similar conversion and virtually identical *ee* of the product amine **60** were observed compared to the reaction performed with complex **86**.

Addition of a catalytic amount of imine **59** to complex **86** resulted in the generation of iridacycle **325** *in situ*. It also improved the conversion of aliphatic imine **328** to **331**. Furthermore, it altered the enantiomeric excess in one example. It also inhibited the reduction of trisubstituted olefin **332**.

Chapter 3 – Mechanistic Investigations

Imines as possible *in situ* additives for improved aliphatic imine hydrogenation

F. Barrios had demonstrated that using iridium PHOX complex **86** in combination with imine **59** afforded higher yields in the asymmetric hydrogenation of aliphatic imines. This was explained by the *in situ* formation of iridacycle **325** which was postulated to be the active catalyst in solution (Figure 18).

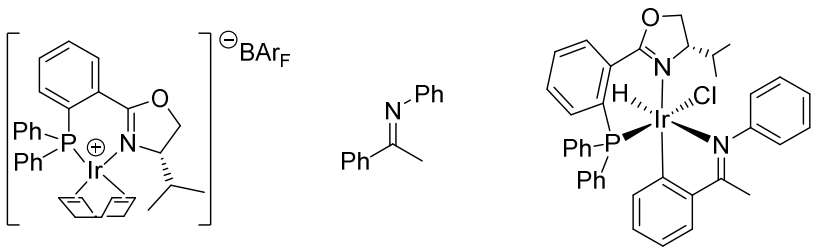

86 **59** **Δ-325**

Figure 18: Complexes **86** and **325** and imine **59**

To verify these previous findings, hydrogenations with the combinations of complex **86** with imine **59** as well as iridacycle **325** with $NaBAr_F$ were tested as shown in Table 7. Since virtually identical enantiomeric excesses as well as similar conversion were obtained, it indicated that a common intermediate must be present in both reaction setups. The omittance of either $NaBAr_F$ when using **325** or imine **59** when using **86** resulted in significantly reduced conversions. Furthermore, different enantiomeric excesses were obtained. This confirmed the hypothesis that only a cationic iridacycle derived from neutral iridacycle **325** is an efficient catalyst for hydrogenation of aliphatic imines **329** to **331**.

Table 7: Asymmetric hydrogenation of *N*-Phenyl aliphatic imines with either iridacycle **325** or generation of **325** *in situ*

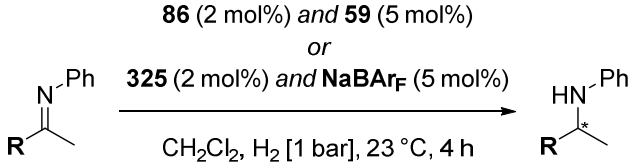

Entry	Catalyst	Imine	Conv. [%][a]	*ee* [%][b]
1	**86** and **59**	**329** (R = Cy)	13	71 (*R*)
2	**86** and **59**	**330** (R = *i*Pr)	8	60 (*R*)
3	**86** and **59**	**331** (R = *n*-Bu)	10	20 (-)
4	**325** and **NaBAr$_F$**	**329** (R = Cy)	20	71 (*R*)
5	**325** and **NaBAr$_F$**	**330** (R = *i*Pr)	11	60 (*R*)
6	**325** and **NaBAr$_F$**	**331** (R = *n*-Bu)	10	21 (-)

a) Determined by GC analysis. b) determined by HPLC analysis on a chiral stationary phase.

The stability of the *in situ* formed iridacycle was demonstrated in cross-over experiments when reducing imine **322** with iridacycle **325** (Scheme 114). By GC analysis, neither imine **59** nor amine **60** could be detected even in trace amounts in the course of the reaction. These results are consistent with the hypothesis that cyclometalation is irreversible and the imine remains bound to iridium throughout the catalytic reaction. The enantiomeric excess of **333** remained constant throughout the reaction as verified by aliquot HPLC analysis.

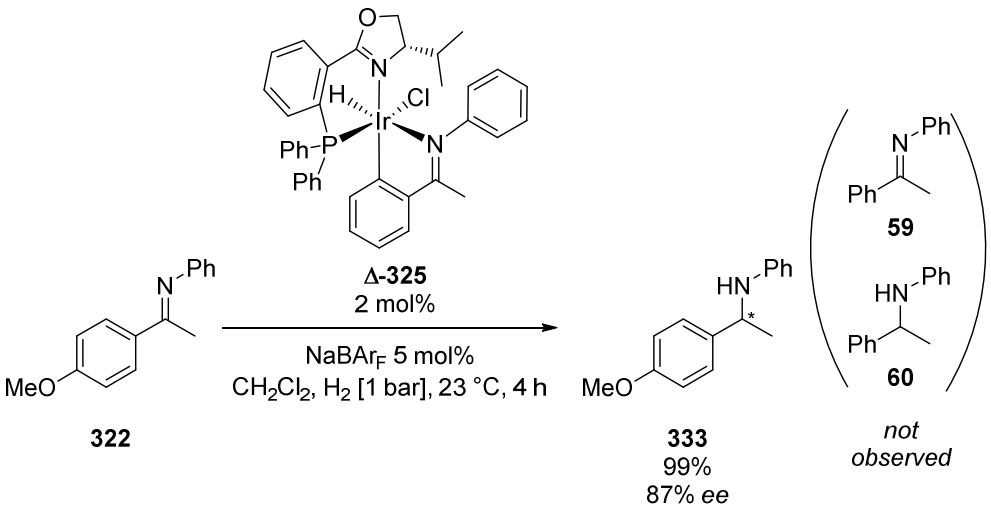

Scheme 114: Asymmetric hydrogenation of imine **322** with iridacycle **325** without observation of imine **59** or amine **60**

To verify that the product amine would not affect any enantiodiscrimination, control experiments using enantiopure amine **60** as an additive in the hydrogenation of imine **334** were conducted (Scheme 115). While full conversion was observed when adding imine **59**[8], racemic amine **335** was obtained in low conversion with enantiopure amine **60**.

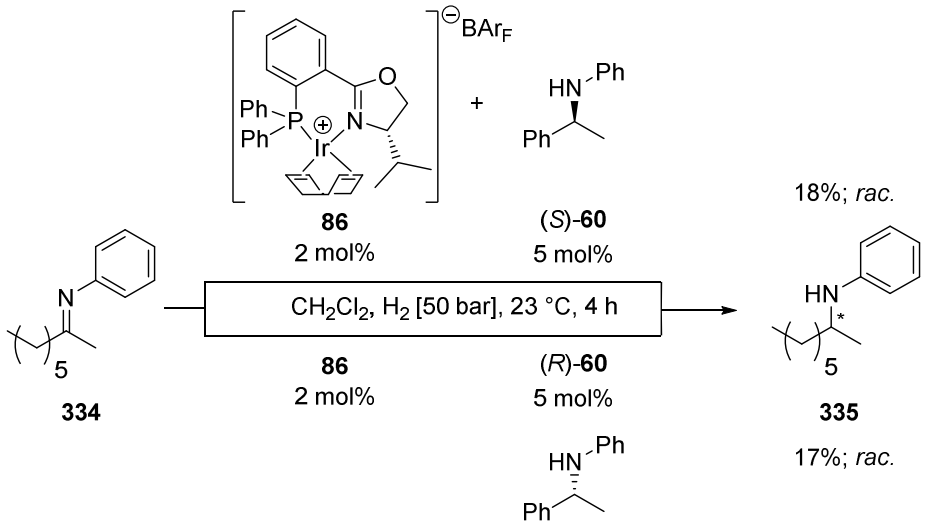

Scheme 115: Investigation of the influence of chiral amine **60** on aliphatic imine **334**

The same results were observed with achiral complex **336** and enantiopure amine **60** (Scheme 116). Therefore, it was concluded that the chiral amine **60** produced in the hydrogenation of **59** (and thus present in solution) does not cyclometalate onto the iridium centre in the presence of imine and form an active catalyst. Reversible cyclometalation of amine **60** has been observed, however with a strong favour of the amine being replaced by an imine.[9]

[8] See chapter 5
[9] See chapter 2

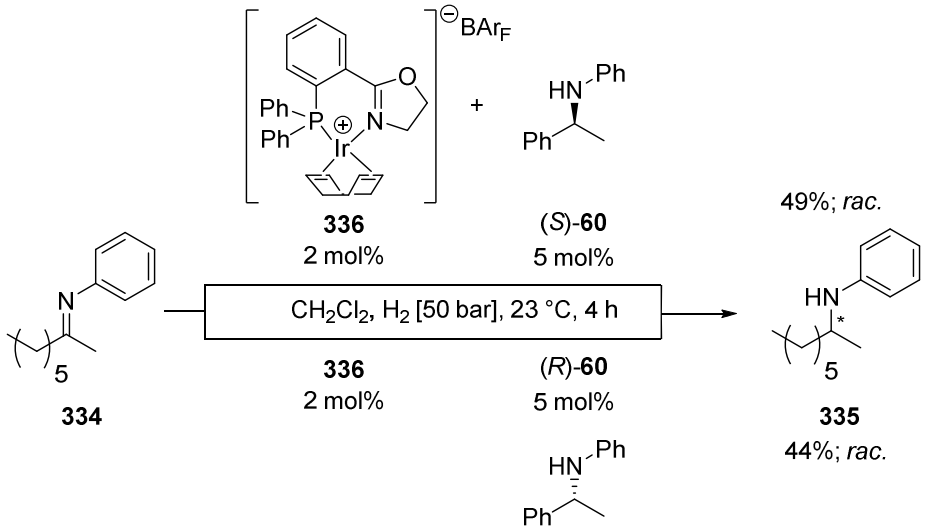

Scheme 116: Investigation of the influence of enantiopure amine **60** with achiral catalyst **336**

F. Barrios had conducted comparison experiments between complex **86** and iridacycle **325** on the hydrogenation of imine **59.** The discrepancy between the conversions of 99% and 80% when comparing complex **86** and **325** with NaBAr$_F$ could not be explained (Scheme 117). However, no detailed kinetic investigations have been conducted.

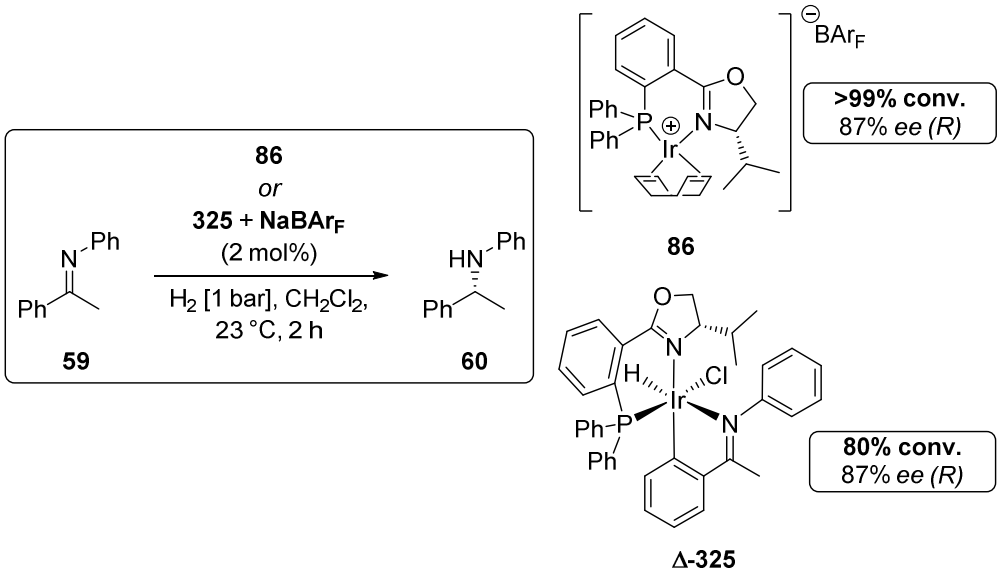

Scheme 117: Comparison of complexes **86** and **325** for the asymmetric hydrogenation of imine **59**

To test whether residual chloride in solution would coordinate to the metal centre and thus reduce its reactivity, lithium chloride was added to the hydrogenation (Scheme 118). The amount of LiCl was varied from 0, 20, **364** up to 100 mol% and aliquots were collected during the reaction. In all cases the reaction proceeded with similar rate irrespective of the amount of LiCl added. This could be explained by limited solubility of LiCl in CH_2Cl_2. A more pronounced effect could possibly be observed with a soluble chloride source, such as tetrabutyl ammonium chloride, but this experiment has not been conducted.

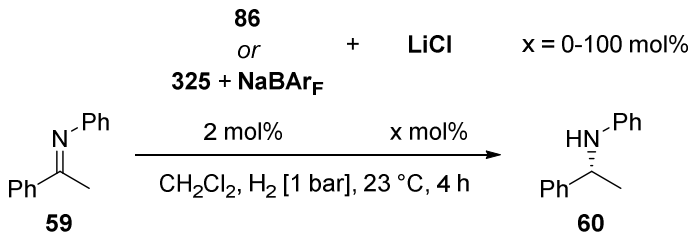

Scheme 118: Testing the possible effect of residual chloride in solution

In order to exclude aniline, a byproduct resulting from hydrolysis, affecting the conversion of the hydrogenation, varying amounts of aniline from 0, 5, 10 up to 20 mol% were added to the reaction to test for competitive coordination to the catalyst (Scheme 119). In all reactions, full conversion with identical *ee* of 40% was observed. Therefore, the presence of aniline in the reaction mixture had no influence on either the reactivity or selectivity of the iridacycle catalyst **337**.

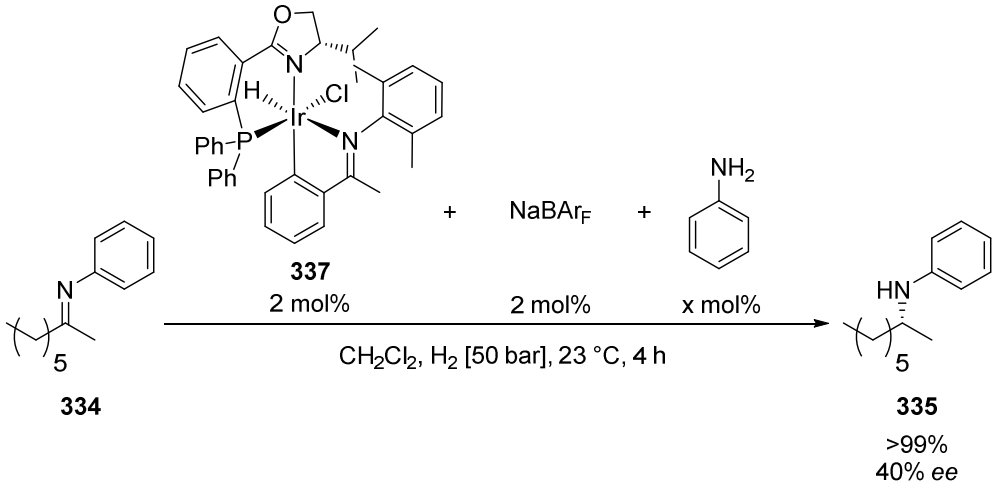

Scheme 119: Testing the possible effect of aniline in solution

Since the active catalyst was generated *in situ* from complex **86** and imine **59** in the studies presented above, an approach for a general ligand screening was targeted. Therefore, the catalyst was generated *in situ* from $[Ir(COD)_2]BAr_F$ (**109**), PHOX ligand **338** and imine **59** and tested in the asymmetric hydrogenation of imine **329** (Scheme 120). Both conversion and enantioselectivity were identical to a reaction employing complex **86** and imine **59.**

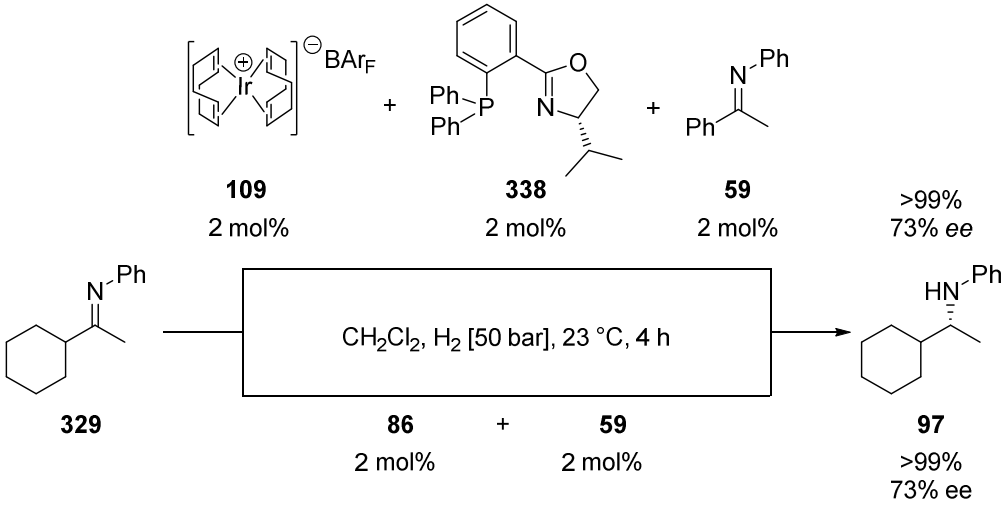

Scheme 120: Comparison of generating iridacycle **325** *in situ* from either **109** and **338**, or **86**

Unfortunately, when applying imine **340**[10], identical conversion but significantly lower *ee* were obtained compared to using **86** with **340** (Scheme 121). Possibly the larger steric bulk from imine **340** did affect iridacycle formation under these conditions. No further optimisation studies were conducted.

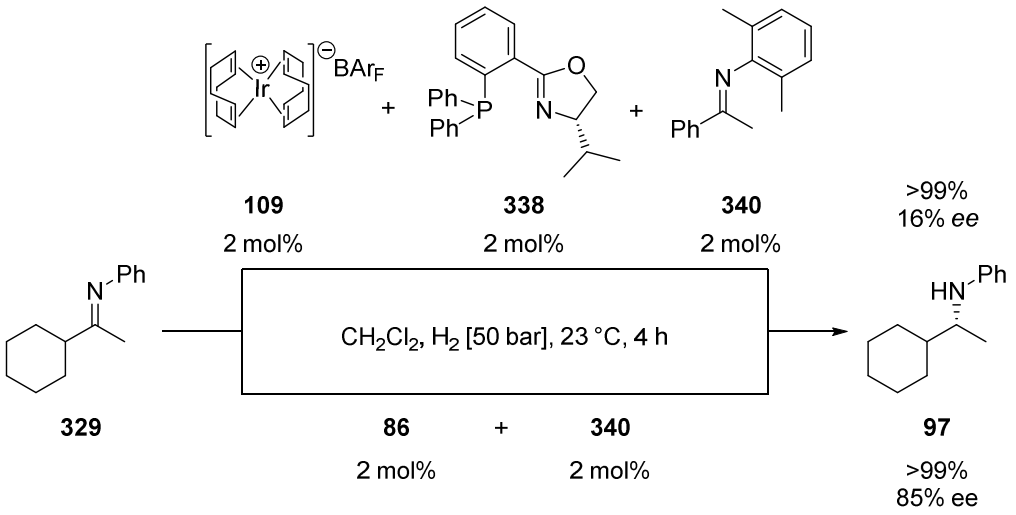

Scheme 121: Comparison of generating iridacycle **337** *in situ* from either **109** and **338**, or **86** with bulky imine **340**

Cyclometalation of different imines

The mechanistic investigations of *F. Barrios* concluded that cyclometalated Ir(III) complexes such as **308** represent catalytically active structures in solution for the hydrogenation of imines (Scheme 122). Since dissociation of the imine **59** was not observed in the course of the reaction by ESI-MS experiments, the catalyst was assumed to be stable and bear imine **59** cyclometalated throughout the reaction at the iridium centre. This would indicate that the cyclometalated imine **59** is also involved in the enantiodiscriminating step.

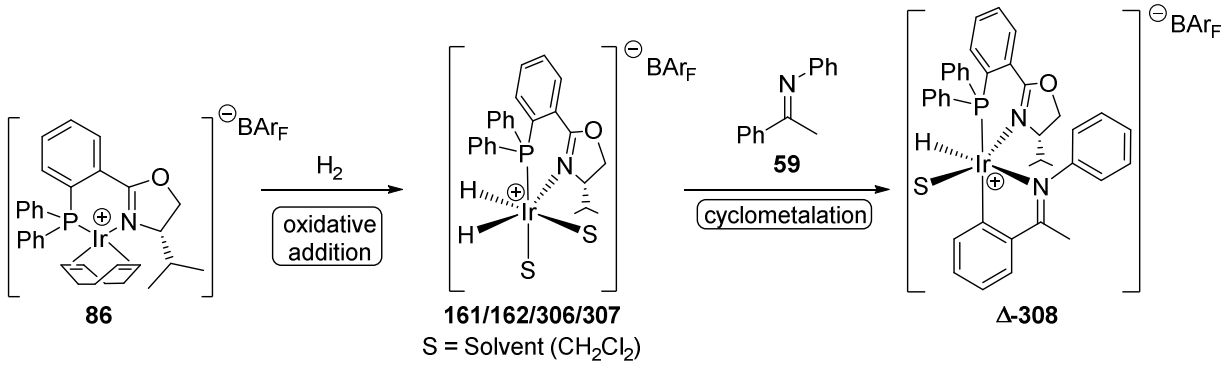

Scheme 122: Activation of complex **86** to iridacycle **308** by cyclometalation of imine **59**

This is highlighted in Scheme 123 where the aliphatic imine is approaching the iridacycle. Upon coordination to the metal centre in structure **341**, the hydride is transferred to the prochiral iminoyl carbon atom, and the electrons from the C=N double bond coordinate the amide to the iridium centre to provide the amide complex **342**. The oxidation state of iridium is not changed overall and the vacant coordination site is occupied by a solvent molecule.

[10] See chapter 5

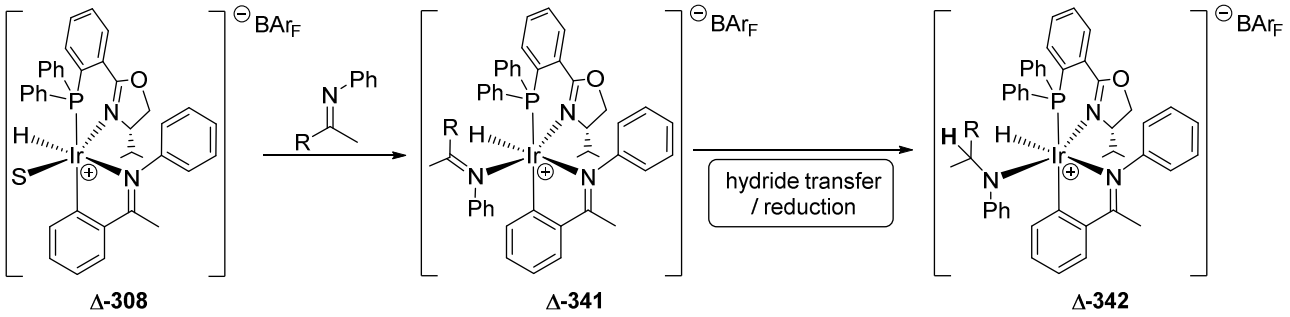

Scheme 123: Hydride transfer to aliphatic imine on iridacycle **308**

In order to verify the participation of the imine in the enantiodiscriminating step, an iridacycle such as **344** with an achiral PHOX ligand and a chiral imine such as **343** should generate a chiral catalyst for asymmetric imine hydrogenation. If the imine remains cyclometalated during the catalytic reaction, asymmetric induction on imine **59** from the chiral imine **343** should be observed in the enantioenriched amine product **60** (Scheme 124).

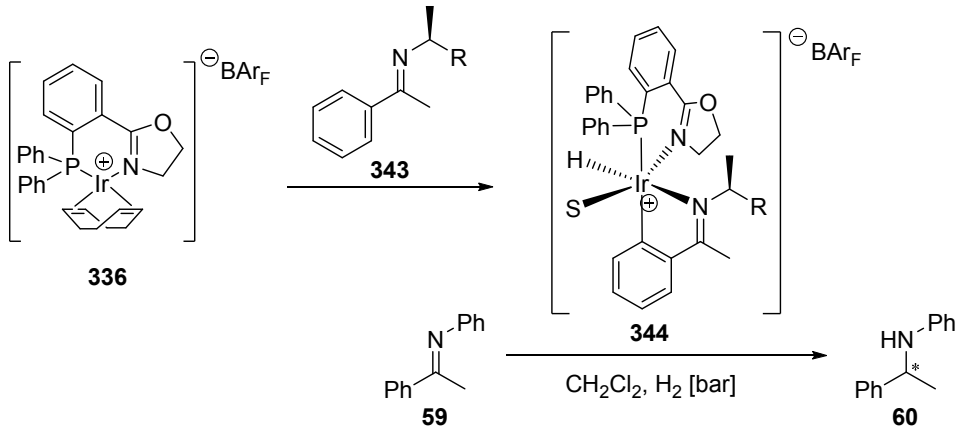

Scheme 124: Asymmetric hydrogenation with iridacycle **344** bearing a chiral imine

To investigate this, chiral imine **346** was prepared by condensation of acetophenone (**117**) and 1-naphtylethylamine (**345**) (Scheme 125). The corresponding chiral imines had been shown to induce high diastereoselectivity, *e.g.* in asymmetric addition of alkyl lithium reagents[90] or asymmetric addition to aldehydes.[91]

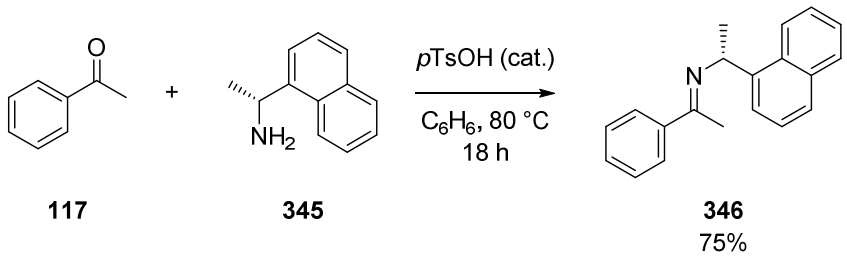

Scheme 125: Preparation of chiral imine **346**

Prior to cyclometalation, they were tested in hydrogenation. No amine product **347** was observed (Scheme 126). Nevertheless, the reaction mixture underwent a colour change from red to yellow. This is accounted by the activation of the iridium PHOX complex undergoing cyclooctadiene hydrogenation, thus generating di-hydride intermediates (Scheme 122).

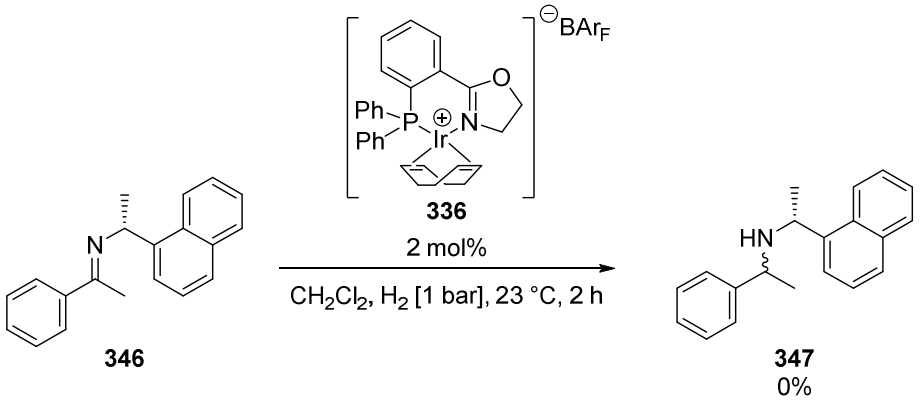

Scheme 126: Hydrogenation of imine **346** using **336**

When the catalyst was changed from **336** to a complex with a sterically more demanding ligand such as **348** or **312** and hydrogenations were conducted at higher pressure, full conversion to the amine was observed (Scheme 127).

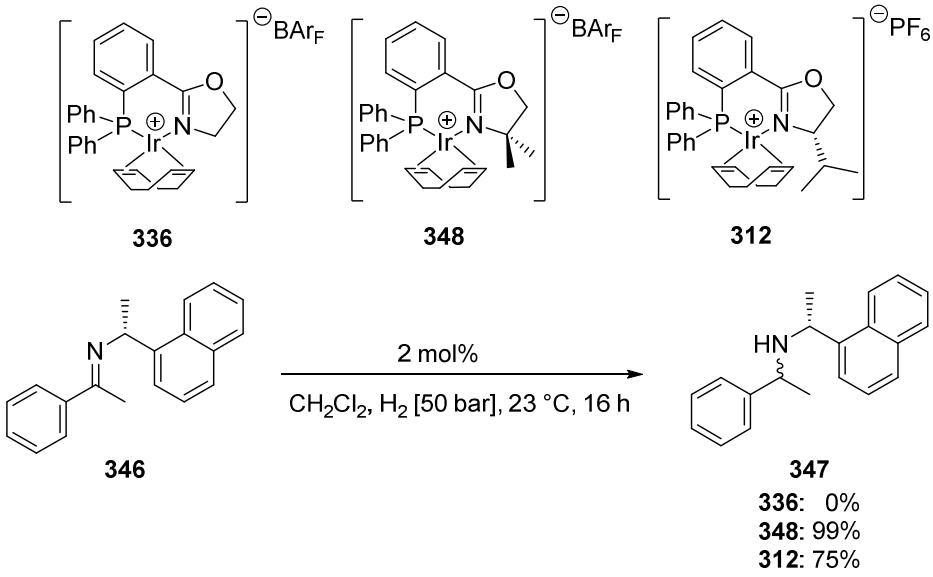

Scheme 127: Hydrogenation of imine **346** using **12**, **348** and **312** at elevated hydrogen pressure

Only complexes **348** and **312** with substituents in the oxazoline ring showed high conversion. Therefore, cyclometalation was conducted with these complexes. Two observations were made: Instead of one single hydride ^{1}H-NMR and one ^{31}P-NMR signal more than 5 hydride signals were observed. Additionally, the expected colour change from red to yellow, caused by iridium oxidation, was not observed to a sufficient extent. The reaction mixtures remained red or dark orange. This indicated that either activation of the complex **312** or cyclometalation of **346** did not occur.

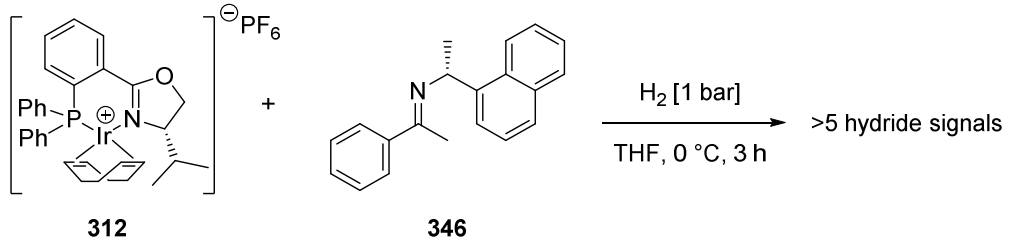

Scheme 128: Attempted iridacycle generation from **312** and **346**

Analysis of the reaction mixture showed that activation of the complex **312** had occurred but no iridacycle formation ensued. Instead, formation of the trinuclear complex **350** was observed (Scheme 129). This

structure had earlier been identified as a degradation product of complex **349** and was shown to be catalytically inactive.[92]

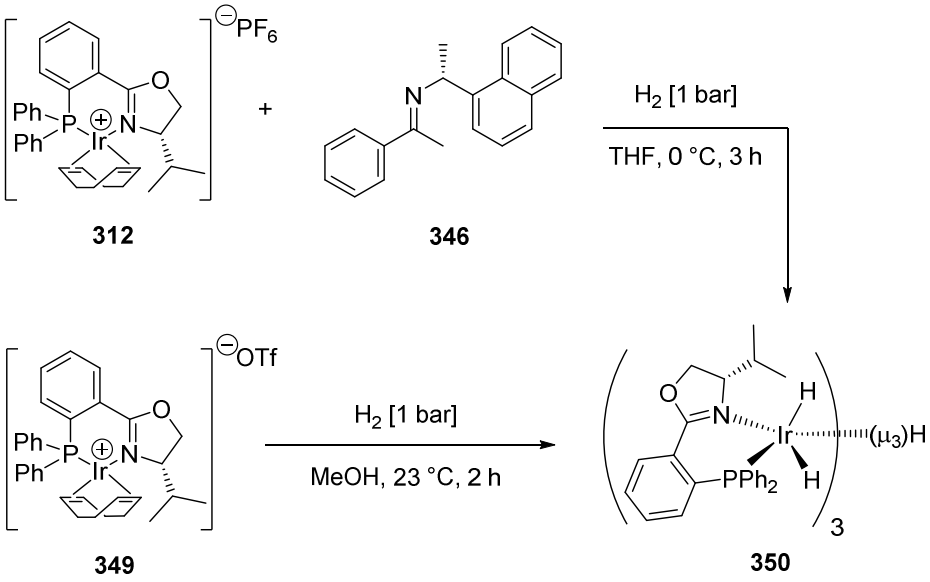

Scheme 129: Deactivation product **350** observed in attempted cyclometalation of **346** to **312**

Therefore, the reaction was conducted in a step-wise manner with the sterically less-demanding complex **336**. Activation with hydrogen gas depicted the expected hydride signals for the different iridium species in solution at low temperature, cyclooctadiene-bound complex **160** and di-hydride disolvent complexes **306** and **307** (Scheme 130 and Spectrum 15). The origin of the broad signals was not investigated further and these signals were not assigned.

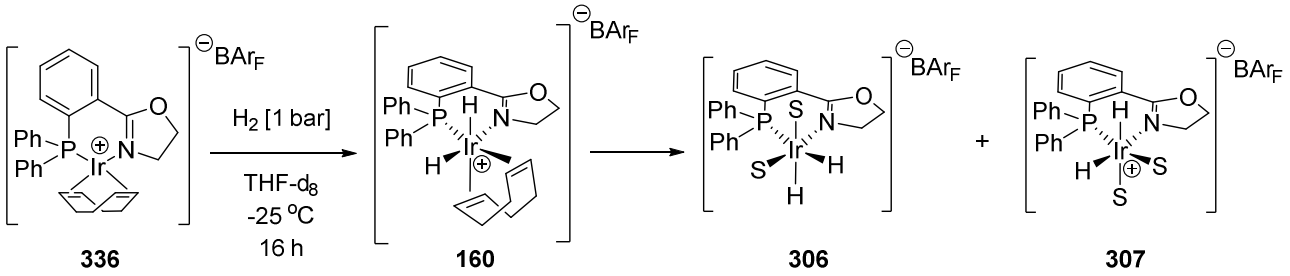

Scheme 130: Activation of complex **336** to dihydride species **160**, **306** and **307**

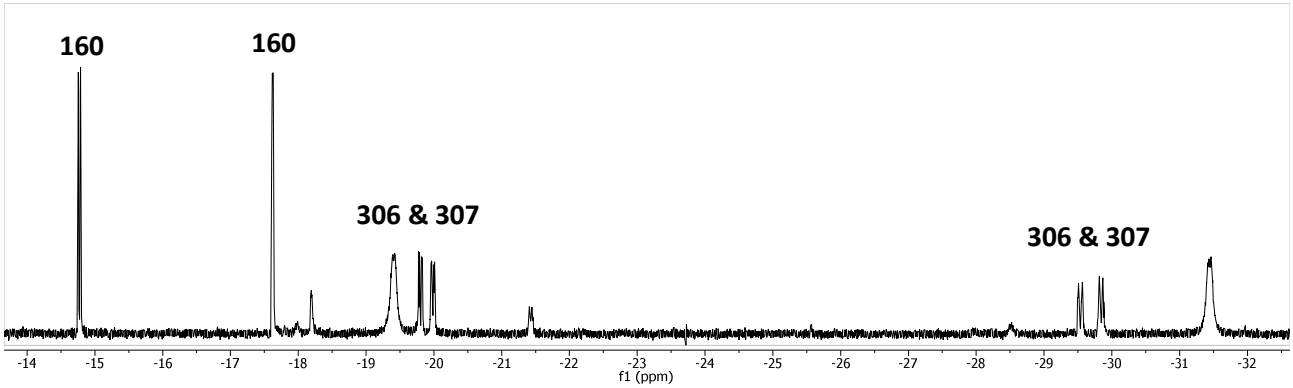

Spectrum 15: Hydride region in ^{1}H-NMR in the activation of **12**

Upon addition of imine **346,** two new peaks were observed which were assigned to configurational isomers of the newly formed iridacycle. While clear spectra could be obtained at -13 °C (Spectrum 16), warming the sample to room temperature resulted in the formation of other species and a plethora of hydride signals was observed (Spectrum 17).

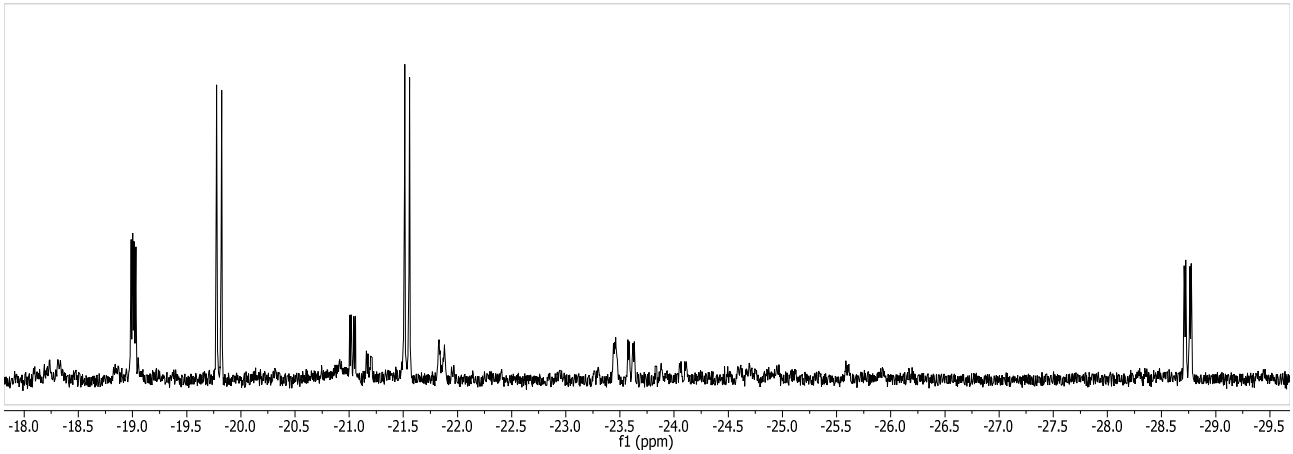

Spectrum 16: Hydride region in ^{1}H-NMR in the activation of **336** upon addition of imine **346**

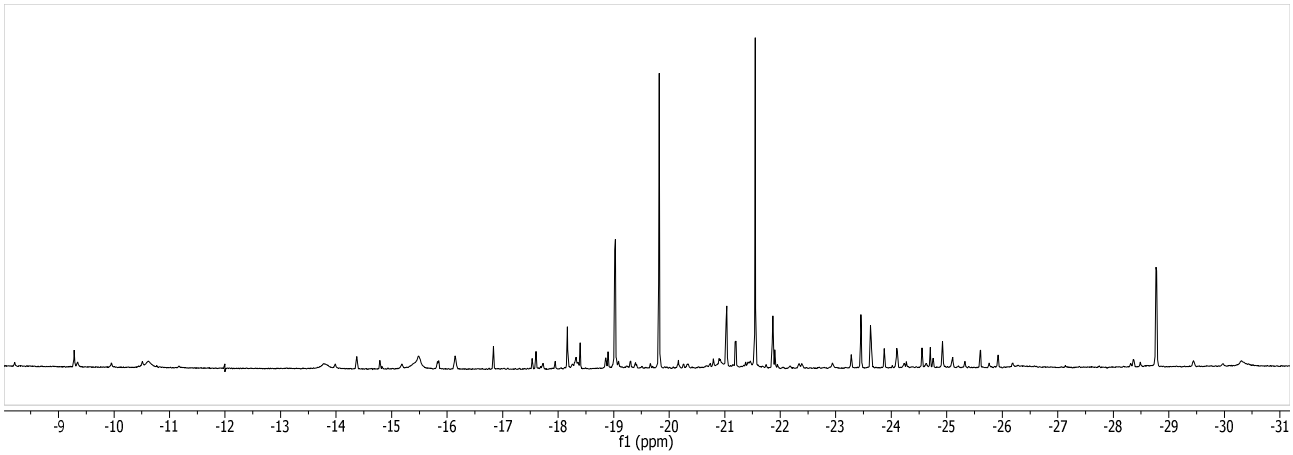

Spectrum 17: Hydride region as in Spectrum 16 upon warming to room temperature

To facilitate cyclometalation, the size of the cyclometalating imine was reduced. Preparation of aldimine **352** proceeded with 87% yield. The corresponding ketimine **353** was prepared in 29% yield (Scheme 131).

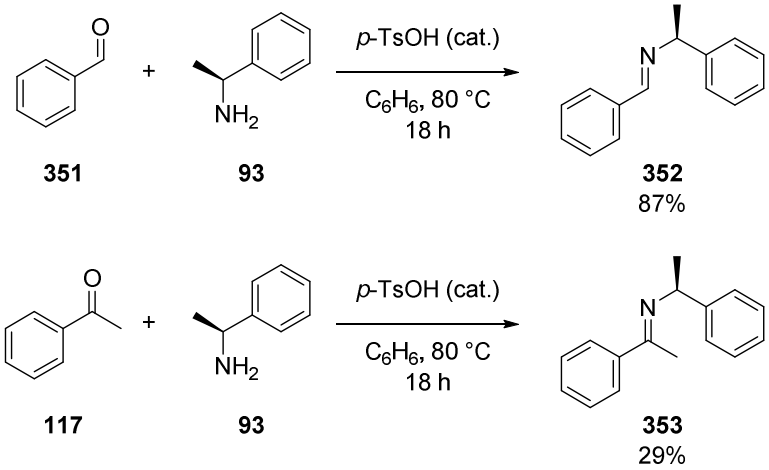

Scheme 131: Preparation of chiral imines **352** and **353**

Aldimine **352** was subjected to cyclometalation with iridium PHOX complex **336** (Scheme 132). The crude reaction mixture displayed two overlapped hydride signals and two ^{31}P-NMR signals along with smaller ones (Spectrum 18 and Spectrum 19). These were assigned to the configurational isomers of complexes **354** and **355**.

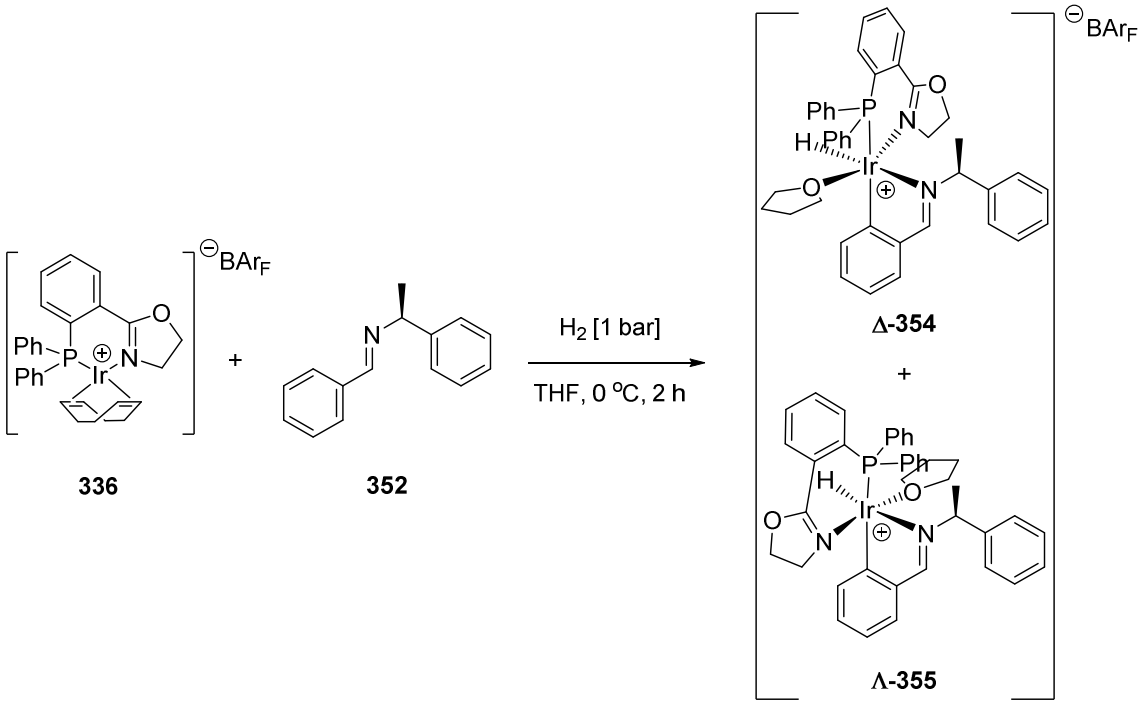

336 352

Scheme 132: Generation of configurational isomers **354** and **355**

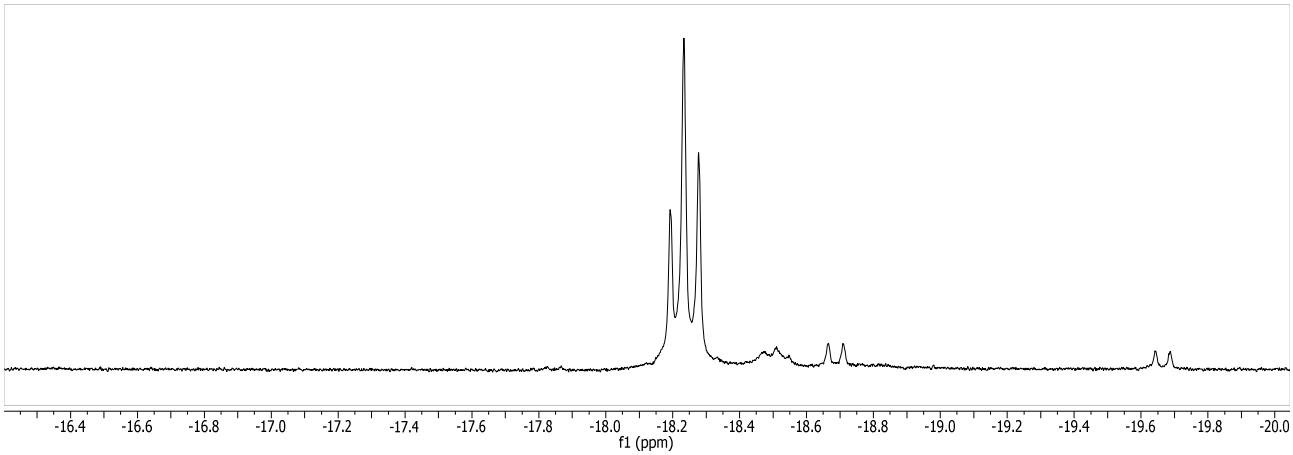

Spectrum 18: Hydride region in the ^{1}H-NMR of complex mixture of **354** and **355**

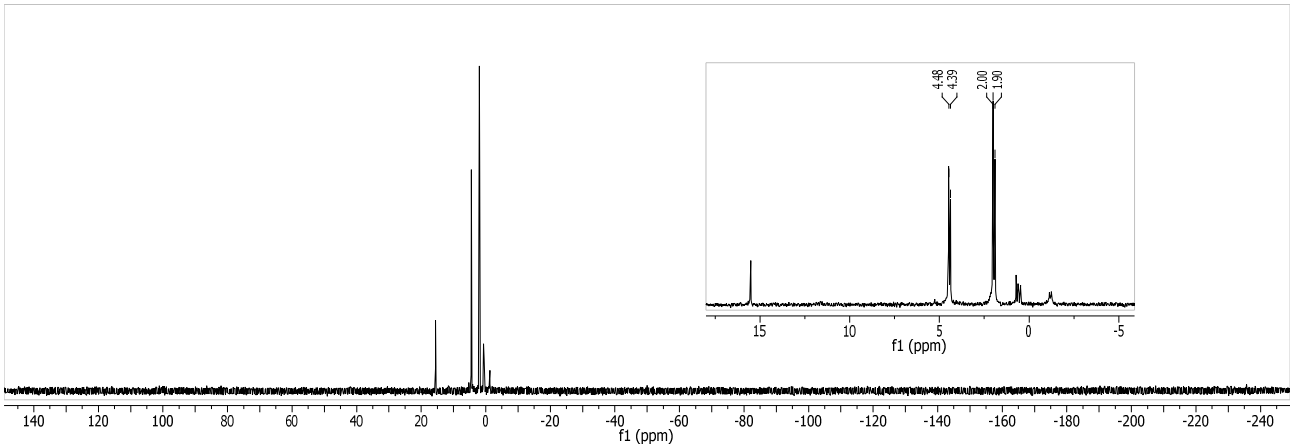

Spectrum 19: ^{31}P{^{1}H}-NMR of complex mixture of **354** and **355**

The crude reaction mixture of complexes **354** and **355** was subjected to flash chromatography and a new single hydride signal (Spectrum 20) as well as one single ^{31}P-NMR signal (Spectrum 21) was observed for

complex **356** (Scheme 133). The counterion was tentatively assigned as a chloride but could not be conclusively identified. MALDI-MS analysis showed two main mass signals at *m/z* 729 and 765. The molecular mass of complex **356** is expected at 768. While the isotopic pattern of the MALDI-MS analysis supported the postulated structure of [**356**-3u]$^{+}$ or [**356**-39u]$^{+}$, the exact masses corresponding to the species [**356**-H]$^{+}$ (*m/z* 767) or [**356**-Cl]$^{+}$ (*m/z* 733) could not be observed. 2D-NMR experiments showed NOE contacts between the hydride and the *ortho*-protons of the iridacycle, the *ortho*-protons of one phenyl substituent at the phosphorus atom as well as one weak NOE contact to a proton of the oxazoline. No NOE contacts to the stereogenic centre of the imine were detected. This led to the postulated structure **356** (Figure 19).

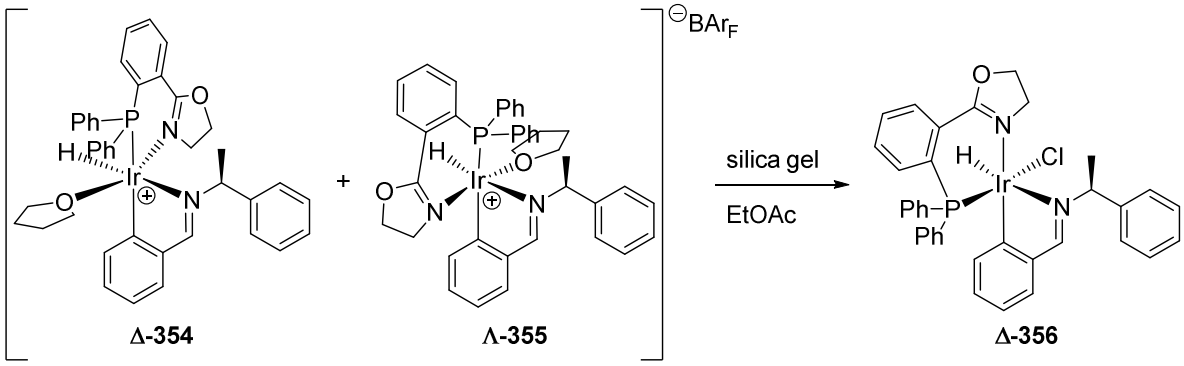

Scheme 133: Generation of chloride iridacycle **356** by elution on silica gel

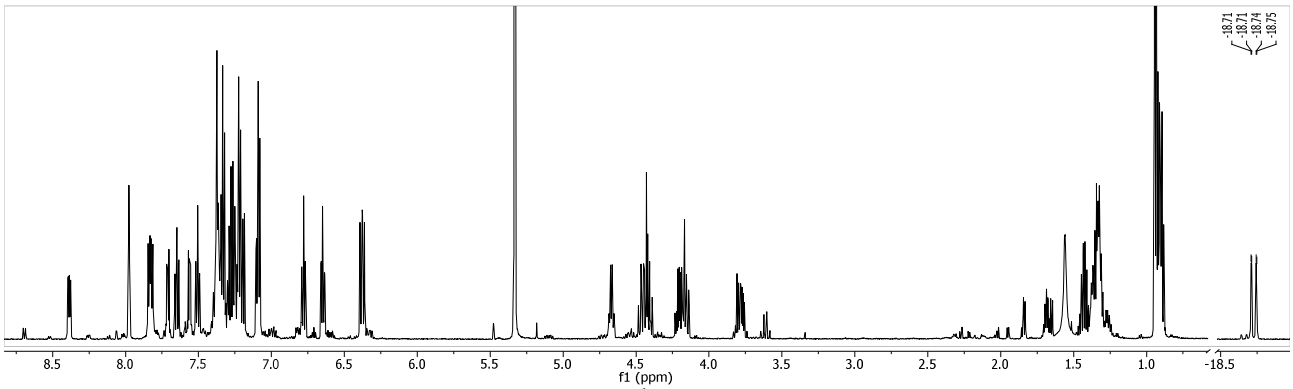

Spectrum 20: ^{1}H-NMR of **356**

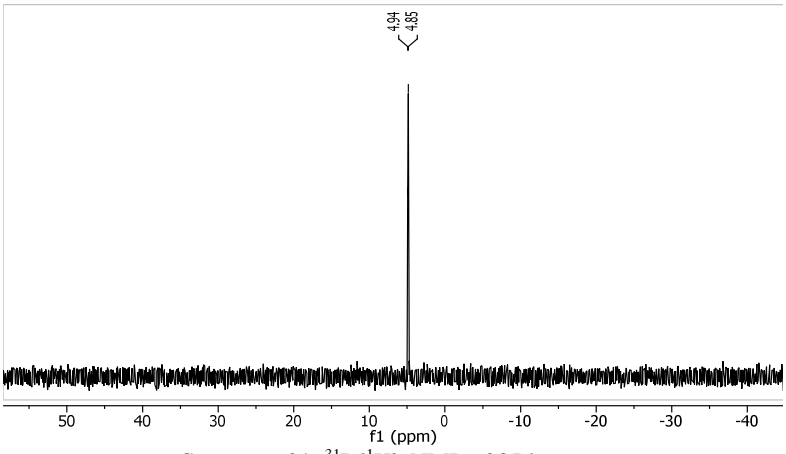

Spectrum 21: ^{31}P{^{1}H}-NMR of **356**

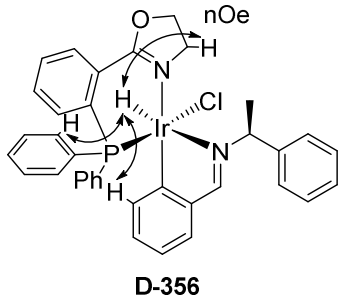

Figure 19: Observed NOE contacts in **356**

Due to loss of the BAr$_F$ counterion during the work-up procedure, the reaction was attempted with complexes **357** or **358** and the crude was eluted on silica gel. More than one hydride ^{1}H-NMR and many ^{31}P-

NMR signals were observed (Figure 20). Therefore, complexes **357** and **358** were no longer evaluated in cyclometalations.

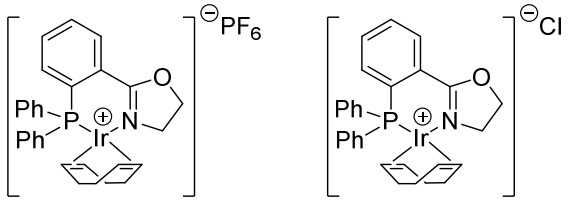

357 **358**

Figure 20: Iridium PHOX complexes **357** and **358**

Cyclometalation was also carried out with ketimine **353**. After elution on silica gel, two hydride signals and two ^{31}P-NMR signals were observed (Spectrum 22). These were assigned to configurational isomers of complex **359** (Scheme **134**).

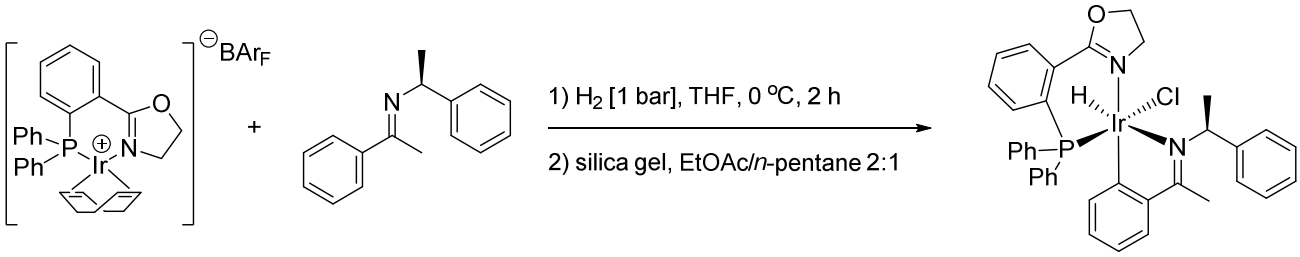

336 **353** **Δ-359**

Scheme 134: Preparation of iridacycle **359**

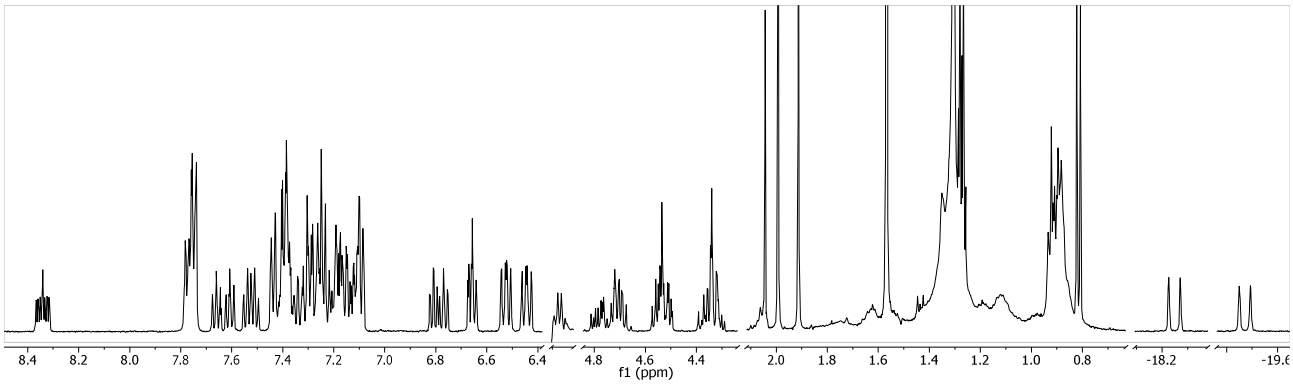

Spectrum 22: ^{1}H-NMR of both configurational isomers of **359**

2D-NMR analysis of **359** is shown in Figure 21. Overlapping signals did not allow for accurate identification of all protons. Furthermore, NOE experiments showed three contacts which could not be assigned to specific protons due to very similar chemical shifts. MALDI-MS analysis showed one mass signal at *m/z* 744. Complex **359** has a molecular weight of 782 g mol^{-1}. FAB-MS analysis showed one mass signal at *m/z* 745. ESI-MS also showed one mass signal at *m/z* 747. This signal would correspond to [**359**-Cl]$^{+}$. No mass signal of [**359**-H]$^{+}$ was found. The isotope distribution fitted well with the postulated structures of **359**. Only soft ionisation techniques such as ESI-MS allowed for the identification of the correct structure from solution.

Cyclometalation was also attempted with complex **348** (Scheme 127). More than five hydride ^{1}H-NMR signals were observed as well as formation of the trinuclear complex deactivation product similar to **350** (Scheme 129). Therefore, complex **348** was no longer considered in cyclometalation reactions.

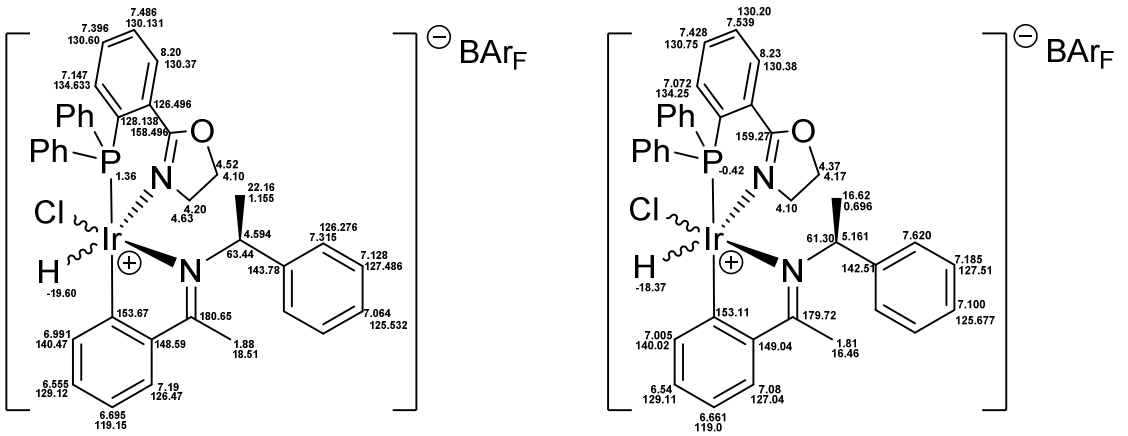

Figure 21: Chemical shifts for both configurational isomers of iridacycle **359**

In order to study the behaviour of complex **359** in solution, it was mixed with an equimolar amount of $NaBAr_F$ in CD_2Cl_2. A rearrangement was observed and only one species **360** ensued. NMR analysis (Spectrum 23 and Spectrum 24) depicted the presence of a single isomer by one ^{1}H-NMR hydride and one ^{31}P-NMR signal in solution. When using $AgPF_6$ instead of $NaBAr_F$ as the chloride abstraction reagent, >4 hydride ^{1}H-NMR and ^{31}P-NMR signals were observed.

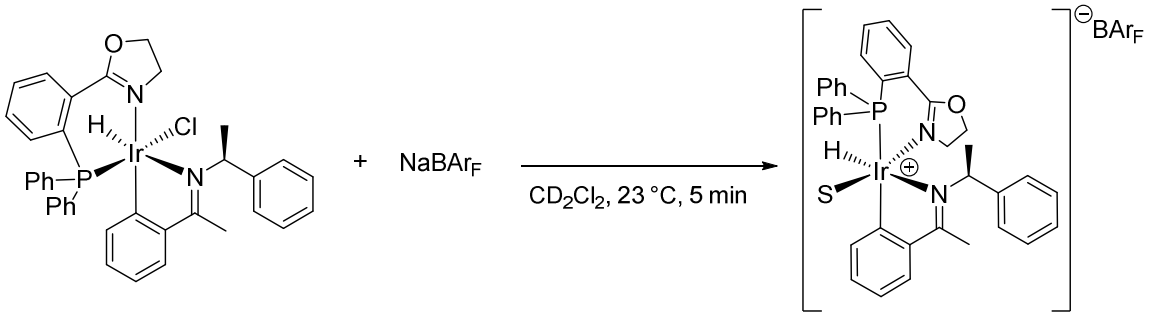

Δ-359 **Δ-360**

(S = CD_2Cl_2)

Scheme 135: Generation of **360** from **359** upon addition of $NaBAr_F$ in CD_2Cl_2

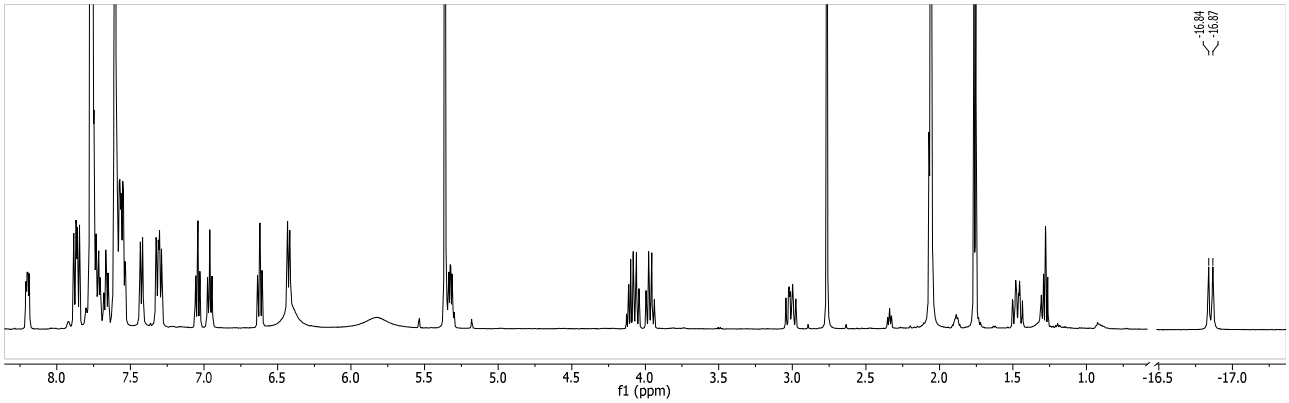

Spectrum 23: ^{1}H-NMR of **360**

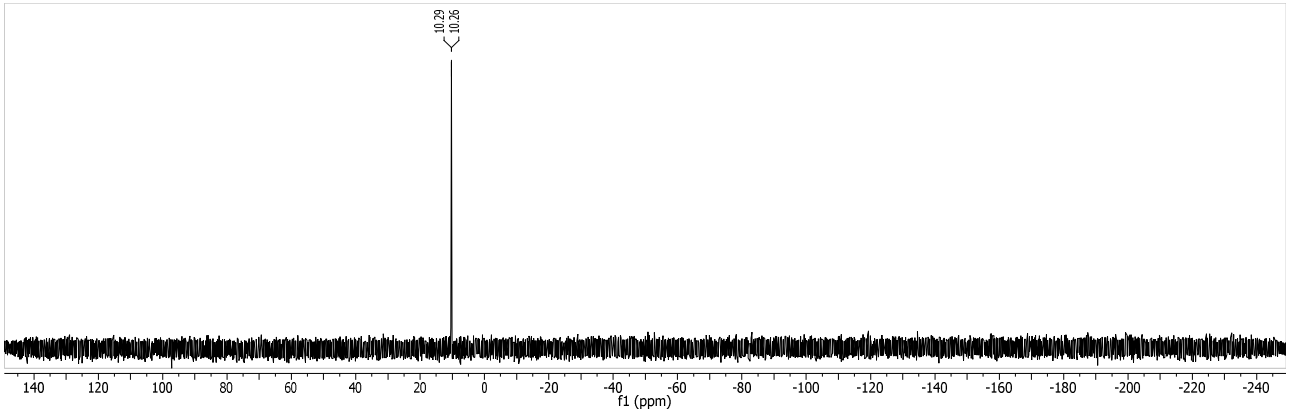

Spectrum 24: $^{31}P\{^{1}H\}$-NMR of **360**

Formation of one single species **360** in solution from configurational isomers of **359** showed that, upon addition of $NaBAr_F$, chloride abstraction and rearrangement of the complex occurred. The observed species **360** was believed to resemble the active catalyst structure in solution. This also demonstrated that the formation of configurational isomers in the preparative cyclometalation is irrelevant for the observed structure in solution. Upon chloride abstraction, a rearrangement of all configurational isomers to a single species is observed. Therefore, all complexes, isolated as mixtures of configurational isomers, where used as precursors in hydrogenation reactions.

To test the catalytic activity of species such as **360**, hydrogenation of imine **59** was carried out (Table 8): While no conversion was observed at atmospheric hydrogen pressure, increasing the pressure to 2.5 bar afforded partial conversion. Full conversion was observed at further elevated hydrogen pressure (6 bar).

Table 8: Asymmetric hydrogenation of imine **59** using iridacycles **356** and **359** as catalysts

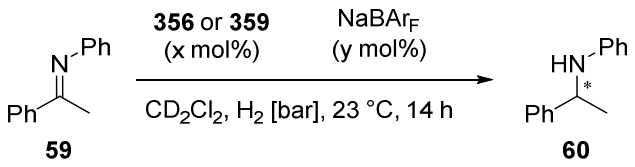

59 **60**

Entry	Catalyst [mol %]	$NaBAr_F$ [mol %]	*p* [bar]	Conv. [%][a]	*ee* [%][b]
1	(*S*)-(Δ)-**356** [2 mol%]	5	2.5	87	4 (*S*)
2	(*S*)-(Δ)-**356** [10 mol%]	10	2.5	>99	4 (*S*)
3	(*S*)-(Δ)-**359** [2 mol%]	5	2.5	40	6 (*R*)
4	(*S*)-(Δ)-**359** [10 mol%]	10	2.5	>99	8 (*R*)
1	(*S*)-(Δ)-**356** [2 mol%]	5	6	94	3 (*S*)
2	(*S*)-(Δ)-**356** [10 mol%]	10	6	>99	4 (*S*)
3	(*S*)-(Δ)-**359** [2 mol%]	5	6	>99	6 (*R*)
4	(*S*)-(Δ)-**359** [10 mol%]	10	6	>99	8 (*R*)

a) Determined by GC analysis. b) determined by HPLC analysis on a chiral stationary phase.

Consistent enantiomeric excesses were observed both at 2.5 and 6 bar hydrogen pressure. In order to induce higher enantioselectivity, the size of the substituent in the benzylic position was changed to an ethyl group. Preparation of imines **362** and **363** is shown in Scheme 136.

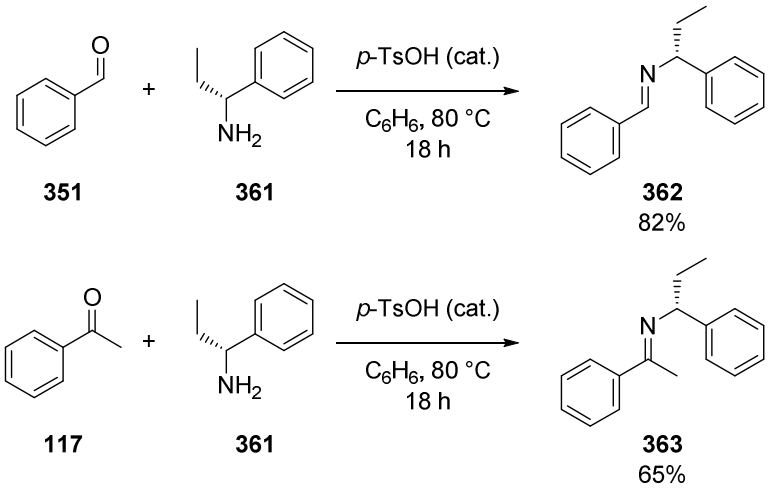

Scheme 136: Preparation of chiral imines **362** and **363**

Cyclometalation of imine **362** delivered complex **364** as a single isomer (Scheme 137). 2D-NMR analysis showed three key NOE contacts between the hydride and several protons. Furthermore, the nitrogen substituent of the imine is either freely rotating or the phenyl ring is rotated towards the oxazoline ligands since strong NOE contacts between the aldimine proton and the ethyl group of the chiral imine are observed (Figure 22).

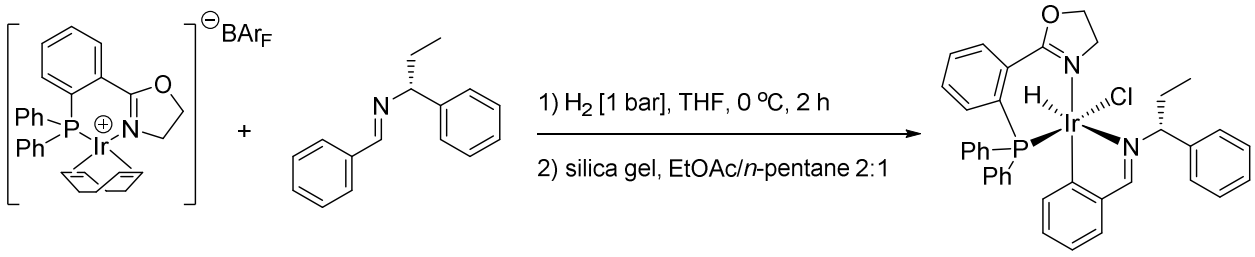

Scheme 137: Preparation of iridacycle **364**

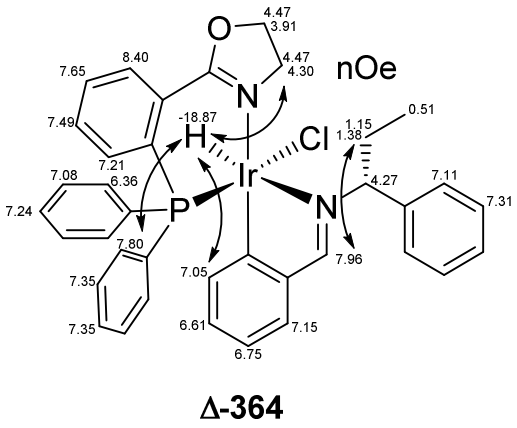

Figure 22: NOE contacts observed in complex **364**

Cyclometalation of imine **363** afforded complex **365**. One dominant ^{1}H-NMR hydride signal and one ^{31}P-NMR signal were observed along with some minor impurities. Upon mixing with $NaBAr_F$, a single species **366** was observed by ^{1}H-NMR (Spectrum 25). 2D analysis depicted three NOE contacts which could be

assigned (Figure 23). The phenyl ring of the nitrogen substituent experiences hindered rotation which is observed by EXSY signals. Therefore, complete assignment of species **366** is hampered by transferred NOE contacts which cannot be definitively assigned.

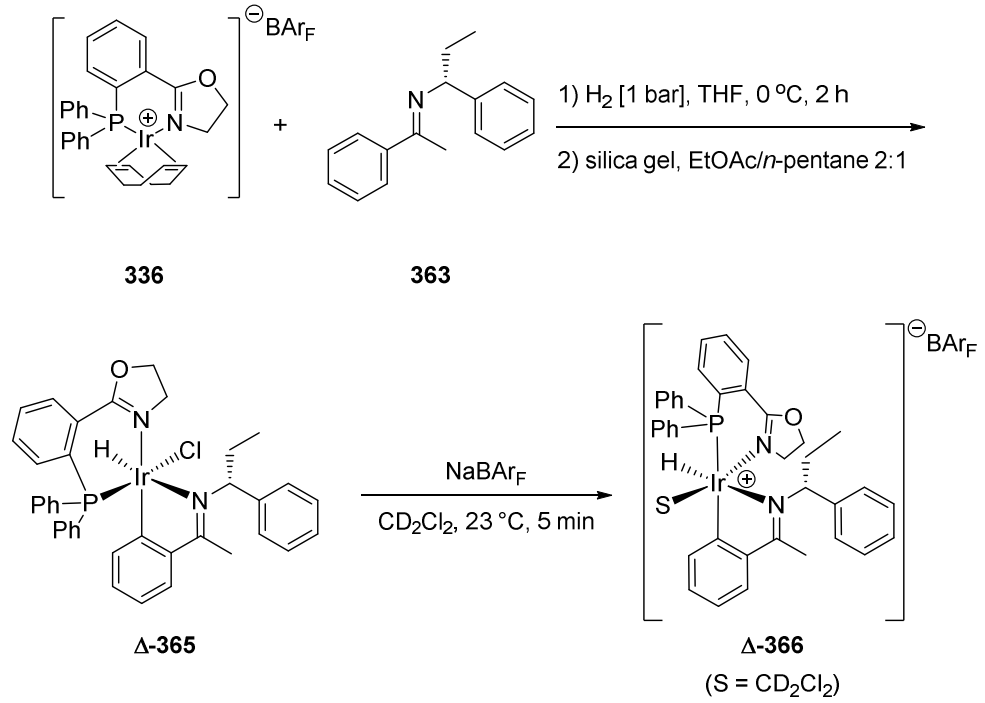

336 **363**

Δ-365 **Δ-366**

Scheme 138: Generation of complex **366** in CD_2Cl_2

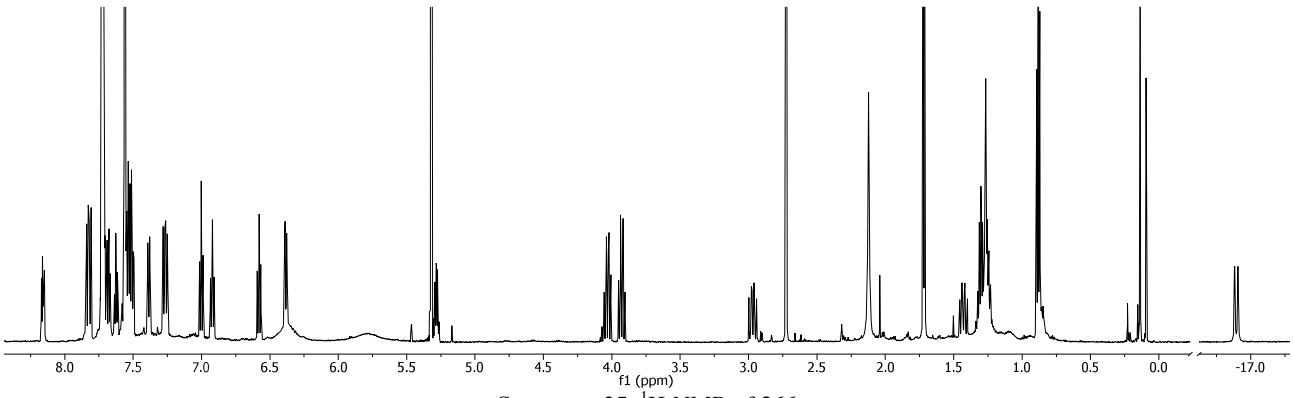

Spectrum 25: ^{1}H-NMR of **366**

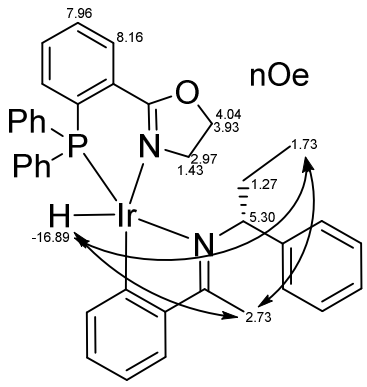

Δ-366

Figure 23: Observed NOE contacts in **366**

With the new complexes **364** and **365** in hand hydrogenations were reinvestigated (Table 9). In order to obtain higher *ee*'s, hydrogenations were conducted at lower temperature. Contrary to the results in Table 8 the (*R*)-amine **60** was observed with complex **356** and the (*S*)-amine **60** with complex **359**. Complexes **364** and **365** gave lower *ee*'s at low temperature (Entries 5 and 6) and comparable ones to **356** and **359** (Entries 7 and 8) at ambient temperature. The reason for the observation of opposed enantioselectivity in the hydrogenation with complex **356** (Entries 1 and 2) and **359** (Entries 3 and 4) could not be rationalised.

Table 9: Asymmetric hydrogenation of imine **59** using iridacycles **356**, **359**, **363** and **365** as catalysts

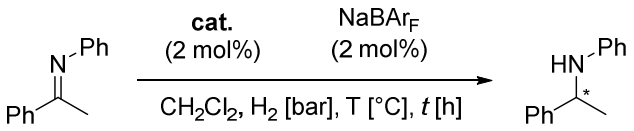

59 **60**

Entry	Catalyst [mol %]	*p* [bar]	T [°C]	*t* [h]	Conv. [%][a]	*ee* [%][b]
1	(*S*)-(Δ)-**356**	6	-20	14	>99	6 (*R*)
2	(*S*)-(Δ)-**356**	6	-20	14	>99	5 (*R*)
3	(*S*)-(Δ)-**359**	1	23	4	20	6 (*S*)
4	(*S*)-(Δ)-**359**	5	23	4	>99	4 (*S*)
5	(*R*)-(Λ)-3**64**	6	-20	14	>99	4 (*R*)
6	(*R*)-(Λ)-**364**	6	-20	14	>99	2 (*R*)
7	(*R*)-(Λ)-**365**	1	23	4	5	6 (*R*)
8	(*R*)-(Λ)-**365**	5	23	4	40	4 (*R*)

a) Determined by GC analysis. b) determined by HPLC analysis on a chiral stationary phase.

To confirm the enantioinduction of complex **359**, both enantiomers of imine **353** were prepared. They were subsequently cyclometalated onto complex **336** and the obtained iridacycles **359** used as catalysts in crude form after elution on silica gel. Reproducible enantioselectivities between 4 to 6% were observed (Table 10). This clearly demonstrated the participation of the cyclometalated chiral imine in the enantiodiscriminating step of the hydrogenation.

Table 10: Asymmetric hydrogenation of imine **59** using iridacycles (*S*)-**359** and (*R*)-**359**

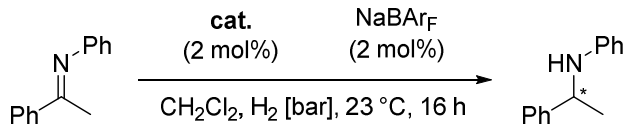

59 **60**

Entry	Catalyst	*p* [bar]	Conv. [%][a]	*ee* [%][b]
1	(*S*)-(Δ)-**359**	1	16	4 (*S*)
2	(*S*)-(Δ)-**359**	5	54	6 (*S*)
3	(*R*)-(Λ)-**359**	1	18	4 (*R*)
4	(*R*)-(Λ)-**359**	5	44	6 (*R*)

a) Determined by GC analysis. b) determined by HPLC analysis on a chiral stationary phase.

In order to obtain higher enantioselectivities in the hydrogenation, other cyclometalating ligands were tested in the following.

Other ligands for cyclometalation

Apart from the chiral imine ligands already presented, structurally similar ligands with a C=N double bond were tested in cyclometalation and the corresponding iridacycles tested in hydrogenations. All complexes were isolated by elution chromatography and used as catalysts without further purification. Oxazolines **367**, **368** and **369** were evaluated since oxazolines in general have been demonstrated to effect high stereoselectivity in a number of transformations. Furthermore, oxazoline **369** would form a six-membered iridacycle.[11] Imine **370** was believed to facilitate cyclometalation due to eased rotation of the nitrogen substituent compared to imine **346**. Imines **371** and **372** were evaluated to investigate the possibility of exocyclic iridacycle formation.[12] The 2,6-dimethyl benzaldehyde moiety was used to force cyclometalation to occur in an endocyclic fashion.

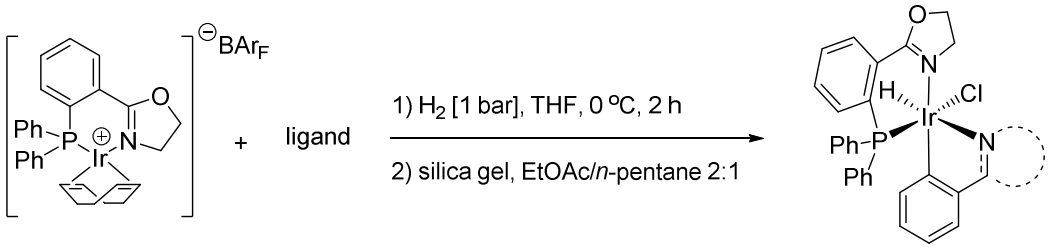

336 **367-372** **373-378**

Scheme 139: Preparation of iridacycles **373**-**378**

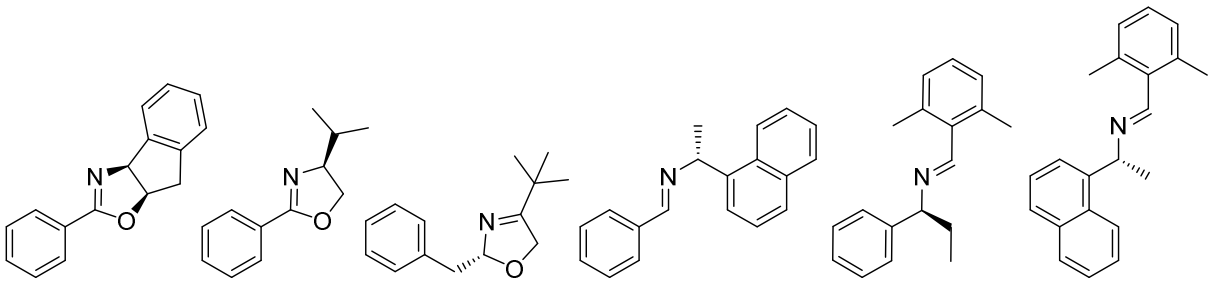

367 **368** **369** **370** **371** **372**

Scheme 140: Ligands **367**-**372**

The yellow precipitate of crude complex **373** showed four ^{1}H-NMR hydride resonances and four ^{31}P-NMR signals as well as a strong BAr_F signal in the ^{19}F-NMR. The crude complex **374** did not show any hydride signal. More than four yellow spots were observed in TLC and a BAr_F signal was observed by ^{19}F-NMR indicating incomplete counterion metathesis or impurities present in the isolated iridacycle **374**. Complex **375** could not be obtained. Instead an iridium tri-hydride trinuclear complex such as **350** was isolated (Figure 24).

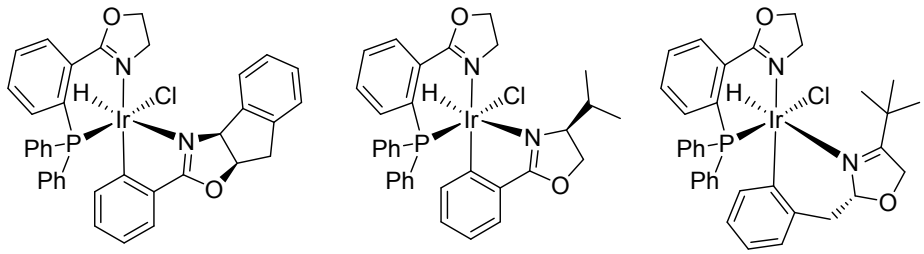

Δ-373 **Δ-374** **Δ-375**

Figure 24: Iridacycles **373**, **374** and **375**

[11] Six-membered iridacycles are commonly observed in alkene-isomerisation chemistry

[12] exocyclic with regards to the C=N double bond not being part of the ring/metallacycle.

Quite differently, iridacycle formation of **376** proceeded smoothly furnishing a crude complex with two hydride ^{1}H-NMR resonances and one ^{31}P-NMR signal. No ^{19}F-NMR signal was detected. Complex **377** was readily formed. Three weak hydride ^{1}H-NMR signals, but no ^{31}P-NMR, as well as no ^{19}F-NMR signal was observed. Complex **378** could not be obtained as no crystalline material was isolated (Figure 25).

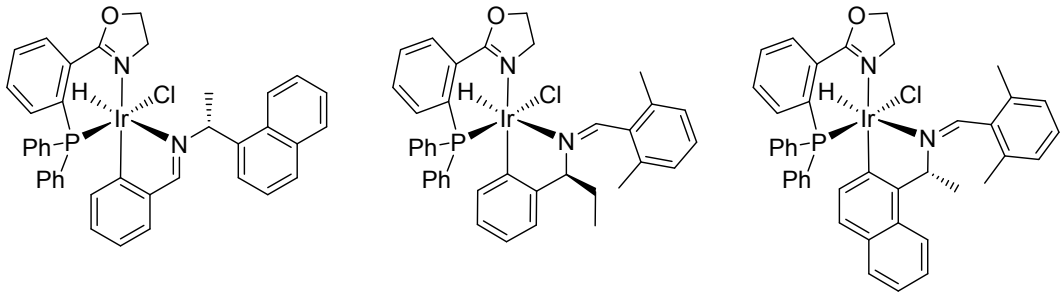

Δ-376 **Δ-377** **Δ-378**

Figure 25: Iridacycles **376**, **377** and **378**

Table 11 summarizes the results. Apart from complex **373** (Entries 1 and 2), low conversions were observed. Additionally, the low enantioselectivities render it hard to draw any conclusions. When comparing imine to oxazoline ligands with regards to the stability of the formed iridacycles, only complex **376** gives consistent enantioselectivities both at atmospheric as well as at elevated hydrogen pressure (Entries 4 and 5). Virtually racemic product is obtained with complex **373** at 5 bar hydrogen pressure (Entry 2). Complex **374** and **377** also depicted an enantioselectivity of maximum 2% at atmospheric hydrogen pressure (Entry 3 and 6). This might originate from exchange of the cyclometalating ligand to the achiral imine forming a catalyst which leads to formation of racemic amine.

Table 11: Asymmetric hydrogenation of imine **59** using iridacycles **373**, **374**, **376** and **377**

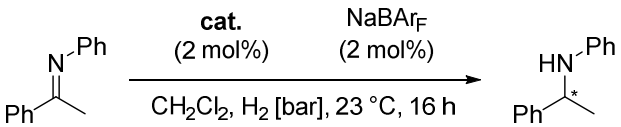

59 **60**

Entry	Catalyst	*p* [bar]	Conv. [%][a)]	*ee* [%][b)]
1	**373**	1	21	6 (*R*)
2	**373**	5	99	2 (*R*)
3	**374**	1	15	2 (*R*)
4	**376**	1	2	9 (*S*)
5	**376**	5	16	9 (*S*)
6	**377**	1	8	2 (*S*)

a) Determined by GC analysis. b) determined by HPLC analysis on a chiral stationary phase.

Imine **370** was also reacted with [Ir(Cp*)Cl$_2$]$_2$ (**279**) to afford the half-sandwich Cp*-complex (*R*)-**379** (Scheme 141).

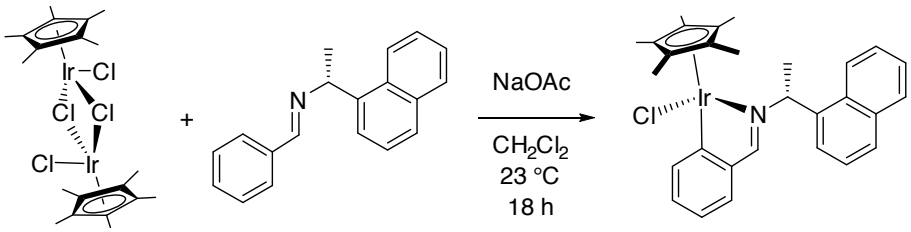

279 **370** (*R*)-**379**

Scheme 141: Preparation of complex (*R*)-**379**

The crystal structure of (*R*)-**379** is shown in Figure 26 and Figure 27.

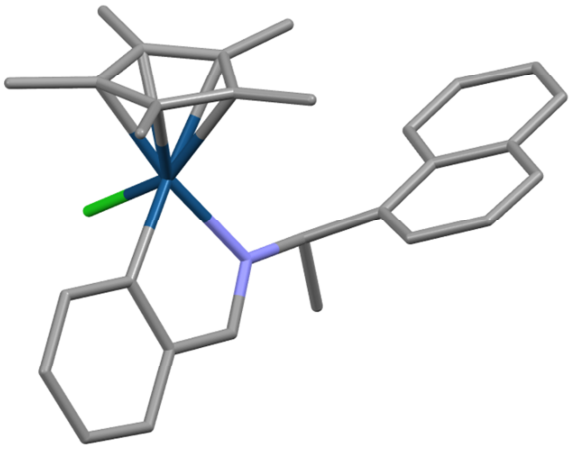

Figure 26: Front view of (*R*)-**379**

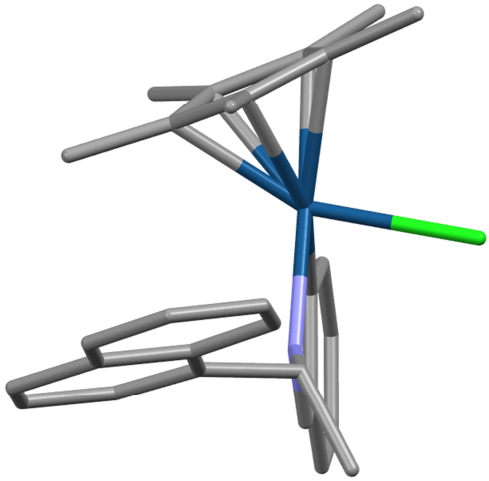

Figure 27: Side view of (*R*)-**379**

On the other hand, the combination of a chiral ligand and an achiral imine provided high enantioselectivities of 87% *ee*.[13] In an attempt to increase the *ee*, the introduction of a sterically demanding group in the cyclometalating imine was pursued (Scheme 142). Imine **383** was prepared from α-tetralone (**380**). Silyl enol ether formation employing mesityl magnesium bromide as a mild base afforded **381** in 82% yield.[93] Subsequent titanium(IV)-mediated *C*-alkylation delivered the tetralone **382** in 34% yield.[94] Ultimately condensation with aniline afforded imine **383** in 29% yield.

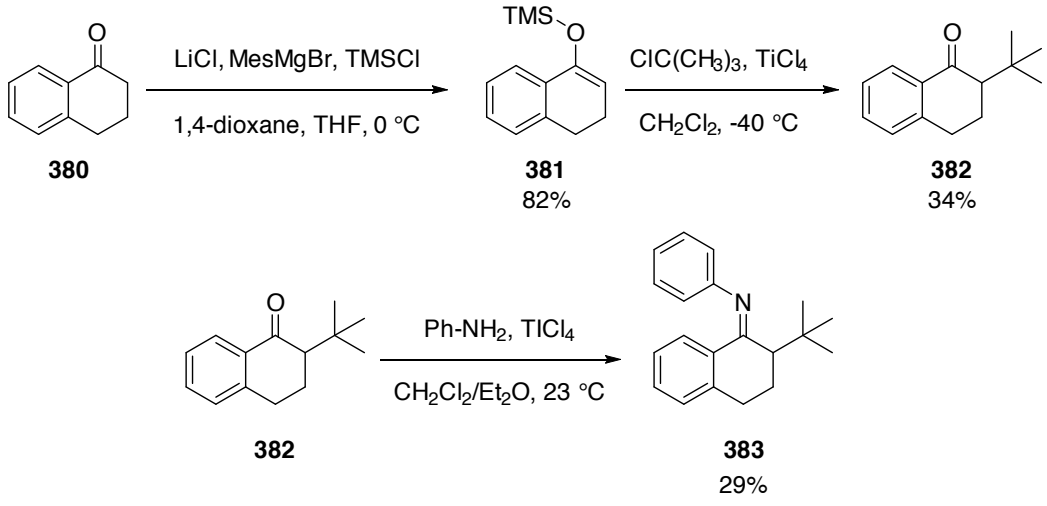

380 **381** 82% **382** 34%

382 **383** 29%

Scheme 142: Synthesis of imine **383**

[13] See chapter 2

Cyclometalation was performed with 1 eq. of complex **86** and 2 eq. of imine **383** to selectively afford the matched pair of the two possible diastereomers of complex **384** (Scheme 143). The isolated complex **384** showed two hydride ^{1}H-NMR resonances. Upon addition of $NaBAr_F$ one hydride signal remained.

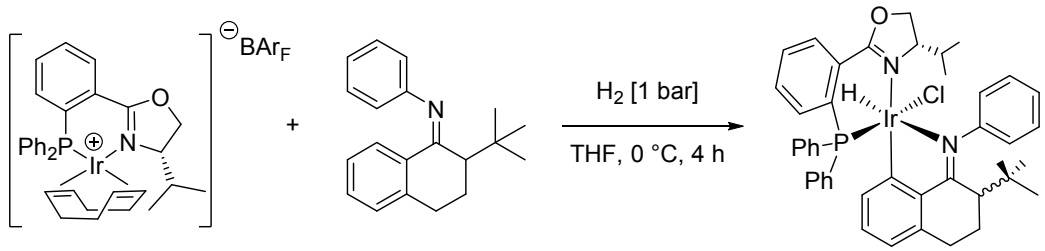

86 **383** **Δ-384**

Scheme 143: Iridacycle preparation of **384**

Complex **384** was tested as a catalyst for imine hydrogenation. Compared to using complex **86** without an additive, both significantly lower conversion and lower enantioselectivity were observed (Scheme 144).

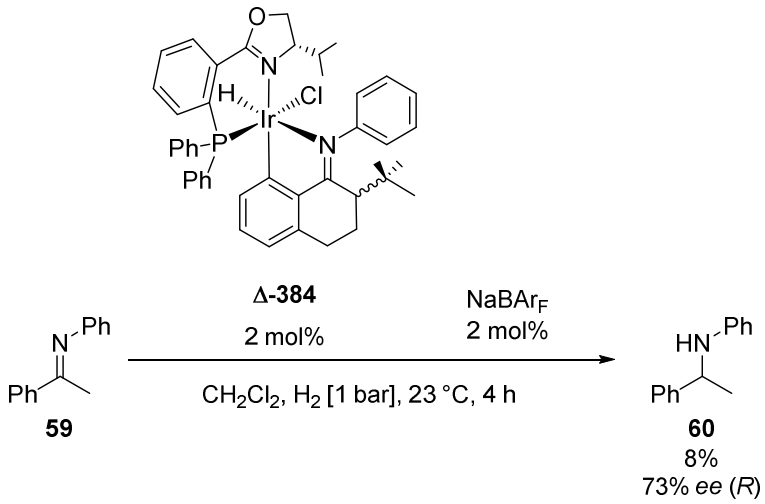

Scheme 144: Asymmetric hydrogenation of imine **59** with iridacycle **384**

When the experiment was conducted in a stepwise fashion, similar conversion and even lower enantioselectivity were observed (Scheme 145).

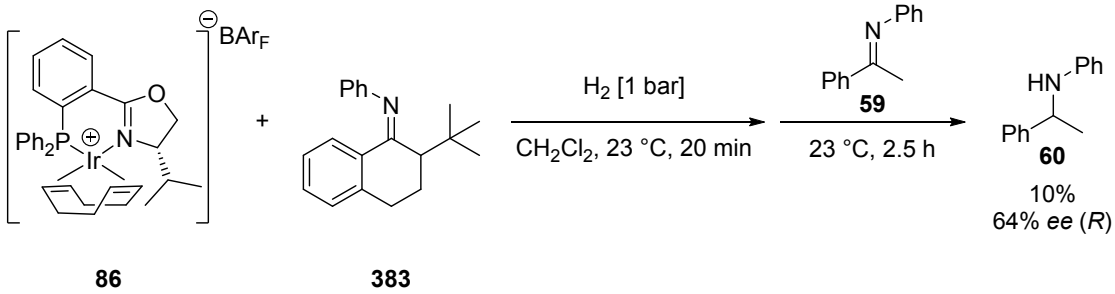

86 **383**

Scheme 145: Stepwise procedure of iridacycle generation from **86** and **383** and subsequent hydrogenation of imine **59**

In order to obtain a better understanding in the role of the cyclometalated imine, two different model imines **80** and **322** were selected (Figure 28) and the corresponding iridacycles prepared. It was desired to influence the *ee* in the hydrogenation by the cyclometalated imine. In the hydrogenation of aryl-alkyl *N*-phenyl imines,

imine **80** displayed the highest enantioselectivity of 90% *ee* using complex **86** while imine **322** gave the lowest enantioselectivity of 78% *ee* with complex **86**.

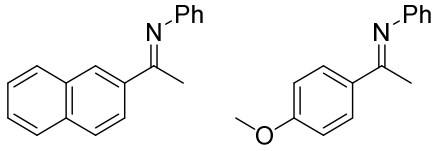

80 **322**

Figure 28: Imines **391** and **322**

Table 12 displays the enantioselectivities obtained for imines **59**, **391** and **73** (Entries 1, 4 and 7). Both iridacycles, with imine **80** or **322**, afforded amine **60** with slightly lower enantioselectivity compared to *in situ* generated **325** (Entry 1 vs. 2 and 3). On the other hand, imine **80** was reduced with high enantioselectivity regardless of the iridacycle catalyst used (Entries 4 to 6). Additionally, imine **322** was reduced with lower enantioselectivity by all iridacycles (Entries 7 to 9). Apparently the structure of the imine being hydrogenated does have a strong influence on the enantioselectivity of the catalyst.

Table 12: Asymmetric hydrogenation of imines **59**, **80** and **322** using iridacycles derived from imines **80** and **322**

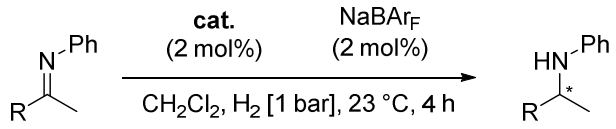

Entry	Catalyst	Imine	Conv. [%][a]	*ee* [%][b]
1	**86**	**59** (R = Ph)	>99	87 (*R*)
2	[Ir(PHOX)(**80**)(H)(Cl)]	**59** (R = Ph)	>99	81 (*R*)
3	[Ir(PHOX)(**322**)(H)(Cl)]	**59** (R = Ph)	>99	82 (*R*)
4	**86**	**80** (R = 2-Naph)	>99	90 (-)
5	[Ir(PHOX)(**80**)(H)(Cl)]	**80** (R = 2-Naph)	>99	90 (-)
6	[Ir(PHOX)(**322**)(H)(Cl)]	**80** (R = 2-Naph)	>99	90 (-)
7	**86**	**322** (R = 4-MeO-Ph)	>99	78 (-)
8	[Ir(PHOX)(**80**)(H)(Cl)]	**322** (R = 4-MeO-Ph)	>99	82 (-)
9	[Ir(PHOX)(**322**)(H)(Cl)]	**322** (R = 4-MeO-Ph)	85	78 (-)

a) Determined by GC analysis. b) determined by HPLC analysis on a chiral stationary phase.

Cyclometalation of aliphatic C-H bonds was also evaluated. C(sp^3)-H activation and metalation with iridium has been observed in iridium-catalysed allylic substitution.[95] Therefore, imine **329** was subjected to cyclometalation reaction conditions (Scheme 146). A strongly yellow coloured band was observed during elution chromatography. However, it did not show a hydride ^{1}H-NMR resonance. Instead three weak signals were detected between -20 and -30 ppm. Furthermore no ^{31}P-NMR signal could be observed with sufficient intensity. Therefore, it was concluded that other products than the desired iridacycle **385** had been formed.

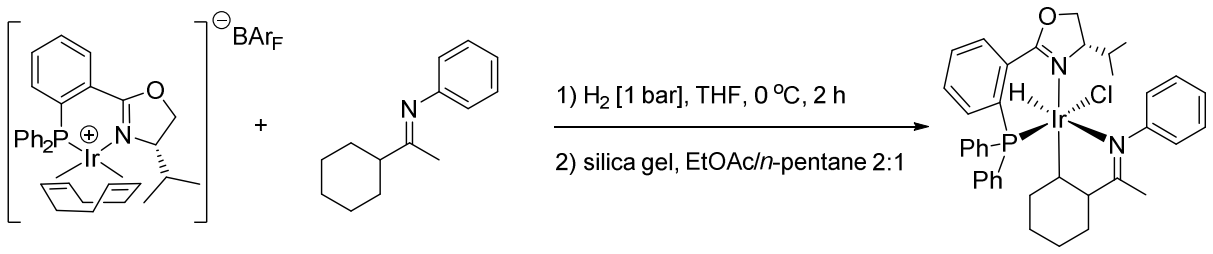

86 **329** **385**

Scheme 146: Attempted preparation of iridacycle **385** with an Ir-C(sp^3) bond

To test the C-H activation of a C(sp^2)-hybridized carbon centre other than aryl, imine **386** was subjected to cyclometalation conditions (Scheme 147). In the ^{1}H-NMR spectrum of the crude complex **387** one hydride signal was observed. However, the integrals of the aromatic region did not match the expected numbers. Five protons too few were counted. The structure was tentatively assigned as the cyclometalated benzylidene acetone complex **387** (Figure 29). Further studies to characterize the complex are required. Nevertheless, cyclometalation of an olefinic C(sp^2)-hybridized C-H bond was observed.

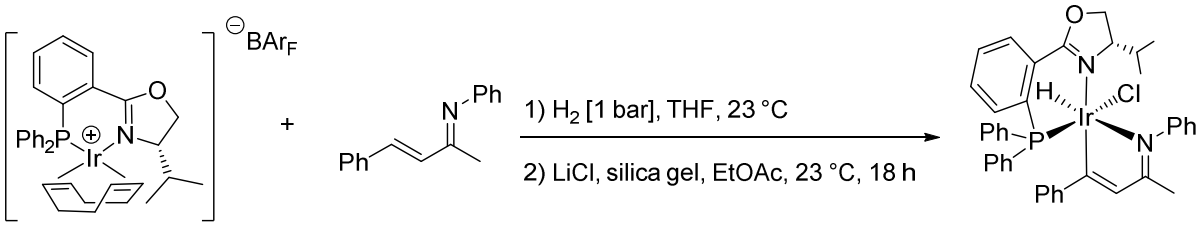

86 **386** **Δ-387**

Scheme 147: Preparation of iridacycle **387** via olefinic C-H bond activation

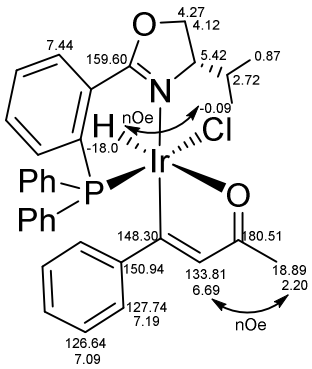

D-387

Figure 29: NMR shifts and key NOE contacts in complex **387**

Improving iridacycle synthesis by counterion metathesis

The previously conducted preparation of the iridacycles featured an elution chromatography to exchange the BAr_F counterion to a chloride. Significant variations in isolated yields were observed. Therefore, a counterion metathesis was investigated (Scheme 148). Complex **86** and imine **59** were thus activated to afford **308** in the presence of hydrogen. Subsequently, different chloride salts were added to afford iridacycle **325**.

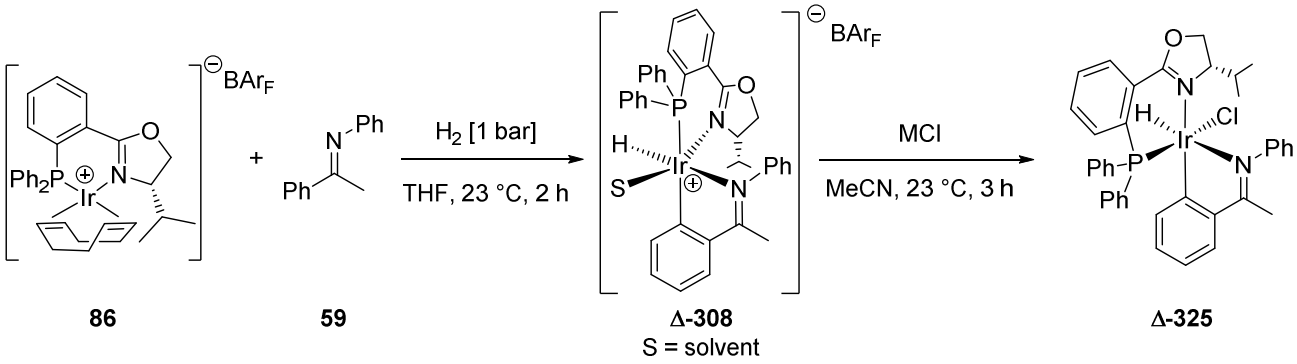

Scheme 148: Preparation of iridacycle **325** involving counterion metathesis

Lithium chloride, ammonium chloride and sodium chloride all furnished the same product as usually obtained after elution of the crude iridacycle by flash chromatography.[14] The procedure was further optimised by switching the solvent to ethyl acetate and adding silical gel to facilitate the counterion metathesis. With this protocol in hand, a number of iridacycles were prepared in yields of 55-60% (Scheme 149).

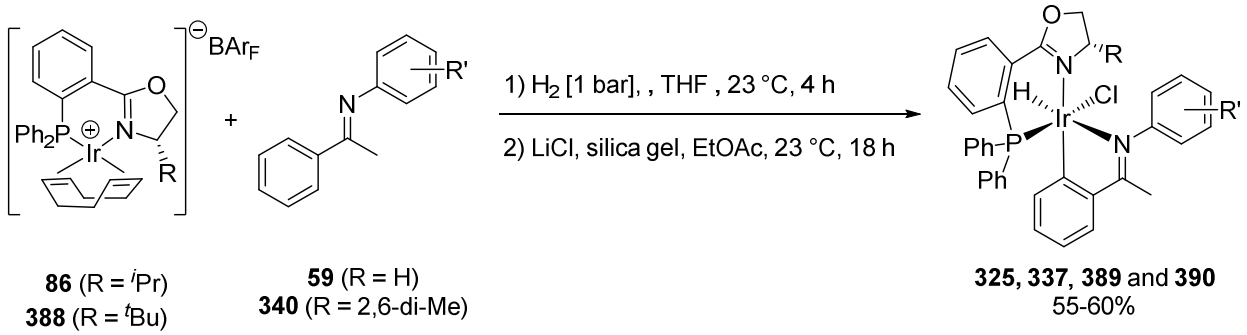

Scheme 149: Preparation of iridacycles **325**, **337**, **389** and **390** *via* counterion metathesis

Iridacycles **325**, **337** and **390**-**391** where isolated as yellow amorphous solids. NMR analysis showed one to three hydride ^{1}H-NMR resonances and the corresponding ^{31}P-NMR signals. NOE analysis depicted several key contacts which facilitated determination of the structure in solution. Complex **325** (Figure 30) was observed as one single isomer in solution (Spectrum 26 and Spectrum 27).

[14] With lithium iodide a distinct colour change of the reaction mixture was observed. The ^{1}H-NMR displayed a differnt hydride resonance.

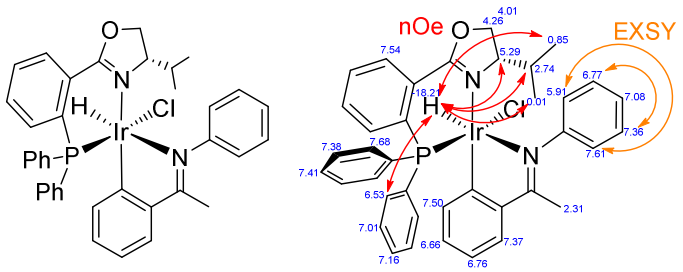

Δ-325

Figure 30: NMR shifts and key NOE contacts in iridacycle **325**

Since no NOE contacts were found between the hydride and the cyclometalated imine, they were assigned as *trans* to each other. The phenyl rings at the phosphorus atom could be fully assigned and each phenyl ring depicted three resonances which indicates free rotation. Furthermore one NOE contact between the hydride and the *ortho*-protons of one *P*-phenyl ring was observed. Thus, they were assigned *cis* to each other. The *N*-phenyl ring of the cyclometalated imine displayed chemical exchange but no NOE contacts to either the oxazoline moiety or any *P*-phenyl substituent.

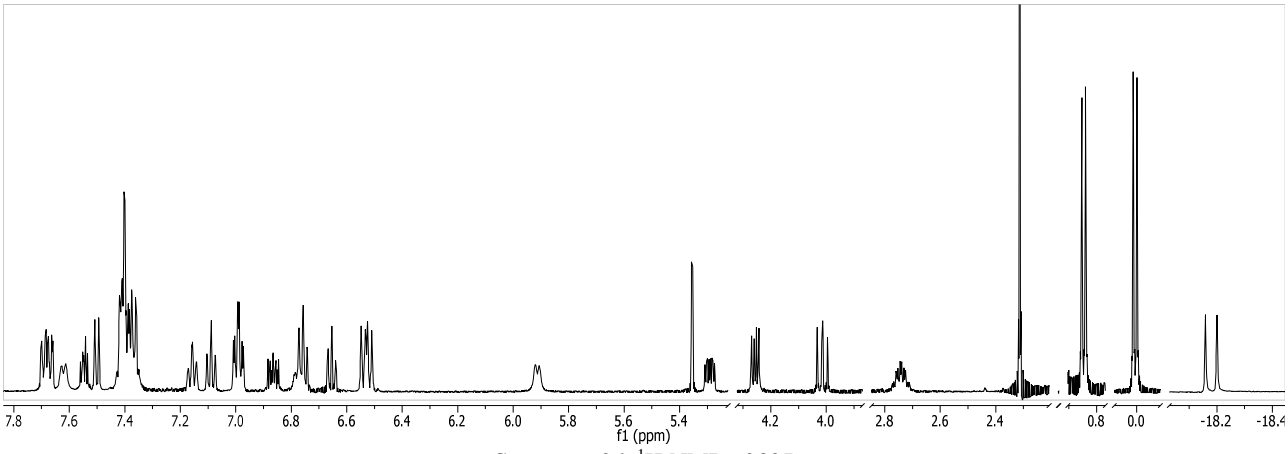

Spectrum 26: ^{1}H-NMR of **325**

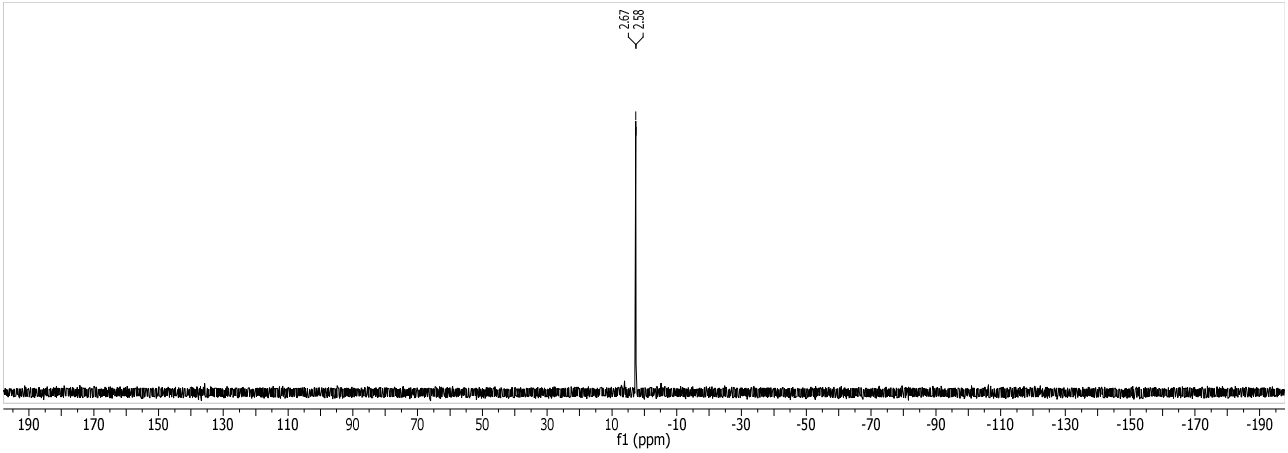

Spectrum 27: ^{31}P{^{1}H}-NMR of **325**

Iridacycle **337** displayed virtually identical features as **325**. Again one single isomer was observed in solution (Spectrum 28 and Spectrum 29). Key NOE contacts are given in Figure 31 which confirmed the postulated structure. An additional NOE contact with the *ortho*-proton of the cyclometalated phenyl ring was also observed.

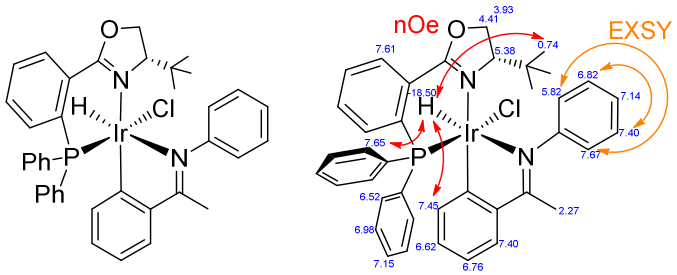

Δ-337

Figure 31: NMR shifts and key NOE contacts in iridacycle **337**

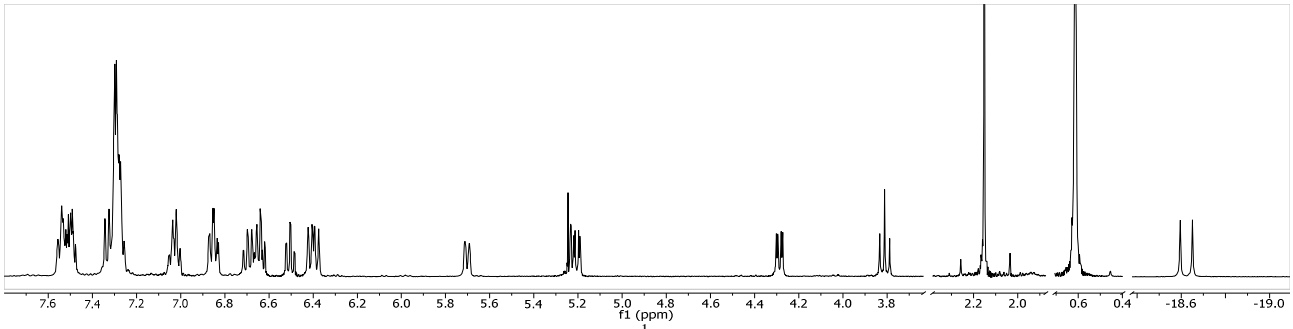

Spectrum 28: ^{1}H-NMR of **337**

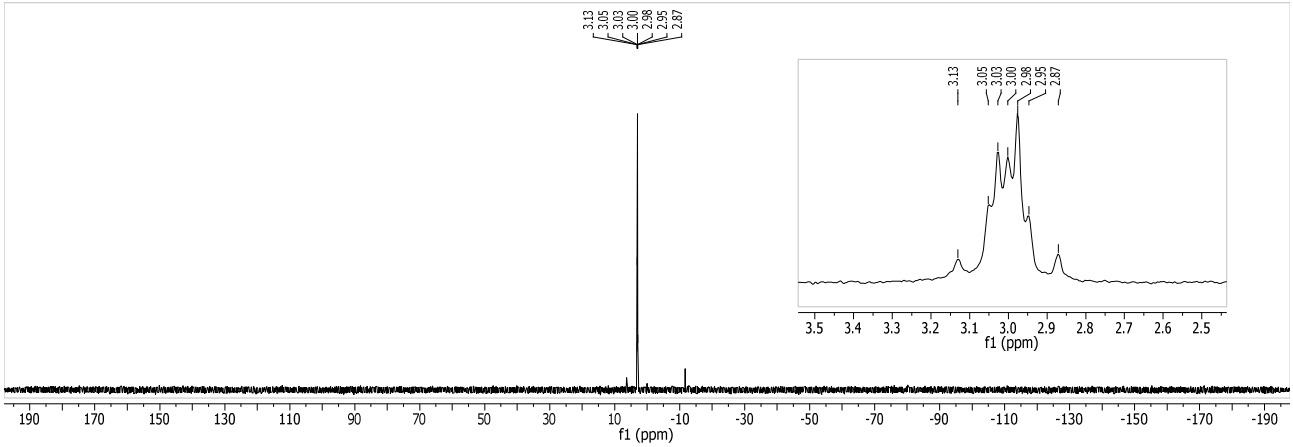

Spectrum 29: ^{31}P{^{1}H}-NMR of **337**

A different picture was observed upon cyclometalation of the more bulky imine **340**. The *N*-Aryl substituent resulted in the formation of three configurational isomers of complex **389** (Spectrum 30 and Spectrum 31). Contrary to complexes **325** and **337**, NOE contacts between the hydride and the aryl ring of the cyclometalated imine were observed. This isomer was assigned as shown in Figure 32 on the left side. The cyclometalated imine and the hydride are *cis* to each other. Additionally, the *P*-phenyl ring experiences hindered rotation which is depicted in the EXSY signals of the *ortho*-protons. This is also observed in the other configurational isomer shown on the right side in Figure 32. Probably also due to this fluxional behaviour, no NOE contact between the hydride and the *P*-phenyl ring was observed.

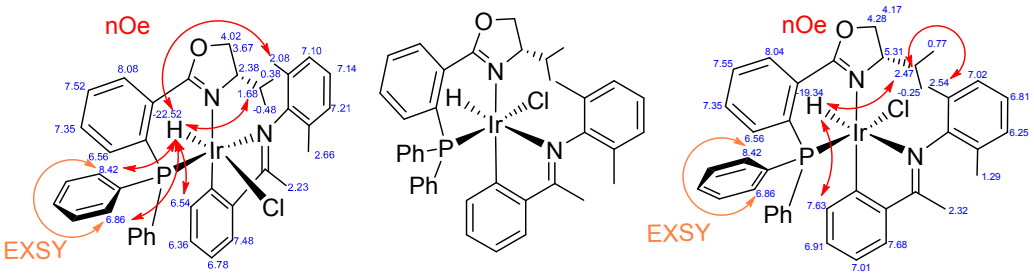

Δ-389

Figure 32: NMR shifts and key NOE contacts of two configurational isomers of iridacycle **389**

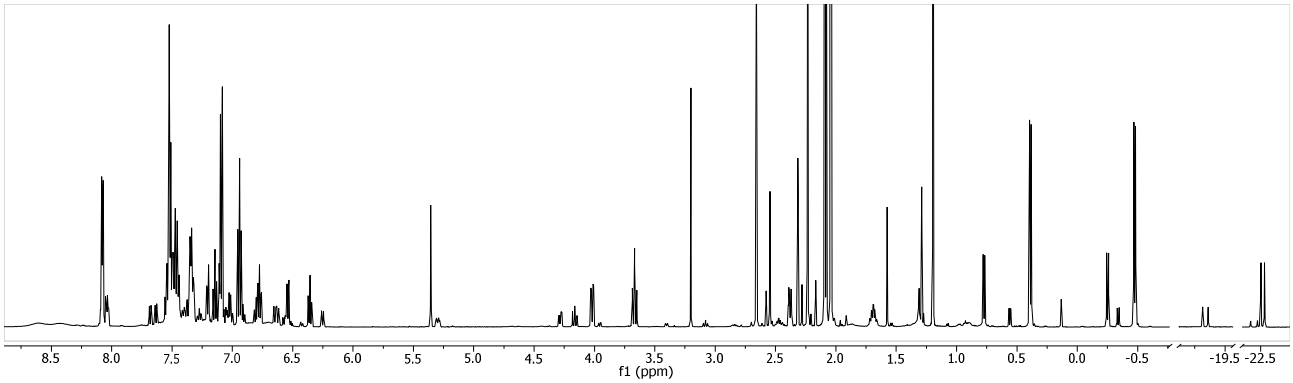

Spectrum 30: ^{1}H-NMR of **389**

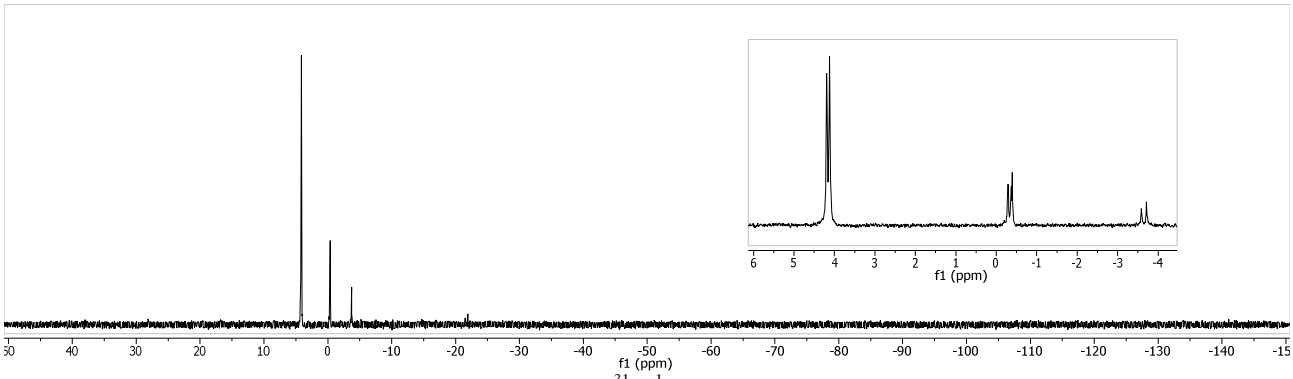

Spectrum 31: ^{31}P{^{1}H}-NMR of **389**

Complex **390** displayed similar structural features compared to **389**. Two configurational isomers were observed in solution (Spectrum 32 and Spectrum 33). No fluxional behaviour of the *P*-phenyl ring was observed. The NOE contacts are given in Figure 33.

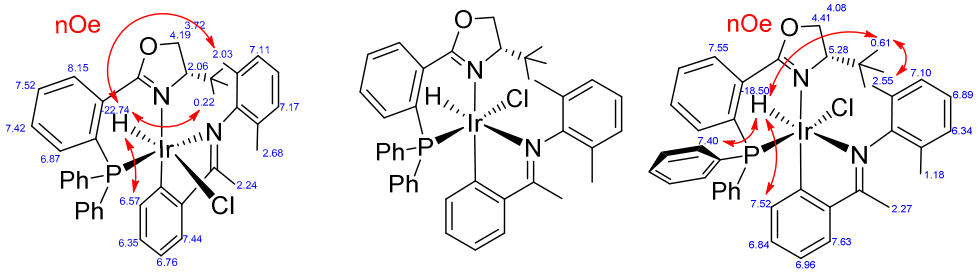

Δ-390

Figure 33: NMR shifts and key NOE contacts of two configurational isomers of iridacycle **390**

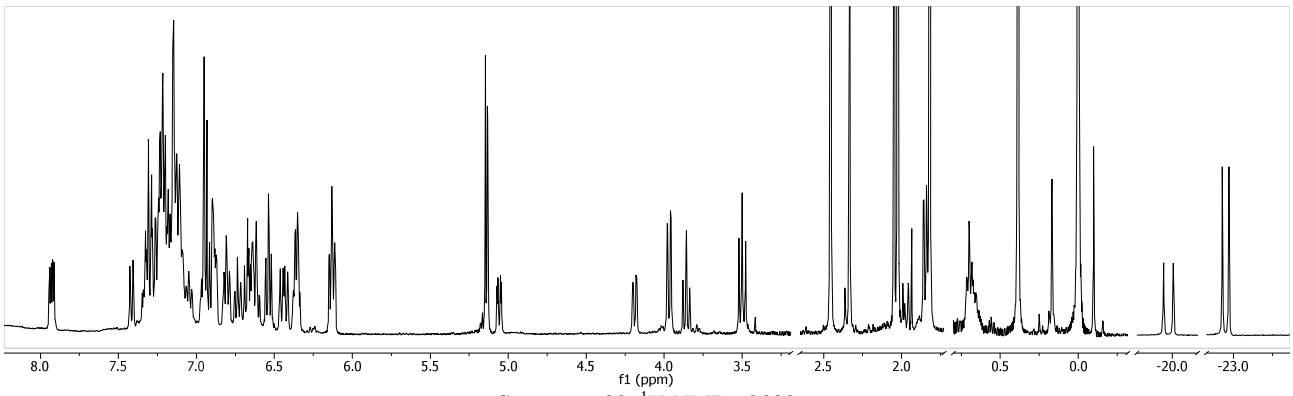

Spectrum 32: ^{1}H-NMR of **390**

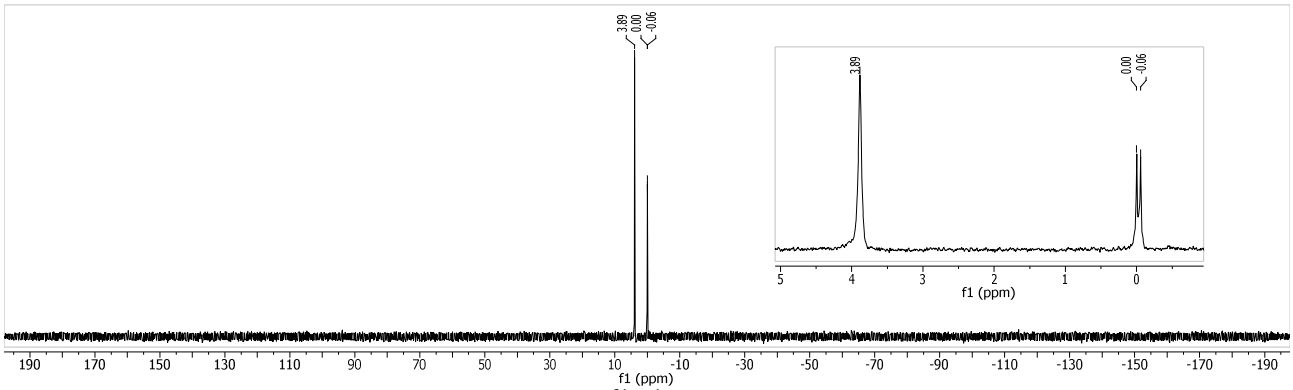

Spectrum 33: ^{31}P{^{1}H}-NMR of **390**

Numerous attempts to crystallize complexes **325**, **337**, **389** and **390** failed. Instead, only oily residual solids were obtained when crystallisation was attempted from chlorinated solvents to apolar solvents (e.g. alkanes or ethers). All iridacycles could be obtained as solids by trituration with *n*-pentane. In the course of investigating other ligand structures as potential catalysts for imine hydrogenation, crystal formation of complex **391** was observed after leaving the oily residue on the bench for a few weeks. NMR analysis of complex **391** displayed one isomer in solution (Spectrum 34 and Spectrum 35). NMR shifts and key NOE contacts are given in Figure 34.

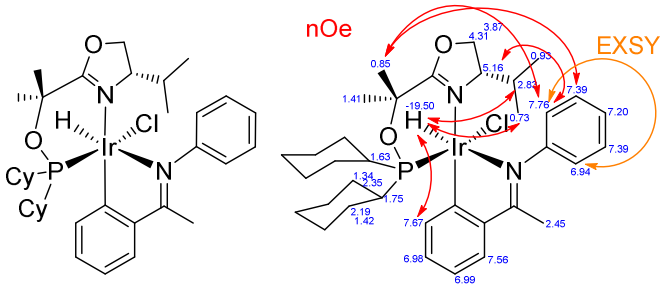

Δ-391

Figure 34: NMR shifts and key NOE contacts in iridacycle **391**

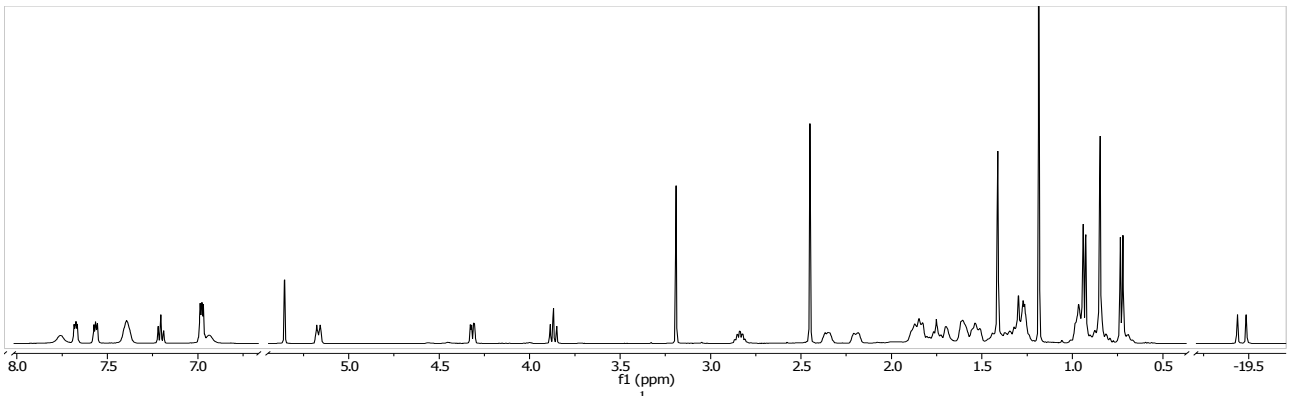

Spectrum 34: ^{1}H-NMR of **391**

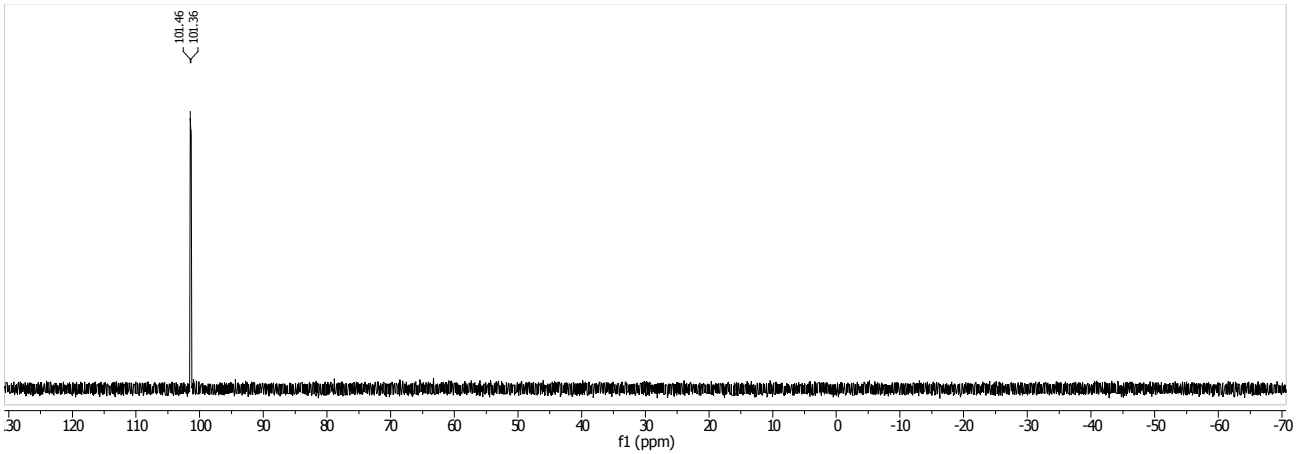

Spectrum 35: ^{31}P{^{1}H}-NMR of **391**

The unit cell obtained from complex **391** contained twelve complexes and is shown in Figure 35, Figure 36 and Figure 37. Schematically, it consisted of layers with four complexes with central mirror point symmetry. These layers are twisted in a helical structure. Between those layers dichloromethane molecules can be observed. It depicts well the problematic nature of such crystalline materials. Instead of forming tightly packed solids, these structures are isolated as layers of monomers which results in the formation of oily sticky material.

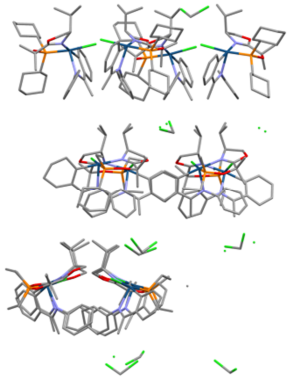

Figure 35: Bottom four complexes in unit cell of iridacycle **391** superimposed

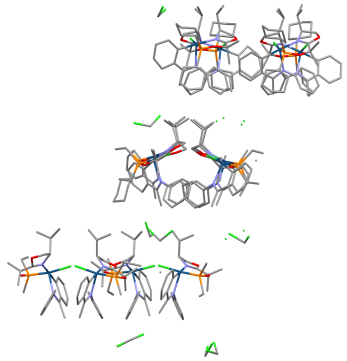

Figure 36: Center four complexes in unit cell of iridacycle **391** superimposed

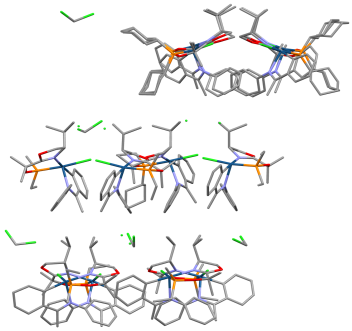

Figure 37: Top four complexes in unit cell of iridacycle **391** superimposed

The quality of the obtained crystals was poor and therefore several restrictions were introduced to solve the structure.[15] When superimposing the three layers and again superimposing these four crystal structures the structure displayed in Figure 38 is obtained. The crystal structure supported the previously postulated structures by NOE NMR experiments. No discussion on bond length or angles is given due to the preliminary character of the structure and the poor data quality. Nevertheless, the same octahedral geometry was observed in all complexes of the unit cell and can thus be confirmed.

All complexes displayed are iridacycles with a hydride-chloride *cis*-relationship. This has not been observed in the literature yet with P'N-ligands but only with NHC-ligands. Otherwise, a hydride and a chloride are usually observed *trans* to each other.[96]

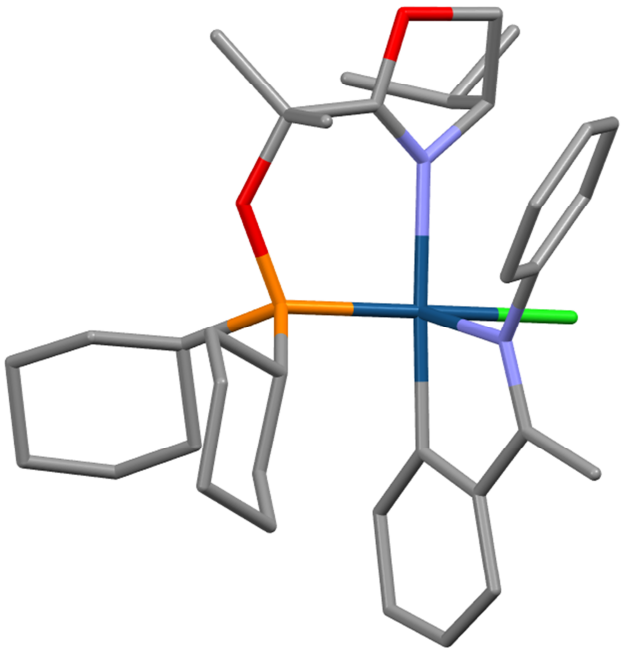

Figure 38: Preliminary crystal structure of iridacycle **391**

[15] Comment from the crystallographer Dr. Markus Neuburger: *„Apart from the fact that diffraction stopped to be observable at quite low Theta values it also seems that they were multiply twinned. The triclinic unit cell did not permit transformation to higher symmetry, even if the structure vaguely suggested the presence of a 3_1 axes as a symmetry element. Attempts to use alternative methods to determine the unit cell, for instance the program "cell_now", always confirmed the strange unit cell with two axes a and b of approximately the same dimension and the angle γ of about 120 degrees, but angles α and β far away from 90 degrees which makes transformation to a higher symmetry impossible. The Z value of the structure is 12. The data quality did not permit to locate all atoms, and like that the refinement finished at some intermediate state. Nevertheless the structure seems to demonstrate that all 12 complex molecules have the same configuration. While all peripheral groups are fuzzy the coordination sphere seems to be determined well enough to identify the compound and confirm its main geometrical features."*

Chiral ligands as cyclometalating reagents

With imine **353** applied as a chiral cyclometalating ligand for imine hydrogenation, selectivities not higher than 6% *ee* were achieved (Table 8). Therefore, a new ligand scaffold was designed. It should resemble the structure of the chiral imines **353** but be more rigid. A connection as shown in red in **353** (Figure 39) was desired. Therefore, an isoquinoline structure with a chiral benzylic position was chosen. The steric hindrance of the chiral imine ligand was increased by the introduction of an isopropyl group at the stereogenic center. The two geminal methyl groups in **392** were incorporated to avoid oxidation and subsequent aromatisation of the isoquinoline.

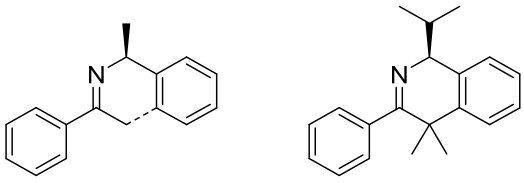

353 **392**

Figure 39: Desired dashed connection in imine **353** leading to isoquinoline ligand **392**

The synthesis of ligand **392** is outlined in chapter 4. Cyclometalation of both enantiomers of ligand **392** proceeded smoothly and afforded an amorphous yellow solid of complex **393** (Scheme 150). The absolute configuration of ligand **392** was not determined. One hydride was observed in solution as shown in Spectrum 36.

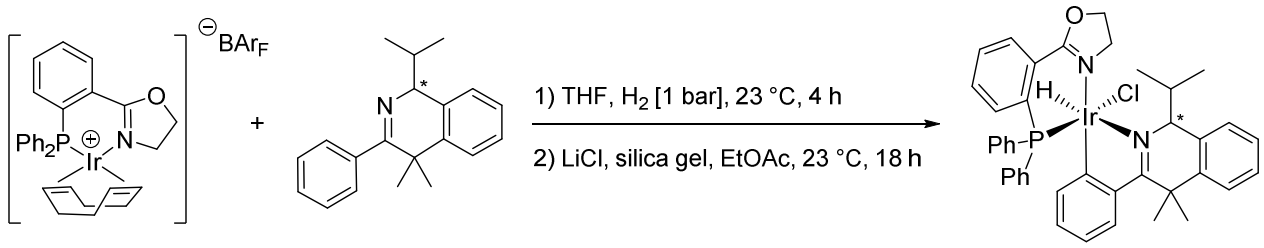

336 **392** **Δ-393**

Scheme 150: Preparation of iridacycle **393**

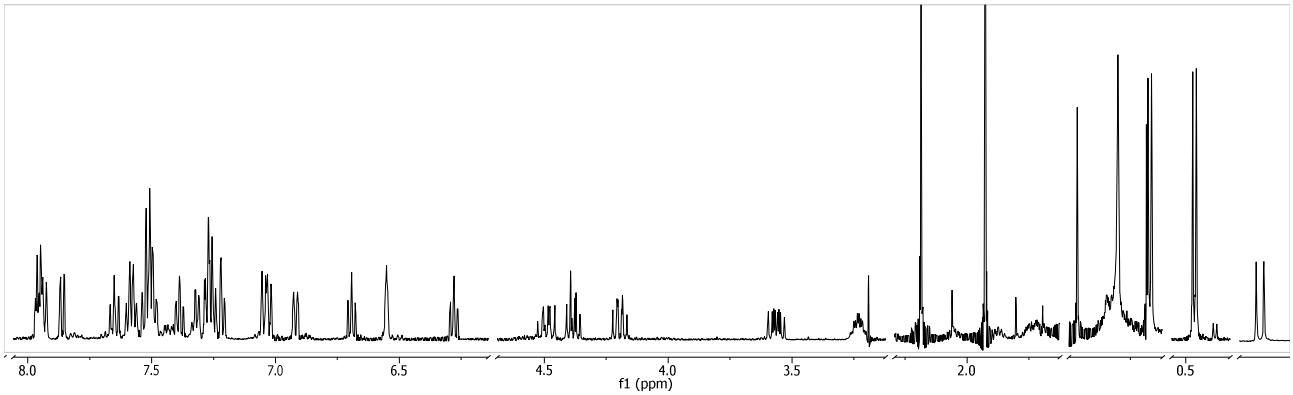

Spectrum 36: ^{1}H-NMR of **393**

Both enantiomers of complexs **393** were tested as catalysts in asymmetric hydrogenation of imine **59.** Both the absolute configuration of ligand **392**, as well as the optical rotation of complexes **393**, was not determined. The optical orientation in brackets refers to the optical rotation of ligand **392**. At 1 bar pressure the enantiodiscriminating role of the cyclometalated ligand was clearly observed (Scheme 151). Similar conversions with opposite but identical enantioselectivity were obtained.

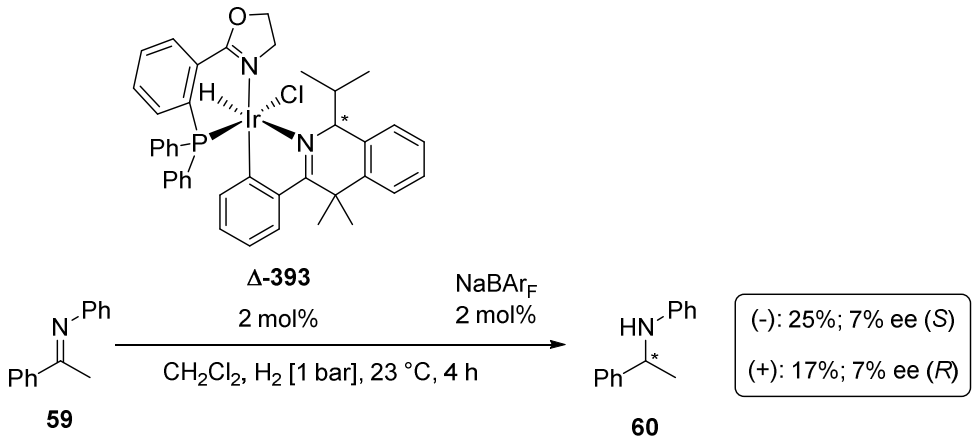

Scheme 151: Asymmetric hydrogenation of imine **59** employing iridacycle **393**

When the reaction was conducted at 5 bar hydrogen pressure, full conversion of the imine was observed. Unfortunately racemic amine was obtained. This is probably due to catalyst decomposition and cyclometalation of imine **59**, thus rendering the catalyst achiral producing racemic amine. With these low conversions and enantioselectivites as well as the postulated decomposition of the complex at elevated pressure the ligand structure was no longer investigated.[16]

In order to obtain higher *ee* values for amine **60** using iridacycle complexes with a chiral imine ligand and an achiral PHOX ligand as catalysts, efforts were devoted to other ligand structures. Two important aspects were maintained. The stereogenic centre is situated in the α-position to the imine nitrogen and the C=N double bond is incorporated into a ring structure to maintain a rigid ligand scaffold. As it was unclear to what extent electronic properties of the ligand would influence the reactivity of the catalyst, Therefore, two structurally analogous ligands **394** and **395** were prepared (Figure 40).

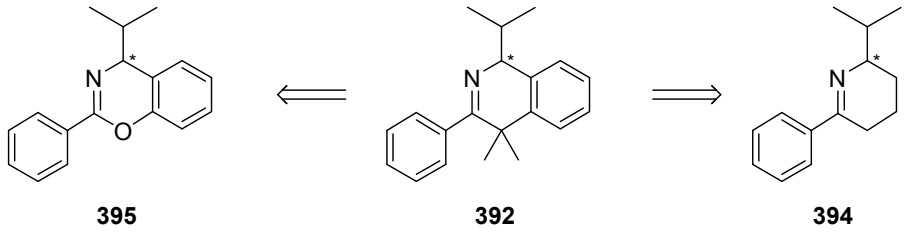

Figure 40: Structurally similar (to **392**) ligands **394** and **395**

The tetrahydropyridine **394** features the same imine C=N double bond as **392** while reducing the sterical demand of the ligand itself. The benzoxazine **395** resembles the isoquinoline **392** structurally but the heterocycle alters the electronic properties of the ligand significantly and thus might strongly influence the reactivity of the catalyst. The synthesis of tetrahydropyridine **394** is outlined in chapter 4. Cyclometalation afforded iridacycle **396** as a yellow amorphous solid after trituration with *n*-pentane (Scheme 152).

[16] The analogous *tert*-butyl variant of ligand **392** precursor was not subjected to enantiomer separation by semi-preparative HPLC.

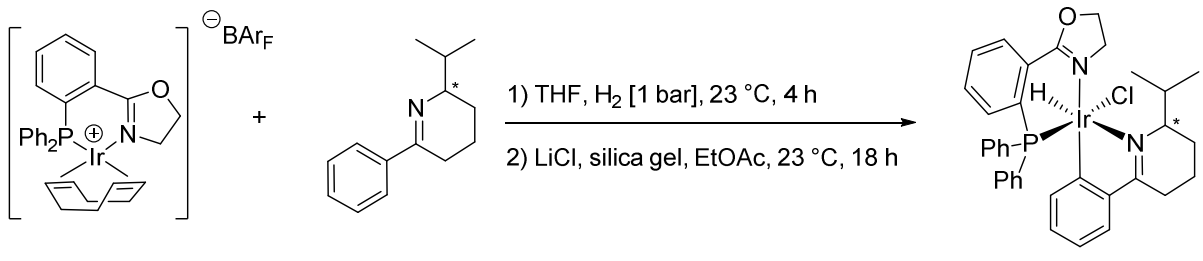

336 **394** **Δ-396**

Scheme 152: Preparation of iridacycle **396**

Similar ^{1}H- and ^{31}P-NMR signals (Spectrum 37 and Spectrum 38) were observed for complexes **396** derived from both enantiomers of **394**. However, the hydride signal was of very low intensity and integrals did not match with other protons in the aliphatic or aromatic region. From the NMR data no conclusions could be drawn.

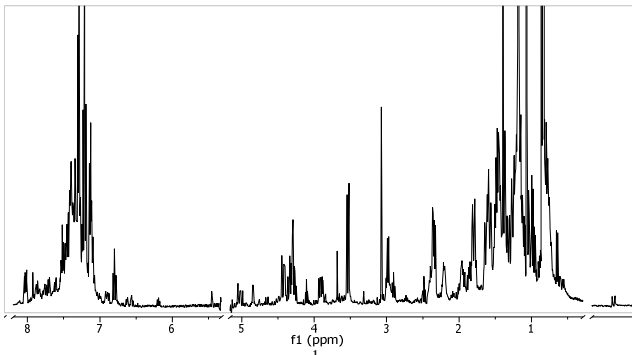

Spectrum 37: ^{1}H-NMR of **396**

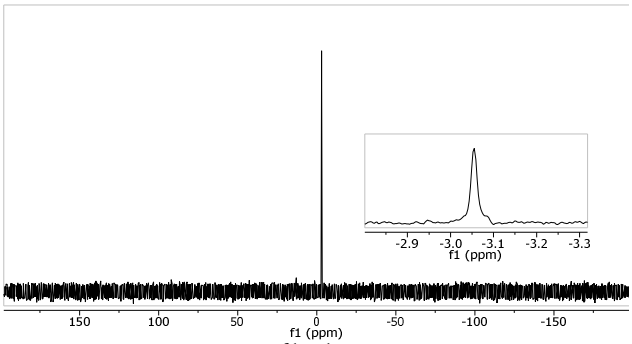

Spectrum 38: ^{31}P{^{1}H}-NMR of **396**

Both enantiomers of complex **396** were tested as catalysts for asymmetric hydrogenation of imine **59** (Scheme 153). The absolute configuration in brackets refers to tetrahydropyridine **394**. In both cases racemic amine was obtained.

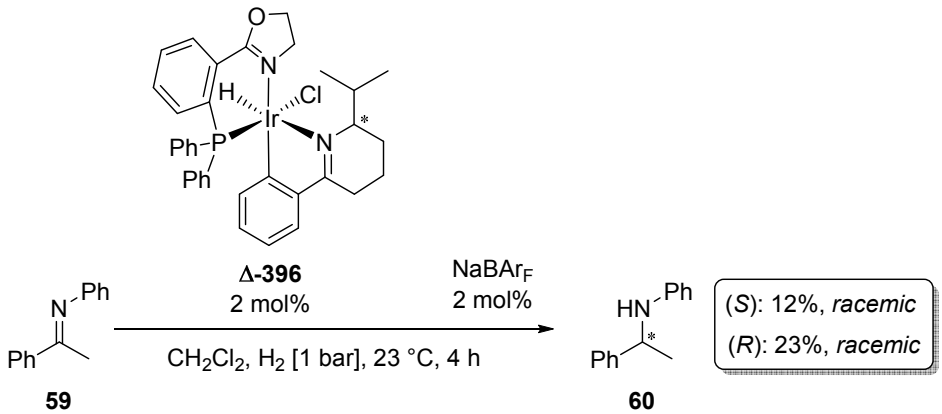

59 **60**

Scheme 153: Asymmetric hydrogenation of imine **59** with iridacycle **396**

The generation of racemic amine could occur for a number of reasons. Most likely, the desired iridacycle **396** has not been formed as the NMR data indicated. Instead, an unidentified iridium complex was applied as the catalyst, or coordination of ligand **394** to the metal centre is labile and thus **394** is readily replaced by **59.** Another possibility is that ligand **394** is too small to induce any enantiodiscrimination in imine hydrogenation when cyclometalated onto iridium.

In order to obtain an idea of the chiral environment around the metal centre, ligand **394** was attempted to cyclometalate onto [Ir(Cp*)Cl]$_2$ **279**. Such Cp*-complexes have been reported on a large variety of imine

ligands which would facilitate comparison with other ligand structures.[17] Therefore, **279** and (*S*)-**394** were mixed to prepare complex **397** (Scheme 154). While NMR analysis showed the formation of a single isomer, crystallisation remained unsuccessful. Instead, a homogeneous solution of a saturated $CHCl_3$/*n*-pentane solution was observed in all attempts. To enforce crystallisation, the cationic hexafluorophosphate complex **398** was prepared. Unfortunately, only black precipitate had formed during the crystallisation period. NMR analysis indicated decomposition and generation of impurities. All other crystallisation attempts failed.

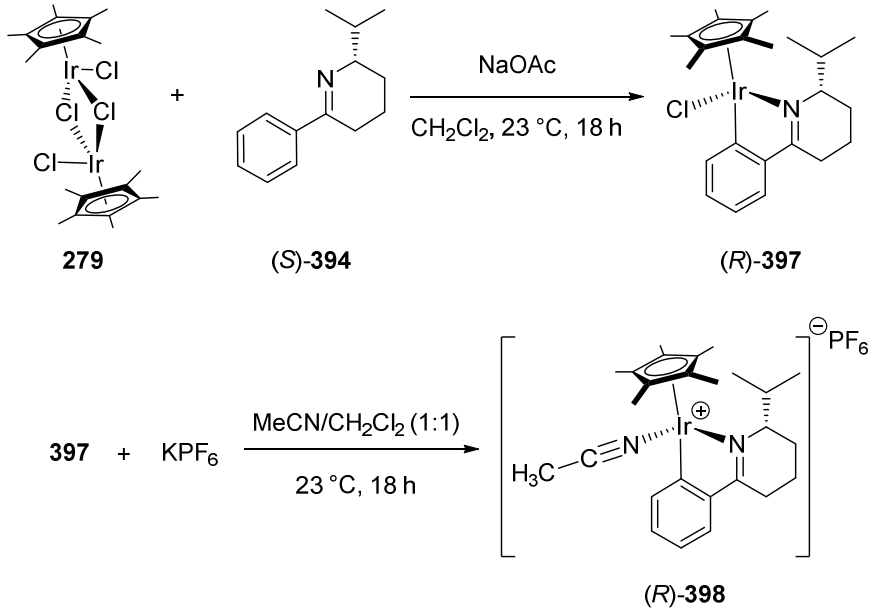

Scheme 154: Preparation of complexes **397** and **398**

Since tetrahydropyridine ligand **394** did not afford the desired iridacycle catalysts which afforded higher *ee*'s in asymmetric imine hydrogenation, efforts were devoted to benzoxazines such as **395** (Figure 41). Syntheses of benzoxazine ligands **395**, **399** and **400** are outlined in chapter 4. With these three benzoxazine ligands it was intended to obtain a better idea of the influence of the substituent at the stereogenic centre in the benzylic position with regards to enantioinduction.

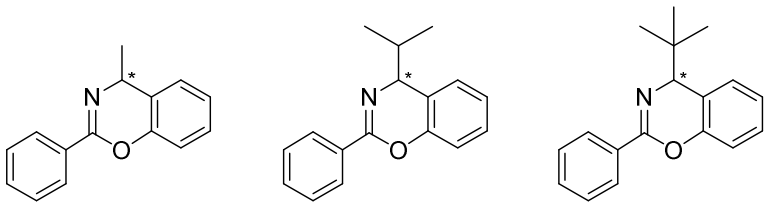

Figure 41: Benzoxazine ligands **395**, **399** and **400**

All six enantiomers were prepared and the corresponding iridacycles **401** to **403** formed (Scheme 155). All iridacycles were obtained as single configurational isomers in solution.

[17] See chapter 1

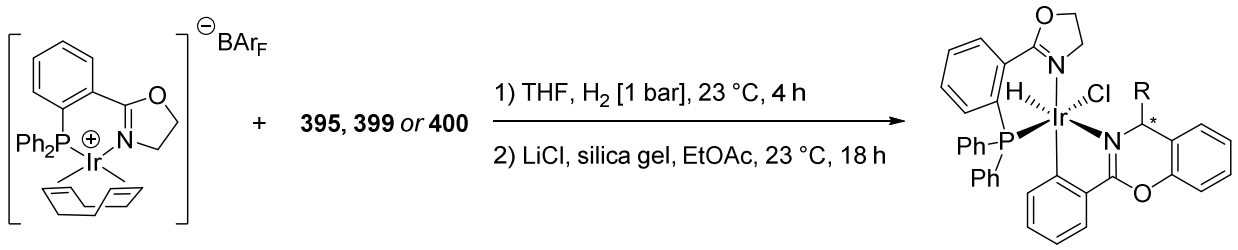

336 **401, 402 *or* 403**

Scheme 155: Preparation of iridacycles **401**-**403**

Iridacycles **401** to **403** (Figure 42) were tested as catalysts for asymmetric hydrogenation of imine **59** (Table 13). [18]

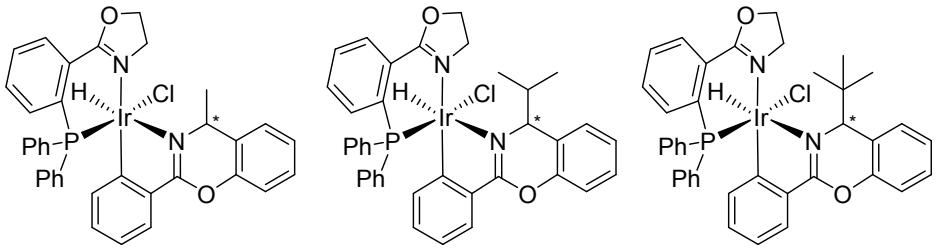

Δ-401 **Δ-402** **Δ-403**

Figure 42: Benzoxazine iridacycles **401**-**403**

Table 13: Asymmetric hydrogenation of imine **59** with iridacycle **401** to **403**

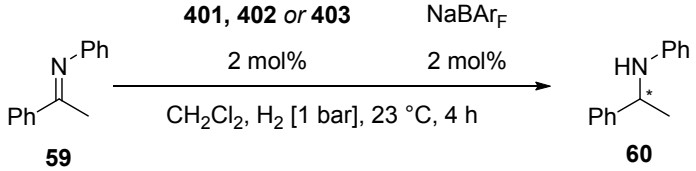

59 **60**

Entry	Catalyst	*p* [bar]	Conv. [%][a]	*ee* [%][b]
1	(+)-**401**	1	63	15 (*S*)
2	(*S*)-(Δ)-**402**	1	31	23 (*R*)
3	(*S*)- (Δ)-**402**	5	97	14 (*R*)
4	(*R*)-(Λ)-**402**	1	20	23 (*S*)
5	(*R*)-(Λ)-**402**	5	>99	14 (*S*)
6	(*S*)-(Δ)-**403**	1	15	17 (*R*)
7	(*S*)-(Δ)-**403**	5	94	2 (*R*)
8	(*R*)-(Λ)-**403**	1	20	16 (*S*)
9	(*R*)-(Λ)-**403**	5	95	5 (*S*)

a) Determined by GC analysis. b) determined by HPLC analysis on a chiral stationary phase.

Several interesting observations were made. The enantioselectivity could be increased when replacing the methyl-substituent in **401** (Entry 1) with a sterically more demanding isopropyl group as in **402** (Entry 2). Consistent enantioselectivities were obtained for both enantiomers of **402** as seen in entries 2-5. However, upon increasing the hydrogen pressure to 5 bar a lower *ee* of 14% was obtained (Entries 3 and 5). And the

[18] The absolute configuration of benzoxazine **399** was not determined. The optical rotation in brackets in Table 13 (Entry 1) refers to the benzoxazine **399** and not to the iridacycle **401**.

sterically even more demanding iridacycle **403** afforded a lower *ee* than **402**. Conducting the reaction at 5 bar hydrogen pressure afforded almost racemic product (Entries 7 and 9).

In order to gain more insight into the catalyst performance of complexes **402** and **403** during the reaction, samples were taken at regular intervals and the *ee* and conversion determined by GC and HPLC analysis. The conversion and enantiomeric excess are displayed in Figure 43.

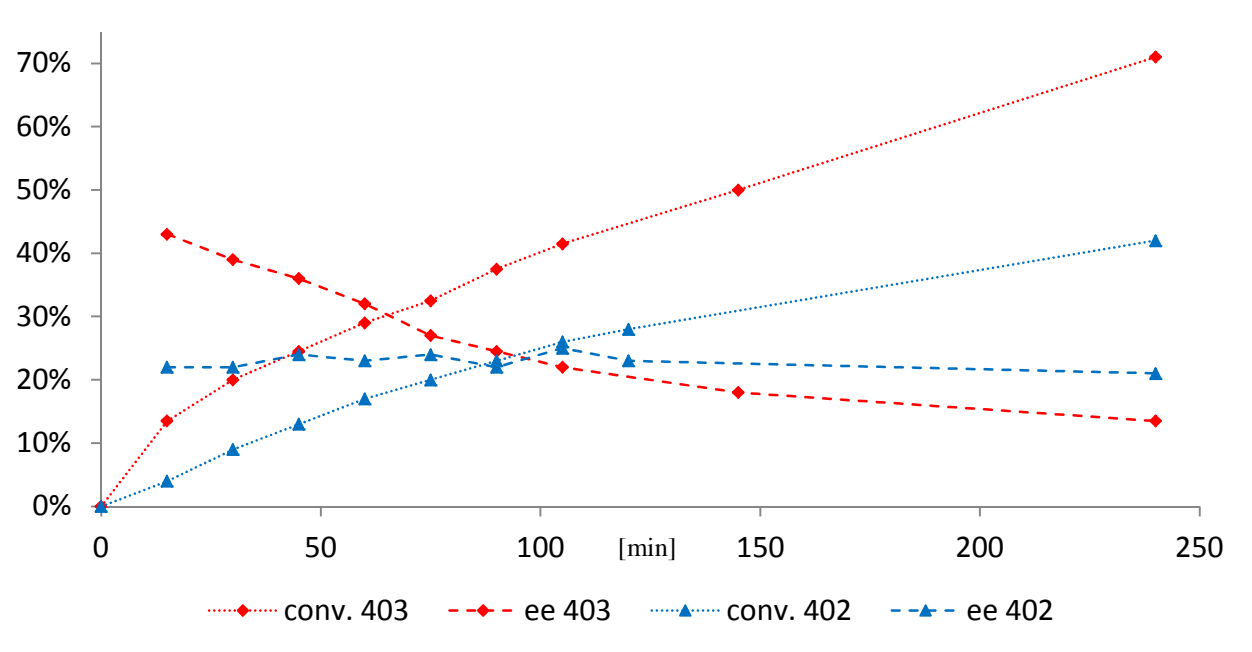

Figure 43: Development of *ee* and conversion over the course of the hydrogenation of imine **59** with **402** and **403**

From the first aliquot of the hydrogenation using **403** as a catalyst, a high *ee* of 44% was detected for both enantiomers. But as the reaction proceeded the enantiomeric excess eroded and flattened to a level of about 12%. This also explained the observed *ee* of 17% which corresponds well to the *ee* between 3 to 4 hours reaction time in the hydrogenation in Table 13.
On the other hand, complex **402** showed a constant *ee* throughout the reaction, within experimental error. Additionally, a lower conversion and reaction rate was observed within the same reaction time. This allows for two significant conclusions: The *tert*-butyl ligand in **403** readily becomes replaced by an achiral ligand which results in a more active achiral catalyst producing racemic amine. This explains the erosion of enantioselectivity. Benzoxazine complexes **402** and **403** are catalytically less active than the iridacycles derived from imines such as **353** or **59.**
The instabilty of the *tert*-butyl benzoxazine complex **403** was also investigated in the hydrogenation of acyclic aliphatic imine **329** (Scheme 156). Imine **329** cannot undergo cyclometalation to form the corresponding iridacycle. Due to rapid decomposition of complex **403** very low conversions of amine **97** were obtained.

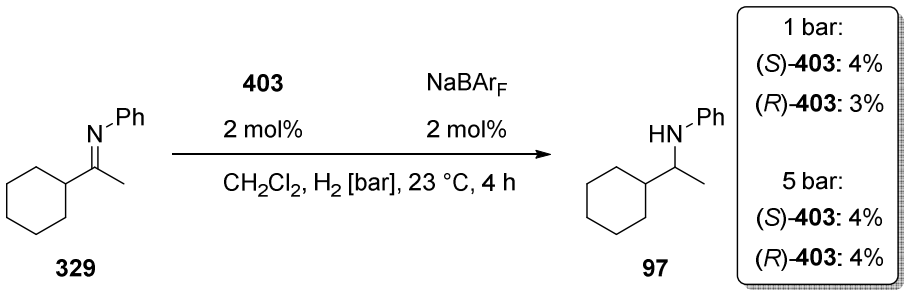

Scheme 156: Asymmetric hydrogenation of imine **329** with iridacycle **403**

In the context of comparing the different imine ligands and their chiral environment upon iridacycle formation, benzoxazine (*S*)-**395** was reacted with $[Ir(Cp^*)Cl_2]_2$ (**279**) to afford complex (*S*)-**404** (Scheme 157). The crystal structure is shown in Figure 44 and Figure 45.

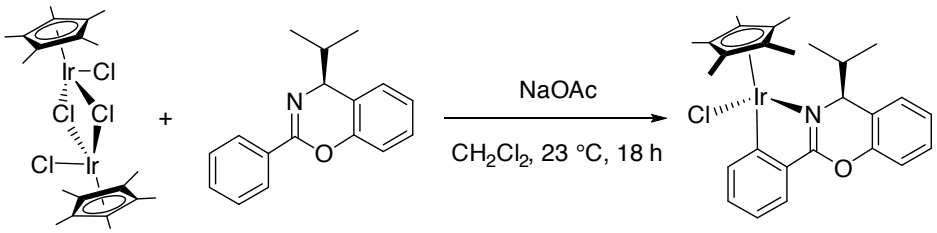

279 (*S*)-**395** (*S*)-**404**

Scheme 157: Preparation of iridium complex (*S*)-**404**

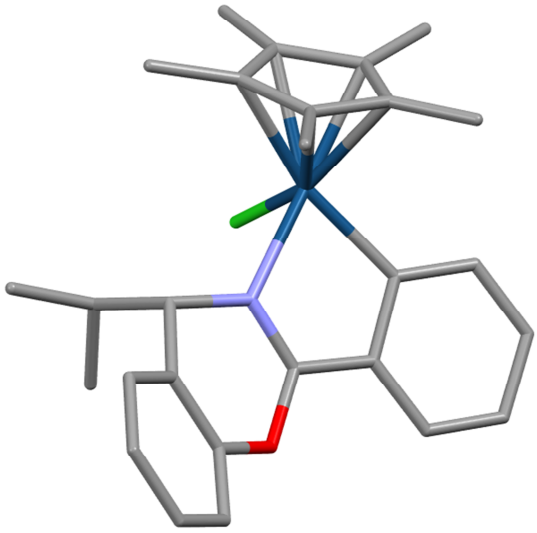

Figure 44: Front view of (*S*)-**404**

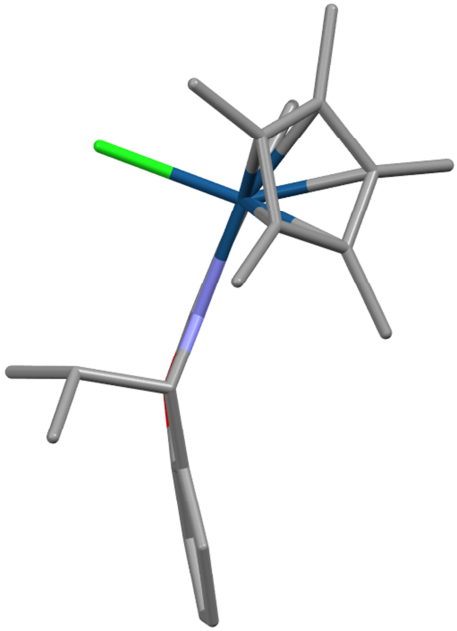

Figure 45: Top view of (*S*)-**404**

Since complex **402** afforded moderate *ee*'s for the asymmetric hydrogenation of imine **59**, benzoxazine **395** was tested as a chiral additive in combination with PHOX catalyst **86** (Scheme 158). Both enantiomers of **395** were cyclometalated onto **86** to identify the match/mismatch case. For comparison, iridacycle **325** is also listed (Table 14).

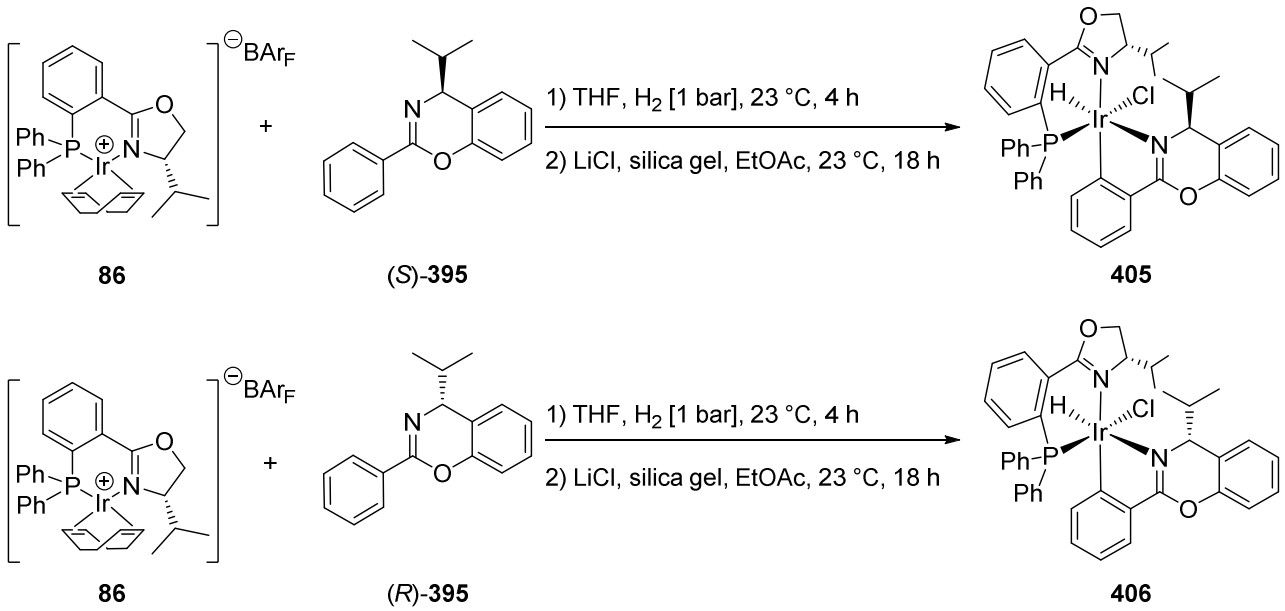

Scheme 158: Preparation of diastereomeric complexes **405** and **406**

Table 14: Asymmetric hydrogenation of imines **325**, **329**, **330** and **331** using diastereomeric benzoxazine iridacycles **405** and **406**

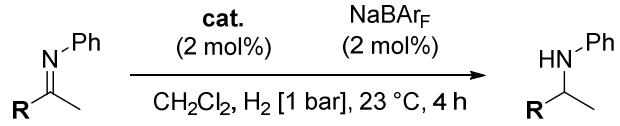

Entry	Catalyst	Imine	Conv. [%][a]	*ee* [%][b]
1	**405**	**329** (R = Cy)	1	-
2	**405**	**330** (R = *i*Pr)	2	-
3	**405**	**331** (R = *n*-Pr)	1	-
4	**405**	**59** (R = Ph)	20	20 (R)
5	**406**	**329** (R = Cy)	4	60 (-)
6	**406**	**330** (R = *i*Pr)	11	54 (-)
7	**406**	**331** (R = *n*-Pr)	19	10 (-)
8	**406**	**59** (R = Ph)	>99	81 (R)
9	**325**	**329** (R = Cy)	13	71 (-)
10	**325**	**330** (R = *i*Pr)	8	60 (-)
11	**325**	**331** (R = *n*-Pr)	10	20 (-)
12	**325**	**59** (R = Ph)	80	87 (*R*)

a) Determined by GC analysis. b) determined by HPLC analysis on a chiral stationary phase.

Complex **406** was identified as the match case and complex **405** as the mismatch case due to the observed reactivity. Nevertheless iridacycle **325** delivers superior results. Therefore, the benzoxazines such as **395** were no longer considered as additional ligands for further reaction condition optimisation.

Effects of chiral Binol-phosphoric acids on imine hydrogenation

The highest *ee*'s in the asymmetric hydrogenation of aliphatic imines to date have been reported by *Xiao* and co-workers.[41] They applied a chiral diamine-Cp* half-sandwich iridium complex with an elaborate chiral Brönsted acid. While the ligand alone did provide the amine in high selectivity with low conversion, addition of a chiral phosphoric acid resulted in high conversion while maintaining the enantioselectivity. The phosphoric acid was postulated to differentiate the prochiral faces of the imine as well as activate the imine by protonation. High selectivities were obtained due to the application of the matched pair of catalyst and iminium activating acid. Chiral phosphoric acids have also been reported to provide enantiomerically enriched amines with high *ee* in asymmetric reductions.[97]
In order to evaluate the potential of chiral phosphoric acids in iridium PHOX catalysed asymmetric imine hydrogenation, two representative chiral phosphoric Brönsted acids **407** and **408** were prepared according to literature procedures (Figure 46). The synthesis is outlined in chapter 4. The chiral phosphoric acids were tested both in combination with chiral complexes **86** and **87** as well as achiral complex **336** (Table 15).

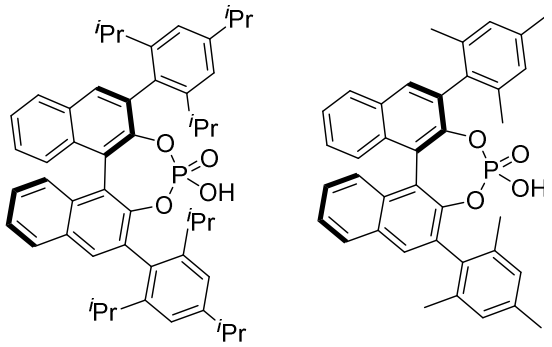

(*R*)-**407** (*R*)-**408**

Figure 46: Chiral phosphoric acids **407** and **408**

The addition of a catalytic amount of phosphoric acid **407** in combination with chiral catalyst **86** afforded amine **60** in only 11% conversion and 82% *ee*. While the *ee* is slighty lower than using **86** alone, the poor conversion was surprising. If the reaction was carried out at 50 bar hydrogen pressure, 93% conversion and 78% *ee* were observed. To test the chiral induction potential of the phosphoric acids **407** and **408** alone they were used along with complex **336**. Very poor conversion and low enantioselectivity were observed. At atmospheric hydrogen pressure only one to two turnover numbers (TON) were achieved.[19][98] This is in strong contrast to using complex **86** without **407** or **408** resulted in full conversion within 2 hours at 1 bar.

[19] Complex **336** was demonstrated to be less active compared to **86** or **348**

Table 15: Asymmetric hydrogenation of imine **59** employing combinations of iridium complexes **86**, **87** or **336** with **407** or **408**

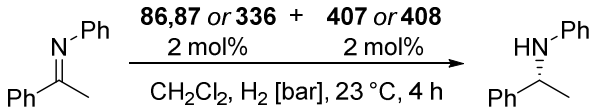

59 **60**

Entry	Catalyst	Acid	Solvent	*p* [bar]	Conv. [%][a]	*ee* [%][b]
1	**336**	(*R*)-**408**	CH_2Cl_2	1	2	9 (*R*)
2	**336**	(*R*)-**407**	CH_2Cl_2	1	2	5 (*R*)
3	**336**	(*R*)-**408**	CH_2Cl_2	50	49	2
4	**336**	(*R*)-**407**	CH_2Cl_2	50	52	2
5	**86**	(*R*)-**407**	CH_2Cl_2	1	11	82 (*R*)
6	**86**	(*R*)-**408**	Toluene	1	10	70 (*R*)
7	**86**	(*R*)-**408**	Toluene	50	93	78 (*R*)
8	**86**	(*R*)-**407**	CH_2Cl_2	1	7-11	82 (*R*)
9	**86**	(*R*)-**407**	CH_2Cl_2	50	92	78 (*R*)
10	**87**	(*R*)-**408**	CH_2Cl_2	1	3	-
11	**87**	(*R*)-**408**	CH_2Cl_2	50	88	87 (*R*)
12	**87**	(*R*)-**407**	CH_2Cl_2	1	1	-
13	**87**	(*R*)-**407**	CH_2Cl_2	50	86	88 (*R*)
14	**87**	(*R*)-**407**	Toluene	1	3-6	-
15	**87**	(*R*)-**407**	Toluene	50	71-88	80 (*R*)

a) Determined by GC analysis. b) determined by HPLC analysis on a chiral stationary phase.

The results did not fit any obvious trend. In order to better understand the role of the phosphoric acid, different catalyst loadings were examined (Table 16). Increased quantities of phosphoric acid resulted in lower conversion as well as hydrolysis of imine **59** in CH_2Cl_2 (Entries 1 to 12). In toluene, hydrolysis appears to be less pronounced. Furthermore, with high loadings of phosphoric acid, no effect on the enantioselectivity was observed and hydrolysis remained dominant. Apparently, chiral phosphoric acids alone did not exhibit significant enantiodiscrimination when being used along with an achiral catalyst such as **86**. In combination with an iridium PHOX catalyst hydrolysis was favoured over hydrogenation even at high pressure. The difference between the **407** and **408** with regards to enantioselectivity can be neglected. Therefore, the effect of chiral phosphoric acids was no longer investigated.

Table 16: Asymmetric hydrogenation of imine **59** employing combinations of iridium complexes **336** with **407** or **408**

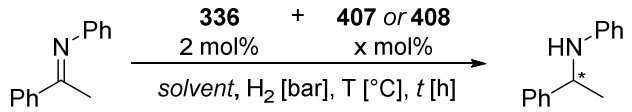

59 **60**

Entry	Acid	Acid [mol %]	Solvent	*p* [bar]	*t* [h]	Conv. [%][a]	Amine [%]	*ee* [%][b]
1	**407**	1	CH_2Cl_2	50	2	36	n.d.	*rac*.
2	**407**	2	CH_2Cl_2	50	2	15	n.d.	*rac*.
3	**407**	5	CH_2Cl_2	50	2	7	n.d.	*rac*.
4	**407**	10	CH_2Cl_2	50	2	5	n.d.	6
5	**408**	1	CH_2Cl_2	50	12	>99	97	*rac.*
6	**408**	2	CH_2Cl_2	50	12	98	89	*rac.*
7	**408**	5	CH_2Cl_2	50	12	73	54	*rac.*
8	**408**	10	CH_2Cl_2	50	12	67	49	*rac.*
9	**407**	1	CH_2Cl_2	50	12	74	62	*rac.*
10	**407**	2	CH_2Cl_2	50	12	62	36	*rac.*
11	**407**	5	CH_2Cl_2	50	12	37	1	n.d.
12	**407**	10	CH_2Cl_2	50	12	53	1	n.d.
13	**408**	1	toluene	50	12	>99	93	*rac.*
14	**408**	2	toluene	50	12	59	37	3
15	**408**	5	toluene	50	12	48	20	7
16	**408**	10	toluene	50	12	43	13	10
17	**407**	1	toluene	50	12	>99	52	*rac.*
18	**407**	2	toluene	50	12	67	38	12
19	**407**	5	toluene	50	12	82	30	20
20	**407**	10	toluene	50	12	>99	20	20
21	**408**	10	toluene	100	24	52	18	12
22	**408**	20	toluene	100	24	55	15	18
23	**408**	30	toluene	100	24	69	16	18
24	**408**	40	toluene	100	24	82	17	n.d.
25	**407**	10	toluene	100	24	50	16	*rac.*
26	**407**	20	toluene	100	24	62	13	*rac.*
27	**407**	30	toluene	100	24	74	12	*rac.*
28	**407**	40	toluene	100	24	75	12	*rac.*

a) Determined by GC analysis. b) determined by HPLC analysis on a chiral stationary phase.

Deuterium labelling studies

F. Barrios had investigated imine hydrogenation by deuterium labelling experiments to better understand the hydride transfer process in the catalytic cycle. As one would expect introduction along the C=N double bond, incorporation of deuterium in the α-position should be observed to a very high extent. A deuterium incorporated at the nitrogen atom would be exchanged during workup. However, the observed deuterium incorporation at the methyl position was contradictory to a simple H_2 addition across the C=N double bond.[20] Since inconsistent numbers were obtained by *F. Barrios*, deuteration experiments were repeated using different iridacycle catalysts (Table 17). Imine **322** was chosen to additionally study the stability of the iridacycle catalysts. GC analysis would depict even trace amounts of imine **59** or amine **60**.

Table 17: Asymmetric hydrogenation of imine **322** with iridacycles **325**, **391** and **403**

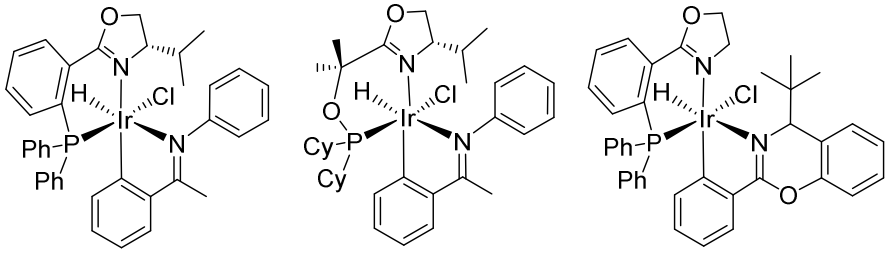

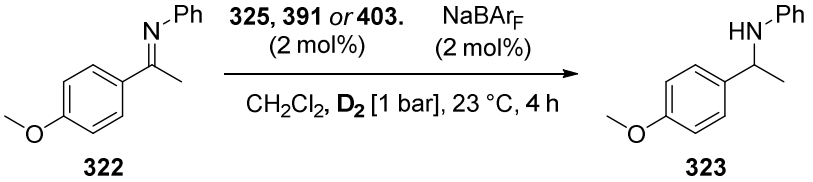

322 323

Entry	Catalyst	*ortho* [% D]	α [% D]	Methyl [% D]	Conv. [%][a]
1	**325**	0	41	13	>99
2	**325**	0	48	17	>99
3	**391**	10	55	0	>99
4	**391**	25	55	0	>99
5	**391**	25	58	0	>99
6	**391**	50	50	0	>99
7	**403**	5	35	17	>99
8	**403**	9	41	20	>99
9	**403**	12	43	22	>99
10	**403**	20	48	24	>99

a) Determined by GC analysis.

Quite large discrepancies were observed over the course of four setups. Whereas **325** did not show any incorporation at the *ortho*-position (Entries 1 and 2), the analogue **391** did not show any incorporation at the methyl position (Entries 3 to 6). With **391**, substitution of imine **59** by (most likely) imine **322** was observed by detection of **59** and **60** in GC analysis after the reaction. No aliquot analysis during the reaction was conducted. Whether such a replacement had happened during the reaction or after full conversion of imine **322** was not clear. However the large amount of deuterium-incorporation in the *ortho*-position is supportive

[20] See chapter 2

of rapid reversible amine cyclometalation indicating such a substitution after the reaction. No reversible cyclometalation was observed with **325**. The lack of deuterium incorporation at the *ortho*-position with **325** was in contrast to previously obtained results by *F. Barrios*. Complex **403** was demonstrated to decompose under hydrogenation conditions. Therefore, these results are not interpreted.

The low extent of deuterium incorporated at the α–position in the hydrogenation with deuterium was somewhat contradictory. Where else would a deuterium atom be incorporated? Where would a proton under deuteration conditions originate from? An issue in experiments with **59**-CD_3 labelled and **59**-d_{13} labelled imine were trace amounts of residual KO^{t}Bu used in the preparation of these deuterated imines.[21] Hydrogenations of these substrates gave brownish coloured reaction mixtures. Residual KO^{t}Bu possibly biased the outcome of these reactions. On the other hand, no such phenomena were observed with **59**-d_{10}.

All experiments by *F. Barrios* were re-examined. Instead of iridium complex **86**, iridacylce **325** was used as the catalyst in combination with an equimolar amount of $NaBAr_F$. Primarily, deuterium labelled derivatives of imine **59** (**59**-CD_3, **59**-d_{10} and **59**-d_{13}) were subjected to hydrogen gas (Scheme 159).

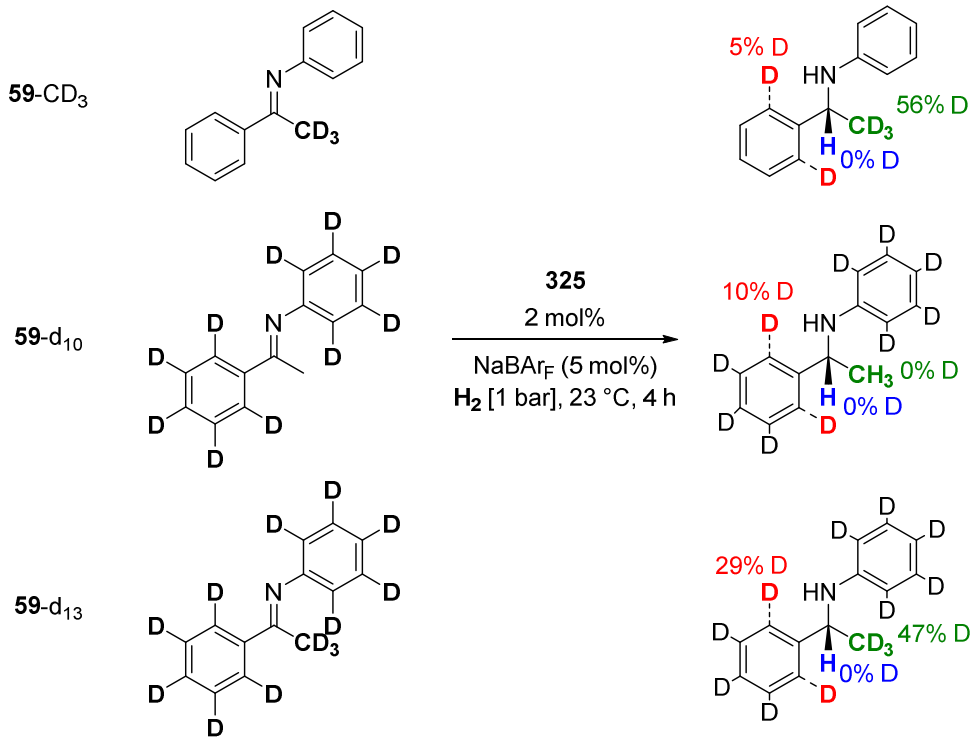

Scheme 159: Re-examination of deuterium labelling experiments previously conducted by *F. Barrios*

In all three cases, no deuterium incorporation at the α–position was observed. This is consistent with dihydrogen being added across the C=N double bond. Moreover, **59**-CD_3 as well as **59**-d_{13} displayed about 50% residual deuterium incorporation (by ^{1}H-NMR). This might originate from imine-enamine tautomerism prior to catalytic reduction. The incorporation of deuterium in the *ortho*-position in **59**-CD_3 demonstrates that the deuterium is transferred from the methyl position to the *ortho*-postion to a small extent. While 44% of deuterium was removed from the methyl group, only 5% could be found in the molecule. Apparently the rest was removed from the molecule to an unknown destination.

When evaluating the corresponding hydrogenation with D_2, conclusions are diffuclt to draw (Scheme 160). In the case of **59**-CD_3, deuterium incorporation at the α-position occurred to a large extent of 80%. However, only 80% residual deuterium incorporation at the methyl position was observed. On the other hand,

[21] Labelled imines were isolated by Kugelrohr distillation.

deuteration of **59**-d_{10} afforded 50% deuterium incorporation at the α-position and 20% at the methyl position. Obviously, the protons from the methyl group were partially transferred to the α-position. Another possibility is the presence of the enamine tautomer in the catalytic cycle. The final experiment with **59**-d_{13} raised some significant questions: How can one observe hydrogen incorporation when conducting hydrogenation with D_2 on a fully deuterated substrate? The origin of hydrogen in such a setup could not be explained. The glass surface of the reaction vial might be possible origin of protons. Such a situation has been observed in studies of trifluoroborate coupling reagents.[99] However this was not investigated in detail and remains speculative.

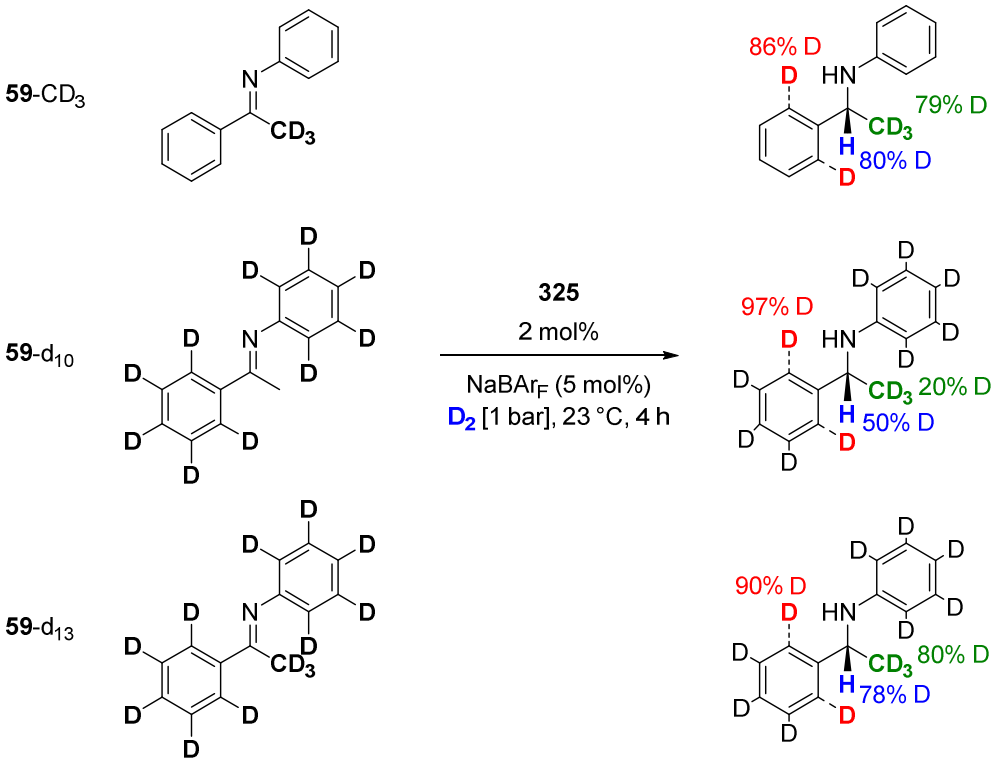

Scheme 160: Deuterium labelling experiments with partially labelled variations of imine **59**

In order to gain further insight into the role of the iridacycle catalyst in such labelling experiments, a labelled derivative of **325** was prepared (Scheme 161). NMR analysis revealed hydrogen incorporation of about 30% in the hydride ligand. Furthermore, about 30% deuterium incorporation was observed at the methyl position of the cyclometalated imine **59**-d_{10} (Spectrum 39 and Spectrum 40). Other sources of hydrogen can be excluded since the reaction was set up under inert conditions and 99.99% Deuterium gas quality was used.

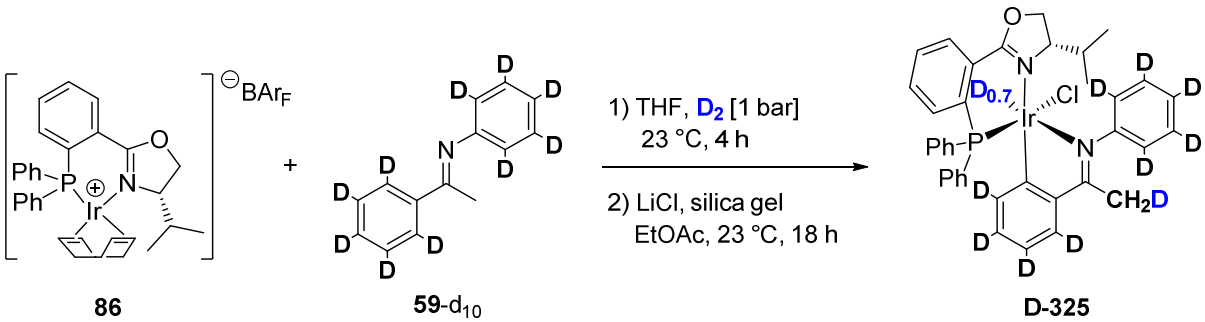

86 **59**-d_{10} **D-325**

Scheme 161: Preparation of iridacycle **325** bearing a deuterium-labelled imine ligand

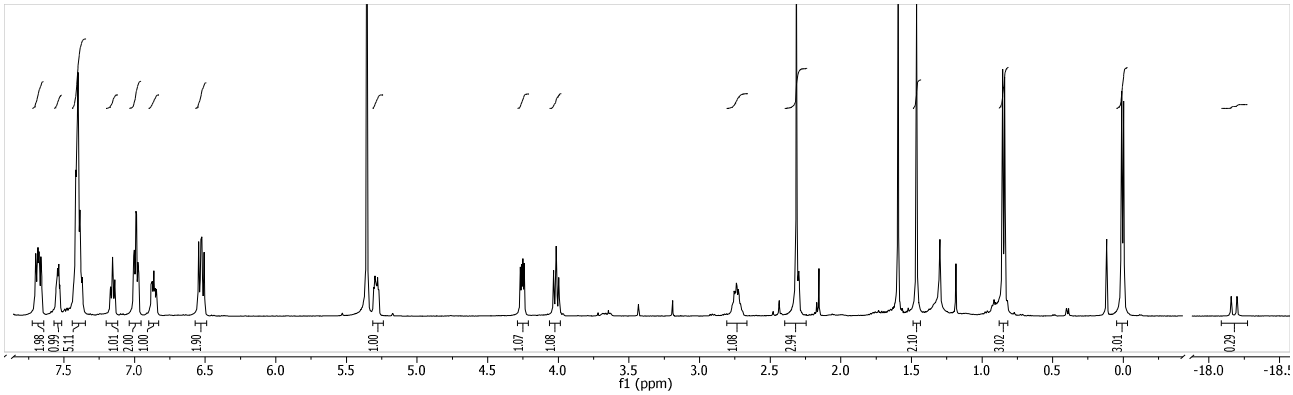

Spectrum 39: ^{1}H-NMR of labelled **325**

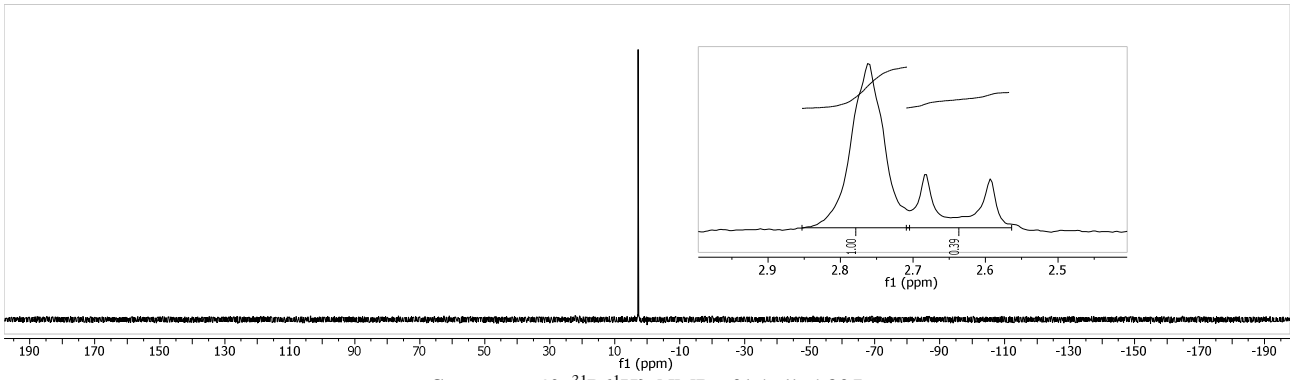

Spectrum 40: ^{31}P{^{1}H}-NMR of labelled **325**

This experiment demonstrated that already during cyclometalation an exchange between the protons of the methyl group and the hydride is occurring. In order to observe such an exchange process also in the course of a hydrogenation, imine **59** (Scheme 162) was analysed by collection of aliquots.

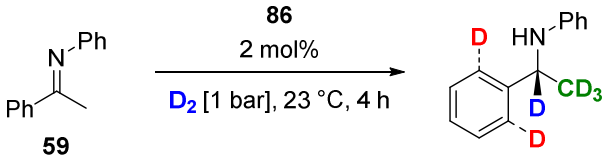

Scheme 162: Deuteration of imine **59** with **86** for aliquot analysis

Spectrum 41 displays the incorporation of deuterium over time. While the deuterium-incorporation at the methyl position (green) and the α-position (blue) remains constant, the erosion of hydrogen content in the *ortho*-position can be depicted (red). Unfortunately this experiment did not deliver the desired information about possible exchange between the methyl-protons and the hydride, since the amine was demonstrated to remain unaffected in the presence of the catalyst.

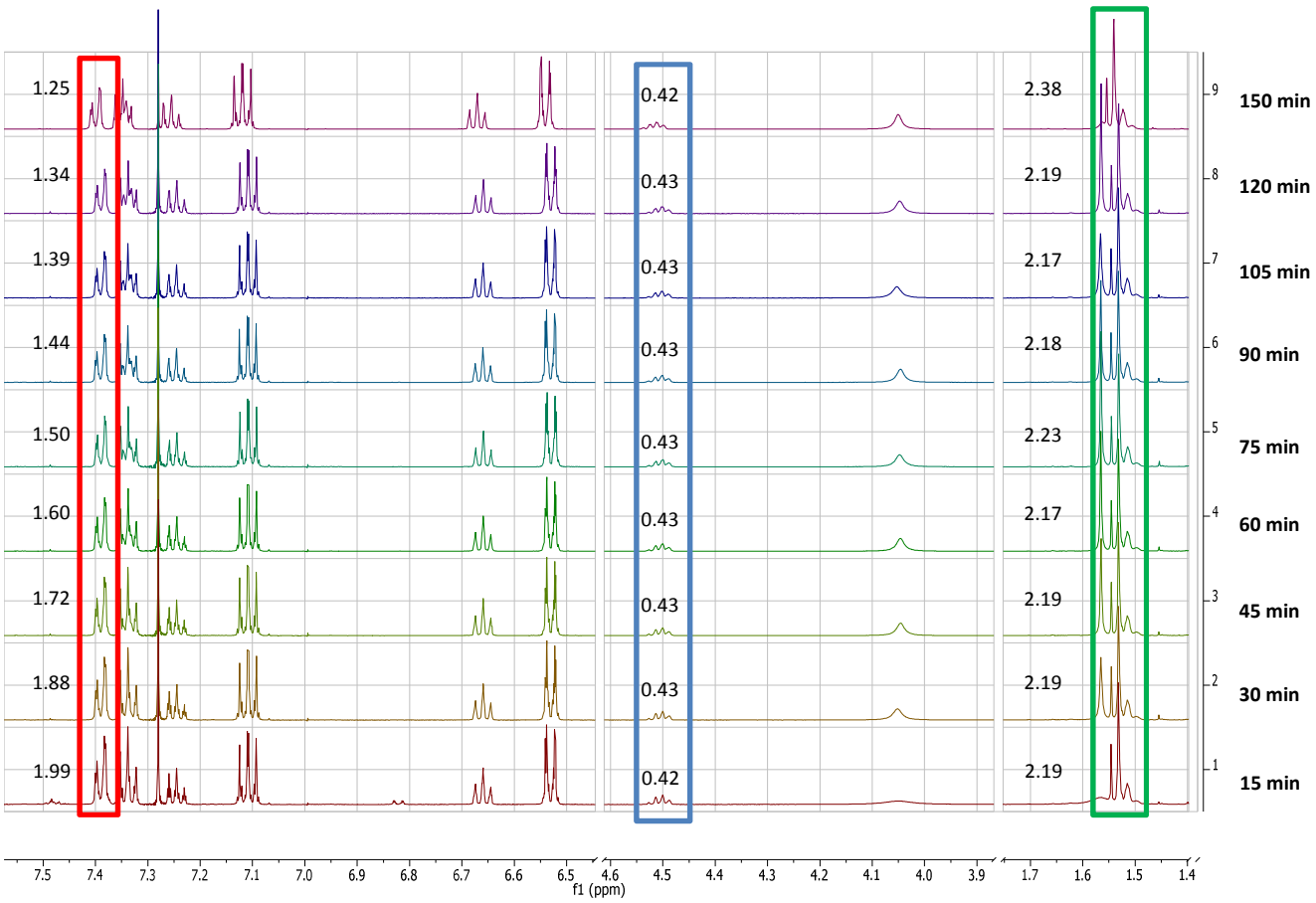

Spectrum 41: ^{1}H-NMR traces of the hydrogenation shown in Scheme 162; methyl group (green), *ortho*-Aryl (red), α-position (blue)

On the other hand, the reaction with H_2 and **59**-d_{10} (Scheme 163) revealed several important features. While progressive incorporation of hydrogen at the *ortho*-position (red) can be explained by reversible cyclometalation of the product amine, incorporation of hydrogen remained constant at both the α- (blue) and the methyl position (green) (Spectrum 42).

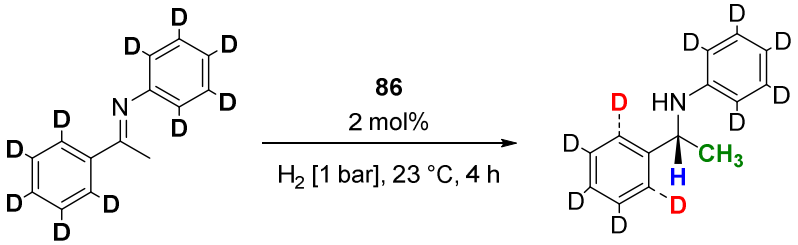

59-d_{10}

Scheme 163: Hydrogenation of imine **59**-d_{10} with **86** for aliquot analysis

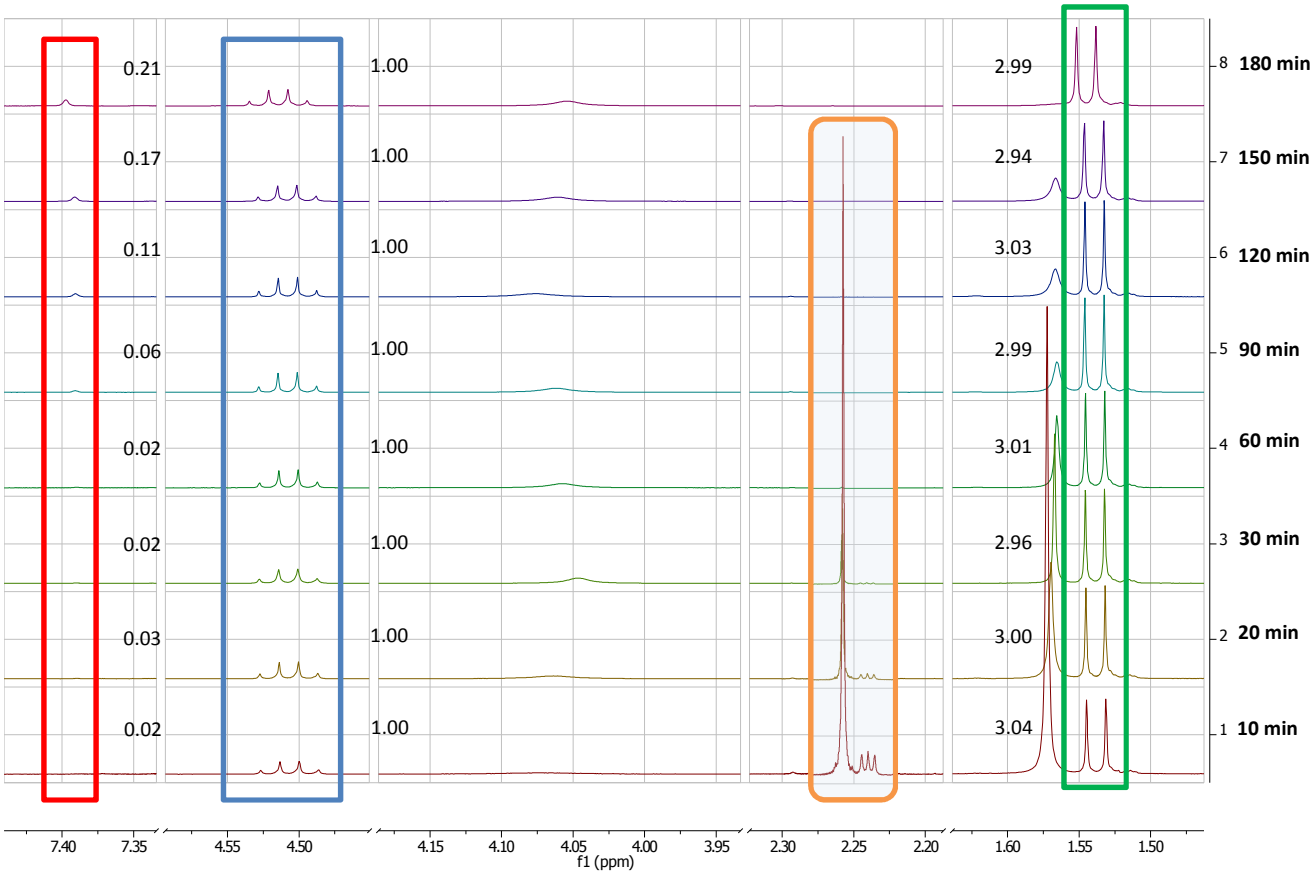

Spectrum 42: ^{1}H-NMR traces of the hydrogenation shown in Scheme 163; methyl group (green), *ortho*-Aryl (red), α-position (blue)

When taking a closer look at the orange frame, partially Me-labelled **59**-d_{10} can be observed. The amount of Me-labelled **59**-d_{10} was about 13% and remained constant in the aliquots taken after 10, 20 and 30 minutes. Imine was no longer detected after 60 minutes. Therefore, incorporation of deuterium is occurring prior to catalysis and possibly involves the transfer of the deuteride from the *ortho*-position to the methyl position of the substrate. However, in the chosen setup of Scheme 163 it does not affect the overall label incorporation significantly.

These experiments demonstrate that addition of hydrogen occurs along the C=N double bond. Minor isomerisation processes prior to hydrogenation strongly affect the extent of incorporation and thus bias results in a way that interpretation becomes very difficult.

Stochiometric Hydride Transfer studies

In previous experiments it was demonstrated that addition of $NaBAr_F$ is necessary to generate the active catalyst in solution from iridacycle **325**. In order to gain an understanding of the structure in solution, chloride abstraction was studied in NMR experiments. Therefore, iridacycle **325** and $NaBAr_F$ were dissolved in CD_2Cl_2 to generate **308** (Scheme 164).

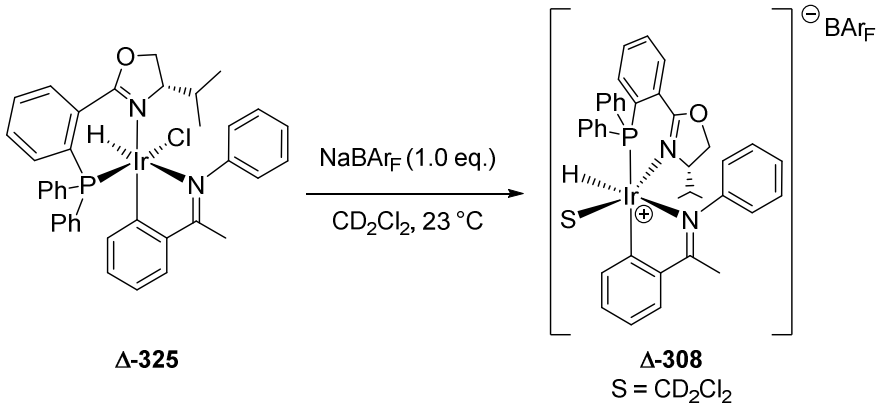

Δ-325 **Δ-308** S = CD_2Cl_2

Scheme 164: Generation of complex **308** in solution

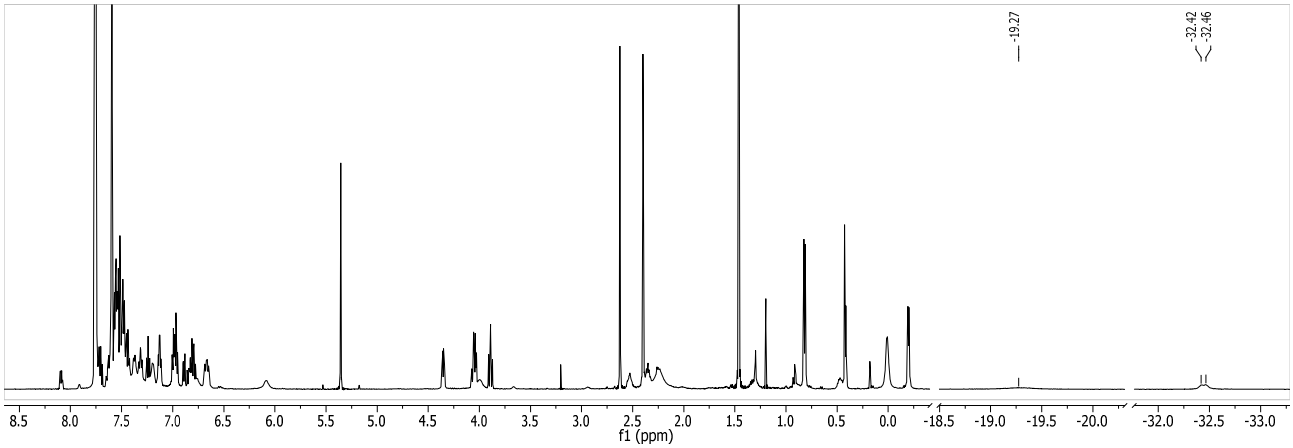

Spectrum 43: ^{1}H-NMR of **308**

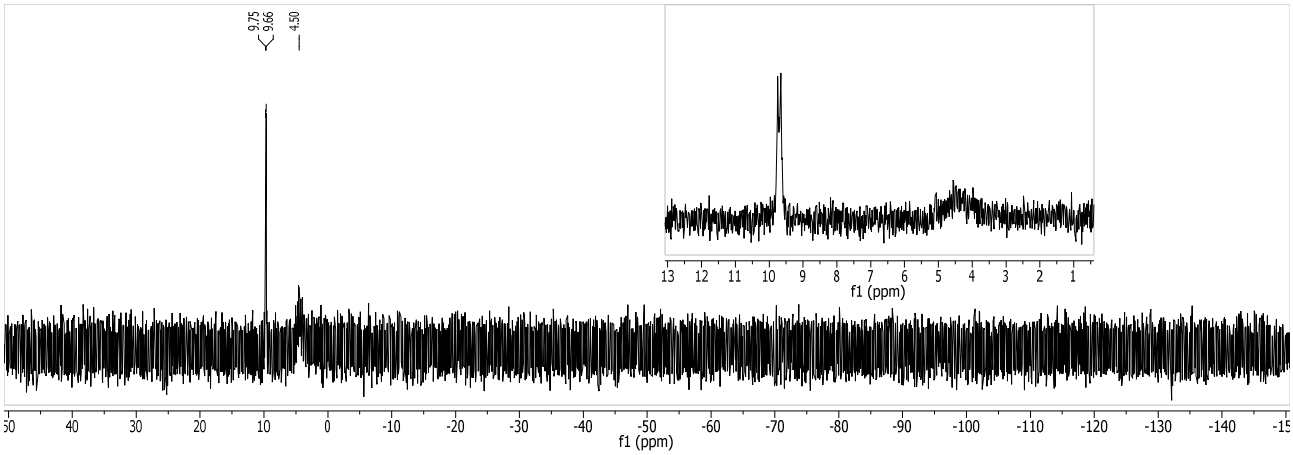

Spectrum 44: $^{31}P\{^1H\}$-NMR of **308**

Spectrum 43 and Spectrum 44 depict two configurational isomers of **308** in solution. CH_2Cl_2 is known to coordinate to iridium centres but in a weak fashion.[22] Therefore, isomers of the iridium complex in solution

[22] See chapter 1 (introduction)

as well as interconverting species can be present. No EXSY signals could be observed with mixing times up to 750 ms. Judging from the chemical shifts of the hydrides, in one case the hydride is situated *trans* to a weak donor such as the nitrogen of the oxazoline or the imine. In the other case, the high field resonance indicates its orientation *trans* to an empty coordination site.

A different picture is obtained when chloride abstraction is conducted in THF (Scheme 165). One single configurational isomer of **308** is observed in solution (Spectrum 45 and Spectrum 46) which depicts similar NOE contacts to the previously characterised complex by *F. Barrios*. The *N*-phenyl ring is experiencing hindered rotation as observed by EXSY signals.

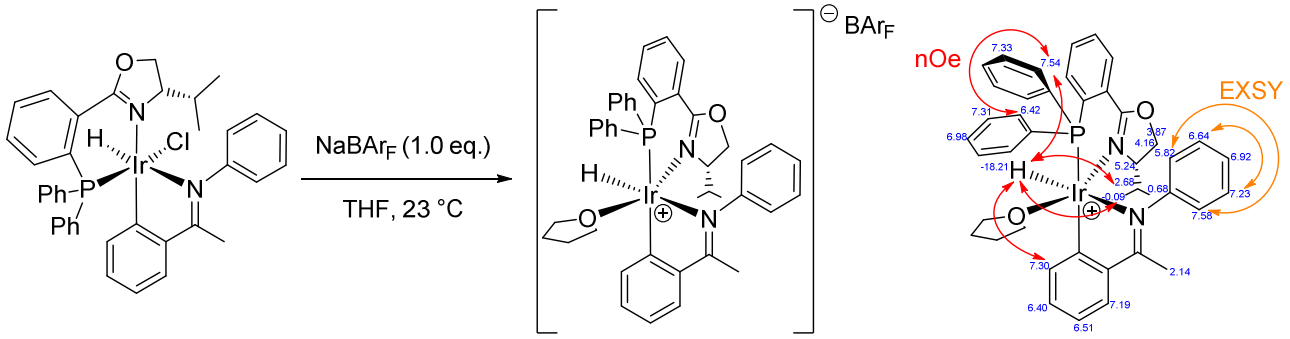

Scheme 165: Generation of complex **308** in solution, key NOE contacts depicted on the right

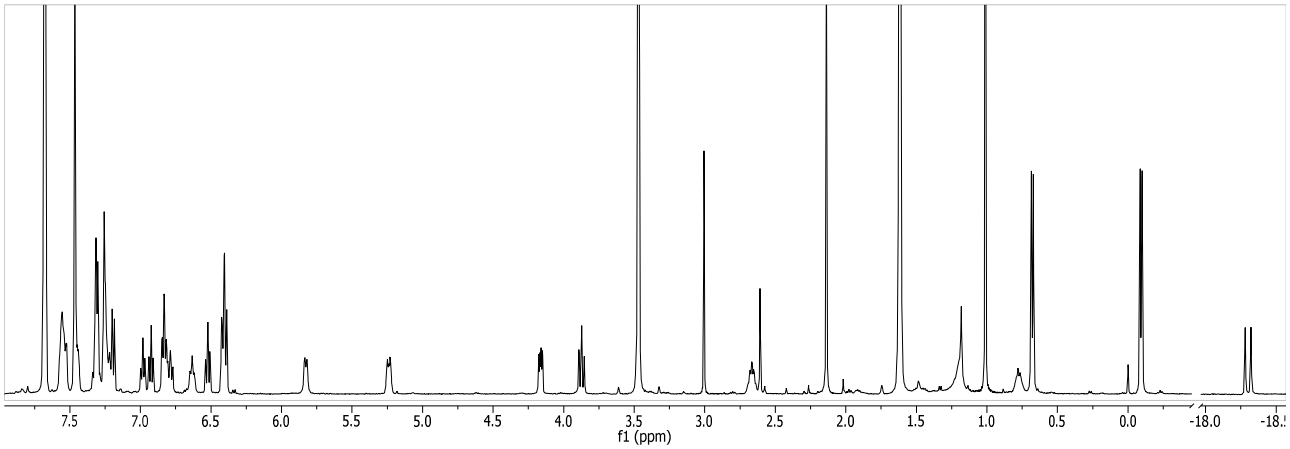

Spectrum 45: ^{1}H-NMR of **308**

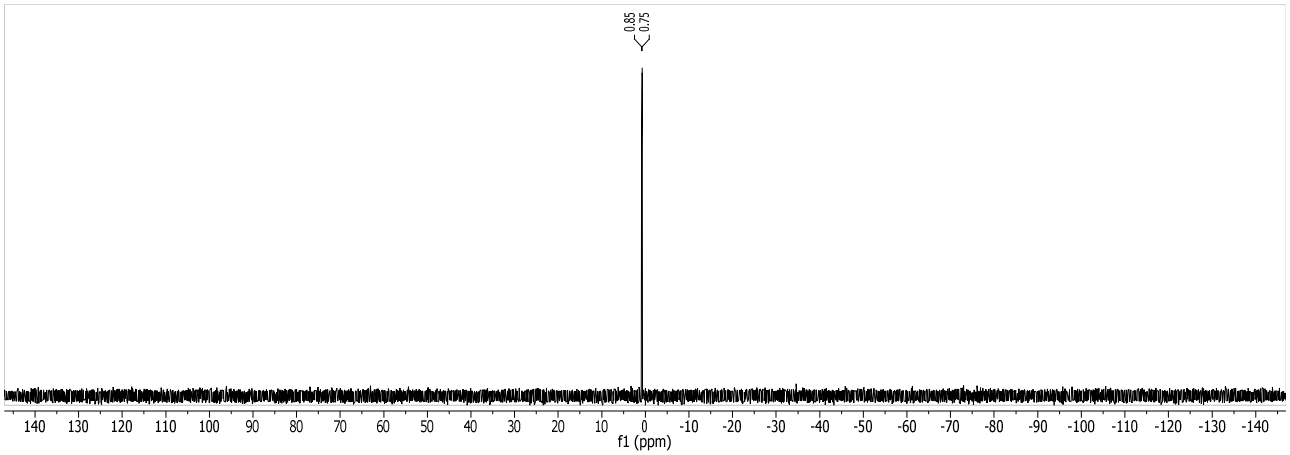

Spectrum 46: ^{31}P{^{1}H}-NMR of **308**

While chloride abstraction afforded two configurational isomers of **308** in CH_2Cl_2 and one isomer in THF, the catalytic reaction is only observed in CH_2Cl_2 at room temperature. This would allow the study of the hydride transfer of "naked" complex **308** in the presence of imine **59.**

Iridacycle **325**, $NaBAr_F$ and **59**-^{15}N were added to a Young's NMR tube and dissolved in CD_2Cl_2. Iridacycle **325** shows one ^{1}H-NMR hydride doublet signal at -18.2 ppm and one ^{31}P-NMR singal at 2.63 ppm. Upon dissolution in CD_2Cl_2, those signals are no longer observed. After 30 minutes, four hydride signals can be observed, all of them doublets (Spectrum 47). Thus the coupling constant between the ^{1}H-hydride and the ^{15}N of the imine is too small to be observed. On the other hand, the $^{31}P\{^1H\}$-NMR depicts doublets of doublets which are indicative of the coupling to both the hydride and the imine nitrogen atom (Spectrum 48). The signals in the blue frame are of specific interest. Since the $^{31}P\{^1H\}$-NMR depicts doublets of doublets and the signal is only observed for a limited amount of time, it was assigned to complex **409** (Scheme 166).

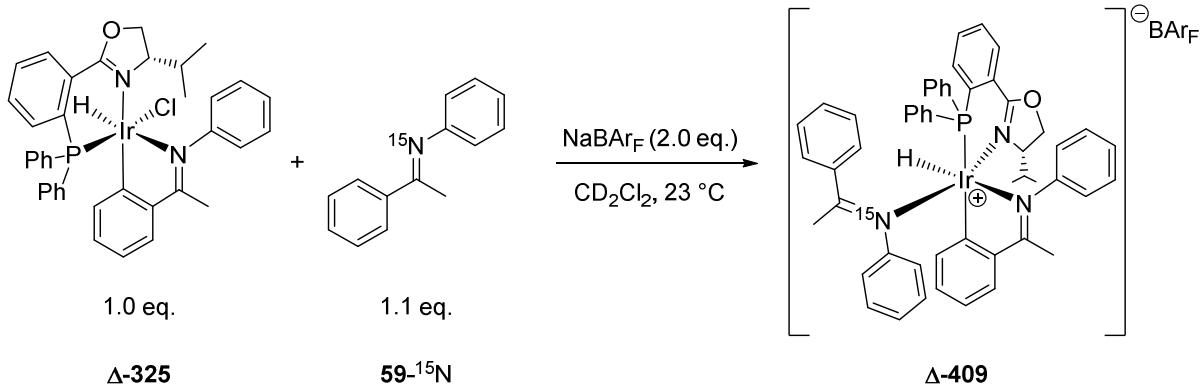

Scheme 166: Generation of complex **409** observed for a limited time period in CD_2Cl_2

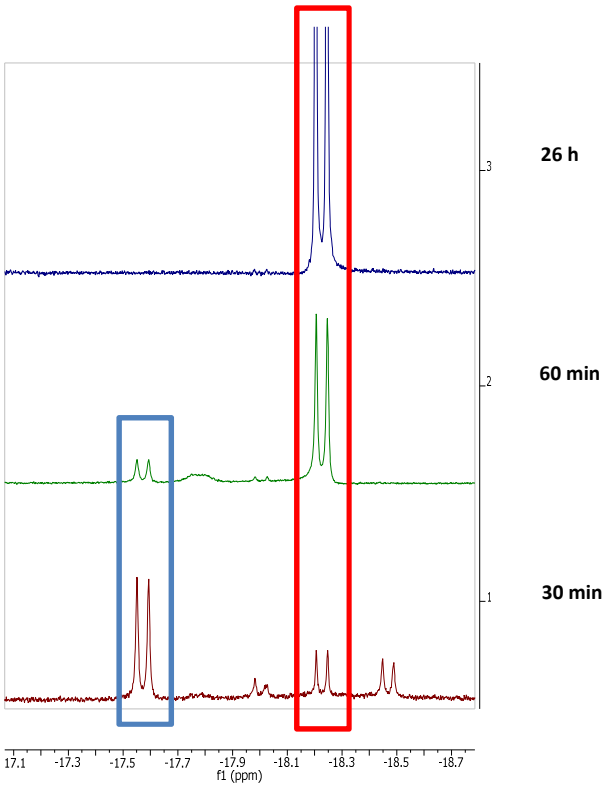

Spectrum 47: ^{1}H-NMR of **409** (blue) and **410** (red)

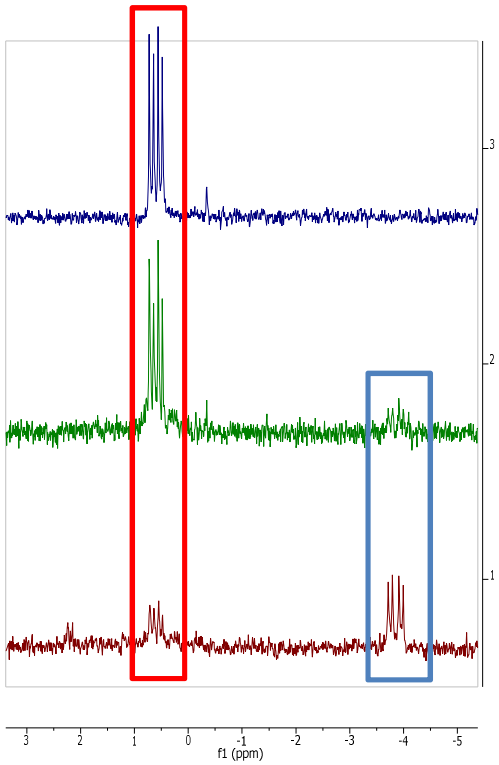

Spectrum 48: $^{31}P\{^1H\}$-NMR of **409** (blue) and **410** (red)

Over the course of 26 hours, only one ^{1}H-NMR hydride signal and one $^{31}P\{^1H\}$-NMR resonance remained (red frame). The structure of this new complex **410** was unclear. When taking a closer look at the ^{1}H-NMR

spectrum, a distinctive coupling pattern of two new signals at around 5 ppm was observed (orange frame, Spectrum 49). A doublet of doublets of doublets (ddd) was observed. It was reduced to a set of doublets of doublets with in the $^{1}H\{^{31}P\}$-NMR decoupling experiment (Spectrum 50).

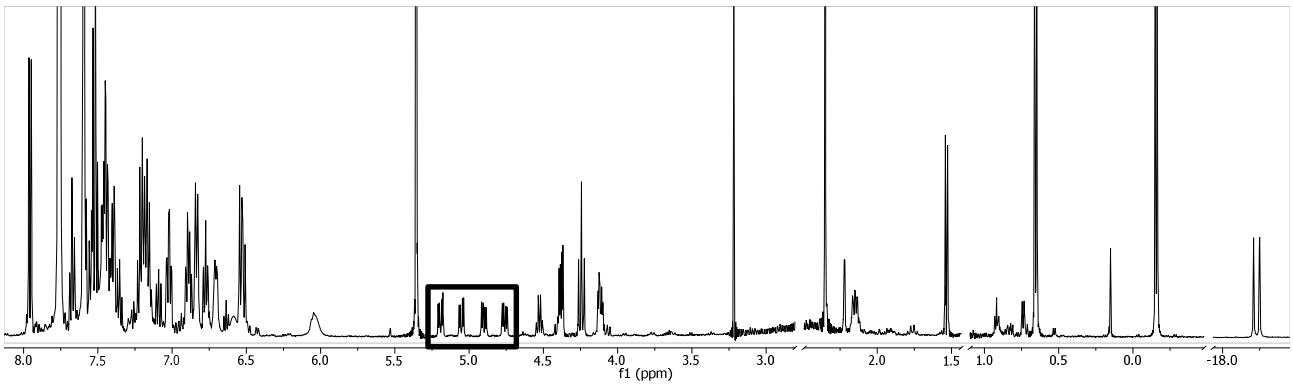

Spectrum 49: ^{1}H-NMR of **410**

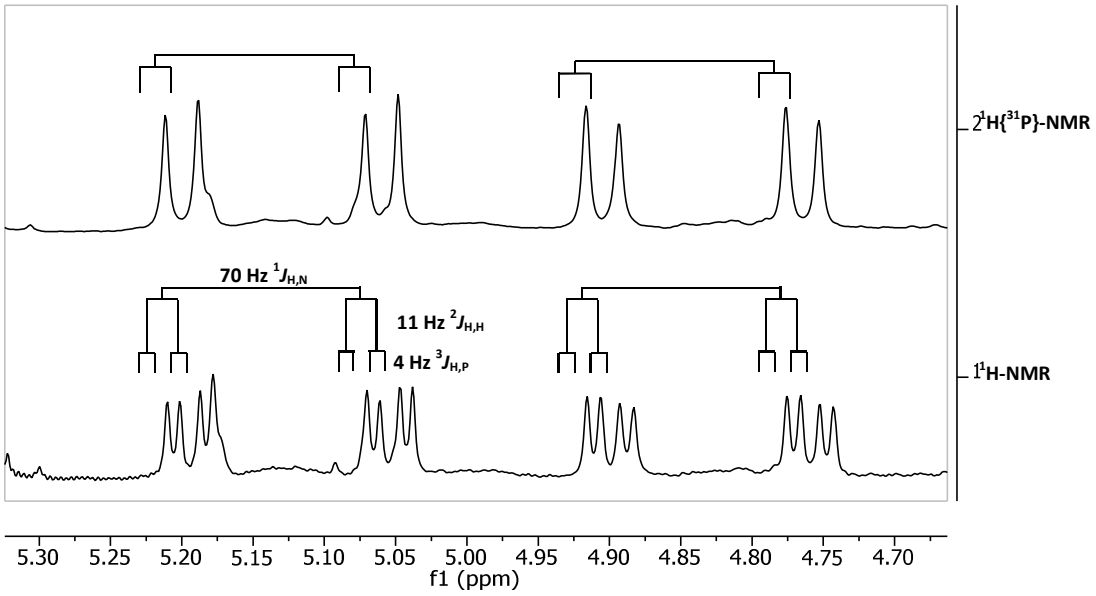

Spectrum 50: Detailed section from 4.7 to 5.3 ppm in the ^{1}H-NMR of **410**

The large coupling constant of 70 Hz indicated a $^{1}J_{N,H}$ coupling. Therefore, the new complex was assigned to an aniline bound species **410** with two inequivalent NH_2 protons (Scheme 167). In a different setup, the existence of the coordinated aniline could be further confirmed by a ^{1}H-^{15}N HMBC correlation experiment.[23] No residual water signal was detected. Two new signals were observed at 3.22 and 1.52 ppm. These were assigned to the methyl group resonances of the product amine **60** and acetophenone (**117**). Thus, no more labelled imine **59**-^{15}N was observed in solution since it was completely hydrolysed. Imine hydrolysis by a rhodium diphosphine complex in imine hydrogenation had been reported by James and co-workers.[64] Thus, the NMR sample was worked up and subsequent GC analysis depicted aniline, acetophenone (**117**) and amine **60**.

[23] Whereas free aniline is expected to have a chemical shift of -330 ppm, the coordinated aniline showed a high-field shift of more than 100 ppm to a resonance of -230 ppm. The signal at -325 ppm corresponds to residual imine **59**-^{15}N, where the *ortho*-protons of the aniline ring as well as the methyl group show correlation signals to the labelled nitrogen atom.

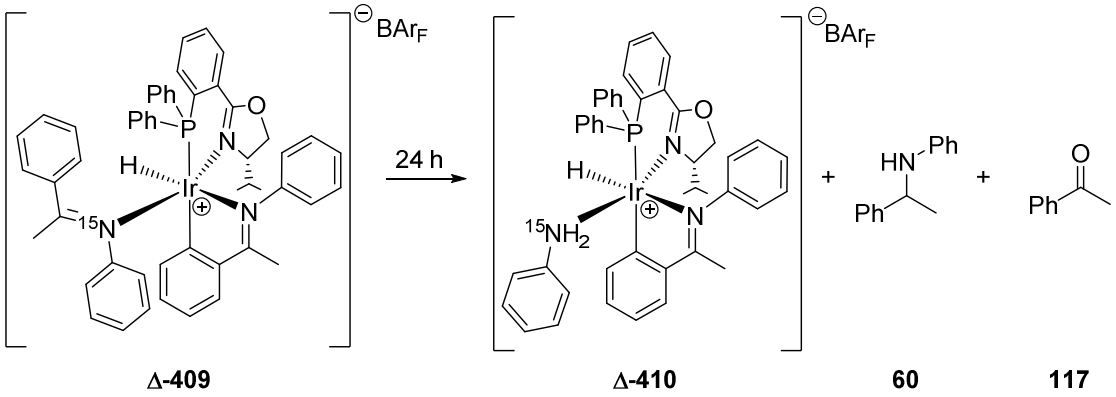

Scheme 167: Hydrolysis of imine **59**-^{15}N in hydride transfer studies

HPLC analysis showed that amine **60** was obtained predominantly as the (*R*)-enantiomer with an *ee* of 67%. The (*R*)-enantiomer is also obtained in the catalytic reaction. Additionally, hydrolysed ^{15}N-aniline is observed as the main component. The mass spectra recorded from GC-MS analysis indicate a *m/z* ratio of the amine (**^{14}N:197** and **^{15}N:198)** of three to one. Therefore, both **60**-^{14}N and some **60**-^{15}N labelled amine are detected. This amine could originate from the added imine as well as from the cyclometalated imine. Therefore, decomposition processes of the catalyst have to be taken into account.
Since stochiometric amounts of imine were added to the mixtures and only very small portions of amine were detected, concomitant hydrolysis must occur during reduction of the imine. In attempts to reproduce generation of complex **410**, amine **60** was not observed in every batch. When working under strict exclusion of water, species **409** could be observed for 24 hours before decomposition processes occurred. Therefore, the reduction of imine **59** to amine **60** is not the dominant process observed in a stochiometric reaction.

The role of imine-enamine tautomerism in the hydrogenation of imines

F. Barrios had raised the concern that imines which cannot undergo imine-enamine tautomerism cannot be hydrogenated, indicating that not the imine but the enamine is the actual species being reduced. Deuterium labelling experiments supported this hypothesis by deuterium incorporation at the methyl group of imine **59.** Furthermore, substrates preventing imine-enamine tautomerism, such as **326** or **327** could not be reduced even at 50 bar hydrogen pressure (Figure 47).

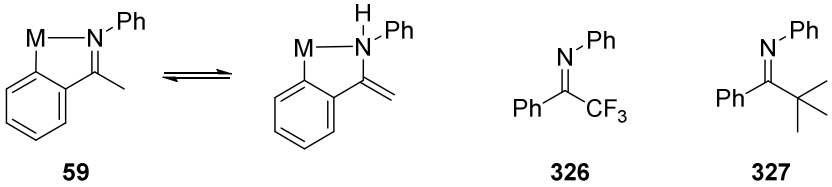

Figure 47: Imine-enamine tautomerism upon cyclometalation and imine **326** and **327** preventing enamine formation

In a re-evaluation, imines **326** and **327** were subjected to hydrogenation conditions in combination with imine **59** to afford iridacycle catalyst **325** *in situ* (Table 18). When comparing entries 1 to 2 as well as 3 to 4, conversion of the imine was achieved in the presence of **59.** This demonstrated that hydrogenation occurs along the C=N double bond. No conversion in the absence of imine **59** could be explained by the difficult formation of the iridacycle with imines **326** and **327**. Iridacycle formation was shown to involve the methyl group as deuterium incorporation was detected in partially deuterated iridacycle **325** in Scheme 161.

When investigating a series of imine **411** to **413** able to undergo imine-enamine tautomerism, conversion was observed at elevated hydrogen pressure in all cases (Entries 6, 8, 10). Similarly, imine **414** afforded the corresponding amine in low yield at atmospheric hydrogen pressure, whereupon imine-enamine tautomerism would result in dearomatization of one aryl substituent. Imine **320** could only be hydrogenated upon addition

of imine **59** (Entry 14). This demonstrates that addition of imine **59** extended the substrate scope to di-*ortho*-substituted imines which cannot form the corresponding iridacycle themselves.

Table 18: Hydrogenation of imines undergoing/preventing imine-enamine tautomerism

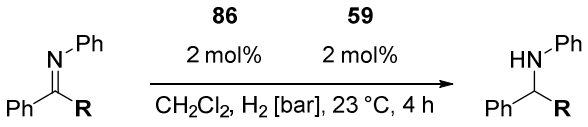

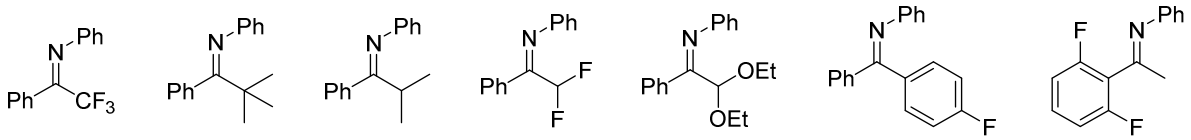

326 **327** **411** **412** **413** **414** **320**

Entry	Imine	59	p [bar]	Conv. [%][a)]
1	**326**	-	50	0
2	**326**	2 mol%	50	10
3	**327**	-	50	0
4	**327**	2 mol%	50	30
5	**411**	-	1	8-13
6	**411**	-	50	28-35
7	**412**	-	1	0
8	**412**	-	50	>99
9	**413**	-	1	25
10	**413**	-	50	>99
11	**414**	-	1	27
12	**414**	-	50	>99
13	**320**	-	50	0
14	**320**	2 mol%	50	>99

a) Determined by GC analysis.

Chapter 4 – Ligand Synthesis

Synthesis of isoquinoline ligand

The retrosynthetic analysis of the isoquinoline ligand **414** is outlined in Scheme 168. **414** would be obtained from intramolecular imine condensation of **415** which in turn would be obtained by Mitsunobu substitution of an alcohol of **416** to an amine. Alcohol **416** would be obtained after deprotection of **417** which was intended to be prepared by a Pd-catalysed α-arylation of isobutyrophenone (**418**) and enantiopure aryl bromide **419**.

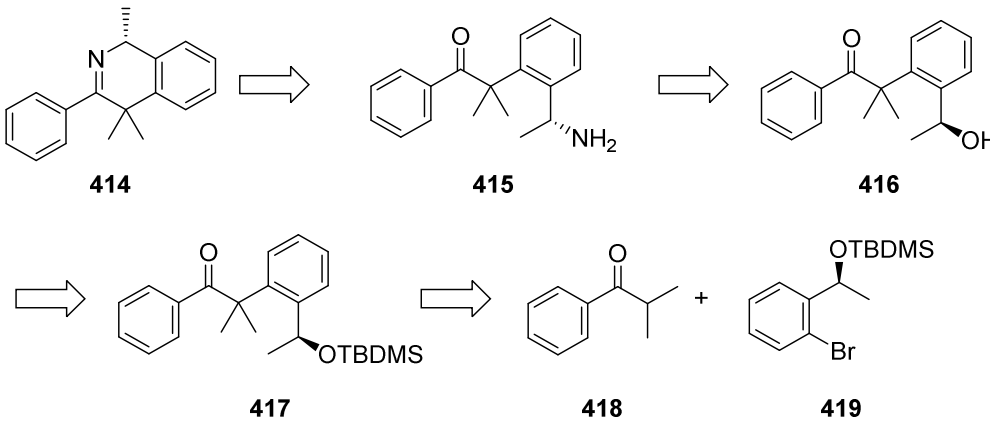

Scheme 168: Retrosynthetic analysis of isoquinoline ligand **414**.

Scheme 169 depicts a short literature research which provided established Buchwald-Hartwig coupling reaction conditions both for **418**[100] and **419**.[101],[102]

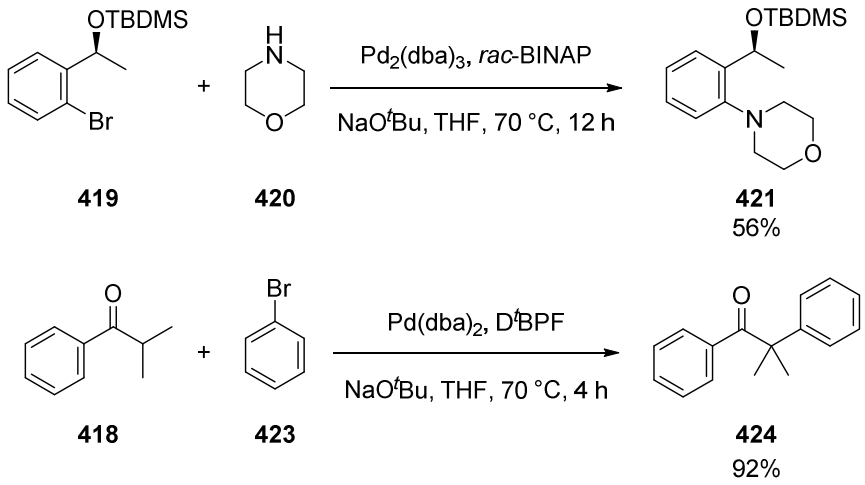

Scheme 169: α-Arylation of protected alcohol **419** and isobutyrophenone (**418**).

Protection of benzylic alcohol **424** with chlorosilane **425** proceeded smoothly in full conversion to afford the protected racemic alcohol **419** (Scheme 170).

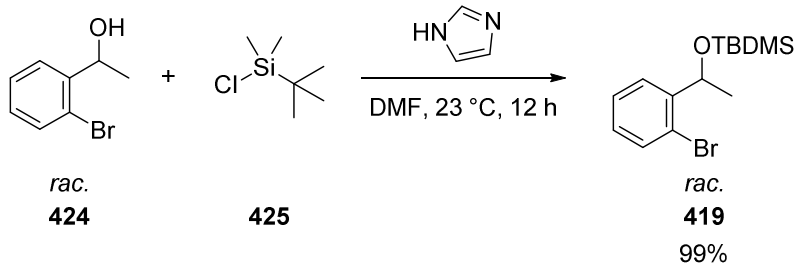

Scheme 170: Preparation of protected aryl bromide **419**.

Subsequently, aryl bromide **419** was subjected to Buchwald-Hartwig α-arylation (Table 19).[101],[103]

Table 19: α-Arylation of protected benzylic alcohol **419** and ketones **117**, **418** and **426**.

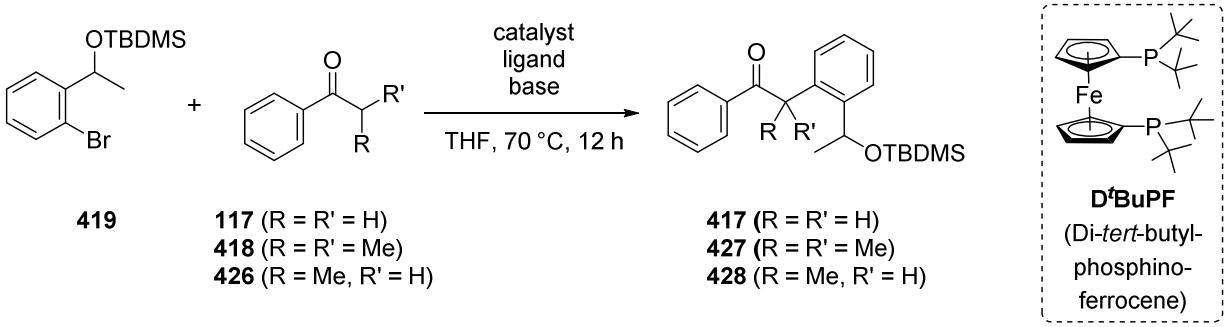

419

117 (R = R' = H)
418 (R = R' = Me)
426 (R = Me, R' = H)

417 (R = R' = H)
427 (R = R' = Me)
428 (R = Me, R' = H)

Entry	Ketone	Catalyst		Ligand		Base		yield
1	**418**	$Pd(OAc)_2$	(10 mol%)	$P(^tBu)_3 \bullet HBF_4$	(25 mol%)	NaO^tBu	(1.5 eq.)	0%
2	**418**	$Pd(OAc)_2$	(10 mol%)	*rac*-BINAP	(12.5 mol%)	KO^tBu	(3.0 eq.)	0%
3	**418**	$Pd_2(dba)_3$	(10 mol%)	D^{t}BuPF	(12.5 mol%)	KO^tBu	(3.0 eq.)	0%
4	**426**	$Pd_2(dba)_3$	(5 mol%)	*rac*-BINAP	(6 mol%)	NaO^tBu	(1.3 eq.)	0%
5	**117**	$Pd_2(dba)_3$	(5 mol%)	*rac*-BINAP	(6 mol%)	NaO^tBu	(1.3 eq.)	0%

Surprisingly, no conversion was observed even when employing sterically less demanding ketones such as **426** or **117**. Partial decomposition of aryl halide **419** was observed. Therefore, the aryl bromide was replaced by 2-bromobenzonitrile (**429**) and attempted to couple with acetophenone (**117**). Again, no conversion was observed (Scheme 171).

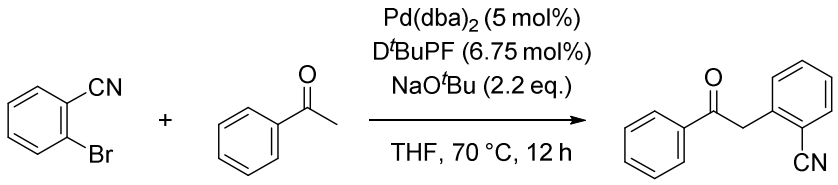

429 **117** **430**
0%

Scheme 171: α-Arylation of aryl bromide **429** and acetophenone (**117**).

Only decomposition of the aryl bromide was observed. Literature search revealed that *ortho*-substituted aryl halides such as **431** undergo α-arylation in 1,4-dioxane to afford **432** (Scheme 172).[104]

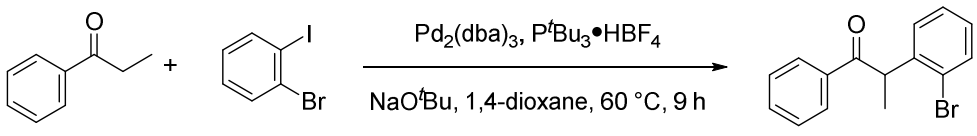

426 **431** **432**
70%

Scheme 172: α-Arylation of 2-bromoiodobenzene (**431**) and propiophenone (**426**).

Therefore, both propiophenone (**426**) and isobutyrophenone (**418**) were subjected to α-arylation with 2-bromoiodobenzene (**431**). Furthermore, aryl bromide **419** was also evaluated as a coupling partner (Table 20).

Table 20: α-Arylation of protected benzylic alcohol **419** and aryl halide **431** with ketones **418** and **426**.

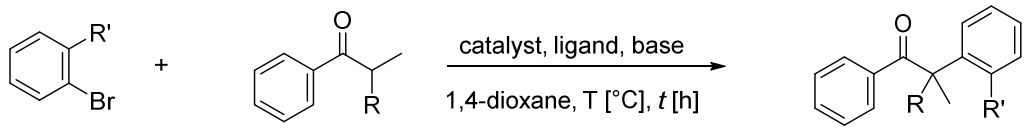

419 (R' = $CH(OTBDMS)CH_3$)
431 (R' = I)

418 (R = Me)
426 (R = H)

427 (R = Me; R' = $CH(OTBDMS)CH_3$)
428 (R = H; R' = $CH(OTBDMS)CH_3$)
432 (R = Me; R' = Br)
433 (R = H; R' = Br)

Entry	Aryl halide	Ketone	Catalyst	Ligand	base	T [°C]	*t* [h]	yield
1	**431**	**426**	$Pd_2(dba)_3$ (0.5 mol%)	$P(^tBu)_3 \bullet HBF_4$ (2.5 mol%)	NaO^tBu (1.3 eq.)	60 °C	9 h	0%
2	**431**	**426**	$Pd_2(dba)_3$ (0.5 mol%)	$P(^tBu)_3 \bullet HBF_4$ (2.5 mol%)	NaO^tBu (1.3 eq.)	80 °C	14 h	70%
3	**431**	**418**	$Pd_2(dba)_3$ (5 mol%)	$P(^tBu)_3 \bullet HBF_4$ (12 mol%)	NaO^tBu (1.5 eq.)	80 °C	12 h	0%[a]
4	**431**	**418**	$Pd(dba)_2$ (7.5 mol%)	D^tBuPF (9 mol%)	KHMDS (1.5 eq.)	85 °C	18 h	0%[a]
5	**419**	**426**	$Pd(dba)_2$ (5 mol%)	D^tBuPF (6 mol%)	NaO^tBu (1.6 eq.)	80 °C	12 h	44%
6	**419**	**426**	$Pd(dba)_2$ (5 mol%)	D^tBuPF (6 mol%)	NaO^tBu (1.6 eq.)	90 °C	24 h	85%
7	**419**	**418**	$Pd(dba)_2$ (5 mol%)	D^tBuPF (6 mol%)	NaO^tBu (1.6 eq.)	80 °C	12 h	10%
8	**419**	**418**	$Pd(dba)_2$ (5 mol%)	D^tBuPF (6 mol%)	NaO^tBu (1.6 eq.)	100 °C	24 h	28%
9	**419**	**418**	$Pd(dba)_2$ (5 mol%)	D^tBuPF (6 mol%)	NaO^tBu (1.6 eq.)	100 °C	24 h	0%[b]
10	**419**	**418**	$Pd(dba)_2$ (10 mol%)	$P(^tBu)_3 \bullet HBF_4$ (12 mol%)	NaO^tBu (1.6 eq.)	100 °C	48 h	43%

[a] no conversion and partial aryl halide decomposition. [b] in toluene

While ketone **426** afforded the arylated product in 70% yield at slightly higher temperatures (Entry 2), ketone **418** displayed no conversion (Entries 3 and 4). Satisfyingly, when reacting propiophenone (**426**) with sterically demanding aryl bromide **419**, the desired arylated product **428** was obtained in 85% yield when conducting the reaction at 90 °C for 24 hours (Entry 6). Under these conditions, reactivity was also observed for isobutyrophenone (**418**) in combination with **419** (Entries 7 and 8). Prolonged reaction times (48 h) and further increase of reaction temperature to 100 °C afforded the desired arylated product **427** in 43% yield (Entry 10).

Deprotection of **427** afforded the undesired hemiacetal **435** *via* intermediate alcohol **434** in full conversion (Scheme 173).

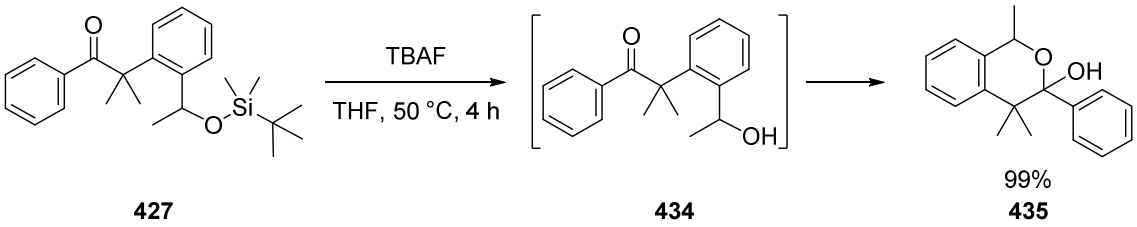

Scheme 173: Deprotection of **427** affording hemi-acetal **435**.

The hemi acetal **435** was subjected to acidic workup but the free alcohol **434** could not be observed by NMR. Since hemiacetals are known to be in equilibrium with the corresponding ketone, **435** was subjected to a number of reaction conditions to either afford the Mitsunobu product[105] or the mesylated acetal as depicted in Scheme 174. However, in all attempts no conversion was observed. Therefore this synthetic route was no longer followed.

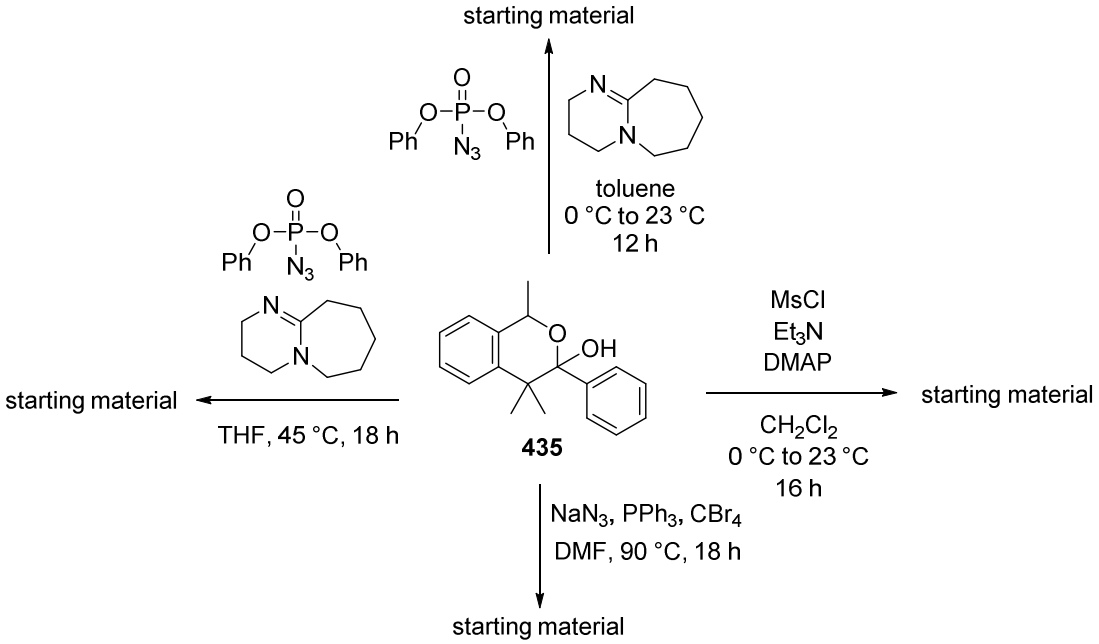

Scheme 174: Attempted derivatisation of hemi-acetal **435**.

While isobutyrophenone (**418**) and 2-bromoiodobenzene (**431**) showed no reaction, propiophenone (**426**) and **431** afforded the desired arylated product **432** in high yield (Table 20). Thus methylation of the α-carbon to obtain **433** was investigated (Table 21).

Table 21: Methylation of **432**.

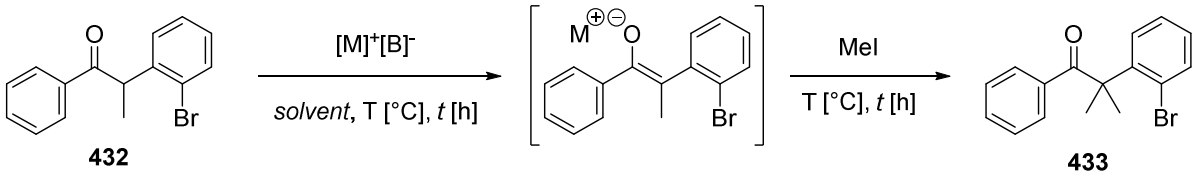

432 **433**

Entry	Base	Solvent	T [°C]	*t* [h]	T [°C]	*t* [h]	yield
1	LDA	THF	-78 °C	30 min	-78 °C 23 °C	60 min overnight	0%
2	LDA	THF	-78 °C	30 min	-78 °C 23 °C	30 min overnight	0%
3	NaH	THF	-78 °C 0 °C	35 min 30 min	-78 °C 23 °C	45 min 2 h	0%
4	LiHMDS	THF	-78 °C 0 °C	15 min 10 min	-78 °C 23 °C	40 min overnight	3%
5	LiHMDS	THF	-78 °C 23 °C	60 min 10 min	-78 °C 23 °C	-78 °C overnight	0%
6	KHMDS	toluene	-78 °C 23 °C	45 min 20 min	-78 °C	60 min H_2O quench	0%
7	KHMDS	toluene	-78 °C 23 °C	60 min 10 min	-78 °C 23 °C	-78 °C overnight	0%
8	KO^{t}Bu, 18-crown-6	THF	23 °C	15 min	23 °C	15 min	12% (48% O-alkylated; 22% rec. sm)

While methylation with strong bases failed at lower temperatures (Entries 1-7), KO^{t}Bu and 18-crown-6 ether in THF afforded the desired ketone **433** at room temperature in 12% yield (Entry 8).[106] By alternating the order of addition and lowering the reaction temperature to 0 °C, methylation of ketone **432** proceeded in 91% conversion providing the desired ketone **433** in 19% yield along with 72% *O*-methylated **436** displayed in Scheme 175. The reaction was not investigated in the absence of 18-crown-6 ether. The presence of crown-ether might be responsible for the high excess of *O*-alkylation.

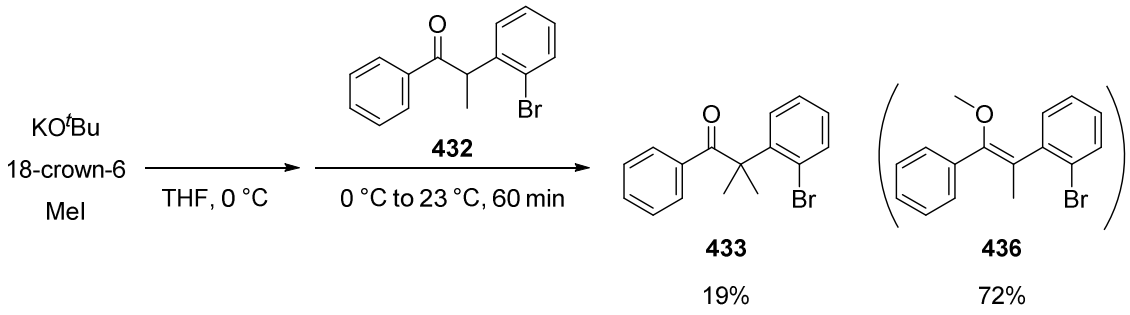

Scheme 175: Methylation of **432**.

In order to obtain the *C*-alkylated product **433** selectively, enamine formation of **432** with pyrrolidine was attempted but enamine **437** could not be obtained (Scheme 176).

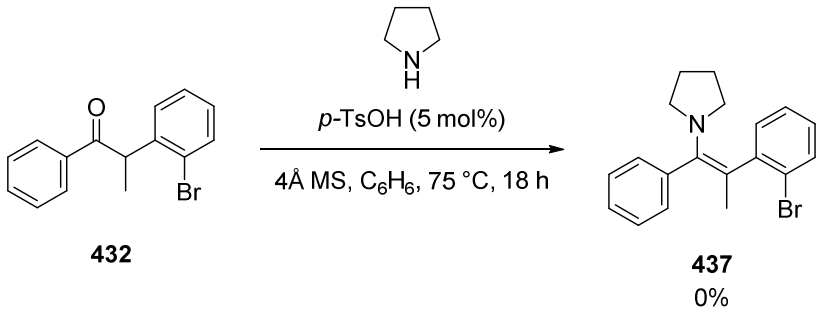

432 **437** 0%

Scheme 176: Attempted enamine formation of **432** to afford **437**.

Due to the poor selectivity of the alkylation, recovery of **432** was investigated. Scheme 177 displays the results: While boron tribromide afforded a 7:3 ratio of **432** and **437**, trimethylsilyl iodide provided ketone **432** alone in 89% yield.[107],[108]

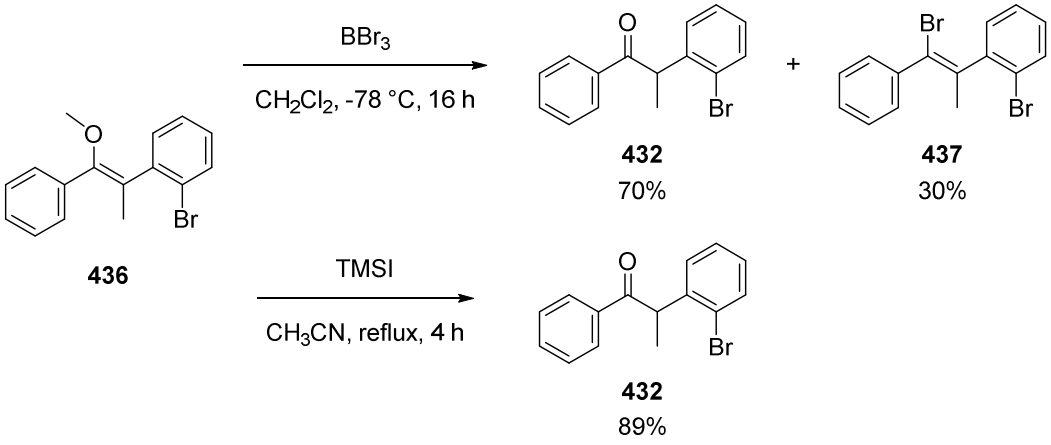

Scheme 177: Regeneration of ketone **432** by demethylation.

With **433** in hand, lithium-halogen exchange and subsequent addition of an electrophile was investigated. As the electrophile *N*-(4-methoxyphenyl)ethanimine **439** was chosen. Deprotection of the PMP-group of **440** under oxidative acidic conditions[109] would form **415** which should directly undergo intramolecular imine condensation to afford the desired isoquinoline ligand **414** as shown in Scheme 178.

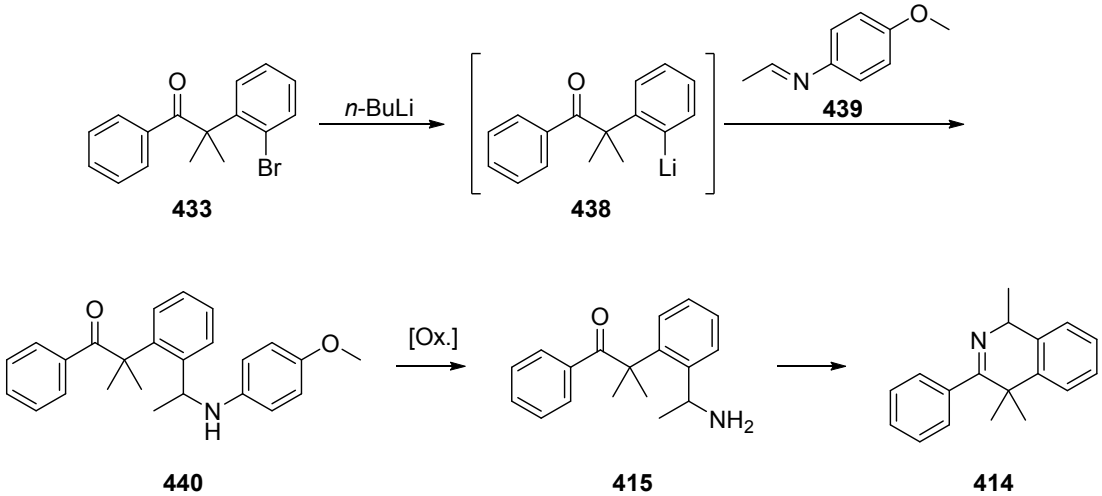

440 **415** **414**

Scheme 178: Revised synthetic route involving lithiation of **438**, subsequent electrophilic attack of **439** and PMP-deprotection to afford **414**.

However, when **433** was lithiated and freshly prepared **439** added, a different product **444** was isolated. Condensation of acetaldehyde and *para*-anisidine did afford the α,β-unsaturated crotonaldehyde-derived aldimine **443** and not **439**. Furthermore, the lithiated species **438** is prone to intramolecular attack to the ketone and rearranged into species **442** with a benzylic anion, in equilibrium with the tertiary lithium alkoxide **441**. **441** underwent Michael addition and subsequent cyclisation to afford **444** as a single diastereomer. Scheme 179 outlines the potential side reaction.

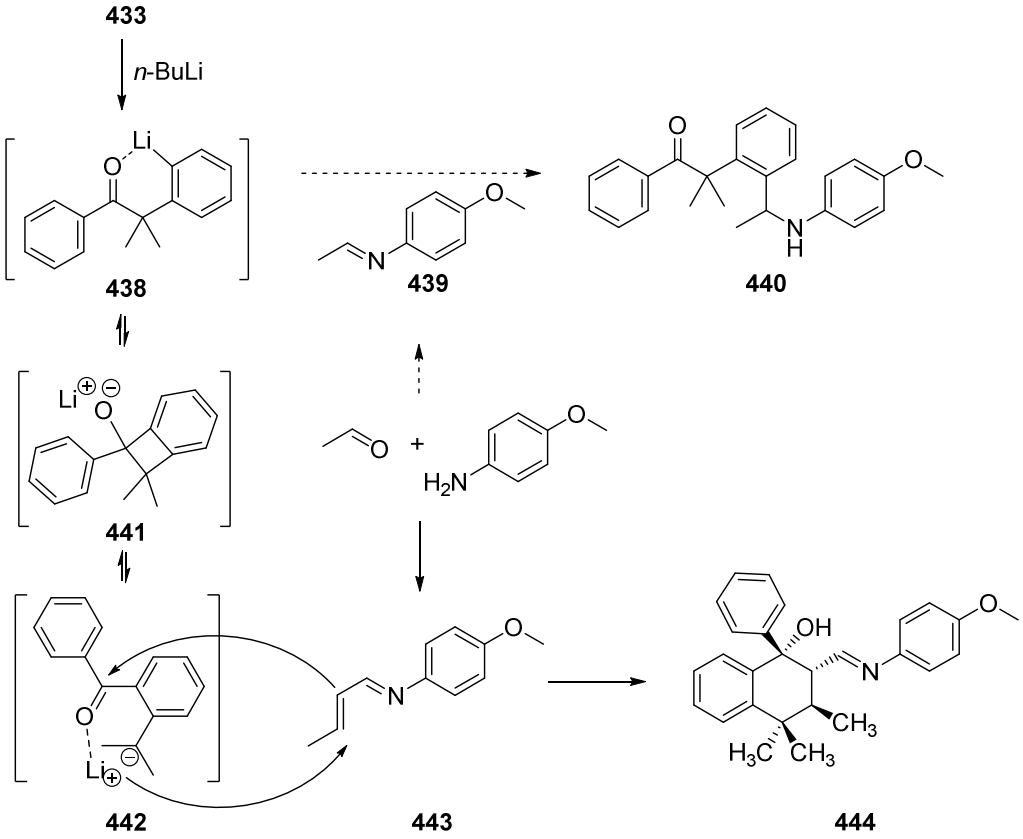

Scheme 179: Potential side reaction upon lithiation and electrophile addition to **433**.

The reaction of aryl bromide **433** with *n*-BuLi and other electrophiles such as isopropylaldehyde or acetaldehyde gave a mixture of products. Therefore lithiation of **433** was no longer investigated.

In order to introduce an amino group, α-arylation of aryl bromides **445** and **446** was investigated (Scheme 180). Upon coupling of **445** isobutyrophenone (**418**), hydrogenation with Pd/C would afford **415**. With aryl bromide **446**, coupling to **418** and subsequent hydrolysis would allow for reductive amination of the ketone to give **415**. When aryl halide **445** was α-arylated with isobutyrophenone (**418**) a complex product mixture was obtained. Aryl halide **446** decomposed under the reaction conditions. The desired products were not observed by GC-MS analysis and could not be isolated by flash chromatography.

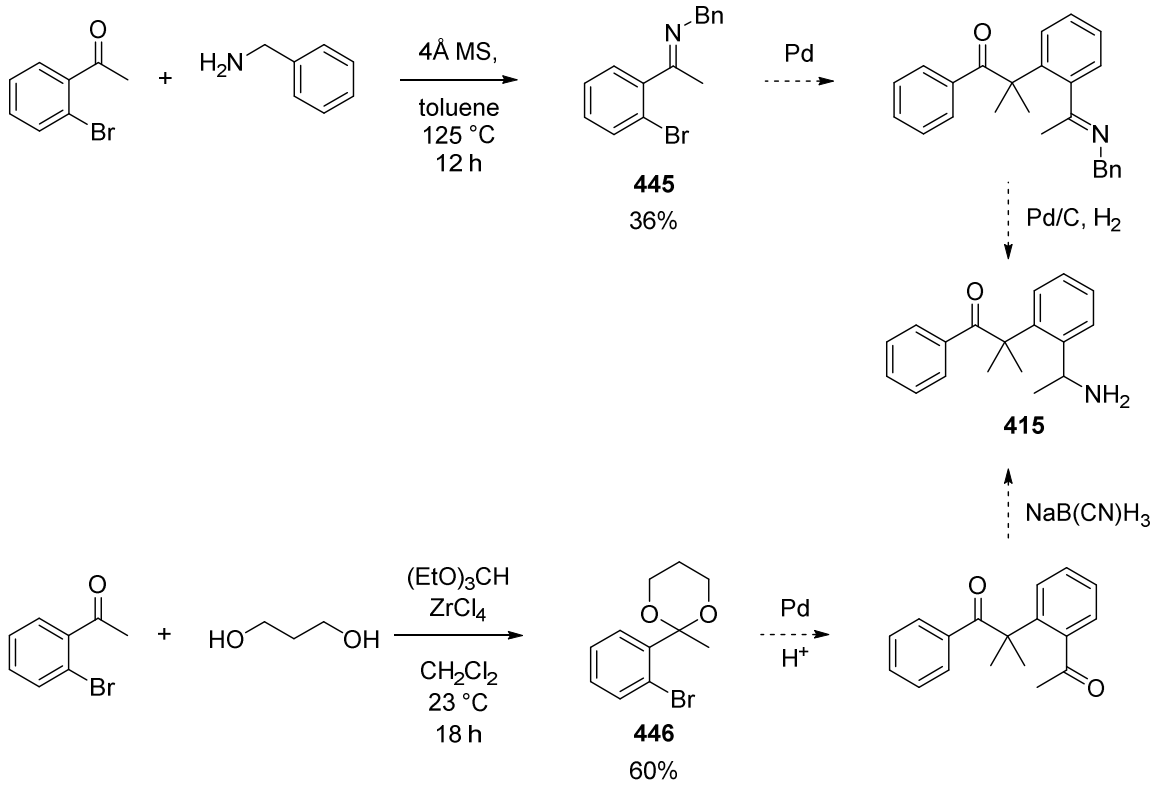

Scheme 180: Preparation of aryl bromides **445** and **446**.

Additionally, aryl bromides **447** and **448** were prepared (Scheme 181).[110] Both **447** and **448** did not afford the desired coupling products, but decomposition of the aryl bromides occurred.

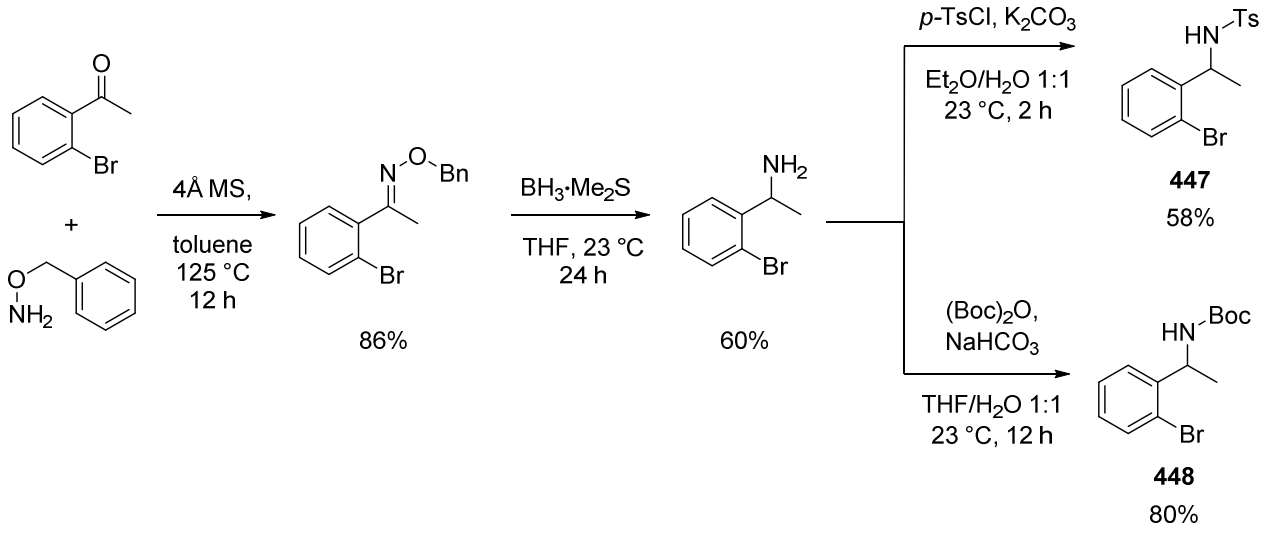

Scheme 181: Preparation of aryl bromides **447** and **448**.

Since coupling of aryl halides **445**, **446**, **447** and **448** was not successful; efforts were devoted towards protection of the keto functionality in order to re-investigate bromine-lithium exchange. Primarily, acetal- and thioacetal formation were investigated (Table 22). No acetal or thioacetal formation was observed.

Table 22: Efforts towards acetal protection of ketone **433**.

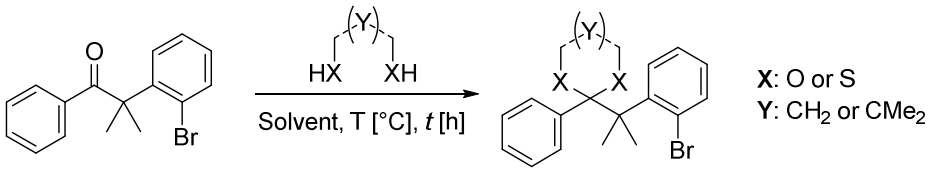

433

Entry	Alcohol	Reagent	Catalyst	Solvent	Temp.	time	yield
1[111]	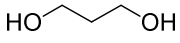	$(MeO)_3CH$	$ZrCl_4•(THF)_2$	CH_2Cl_2	23 °C	18 h	0%
2	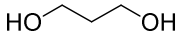	4Å MS	*p*-TsOH	toluene	115 °C	12 h	0%
3[112]	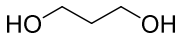	$(MeO)_3CH$	$(nBu)_3NBr_3$	CH_2Cl_2	23 °C	24 h	0%
4[113]	MeOH	$(MeO)_3CH$	CF_3SO_3H	$MeNO_2$	115 °C	6 h	0%
5[113]		$(MeO)_3CH$	CF_3SO_3H	$MeNO_2$	115 °C	6 h	0%
6		4Å MS	*p*-TsOH	toluene	115 °C	12 h	0%
7[114]		Silica gel	*p*-TsOH	CH_2Cl_2	55 °C	24 h	0%

Therefore, protection by methylenation was attempted (Table 23). The desired 1,1,-disubstituted terminal olefin **449** or **450** would be converted to the ketone at a later stage in the synthesis by ozonolysis. While attempts with titanium-mediated carbene generation from dichloromethane were unsuccessful (Entries 1 and 2)[115], the *Tebbe* reagent provided the desired olefin **449** in up to 39% yield (Entry 6). Exclusion of light significantly enhanced the life-time of the *Tebbe* reagent in solution.[116],[117],[118],[119]

Table 23: Methylenation of **427** and **433**.

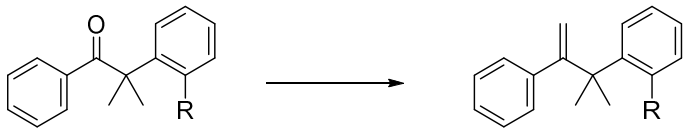

427 (R = $CH(OTBDMS)CH_3$)
433 (R = Br)

449 (R = $CH(OTBDMS)CH_3$)
450 (R = Br)

Entry	Substrate	Reagent	Solvent	T [°C]	*t* [h]	yield
1	**427**	Mg, $TiCl_4$, CH_2Cl_2	THF	0 °C to 23 °C	1 h	0%
2	**433**	Mg, $TiCl_4$, CH_2Cl_2	THF	0 °C to 23 °C	1 h	0%
3	**433**	$(Cp)_2Ti(Me)_2$	toluene	75 °C	24 h	0%
4	**433**	$(Cp)_2Ti(Me)_2$, *exlusion of light*	toluene	75 °C	24 h	0%
5	**433**	$(Cp)_2Ti(Me)_2$, *exlusion of light*	toluene	85 °C	72 h	16%
6	**433**	$(Cp)_2Ti(Me)_2$, *exlusion of light*	toluene/THF 1:1	70 °C	48 h	39%

Reactions were very sluggish and the olefin products difficult to purify due to their high lipophilic character. Therefore, subsequent one-pot deprotection of the olefin to the free secondary alcohol **451** was conducted. Isolated yields lower than 50% were achieved (Scheme 182). **451** was subjected to Mitsunobu reaction

conditions[120],[121],[122] to afford the *N*-Boc-protected amine. Instead the elimination product **452** was formed exclusively.

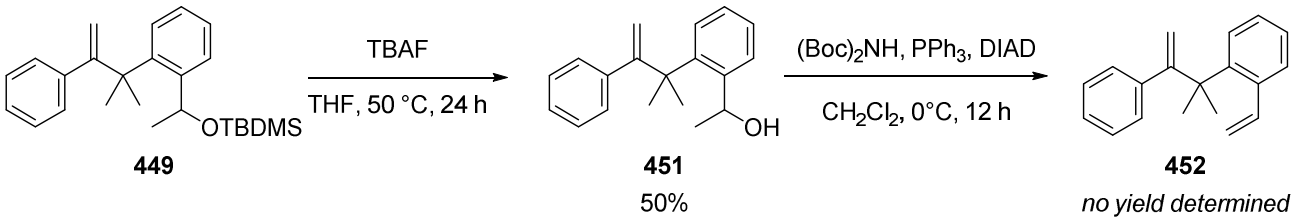

449 **451** 50% **452** *no yield determined*

Scheme 182: Deprotection and attempted Mitsunobu reaction on **449**.

Robin Wehlauch observed formation of **454** by α-arylation of **418** and **453** during his internship. Under optimized conditions, **454** was obtained in 67% yield as shown in Scheme 183.

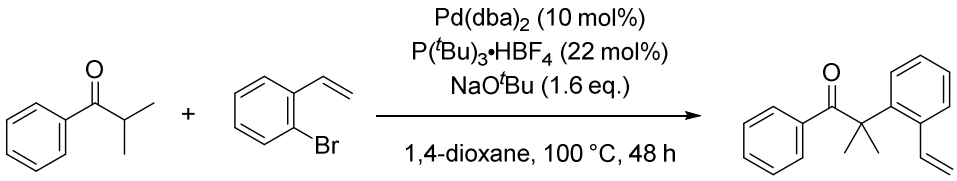

418 **453** **454** 67%

Scheme 183: α-arylation of isobutyrophenone (**418**) and 2-bromostyrene (**453**).

Subsequent ozonolysis followed by treatment with triphenylphosphine afforded the keto-aldehyde **455** (Scheme 184). Under optimized reaction conditions, **455** was obtained in 89% yield.[123]

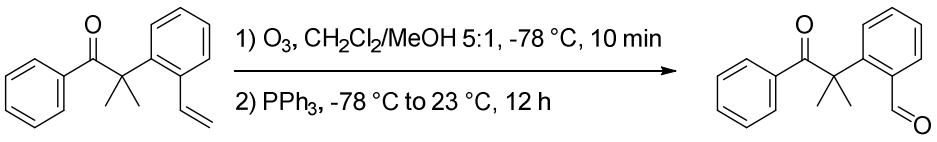

454 **455** 89%

Scheme 184: Ozonolysis of **454**.

Keto-Aldehyde **455** was condensed with *para*-anisidine to afford **456**. On the other hand, condensation with $BocNH_2$ to obtain **457** failed. *N*-PMP aldimine formation of **456** proceeded smoothly in >95% conversion determined by NMR (Scheme 185). The PMP protection group was chosen since it can be oxidized and cleaved under acidic conditions. Furthermore, the aldimine offered the possibility of introducing a variety of substituents by nucleophilic addition.

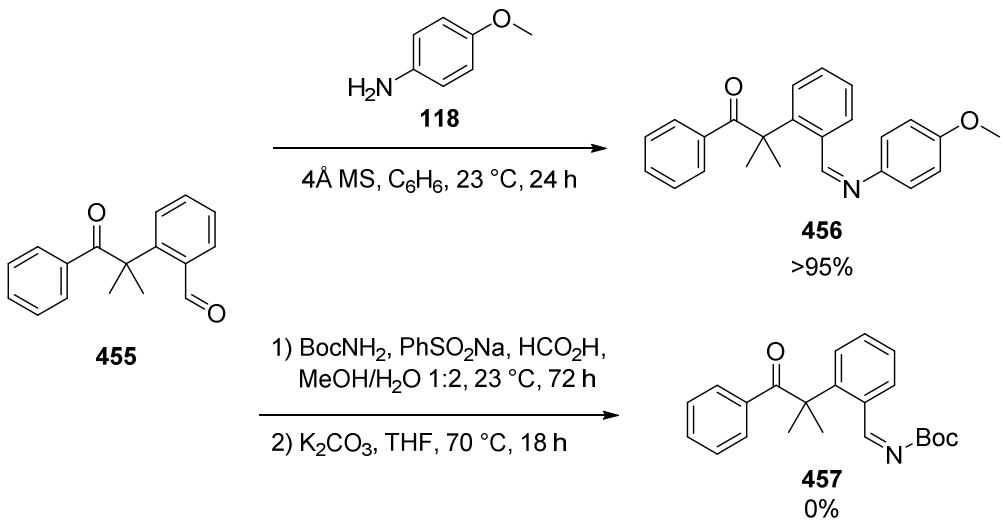

Scheme 185: Condensation of **455** with amines.

Hence, aldimine **456** was generated *in situ* and dried *in vacuo*. The corresponding nucleophile was added to afford the desired protected secondary amine. Scheme 186 gives an overview of attempted nucleophilic additions. Addition of alkyl Grignard and alkyl lithium reagents showed different reactivity. With methyl lithium, the hemi-aminal **458** was obtained in 30% yield. This observation is similar to hemi-acetal **435** obtained from **427** (Scheme 173). It appears that the methyl group is small enough to facilitate nucleophilic attack of the generated amide or alkoxide. Contrary to methyl lithium, methyl magnesium bromide gave a complex product mixture. On the other hand, isopropyl magnesium chloride afforded the corresponding secondary amine **459** under mild reaction conditions in 53% yield. A similar reactivity was observed with *tert*-butyl magnesium chloride delivering amine **460** in 25% yield. The same reaction with *tert*-butyl lithium did not give any product probably due to the high basicity of the lithium reagent.

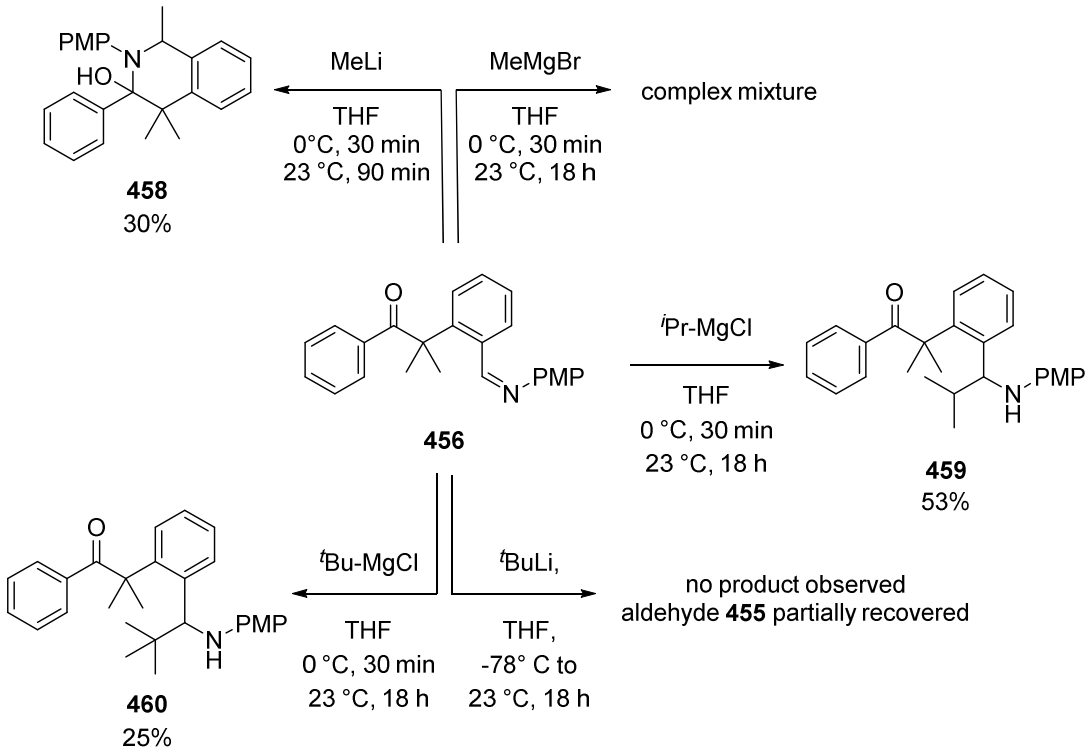

Scheme 186: Addition of alkyl Grignard and lithium reagents to **456**.

Different reagents with moderate oxidizing strength to deprotect **459** were tested. The free amine generated *in situ* directly underwent intramolecular imine condensation to afford the isoquinoline ligand **392** (Scheme 187).

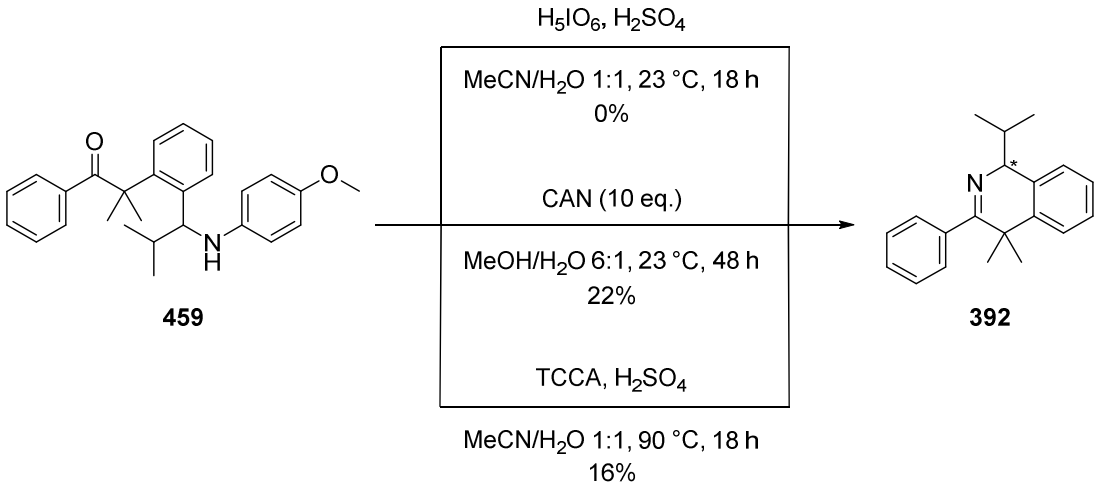

Scheme 187: Oxidative deprotection of **459** and subsequent intramolecular imine condensation.[24]

In order to obtain enantiomerically pure isoquinoline ligand **392**, separation of **459** by semipreparative HPLC on a chiral stationary phase was performed. However, when converting enantiopure **459** to **392** partial racemisation was observed with CAN (Scheme 188). Therefore separation of enantiomers was performed with isoquinoline **392**. Reactions with enantiopure **459** gave higher yields of **392** even though the racemate of **459** was purified by flash chromatography. The contaminant in the racemic material could not be identified by NMR or GC analysis.

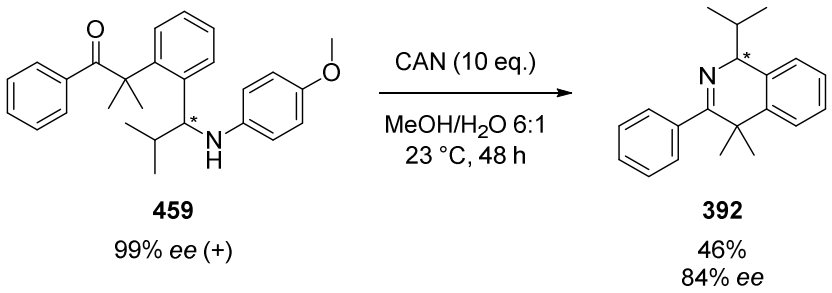

Scheme 188: Oxidative deprotection of enantiomerically enriched **459** giving **392** with erosion of enantiomeric excess.

[24] CAN = Cerium Ammonium Nitrate; TCCA = Trichloroisocyanuric acid

Synthesis of tetrahydropyridine ligand

The retrosynthetic analysis of ligand **394** is depicted in Scheme 189. **394** would be obtained from intramolecular imine condensation of **462** which in turn would be generated from **463**. Diastereoselective reduction of **464** and subsequent re-oxidation of to the ketone would afford **463**. **464** would be obtained from Michael addition of *N*-sulfinimine **465** and Michael acceptor **466**.

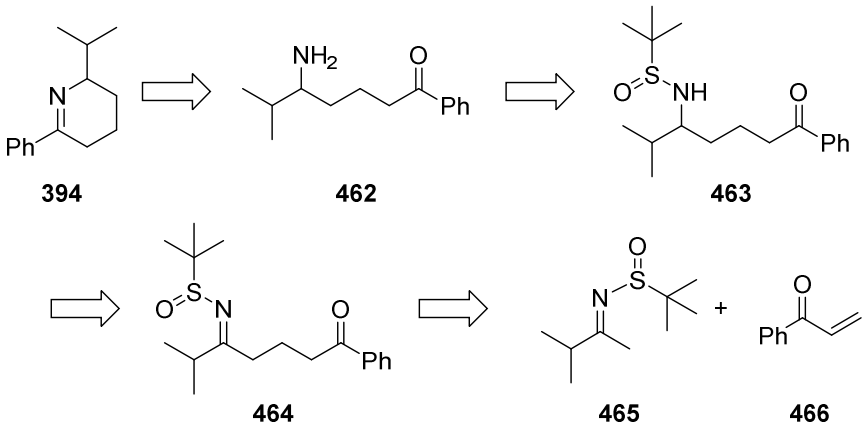

Scheme 189: Retrosynthetic analysis of ligand **394**.

The synthetic route is based on the synthesis of 1,3,5-substituted piperidines like **472** reported by *Ellman* and co-coworkers (Scheme 190).[124] The application of enantiopure *N*-sulfinamides **468** to generate *N*-sulfinimines like **465** as chiral auxiliaries afforded the corresponding Michael addition products **470** in excellent diastereoselectivities. While *Ellman* and co-workers reduced the imine directly *in-situ*, no efforts to isolate such structures have been reported.

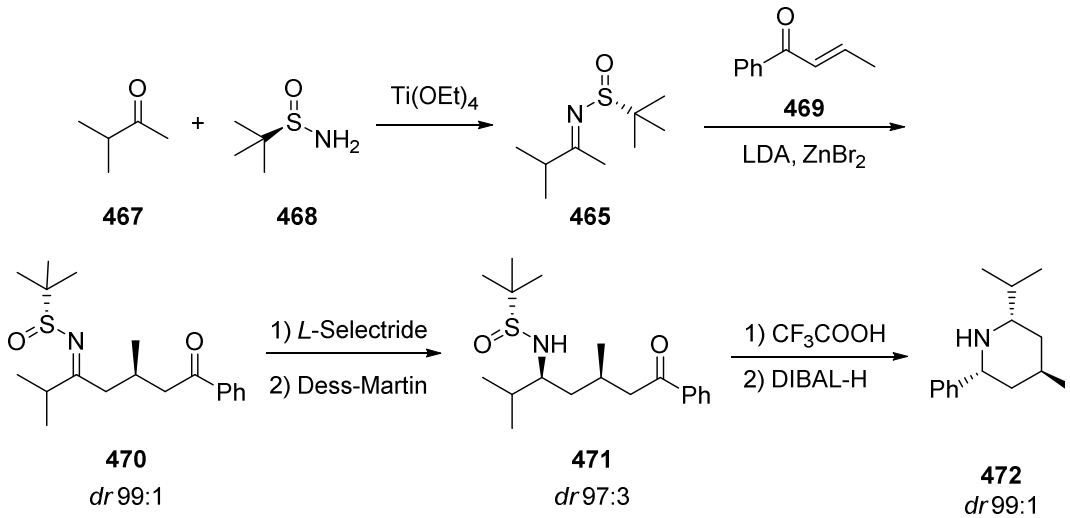

Scheme 190: Preparation of 1,3,5-substituted piperidines such as **472** by *Ellman* and co-workers.

With enantiopure sulfinimine **465** the direct preparation of each enantiomer of the desired ligand could be envisioned. A similar route as the one by *Ellman* was followed to afford the corresponding tetrahydropyridines. Preparation of the *N*-sulfinyl imines **465** and **474** proceeded with moderate to high yields as shown in Scheme 191.

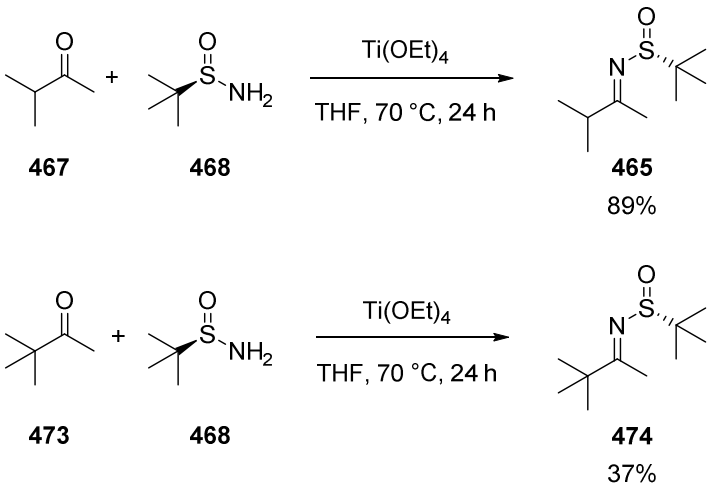

Scheme 191: Preparation of *N*-sulfinyl imines **465** and **474**.

The subsequent addition of the lithium enamide of **465** to phenyl vinyl ketone **466** presented several challenges. While isolated yields of up to 54% were obtained for Michael adduct **464** (Scheme 192), the product could not be isolated in pure form by flash chromatography. Co-elution of unreacted starting material and side products was observed. Repetitive flash chromatography still resulted in co-elution of product and side products due to similar R_f values.

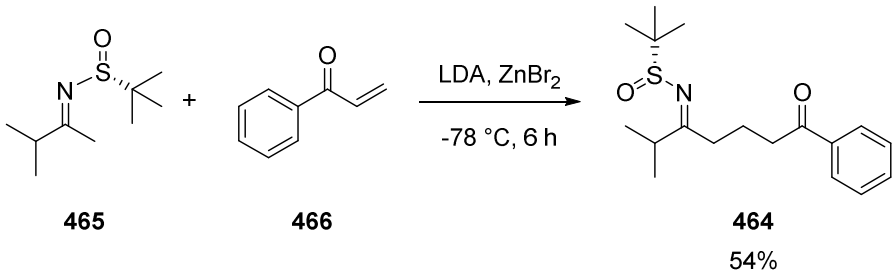

Scheme 192: Michael addition of lithium enolate of **465** to **466** affording **464**.

In order to elucidate possible impurities in phenyl vinyl ketone **466**, the synthesis thereof was varied (Scheme 193).[125],[126] Furthermore, **466** was purified by flash chromatography as well as distillation. No difference in reactivity was observed with regards to the isolation protocol or purity of **466**. In all cases, low to moderate yields were obtained with a maximum of 54%. Therefore, the poor reactivity was accounted to the substrate **466** itself. *Ellman* and co-workers did not apply phenyl vinyl ketone in their substrate scope, therefore the results could not be compared. All substrates employed by *Ellmann* featured *trans-* or *cis-*disubstituted double bonds.

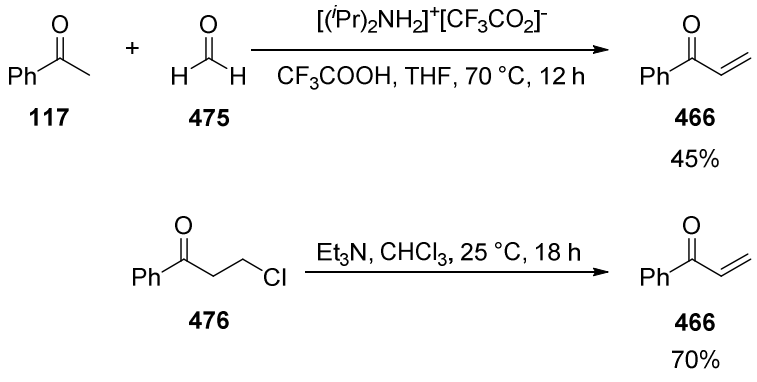

Scheme 193: Preparation of phenyl vinyl ketone **466**.

The crude Michael adduct **464** was reduced with *L*-Selectride. *Ellmann* and co-workers had reported diastereoselectivities higher than 97:3 for all substrates employed for reactions performed at -40 °C. With **464**, yields of up to 44% were obtained, even up to 5 equivalents of *L*-Selectride (Scheme 194). Reactions at -40 °C provided the amine **477** with a *dr* of 83:17. Lowering the reaction temperature to -50 °C improved the diastereoselectivity to 97:3 while maintaining the reactivity. Subsequent re-oxidation of the benzylic alcohol **477** to the ketone **463** with Dess-Martin periodane proceeded in 75% yield and allowed for an accurate determination of diastereomeric excess by ^{1}H-NMR. Diastereomers were also separated by semipreparative HPLC on a chiral stationary phase in case of mixtures with a *dr* lower than 97:3.

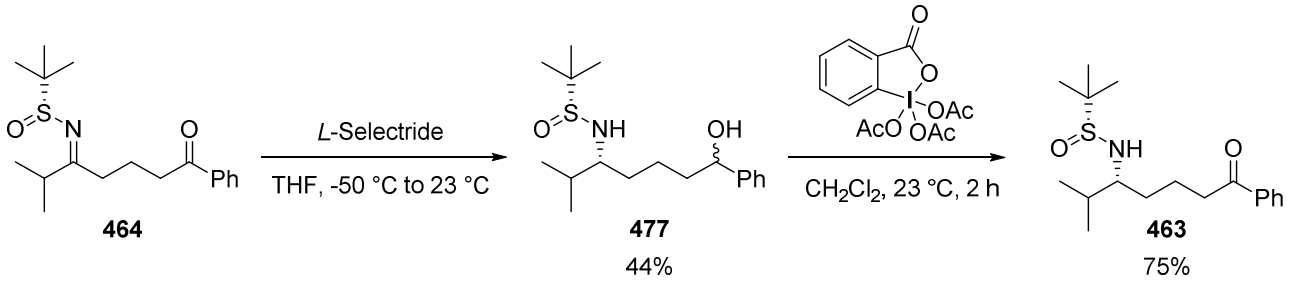

Scheme 194: Diastereoselective reduction of imine **464** and subsequent re-oxidation to ketone **463**.

Deprotection of the sulfinyl amine (*S*)-**463** or (*R*)-**463** and subsequent intramolecular condensation delivered the corresponding tetrahydropyridines (*S*)-**392** and (*R*)-**392** as shown in Scheme 195. Basic workup followed by dichloromethane extraction was used to remove any polar side products.

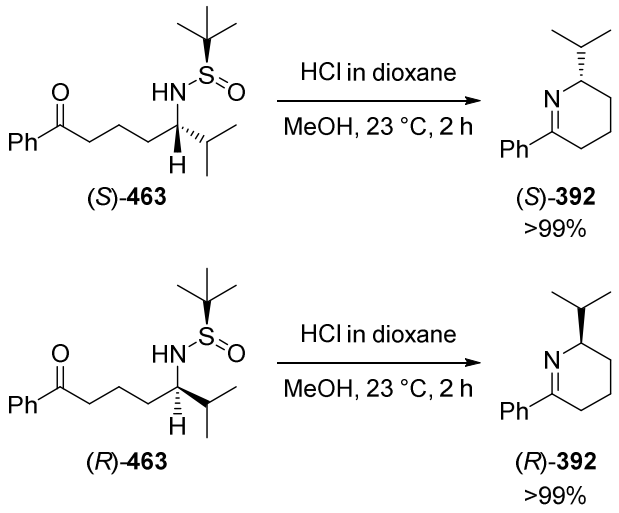

Scheme 195: Imine condensation with (*S*)-**463** and (*R*)-**463**.

Synthesis of benzoxazine ligand

The retrosynthetic analysis of benzoxazine ligand **395** is outlined in Scheme 196. **395** would be generated by benzoxazine condensation from amide **478**. **478** would be obtained by benzoylation of amine **479** which in turn would be prepared from 2-methoxybenzoic acid (**480**).

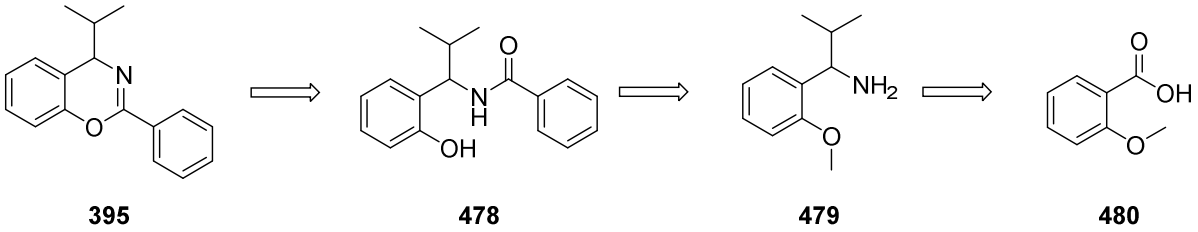

Scheme 196: Retrosynthetic analysis of benzoxazine ligand **395**.

The synthetic route is based on the preparation of (phosphinophenyl)benzoxazine ligands developed by *P. Kündig* and co-workers as shown in Scheme 197.[127],[128],[129] Acyl chloride formation of **481** from 2-methoxybenzoic acid (**480**) was followed by nucleophilic addition of isopropyl zinc iodide to afford **482**. Subsequent reductive amination provided benzylic amine **479**, which was separated to its enantiomers by recrystallization with mandelic acid. After benzoylation of (*R*)-**479** to amide (*R*)-**484**, deprotection of the methoxy group to obtain (*R*)-**485** was conducted with $AlBr_3$ to prevent racemization. Benzoxazine formation of (*R*)-**486** was followed by an *ipso*-substitution to obtain the (phosphinophenyl)benzoxazine ligand (*R*)-**487**.

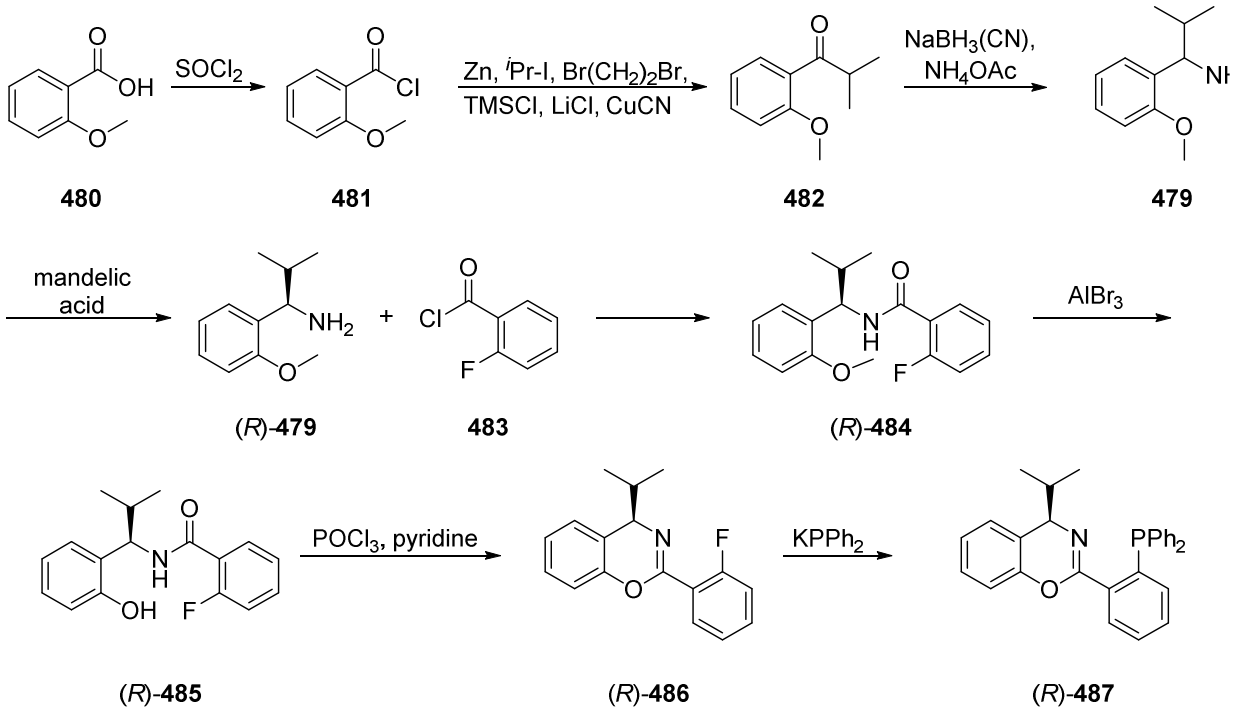

Scheme 197: Synthesis of ligand **487**.

Since no phosphine introduction was intended, amide formation with benzoyl chloride followed by benzoxazine formation would provide the desired ligands. In order to vary the alkyl substituent in the benzylic position, a modular synthesis was conducted. Nucleophilic addition of Grignard reagents to nitriles (Scheme 198) and subsequent one-pot Birch reduction afforded the benzylic amines **479** and **489**.[130] This also significantly reduced the number of steps compared to *P. Kündig*'s synthetic route.

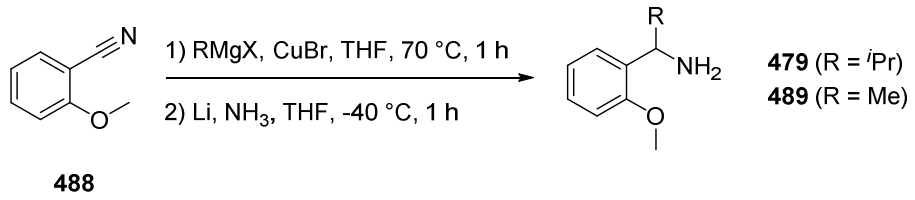

Scheme 198: Intended preparation of **479** and **489**.

Demethoxylation was observed for **489**, which was obtained as a 1:4.5 mixture along with **490** (Scheme 199). Electron-transfer-induced reductive demethylation of methyl ethers has been observed for a number of alkali metals in anhydrous solvents as well as for reactions under Birch conditions.[131],[132]

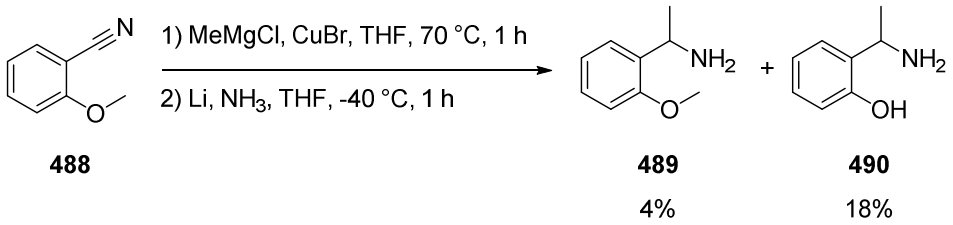

Scheme 199: Preparation of **489** and observation of **490**.

On the other hand, nucleophilic addition of isopropyl magnesium chloride to **488** and subsequent Birch reduction afforded the desired benzylic amine **479** in 86% yield (Scheme 200).

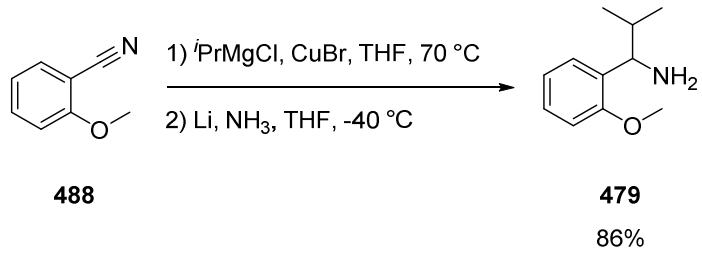

Scheme 200: Preparation of **479**.

Introduction of a *tert*-butyl group was conducted *via* the synthetic route reported by *P. Kündig* and co-workers as depicted in Scheme 201. Condensation of **491** and benzylamine afforded imine **492** in 88% yield. Subsequent addition of *tert*-butyl lithium required solvent exchange from pentane to THF and slow addition of **492** to afford *N*-benzylamine **493** in 77% yield. Deprotection of the amine **493** by Pd/C and hydrogen gas delivered benzylic amine **494** in 89% yield.

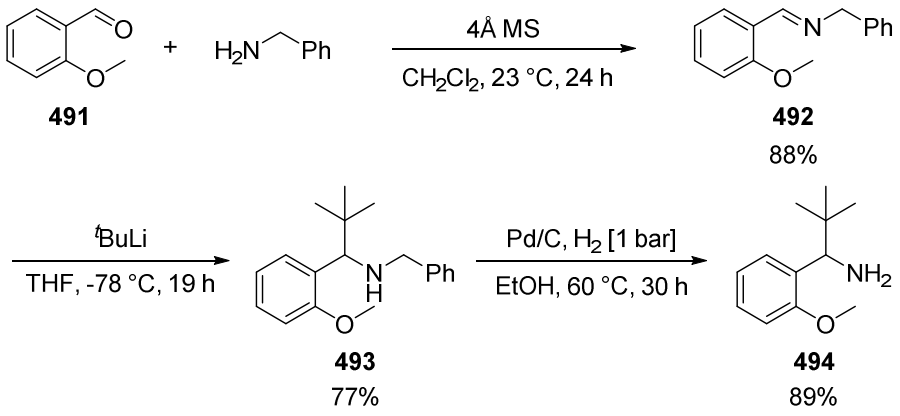

Scheme 201: Preparation of **494**.

While *P. Kündig* and co-workers separated enantiomers at that stage, yields of enantiomerically enriched amines were very low in the case of **479**. Furthermore, **489** and **490** were isolated as a mixture. Therefore **489** was transformed to **490** with boron tribromide in 96% yield and treated with benzoyl chloride to afford the benzamide **495** in 85% yield (Scheme 202). Enantiomers of **495** were separated by semipreparative HPLC on a chiral stationary phase.

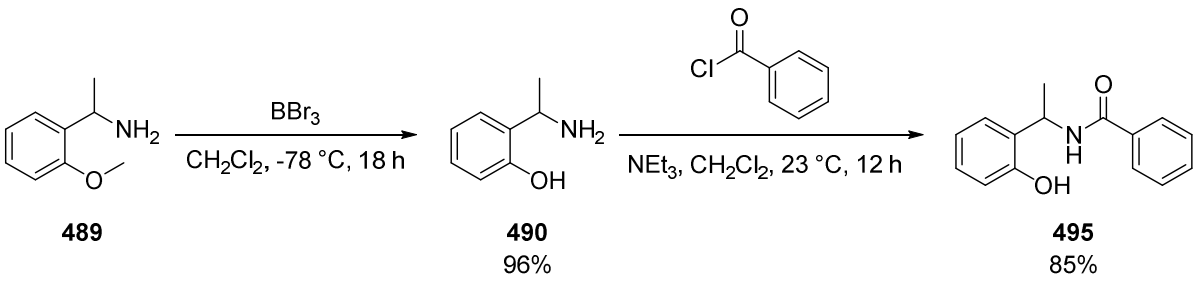

489 | **490** 96% | **495** 85%

Scheme 202: Amide formation of **495** and separation of enantiomers by SemiPrep HPLC.

In a similar fashion, **479** was deprotected using boron tribromide to afford **496** in 80% yield as shown in Scheme 203. Subsequent addition of benzoyl chloride gave benzamide **497** in essentially quantitative yield. Enantiomers were separated by semipreparative HPLC on a chiral stationary phase.

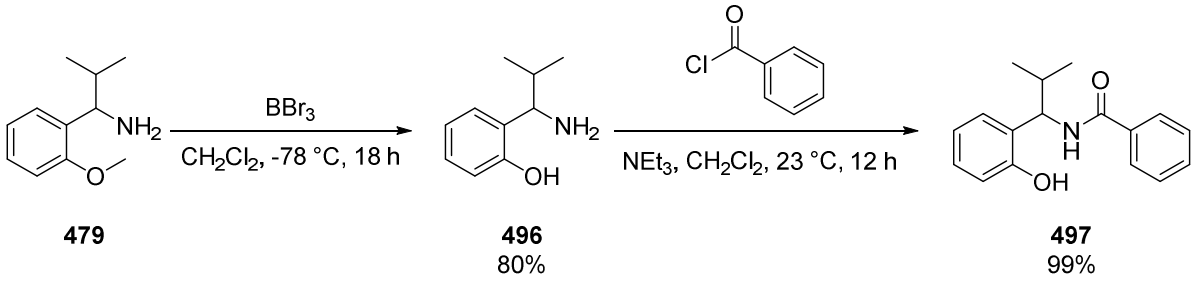

479 | **496** 80% | **497** 99%

Scheme 203: Deprotection of **489**, amide formation and separation of enantiomers to afford (*R*)-**497**.

Enantiomers of **494** were separated by recrystallisation with enantiopure mandelic acid **498** to afford the diastereomerically enriched mandelic acid salts. The free amine (*R*)-**494** was demethylated using boron tribromide to afford (*R*)-**499** in 90% yield. Addition of benzoyl chloride then furnished benzamide (*R*)-**500** in essentially quantitative yield (Scheme 204).

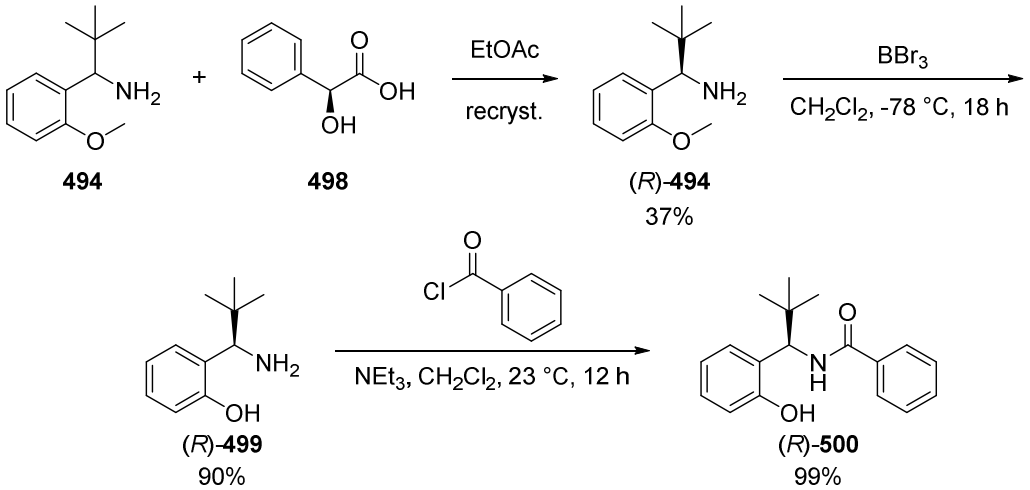

494 | **498** | (*R*)-**494** 37%

(*R*)-**499** 90% | (*R*)-**500** 99%

Scheme 204: Preaparation of (*R*)-**500**.

With the benzamides **495**, **497** and **500** in hand, cyclisation employing phosphorus oxychloride was investigated. Depending on the alkyl substituent, quite different yields were observed. Whereas cyclisation

of the methyl-substituted benzamide **495** with $POCl_3$ to deliver **399** gave poor yields of only up to 6% yield, cyclisation with triflic anhydride failed. Moderate yields up to 42% were obtained with **497** affording **398** and up to 29% in the case **500** giving benzoxazine **400**.

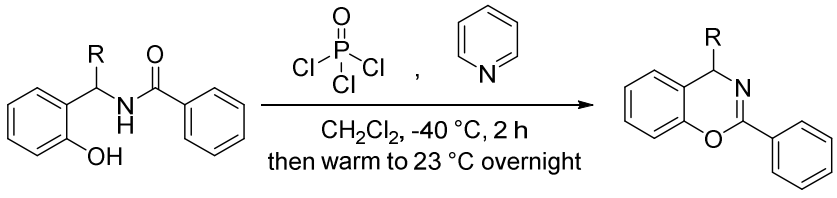

495 (R = Me)
497 (R = ^{i}Pr)
500 (R = ^{t}Bu)

399 (R = Me) 6%
398 (R = ^{i}Pr) 42%
400 (R = ^{t}Bu) 29%

Scheme 205: Cyclisation of benzamides **495**, **497** and **500**.

Preparation of chiral BINOL-based phosphoric acids

The synthesis of BINOL-derived chiral phosphoric acids is well documented in the literature. Therefore, literature procedures for the preparation of **408** and **407** were performed (Figure 48).

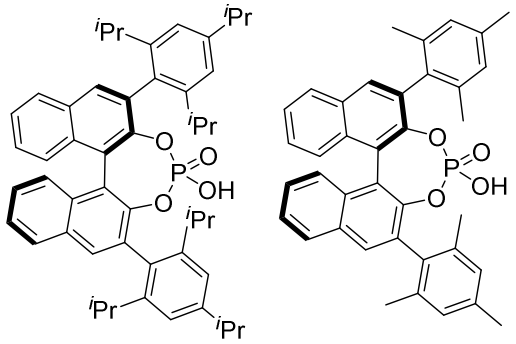

(*R*)-**407** (*R*)-**408**

Figure 48: Chiral phosphoric acids **407** and **408**.

At the outset, (*R*)-BINOL **501** was methylated using methyl iodide and potassium carbonate to afford (*R*)-**502** in 98% yield. Subsequent deprotonation at the *ortho*-position and halogen quenching provided (*R*)-**503** in 71% yield (Scheme 206). Attempts to introduce boron by addition of triethyl boronate instead of iodine failed. (*R*)-**503** is used as a general building block for preparation of BINOL-based ligands and acids.

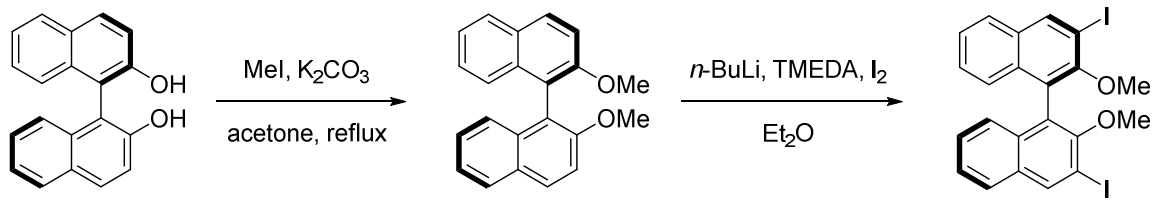

(*R*)-**501** (*R*)-**502** (*R*)-**503**

98% 71%

Scheme 206: Preparation of building block (*R*)-**503**.

(*R*)-**503** was arylated by Kumada coupling with mesityl magnesium bromide (**504**) using nickel catalyst **505** to afford (*R*)-**506** (Scheme 207). Deprotection of the methyl ether (*R*)-**506** was demonstrated to result in higher yields when conducted in a one-pot fashion.[133] Hence, (*R*)-**506** was directly subjected to boron tribromide to afford (*R*)-**507** in 52% yield over two steps.

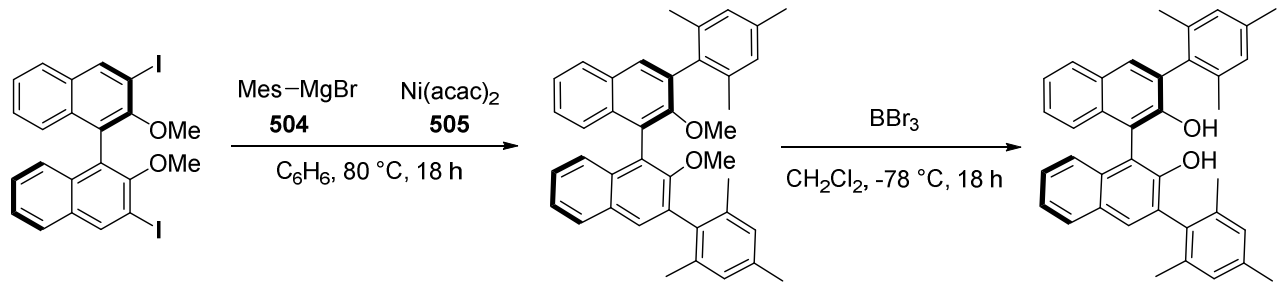

(*R*)-**503** (*R*)-**506** (*R*)-**507**

52%
(over 2 steps)

Scheme 207: Synthesis of BINOL (*R*)-**507**.

In a similar fashion, (*R*)-**503** was reacted with zinc bromide **508**. **508** was freshly prepared from 1,3,5-triisopropylbromobenzene and zinc bromide, and reacted with (*R*)-**503** in a Negishi coupling using *Fu*'s palladium-catalyst **509** to afford (*R*)-**510** (Scheme 208). One-pot demethylation with boron tribromide afforded (*R*)-**511** in 50% yield over two steps.[134]

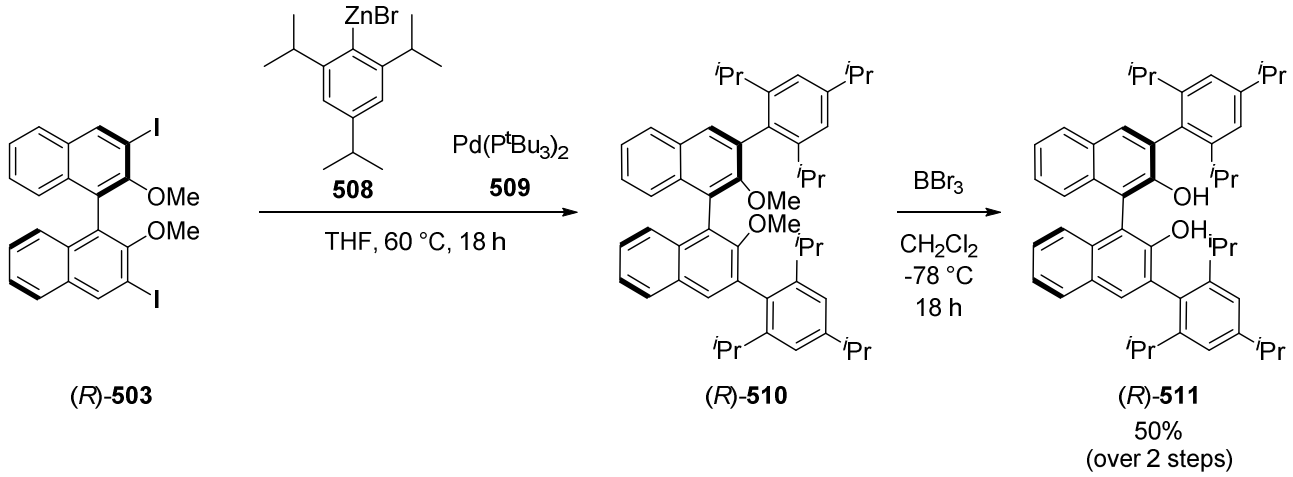

Scheme 208: Synthesis of BINOL (*R*)-**511**.

Ultimately, preparation of the phosphoric acid was performed in a three-step one-pot procedure (Scheme 209). Phosphorylation with phosphorus oxychloride, subsequent hydrolysis of the phosphine chloride and acidification followed by recrystallisation in aqueous hydrogen chloride furnished the chiral phosphoric acids (*R*)-**407** in 55% and (*R*)-**408** in 25% yield.[135]

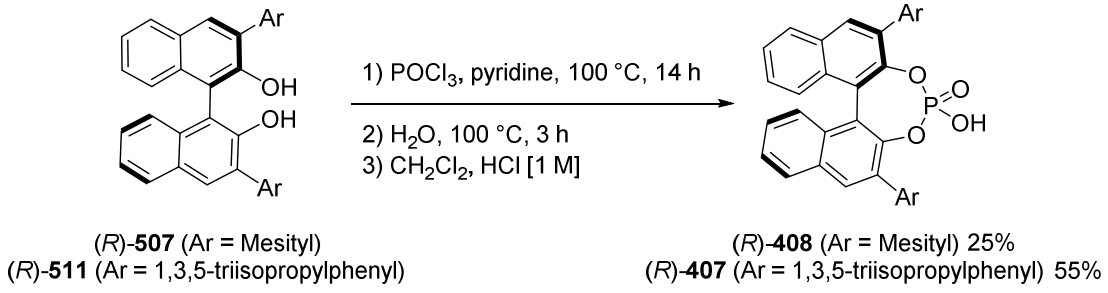

Scheme 209: Preparation of chiral phosphoric acids (*R*)-**407** and (*R*)-**408**.

Chapter 5 – Synthetic Investigations

Asymmetric Hydrogenation of acyclic aliphatic imines

In the previous chapter the *in situ* formation of iridacycle catalysts for the hydrogenation of aliphatic imines has been demonstrated. In order to render the gained knowledge into a synthetically useful methodology, optimisation studies were conducted. In a primary attempt, the cyclometalating imine was varied. Different substituents at the acetophenone-derived aryl ring as well as at the *N*-aryl ring were introduced. *In situ* cyclometalation and iridacycle formation prior to catalysis would form the active catalyst.
The structurally related PHOX and SimplePHOX catalysts were demonstrated to afford the highest enantioselectivities in imine hydrogenation of acetophenone-derived *N*-aryl imines.[31] They were evaluated as catalysts. The influence on both enantioselectivity and reactivity of a large variety of imines as additives was tested. Cyclohexyl methyl *N*-phenyl imine **329** was chosen as the test substrate. Full conversion and 73% enantiomeric excess were obtained with PHOX catalyst **86** in the presence of imine **59**. Using SimplePHOX catalyst **87**, 74% enantiomeric excess was observed along with full conversion (Scheme 210).

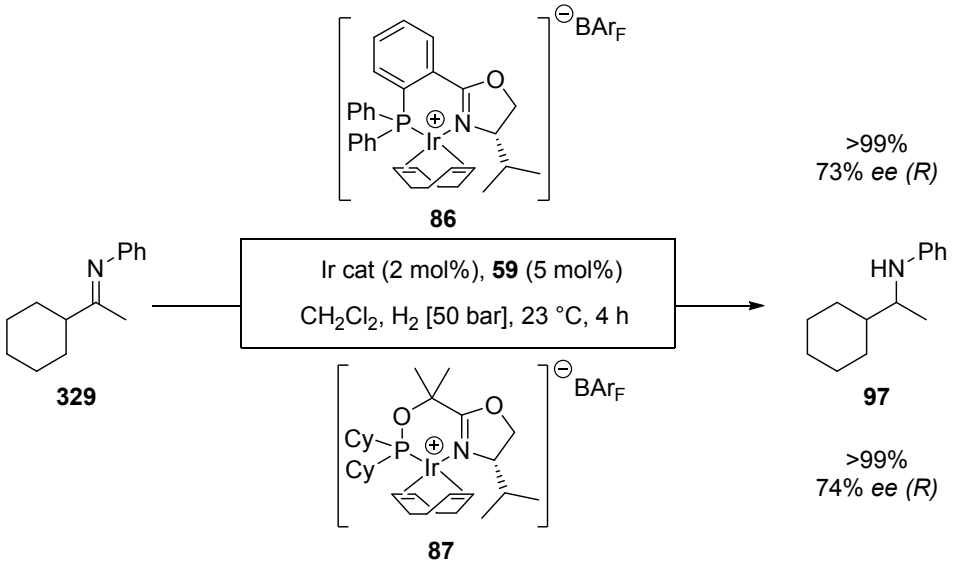

Scheme 210: Asymmetric hydrogenation of cyclohexyl methyl *N*-phenyl imine **329** with iridium catalysts **86** or **512** and imine additive **59**

The first variation of the catalytic system was the introduction of a sterically more demanding acetophenone-derived aryl ring.

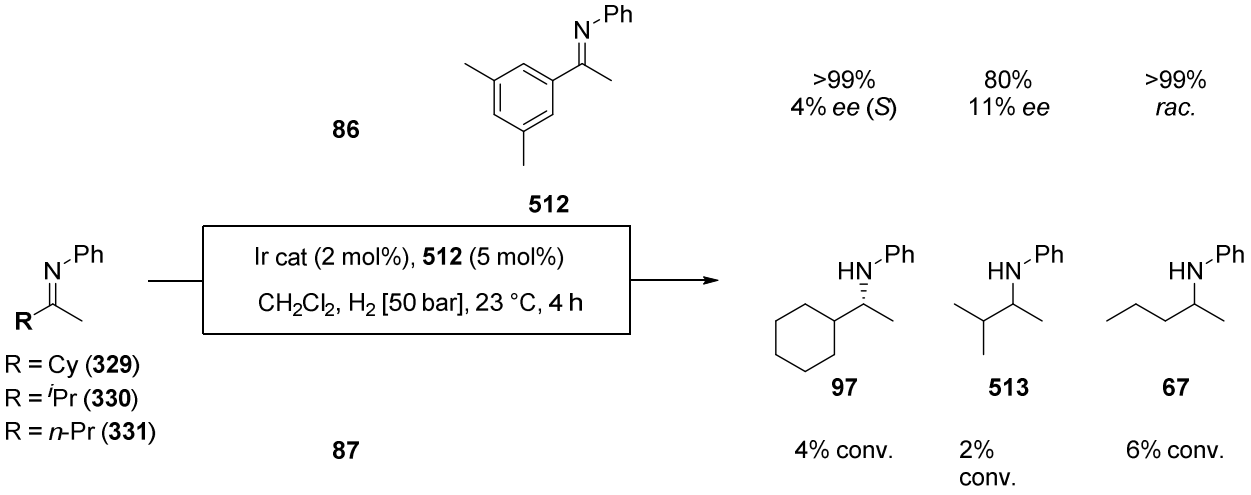

Scheme 211: Asymmetric hydrogenation of imines **329**, **330** and **331** with iridium catalysts **86** or **87** and imine additive **512**

3,5-Dimethylacetophenone-derived imine **512** was used as an additive (Scheme 211). When applying PHOX catalyst **86**, full conversion with low, inverted enantioselectivity of 4% was observed. On the other hand, very low conversions were obtained when using SimplePHOX catalyst **87**. In order to exclude substrate

incompatibility, imines **330** and **331** were also tested. When comparing catalysts **86** and **87**, imines **329**, **330** and **331** were significantly less reactive with the combination of **87** and **512**. This was somewhat surprising since catalyst **87** and imine **59** afforded amine **97** in full conversion and 74% enantiomeric excess, virtually identical to the results obtained with PHOX catalyst **86** (Scheme 210). While the electronic properties of the PHOX and the SimplePHOX ligands are quite different with regards to the phosporus moiety, it rather seemed that the two additional methyl group at the acetophenone-derived aryl ring exhibit too large steric bulk and thus prevent iridacycle formation.

In order to test this hypothesis, the corresponding iridacycles were prepared. Iridacycle preparation of **514** and **515** provided yellow solids displaying one hydride ^{1}H- and one ^{31}P-NMR signal (Scheme 212).

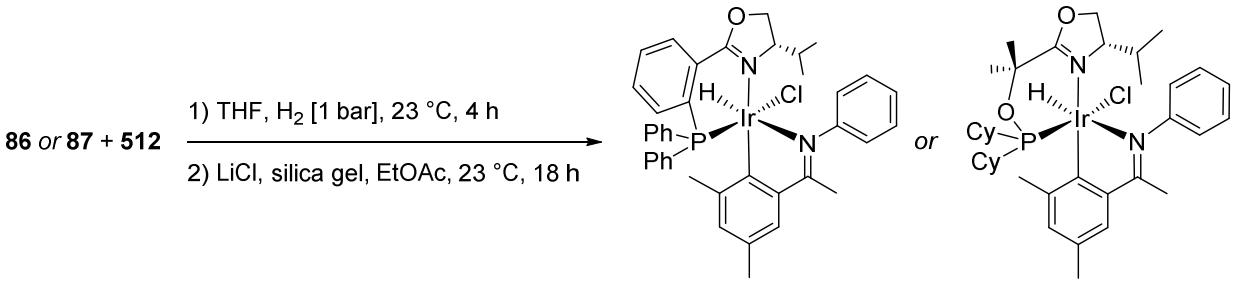

514 **515**

Scheme 212: Preparation of iridacycles **514** and **515**

Table 24 displays the results of testing them as catalysts in the hydrogenation of different aliphatic imines. Reactions were performed at lower pressure to obtain a clear picture of the reactivity or possible decomposition processes. At higher hydrogen pressure, other mechanisms might be operating and thus **514** and **515** show a similar reactivity. *In situ* iridacycle formation can not be verified at high pressure. Only imine **59** (entries 3, 11 and 12) was reduced with moderate to high yields, albeit still with lower enantioselectivity compared to using **86** or **87** alone.

Table 24: Asymmetric hydrogenation of imines **59**, **329**, **330** and **331** with iridacycles **514** and **515**

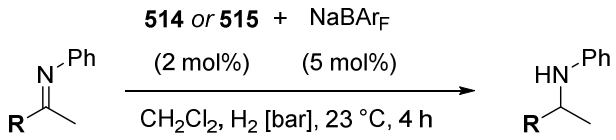

Entry	Catalyst	Imine	*p* [bar]	Conv. [%][a)]	*ee* [%][b)]
1	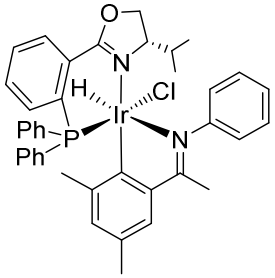	**329**	1	0	-
2			7	15	-
3		**59**	1	4	-
4			7	60	58 (*R*)
5		**330**	1	0	-
6			7	8	-
7		**331**	1	3	-
8			7	20	-

514

9	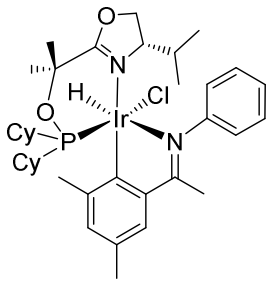	**329**	1	0	-
10			7	2	-
11		**59**	1	25	86 (*R*)
12			7	98	86 (*R*)
13		**330**	1	0	-
14			7	0	-
15		**331**	1	6	-
16	**515**		7	12	-

a) Determined by GC analysis. b) determined by HPLC analysis on a chiral stationary phase.

These results indicated that the steric repulsion of the acetophenone-derived aryl ring is too large and thus hydrogenation only takes place at high pressure. Despite these disappointing preliminary results, other imine substrates with larger substituents were prepared. The synthesis of the 3,5-di-isopropyl imine **522** was conducted as shown in Scheme 213. 2,6-diisopropylaniline **516** was brominated to 4-bromo-2,6-diisopropylaniline **517** with tetra-*n*-butyl ammonium perbromide in 91% isolated yield. Sandmeyer de-azonation (Meerwein reduction) with hypophosphorous acid provided 3,5-di-isopropylbromobenzene **518** in 56% yield. Subsequent Vilsmeier-Haack-type formylation with *n*-butyl lithium and dimethylformamide furnished the corresponing aldehyde **519** in 66% yield. Nucleophilic addition of methyl magnesium bromide gave the benzylic alcohol **520** in 85% yield. Oxidation of the benzylic alcohol **520** to the desired ketone **521** with Dess-Martin-Periodane performed smoothly in 95% yield. Ultimately, condensation of ketone **521** with aniline (**142**) in refluxing toluene provided imine **522** as a yellow oil in 45% yield.

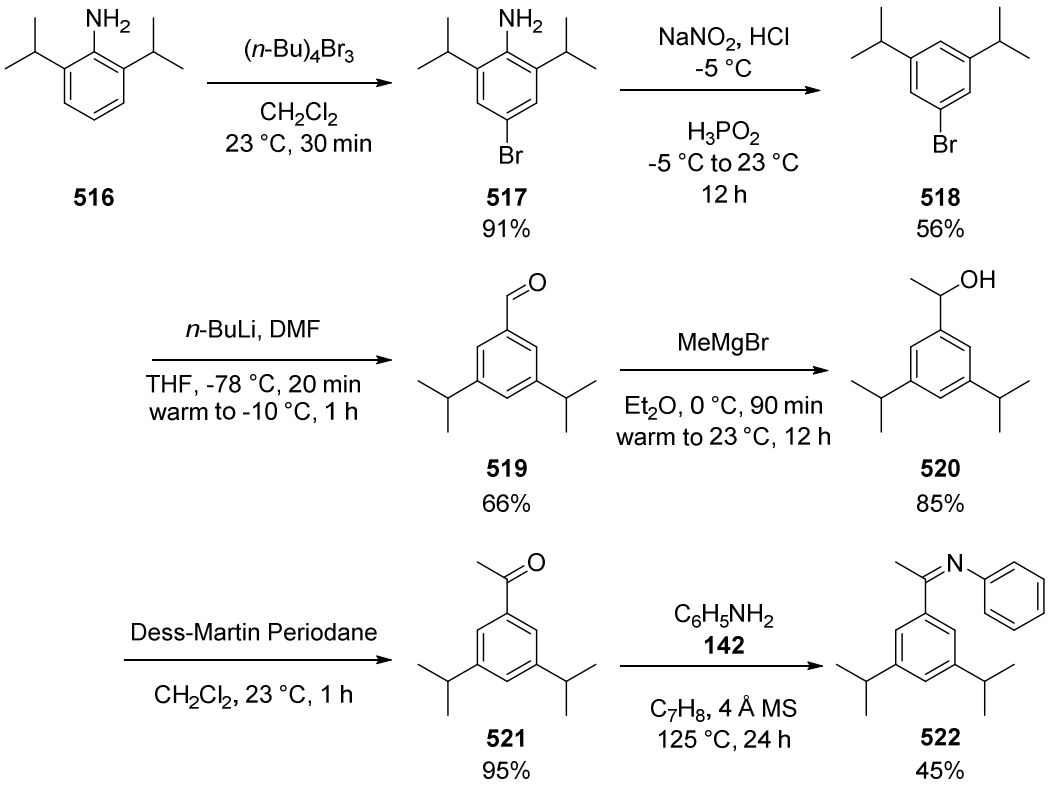

Scheme 213: Synthesis of imine **522**

Identical to the conducted synthetic route delivering **522**, 3,5-di-*tert*-butylbenzaldehyde **523** was reacted with methyl magnesium bromide to provide the benzylic alcohol **524** in 96% yield (Scheme 214). Subsequent oxidation with Dess-Martin Periodane to the ketone **525** in 96% and condensation with aniline (**142**) to the imine **526** in 56% yield proceeded as expected.

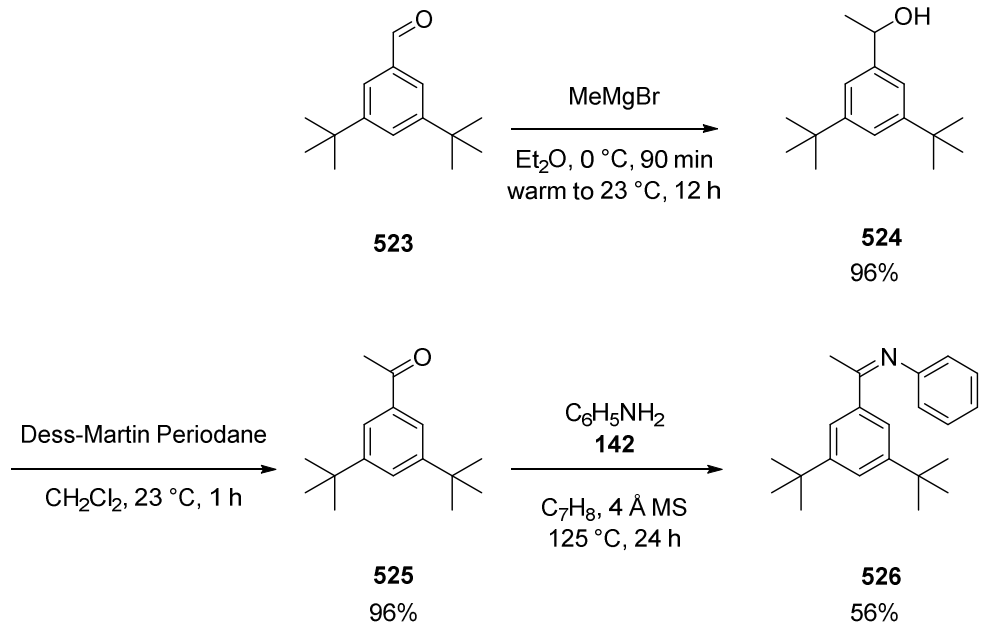

Scheme 214: Preparation of imine **526**

The influence of imines **522** and **526** as additives was subsequently tested in the hydrogenation of aliphatic imines (Table 25). They were only tested with the PHOX catalyst **86**, since the SimplePHOX analogue **87** had already shown very poor conversions in combination with the sterically less demanding imines **330** and **331** in test reactions (Scheme 211).

Table 25: Asymmetric hydrogenation of imines **329**, **330** and **331** using **86** and **522** or **526**

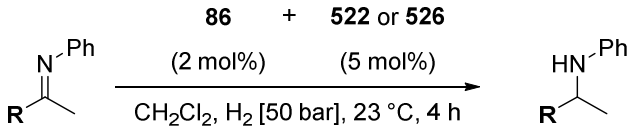

Entry	Imine Additive	Imine	Conv. [%][a)]	*ee* [%][b)]
1		**329**	45	26 (*S*)
2	**522**	**330**	29	4 (*R*)
3		**331**	23	*rac.*
4		**329**	10	20 (*R*)
5	**526**	**330**	13	5 (*R*)
6		**331**	13	4

a) Determined by GC analysis. b) determined by HPLC analysis on a chiral stationary phase.

With both imines **522** and **526** lower conversions than with imine **512** were obtained. Again, the enantioselectivity was inverted in the case of the **522** but not with **526**. The overall low yields compared to the results obtained using imines **59** and **512** strenghtened the concern that such imines exert too much steric bulk. The poor conversion could be explained by the inability of iridacycle formation with imine **522** or **526**. Indeed, when attempting to prepare the corresponding iridacycle of imine **526** no iridacycle could be isolated.

On the contrary, the corresponding iridacycle **527** of imine **522** was obtained as a single species displaying one hydride ^{1}H- and one ^{31}P-NMR signal. When using iridacycle **527** as a catalyst, full conversion was observed (Table 26). The enantioselectivity was increased from 26% to 42% of the (*S*)-enantiomer for imine **329**. The same enantiomer was also obtained when the iridacycle catalyst was formed *in situ*. Inversion of

enantioselectivity was observed as well in the case of the imine **330**. This had not been the case when the catalyst was formed *in situ*.

Table 26: Asymmetric hydrogenation of imines **329**, **330** and **331** using iridacycle **527**

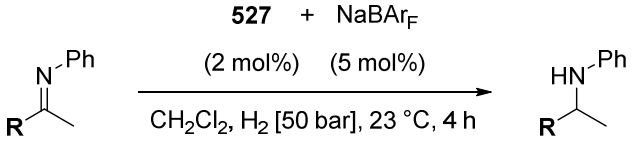

Entry	Catalyst	Substrate	Conv. [%][a)]	*ee* [%][b)]
1	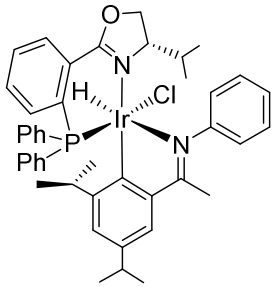	**329**	>99	42 (*S*)
2		**330**	>99	10 (*S*)
3		**331**	>99	*rac.*
	527			

a) Determined by GC analysis. b) determined by HPLC analysis on a chiral stationary phase.

The origin of inverted enantioselectivty of the catalyst was unclear. The two isopropyl groups of imine **522** might result in a change of the overall catalyst conformation. The high impact on enantiodiscrimination with such imine additives is displayed in the inversion of enantioselectivity with imines **512** and **522**. However, when attempting to further increase the steric bulk of the additive only poor yields are observed and iridacycle formation does not occur in the case of imine **526**. This is possibly due to steric repulsion of the additive imine to the ligand.

Since increasing the steric bulk of the acetophenone aryl ring did not afford higher selectivities, electronic effects of the imine additive were studied. Therefore, the substituent in the *para*-position of the acetophenone aryl ring was varied (Table 27). All enantioselectivites obtained have to be compared to the *ee* of 73% for the (*R*)-isomer obtained in full conversion with acetophenone-derived *N*-phenyl imine **59** (Entry 1). 3,5-Alkyl di-substituted imines **512**, **522** and **526** gave lower conversions and lower (opposite) enantioselectivities (Entries 2, 3 and 4). With regards to substituents in the *para*-position of the acetophenone-derived aryl ring, electron–rich or electron–neutral imines **528**, **314** and **322** (Entries 5, 6 and 7) as well as electron–poor imines **323** and **310** (Entries 8 and 9) furnished amine **97** in full conversion in enantiomeric excesses of 56-66%. Only strongly electron–withdrawing imines such as **324**, **529**, **530** and **531** (Entries 10 to 13) lowered both conversion and enantioselectivity. Overall no improvement in terms of enantioselectivity was observed. A trend of decreased reactivity and selectivity can be drawn from the table disfavouring imine additives with strongly electron-withdrawing substituents. Similar to substituents in the *para*-position of the acetophenone-derived aryl ring, electron–poor imines reduce the reactivity and selectivity of the formed iridacycle catalyst. Whereas alkyl-substituents in the *meta*-position seem to significantly influence the enantiodiscrimination of the catalyst by their steric bulk, imines such as **530** and **531** could as well explain the poor conversion due to their electron-withdrawing substituents. Especially NO_2-substituted imines **529**-**531** showed lower conversion and poor enantioselectivity.

Moreover, virtually no difference between a methyl- and a fluoro-substituent in the *ortho*-position in terms of selectivity is observed (Entries 13 and 14). Especially with **319**, a strong effect on the enantiodiscrimination would be expected due to the electronic difference to imine **59**. However, the obtained reactivity and selectivity are virtually identical to imine **59**.

Table 27: Asymmetric hydrogenation of **329** with **86** forming iridacycles with electronically varied imines

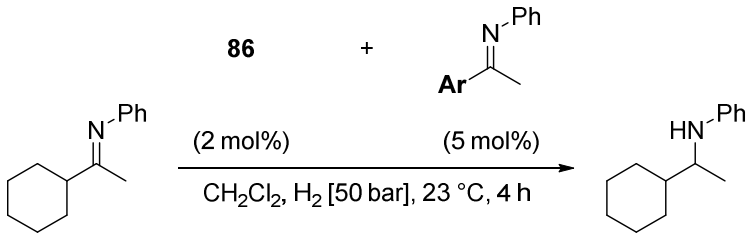

329 **97**

Entry	Imine Additive	Conv. [%][a)]	*ee* [%][b)]
1	**59** (Ar = Ph)	>99	73 (*R*)
2	**512** (Ar = 3,5-di-Me-Ph)	>99	4 (*S*)
3	**522** (Ar = 3,5-di-^{i}Pr-Ph)	45	26 (*S*)
4	**526** (Ar = 3,5-di-^{t}Bu-Ph)	10	20 (*R*)
5	**528** (Ar = 4-^{t}Bu-Ph)	>99	64 (*R*)
6	**314** (Ar = 4-Me-Ph)	>99	63 (*R*)
7	**322** (Ar = 4-OMe-Ph)	>99	67 (*R*)
8	**323** (Ar = 4-Cl-Ph)	>99	56 (*R*)
9	**310** (Ar = 4-F-Ph)	>99	66 (*R*)
10	**324** (Ar = 4-CF_3-Ph)	95	50 (*R*)
11	**529** (Ar = 4-NO_2-Ph)	40	45 (*R*)
12	**530** (Ar = 3,5-di-NO_2-Ph)	15	15 (*R*)
13	**531** (Ar = 3-NO_2-Ph)	75-99[c)]	48 (*R*)
14	**319** (Ar = 2-F-Ph)	90-95[c)]	70 (*R*)
15	**318** (Ar = 2-Me-Ph)	>99	69 (*R*)

a) Determined by GC analysis;
b) determined by HPLC analysis on a chiral stationary phase;
c) range observed over three reactions.

In further optimisation attempts, the *N*-aryl-ring was varied as can be seen in Table 28. Primarily, electronically different substituents in the *para*-position were evaluated. A similar trend to previous results with electronically different imine additives was observed. Electron–withdrawing substituents as with imine **532** (Entry 2) lower both reactivity and enantioselectivity. Electron-neutral substitution, e.g. with a methoxy substituent from *para* (**99**) to *meta* (**533**) and *ortho* (**534**) (Entries 1, 3 and 4) substitution did not alter reactivity or enantioselectivity significantly. Neither did a large halogen atom in ortho-position (Entry 5) as in **535**. On the other hand, introduction of an alkyl substituent in the *ortho*-position as with the imine **536** (Entry 6) did increase the enantioselectivity while maintaining reactivity. A sterically more demanding isopropyl substituent of imine **537** (Entry 7) further increased the enantioselectivity. Ultimately, application of acetophenone *N*-2,6-dimethylphenyl imine **340** (Entry 8) gave the highest enantioselectivity of 85%. Overall, substitution at the *N*-aryl ring did increase enantioselectivity with sterically demanding alkyl groups. Attempts to prepare sterically more demanding imines such as *N*-2,6-diisopropyl or *N*-2,6-dimethoxy failed.

Table 28: Asymmetric hydrogenation of **329** using **86** and electronically and sterically varied imines **99, 340** and **532-537**

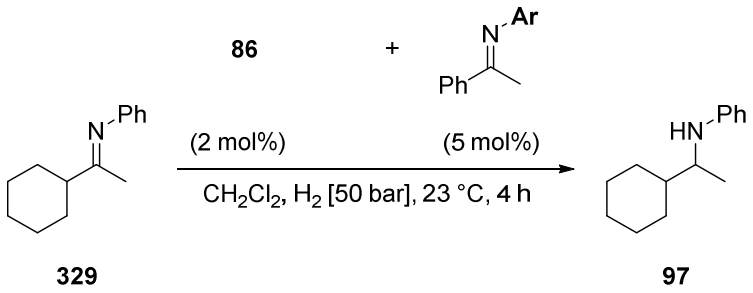

329 **97**

Entry	Imine Additive	Conv. [%][a]	*ee* [%][b]
1	**99** (Ar = 4-OMe-Ph)	>99	69 (*R*)
2	**532** (Ar = 4-CF_3-Ph)	60	59 (*R*)
3	**533** (Ar = 3-OMe-Ph)	>99	68 (*R*)
4	**534** (Ar = 2-OMe-Ph)	>99	71 (*R*)
5	**535** (Ar = 2-Br-Ph)[c]	>99	68 (*R*)
6	**536** (Ar = 2-Me-Ph)	>99	78 (*R*)
7	**537** (Ar = 2-^{i}Pr-Ph)	>99	81 (*R*)
8	**340** (Ar = 2,6-di-Me-Ph)	>99	85 (*R*)

a) Determined by GC analysis;
b) determined by HPLC analysis on a chiral stationary phase;
c) *p*-tolyl acetophenone-derived moiety.

For comparison, complex **87** was also evaluated as a catalyst in this application (Table 29). While substituents at the acetophenone-derived aryl ring as **322**, **529** and **531** (Entries 2, 3 and 4) gave similar reactivities and slightly increased enantioselectivities compared to complex **86**, the sterically more demanding imines **512**, **536**, **537** and **340** (Entries 5 to 8) gave lower to no turnovers. This is possibly due to steric repulsion and thus prevented iridacycle formation with complex **87**. While complex **87** and imine **536** provide amine **97** in the same enantioselectivity as complex **86** and imine **340**, several aspects disfavour this combination. Preparation of the SimplePHOX complex **87** requires more synthetic steps than the PHOX complex **86**. Additionally, imine **536** is isolated as an oil and prone to hydrolysis when handled in air. On the contrary, imine **340** is isolated as a solid relatively stable and inert to decomposition processes when handled in air.

Table 29: Asymmetric Hydrogenation of **329** using **87** and different imine additives.

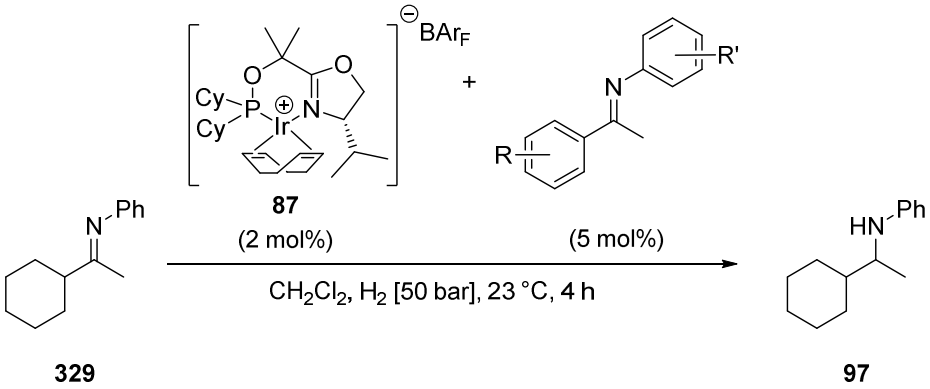

329 **97**

Entry	Imine Additive	Conv. [%][a)]	*ee* [%][b)]
1	**59** (R = H; R' = H)	>99	74 (*R*)
2	**322** (R = 4-OMe; R' = H)	>99	73 (*R*)
3	**529** (R = 4-NO_2; R' = H)	>99	58 (*R*)
4	**531** (R = 3-NO_2; R' = H)	>99	55 (*R*)
5	**512** (R = 3,5-di-Me; R' = H)	3	-
6	**536** (R = H; R' = 2-Me)	60	85 (*R*)
7	**537** (R = H; R' = 2-^{i}Pr)	40	70 (*R*)
8	**340** (R = H; R' = 2,6-di-Me)	0	-

a) Determined by GC analysis; b) determined by HPLC analysis on a chiral stationary phase.

The next goal was to optimize reaction conditions with regard to reaction temperature. To better compare the results obtained, imine **59** and **340** were used as additives. Both complexes **86** and **87** were tested as catalysts systematically (Table 30). Optimal conditions were found when the reaction was carried out at -5 °C. Full conversion to amine **97** with high enantioselectivity of 92% was achieved with catalyst **86** and imine **340** (Entry 4). The same enantioselectivity could also be reached with the combination of catalyst **87** and imine **536** albeit with incomplete conversion (Entry 6). Complex **87** and imine **59** provide amine **97** at temperatures as low as -20 °C, but enantioselectivities no higher than 87% were obtained (Entry 10). On the other hand, the iridacycle generated from PHOX catalyst **86** show low (with **340**, Entry 9) to no (with **59**, Entry 8) catalytic activity at -20 °C.

Table 30: Optimization of reaction parameters for asymmetric hydrogenation of imine **329**

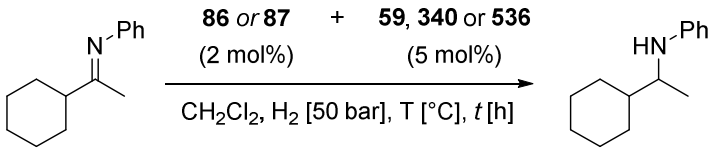

329 **97**

Entry	Catalyst	Imine Additive	T [°C]	*t* [h]	Conv. [%][a)]	*ee* [%][b)]
1	**86**	-	23	4	27	36 (*R*)
2	**87**	-	23	4	3	-
3	**86**	**59**	-5	12	>99	73 (*R*)
4	**86**	**340**	-5	12	>99	92 (*R*)
5	**87**	**59**	-5	12	>99	85 (*R*)
6	**87**	**536**	-5	12	77	92 (*R*)
7	**87**	**340**	-5	12	0	-
8	**86**	**59**	-20	4	2	-
9	**86**	**340**	-20	4	35	90 (*R*)
10	**87**	**59**	-20	4	>99	87 (*R*)
11	**87**	**340**	-20	4	0	-

a) Determined by GC analysis; b) determined by HPLC analysis on a chiral stationary phase.

Table 31 summarizes all the optimisation experiments. While initially no conversion was observed in the absence of imine **59** even at elevated pressure (Entry 2), the conversion was drastically improved upon the addition of imine **59** (Entry 3) and full conversion was observed when conducting the reaction at higher

pressure (Entry 4). Furthermore, optimisation of the imine additive structure leading to sterically demanding *N*-aryl imine additive **340** improved the enantioselectivity of the reaction (Entry 5). Ultimately, conducting the reaction at low temperature further improved the enantioselectivity while maintaining the reactivity (Entry 6). The reaction conditions are exceptionally mild.

Table 31: Summary of optimization efforts towards the asymmetric hydrogenation of imine **329**

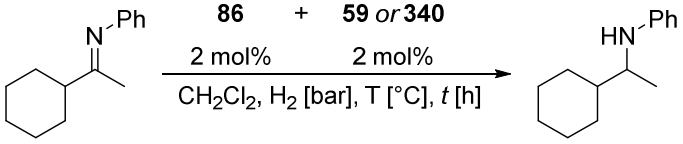

329 **97**

Entry	Imine Additive	*p* [bar]	T [°C]	*t* [h]	Conv. [%][a)]	*ee* [%][b)]
1	-	1	23	4	5	69 (*R*)
2	-	50	23	4	27	35 (*R*)
3	**59**	1	23	4	50	69 (*R*)
4	**59**	50	23	4	>99	73 (*R*)
5	**340**	50	23	4	>99	85 (*R*)
6	**340**	50	-5	18	>99	92 (*R*)

a) Determined by GC analysis; b) determined by HPLC analysis on a chiral stationary phase.

While PHOX complex **86** and SimplePHOX complex **87** have been demonstrated to be the most selective catalysts for acetophenone-derived *N*-aryl imine[31] no such evaluation has been conducted for aliphatic imines. Therefore many complexes available within the *Pfaltz* group were tested on a substrate with two alkyl chains, *n*-hexyl methyl *N*-phenyl imine **334** (Table 32). Such a substrate has a different scaffold compared to acetophenone-derived *N*-aryl imines or imine **59**. It was intended to obtain a better picture of the general ability of the ligands to differentiate between to alkyl groups which exert akin steric bulk. [25]

As can be seen from Table 32, the initially used PHOX and SimplePHOX catalysts displayed the highest enantioselectivites (Entries 1 to 5). In many cases the combination of the iridium catalyst and imine **340** resulted in poor yields and enantioselectivities, especially when the hydrogenation was conducted at lower reaction temperatures. An explanation might be the inability of the correspong iridacycle formation or the fact that the resultant iridacycle is not reactive. The preparative cyclometalation of all possible combinations has not been studied. Some ligands (e.g. **L5** and **L6**) did already show low conversion and selectivity with acetophenone-derived *N*-aryl imines[31] and thus some ligands might inherently be less active towards imine hydrogenation.

The best ligand found for imine **334** turned out to be the ^{t}Bu-PHOX ligand **L1** (Entries 1 to 3). Only ligand **L18** also provided an enantioselectivity above 20% (Entry 30). Since the synthesis of such a ligand is more elaborate than **L1**, complex [Ir(**L1**)(COD)]BAr$_F$ **388** in combination with imine **340** was selected as the most potent combination forming the active iridacycle catalyst *in situ* for imine hydrogenation of acyclic substrates.

[25] Imine **334** was freshly prepared and stored as a stock solution. All screening reactions were conducted with the same stock solution. Reactions were setup while being purged with argon. Over the course of a few days, the stock solution of imine **334** did turn yellow while being stored under argon atmosphere in the freezer. The poor yields are due to competitive hydrolysis which occurred to a large extent at lower reaction temperatures. On re-examination by freshly preparing imine **334** via distillation under inert atmosphere and setting up all hydrogenation in the glove box, no competitive hydrolysis was observed.

Table 32: Screening of iridium catalysts for asymmetric hydrogenation of imine **334**

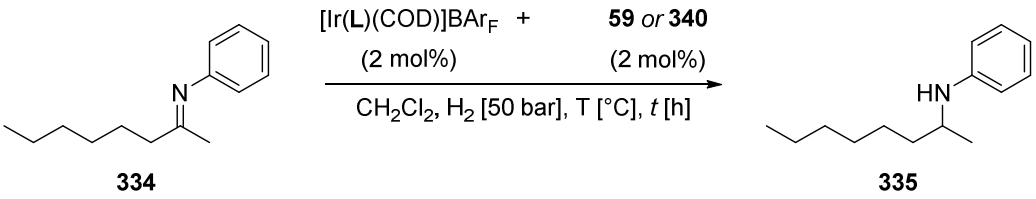

334 **335**

Entry	L (Ligand)		Imine Additive	T [°C]	*t* [h]	Conv. [%][a]	*ee* [%][b]
1	**L1**	R_2 = ^{t}Bu, R_1 = Ph	**59**	23	4	>99	24 (*R*)
2			**340**	23	4	84	47 (*R*)
3			**340**	-5	18	21	53 (*R*)
4	**L2**	R_2 = ^{i}Pr, R_1 = Ph	**59**	23	4	>99	18 (*R*)
5			**340**	23	4	>99	36 (*R*)
6			**340**	-5	18	60	44 (*R*)
7	**L3**	R_2 = ^{t}Bu, R_1 = Cy	**59**	23	4	>99	18 (*R*)
8			**340**	23	4	79	7 (*R*)
9	**L4**	R_2 = ^{i}Pr, R_1 = Cy	**59**	23	4	>99	14 (*R*)
10			**340**	23	4	84	4 (*R*)
11	**L5**	R = *o*-Tol	**59**	23	4	97	7 (*R*)
12	**L6**	R = Cy	**59**	23	4	>99	8 (*R*)
13	**L7**	R_2 = ^{t}Bu, R_1 = *o*-Tol	**59**	23	4	39	-
14	**L8**	R_2 = ^{t}Bu, R_1 = Ph	**59**	23	4	51	-
15			**59**	23	4	>99	14 (*R*)
16	**L9**	R_2 = ^{i}Pr, R_1 = Ph	**340**	23	4	80	8 (*S*)
17			**340**	-5	18	3	5 (*S*)
18	**L10**	R_2 = ^{t}Bu, R_1 = Cy	**59**	23	4	13	-
19	**L11**	R_2 = ^{i}Pr, R_1 = Cy	**59**	23	4	95	10 (*R*)
20			**340**	23	4	28	-
21	**L12**	R_2 = ^{t}Bu, R_1 = ^{t}Bu	**59**	23	4	33	-
22	**L13**	R_2 = ^{i}Pr, R_1 = ^{t}Bu	**59**	23	4	43	-
23	**L14**	R_2 = ^{t}Bu, R_1 = *o*-Tol	**59**	23	4	>99	3 (*R*)
24	**L15**	R_2 = ^{i}Pr, R_1 = Ph	**59**	23	4	>99	13 (*R*)
25			**340**	23	4	51	-
26			**340**	-5	18	12	16 (*R*)
27	**L16**	R_2 = ^{t}Bu, R_1 = ^{t}Bu	**59**	23	4	31	rac.
28	**L17**	R_2 = ^{t}Bu, R_1 = Cy	**59**	23	4	97	11 (*R*)
29	**L18**	R_2 = ^{i}Pr, R_1 = Cy	**59**	23	4	>99	21 (*R*)
30			**340**	-5	18	1	33 (*R*)

31	**L19**	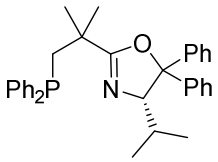	**59**	23	4	>99	18 (*R*)
32			**340**	23	4	27	-
33			**340**	-5	18	3	8 (*R*)
34	**L20**	$R_2 = {}^t$Bu, R_1 = *o*-Tol	**59**	23	4	>99	17 (*R*)
35			**340**	-5	18	4	8 (*R*)
36	**L21**	$R_2 = {}^t$Bu, R_1 = Ph	**59**	23	4	>99	11 (*R*)
37			**340**	23	4	14	4 (*R*)
38	**L22**	$R_2 = {}^i$Pr, R_1 = Ph	**59**	23	4	>99	10 (*R*)
39			**340**	23	4	80	12 (*R*)
40			**340**	-5	18	9	7 (*R*)
41	**L23**	n = 1, R = ^{t}Bu	**59**	23	4	>99	2 (*R*)
42	**L24**	n = 1, R = Ph	**59**	23	4	>99	5 (*R*)
43	**L26**	n = 2, R = *o*-Tol	**59**	23	4	>99	3 (*R*)
44	**L27**	n = 2, R = ^{t}Bu	**59**	23	4	>99	2 (*R*)
45	**L25**	n = 1	**59**	23	4	30	-
46	**L28**	n = 2	**59**	23	4	>99	12 (*R*)
47	**L29**	R = Cy	**59**	23	4	>99	3 (*R*)
48	**L30**	R = Ph	**59**	23	4	>99	15 (*R*)

a) Determined by GC analysis; b) determined by HPLC on a chiral stationary phase.

Subsequently this combination of complex **388** and imine **340** was tested under optimised reaction conditions on imine **329** (Scheme 215). Surprisingly, significantly lower yield and different enantioselectivity were obtained. The enantioselectivity was in the same range as when the reaction was carried out in the absence of an additive imine. Without the additive, higher conversion was observed. Therefore, formation of the iridacycle might have occurred but imine **329** exhibits too much steric bulk to undergo hydrogenation by the *in situ* formed iridacycle catalyst. This would also explain the poor yield.

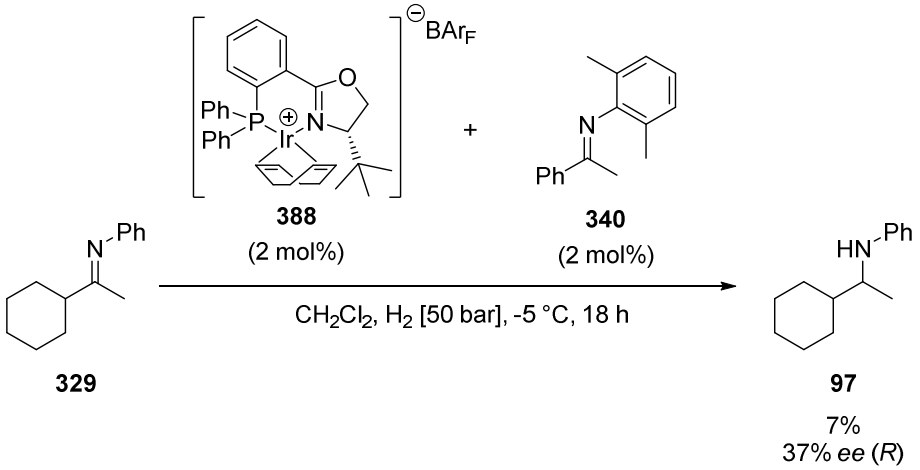

Scheme 215: Asymmetric hydrogenation of imine **329** employing combination of complex **388** and additive **340**

The next substrate evaluated was cyclopentyl methyl *N*-phenyl imine **538** (Table 33). At room temperature, full conversion with moderate enantioselectivities between 42% and 52% were obtained. Importantly, the substrate itself proved to be particularly air- and moisture-sensitive and thus could only be handled in the glove box. When hydrogenations were conducted at lower temperature, poor conversion along with hydrolysis of imine **538** to a large extent was observed. Residual water from the imine additive, the catalyst or even the hydrogen gas applied represent possible origins. Nevertheless, the substrate is less robust than other *di*-alkyl acyclic imines. This can be observed when storing imine **538** under an argon atmosphere in the fridge. Decomposition to a brown material is observed within 12 hours.
The best results were obtained using the combination of either complex **86** and imine **340** or complex **87** and imine **59**. With catalyst **388** and imine **59**, no conversion was observed at all. Similar to imine **329** the cyclopentyl ring might result in too much steric repulsion between the formed iridacycle catalyst and the imine substrate **538**.

Table 33: Asymmetric Hydrogenation of imine **538**

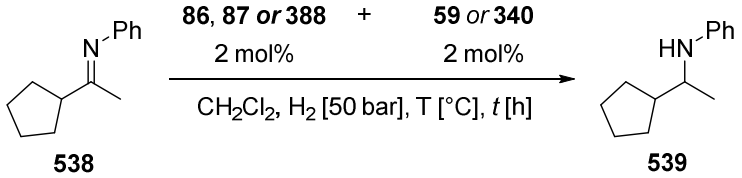

538 **539**

Entry	Catalyst	Imine Additive	T [°C]	*t* [h]	Conv. [%][a)]	*ee* [%][b)]
1	**86**	-	23	4	2	-
2	**87**	-	23	4	0	-
3	**86**	**59**	23	12	>99	50 (-)
4	**86**	**340**	23	12	>99	52 (-)
5	**87**	**59**	23	12	>99	42 (-)
6	**87**	**340**	23	12	0	-
7	**86**	**59**	-5	12	6	56 (-)
8	**87**	**59**	-5	12	28	63 (-)
9	**86**	**340**	-5	18	8	63 (-)
10	**388**	**340**	-5	18	0	-

a) Determined by GC analysis; b) determined by HPLC analysis on a chiral stationary phase.

Imine **331** represents a challenging substrate as it contains two short alkyl chains (Table 34). Surprisingly, full conversion to amine **67** was observed in the absence of an imine additive such as **59**. A possible explanation might be formation of a different catalyst with this particular substrate or a different mechanism operating. The different enantioselectivity observed (Entry 1) in the absence of imine **59** depicts the discrepancy. The best results were obtained with identical reaction conditions used for imine **334** giving similar enantioselectivity (Entry 9).

Table 34: Asymmetric Hydrogenation of imine **331**

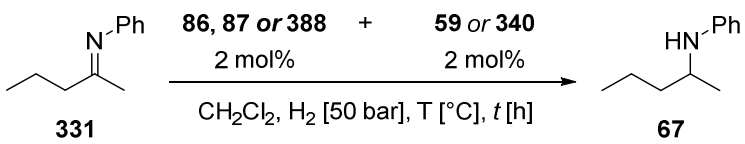

331 **67**

Entry	Catalyst	Imine Additive	T [°C]	*p* [bar]	*t* [h]	Conv. [%][a)]	*ee* [%][b)]
1	**86**	-	23	50	4	>99	30 (-)
2	**86**	**59**	23	1	4	16	21 (-)
3	**86**	**59**	23	50	4	>99	23 (-)
4	**87**	**59**	23	50	12	>99	19 (-)
5	**86**	**340**	23	50	4	>99	35 (-)
6	**86**	**59**	-5	50	12	>99	31 (-)
7	**388**	**59**	-5	50	12	>99	20 (-)
8	**86**	**340**	-5	50	12	>99	40 (-)
9	**388**	**340**	-5	50	12	>99	52 (-)
10	**87**	**59**	-5	50	12	>99	25 (-)
11	**87**	**340**	-5	50	12	5	-

a) Determined by GC analysis; b) determined by HPLC analysis on a chiral stationary phase.

Table 35 depicts the results of *sec*-butyl methyl *N*-phenyl imine **540** with an additional methyl group in the alkyl side chain. The best enantioselectivity of 80% was obtained using **388** with imine **340** (Entry 11).

Table 35: Asymmetric Hydrogenation of imine **540**

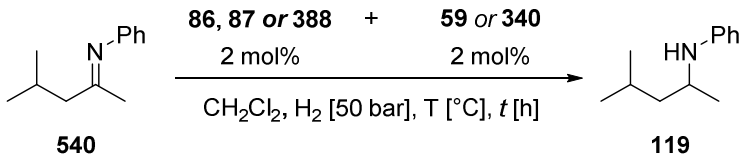

540 **119**

Entry	Catalyst	Imine Additive	T [°C]	*p* [bar]	*t* [h]	Conv. [%][a)]	*ee* [%][b)]
1	**86**	-	23	1	4	1	-
2	**86**	**59**	23	1	4	13	42 (-)
3	**86**	-	23	50	4	30	41 (-)
4	**86**	**59**	23	50	12	>99	41 (-)
5	**86**	**340**	23	50	12	>99	62 (-)
6	**87**	**59**	23	50	12	>99	43 (-)
7	**87**	**340**	23	50	12	22	37 (-)
8	**86**	**59**	-5	50	12	>99	50 (-)
10	**86**	**340**	-5	50	12	>99	70 (-)
11	**388**	**340**	-5	50	12	>99	80 (-)
12	**87**	**59**	-5	50	12	>99	51 (-)
13	**87**	**340**	-5	50	12	0	-

a) Determined by GC analysis; b) determined by HPLC analysis on a chiral stationary phase.

Yet another substrate tested was isopropyl methyl *N*-phenyl imine **330** shown in Table 36

Table 36. Whereas full conversion could be observed when the reaction was conducted at room temperature, lowering the reaction temperature to -5° already resulted in decreased conversion. Imine **330** is not particularly sensitive to hydrolysis. Longer reaction times than 12 hours have not been studied. Best results

were obtained using the combination of PHOX complex **86** and imine **340**. Yields varied over the range of 33-43% in the reaction conducted within the time-frame of 12 hours on an average of four runs.

Table 36: Asymmetric Hydrogenation of imine **330**

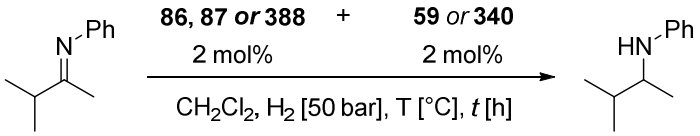

330 **513**

Entry	Catalyst	Imine Additive	T [°C]	*t* [h]	Conv. [%][a]	*ee* [%][b]
1	**86**	-	23	4	8	19 (*R*)
2	**86**	**59**	23	4	>99	59 (*R*)
3	**87**	**59**	23	4	52	57 (*R*)
4	**86**	**59**	-5	12	30	66 (*R*)
5	**87**	**59**	-5	12	96	75 (*R*)
6	**86**	**340**	-5	12	33-43[c]	84 (*R*)
7	**388**	**340**	-5	12	3	-

a) Determined by GC analysis; b) determined by HPLC analysis on a chiral stationary phase; c) 4 runs were performed.

A particularly challenging substrate is the *tert*-butyl methyl *N*-phenyl imine **541** (Table 37). Indeed the large steric bulk exerted by the substrate is displayed in the poor conversions over all hydrogenations conducted. Whereas moderate yields of 30% with 38% *ee* are obtained at room temperature (Entry 3) , the energy barrier seems to be too high to afford any reaction at -5 °C (Entries 5 to 7). Furthermore, similar to imines **329** and **538**, no conversion is observed using complex **388** in combination with imine **340**.

Table 37: Asymmetric Hydrogenation of imine **541**

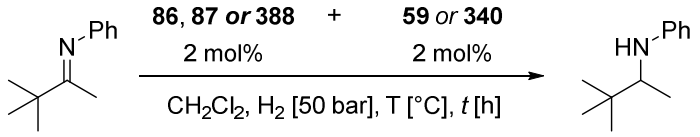

541 **98**

Entry	Catalyst	Imine Additive	T [°C]	*p* [bar]	*t* [h]	Conv. [%][a]	*ee* [%][b]
1	**86**	**59**	23	1	4	3	-
2	**86**	-	23	50	4	6	4 (*R*)
3	**86**	**59**	23	50	4	30	38 (*R*)
4	**87**	**59**	23	50	12	20	8 (*R*)
5	**86**	**59**	-5	50	18	8	46 (*R*)
6	**86**	**340**	-5	50	18	4	35 (*R*)
7	**388**	**340**	-5	50	18	0	-

a) Determined by GC analysis; b) determined by HPLC analysis on a chiral stationary phase.

As reported in chapter 2, the iridacycle catalyst formed under hydrogenation conditions was demonstrated to be a selective reduction catalyst for C=N imine double bonds leaving olefins untouched. To apply this hypothesis to a more challenging substrate, 6-Methyl-5-hepten-2-one *N*-phenyl imine **542** was tested in hydrogenation (Table 38).

Table 38: Asymmetric Hydrogenation of imine **542**

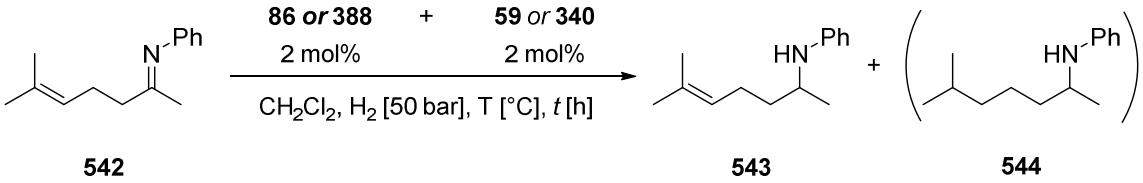

542 **543** **544**

Entry	Catalyst	Imine Additive	T [°C]	*t* [h]	Conv. [%][a]	59 *vs.* 60 [a)]	*ee* [%][b)]
1	**86**	**340**	23	4	>99	74.4 : 17.3	~20-40
2	**388**	**340**	23	4	>99	58.1 : 33.8	~20-40
3	**388**	**340**	-5	18	>99	90.4 : 2.8	56 (-)

a) Determined by GC analysis; b) determined by HPLC analysis on a chiral stationary phase.

The mono-hydrogenated **543** and the *di*-hydrogenated product **544** could not be separated by flash chromatography. The product mixtures were directly subjected to HPLC analysis. Enantiomers of **543** and **544** overlayed in the HPLC chromatogram. *Ee*'s between 20 to 40% (estimated) were observed. Therefore, reaction conditions optimisation was conducted by lowering the reaction temperature to -5 °C. Satisfyingly, virtually selective imine hydrogenation was observed with an enatioselectivity of 56%. This is in the range of substrates tested with two alkyl chains such as imines **334** and **331**.

Another example for competitive olefin and imine reduction is the reaction of (2*E*,3*E*)-*N*,4-diphenylbut-3-en-2-imine **545** (Scheme 216). While cyclometalation was expected to occur prior to olefin hydrogenation based on the results of *F. Barrios*, a mixture of products was obtained in the hydrogenation at atmospheric hydrogen pressure. The findings of *F. Barrios* cannot be applied with this particular substrate due to conjugation of the C=N double bond, the olefin and the aromatic ring.

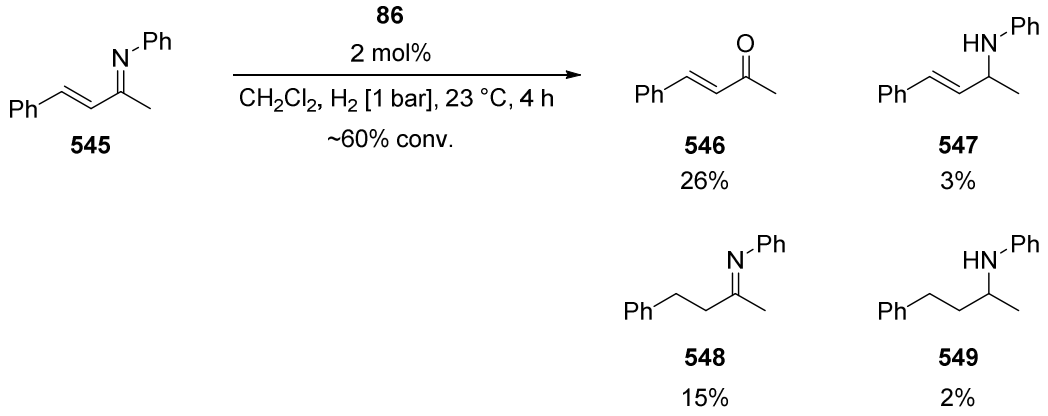

545

546 26%

547 3%

548 15%

549 2%

Scheme 216: Hydrogenation of α,β-unsaturated imine **545**

A clear preference for olefin reduction towards **548** can be observed. Whether this originates from steric or electronic reasons cannot be explained. The hydrogenation itself appears to be disfavoured since about 26% of hydrolysed imine are detected in the form of the α,β-unsaturated ketone **546**. In contrast, if the reaction is carried out at elevated hydrogen pressure (50 bar), complete conversion to the saturated amine **549** without hydrolysis is observed (Scheme 217). For this particular imine **545**, olefin hydrogenation occurs prior to imine hydrogenation. Nevertheless, cyclometalation of the imine substrate is possible. However, the exact nature of the iridacycle could not be determined by NMR spectroscopy (see iridacycle chapter).

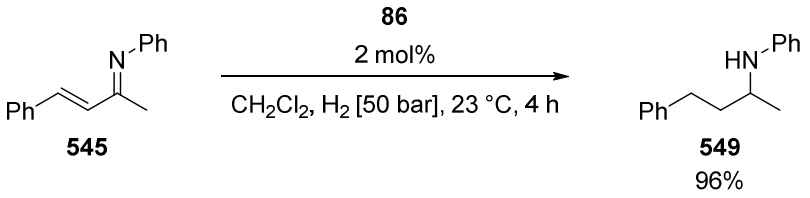

545 **549** 96%

Scheme 217: Hydrogenation of α,β-unsaturated imine **545** at elevated hydrogen pressure

Amine **82** belongs to the structure family of methamphetamines. Such substances are of particular interest in psychopharmacological applications. No enantioselective hydrogenation of this structure class has been reported yet (Jan 2013). Imine **550** is particularly sensitive to moisture and requires strict handling under inert atmosphere. Table 39 summarizes the results. The highest enantioselectivity was observed when the reaction was carried out at -5 °C with complex **388** and imine **340**. If the hydrogenation was carried out at room temperature using **388**, a plethora of side products was obtained. Only at lower temperature selective hydrogenation could be achieved.

Table 39: Asymmetric Hydrogenation of imine **550**

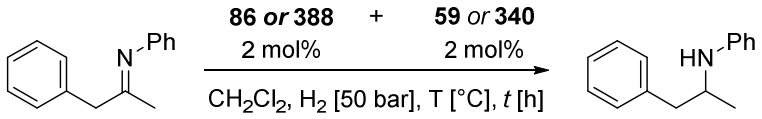

550 **82**

Entry	Catalyst	Imine Additive	T [°C]	*t* [h]	Conv. [%][a)]	*ee* [%][b)]
1	**86**	**59**	23	4	>99	22 (+)
2	**86**	**59**	-5	12	97	26 (+)
3	**86**	**340**	23	4	>99	34 (+)
4	**86**	**340**	-5	12	>99	62 (+)
5	**388**	**59**	23	4	>99	18 (+)
6	**388**	**59**	-5	12	>99	29 (+)
7	**388**	**340**	23	4	<5[c)]	-
8	**388**	**340**	-5	18	94	72 (+)

a) Determined by GC analysis;
b) determined by HPLC analysis on a chiral stationary phase;
c) large amount of side products observed

Scheme 218 summarizes the best results for all acyclic aliphatic *N*-phenyl imines. Imine substrates with two alkyl chains such as **334**, **331**, **540**, **542** and **550** are fully converted to the corresponding amines under optimised reaction conditions. An improvement in reactivity and enantioselectivity was obtained in all cases when comparing to the reaction of the iridium catalyst without additive. When attempting to hydrogenate substrates with sterically more demanding substituents, only imine **329** is fully reduced while other imines such as **538**, **330** and **541** experience only partial conversion. This can be explained by the steric repulsion of the imine substituent and the catalyst. In such a case, hydrolysis becomes favoured and substrates particularly prone to side reactions decompose under hydrogenation reaction conditions.

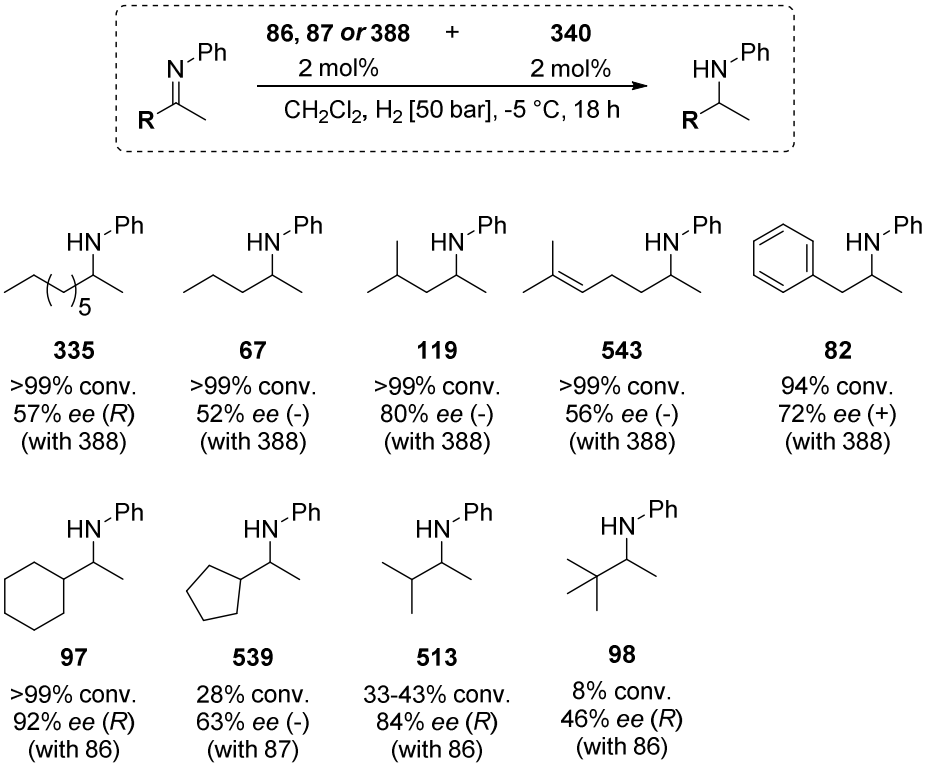

Scheme 218: Summary of asymmetric hydrogenation of aliphatic *N*-phenyl imines

To investigate whether the *N*-phenyl substituent was essential, acyclic all-aliphatic imines were prepared. The corresponding *N*-methyl and *N*-adamantyl substrates could not be prepared. In contrary to the *N*-phenyl derivatives, all-aliphatic imines are particularly air- and moisture-sensitive. Strict exclusion – except for the *N*-benzyl derivative – of water and air was necessary. Therefore, hydrogenations had to be set up in a glove box. Otherwise complete hydrolysis of the substrate was observed under hydrogenation reaction conditions.

The first example is cyclohexyl methyl *N*-benzyl imine **551**. *N*-benzyl imines have been intensively investigated by many research groups. High enantioselectivities with full conversion are generally obtained.[136] In the same tenor, full conversion was observed using catalyst **86** and imine **59** as shown in Table 40. However, reducing the reaction temperature or modifying the imine to a more bulky structure did result in reduced reactivity of the catalyst. Furthermore, hydrolysis of the imine is observed to a large extent. While slightly higher enantioselectivity of 48% was obtained using imine **340**, the reduced reactivity and thus resulting hydrolysis limit the choice of catalyst and imine for this specific substrate.

Table 40: Asymmetric Hydrogenation of imine **551**

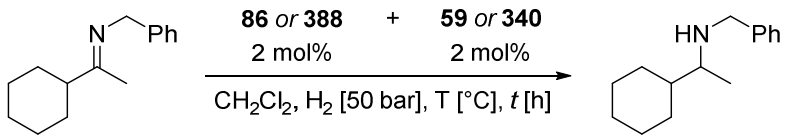

551 **84**

Entry	Catalyst	Imine Additive	T [°C]	*t* [h]	Conv. [%][a)]	Hydrolysis [%]	*ee* [%][b)]
1	**86**	**59**	23	4	>99	-	44 (*R*)
2	**86**	**59**	-5	18	98	58	39 (*R*)
3	**86**	**340**	23	4	>99	48	36 (*R*)
4	**86**	**340**	-5	18	>99	83	48 (*R*)
5	**388**	**59**	23	4	>99	-	18 (*R*)
6	**388**	**59**	-5	18	>99	-	31 (*R*)
7	**388**	**340**	23	4	>99	56	16 (*R*)
8	**388**	**340**	-5	18	96	64	39 (*R*)

a) Determined by GC analysis;
b) determined after derivatisation to the 1-naphtoylamide by HPLC analysis on a chiral stationary phase.

The next example is cyclohexyl methyl *N*-*n*-butyl imine **552**. This substrate prooved to be particularly sensitive to moisture. Similar to the results obtained with imine **551**, only the combination of catalyst **86** and imine **59** gave the corresponding amine **553** in full conversion (Table 41). A low enantioselectivty of 33% was observed. This is significantly lower than the corresponding *N*-phenyl substrate. Nevertheless, the low steric bulk and flexibility of the *N*-alkyl chain can explain the low enantioselectivity observed.

Table 41: Asymmetric Hydrogenation of imine **552**

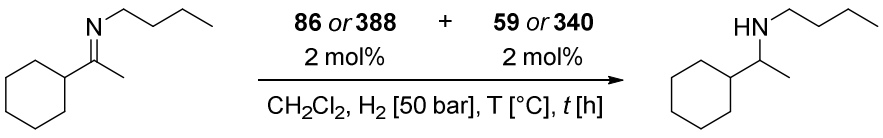

552 **553**

Entry	Catalyst	Imine Additive	Conv. [%][a)]	*ee* [%][b)]
1	**86**	**59**	>99	33 (*R*)
2	**86**	**340**	38	23 (*R*)
3	**388**	**59**	63	*rac.*
4	**388**	**340**	43	26 (*R*)

a) Determined by GC analysis; b) determined by GC analysis on a chiral stationary phase.

The steric bulk of the *N*-substituent was then increased by investigating cyclohexyl methyl *N*-isopropyl imine **554** (Table 42). Indeed, the first catalytic hydrogenation furnished the corresponding amine **55** in full conversion and good enantioselectivity of 72% (Entry 1). Unfortunately, all attempts to improve the enantioselectivity were unsucessful. Similar trends as with imines **551** and **552** were observed.

Table 42: Asymmetric Hydrogenation of imine **554**

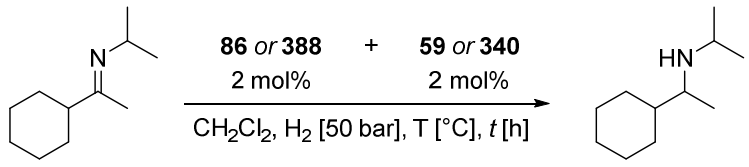

554 **555**

Entry	Catalyst	Imine Additive	Conv. [%][a)]	*ee* [%][b)]
1	**86**	**59**	>99	72 (*R*)
2	**86**	**340**	39	68 (*R*)
3	**388**	**59**	96	44 (*R*)
4	**388**	**340**	32	34 (*R*)

a) Determined by GC analysis;
b) determined after derivatisation to the acetamide by GC analysis on a chiral stationary phase;

Ultimately, to further investigate effect of the steric bulk exhibited by the nitrogen substituent, cyclohexyl methyl *N*-cyclohexyl imine **556** was subjected to hydrogenation. Full conversion to amine **557** in good enantioselectivity of 77% was observed (Entry 1, Table 43). This is in a similar range to the comparable *N*-phenyl analogue imine **329** which is reduced with 73% enantiomeric excess (Scheme 210).

Table 43: Asymmetric Hydrogenation of imine **556**

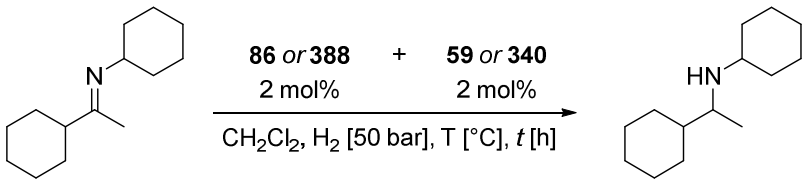

556 **557**

Entry	Catalyst	Imine Additive	Conv. [%][a]	*ee* [%][b]
1	**86**	**59**	>99	77 (*R*)
2	**86**	**340**	0	-
3	**388**	**59**	96	51 (*R*)
4	**388**	**340**	13	-

a) Determined by GC analysis;
b) determined after derivatisation to the 1-naphtamide by HPLC analysis on a chiral stationary phase.

Scheme 219 summarizes results for acyclic aliphatic *N*-alkyl imines. In all reactions, the (*R*)-enantiomer was observed as the major product. In case of the *N*-isopropyl amine **555** or *N*-cyclohexyl amines **557** similar enantioselectivities to *N*-phenyl amine **97** were obtained. This suggests, that the nitrogen substituent plays a crucial role for the selectivity of the hydrogenation reaction. In this context, the lower enantioselectivities of amine **84** and **553** can be explained by the flexibility of the nitrogen substituent.
N-alkyl substituents lower the reactivity of the C=N imine double bond towards hydrogenation so that side reactions such as hydrolysis are observed. Nevertheless, the reactivity can be fine-tuned by the appropiate choice of the catalyst and the imine additive.

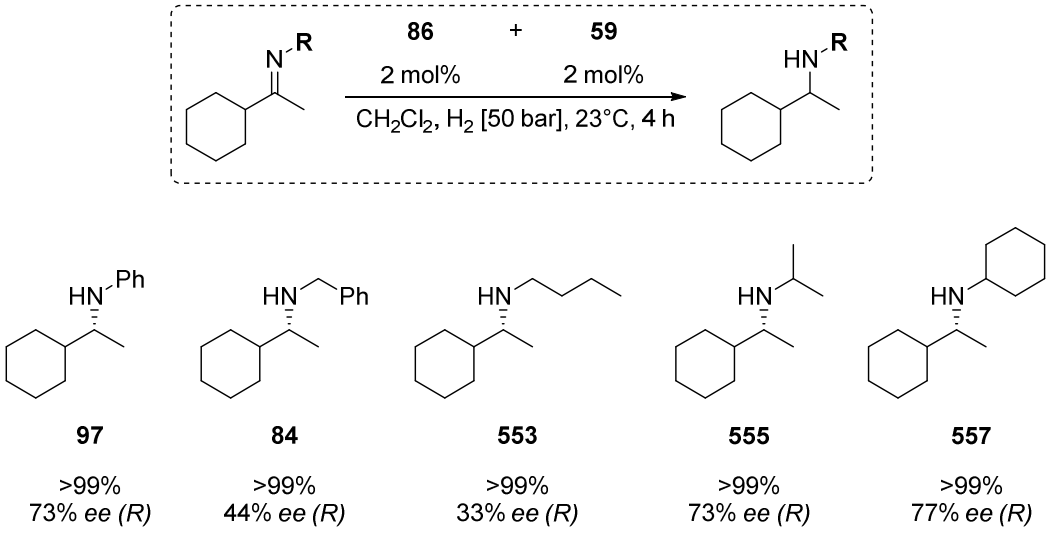

Scheme 219: Summary of asymmetric hydrogenation of aliphatic *N*-alkyl imines

Asymmetric Hydrogenation of cyclic aliphatic imines

Cyclic amines frequently appear in natural products and biologically important molecules, e.g. tetrahydroquinolines or more complex alkaloids such as nicotine, levofloxacine or morphine. To extend the application of the methodology developed, cyclic imines with aliphatic and aromatic substituents were evaluated. Preparation of cyclic aliphatic imines such as **560** was prepared from piperidin-2-one **558** and is shown in Scheme 220. After *N*-silylation with trimethylchlorosilane to afford **559** in 95% yield, subsequent treatment with methyl lithium afforded the desired cyclic imine **560** in low yield (20%). Attempts to introduce other substituents with the corresponding alkyl lithium reagent failed.

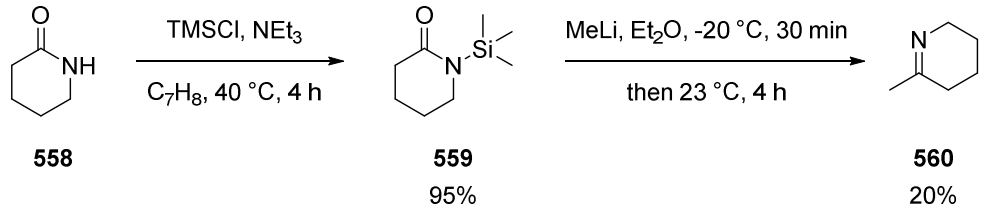

Scheme 220: Preparation of cyclic imine **560**

Therefore **558** was *N*-Boc protected to afford **561** in 71% yield. Nucleophilic attack of phenyl magnesium bromide furnished the desired acyclic NH-Boc precursor **562** in 45% yield. Deprotection and intramolecular imine condensation gave **563** in quantitative yield (Scheme 221).

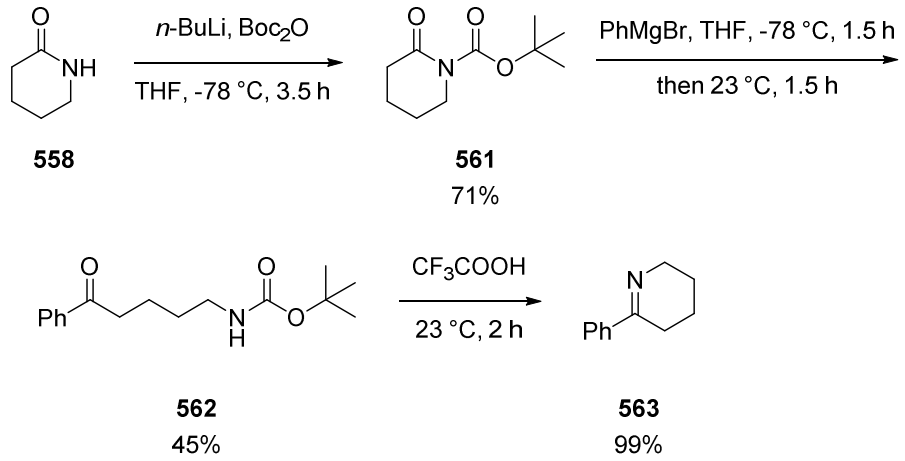

558 **561** 71% **562** 45% **563** 99%

Scheme 221: Preparation of cyclic imine **563**

In an analogous fashion as shown in Scheme 222, **561** was treated with *n*-butyl magnesium chloride to afford **564** in 33% yield. Deprotection and imine condensation afforded **565** in quantitative yield.

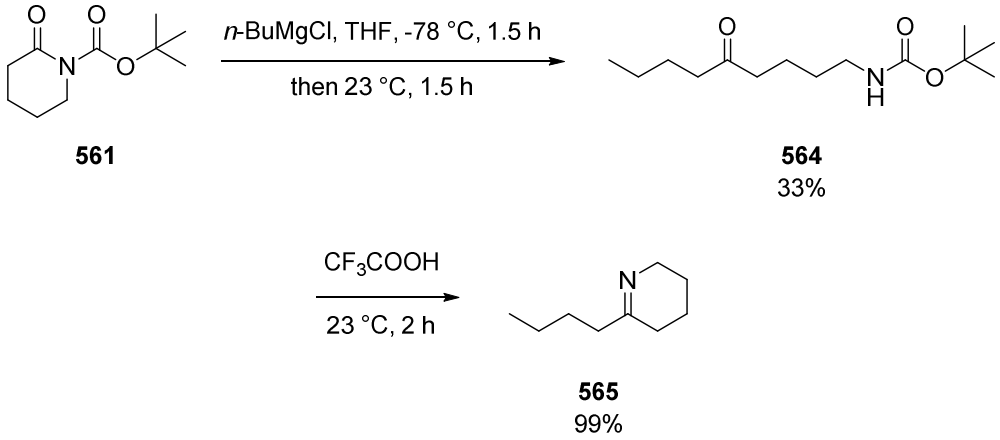

561 **564** 33% **565** 99%

Scheme 222: Preparation of cyclic imine **565**

Purification of 6-membered cyclic imines **560**, **563** and **565** was performed *via* Kugelrohr distillation. Imines **560** and **565** proved to be particularly sensitive to air and moisture. Literature study revealed that such aliphatic cyclic substrates have been studied in transition-metal catalysed imine hydrogenation only by *Buchwald*.[136] On the other hand, quinolines as well as 2-aryl cyclic imines were frequently studied.[136] When imines **560** and **565** were stored under argon in the freezer, slow brownish colorisation was observed over the course of a few days. The corresponding NMR spectra indicated small amounts of unidentified side products. Therefore, cyclic imines were subjected to hydrogenation experiments in 90-95% purity.

In addition to the 6-membered cyclic imines **560**, **563** and **565** the four 5-membered cyclic imines **566**, **567**, **568** and **569**[26] were also tested in hydrogenation reactions (Scheme 223). Similar to the 5-membered cyclic imines, substrates **567**, **568** and **569** proved to be highly senstitve to moisture and air. Imine **566** was freshly distilled prior to hydrogenation experiments. Neither the imine nor the corresponding amine eluted on a short silica plug during work-up. Therefore derivatisation to the *N*-acetamide or *N*-trifluoroacetamide was required. Reaction mixture analysis was performed with the corresponding amide and enamide.

[26] kindly provided by *V. Köhler*, Research group of *Prof. T. Ward*

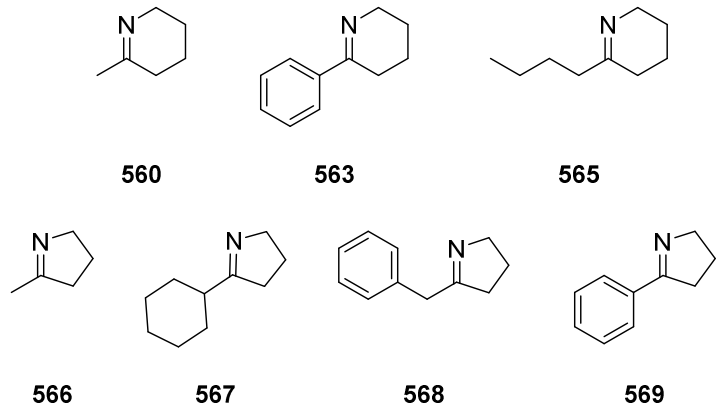

Scheme 223: Cyclic imines evaluated with *in situ* formed iridacycles as catalysts.

Initial hydrogenation experiments were conducted on imine **567** given in Table 44. At room temperature, employing similar reaction conditions as with acyclic aliphatic imines, no conversion was observed. In a related iridium-(f)-binaphane catalysed hydrogenation of cyclic imines, only a solvent mixture of dichloromethane and ethyl acetate at 50 °C displayed sufficient reactivity.[137] Conducting hydrogenations under these conditions afforded the corresponding amine **570** in somewhat higher but still low conversions (Entries 8-11). Conversions were calculated from observed enamide and amide peaks of GC analysis. No isolation by flash chromatography was performed. When attempting to reproduce these results, no conversion of imine **567** was observed. The reason thereof could not be determined. Due to varying conversions and low enantiomeric excesses, no further optimisation studies were conducted.

Table 44: Asymmetric hydrogenation of cyclic imine **567**

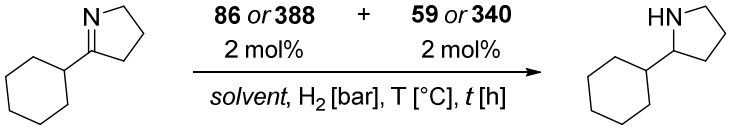

567 **570**

Entry	Catalyst	Additive	Solvent	*p* [bar]	T [°C]	*t* [h]	Conv. [%][a)]	*ee* [%][b)]
1	**86**	**59**	CH_2Cl_2	50	23	24	0	-
2	**86**	**59**	CH_2Cl_2	50	50	24	1	-
3	**86**	**340**	CH_2Cl_2	100	23	24	0	-
4	**388**	**59**	CH_2Cl_2	100	23	24	0	-
5	**388**	**340**	CH_2Cl_2	100	23	24	0	-
6	**86**	**59**	$Cl_2HCCHCl_2$	50	50	24	2	-
7	**86**	**59**	EtOAc	50	50	24	2	-
8	**86**	**59**	EtOAc/CH_2Cl_2 (2:1)	100	50	24	0-11	12
9	**86**	**340**	EtOAc/CH_2Cl_2 (2:1)	100	50	24	0-20	12
10	**388**	**59**	EtOAc/CH_2Cl_2 (2:1)	100	50	24	0-12	18
11	**388**	**340**	EtOAc/CH_2Cl_2 (2:1)	100	50	24	0-3	5

a) Determined after derivatisation to the *N*-trifluoroacetamide by GC analysis;
b) determined after derivatisation to the *N*-trifluoroacetamide by GC analysis on a chiral stationary phase.

Next, imine **560** was evaluated. No conversion was observed when conducting the reaction in dichloromethane in the presence or absence of imine **59** (Table 45, Entries 1 and 2). The reactivity drastically changed upon employing the solvent mixture of CH_2Cl_2/EtOAc in the presence or absence of imine **59** (Entries 3 and 4).

Table 45: Asymmetric hydrogenation of cyclic imine **560**

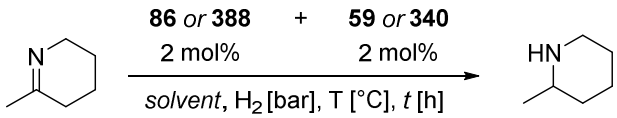

560 **571**

Entry	Catalyst	Additive	Solvent	*p* [bar]	T [°C]	*t* [h]	Conv. [%][a)]	*ee* [%][b)]
1	**86**	-	CH_2Cl_2	50	50	24	0	-
2	**86**	**59**	CH_2Cl_2	50	50	24	0	-
3	**86**	-	EtOAc/CH_2Cl_2 (2:1)	100	50	24	0	-
4	**86**	**59**	EtOAc/CH_2Cl_2 (2:1)	100	50	24	>99	0-3 (*R*)
5	**86**	**340**	EtOAc/CH_2Cl_2 (2:1)	100	50	24	>99	rac.
6	**388**	**59**	EtOAc/CH_2Cl_2 (2:1)	100	50	24	>99	rac.
7	**388**	**340**	EtOAc/CH_2Cl_2 (2:1)	100	50	24	>99	rac.
8	**86**	**I_2**	EtOAc/CH_2Cl_2 (2:1)	100	50	24	13	24 (*R*)
9	**86**	**59 + I_2**	EtOAc/CH_2Cl_2 (2:1)	100	50	24	5	26 (*R*)

a) Determined after derivatisation to the *N*-acetamide by GC analysis;
b) determined after derivatisation to the *N*-acetamide by GC analysis on a chiral stationary phase.

While virtually racemic amine was observed, the desired reactivity could be observed employing the combination complex **86** and imine **59**. Optimisation attempts with complex **388** or imine **340** still furnished racemic amine (Entry 5 to 7). Surprisingly, iodine addition resulted in formation of a less reactive but more selective catalyst compared to the combination **86** and **59** (Entries 8 and 9). Reduced reactivity upon iodine addition has been observed on iridium-PHOX catalysed hydrogenation of imines.[30]

Imine **560** demonstrated the desired reactivity upon addition of 2 mol% imine **59** as an additive. However, with other substrates, quite different reactivties were observed as can be seen in Table 46. While imines **565**, **566** and **568**, even under forcing conditions of 100 bar hydrogen pressure, showed no conversion, phenyl-substituted imines **563** and **569** gave very surprising results.

Table 46: Asymmetric hydrogenation of cyclic imine **563**, **565**, **566**, **568** and **569**

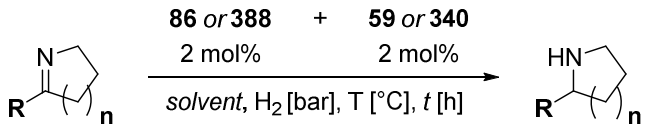

Entry	Imine	Catalyst	Additive	Solvent	*p* [bar]	Conv. [%][a)]	*ee* [%][b)]
1	**565** n = 2 R = *n*-Bu	**86**	-	CH_2Cl_2	50	0	-
2		**86**	**59**	CH_2Cl_2	50	0	-
3		**86**	-	EtOAc/CH_2Cl_2 (2:1)	50	0	-
4		**86**	**59**	EtOAc/CH_2Cl_2 (2:1)	50	0	-
5	**566** n = 1 R = Me	**86**	-	CH_2Cl_2	50	0	-
6		**86**	**59**	CH_2Cl_2	50	0	-
7		**86**	-	EtOAc/CH_2Cl_2 (2:1)	50	0	-
8		**86**	**59**	EtOAc/CH_2Cl_2 (2:1)	100	2	-
9		**86**	**340**	EtOAc/CH_2Cl_2 (2:1)	100	0	-
10		**388**	**59**	EtOAc/CH_2Cl_2 (2:1)	100	0	-
11		**388**	**340**	EtOAc/CH_2Cl_2 (2:1)	100	0	-
12	**568** n = 1 R = Bn	**86**	-	CH_2Cl_2	100	0	-
13		**86**	**59**	CH_2Cl_2	100	0	-
14		**86**	-	EtOAc/CH_2Cl_2 (2:1)	100	0	-
15		**86**	**59**	EtOAc/CH_2Cl_2 (2:1)	100	0	-
16	**563** n = 2 R = Ph	**86**	-	CH_2Cl_2	50	>99	80
17		**86**	**59**	CH_2Cl_2	50	>99	80
18		**86**	-	EtOAc/CH_2Cl_2 (2:1)	50	98	51
19		**86**	**59**	EtOAc/CH_2Cl_2 (2:1)	50	95	48
20	**569** n = 1 R = Ph	**86**	-	CH_2Cl_2	50	90	74
21		**86**	**59**	CH_2Cl_2	50	85	74
22		**86**	-	EtOAc/CH_2Cl_2 (2:1)	50	81	38
23		**86**	**59**	EtOAc/CH_2Cl_2 (2:1)	50	55	37

a) Determined after derivatisation to the *N*-acetamide by GC analysis;

b) determined after derivatisation to the *N*-acetamide by GC analysis on a chiral stationary phase;

Already in dichloromethane high conversion of 90% along with reasonable enantioselectivity of 74% was observed for the 5-membered cyclic imine **569** (Entry 20). Moreover, no additional imine was required for achieving high conversions (Entries 20 *vs*. 21). This suggests that either imine **569** itself forms the corresponding iridacycle catalyst (due to less steric bulk compared to **59** or **340**) or hydrogenation proceeds *via* a different mechanism. Interestingly, the solvent mixture of CH_2Cl_2 and EtOAc resulted in lower conversions than CH_2Cl_2 alone (entries 16-17 vs. 18-19).

In a similar fashion to **569**, the analogous 6-membered imine **563** is fully reduced in dichloromethane both in the absence or presence of imine **59**. Again, formation of the iridacycle catalyst with imine **563** might occur or hydrogenation proceed via a different mechanism. A good enantioselectivity of 80% was observed. Furthermore, higher conversions compared to imine **569** were obtained. This can be an evidence for iridacycle formation with the cyclic imine **563**. An iridacycle with imine **563** benefits from a favourable overall geometry with regards to the iridacycle angle (C-Ir-N) and the iridium-nitrogen atom distance compared an iridacycle formed with **569** and results in a more stable and more reactive iridacycle.

Scheme 224 summarizes results for cyclic aliphatic imines. In the series of *N*-phenyl, *N*-alkyl and cyclic aliphatic imines, these substrates exhibit the lowest reactivity. While no conversion was observed for imines **565**, **566**, **567** and **568**, the methodology employing an iridium(I) precatalyst and an acetophenone *N*-aryl imine was sucessfully applied on imine **560** although only racemic amine could be obtained. Furthermore, imines **563** and **569** were fully reduced with good enantioselectivities. With **563** and **569** no imine additive is required, most likely due to the ability of the substrate to form the corresponding iridacycle catalyst with the iridium(I) complex under reaction conditions.

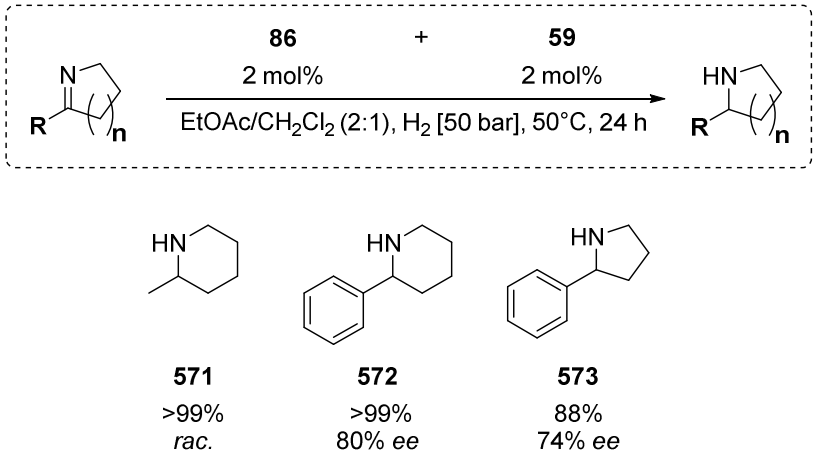

571 >99% *rac.*

572 >99% 80% *ee*

573 88% 74% *ee*

Scheme 224: Summary of asymmetric hydrogenation of cyclic aliphatic imines

Chapter 6 – Experimental Part

Working Techniques, solvents and reagents

The synthesis of air- and moisture sensitive compounds were carried out in oven- or flame-dried glassware under an athmosphere of argon employing standard Schlenk techniques or under nitrogen athmosphere in a glove box (MBraun Labmaster 130).
Flash and elution chromatography was performed on Merck Silica gel 60 (particle size 40-64 μm). Solvents were of technical grade.
Solvents employed in chemical transformations were obtained from a solvent purification system (PureSolv, Innovative Technology Inc.) or from septum sealed bottles over molecular sieves (Sigma-Aldrich, crown-cap). THF was distilled over potassium/benzophenone prior to use and 1,4-dioxane was distilled over CaH_2 prior to application.
Deuterated solvents were purchased from Cambridge Isotope Laboratories or Arma. CD_2Cl_2 was stored over molecular sieves under an athmosphere of argon.
Commercially available reagents were purchased from various suppliers and used without further purification.

Analytical Methods

Thin layer chromatography (TLC): TLC plates were obtained from Machrey-Nagel (Polygram SIL/UV254, 0.2 mm silica with fluorescence indicator). UV light (254 nm) or stain solutions ($KMnO_4$, $Ce(SO_4)_2$, Ninhydrine) were used to visualize the respective compounds.

Melting point (m.p.): Melting points were determined on a Büchi 535 and Büchi 545 (*Gademann* group) apparatus. The values are not corrected.

NMR spectroscopy: NMR spectea were recorded on a Bruker Avance 400 (400 MHz) and Avance 500 (500 MHz) NMR spectrometer. The chemical shifts (δ) are indicated in parts per million (ppm). The chemical shift values have been corrected to internal standard signals of deuterated solvents : 7.26 (^{1}H) and 77.16 (^{13}C) for $CDCl_3$; 5.32 (^{1}H) and 53.84 (^{13}C) for CD_2Cl_2 ; 3.58 (^{1}H) and 67.21 (^{13}C) for THF ; 2.50 (^{1}H) and 39.52 (^{13}C) for DMSO. ^{31}P-NMR spectra are corrected to 85% phopsphoric acid (δ = 0.0 ppm). ^{19}F-NMR spectra are corrected to $CFCl_3$ (δ = 0.0 ppm). Calibration has been performed with external standards. 1D-routine ^{13}C- and ^{31}P-NMR spectra are recorded ^{1}H-decoupled. 2D-routine correlation experiments (COSY, NOESY, HMQC, HMBC) were run without accurate pulse determination. Advanced two-dimensional correlation experiments (EXSY, ^{1}H-^{31}P HMBC) were carried out with prior ^{1}H-90° pulse determination. Multiplets are assigned as s (singlet), d (doublet), t (triplet) and q (quartet). All higher coupling patterns are indicated as m (multiplet). Broad peaks are assigned as br (broad).

Infrared spectroscopy (IR): Infrared spectra were collected on a Shimadzu FTIR-8400S spectrometer. The compounds were measured as pure substance *via* Specac ATR attachment. When, the solid samples were measured as potassium bromide discs, the spectra were collected on a Perkin Elmer 1600 series FTIR spectrometer. The absorption bands are given in wave numbers (ν [cm^{-1}]). The peak intensity is described by: s (strong), m (medium), w (weak).

Mass spectroscopy (MS): Mass Spectra were recorded by H. Nadig (Uni Basel) and Mass Spectrometry Service Facility (LOC, ETH Zurich). Electron impact ionixzation (EI) was measured on a VG70-250 spectrometer. Fast atom bombardement (FAB) was measured on a MAR 312 spectrometer. 3-nitrobenzyl alcohol was used as matrix in FAB. Electron spray ionization (ESI) was measured by C. Ebner, F. Bächle and P. Isenegger (Uni Basel) on an open source Finnigan MAT LCQ and on a Varian 1200L triple Quad MS/MS. The signals are given in mass to charge ratio (*m/z*). The fragments and intensities are given in brackets. All values are rounded tot he nearest number.

High Resolution Mass Spectrometry (HRMS): High resolution mass spectra were recorded by Mass Spectrometry Service Facility (LOC, ETH Zurich) on a Bruker Daltonics maXis (UHR-TOF) and Bruker solariX 94 ESI/MALDI-FT-ICR spectrometer and by H. Nadig (University of Basel) on a bruker maXis 4G QTOF-ESI Spectrometer.

Elemental analysis (EA): Elemental analyses were performed by W. Kirsch (Uni Basel), S. Mittelheisser (Uni Basel) and M. Schneider (ETHZ) in the microlaboratory on a Leco CHN-900 (Kirsch, Schneider) as well as a Vario Micro Cube by Elementar.

Optical rotations: Optical Rotations were measured on a Perkin Elmer Polarimeter 341 in a cuvette (ø = 1 dm) at 20 °C and 589 nm (sodium lamp). The concentration c is given in g/100 mL. The values are the average of three consecutive measurements and uncorrected.

High Performance Liquid Chromatography (HPLC): HPLC analyses were performed on Shimadzu systems with SLC-10A/SIL-20AHT system controller, CTO-10AC/AS column oven, LC10-AD/20-AD pump system, DGU-14A/20AD3 degasser and SPD-M10A/M20A diode array- or UV/VIS detector. Chiral columns Chiracel AD-H, AS-H, OB-H, OD-H, OJ or OJ-H (4.6 x 250 mm) from Daicel Chemical Industries were used. Semipreparative separations were on a Shimadzu system with SIL-10ADvp autosampler, LC-10ATvp pump system, CTO-10ACvp column oven, SPD-10Avp diode array detector and FRC-10Avp fraction collector) Daicel Chiracel AD or OD (2 x 25 cm) columns were used.

Gas Chromatography (GC): Gas chromatograms were recorded on Carlo Erba HRGC Mega2 Series 800 (HRGS Mega2), on CarboErga GC8000Top and on Shimadzu GC-2010 plus instruments, Separations on achiral phases were performed on a Restek Rtx-1701 (30 m x 0.25 mm x 0.25 µmol) or a Macherey-Nagel Optima 5-Amin (0.25 mm x 0.25 µm x 30 m) column. Separations of enantiomers were achieved on a *Chiraldex* γ-cyclodextrin TFA G-TA (30 m x 0.25 mm x 0.12 µm) or a *Brechbühler* β-cyclodextrin DEtTButSil (SE54), (0.25 mm x 0.25 µm x 25 m) column.

Gas Chromatography / Mass Spectroscopy (GC-MS): GC-MS analysis was performed on open-source 5890 Series II (GC-columns : Macherey-Nagel OPTIMA1 Me_2Si, 25 m x 0.2 mm, 0.35 um, 20 psi, split ca. 20 :1, carrier gas : 1 mL/min helium, 5971 series mass selective detector (EI) ; Macherey-Nagel Optima5 5% PhMeSi, 25 m 0.2 mm, 0.35 um, 20 psi, split ca 20:1, carrier gas : 1 mL/min helium, 5970A series mass selective detector (EI)) and Shimadzu GC 2010 plus with GCMS-QP2010 SE mass detectors. The signals are given in mass-to-charge ratios (*m*/*z*) and often with the relative intensity in brackets.

Imines

General Method:
A 25mL oven-dried two-neck round-bottom flask equipped with a stirrer, reflux condenser and a stopper was evacuated and purged with Argon gas three times. Freshly activated 4Å mol sieves were added under an argon counterflow. The stopper was replaced with a septum and ketone, aniline and solvent were added. A spatula tip of *p*-toluenesulfonic acid was added. The septum was replaced by a stopper and the solution was heated to reflux for 24 to 48 hours. After cooling to room temperature under argon the solution was filtered through a paper filter and rinsed with toluene. The solvent was removed under reduced pressure and the product was purified by Kugelrohr distillation.

Compounds **59**[30], **534**[138], **533**[139], **99**[30] had been prepared previously in our laboratories.

***N*-(1-(4-methoxyphenyl)ethylidene)aniline (322)**[140]

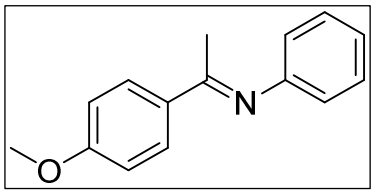

By general method 4-methoxyacetophenone (2.7 g, 18 mmol, 1.0 eq.) and aniline (2 g, 21.9 mmol, 1.21 eq.) were dissolved in dry benzene (7.5 mL). Purification by Kugelrohr distillation (110-180 °C at 0.07 mbar) afforded 3.4 g (15.1 mmol, 83%) of **322** as a yellow solid.

$C_{15}H_{15}NO$ (M_W = 225.29 g/mol):
m.p.: 91-92 °C (Lit. 92-94°C); **^{1}H-NMR** (500 MHz, $CDCl_3$): 7.85 (d, *J* = 8.6 Hz, 2H, CH_{Ar}C$_{Ar}$C=N), 7.25 (t, *J* = 7.7 Hz, 2H, CH_{Ar}CH$_{Ar}$C$_{Ar}$-N), 6.98 (t, *J* = 7.4 Hz, 1H, CH_{Ar}CH$_{Ar}$CH$_{Ar}$C$_{Ar}$-N), 6.86 (d, *J* = 8.6 Hz, 2H, CH_{Ar}C$_{Ar}$OMe), 6.70 (d, *J* = 7.7 Hz, 2H, CH_{Ar}C$_{Ar}$-N), 3.77 (s, 3H, OCH_3), 2.11 (s, 3H, CH_3C=N); **^{13}C{^{1}H}-NMR** (126 MHz, $CDCl_3$) δ 164.65 (*C*=N), 161.62 (*C*$_{Ar}$OMe), 151.99 (*C*$_{Ar}$-N), 132.30 (*C*$_{Ar}$C=N), 129.02 (C*H*$_{Ar}$CH$_{Ar}$C$_{Ar}$-N), 128.94 (*C*H$_{Ar}$C$_{Ar}$C=N), 123.12 (*C*H$_{Ar}$CH$_{Ar}$CH$_{Ar}$C$_{Ar}$-N), 119.71 (*C*H$_{Ar}$C$_{Ar}$-N), 113.70 (*C*H$_{Ar}$C$_{Ar}$OMe), 55.51 (O*C*H$_3$), 17.30 (*C*H$_3$C=N).

***N*-(1-cyclohexylethylidene)aniline (329)**[141]

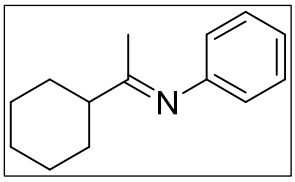

By general method cyclohexyl methyl ketone (1.83 g, 14.53 mmol, 1.0 eq.) and aniline (1.49 g, 15.98 mmol, 1.1 eq.) were dissolved in dry toluene (10 mL). Purification by Kugelrohr distillation (130 °C at 0.15 mbar) afforded 1.30 g (6.44 mmol, 44%) of **329** as a colourless oil.

$C_{14}H_{19}N$ (M_W = 201.31 g/mol):
^{1}H-NMR (400 MHz, $CDCl_3$) δ 7.32 – 7.22 (m, 2H), 7.05 – 6.98 (m, 1H), 6.71 – 6.63 (m, 2H), 2.30 (tt, *J* = 11.5, 3.2 Hz, 1H), 1.93 (dd, *J* = 6.7, 5.5 Hz, 2H), 1.89 – 1.80 (m, 2H), 1.74 – 1.70 (m, 3H), 1.49 – 1.16 (m, 6H); **^{13}C{^{1}H}-NMR** (101 MHz, $CDCl_3$) δ 175.75, 151.94, 128.96, 122.91, 119.52, 49.53, 30.39, 26.30, 26.28, 17.81; **GC** (Machary-Nagel Optima-5-Amin (0.50 µm x 0.25 µm x 30 m), 60 kPa H_2, 100 °C/2 min, 10 °C/min, 250 °C/7 min): t_R = 18.5 min; **HRMS**: calculated: 201.1512; found: 201.1512.

***N*-(1-(o-tolyl)ethylidene)aniline (318)**[142]

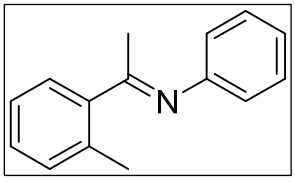

By general method acetophenone (2.29 g, 17 mmol, 1.0 eq.) and aniline (2 g, 22 mmol, 1.3 eq.) were dissolved in dry benzene (20 mL). Purification by Kugelrohr distillation (100-160 °C at 0.1 mbar) afforded 2.74 g (13.1 mmol, 77%) of **318** as a yellow oil.

$C_{15}H_{15}N$ (M_W = 209.29 g/mol):
Major: **^{1}H-NMR** (500 MHz, $CDCl_3$) δ 7.419 (m, 1H, CH_{Ar}C$_{Ar}$C=N), 7.392 (m, 2H, CH_{Ar}CH$_{Ar}$C$_{Ar}$-N), 7.297 (m, 1H, CH_{Ar}CH$_{Ar}$C$_{Ar}$CH$_3$), 7.280 (m, 1H, CH_{Ar}C$_{Ar}$CH$_3$), 7.278 (m, 1H, CH_{Ar}CH$_{Ar}$C$_{Ar}$C=N), 7.127 (m, 1H, CH_{Ar}CH$_{Ar}$CH$_{Ar}$C$_{Ar}$-N), 6.876 (m, 2H, CH_{Ar}C$_{Ar}$-N), 2.543 (s, 3H, C$_{Ar}$CH_3), 2.18 (s, 3H CH_3C=N);

^{13}C{^{1}H}-NMR (126 MHz, $CDCl_3$) δ 170.036 (*C*=N), 151.291 (C_{Ar}-N), 141.571 (C_{Ar}C=N), 135.04 ($C_{Ar}CH_3$), 131.111 ($CH_{Ar}C_{Ar}CH_3$), 129.103 ($CH_{Ar}CH_{Ar}C_{Ar}$-N), 128.683 ($CH_{Ar}CH_{Ar}C_{Ar}CH_3$), 127.183 ($CH_{Ar}C_{Ar}C$=N), 125.849 ($CH_{Ar}CH_{Ar}C_{Ar}C$=N), 123.459 ($CH_{Ar}CH_{Ar}CH_{Ar}C_{Ar}$-N), 119.303 ($CH_{Ar}C_{Ar}$-N), 21.23 ($CH_3$C=N), 20.51 ($C_{Ar}CH_3$).
Minor: **^{1}H-NMR** (500 MHz, $CDCl_3$) δ 7.122 (m, 1H, $CH_{Ar}CH_{Ar}C_{Ar}CH_3$), 7.115 (m, 1H, $CH_{Ar}CH_{Ar}C_{Ar}C$=N), 7.107 (m, 2H, $CH_{Ar}CH_{Ar}C_{Ar}$-N), 7.052 (m, 1H, $CH_{Ar}C_{Ar}C$=N), 7.036 (m, 1H, $CH_{Ar}C_{Ar}CH_3$), 6.906 (m, 1H, $CH_{Ar}CH_{Ar}CH_{Ar}C_{Ar}$-N), 6.687 (m, 2H, $CH_{Ar}C_{Ar}$-N), 2.493 (s, 3H CH_3C=N), 2.133 (s, 3H, $C_{Ar}CH_3$); **^{13}C{^{1}H}-NMR** (126 MHz, $CDCl_3$) δ 171.106 (*C*=N), 150.290 (C_{Ar}-N), 139.050 (C_{Ar}C=N), 133.01 ($C_{Ar}CH_3$), 130.208 ($CH_{Ar}C_{Ar}CH_3$), 128.251 ($CH_{Ar}CH_{Ar}C_{Ar}$-N), 128.162 ($CH_{Ar}CH_{Ar}C_{Ar}CH_3$), 127.069 ($CH_{Ar}C_{Ar}C$=N), 125.379 ($CH_{Ar}CH_{Ar}C_{Ar}C$=N), 123.498 ($CH_{Ar}CH_{Ar}CH_{Ar}C_{Ar}$-N), 120.841 ($CH_{Ar}C_{Ar}$-N), 29.32 ($CH_3$C=N), 21.33 ($C_{Ar}CH_3$); **GC-MS**: (Optima-5-Amine, 100.2/10.270/10): t_R = 14.6 min, *m/z* = 209 ($[M]^+$), 194 ($[M\text{-}CH_3]^+$), 118 (($[M\text{-}NPh]^+$).

***N*-(1-(2-fluorophenyl)ethylidene)aniline (319)**

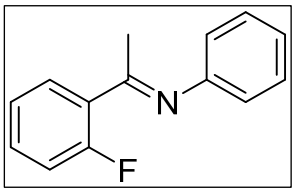

By general method 2-fluoroacetophenone (2.5 g, 18.1 mmol, 1.0 eq.) and aniline (2 g, 22 mmol, 1.2 eq.) were dissolved in dry benzene (20 mL). Purification by Kugelrohr distillation (110-160 °C at 0.1 mbar) afforded 3.08 g (14.5 mmol, 80%) of **319** as a yellow oil.

$C_{14}H_{12}FN$ (M_W = 213.25 g/mol):
E/Z mixture 7:1, signals overlapping, only *major* isomer characterised: **^{1}H-NMR** (500 MHz, $CDCl_3$) δ 7.85 (td, *J* = 7.7, 1.9 Hz, 1H, $CH_{Ar}C_{Ar}C$=N), 7.41 (dddd, 1H, *J* = 8.2, 7.1, 5.1, 1.8 Hz, $CH_{Ar}CHArC_{Ar}F$), 7.37 (t, *J* = 7.7 Hz, 2H, $CH_{Ar}CH_{Ar}C_{Ar}$-N), 7.22 (t, *J* = 7.5 Hz, 1H, $CH_{Ar}CH_{Ar}CH_{Ar}C_{Ar}C$-N), 7.15 (m, 1H, $CH_{Ar}C_{Ar}$-F), 7.12 (m, 1H, $CH_{Ar}CH_{Ar}C_{Ar}C$=N), 6.83 (d, *J* = 7.7 Hz, 2H, $CH_{Ar}C_{Ar}$-N), 2.25 (d, *J* = 3.5 Hz, 3H, CH_3C=N); **^{13}C{^{1}H}-NMR** (126 MHz, $CDCl_3$): 165.37 (*C*=N), 161.22 (d, *J* = 250.6 Hz, C_{Ar}-F), 150.85 (C_{Ar}-N), 131.70 (d, *J* = 8.6 Hz, $CH_{Ar}CHArC_{Ar}F$), 130.18 (d, *J* = 3.5 Hz, $CH_{Ar}C_{Ar}C$=N), 129.15 ($CH_{Ar}CH_{Ar}C_{Ar}$-N) , 124.42 ($CH_{Ar}CH_{Ar}CH_{Ar}C_{Ar}C$-N), 123.69 ($CH_{Ar}CH_{Ar}C_{Ar}C$=N), 119.43 ($CH_{Ar}C_{Ar}$-N), 116.37 (d, *J* = 22.9 Hz, $CH_{Ar}C_{Ar}$-F), 20.80 (d, *J* = 6.8 Hz, CH_3C=N); **^{19}F NMR** (376 MHz, $CDCl_3$) δ -113.34 (major), -113.43 (minor); **IR** (neat, ATR) ν/cm^{-1} = 3060 (w), 3031 (w), 2997 (w), 1634 (s), 1610 (m), 1593 (s), 1576 (m), 1485 (s), 1450 (m), 1368 (m), 1293 (m), 1211 (s), 1169 (w), 1113 (m), 1072 (m). 801 (m), 759 (s), 716 (m), 696 (s); **MS** (EI, 70 eV): 213.1 (55.7%), 198.1 (100%), 118.1 (8.1%); **EA**: calc. C, 78.85; H, 5.67; N, 6.57, found C, 78.68; H, 5.86; N, 6.47

***N*-(1-(3-nitrophenyl)ethylidene)aniline (531)**

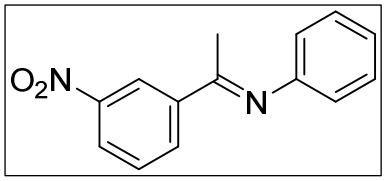

By general method 3-nitroacetophenone (0.5 g, 3 mmol, 1.0 eq.) and aniline (0.33 g, 3.6 mmol, 1.2 eq.) were dissolved in dry toluene (10 mL). Purification by Kugelrohr distillation (170 °C at 0.1 mbar) afforded 0.357 g (1.49 mmol, 49%) of **531** as a yellow solid.

$C_{14}H_{12}N_2O_2$ (M_W = 240.26 g/mol):
m.p.: 96 °C; **^{1}H-NMR** (400 MHz, $CDCl_3$) δ 8.89 – 8.70 (m, 1H, $CH_{Ar}C_{Ar}NO_2$), 8.44 – 8.22 (m, 2H, $CH_{Ar}C_{Ar}NO_2$&$CH_{Ar}C_{Ar}C$=N), 7.64 (t, *J* = 8.0 Hz, 1H, $CH_{Ar}CH_{Ar}C_{Ar}C$=N), 7.38 (t, *J* = 7.8 Hz, 2H, $CH_{Ar}CH_{Ar}C_{Ar}$-N), 7.13 (t, *J* = 7.4 Hz, 1H, $CH_{Ar}CH_{Ar}CH_{Ar}C_{Ar}$-N), 6.80 (d, *J* = 7.3 Hz, 2H, $CH_{Ar}C_{Ar}$-N), 2.30 (s, 3H, CH_3C=N); **^{13}C{^{1}H}-NMR** (101 MHz, $CDCl_3$) δ 163.33 (*C*=N), 150.91 (C_{Ar}-N), 141.21 (C_{Ar}C=N), 133.10 ($CH_{Ar}C_{Ar}C$=N), 129.51 ($C_{Ar}C$=N$CH_{Ar}C_{Ar}NO_2$), 129.24 ($CH_{Ar}CH_{Ar}C_{Ar}$-N), 125.12 ($CH_{Ar}CH_{Ar}CH_{Ar}C_{Ar}$-N), 124.01 ($CH_{Ar}C_{Ar}NO_2$), 122.38 ($CH_{Ar}CH_{Ar}C_{Ar}C$=N), 119.31 ($CH_{Ar}C_{Ar}$-N), 17.50 ($CH_3$C=N); **IR** (neat, ATR) ν/cm^{-1} = 3114 (w), 3099 (w), 3076 (w), 3070 (w), 3017 (w), 1623 (m), 1593 (m), 1576 (m), 1521 (s), 1483 (s), 1473 (s), 1432 (m), 1368 (m), 1345 (s), 1317 (m), 1286 (m), 1258 (m), 1213 (m), 1170 (w), 1111 (m), 1060 (m), 1024 (w), 900 (m), 818 (m), 744 (s), 735 (s), 693 (s); **MS** (EI, 70 eV): 240.1 (84.2%), 225.1 (100%), 179.1 (42.5%); **HRMS**: calculated: 240.0894; found: 240.0900; **EA**: calc. C, 69.99; H, 5.03; N, 11.66; found: C, 69.81; H, 5.14; N, 11.56

***N*-(1-(3,5-dinitrophenyl)ethylidene)aniline (530)**

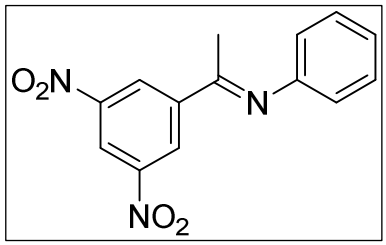

By general method 3,5-dinitroacetophenone (0.5 g, 2.38 mmol, 1.0 eq.) and aniline (0.26 g, 2.85 mmol, 1.2 eq.) were dissolved in dry toluene (10 mL). Purification by recrystallisation from ethanol afforded 0.291 g (1.02 mmol, 43%) of **530** as an orange solid.

$C_{14}H_{11}N_3O_4$ (M_W = 285.25 g/mol):
m.p.: 132-133 °C; **^{1}H-NMR** (400 MHz, $CDCl_3$) δ 9.19 – 9.08 (m, 3H, CH_{ArNO2}), 7.48 – 7.34 (m, 2H, CH_{Ar}CH_{Ar}C$_{Ar}$-N), 7.22 – 7.13 (m, 1H, CH_{Ar}CH_{Ar}CH_{Ar}C$_{Ar}$-N), 6.82 (dd, J = 8.3, 1.0 Hz, 2H, CH_{Ar}C$_{Ar}$-N), 2.38 (s, 3H, CH_3C=N); **^{13}C{^{1}H}-NMR** (101 MHz, $CDCl_3$) δ 161.25 (*C*=N), 150.01 (*C*$_{Ar}$-N), 148.83 (C$_{Ar}$-NO_2), 143.01 (*C*$_{Ar}$C=N), 129.37 (CH_{Ar}CH_{Ar}C$_{Ar}$-N), 127.24 (CH_{Ar}C$_{Ar}$C=N), 124.68 (CH_{Ar}CH_{Ar}CH_{Ar}C$_{Ar}$-N), 120.02 (C$_{Ar\text{-}NO2}$CH_{Ar}C$_{Ar\text{-}NO2}$), 119.22 (CH_{Ar}C$_{Ar}$-N), 17.48 (CH_3C=N); **IR** (neat, ATR) ν/cm^{-1} = 3117 (w), 3101 (w), 3059 (w), 3050 (w), 1646 (m), 1625 (m), 1590 (m), 1535 (s), 1481 (w) 1461 (w), 1438 (w), 1367 (m), 1345 (s), 1334 (s), 1285 (m), 1237 (w), 1209 (m), 1169 (w), 1144 (m), 1100 (w), 1073 (m), 910 (m), 903 (m), 810 (m), 795 (m), 753 (s), 728 (s), 654 (s); **MS** (EI, 70 eV): 285.1 (100%), 270.1 (82.8%), 224.1 (18.1%), 178.1 (24.1%); **HRMS**: calculated: 285.0744; found: 285.0740; **EA**: calc. C, 58.95; H, 3.89; N, 14.73; found: C, 58.93; H, 3.99; N, 14.64

***N*-(1-(3,5-dimethylphenyl)ethylidene)aniline (512)**

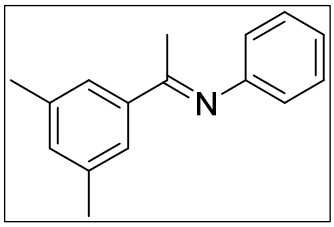

By general method 3,5-dimethylacetophenone (0.3 g, 2 mmol, 1.0 eq.) and aniline (0.2 g, 2.2 mmol, 1.1 eq.) were dissolved in dry toluene (7.5 mL). Purification by Kugelrohr distillation (137 °C at 0.08 mbar) afforded 0.165 g (0.74 mmol, 37%) of **512** as an off-yellow solid.

$C_{16}H_{17}N$ (M_W = 223.31 g/mol):
b.p.: 137 °C at 0.08 mbar; **m.p.**: 44 °C; **^{1}H-NMR** (400 MHz, $CDCl_3$) δ 7.58 (s, 2H, CH_{Ar}C$_{Ar}$C=N)), 7.40 – 7.29 (m, 2H, CH_{Ar}CH_{Ar}C$_{Ar}$-N), 7.11 (s, 1H, C$_{Ar}$CH_3CH_{Ar}C$_{Ar}$CH_3), 7.10 – 7.05 (m, 1H, CH_{Ar}CH_{Ar}CH_{Ar}C$_{Ar}$-N), 6.79 (dt, *J* = 8.3, 1.6 Hz, 2H, CH_{Ar}C$_{Ar}$-N), 2.38 (s, 6H, C$_{Ar}$CH_3), 2.21 (s, 3H, CH_3C=N); **^{13}C{^{1}H}-NMR** (101 MHz, $CDCl_3$) δ 166.10 (*C*=N), 151.95 (*C*-N), 139.68 (*C*$_{Ar}$C=N), 138.05 (*C*$_{Ar}$CH$_3$), 132.25 (C$_{Ar}$CH$_3$CH_{Ar}C$_{Ar}$CH$_3$), 129.07 (CH_{Ar}CH_{Ar}C$_{Ar}$-N), 125.14 (*C*H$_{Ar}$C$_{Ar}$C=N), 123.27 (*C*H$_{Ar}$CH$_{Ar}$CH$_{Ar}$C$_{Ar}$-N), 119.54 (*C*H$_{Ar}$C$_{Ar}$-N), 21.49 (C$_{Ar}$*C*H$_3$), 17.70 (*C*H$_3$C=N); **IR** (neat, ATR) ν/cm^{-1} = 3027 (w), 3010 (w), 2959 (w), 2917 (w), 1628 (s), 1600 (m), 1590 (s), 1576 (m), 1480 (m), 1447 (m), 1438 (m), 1376 (w), 1363 (m), 1321 (m), 1272 (w), 1208 (s), 1167 (m), 1155 (m), 1071 (m), 1026 (m), 906 (m), 852 (s), 800 (s), 761 (s), 694 (s); **MS** (EI, 70 eV): 223.1 (43.9%), 208.1 (100%); **GC-MS**: (Rtx-5MS, 100.2/10.270/10): t_R = 19.1 min, *m/z* = 223 ([M]$^+$); **EA**: calc. C, 86.06; H, 7.67; N, 6.27, found C, 86.19; H, 7.65; N, 6.28

***N*-(1-(3,5-diisopropylphenyl)ethylidene)aniline (522)**

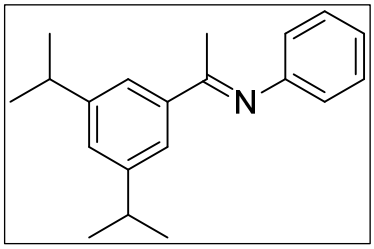

By general method **521** (0.5 g, 2.45 mmol, 1.0 eq.) and aniline (0.29 g, 3.18 mmol, 1.3 eq.) were dissolved in dry toluene (10 mL). Purification by Kugelrohr distillation (160 °C at 0.08 mbar) afforded 0.310 g (1.11 mmol, 45%) of **522** as a yellow oil.

$C_{20}H_{25}N$ (M_W = 279.42 g/mol):
E/*Z* mixture 8:1, signals overlapping; *Major*: **^{1}H-NMR** (500 MHz, $CDCl_3$) δ: 7.65 (d, *J* = 4.0 Hz, 2H, CH_{Ar}C$_{Ar}$C=N), 7.35 (t, *J* = 7.7 Hz, 2H, CH_{Ar}CH_{Ar}C$_{Ar}$-N), 7.20 (s, 1H, C$_{Ar}$CH(CH$_3$)$_2$CH_{Ar}C$_{Ar}$CH(CH$_3$)$_2$), 7.08 (t, *J* = 7.4 Hz, 1H, CH_{Ar}CH_{Ar}CH_{Ar}C$_{Ar}$-N), 6.80 (d, *J* = 7.7 Hz, 2H, CH_{Ar}C$_{Ar}$-N), 2.97 (hept, *J* = 6.9 Hz, 2H, C*H*(CH$_3$)$_2$), 2.23 (d, *J* = 7.0 Hz, 3H, CH_3C=N), 1.30 (d, *J* = 7.1 Hz, 12H, CH(CH_3)$_2$); **^{13}C{^{1}H}-NMR** (125 MHz, $CDCl_3$) δ:166.23 (*C*=N), 152.10 (*C*$_{Ar}$-N), 149.18 (*C*$_{Ar}$CH(CH$_3$)$_2$), 139.68 (*C*$_{Ar}$C=N), 129.07 (CH_{Ar}CH_{Ar}C$_{Ar}$-N), 127.05 (*C*H$_{Ar}$CH_{Ar}CH_{Ar}C$_{Ar}$-N), 123.19 (C$_{Ar}$CH(CH$_3$)$_2$C*H*ArC$_{Ar}$CH(CH$_3$)$_2$), 123.07 (C$_{Ar}$CH(CH$_3$)$_2$CH_{Ar}C$_{Ar}$C=N), 119.54 (CH_{Ar}C$_{Ar}$-N), 34.48 (C*H*(CH$_3$)$_2$), 24.23 (CH(*C*H$_3$)$_2$), 17.84 (*C*H$_3$C=N); **IR** (neat, ATR) ν/cm^{-1} = 3058 (w), 2960 (s), 2927 (m), 2869 (m), 1634 (s), 1595 (s), 1485 (m), 1465 (m), 1440 (w), 1364 (m), 1255 (w), 1209 (s), 875 (w), 802 (w), 759 (w), 699 (m); **MS** (EI, 70 eV): 279.2

(40.79%), 264.2 (100%), 248.1 (9.7%); **HRMS**: calculated: 279.1982; found: 279.1983; **EA**: calc. C, 85.97; H, 9.02; N, 5.01; found: C, 85.71; H, 8.91; N, 5.01.

***N*-(1-(3,5-di-*tert*-butylphenyl)ethylidene)aniline (526)**

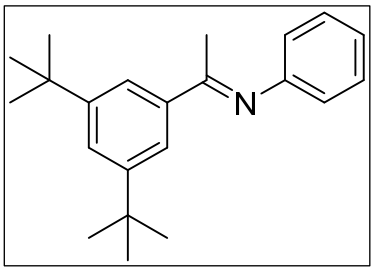

By general method **525** (0.5 g, 2.15 mmol, 1.0 eq.) and aniline (0.25 g, 2.8 mmol, 1.3 eq.) were dissolved in dry toluene (10 mL). Purification by Kugelrohr distillation (170 °C at 0.1 mbar) afforded 0.368 g (1.2 mmol, 56%) of **526** as a yellow-white solid.

$C_{22}H_{29}N$ (M_W = 307.47 g/mol):
m.p.: 86-90 °C; **^{1}H-NMR** (500 MHz, $CDCl_3$) δ:7.84 (s, 2H, CH_{Ar}C$_{Ar}$C=N)), 7.58 (s, 1H, C$_{Ar}$C(CH$_3$)$_3$CH_{Ar}C$_{Ar}$C(CH$_3$)$_3$), 7.36 (t, *J* = 7.7 Hz, 2H, CH_{Ar}CH$_{Ar}$C$_{Ar}$-N), 7.09 (t, *J* = 7.5 Hz, 1H, CH_{Ar}CH$_{Ar}$CH$_{Ar}$C$_{Ar}$-N), 6.82 (d, *J* = 7.7 Hz, 2H, CH_{Ar}C$_{Ar}$-N), 1.40 (s, 18H, C(CH_3)$_3$); **^{13}C{^{1}H}-NMR** (125 MHz, $CDCl_3$) δ: 166.42 (*C*=N), 152.23 (*C*$_{Ar}$-N), 150.93 (*C*$_{Ar}$C(CH$_3$)$_3$), 139.13 (*C*$_{Ar}$C=N), 129.07 (*C*H$_{Ar}$CH$_{Ar}$C$_{Ar}$-N), 124.88 (C$_{Ar}$C(CH$_3$)$_3$CH_{Ar}C$_{Ar}$C(CH$_3$)$_3$), 123.12 (*C*H$_{Ar}$CH$_{Ar}$CH$_{Ar}$C$_{Ar}$-N), 121.54 (*C*H$_{Ar}$C$_{Ar}$C=N), 119.52 (*C*H$_{Ar}$C$_{Ar}$-N), 35.14 (*C*(CH$_3$)$_3$), 31.63 (C(*C*H$_3$)$_3$), 17.92 (*C*H$_3$C=N); **IR** (neat, ATR) ν/cm^{-1} = 3061 (w), 2961 (m), 2934 (w), 2905 (w), 2865 (w), 1685 (w), 1636 (m), 1590 (m), 1477 (m), 1447 (m), 1393 (w), 1362 (m), 1323 (m), 1247 (m), 1212 (s), 1168 (m), 1068 (m), 1024 (m), 903 (m), 879 (m), 798 (m), 755 (s), 701 (s); **MS** (EI, 70 eV): 307.2 (52.7%), 292.2 (100%), 276.2 (12.6%); **HRMS**: calculated: 307.2295; found: 307.2294; **EA**: calc. C, 85.94; H, 9.51; N, 4.56; found: C, 85.93; H, 9.49; N, 4.44.

***N*-(1-(4-(*tert*-butyl)phenyl)ethylidene)aniline (528)**

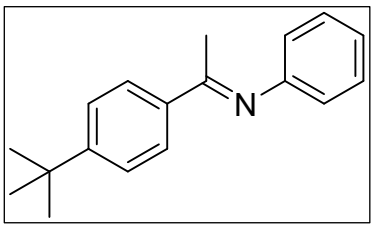

By general method 4-*tert*-butyl acetophenone (0.48 g, 2.72 mmol, 1.0 eq.) and aniline (0.35 g, 3.93 mmol, 1.44 eq.) were dissolved in dry toluene (10 mL). Purification by Kugelrohr distillation (125 °C at 0.08 mbar) afforded 0.28 g (1.11 mmol, 41%) of **528** as yellow-white solid.

$C_{18}H_{21}N$ (M_W = 251.37 g/mol):
b.p.: 125 °C at 0.08 mbar; **m.p.**: 63-64 °C; **^{1}H-NMR** (400 MHz, $CDCl_3$) δ 7.93 (d, *J* = 8.5 Hz, 2H, CH_{Ar}C$_{Ar}$C=N), 7.48 (d, *J* = 8.5 Hz, 2H, CH_{Ar}C$_{Ar}$C(CH$_3$)$_3$), 7.35 (t, *J* = 7.8 Hz, 2H, CH_{Ar}CH$_{Ar}$C$_{Ar}$-N), 7.08 (t, *J* = 7.4 Hz, 1H, CH_{Ar}CH$_{Ar}$CH$_{Ar}$C$_{Ar}$-N), 6.79 (t, *J* = 7.4 Hz, 2H, CH_{Ar}C$_{Ar}$-N), 2.22 (s, 3H, CH_3C=N), 1.36 (s, 9H, C(CH_3)$_3$);
^{13}C{^{1}H}-NMR (101 MHz, $CDCl_3$) δ 165.31 (*C*=N), 154.01 (*C*$_{Ar}$C(CH$_3$)$_3$), 152.01 (*C*$_{Ar}$-N), 136.88 (*C*$_{Ar}$C=N), 129.06 (*C*H$_{Ar}$CH$_{Ar}$C$_{Ar}$-N), 127.12 (*C*H$_{Ar}$C$_{Ar}$C=N), 125.44 (*C*H$_{Ar}$C$_{Ar}$C(CH$_3$)$_3$), 123.21 (*C*H$_{Ar}$CH$_{Ar}$CH$_{Ar}$C$_{Ar}$-N), 119.58 (*C*H$_{Ar}$C$_{Ar}$-N), 34.97 (*C*(CH$_3$)$_3$), 31.38 (C(*C*H$_3$)$_3$), 17.40 (*C*H$_3$C=N); **IR** (neat, ATR) ν/cm^{-1} = 3053 (w), 2971 (w), 2952 (m), 2902 (w), 2864 (w), 1623 (m), 1601 (m), 1589 (m), 1560 (m), 1509 (w), 1478 (m), 1434 (m), 1360 (m), 1312 (w), 1290 (m), 1216 (m), 1199 (m), 1126 (m), 1024 (m), 1011 (m), 852 (m), 824 (s), 699 (s); **MS** (EI, 70 eV): 251.2 (46.7%), 236.1 (100%); **HRMS**: calculated: 251.1669; found: 251.1670; **EA**: calc. C, 86.01; H, 8.42; N, 5.57; found: C, 85.83; H, 8.49; N, 5.59.

***N*-(1-(*p*-tolyl)ethylidene)aniline (314)[143]**

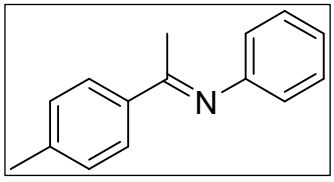

By general method 4-methyl acetophenone (1.3 mL, 10 mmol, 1 eq.) and aniline (1.1 ml, 12 mmol, 1.2 eq.) were dissolved in dry benzene (5 mL). Purification by Kugelrohr distillation (130 °C at 0.08 mbar) afforded 1.67 g (7.98 mmol, 79 %) of **314** as a yellow oil.

$C_{15}H_{15}N$ (M_W = 209.29 g/mol):
^{1}H-NMR (400 MHz, CD_2Cl_2): 7.90 (d, *J* = 8.0 Hz, 2H,CH_{Ar}C$_{Ar}$C=N); 7.37 (t, *J* = 7.25 Hz, 2H, CH_{Ar}CH$_{Ar}$C$_{Ar}$-N); 7.28 (d, *J* = 7.75 Hz, 2H, CH_{Ar}C$_{Ar}$CH$_3$); 7.10 (t, *J* = 7.5 Hz, 1H, CH_{Ar}CH$_{Ar}$CH$_{Ar}$C$_{Ar}$-N); 6.81 (d, *J* = 7.75 Hz, 2H, CH_{Ar}C$_{Ar}$-N); 2.43 (s, 3H, C$_{Ar}$CH_3); 2.21 (s, 3H, CH_3C=N); **^{13}C{^{1}H}-NMR** (100 MHz, CD_2Cl_2): 164.9 (*C*=N); 152.0 (*C*$_{Ar}$-N); 140.7 (*C*$_{Ar}$CH$_3$); 136.8 (*C*$_{Ar}$C=N); 128.9 (*C*H$_{Ar}$C$_{Ar}$CH$_3$); 128.8

($CH_{Ar}CH_{Ar}C_{Ar}$-N); 127.0 ($CH_{Ar}C_{Ar}C$=N); 122.9 ($CH_{Ar}CH_{Ar}CH_{Ar}C_{Ar}$-N); 119.3 ($CH_{Ar}C_{Ar}$-N); 21.1 ($C_{Ar}CH_3$); 16.9 ($CH_3C$=N).

***N*-(1-(4-chlorophenyl)ethylidene)aniline (323)[144]**

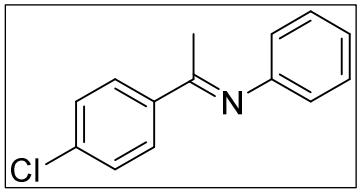

By general method 1-(4-chlorophenyl)ethanone (1.3 mL, 10 mmol, 1 eq.) and aniline (1.1 mL, 12 mmol, 1.2 eq.) were dissolved in dry benzene (5 mL). Purification by Kugelrohr distillation (145 °C at 0.08 mbar) afforded 1.87 g (8.1 mmol, 81 %) of **323** as a yellow solid.

$C_{14}H_{12}ClN$ (M_W = 229.70 g/mol):
m.p.: 93 °C (Lit. 93-95°C); **^{1}H-NMR** (600 MHz, CD_2Cl_2): 7.95 (d, *J* = 8.0 Hz, 2H, $CH_{Ar}C_{Ar}C$=N); 7.45 (d, *J* = 8.0 Hz, 2H, $CH_{Ar}C_{Ar}Cl$); 7.38 (t, *J* = 7.75 Hz, 2H, $CH_{Ar}CH_{Ar}C_{Ar}$-N); 7.12 (t, *J* = 7.25 Hz, 1H, $CH_{Ar}CH_{Ar}CH_{Ar}C_{Ar}$-N); 6.79 (d, *J* = 7.75 Hz, 2H, $CH_{Ar}C_{Ar}$-N); 2.21 (s, 3H, CH_3C=N); **^{13}C{^{1}H}-NMR** (100 MHz, CD_2Cl_2): 163.88 (C=N); 151.40 (C_{Ar}-N); 137.87 ($C_{Ar}C$=N); 136.21 ($C_{Ar}Cl$); 128.81 ($CH_{Ar}CH_{Ar}C_{Ar}$-N); 128.45 ($CH_{Ar}C_{Ar}C$=N); 128.27 ($CH_{Ar}C_{Ar}Cl$); 123.11 ($CH_{Ar}CH_{Ar}CH_{Ar}C_{Ar}$-N); 119.08 ($CH_{Ar}C_{Ar}$-N); 16.81 ($CH_3C$=N).

***N*-(1-(4-fluorophenyl)ethylidene)aniline (310)[141]**

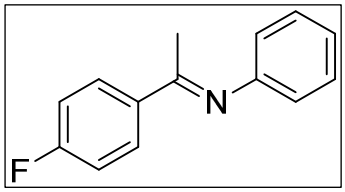

By general method 1-(4-fluorophenyl)ethanone (2.517 g, 18.22 mmol, 1.0 eq.) and aniline (2 g, 21.9 mmol, 1.2 eq.) were dissolved in dry benzene (7 mL). Purification by Kugelrohr distillation (120-160° C at 0.1 mbar) afforded 3.21 g (15 mmol, 82 %) of **310** as a off-white solid.

$C_{14}H_{12}FN$ (M_W = 213.25 g/mol):
m.p.: 81 °C (Lit. 86-87°C); **^{1}H-NMR** (500 MHz, CD_2Cl_2) δ 8.03 – 7.81 (m, 2H, $CH_{Ar}C_{Ar}C$=N), 7.27 (t, *J* = 7.2 Hz, 2H, $CH_{Ar}CH_{Ar}C_{Ar}$-N), 7.03 (m, 3H, $CH_{Ar}C_{Ar}F$&$CH_{Ar}CH_{Ar}CH_{Ar}C_{Ar}$-N), 6.69 (d, *J* = 7.4 Hz, 2H, $CH_{Ar}C_{Ar}$-N), 2.12 (s, 3H, CH_3C=N); **^{13}C{^{1}H}-NMR** (126 MHz, CD_2Cl_2) δ 164.64 (d, *J* = 249.7 Hz, C_{Ar}-F), 164.33 (*C*=N), 152.07 (C_{Ar}-N), 136.22 ($C_{Ar}C$=N), 129.69 (d, *J* = 8.6 Hz, $CH_{Ar}C_{Ar}C$=N), 129.34 ($CH_{Ar}CH_{Ar}C_{Ar}$-N), 123.56 ($CH_{Ar}CH_{Ar}CH_{Ar}C_{Ar}$-N), 119.68 ($CH_{Ar}C_{Ar}$-N), 115.50 (d, *J* = 21.6 Hz, $CH_{Ar}C_{Ar}F$), 17.41 (CH_3C=N).

***N*-(1-(4-(trifluoromethyl)phenyl)ethylidene)aniline (324)[144]**

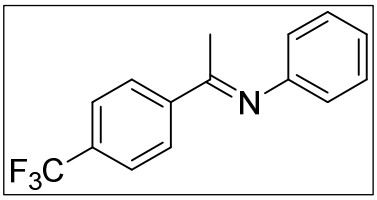

By general method 1-(4-trifluoromethylphenyl)ethanone (1.135 g, 6.03 mmol, 1.0 eq.) and aniline (0.67 g, 7.2 mmol, 1.2 eq.) were dissolved in dry benzene (7 mL). Purification by Kugelrohr distillation (100-150 °C at 0.07 mbar) afforded 1.23 g (4.7 mmol, 78 %) of **324** as a yellow white solid.

$C_{15}H_{12}F_3N$ (M_W = 263.26 g/mol):
m.p.: 72-74 °C (Lit. 75-77°C); **^{1}H-NMR** (400 MHz, CD_2Cl_2) δ 8.13 (d, *J* = 8.0 Hz, 2H, $CH_{Ar}C_{Ar}C$=N), 7.73 (d, *J* = 8.0 Hz, 2H, $CH_{Ar}C_{Ar}$-CF_3), 7.39 (t, *J* = 7.5 Hz, 2H, $CH_{Ar}CH_{Ar}C_{Ar}$-N), 7.13 (t, *J* = 7.2 Hz, 1H, $CH_{Ar}CH_{Ar}CH_{Ar}C_{Ar}$-N), 6.82 (t, *J* = 7.0, 2H, $CH_{Ar}C_{Ar}$-N), 2.27 (s, 3H, CH_3=N); **^{13}C{^{1}H}-NMR** (126 MHz, CD_2Cl_2) δ 164.61 (*C*=N), 151.72 (C_{Ar}-N), 143.24 ($C_{Ar}C$=N), 131.98 (q, *J* = 32.5 Hz, C_{Ar}-CF_3), 129.41 ($CH_{Ar}CH_{Ar}C_{Ar}$-N), 127.98 ($CH_{Ar}C_{Ar}C$=N), 125.62 (q, *J* = 3.8 Hz, $CH_{Ar}C_{Ar}$-CF_3), 123.90 ($CH_{Ar}CH_{Ar}CH_{Ar}C_{Ar}$-N), 119.52 ($CH_{Ar}C_{Ar}$-N), 17.57 ($CH_3C$=N); **^{19}F{^{1}H}-NMR** (376 MHz, CD_2Cl_2) δ -64.16.

_N_-(1-(4-nitrophenyl)ethylidene)aniline (529)[140]

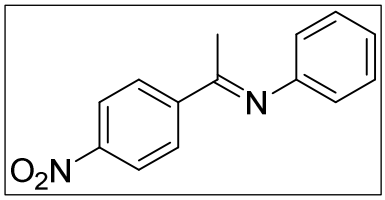

By general method 4-nitroacetophenone (0.5 g, 3.03 mmol, 1.0 eq.) and aniline (0.33 g, 3.55 mmol, 1.2 eq.) were dissolved in dry toluene (10 mL). Purification by recrystallisation from ethanol and pentane-washing afforded 0.456 g (1.89 mmol, 63 %) of **529** as an orange solid.

$C_{14}H_{12}N_2O_2$ (M_W = 240.26 g/mol):
m.p.: 110-114 °C (Lit. 113-115°C); **^{1}H-NMR** (400 MHz, $CDCl_3$) δ 8.30 (d, *J* = 8.8 Hz, 2H, CH_{Ar}C$_{Ar}$-NO_2), 8.14 (d, *J* = 8.8 Hz, 2H, CH_{Ar}C$_{Ar}$C=N), 7.38 (t, *J* = 7.7 Hz, 2H, CH_{Ar}CH$_{Ar}$C$_{Ar}$-N), 7.14 (t, *J* = 7.4 Hz, 1H, CH_{Ar}CH$_{Ar}$CH$_{Ar}$C$_{Ar}$-N), 6.80 (d, *J* = 7.5 Hz, 2H, CH_{Ar}C$_{Ar}$-N), 2.29 (s, 3H, CH_3C=N); **^{13}C{^{1}H}-NMR** (101 MHz, $CDCl_3$) δ 163.77 (*C*=N), 150.93 (*C*$_{Ar}$-N), 149.12 (*C*$_{Ar}$-NO_2), 145.10 (*C*$_{Ar}$C=N), 129.25 (*C*H$_{Ar}$CH$_{Ar}$C$_{Ar}$-N), 128.29 (*C*H$_{Ar}$C$_{Ar}$C=N), 124.10 (*C*H$_{Ar}$CH$_{Ar}$CH$_{Ar}$C$_{Ar}$-N), 123.70 (*C*H$_{Ar}$C$_{Ar}$-NO_2), 119.21 (*C*H$_{Ar}$C$_{Ar}$-N), 17.67 (*C*H_3C=N).

_N_-(2-bromophenyl)-1-(*p*-tolyl)ethan-1-imine (535)

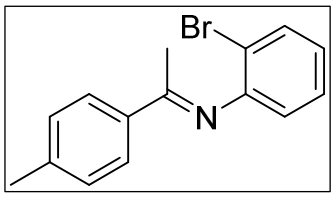

By general method 4-methylacetophenone (1.0 g, 0.745 mmol, 1.0 eq.) and 2-bromoaniline (1.28 g, 0.745 mmol, 1.0 eq.) were dissolved in dry toluene (10 mL). Purification by Kugelrohr distillation (190 °C at 0.1 mbar) afforded 0.215 g (0.75 mmol, 10 %) of **535** as yellow oil.

$C_{15}H_{14}BrN$ (M_W = 287.03 g/mol):
b.p.: 190 °C at 0.1 mbar; **^{1}H-NMR** (500 MHz, $CDCl_3$) δ 7.92 (d, *J* = 8.1 Hz, 2H, CH_{Ar}C$_{Ar}$C=N), 7.59 (d, *J* = 8.0 Hz, 1H, CH_{Ar}C$_{Ar}$-Br), 7.28 (m, 1H, CH_{Ar}CH$_{Ar}$C$_{Ar}$-N), 7.26 (d, *J* = 8.0 Hz, CH_{Ar}C$_{Ar}$-CH_3), 6.94 (t, J = 7.7 Hz, 1H, CH_{Ar}CH$_{Ar}$C$_{Ar}$-Br), 6.79 (d, *J* = 7.8 Hz, 1H, CH_{Ar}C$_{Ar}$-N), 2.42 (s, 3H, CH_3); **^{13}C{^{1}H}-NMR** (126 MHz, $CDCl_3$) δ 167.29 (*C*=N), 150.27 (*C*$_{Ar}$-N), 141.31 (*C*$_{Ar}$-CH_3), 136.32 (*C*$_{Ar}$C=N), 132.97 (*C*H$_{Ar}$C$_{Ar}$-Br), 129.27 (*C*H$_{Ar}$C$_{Ar}$-CH_3), 128.09 (*C*H$_{Ar}$CH$_{Ar}$C$_{Ar}$-N), 127.54 (*C*H$_{Ar}$C$_{Ar}$C=N), 124.44 (*C*H$_{Ar}$CH$_{Ar}$C$_{Ar}$-Br), 120.64 (*C*H$_{Ar}$C$_{Ar}$-N), 114.01 (*C*$_{Ar}$-Br), 21.58 (C$_{Ar}$*C*H_3), 18.16 (*C*H_3C=N); **IR** (neat, ATR) ν/cm^{-1} = 3058 (2), 3027 (w), 2920 (w), 1636 (s), 1608 (m), 1582 (m), 1572 (m), 1462 (s), 1434 (m), 1405 (w), 1365 (m), 1310 (m), 1295 (m), 1256 (m), 1213 (m), 1183 (m), 1116 (w), 1044 (w), 1026 (m); **GC-MS**: (EI, 70 eV, PhMeSi, 100.2/10.270/10): t_R = 17.8 min, *m/z* = 287 ([M]$^+$), 274, 155; **EA**: calc. C, 62.52; H, 4.90; N, 4.86; found: C, 62.20; H, 4.90; N, 4.87.

2-Methyl-_N_-(1-phenylethylidene)aniline (536)[145]

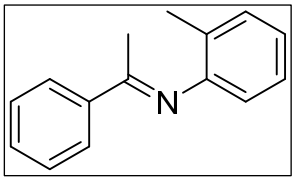

By general method acetophenone (0.515 g, 4.29 mmol, 1.15 eq.) and *o*-toluidine (0.4 g, 3.74 mmol, 1.0 eq.) were dissolved in dry toluene (10 mL). Purification by Kugelrohr distillation (125 °C at 0.08 mbar) afforded 0.678 g (3.24 mmol, 76 %) of **536** as yellow oil.

$C_{15}H_{15}N$ (M_W = 209.29 g/mol):
b.p.: 125°C at 0.08 mbar; **^{1}H-NMR** (400 MHz, $CDCl_3$) δ 8.09 – 7.91 (m, 2H, CH_{Ar}CC=N), 7.45 (m, 3H, CH_{Ar}&CH_{Ar}CHCC=N), 7.19 (m, 2H, C$_{Ar}$(CH$_3$)CH_{Ar}&CH$_{Ar}$CH_{Ar}CH$_{Ar}$), 7.00 (t, *J* = 7.4 Hz, 1H, C$_{Ar}$(CH$_3$)CH$_{Ar}$CH_{Ar}), 6.65 (d, *J* = 7.7 Hz, 1H, CH_{Ar}C-N), 2.16 (s, 3H, C$_{Ar}$CH_3), 2.10 (s, 3H, C=NCH_3).

_N_-(1-phenylethylidene)-4-(trifluoromethyl)aniline (532)[37]

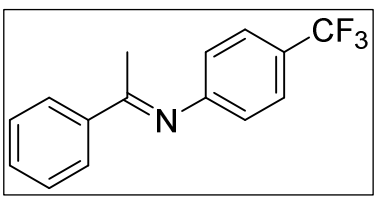

By general method acetophenone (0.373 g, 3.1 mmol, 1.0 eq.) and 4-(trifluoromethyl)aniline (0.5 g, 3.1 mmol, 1.0 eq.) were dissolved in dry toluene (10 mL). Purification by Kugelrohr distillation (150 °C at 0.2 mbar) afforded 0.056 g (0.21 mmol, 6 %) of **532** as yellow-orange solid.

$C_{15}H_{12}F_3N$ (M_W = 263.26 g/mol):

m.p.: 51-52 °C (Lit. 80-81°C); **^{1}H-NMR** (500 MHz, $CDCl_3$) δ 8.01 – 7.94 (m, 2H, CH_{Ar}CC=N), 7.61 (d, *J* = 8.3 Hz, 2H, CH_{Ar}C(CF_3)), 7.54 – 7.42 (m, 3H, CH_{Ar}&CH_{Ar}CH_{Ar}C$_{Ar}$C=N), 6.88 (d, *J* = 8.2 Hz, 2H, CH_{Ar}C-N), 2.24 (s, 3H, CH_3C=N); **^{13}C{^{1}H}-NMR** (126 MHz, $CDCl_3$) δ 166.34 (s, *C*=N), 154.98 (s, C_{Ar}-N), 138.98 (s, C_{Ar}C=N), 131.06 (s, 1CH_{Ar}), 128.62 (s, 2CH_{Ar}), 127.40 (s, 2CH_{Ar}CC=N), 126.42 (d, *J* = 3.7 Hz, CH_{Ar}C(CF_3)), 125.66 (d, *J* = 13.5 Hz, *C*C(CF_3)), 124.45 (q, J = 225.2 Hz, *C*F_3), 119.54 (s, CH_{Ar}C-N), 17.75 (s, *C*H_3C=N); **GC-MS**: (Rtx-5MS, 100.2/10.270/10): t_R = 21.2 min, *m/z* = 263 ($[M]^+$);

2-Isopropyl-*N*-(1-phenylethylidene)aniline (537)

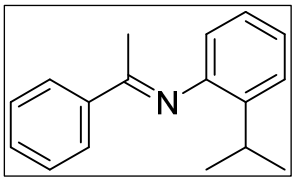

By general method acetophenone (0.515 g, 4.29 mmol, 1.4 eq.) and 2-isopropylaniline (0.418 g, 3.1 mmol, 1.0 eq.) were dissolved in dry toluene (10 mL). Purification by Kugelrohr distillation (138 °C at 0.1 mbar) afforded 0.654 g (2.76 mmol, 89%) of **537** as yellow oil.

$C_{17}H_{19}N$ (M_W = 237.34 g/mol):
b.p.: 138 °C at 0.1 mbar; **^{1}H-NMR** (400 MHz, $CDCl_3$) δ: 8.08 – 7.96 (m, 2H CH_{Ar}CC=N), 7.56 – 7.42 (m, 3H, CH_{Ar}&CH_{Ar}CHCC=N), 7.32 (dd, *J* = 7.6, 1.2 Hz, 1H, C$_{Ar}$(CH(CH_3)$_2$)CH_{Ar}), 7.18 (td, *J* = 7.5, 1.5 Hz, 1H, C$_{Ar}$(CH(CH_3)$_2$)CH_{Ar} CH_{Ar}), 7.10 (td, *J* = 7.5, 1.3 Hz, 1H, C$_{Ar}$(CH(CH_3)$_2$)CH_{Ar} CH$_{Ar}$CH_{Ar}), 6.61 (dd, *J* = 7.7, 1.3 Hz, 1H, C$_{Ar}$-NCH_{Ar}), 3.09 – 2.92 (m, 1H, C$_{Ar}$C*H*(CH_3)$_2$), 2.23 (s, 3H, C=NCH_3), 1.19 (d, *J* = 6.9 Hz, 6H, C$_{Ar}$CH_3); **^{13}C{^{1}H}-NMR** (101 MHz, $CDCl_3$) δ 164.66 (*C*=N), 149.16 (C_{Ar}-N), 139.66 (C_{Ar}C=N), 138.27 (C_{Ar}CH(CH_3)$_2$), 130.50 (*C*H$_{Ar}$CH$_{Ar}$CH$_{Ar}$C$_{Ar}$C=N), 128.51 (*C*H$_{Ar}$CH$_{Ar}$C$_{Ar}$C=N), 127.28 (*C*H$_{Ar}$C$_{Ar}$C=N), 126.19 (*C*H$_{Ar}$CH$_{Ar}$CH$_{Ar}$C$_{Ar}$CH(CH_3)$_2$), 125.76 (*C*H$_{Ar}$CH$_{Ar}$C$_{Ar}$CH(CH_3)$_2$), 123.78 (*C*H$_{Ar}$C$_{Ar}$CH(CH_3)$_2$), 118.78 (*C*H$_{Ar}$C$_{Ar}$-N), 28.48 (C$_{Ar}$*C*H(CH_3)$_2$), 22.97 (C$_{Ar}$CH(*C*H_3)$_2$), 17.71 (*C*H_3C=N); **IR** (neat, ATR) ν/cm^{-1} = 3060 (w), 3021 (w), 2959 (m), 2925 (w), 2866 (w), 1645 (m), 1633 (s), 1594 (m), 1578 (m), 1480 (m), 1447 (m), 1365 (m), 1287 (m), 1220 (m), 1192 (w), 1084 (w), 1033 (w), 753 (m), 692 (m); **MS** (EI, 70 eV): 237.1 (16.5%), 222.1 (100%), 207.1 (15.1%); **HRMS**: calculated: 237.1512; found: 237.1515; **EA**: calc. C, 86.40; H, 7.68; N, 5.93; found: C, 85.90; H, 8.11; N, 5.90.

2,6-Dimethyl-*N*-(1-phenylethylidene)aniline (340)[145]

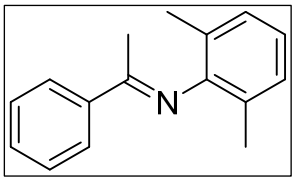

By general method acetophenone (0.98 g, 8.1 mmol, 1.0 eq.) and 2,6-dimethylaniline (0.98 g, 8.1 mmol, 1.0 eq.) were dissolved in dry toluene (10 mL). Purification by Kugelrohr distillation (137.5 °C at 0.1 mbar) afforded 0.4 g (1.8 mmol, 21 %) of **340** as yellow-white solid.

$C_{16}H_{17}N$ (M_W = 223.31 g/mol):
m.p.: 61-62 °C (Lit. 59-60°C); **^{1}H-NMR** (500 MHz, $CDCl_3$) δ 8.08 – 7.99 (m, 2H, CH_{Ar}CC=N), 7.54 – 7.42 (m, 3H, CH_{Ar}&CH_{Ar}CH_{Ar}C$_{Ar}$C=N), 7.06 (d, *J* = 7.5 Hz, 2H, CH_{Ar}C$_{Ar}$(CH_3)), 6.92 (t, *J* = 7.5 Hz, 1H, C$_{Ar}$(CH_3)CHArCH_{Ar}), 2.07 (s, 3H, C=N*C*H_3), 2.03 (s, 6H, C$_{Ar}$(*C*H_3)); **^{13}C{^{1}H}-NMR** (126 MHz, $CDCl_3$) δ 165.39 (*C*=N), 149.13 (C_{Ar}-N), 139.27 (C_{Ar}C=N), 130.60 (CH_{Ar}), 128.54 (CH_{Ar}), 127.96 (CH_{Ar}), 127.22 (CH_{Ar}), 125.88 (CH_{Ar}), 122.88 (CH_{Ar}), 18.11 (C$_{Ar}$(CH_3)), 17.63(*C*H_3C=N);

***N*-(3-methylbutan-2-ylidene)aniline (330)[140]**

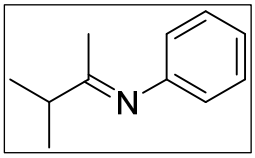

By general method 3-methyl-2-butanone (2.11 g, 24.5 mmol, 1.14 eq.) and aniline (2.0 g, 21.5 mmol, 1.0 eq.) were dissolved in dry benzene (6 mL). Purification by Kugelrohr distillation (75° C at 0.15 mbar) afforded 2.01 g (12.47 mmol, 58%) of **330** as a colourless oil.

$C_{11}H_{15}N$ (M_W = 161.24 g/mol):
E/*Z* mixture 6:1; *Major*: **^{1}H-NMR** (400 MHz, $CDCl_3$) δ 7.32 – 7.24 (m, 2H), 7.05 – 6.98 (m, 1H), 6.70 – 6.64 (m, 2H), 2.62 (hept, *J* = 6.9 Hz, 1H), 1.73 (s, 3H), 1.20 (d, *J* = 6.9 Hz, 6H); **^{13}C{^{1}H}-NMR** (101 MHz, $CDCl_3$) δ 176.31, 151.88, 128.98, 122.95, 119.47, 119.32, 39.32, 20.02, 17.14; *Minor*: **^{1}H-NMR** (400 MHz, $CDCl_3$) δ 7.18 – 7.12 (m, 2H), 6.75 (tt, *J* = 7.5, 1.1 Hz, 1H), 6.71 – 6.64 (m, 2H), 2.72 (dt, *J* = 13.7, 6.9 Hz,

1H), 2.07 (s, 3H), 1.02 (d, *J* = 6.9 Hz, 6H); **GC** (Machary-Nagel Optima-5-Amin (0.50 µm x 0.25 µm x 30 m), 60 kPa H_2, 100 °C/2 min, 10°C/min, 250 °C/7 min): t_R = 12.0 min; **GC-MS** (EI, 70 eV, PhMeSi, 80.2/10.270/10): t_R = 9.2 min, *m/z* = 161 ($[M]^+$), 146, 118 ($[M-(C(CH_3)_3)]^+$); **HRMS**: calculated: 161.1199; found: 161.1200

***N*-(4-methylpentan-2-ylidene)aniline (540)**

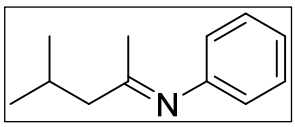

By general method 4-methyl-2-pentanone (3.0 g, 30 mmol, 1.0 eq.) and aniline (2.79 g, 30 mmol, 1.0 eq.) were dissolved in dry toluene (10 mL). Purification by Kugelrohr distillation (95° C at 0.1 mbar) afforded 1.14 g (6.5 mmol, 21%) of **540** as a colourless oil.

$C_{12}H_{17}N$ (M_W = 175.27 g/mol):
E/Z mixture 3.2:1; *Major*: **^{1}H-NMR** (500 MHz, $CDCl_3$) δ 7.30 (t, *J* = 7.8 Hz, 2H), 7.05 (t, *J* = 7.3 Hz, 1H), 6.71 (dd, *J* = 8.3, 1.0 Hz, 2H), 2.31 (d, *J* = 7.3 Hz, 2H), 2.20 – 2.11 (sept, *J* = 7.0 Hz, 1H), 1.78 (s, 3H), 1.03 (d, *J* = 6.6 Hz, 6H); **^{13}C{^{1}H}-NMR** (101 MHz, CDCl3) δ 171.75 (*C*=N), 151.73 (C_{Ar}-N), 128.99 ($CH_{Ar}CH_{Ar}C_{Ar}$-N), 123.08 ($CH_{Ar}CH_{Ar}CH_{Ar}C_{Ar}$-N), 119.64 ($CH_{Ar}C_{Ar}$-N), 50.85 ($CH_2CH(CH_3)_2$), 26.39 ($CH(CH_3)_2$), 22.66 ($CH(CH_3)_2$), 19.90 ($CH_3C$=N); *Minor*: **^{1}H-NMR** (500 MHz, $CDCl_3$) δ 7.28 (m, 2H, $CH_{Ar}CH_{Ar}C_{Ar}$-N), 7.03 (m, 1H, $CH_{Ar}CH_{Ar}CH_{Ar}C_{Ar}$-N), 6.68 (dd, *J* = 8.3, 1.0 Hz, 2H, $CH_{Ar}C_{Ar}$-N), 2.17 (s, 3H, CH_3C=N), 2.08 (d, *J* = 7.2 Hz, 2H, $CH_2C(CH_3)C$=N), 2.00 (sept, *J* = 6.5 Hz, 1H, $(CH_3)_2CHCH_2$), 0.84 (d, *J* = 6.5 Hz, 6H, $(CH_3)_2CHCH_2$); **^{13}C{^{1}H}-NMR** (101 MHz, CDCl3) δ 171.99 (*C*=N), 151.13 (C_{Ar}-N), 128.88 ($CH_{Ar}CH_{Ar}C_{Ar}$-N), 122.86 ($CH_{Ar}CH_{Ar}CH_{Ar}C_{Ar}$-N), 119.75 ($CH_{Ar}rC_{Ar}$-N), 43.07 ($CH_2CH(CH_3)_2$), 26.37 ($CH(CH_3)_2$), 26.16 ($CH_3C$=N), 22.64 ($CH(CH_3)_2$); **IR** (neat, ATR) ν/cm^{-1} = 3075 (w), 3028 (w), 2955 (m), 2869 (w), 1656 (s), 1593 (s), 1483 (m), 1464 (w), 1366 (m), 1252 (w), 1188 (w), 1168 (w), 1103 (w), 1070 (w), 900 (w), 794 (m), 744 (s), 696 (s); **GC** (Machary-Nagel Optima-5-Amin (0.50 µm x 0.25 µm x 30 m), 60 kPa H_2, 100 °C/2 min, 10 °C/min, 250 °C/7 min): t_R = 13.6 min; **GC-MS**: (Rtx-5MS, 100.2/10.270/10): t_R = 8.8 min, *m/z* = 175 ($[M]^+$), 160, 132, 118, 104, 92; **EA**: calc. C, 82.23; H, 9.78; N, 7.99; found: C, 81.84; H, 9.60; N, 8.32

***N*-(1-phenylpropan-2-ylidene)aniline (550)[146]**

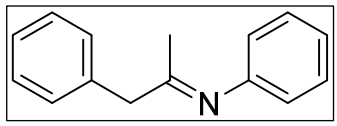

By general method phenylacetone (2.7 g, 20 mmol, 1.0 eq.) and aniline (2 g, 22 mmol, 1.1 eq.) were dissolved in dry benzene (7 mL). Purification by Kugelrohr distillation (125° C at 0.1 mbar) afforded 1.58 g (7.55 mmol, 38%) of **550** as a yellow-orange clear oil.

$C_{15}H_{15}N$ (M_W = 209.29 g/mol):
E/Z mixture 3:1, *Major*: **^{1}H-NMR** (400 MHz, CD_2Cl_2) δ 7.42 – 7.28 (m, 7H), 7.10 – 7.04 (m, 1H), 6.73 (d, *J* = 7.7 Hz, 2H), 3.74 (s, 2H), 1.74 (s, 3H); **^{13}C{^{1}H}-NMR** (126 MHz, CD_2Cl_2) δ 170.63, 151.93, 137.74, 129.63, 129.23, 128.93, 127.02, 123.34, 119.70, 48.73, 19.02; *Minor*: **^{1}H-NMR** (400 MHz, CD_2Cl_2) δ 7.14 (d, *J* = 7.5 Hz, 1H), 6.81 (d, *J* = 7.7 Hz, 1H), 3.51 (s, 1H), 2.07 (s, 2H), *other signals overlayed by major isomer*; **^{13}C{^{1}H}-NMR** (126 MHz, CD_2Cl_2) δ 169.58, 151.60, 137.27, 129.41, 129.38, 129.02, 126.87, 119.82, 115.15, 40.65, 25.99; **GC** (Machary-Nagel Optima-5-Amin (0.50 µm x 0.25 µm x 30 m), 60 kPa H_2, 100 °C/2 min, 10°C/min, 250 °C/10 min): t_R = 20.2 min; **GC-MS** (Rtx-5MS, 50.2/30.250/5): t_R = 8.9 min, *m/z* = 209 ($[M]^+$), 193, 167, 118, 91, 77.

***N*-(pentan-2-ylidene)aniline (331)**

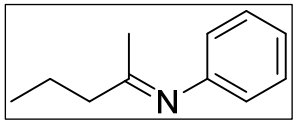

By general method 2-pentanone (1.62 g, 18.8 mmol, 1.0 eq.) and aniline (2 g, 21.5 mmol, 1.14 eq.) were dissolved in dry toluene (10 mL). Purification by Kugelrohr distillation (75° C at 0.1 mbar) afforded 1.16 g (7.2 mmol, 38%) of **331** as a colourless oil.

$C_{11}H_{15}N$ (M_W = 161.24 g/mol):

3:1 *E/Z* mixture, *Major*: **^{1}H-NMR** (400 MHz, $CDCl_3$) δ 7.30 (m, 2H, CH_{Ar}CH$_{Ar}$C$_{Ar}$-N), 7.03 (t, *J* = 7.4 Hz, 1H, CH_{Ar}CH$_{Ar}$CH$_{Ar}$C$_{Ar}$-N), 6.68 (d, *J* = 7.3, 2H, CH_{Ar}C$_{Ar}$-N), 2.41 (t, *J* = 7.5 Hz, 2H, CH_2C=N), 1.77 (s, 3H, CH_3C=N), 1.70 (tq (m), 2H, CH_2CH$_2$C=N), 1.02 (t, *J* = 7.4 Hz, 3H, CH_3CH$_2$CH$_2$C=N); **^{13}C{^{1}H}-NMR** (101 MHz, $CDCl_3$) δ 172.12 (*C*=N), 151.75 (*C*$_{Ar}$-N), 128.96 (*C*H$_{Ar}$CH$_{Ar}$C$_{Ar}$-N), 123.05 (*C*H$_{Ar}$CH$_{Ar}$CH$_{Ar}$C$_{Ar}$-N), 119.64 (*C*H$_{Ar}$C$_{Ar}$-N), 43.74 (*C*H$_2$C=N), 19.83 (*C*H$_3$C=N), 19.52 (*C*H$_2$CH$_2$C=N), 13.91 (*C*H$_3$CH$_2$CH$_2$C=N); *Minor*: **^{1}H-NMR** (400 MHz, $CDCl_3$) δ 7.30 (m, 2H, CH_{Ar}CH$_{Ar}$C$_{Ar}$-N), 7.03 (t, *J* = 7.4 Hz, 1H, CH_{Ar}CH$_{Ar}$CH$_{Ar}$C$_{Ar}$-N), 6.66 (d, *J* = 7.2 Hz, 2H, CH_{Ar}C$_{Ar}$-N), 2.15 (s, 3H, *C*H$_3$C=N), 2.11 (dd, *J* = 8.7, 6.9 Hz, 2H, CH_2C=N), 1.52 (qt (m), 2H, *C*H$_2$CH$_2$C=N), 0.83 (t, *J* = 7.4 Hz, 3H, *C*H$_3$CH$_2$CH$_2$C=N); **^{13}C{^{1}H}-NMR** (101 MHz, $CDCl_3$) δ 173.64 (*C*=N), 151.21 (*C*$_{Ar}$-N), 129.39 (*C*H$_{Ar}$CH$_{Ar}$C$_{Ar}$-N), 122.94 (*C*H$_{Ar}$CH$_{Ar}$CH$_{Ar}$C$_{Ar}$-N), 115.20 (*C*H$_{Ar}$C$_{Ar}$-N), 36.12 (*C*H$_2$C=N), 25.97 (*C*H$_3$C=N), 20.39 (*C*H$_2$CH$_2$C=N), 14.14 (*C*H$_3$CH$_2$CH$_2$C=N); **IR** (neat, ATR) ν/cm^{-1} = 3075 (w), 3060 (w), 3028 (w), 3018 (w), 2959 (m), 2931 (w), 2872 (w), 1658 (s), 1594 (s), 1483 (m), 1366 (m), 1252 (m), 1225 (w), 1186 (m), 1168 (w), 1093 (w), 1071 (m), 900 (w), 797 (m), 746 (m), 698 (s); **GC** (Machary-Nagel Optima-5-Amin (0.50 µm x 0.25 µm x 30 m), 60 kPa H_2, 100 °C/2 min, 10 °C/min, 250 °C/7 min): t_R = 12.7 min; **GC-MS** (EI, 70 eV, PhMeSi, 100.2/10.270/10): t_R = 7.1 min, *m/z* = 161 ([M]$^+$);
EA: calc. C, 81.94; H, 9.38; N, 8.69; found: C, 81.72; H, 9.33; N, 8.65.

***N*-(6-methylhept-5-en-2-ylidene)aniline (542)**

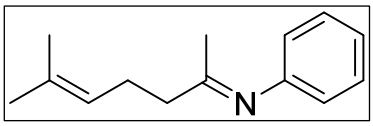

By general method 6-methylhept-5-en-2-one (1.71 g, 13.55 mmol, 1.0 eq.) and aniline (1.26 g, 13.55 mmol, 1.0 eq.) were dissolved in dry toluene (10 mL). Purification by Kugelrohr distillation (112.5° C at 0.1 mbar) afforded 600 mg (3.0 mmol, 22%) of **542** as a yellow clear oil.

$C_{14}H_{19}N$ (M_W = 201.31 g/mol):
E/Z mixture 3:1, *Major*: **^{1}H-NMR** (400 MHz, $CDCl_3$) δ 7.33 – 7.28 (m, 2H), 7.05 (tt, J = 7.5, 1.2 Hz, 1H), 6.70 (dd, J = 8.4, 1.1 Hz, 2H), 5.22 (dddt, J = 6.8, 5.3, 2.8, 1.4 Hz, 1H), 2.48 – 2.43 (m, 2H), 2.42 – 2.37 (m, 2H), 1.79 (s, 3H), 1.74 (d, J = 1.2 Hz, 3H), 1.68 (d, J = 1.2 Hz, 3H); **^{13}C{^{1}H}-NMR** (101 MHz, $CDCl_3$) δ 171.71, 151.63, 132.37, 128.86, 123.28, 122.95, 119.51, 41.59, 25.77, 25.04, 19.66, 17.79;
Minor: **^{1}H-NMR** (400 MHz, $CDCl_3$) δ 7.31 – 7.27 (m, 2H), 7.06 – 7.02 (m, 1H), 6.72 – 6.68 (m, 2H), 4.97 (dddt, J = 7.0, 5.5, 3.0, 1.5 Hz, 1H), 2.47 – 2.45 (m, 2H), 2.39 – 2.36 (m, 2H), 2.18 (s, 3H), 1.67 (d, J = 1.1 Hz, 3H), 1.53 (d, J = 1.2 Hz, 3H); **^{13}C{^{1}H}-NMR** (101 MHz, $CDCl_3$) δ 172.26, 151.09, 132.91, 128.79, 122.85, 122.66, 119.51, 34.02, 26.04, 25.64, 25.43, 17.56; **GC** (Machary-Nagel Optima-5-Amin (0.50 µm x 0.25 µm x 30 m), 60 kPa H_2, 100 °C/2 min, 10°C/min, 250 °C/10 min): t_R = 17.2 min; **GC-MS** (Rtx-5MS, 50.2/30.250/5): t_R = 8.1 min, *m/z* = 201 ([M]$^+$), 186, 158, 144, 132, 118, 109, 93, 77;
IR (neat, ATR) ν/cm^{-1} = 3072 (w), 3057 (w), 3022 (w), 2966 (m), 2914 (m), 2854 (m), 1663 (s), 1593 (m), 1483 (m), 1443 (w), 1367 (w), 1246 (w), 1169 (w); **EA**: calculated: C, 83.53; H, 9.51; N, 6.96, found: C, 83.45; H, 9.31; N, 6.87.

***N*-(octan-2-ylidene)aniline (334)[147]**

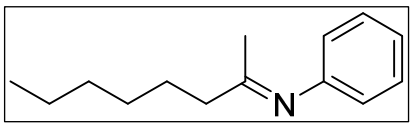

By general method 2-octanone (1.64 g, 12.8 mmol, 1.0 eq.) and aniline (1.19 g, 12.8 mmol, 1.0 eq.) were dissolved in dry toluene (10 mL). Purification by Kugelrohr distillation (125° C at 0.1 mbar) afforded 847 mg (4.17 mmol, 32%) of **334** as a slighty yellowish clear oil.

$C_{14}H_{21}N$ (M_W = 203.32 g/mol):
E/Z mixture 3:1, *Major*: **^{1}H-NMR** (400 MHz, $CDCl_3$) δ 7.30 (m, 2H), 7.05 (m, 1H), 6.70 (m, 2H), 2.42 (m, 2H), 1.79 (s, 3H), 1.69 (m, 2H), 1.41 (m, 2H), 1.36 (m, 4H), 0.92 (m, 3H); **^{13}C{^{1}H}-NMR** (101 MHz, $CDCl_3$) δ 172.35, 151.77, 128.96, 123.03, 119.65, 41.88, 31.83, 29.16, 26.48, 22.73, 19.55, 14.22; M*inor*: **^{1}H-NMR** (400 MHz, $CDCl_3$) δ 7.30 (m, 2H), 7.05 (m, 1H), 6.70 (m, 2H), 2.17 (s, 3H), 2.14 (m, 2H), 1.49 (m, 2H),

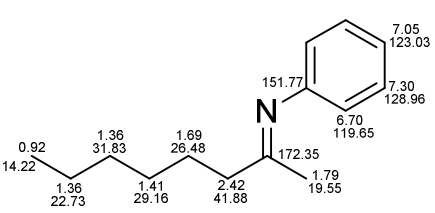

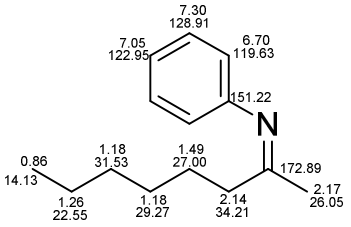

1.18 (m, 4H), 1.26 (m, 2H), 0.86 (m, 3H); **^{13}C{^{1}H}-NMR** (101 MHz, $CDCl_3$) δ 172.89, 151.22, 128.91, 122.95, 119.63, 34.21, 31.52, 29.27, 27.00, 26.05, 22.55, 14.13; **GC** (Machary-Nagel Optima-5-Amin (0.50 µm x 0.25 µm x 30 m), 60 kPa H_2, 100 °C/2 min, 10°C/min, 250 °C/10 min): t_R = 17.3 min; **GC-MS** (Rtx-5MS, 100.2/10.270/10): t_R = 13.3 min, *m/z* = 203 ($[M]^+$), 188, 174, 160, 146, 132, 118, 92, 77.

***N*-(1-cyclopentylethylidene)aniline (538)**

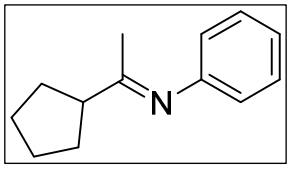

By general method cyclopentyl methyl ketone (0.34 g, 3.125 mmol, 1.0 eq.) and aniline (0.32 g, 3.43 mmol, 1.1 eq.) were dissolved in dry toluene (10 mL). Purification by Kugelrohr distillation (100° C at 0.15 mbar) afforded 0.25 g (1.33 mmol, 42%) of **538** as a colourless oil.

$C_{13}H_{17}N$ (M_W = 187.28 g/mol):
6:1 *E/Z* mixture, M*ajor*: **^{1}H-NMR** (500 MHz, $CDCl_3$) δ 7.27 (m, 2H, CH_{Ar}CH_{Ar}C$_{Ar}$-N), 7.02 (d, *J* = 7.4 Hz, 1H, CH_{Ar}CH_{Ar}CH_{Ar}C$_{Ar}$-N), 6.67 (dd, *J* = 8.3, 1.1 Hz, 2H, CH_{Ar}C$_{Ar}$-N), 2.81 (pent, *J* = 8.1 Hz, 1H, C*H*C=N), 1.95 (m, 2H, C*H*HCHC=N), 1.77 (m, 4H, C*H*HC*H*HCHC=N), 1.76 (s, 3H, CH_3), 1.67 (m, 2H, C*H*HCHHCHC=N); **^{13}C{^{1}H}-NMR** (126 MHz, $CDCl_3$) δ 174.36 (*C*=N), 151.90 (*C*$_{Ar}$-N), 128.85 (*C*H_{Ar}CH_{Ar}C$_{Ar}$-N), 122.75 (*C*H_{Ar}CH_{Ar}CH_{Ar}C$_{Ar}$-N), 119.41 (*C*H_{Ar}C$_{Ar}$-N), 50.61 (*C*HC=N), 30.13 (*C*H_2CHC=N), 25.64 (*C*H_2CH_2CHC=N), 18.24 (*C*H_3); *Minor*: **^{1}H-NMR** (500 MHz, $CDCl_3$) δ 7.27 (m, 2H, CH_{Ar}CH_{Ar}C$_{Ar}$-N), 7.02 (d, *J* = 7.4 Hz, 1H, CH_{Ar}CH_{Ar}CH_{Ar}C$_{Ar}$-N), 6.67 (dd, *J* = 8.3, 1.1 Hz, 2H, CH_{Ar}C$_{Ar}$-N), 2.70 (pent, *J* = 8.0 Hz, 1H, C*H*C=N), 2.10 (s, 3H, *C*H_3), 1.71 (m, 2H, C*H*HCHHCHC=N), 1.70 (m, 2H, C*H*HCHC=N), 1.61 (m, 2H, C*H*HCHC=N), 1.49 (m, 2H, C*H*HCHHCHC=N); **^{13}C{^{1}H}-NMR** (126 MHz, $CDCl_3$) δ 175.40 (*C*=N), 151.90 (*C*$_{Ar}$-N), 128.81 (*C*H_{Ar}CH_{Ar}C$_{Ar}$-N), 122.71 (*C*H_{Ar}CH_{Ar}CH_{Ar}C$_{Ar}$-N), 119.34 (*C*H_{Ar}C$_{Ar}$-N), 43.12 (*C*HC=N), 31.12 (*C*H_2CHC=N), 26.16 (*C*H_2CH_2CHC=N), 22.04 (*C*H_3); **GC** (Machary-Nagel Optima-5-Amin (0.50 µm x 0.25 µm x 30 m), 60 kPa H_2, 100 °C/2 min, 10 °C/min, 250 °C/7 min): t_R = 16.8 min; **GC-MS**: (Rtx-5MS, 100.2/10.270/10): t_R = 12.7 min, *m/z* = 187 ($[M]^+$), 146, 118; **IR** (neat, ATR) ν/cm^{-1} = 3060 (w), 3018 (w), 2950 (m), 2866 (m), 1567 (s), 1594 (s), 1578 (w), 1483 (m), 1447 (w), 1364 (m), 1192 (m), 1166 (m), 1070 (w), 1025 (w), 899 (w), 798 (w), 697 (s); **EA**: calc. C, 83.37; H, 9.15; N, 7.48; found: C, 82.26; H, 8.96; N, 7.88.

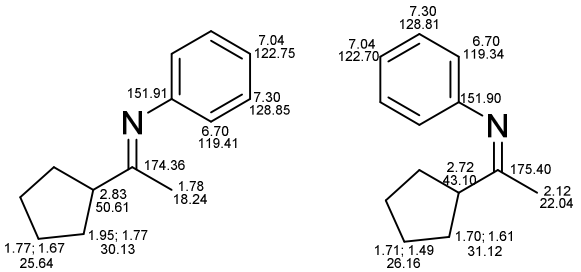

***N*-(3,3-dimethylbutan-2-ylidene)aniline (541)[148]**

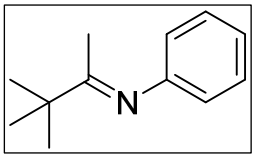

By general method pinacolone (2.15 g, 21.4 mmol, 1.0 eq.) and aniline (2.0 g, 21.5 mmol, 1.0 eq.) were dissolved in dry benzene (6 mL). Purification by Kugelrohr distillation (100-150° C at 0.07 mbar) afforded 1.5 g (8.56 mmol, 40%) of **541** as a colourless oil.

$C_{12}H_{17}N$ (M_W = 175.27 g/mol):
^{1}H-NMR (400 MHz, $CDCl_3$) δ 7.27 (m, 2H, CH_{Ar}CH_{Ar}C$_{Ar}$-N), 7.00 (m, 1H, CH_{Ar}CH_{Ar}CH_{Ar}C$_{Ar}$-N), 6.63 (m, 2H, CH_{Ar}C$_{Ar}$-N), 1.74 (s, 3H, CH_3), 1.22 (s, 9H, C(CH_3)$_3$); **^{13}C{^{1}H}-NMR** (101 MHz, $CDCl_3$) δ 177.60 (*C*=N), 152.34 (*C*$_{Ar}$-N), 129.00 (*C*H_{Ar}CH_{Ar}C$_{Ar}$-N), 122.69 (*C*H_{Ar}CH_{Ar}CH_{Ar}C$_{Ar}$-N), 119.15 (*C*H_{Ar}C$_{Ar}$-N), 40.35 (*C*(CH$_3$)$_3$), 27.95 (*C*H$_3$C=N), 15.38 (C(*C*H$_3$)$_3$); **GC** (Machary-Nagel Optima-5-Amin (0.50 µm x 0.25 µm x 30 m), 60 kPa H_2, 100 °C/2 min, 10°C/min, 250 °C/10 min): t_R = 12.7 min; **GC-MS** (EI, 70 eV, PhMeSi, 100.2/10.270/10): t_R = 7.9 min, *m/z* = 175 ($[M]^+$), 118; **HRMS**: calculated: 175.1356; found: 175.1357.

***N*-(1-cyclohexylethylidene)-1-phenylmethanamine (551)[149]**

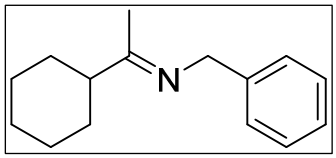

By general method cyclohexyl methyl ketone (1.09 g, 8.6 mmol, 1.0 eq.) and benzylamine (1.02 g, 9.5 mmol, 1.1 eq.) were dissolved in dry toluene (10 mL). Purification by Kugelrohr distillation (125° C at 0.1 mbar) afforded 0.84 g (3.9 mmol, 45%) of **551** as a colourless clear oil.

$C_{15}H_{21}N$ (M_W = 215.33 g/mol):
^{1}H-NMR (400 MHz, $CDCl_3$) δ 7.31 (m, 5H, CH_{Ar}), 4.49 (s, 2H, CH_2), 2.25 (tt, J = 11.6, 3.3 Hz, 1H, C*H*C=N), 1.84 (s, 3H, CH_3), 1.77 (m, 4H, CH_{Aliph}), 1.32 (m, 6H, CH_{Aliph}); **GC** (Machary-Nagel Optima-5-Amin (0.50 µm x 0.25 µm x 30 m), 60 kPa H_2, 100 °C/2 min, 10°C/min, 250 °C/7 min): t_R = 20.6 min (I34); **GC-MS** (Rtx-5MS, 100.2/10.270/10): t_R = 16.8 min, m/z = 215 ($[M]^+$), 200, 186, 174, 160, 147, 124, 91.

***N*-(1-cyclohexylethylidene)butan-1-amine (552)**

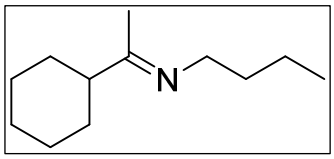

By general method cyclohexyl methyl ketone (0.92 g, 7.27 mmol, 1.0 eq.) and *n*-butylamine (1.6 g, 21.8 mmol, 3.0 eq.) were dissolved in dry toluene (10 mL). Purification by Kugelrohr distillation (87° C at 0.15 mbar) afforded 0.75 g (4.11 mmol, 56%) of **552** as a colourless clear oil.

$C_{12}H_{23}N$ (M_W = 181.32 g/mol):
^{1}H-NMR (400 MHz, $CDCl_3$) δ 3.23 (t, *J* = 7.3 Hz, 2H), 2.17 (ddt, *J* = 11.3, 6.6, 3.3 Hz, 1H), 1.83 – 1.73 (m, 4H), 1.76 (s, 3H), 1.72 – 1.66 (m, 1H), 1.60 (p, J = 7.4 Hz, 2H), 1.39 – 1.34 (m, 2H), 1.30 (ddd, J = 12.2, 8.5, 3.0 Hz, 4H), 1.19 (dddd, J = 15.9, 12.3, 7.4, 3.4 Hz, 1H), 0.94 (t, J = 7.3 Hz, 3H); **^{13}C{^{1}H}-NMR** (101 MHz, $CDCl_3$) δ 173.36, 51.07, 50.87, 33.20, 30.32, 26.31, 26.29, 20.87, 14.91, 14.19; **GC** (Machary-Nagel Optima-5-Amin (0.50 µm x 0.25 µm x 30 m), 60 kPa H_2, 100 °C/2 min, 10°C/min, 250 °C/10 min): t_R = 13.8 min (I35); **GC-MS** (Rtx-5MS, 50.2/30.250/5): t_R = 7.0 min, m/z = 181 ($[M]^+$), 166, 152, 126, 98; **IR** (neat, ATR) ν/cm^{-1} = 2955 (s), 2924 (s), 2851 (s), 1663 (m), 1643 (w), 1447 (m), 1369 (w), 1248 (w), 1198 (w); **EA**: calculated: C, 79.49; H, 12.79; N, 7.72, found: C, 79.61; H, 12.63; N, 7.76.

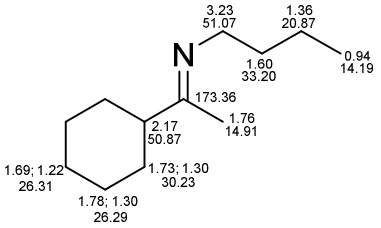

***N*-(1-cyclohexylethylidene)propan-2-amine (554)**

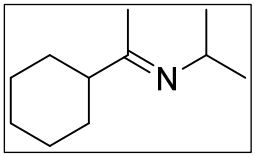

By general method cyclohexyl methyl ketone (0.92 g, 7.27 mmol, 1.0 eq.) and isoproylamine (2.15 g, 36.33 mmol, 5.0 eq.) were dissolved in dry toluene (10 mL) and stirred at room temperature for four days. Purification by Kugelrohr distillation (100° C at 0.15 mbar) afforded 0.52 g (3.1 mmol, 43%) of **554** as a colourless clear oil.

$C_{11}H_{21}N$ (M_W = 167.29 g/mol):
E/Z mixture 16:1, *Major*: **^{1}H-NMR** (400 MHz, $CDCl_3$) δ 3.60 (hept, J = 6.3 Hz, 1H), 2.16 (td, J = 9.6, 8.9, 4.8 Hz, 1H), 1.75 (s, 3H), 1.81 – 1.65 (m, 6H), 1.36 – 1.25 (m, 4H), 1.10 (s, 3H), 1.09 (s, 3H); **^{13}C{^{1}H}-NMR** (101 MHz, $CDCl_3$) δ 170.70, 51.16, 49.81, 30.25, 26.26, 26.20, 23.63, 13.78; **GC** (Machary-Nagel Optima-5-Amin (0.50 µm x 0.25 µm x 30 m), 60 kPa H_2, 100 °C/2 min, 10°C/min, 250 °C/10 min): t_R = 10.8 min; **GC-MS** (Rtx-5MS, 50.2/30.250/5): t_R = 6.0 min, *m/z* = 167 ($[M]^+$), 152, 126, 112, 99, 84; **IR** (neat, ATR) ν/cm^{-1} = 2964 (m), 1924 (s), 1853 (m), 1663 (m), 1643 (m), 1448 (m), 1373 (w), 1364 (w), 1246 (w), 1202 (w), 1159 (w), 808 (w); **EA**: calculated: C, 78.97; H, 12.65; N, 8.37, found: C, 78.44; H, 12.50; N, 8.34.

***N*-(1-cyclohexylethylidene)cyclohexanamine (556)**

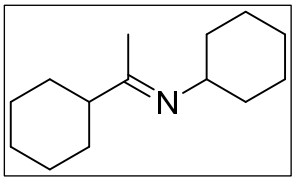

By general method cyclohexyl methyl ketone (1.834 g, 14.53 mmol, 1.0 eq.) and cyclohexylamine (1.439 g, 14.53 mmol, 1.0 eq.) were dissolved in dry toluene (10 mL). Purification by Kugelrohr distillation (100° C at 0.1 mbar) afforded 1.153 g (5.56 mmol, 38%) of **556** as a colourless clear oil.

$C_{14}H_{25N}$ (M_W = 207.35 g/mol):

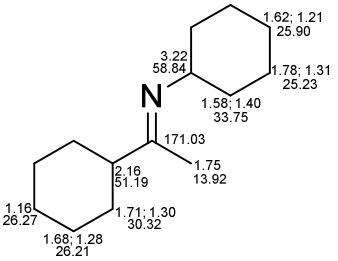

^{1}H-NMR (400 MHz, $CDCl_3$) δ 3.22 (m, 1H, C*H*C-N), 2.19 – 2.12 (m, 1H, C*H*C=N), 1.82 – 1.61 (m, 11H), 1.61 – 1.54 (m, 2H), 1.45 – 1.13 (m, 10H); **^{13}C{^{1}H}-NMR** (101 MHz, $CDCl_3$) δ 171.13, 58.93, 51.29, 33.85, 30.41, 26.36, 26.30, 25.99, 25.33, 14.01; **GC** (Machary-Nagel Optima-5-Amin (0.50 µm x 0.25 µm x 30 m), 60 kPa H_2, 100 °C/2 min, 10°C/min, 250 °C/10 min): t_R = 17.4 min; **GC-MS** (Rtx-5MS, 100.2/10.270/10): t_R = 13.2 min, *m/z* = 207 ($[M]^+$), 192, 178, 166, 152, 126, 124, 83; **IR** (neat, ATR) ν/cm^{-1} = 2922 (s), 2851 (s), 1657 (m), 1447 (m), 1369 (w), 1358 (w), 1240 (w), 1196 (w), 1028 (w), 889 (w), 843 (w); **EA**: calculated: C, 81.09; H, 12.15; N, 6.75, found: C, 80.69; H, 12.04; N, 6.94.

***N*-(2-methyl-1-phenylpropylidene)aniline (411)[150]**

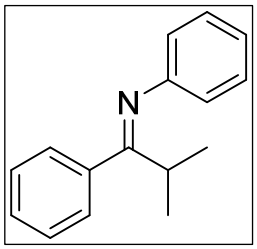

By general method, isobutyrophenone (1.964 g, 1.325 mmol, 1.1 eq.) and aniline (1.12 g, 1.2 mmol, 1.0 eq.) were dissolved in benzene (16 mL). Purification by Kugelrohr distillation (95 °C, 0.1 torr) afforded 1.28 g (0.576 mmol, 48 %) of **441** as a yellowish oil.

$C_{16}H_{17}N$ (M_W = 223.31 g/mol):

^{1}H-NMR (500 MHz, $CDCl_3$) δ 7.20 – 7.17 (m, 3H), 7.08 (t, *J* = 7.6 Hz, 2H), 7.01 (dd, *J* = 7.0, 2.8 Hz, 2H), 6.86 (d, *J* = 7.4 Hz, 1H), 6.59 (d, *J* = 8.1 Hz, 2H), 3.03 (hept, *J* = 6.9 Hz, 1H), 1.24 (d, *J* = 6.9 Hz, 6H); **GC-MS**: (Optima-5-Amine, 80.2/7.270/10): t_R = 19.5 min, *m/z* = 223 $[M]^+$, 208 $[M\text{-}CH_3]^+$, 180 $[M\text{-}C_3H_7]^+$.

***N*-(2,2-difluoro-1-phenylethylidene)aniline (412)[151]**

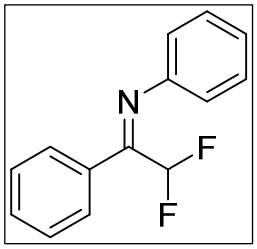

An oven-dried 50 mL two-necked round-bottom flask was purged with Argon three times before being charged with dry THF (2 mL) and cooled to -78 °C. Trimethyl(trifluoromethyl)silane (860 mg, 6.04 mmol, 1.5 eq.) dissolved in fry THF (2.0 M) was added slowly. N-benzylideneaniline (730 mg, 4.03 mmol, 1.0 eq.) was dissolved in THF (5 mL) and added dropwise before stirring was continued at -78 °C for 15 minutes. The reaction was warmed to -60 °C and tetramethyl ammonium fluoride (500 mg, 5.37 mmol, 1.33 eq.) was added in 10 portions over the course of 90 minutes. The reaction was then warmed to -50 °C and stirred for an additional 2 hours. It was then allowed to warm up to room temperature while stirring overnight. The reaction mixture was filtered, the filter cake washed with pentane (25 mL) and solvents reduced under reduced pressure. Purification by flash chromatography afforded 400 mg (1.73 mmol, 43 %) of **412** as a yellow solid.

$C_{14}H_{11}F_2N$ (M_W = 231.24 g/mol):

E/Z mixture 1:1.5: **^{1}H-NMR** (400 MHz, $CDCl_3$) δ 8.08 (d, *J* = 8.1 Hz, 0.7H), 7.68 – 7.26 (m, 4H), 7.26 – 7.13 (m, 2.6H), 7.03 (t, *J* = 7.4 Hz, 0.7H), 6.94 – 6.86 (m, 0.7H), 6.81 – 6.70 (m, 1.2H), 6.38 (t, *J* = 53.0 Hz, 0.4H), 6.37 (t, *J* = 55.3 Hz, 0.6H); **^{19}F-NMR** (376 MHz, $CDCl_3$) δ -116.01 (0.4F), -117.40 (0.6F).

Diethyl 2-(phenyl(phenylimino)methyl)malonate (413)

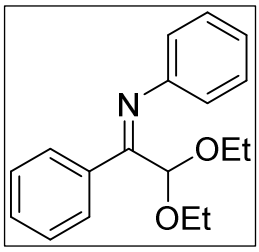

By general method, diethyl 2-benzoylmalonate (1.0 g, 4.8 mmol, 1.0 eq.) and aniline (536 mg, 5.76 mmol, 1.2 eq.) were dissolved in benzene (5 mL). Purification by Kugelrohr distillation (125 °C, 0.1 torr) afforded 310 mg (1.094 mmol, 23 %) of **413** as a yellow oil.

$C_{18}H_{21}NO_2$ (M_W = 283.37 g/mol):
^{1}H-NMR (500 MHz, $CDCl_3$) δ 8.22 (d, *J* = 7.3 Hz, 2H), 7.45 – 7.38 (m, 3H), 7.34 (t, *J* = 7.6 Hz, 2H), 7.24 (s, 1H), 7.23 – 7.17 (m, 2H), 7.12 (dt, *J* = 15.1, 7.6 Hz, 2H), 6.86 (d, *J* = 7.9 Hz, 2H), 6.70 (d, *J* = 7.9 Hz, 1H), 5.18 (s, 1H), 5.11 (s, 1H), 3.84 (dq, *J* = 14.3, 7.2 Hz, 1H), 3.75 – 3.67 (m, 1H), 3.58 (dq, *J* = 14.5, 7.1 Hz, 2H), 3.43 – 3.34 (m, 2H), 1.26 (t, *J* = 7.0 Hz, 4H), 1.14 (t, *J* = 7.0 Hz, 6H); **GC-MS**: (Optima-5-Amine, 50.2/10.270/10): t_R = 21.2 min, *m/z* = 283 $[M]^+$, 281, 255.

***N*-((4-fluorophenyl)(phenyl)methylene)aniline (414)**

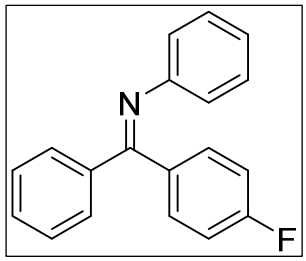

An oven-dried Argon-purged 50 mL two-necked round-bottom flask was charged with (4-fluorophenyl)(phenyl)methanone (1.0 g, 5 mmol, 1.0 eq.), aniline (545 mg, 6 mmol, 1.2 eq.) and dissolved in benzene (10 mL). It was heated to reflux for 24 hours. Purification by Kugelrohr disitllation (165 °C, 0.07 torr) afforded 700 mg (2.55 mmol, 51%) of **414** as a yellow solid.

$C_{19}H_{14}FN$ (M_W = 275.32 g/mol):
m.p.: 124-125 °C; *E/Z* mixture 1:1, signals overlaying: **^{1}H NMR** (400 MHz, $CDCl_3$) δ 7.74 (m, 4H), 7.48 (m, 1H), 7.42 (dd, *J* = 8.2, 6.5 Hz, 2H), 7.26 (m, 5H), 7.12 (m, 10H), 6.94 (m, 4H), 6.71 (m, 4H); **^{13}C{^{1}H}-NMR** (125 MHz, $CDCl_3$) δ 167.35, 167.15, 151.25, 151.18, 139.71, 136.11, 136.01, 132.25, 131.75, 131.67, 131.59, 131.50, 130.99, 129.54, 129.42, 128.83, 128.75, 128.63, 128.41, 128.13, 123.42, 123.36, 121.07, 120.96, 115.44, 115.34, 115.22, 115.13; **^{19}F-NMR** (376 MHz, $CDCl_3$) δ -110.04 (major), -111.83 (minor); **IR** (neat, ATR) ν/cm^{-1} = 3061 (w), 1613 (m), 1590 (s), 1502 (s), 1485 (m), 1444 (m), 1407 (m), 1296 (m), 1270 (m), 1217 (s), 1154 (m), 1144 (m), 1097 (w), 1071 (m), 960 (m); **GC-MS**: (Optima-5-Amine, 80.2/10.270/10): t_R = 20.1 min, *m/z* = 275; **MS** (EI, 70 eV): 275.1 (100%), 198.1 (59%), 183.1 (47%), 180.1 (39%); **EA**: calc.: C, 82.89; H, 5.13; N, 5.09; found: C, 82.70; H, 5.21; N, 4.83

***N*-(2-(tert-butyl)-3,4-dihydronaphthalen-1(2H)-ylidene)aniline (383)**

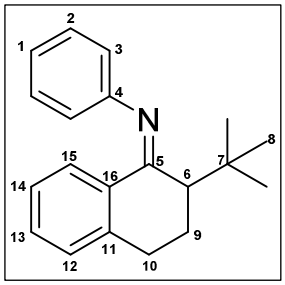

An oven-dried and Argon-purged 25 mL two-necked round-bottom flask was charged with 2-(tert-butyl)-3,4-dihydronaphthalen-1(2H)-one (350 mg, 1.73 mmol, 1.0 eq.) and aniline (472 mg, 5.19 mmol, 3.0 eq.) It was dissolved in dry Et_2O (10 mL) and cooled to 0 °C. A precooled solution (0 °C) of $TiCl_4$ (344 mg, 1.82 mmol, 1.05 eq.) in Et_2O (1.0 M) was added dropwise before the cooling bath was removed and the reaction mixture heated to reflux for 3 days. After cooling to room temperature, the reaction mixture was filtered and the filter cake washed with Et_2O (50 mL). The etheral solution was then washed with NaOH (1.0 M, 20 mL), the aequeous layer re-extracted with Et_2O (2x15 mL) and the combined organic layers dried over K_2CO_3, filtered and solvents removed under reduced pressure. Purification by Kugelrohr distillation (150 °C, 0.08 mbar) afforded 140 mg (0.5 mmol, 29 %) of **383** as a yellow oil.

$C_{20}H_{23}N$ (M_W = 277.40 g/mol):
^{1}H-NMR (500 MHz, DMSO-d_6) 7.96 (d, *J* = 7.7 Hz, 1H, H15), 7.38 (t, *J* = 7.3 Hz, 1H, H13), 7.33 (t, *J* = 7.7 Hz, 2H, H2), 7.27 (t, *J* = 7.4 Hz, 1H, H14), 7.20 (d, *J* = 7.6 Hz, 1H, H12), 7.02 (t, *J* = 7.4 Hz, 1H, H1), 6.76 (d, *J* = 7.6 Hz, 2H, H3), 3.07 (ddd, *J* = 18.2, 11.9, 6.5 Hz, 1H, H10), 2.98 (dd, *J* = 4.9, 2.3 Hz, 1H, H6), 2.88 (dd, *J* = 18.0, 6.9 Hz, 1H, H10'), 2.27 (dd, *J* = 14.4, 6.4 Hz, 1H, H9), 2.11 (ddd, *J* = 19.6, 12.6, 7.1 Hz, 1H, H9'), 0.66 (s, 9H, H8); **^{13}C{^{1}H}-NMR** (126 MHz, DMSO-d_6) 168.44 (C5), 150.80 (C4), 139.82 (C_{Ar}), 136.54 (C_{Ar}), 130.08 (CH_{Ar}), 128.58 (C2), 128.40 (CH_{Ar}), 125.94 (CH_{Ar}), 125.60 (CH_{Ar}), 122.42 (CH_{Ar}), 119.57 (C3), 42.54 (C6), 33.98 (C7), 29.19 (C8), 25.13 (C10), 24.15 (C9).

_N_-((_E_)-4-phenylbut-3-en-2-ylidene)aniline (545)[152]

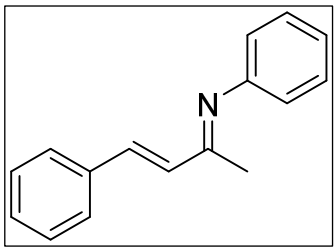

By general method, (*E*)-4-phenylbut-3-en-2-one (2.016 g, 13.79 mmol, 1.0 eq.), aniline (1.282 g, 13.79 mmol, 1.0 eq.) and zinc chloride (20 mg, 0.147 mmol, 0.01 eq.) were dissolved in toluene (10 mL). Purification by recrystallisation from ethanol afforded 80 mg (0.36 mmol, 2.6 %) of **545** as a yellow solid.

$C_{16}H_{15}N$ (M_W = 221.30 g/mol):
E/Z mixture (2:1); **^{1}H-NMR** (400 MHz, $CDCl_3$) δ 7.55 (d, *J* = 7.2 Hz, 2H), 7.39 (t, *J* = 7.3 Hz, 2H), 7.37 – 7.27 (m, 6H), 7.19 (d, *J* = 16.5 Hz, 1H), 7.12 – 7.09 (m, 1H), 7.10 – 7.06 (m, 1H), 7.02 (d, *J* = 16.5 Hz, 1H), 6.84 – 6.80 (m, 1H), 6.80 – 6.76 (m, 2H), 6.71 (d, *J* = 16.3 Hz, 1H), 2.46 (s, 1H), 2.07 (s, 3H); **GC-MS**: (Rtx-5MS, 50.2/30.250/5): t_R = 10.2 min, *m/z* = 220, 206.

(_S_)-1-(naphthalen-1-yl)-_N_-(1-phenylethylidene)ethanamine (346)[90]

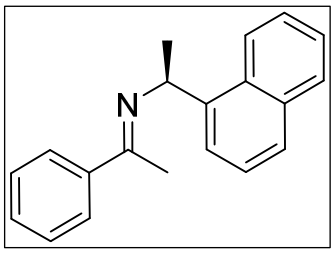

By general method acetophenone (1.03 g, 8.5 mmol, 2.3 eq.) and (*S*)-1-(naphthalen-1-yl)ethanamine (640 mg, 3.74 mmol, 1.0 eq.) were dissolved in dry benzene (10 mL). Purification by Kugelrohr distillation (185 °C at 0.08 torr) afforded 690 mg (2.52 mmol, 75 %) of **346** a as clear oil.

$C_{20}H_{19}N$ (M_W = 273.37 g/mol):
^{1}H-NMR (500 MHz, $CDCl_3$) δ 8.30 (d, *J* = 8.5 Hz, 1H), 7.89 (dd, *J* = 8.0, 5.8 Hz, 3H), 7.80 (d, *J* = 7.2 Hz, 1H), 7.74 (d, *J* = 8.0 Hz, 1H), 7.54 (t, *J* = 7.6 Hz, 1H), 7.47 (dt, *J* = 15.3, 7.8 Hz, 2H), 7.40 (d, *J* = 4.2 Hz, 3H), 5.55 (q, *J* = 6.5 Hz, 1H), 2.26 (s, 3H), 1.73 (d, *J* = 6.6 Hz, 3H); **GC-MS**: (Optima-5-Amine, 100.2/10.270/10): t_R = 20.3 min, *m/z* = 272, 258, 155; **HPLC** (Daicel Chiracel OD-H, *n*-heptane/iso-propanol 99:1, 0.5 mL/min, 25 °C, 208/243 nm): t_R = 11.6 min (*S*); **Optical rotation**: $[a]_D^{20}$ = +54.5 (c = 2.0 in EtOH)

(_R_)-1-(naphthalen-1-yl)-_N_-(1-phenylethylidene)ethanamine (346)[90]

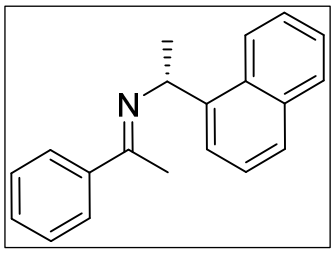

By general method acetophenone (1.05 g, 8.76 mmol, 1.5 eq.) and (*R*)-1-(naphthalen-1-yl)ethanamine (1.0 g, 5.84 mmol, 1.0 eq.) were dissolved in dry benzene (10 mL). Purification by Kugelrohr distillation (185 °C at 0.08 torr) afforded 600 mg (2.2 mmol, 37 %) of **346** a as clear oil.

$C_{20}H_{19}N$ (M_W = 273.37 g/mol):
^{1}H-NMR (500 MHz, $CDCl_3$) δ 8.33 (d, *J* = 8.5 Hz, 1H), 7.91 (dd, *J* = 9.8, 6.2 Hz, 3H), 7.83 (d, *J* = 7.2 Hz, 1H), 7.76 (d, *J* = 8.1 Hz, 1H), 7.56 (t, *J* = 7.6 Hz, 1H), 7.53 – 7.45 (m, 2H), 7.42 (dd, *J* = 7.1, 3.6 Hz, 3H), 5.58 (q, *J* = 6.5 Hz, 1H), 2.28 (s, 3H), 1.75 (d, *J* = 6.6 Hz, 3H); **^{13}C{^{1}H}-NMR** (126 MHz, $CDCl_3$) δ 164.43, 142.49, 141.65, 134.12, 130.80, 129.62, 129.14, 128.36, 127.14, 126.97, 125.96, 125.87, 125.40, 124.14, 123.66, 56.66, 24.82, 16.16; **GC-MS**: (Rtx-1701, 100.2/10.270/10): t_R = 18.6 min, *m/z* = 272, 258, 155; **Optical rotation**: $[a]_D^{20}$ = -284.5 (c 2.2 in $CHCl_3$, 0.75% EtOH).

(*R*)-*N*-benzylidene-1-(naphthalen-1-yl)ethanamine (370)[153]

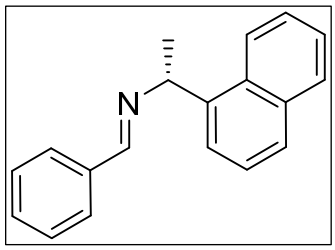

By general method benzaldehyde (277 mg, 2.61 mmol, 1.2 eq.) and (*R*)-1-(naphthalen-1-yl)ethanamine (373 mg, 2.18 mmol, 1.0 eq.) were dissolved in dry benzene (5 mL). Purification by Kugelrohr distillation (165 °C at 0.08 torr) afforded 320 mg (1.23 mmol, 57 %) of **370** as a white solid.

$C_{19}H_{17}N$ (M_W = 259.34 g/mol):
m.p.: 92 °C; **^{1}H-NMR** (500 MHz, $CDCl_3$) δ 8.45 (s, 1H), 8.27 (d, *J* = 8.4 Hz, 1H), 7.91 – 7.86 (m, 1H), 7.86 – 7.80 (m, 3H), 7.78 (d, *J* = 8.2 Hz, 1H), 7.55 (ddd, *J* = 8.4, 6.8, 1.5 Hz, 1H), 7.52 – 7.47 (m, 2H), 7.45 – 7.40 (m, 3H), 5.38 (q, *J* = 6.6 Hz, 1H), 1.76 (d, *J* = 6.7 Hz, 3H); **^{13}C{^{1}H}-NMR** (126 MHz, $CDCl_3$) δ 159.79, 141.30, 136.65, 134.13, 130.80, 130.74, 129.08, 128.69, 128.42, 127.48, 125.95, 125.84, 125.46, 124.17, 123.76, 65.73, 24.68; **GC-MS**: (Optima-5-Amine, 100.2/10.270/10): t_R = 22.0 min, *m/z* = 259, 244, 155; **Optical rotation**: $[a]_D^{20}$ = -218.5 (c 2.2 in $CHCl_3$, 0.75% EtOH).

(*S*)-*N*-benzylidene-1-phenylethanamine (352)[154]

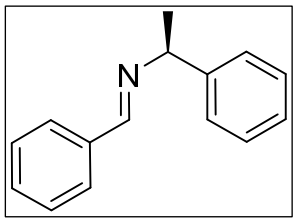

By general method benzaldehyde (478 mg, 4.51 mmol, 1.0 eq.) and (*S*)-1-phenylethanamine (546 mg, 4.51 mmol, 1.0 eq.) were dissolved in dry benzene (15 mL). Purification by Kugelrohr distillation (110 °C at 0.08 torr) afforded 820 mg (3.92 mmol, 87 %) of **352** as a clear oil.

$C_{15}H_{15}N$ (M_W = 209.29 g/mol):
^{1}H-NMR (500 MHz, $CDCl_3$) δ 8.38 (s, 1H), 7.79 (dd, *J* = 6.5, 2.7 Hz, 2H), 7.46 – 7.38 (m, 5H), 7.34 (t, *J* = 7.6 Hz, 2H), 7.28 – 7.21 (m, 1H), 4.55 (q, *J* = 6.6 Hz, 1H), 1.60 (d, *J* = 6.7 Hz, 4H).

(*S*)-1-phenyl-*N*-(1-phenylethylidene)ethanamine (353)[154]

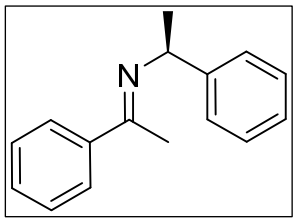

By general method acetophenone (1.96 g, 16.32 mmol, 1.2 eq.) and (*S*)-1-phenylethanamine (1.65 g, 13.6 mmol, 1.0 eq.) were dissolved in dry benzene (20 mL). Purification by Kugelrohr distillation (135 °C at 0.15 mbar) afforded 1.92 g (8.6 mmol, 63 %) of **353** as a clear oil.

$C_{16}H_{17}N$ (M_W = 223.31 g/mol):
b.p.: 135 °C (0.15 mbar); 10:1 *E/Z* mixture, M*ajor*: **^{1}H-NMR** (500 MHz, $CDCl_3$) δ: 7.84 (m, 2H, CH_{Ar}C$_{Ar}$C=N), 7.47 (d, *J* = 7.8 Hz, 2H, CH_{Ar}CH$_{Ar}$C$_{Ar}$C=N), 7.39 (m, 3H, CH_{Ar}C$_{Ar}$CH(CH$_3$) and CH_{Ar}CH$_{Ar}$CH$_{Ar}$C$_{Ar}$C=N), 7.33 (t, *J* = 7.5 Hz, 2H, CH_{Ar}CH$_{Ar}$C$_{Ar}$CH(CH$_3$)), 7.23 (t, *J* = 7.7 Hz, 1H, CH_{Ar}CH$_{Ar}$CH$_{Ar}$C$_{Ar}$CH(CH$_3$)N), 4.84 (q, *J* = 6.5 Hz, 1H, C$_{Ar}$C*H*(CH$_3$)N=C), 2.27 (s, 3H, C=NCH_3), 1.54 (d, *J* = 6.5 Hz, 3H, CH(CH_3)); **^{13}C{^{1}H}-NMR** (126 MHz, $CDCl_3$) δ 163.68 (*C*=N), 146.37 (*C*$_{Ar}$CH(CH$_3$)N), 141.68 (*C*$_{Ar}$C=N), 129.56 (*C*H$_{Ar}$CH$_{Ar}$CH$_{Ar}$C$_{Ar}$C=N), 128.51 (*C*H$_{Ar}$CH$_{Ar}$C$_{Ar}$CH(CH$_3$)N), 128.33 (*C*H$_{Ar}$CH$_{Ar}$C$_{Ar}$C=N), 126.95 (*C*H$_{Ar}$C$_{Ar}$C=N), 126.82 (*C*H$_{Ar}$C$_{Ar}$CH(CH$_3$)N), 126.67 (*C*H$_{Ar}$CH$_{Ar}$CH$_{Ar}$C$_{Ar}$CH(CH$_3$)N), 60.00 (*C*H(CH$_3$)N), 25.25 (CH(*C*H$_3$)N), 15.78 (C=NCH$_3$); **Optical Rotation**: $[a]_D^{20}$ = +92.5 (c 0.75 in $CHCl_3$, 0.75% EtOH) (Lit. +97.7 (c 1.8 in CCl_4)).

(*R*)-1-phenyl-*N*-(1-phenylethylidene)ethanamine (353)[154]

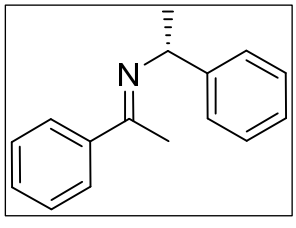

By general method acetophenone (0.98 g, 8.16 mmol, 1.2 eq.) and (*R*)-1-phenylethanamine (0.824 g, 6.8 mmol, 1.0 eq.) were dissolved in dry benzene (10 mL). Purification by Kugelrohr distillation (135 °C at 0.15 mbar) afforded 0.925 g (4.14 mmol, 61 %) of **353** as a clear oil.

$C_{16}H_{17}N$ (M_W = 223.31 g/mol):

^{1}H-NMR (500 MHz, $CDCl_3$) δ: 7.84 (m, 2H, CH_{Ar}C$_{Ar}$C=N), 7.47 (d, *J* = 7.8 Hz, 2H, CH_{Ar}CH$_{Ar}$C$_{Ar}$C=N), 7.39 (m, 3H, CH_{Ar}C$_{Ar}$CH(CH$_3$) and CH_{Ar}CH$_{Ar}$CH$_{Ar}$C$_{Ar}$C=N), 7.33 (t, *J* = 7.5 Hz, 2H, CH_{Ar}CH$_{Ar}$C$_{Ar}$CH(CH$_3$)N), 7.23 (t, *J* = 7.7 Hz, 1H, CH_{Ar}CH$_{Ar}$CH$_{Ar}$C$_{Ar}$CH(CH$_3$)), 4.84 (q, *J* = 6.5 Hz, 1H, C$_{Ar}$C*H*(CH$_3$)N=C), 2.27 (s, 3H, C=NCH_3), 1.54 (d, *J* = 6.5 Hz, 3H, CH(CH_3)); **Optical Rotation**: $[a]_D^{20}$ = -94.0 (c 0.75 in $CHCl_3$, 0.75% EtOH) (Lit. -97.7 (c 1.8 in CCl_4)).

(*R*)-*N*-benzylidene-1-phenylpropan-1-amine (362)

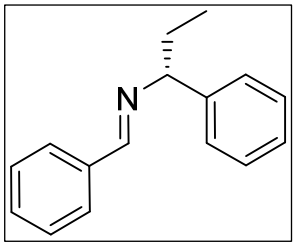

By general method benzaldehyde (1.044 g, 9.84 mmol, 1.0 eq.) and (*R*)-1-phenylpropan-1-amine (1.6 g, 11.8 mmol, 1.2 eq.) were dissolved in dry benzene (10 mL). Purification by Kugelrohr distillation (135 °C at 0.1 mbar) afforded 1.8 g (8.07 mmol, 82 %) of **362** as a clear oil.

$C_{16}H_{17}N$ (M_W = 223.31 g/mol):
^{1}H-NMR (500 MHz, $CDCl_3$) δ 8.35 (s, 1H), 7.83 – 7.76 (m, 2H), 7.45 (dd, *J* = 8.1, 1.0 Hz, 2H), 7.43 – 7.39 (m, 3H), 7.37 – 7.32 (m, 2H), 7.27 – 7.21 (m, 1H), 4.19 (t, *J* = 6.8 Hz, 1H), 1.97 (p, *J* = 7.3 Hz, 2H), 0.90 (t, *J* = 7.4 Hz, 3H); **^{13}C{^{1}H}-NMR** (101 MHz, $CDCl_3$) δ 159.81, 144.65, 136.57, 130.62, 128.64, 128.47, 128.41, 127.19, 126.94, 77.28, 31.81, 11.28; **IR** (NaCl) ν/cm^{-1} = 3082 (m), 3060 (m), 3026 (m), 2964 (s), 2930 (s), 2871 (m), 2845 (m), 1647 (s), 1602 (m), 1580 (s), 1492 (s), 1451 (s), 1380 (m), 1309 (m), 1218 (m), 1169 (w), 1072 (w), 1027 (m), 970 (m); **GC-MS**: (Optima-5-Amine, 100.2/10.270/10): t_R = 21.1 min, *m/z* = 222, 194, 167; **MS** (EI, 70 eV): 223.1 (2.2%, $[M]^+$). 194.1 (100%); **EA**: calc. C, 86.06; H, 7.67; N, 6.27; found: C, 85.93; H, 7.68; N, 6.26.

(*R*)-1-phenyl-*N*-(1-phenylethylidene)propan-1-amine (363)

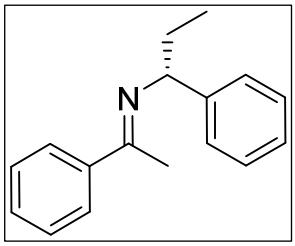

By general method acetophenone (1.03 g, 8.57 mmol, 1.2 eq.) and (*R*)-1-phenylpropan-1-amine (966 mg, 7.14 mmol, 1.0 eq.) were dissolved in dry benzene (10 mL). Purification by Kugelrohr distillation (112 °C at 0.08 torr) afforded 1.1 g (4.64 mmol, 65 %) of **363** as a clear oil.

$C_{17}H_{19}N$ (M_W = 237.34 g/mol):
^{1}H-NMR (500 MHz, $CDCl_3$) δ 7.83 (dd, *J* = 6.6, 3.0 Hz, 2H), 7.42 (d, *J* = 7.4 Hz, 2H), 7.40 – 7.35 (m, 3H), 7.32 (t, *J* = 7.6 Hz, 2H), 7.22 (t, *J* = 7.3 Hz, 1H), 4.54 (t, *J* = 6.7 Hz, 1H), 2.24 (s, 3H), 1.99 – 1.89 (m, 2H), 0.89 (t, *J* = 7.4 Hz, 3H); **^{13}C{^{1}H}-NMR** (126 MHz, $CDCl_3$) δ 164.01, 145.08, 141.81, 129.47, 128.38, 128.30, 127.41, 126.95, 126.69, 66.79, 32.75, 16.12, 11.28; **IR** (neat, ATR) ν/cm^{-1} = 3081 (w), 3058 (w), 3024 (w), 2960 (m), 2929 (m), 2871 (m), 1632 (s), 1601 (m), 1578 (m), 1491 (s), 1447 (s), 1373 (m), 1284 (m), 1264 (m), 1078 (w), 1027 (m), 916 (w), 901 (w), 814 (m); **GC-MS**: (Optima-5-Amine, 80.2/10.270/10): t_R = 17.2 min, *m/z* = 236, 209, 208, 167; **Optical rotation**: $[a]_D^{20}$ = -55.0 (c = 1.0 in $CHCl_3$ with 0.75% EtOH); **EA**: calc.: C, 86.03; H, 8.07; N, 5.90; found: C, 86.03; H, 8.07; N, 5.71.

(*S*)-N-(2,6-dimethylbenzylidene)-1-phenylpropan-1-amine (371)

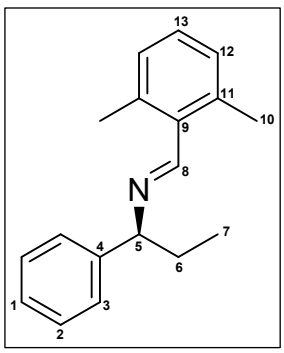

By general method 2,6-dimethylbenzaldehyde (500 mg, 3.73 mmol, 1.0 eq.) and (*S*)-1-phenylpropan-1-amine (504 mg, 3.73 mmol, 1.0 eq.) were dissolved in dry toluene (10 mL). Purification by Kugelrohr distillation (175 °C at 0.08 mbar) afforded 280 mg (1.1 mmol, 30 %) of **371** as a clear oil.

$C_{18}H_{21}N$ (M_W = 251.37 g/mol):
^{1}H-NMR (400 MHz, $CDCl_3$) δ 8.66 (s, 1H, H8), 7.44 (d, *J* = 7.7 Hz, 2H, H3), 7.34 (t, *J* = 7.5 Hz, 2H, H2), 7.24 (m, 1H, H1), 7.13 (t, *J* = 7.5 Hz, 1H, H13), 7.03 (d, *J* = 7.4 Hz, 2H, H12), 4.17 (t, *J* = 6.8 Hz, 1H, H5), 2.39 (s, 6H, H10), 1.96 (p, *J* = 7.2 Hz, 2H, H6), 0.93 (t, *J* = 7.4 Hz, 3H, H7); **^{13}C{^{1}H}-NMR** (101 MHz, $CDCl_3$) δ 160.10 (C8), 144.74 (C4), 137.42 (C11), 134.31 (C9), 128.87 (C13), 128.57 (C12), 128.49 (C2), 127.18 (C3), 126.92 (C1), 78.97 (C5), 32.03 (C6), 20.79 (C10), 11.39 (C7); **IR** (neat, ATR) ν/cm^{-1} = 3063 (w), 3023 (w), 2961 (m), 2920 (m), 2871

(w), 2851 (w), 1644 (s), 1594 (w), 1580 (w), 1491 (m), 1463 (m), 1451 (m), 1375 (m), 807 (m); **GC-MS**: (Rtx-1701, 100.2/10.270/10): t_R = 15.5 min, *m/z* = 251, 222, 132; **Optical rotation**: $[a]_D^{20}$ = +3.2 (c = 1.0 in $CHCl_3$ with 0.75% EtOH).

(*R*)-*N*-(2,6-dimethylbenzylidene)-1-(naphthalen-2-yl)ethanamine (372)

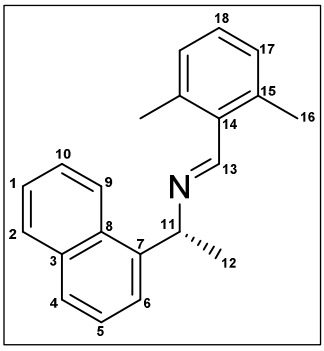

By general method 2,6-dimethylbenzaldehyde (500 mg, 3.73 mmol, 1.28 eq.) and (*R*)-1-(naphthalen-2-yl)ethanamine (500 mg, 2.92 mmol, 1.0 eq.) were dissolved in dry toluene (10 mL). Purification by Kugelrohr distillation (200 °C at 0.15 mbar) afforded 566 mg (1.97 mmol, 67 %) of **372** as a white solid.

$C_{21}H_{21}N$ (M_W = 287.40 g/mol):
m.p.: 53 °C; **^{1}H-NMR** (500 MHz, $CDCl_3$) δ 8.77 (s, 1H, H13), 7.88 (s_{br}, 1H, H10), 7.84 (m, 3H, H5, H1), 7.62 (d, *J* = 8.5 Hz, 1H, H6), 7.45 (m, 2H), 7.14 (t, *J* = 7.5 Hz, 1H, H18), 7.04 (d, *J* = 7.6 Hz, 2H, H17), 4.71 (q, *J* = 6.6 Hz, 1H, H11), 2.41 (s, 6H, H16), 1.70 (d, *J* = 6.6 Hz, 3H, H12); **^{13}C{^{1}H}-NMR** (126 MHz, $CDCl_3$) δ 160.02 (C13), 142.87 (C7), 137.34 (C15), 134.35 (C14), 133.67 (C3), 132.77 (C8), 128.93 (C18), 128.55 (C17), 128.24 (CH_{Ar}), 128.03 (CH_{Ar}), 127.78 (CH_{Ar}), 126.07 (CH_{Ar}), 125.65 (CH_{Ar}), 125.47 (CH_{Ar}), 124.98 (C6), 71.62 (C11), 25.67 (C12), 20.71 (C16); **IR** (neat, ATR) ν/cm^{-1} = 3046 (w), 2973 (w), 2922 (w), 2876 (w), 2861 (w), 1639 (s), 1460 (w), 1374 (m), 1362 (m), 1113 (m), 1073 (w), 960 (m), 928 (w); **EA**: calc.: C, 87.76; H, 7.36; N, 4.87; found: C, 87.81; H, 7.38; N, 5.19; **Optical rotation**: $[a]_D^{20}$ = -4.5 (c = 1.0 in $CHCl_3$ with 0.75% EtOH).

Cyclic Imines

5-methyl-3,4-dihydro-2H-pyrrole (566)

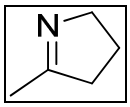

Was purchased and distilled prior to use.

5-cyclohexyl-3,4-dihydro-2H-pyrrole (567)

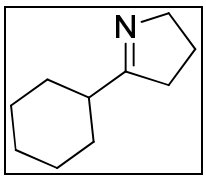

Was obtained from Valentin Köhler, Ward Group, Uni Basel

5-benzyl-3,4-dihydro-2H-pyrrole (568)

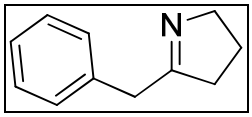

Was obtained from Valentin Köhler, Ward Group, Uni Basel

5-phenyl-3,4-dihydro-2H-pyrrole (569)

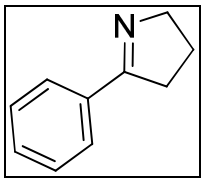

Was obtained from Valentin Köhler, Ward Group, Uni Basel

6-methyl-2,3,4,5-tetrahydropyridine (560)[155]

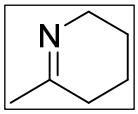

A two-necked 100 mL round-bottom flask was charged with a stirrer, gas inlet and a thermometer and flame-dried with a bunsen burner while evacuating. After cooling to room temperature, the flask was purged with argon three times and 1-(trimethylsilyl)piperidin-2-one (2 g, 11.7 mmol, 1.0 eq.) was added and dissolved in anhydrous Et_2O (15 mL). The reaction mixture was cooled to -20 °C with the aid of an ice/salt bath and methyl lithium (12.8 mmol, 1.6 M, 1.1 eq.) was added dropwise. The reaction mixture was stirred for 30 minutes at -20 °C and then allowed to warm to room temperature to stir for another 4 hours. The reaction mixture was quenched with saturated NH_4Cl (25 mL) and stirred for another hour at room temperature. The organic layer was extracted with CH_2Cl_2 (3x25 mL) and solvents were removed under reduced pressure. Distillation (1 bar, 125 °C) afforded **560** (0.74 g, 7.6 mmol, 65%) as a clear colourless liquid.

$C_6H_{11}N$ (M_W = 97.16 g/mol):
^{1}H-NMR (400 MHz, $CDCl_3$) δ 3.36 (ddd, *J* = 10.3, 6.0, 3.5 Hz, 2H), 1.96 (t, *J* = 6.6 Hz, 2H), 1.75 (s, 3H), 1.55 – 1.47 (m, 2H), 1.43 – 1.35 (m, 2H); **GC** (Machary-Nagel Optima-5-Amin (0.50 µm x 0.25 µm x 30 m), 60 kPa H_2, 60 °C/3 min, 10°C/min to 250 °C/10 min): t_R = 9.4 min; **GC-MS** (Rtx-5MS, 50.2/30.250/5): t_R = 3.7 min, *m/z* = 97 ($[M]^+$), 69.

6-butyl-2,3,4,5-tetrahydropyridine (565)[156]

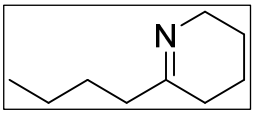

tert-Butyl (5-oxononyl)carbamate (0.86 g, 3.34 mmol, 1.0 eq.) was dissolved in trifluoroacetic acid (2 mL) and stirred for two hours. The reaction mixture was quenched with NaOH (10% wt.) until a pH of 13-14 was observed. Extraction with CH_2Cl_2 (3x10 mL) was followed by drying over $MgSO_4$, filtering and removal of solvents under reduced pressure afforded **565** as a yellow oil.

$C_9H_{17}N$ (M_W = 139.24 g/mol):
^{1}H-NMR (400 MHz, $CDCl_3$) δ 3.55 (t, *J* = 5.8 Hz, 2H), 2.18 – 2.09 (m, 4H), 1.71 – 1.62 (m, 2H), 1.59 – 1.46 (m, 4H), 1.33 (h, *J* = 7.4 Hz, 2H), 0.91 (t, *J* = 7.3 Hz, 3H); **GC** (Machary-Nagel Optima-5-Amin (0.50 µm x 0.25 µm x 30 m), 60 kPa H_2, 100 °C/2 min, 10°C/min, 250 °C/10 min): t_R = 10.2 min; **GC-MS** (Rtx-5MS, 100.2/10.270/10): t_R = 5.3 min, *m/z* = 138 ($[M-1]^+$), 124, 110, 97, 82.

6-phenyl-2,3,4,5-tetrahydropyridine (563)[157]

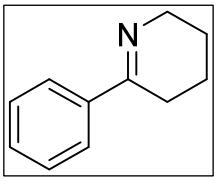

tert-Butyl (5-oxo-5-phenylpentyl)carbamate (0.5 g, 1.8 mmol, 1.0 eq.) was dissolved in trifluoroacetic acid (2 mL) and stirred for two hours at room temperature. The reaction mixture was quenched with NaOH (10% wt.) until a pH of 13-14 and organic components were extracted with CH_2Cl_2 (3x10 mL). After drying over $MgSO_4$, filtration and removal of volatile components under reduced pressure afforded **563** as a yellow oil.

$C_{11}H_{13}N$ (M_W = 159.23 g/mol):
^{1}H-NMR (400 MHz, $CDCl_3$) δ 7.76 (dd, *J* = 6.5, 3.1 Hz, 2H), 7.40 – 7.34 (m, 3H), 3.83 (t, *J* = 5.8 Hz, 2H), 2.63 (t, *J* = 6.6 Hz, 2H), 1.84 (p, *J* = 6.4 Hz, 2H), 1.73 – 1.62 (m, 2H); **GC-MS** (Rtx-5MS, 100.2/10.270/10): t_R = 11.9 min, *m/z* = 159 ($[M]^+$), 144, 130, 103, 91.

Metal Complexes

(η^4-1,5-cyclooctadiene)-{2-(2-(diphenylphosphino)phenyl)-4,4-dimethyl-4,5-dihydrooxazole}-iridium(I)-tetrakis(3,5-bis(trifluoromethyl)phenyl)borate (348)[98]

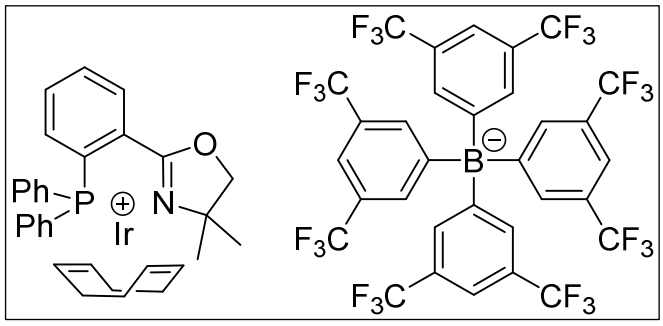

General method:
In an oven-dried and argon-purged 25 mL round-bottomed two-necked flask was placed 2-(2-(diphenyl-phosphanyl)phenyl)-4,4-dimethyl-4,5-dihydrooxazole (100 mg, 0.278 mmol, 2.0 eq.) and $[Ir(COD)Cl]_2$ (93.6 mg, 0.139 mmol, 1.0 eq.) and dissolved in anhydrous CH_2Cl_2 (5 mL). The reaction mixture was heated to reflux for one hour. After cooling to room temperature, $NaBAr_F$ (321 mg, 0.362 mmol, 2.6 eq.) was added and the resultant suspension stirred vigorously. After 5 minutes, water (5 mL) was added and vigorous stirring continued. The organic components were extracted with CH_2Cl_2 (3x20 mL), washed with water (10 mL), dried over $MgSO_4$, filtered and solvent removed under reduced pressure. The residue was purified by elution chromatography (SiO_2, CH_2Cl_2) to afford **348** (294 mg, 0.193 mmol, 69%) as a red solid. Recrystallisation from CH_2Cl_2 to *n*-pentane afforded air-stable needles.

$C_{63}H_{46}BF_{24}IrNOP$ (M_W = 1523.03 g/mol):
^{1}H-NMR (500 MHz, CD_2Cl_2) δ 7.87 – 7.82 (m, 1H), 7.66 – 7.62 (m, 8H), 7.60 (dt, *J* = 7.7, 1.3 Hz, 1H), 7.56 (tt, *J* = 7.6, 1.4 Hz, 1H), 7.53 – 7.49 (m, 2H), 7.47 (dt, *J* = 2.3, 1.3 Hz, 4H), 7.46 – 7.42 (m, 4H), 7.41 – 7.37 (m, 1H), 7.26 (m, 4H), 5.40 – 5.33 (m, 2H), 3.86 (s, 2H), 3.23 – 3.15 (m, 2H), 2.24 – 2.08 (m, 4H), 1.96 (s, 2H), 1.76 (d, *J* = 9.8 Hz, 2H), 1.28 (s, 6H); **^{31}P{^{1}H}-NMR** (202 MHz, CD_2Cl_2) δ 20.98.

(η^4-1,5-cyclooctadiene)-{2-(2-(diphenylphosphino)phenyl)-4,5-dihydrooxazole}-iridium(I)-tetrakis(3,5-bis(trifluoromethyl)phenyl)borate (336)[98]

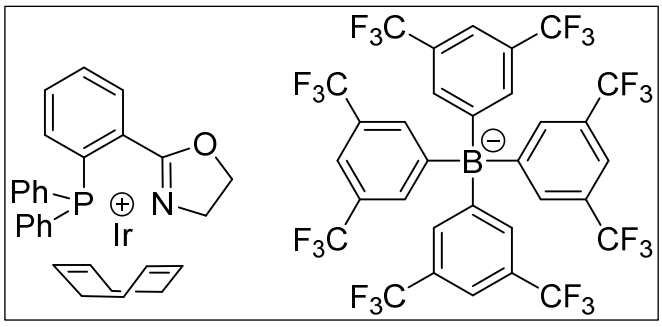

By general method, 2-(2-(diphenylphosphanyl)phenyl)-4,5-dihydrooxazole (400 mg, 1.207 mmol, 2.0 eq.), $[Ir(COD)Cl]_2$ (405.4 mg, 0.604 mmol, 1.0 eq.) and $NaBAr_F$ (1.39 g, 1.57 mmol, 2.6 eq.) afforded **336** (1.543 g, 1.027 mmol, 85%) as a red amorphous solid. Recrystallisation from CH_2Cl_2 to *n*-pentane afforded air-stable crystals which are required to be stored in the fridge under an atmosphere of argon.

$C_{61}H_{42}BF_{24}IrNOP$ (M_W = 1494.98 g/mol):
^{1}H-NMR (500 MHz, CD_2Cl_2) δ 8.05 (ddd, *J* = 7.4, 4.0, 1.6 Hz, 1H), 7.64 (dt, *J* = 4.7, 2.3 Hz, 8H), 7.58 (dtd, *J* = 9.0, 7.6, 6.1 Hz, 2H), 7.50 (dd, *J* = 7.2, 1.8 Hz, 1H), 7.49 – 7.46 (m, 5H), 7.43 (tt, *J* = 7.3, 2.8 Hz, 5H), 7.41 – 7.34 (m, 4H), 5.07 (ddd, *J* = 7.8, 4.9, 2.4 Hz, 2H), 4.51 (t, *J* = 9.9 Hz, 2H), 4.09 (t, *J* = 10.0 Hz, 2H), 3.10 (q, *J* = 3.4 Hz, 2H), 2.31 – 2.14 (m, 4H), 2.07 – 1.98 (m, 2H), 1.88 (dt, *J* = 13.6, 5.9 Hz, 2H); **^{31}P{^{1}H}-NMR** (202 MHz, CD_2Cl_2) δ 15.96.

(η^4-1,5-cyclooctadiene)-{(*S*)-2-(2-(diphenylphosphino)phenyl)-4-isopropyl-4,5-dihydrooxazole}-iridium(I)-tetrakis(3,5-bis(trifluoromethyl)phenyl)borate (86)[158]

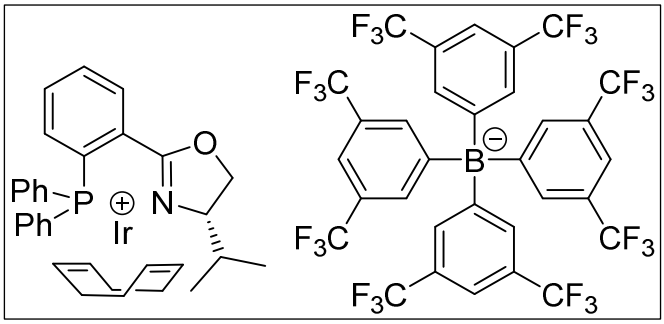

By general method, (*S*)-2-(2-(diphenylphosphanyl)phenyl)-4-isopropyl-4,5-dihydrooxazole (200 mg, 0.536 mmol, 2.0 eq.), $[Ir(COD)Cl]_2$ (180 mg, 0.27 mmol, 1.0 eq.) and $NaBAr_F$ (621 mg, 0.7 mmol, 2.6 eq.) afforded **86** (655 mg, 0.426 mmol, 80%) as a red amorphous solid. Recrystallisation from CH_2Cl_2 to *n*-pentane afforded air-stable crystals.

$C_{64}H_{48}BF_{24}IrNOP$ (M_W = 1537.06 g/mol):
^{1}H-NMR (500 MHz, CD_2Cl_2) δ 8.14 – 8.08 (m, 1H), 7.67 – 7.60 (m, 9H), 7.57 (ddt, *J* = 7.6, 6.3, 1.3 Hz, 3H), 7.54 – 7.49 (m, 1H), 7.47 (q, *J* = 1.4 Hz, 4H), 7.45 (dddd, *J* = 7.8, 6.6, 1.8, 1.0 Hz, 3H), 7.41 – 7.37 (m, 2H), 7.37 – 7.33 (m, 1H), 7.09 – 6.98 (m, 2H), 5.03 – 4.94 (m, 1H), 4.94 – 4.83 (m, 1H), 4.41 (dd, *J* = 9.6, 3.6 Hz, 1H), 4.32 (t, *J* = 9.5 Hz, 1H), 4.09 (ddd, *J* = 9.4, 3.6, 2.4 Hz, 1H), 3.30 – 3.21 (m, 1H), 3.05 – 2.93 (m, 1H), 2.60 – 2.48 (m, 1H), 2.48 – 2.35 (m, 3H), 2.05 (dt, *J* = 12.9, 8.9 Hz, 1H), 2.00 – 1.88 (m, 2H), 1.62 (tt, *J* = 13.8, 7.6 Hz, 1H), 1.50 – 1.35 (m, 2H), 0.80 (d, *J* = 7.1 Hz, 3H), -0.15 (d, *J* = 6.7 Hz, 3H); **^{31}P{^{1}H}-NMR** (202 MHz, CD_2Cl_2) δ 15.90.

(η^4-1,5-cyclooctadiene-{(*S*)-2-(2-((dicyclohexylphosphino)oxy)propan-2-yl)-4-isopropyl-4,5-dihydrooxazole}-iridium(I)-tetrakis(3,5-bis(trifluoromethyl)phenyl)borate (87)[159]

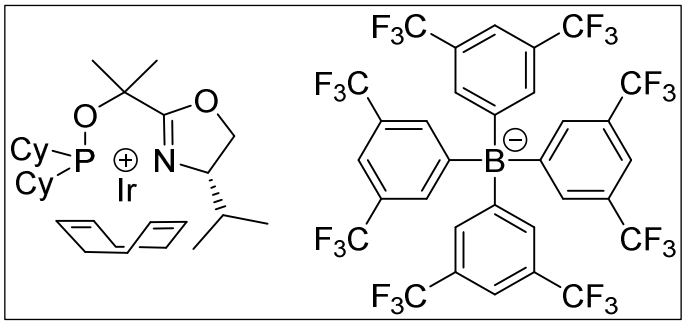

An oven-dried and argon-purged 25 mL Schlenk tube was charged with a magnetic stir bar and brought to the glove box. Dicyclohexyl phosphine (149.6 mg, 0.643 mmol, 1.1 eq.) and NaH (21 mg, 0.876 mmol, 1.5 eq.) and dissolved in anhydrous THF (0.9 mL) and DMF (0.1 mL). Outside the glove box (*S*)-2-(4-isopropyl-4,5-dihydrooxazol-2-yl)propan-2-ol (100 mg, 0.584 mmol, 1.0 eq.) and the reaction mixture stirred overnight at room temperature. The solvents removed *in vacuo* and the reaction mixture suspended in anhydrous toluene. Inside the glove box, the suspension was filtered through a CHROMAFIL HPLC filter and rinsed with anhydrous toluene (2x2 mL). The solvent was removed *in vacuo* and redissolved in anhydrous CH_2Cl_2 (3 mL). In another 25 mL Schlenk tube was placed $[Ir(COD)Cl]_2$ (130 mg, 0.193 mmol, 1.0 eq.) and dissolved in CH_2Cl_2 (1 mL). The ligand mixture was added dropwise and the resultant mixture stirred for one hour before $NaBAr_F$ (444.7 mg, 0.502 mmol, 1.3 eq.) was added and stirring continued for another 60 minutes. Silica gel (3g) was added and solvents removed under reduced pressure. The residue was purified by elution chromatography (SiO_2, 15x2.5 cm, 1st TBME (200 mL), then CH_2Cl_2 (200 mL)) to afford **87** as a dark red oil after removal of solvents. Recrystallisation from CH_2Cl_2 to *n*-pentane afforded air-stable orange crystals (495 mg, 0.323 mmol, 83%).

$C_{61}H_{62}BF_{24}IrNO_2P_2$ (M_W = 1562.11 g/mol):
^{1}H-NMR (400 MHz, CD_2Cl_2) δ 7.64 (dt, *J* = 5.0, 2.2 Hz, 8H), 7.48 (s, 4H), 4.95 (dp, *J* = 8.7, 3.9 Hz, 1H), 4.60 (tt, *J* = 7.6, 3.8 Hz, 1H), 4.53 (dd, *J* = 9.7, 3.9 Hz, 1H), 4.29 (t, *J* = 9.7 Hz, 1H), 3.87 (ddt, *J* = 12.8, 8.8, 3.8 Hz, 2H), 3.42 (tdd, *J* = 8.0, 4.9, 2.6 Hz, 1H), 2.41 – 2.29 (m, 2H), 2.24 (td, *J* = 8.8, 8.3, 5.3 Hz, 2H), 2.08 (dddd, *J* = 20.8, 12.2, 8.7, 3.6 Hz, 2H), 2.01 – 1.92 (m, 1H), 1.87 (ddq, *J* = 10.2, 6.8, 3.4 Hz, 3H), 1.82 – 1.70 (m, 9H), 1.64 (ddt, *J* = 14.2, 8.9, 4.1 Hz, 5H), 1.52 (d, *J* = 1.5 Hz, 3H), 1.39 – 1.09 (m, 10H), 0.96 (d, *J* = 7.0 Hz, 3H), 0.76 (d, *J* = 6.7 Hz, 3H); **^{31}P{^{1}H}-NMR** (162 MHz, CD_2Cl_2) δ 121.27.

(η^4-1,5-cyclooctadiene)-{2-(2-(diphenylphosphino)phenyl)-4,5-dihydrooxazole}-iridium(I)-hexafluorophosphate (357)

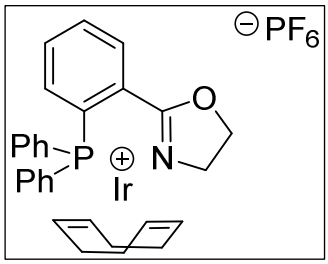

By general method, 2-(2-(diphenylphosphanyl)phenyl)-4,5-dihydrooxazole (200 mg, 0.6 mmol, 2.0 eq.), $[Ir(COD)Cl]_2$ (203 mg, 0.3 mmol, 1.0 eq.) were dissolved in CH_2Cl_2 (5 mL). After cooling to room temperature the reaction mixture was washed with NH_4PF_6 solution (0.4 M, 2x5 mL, 8 mmol). Subsequently the reaction mixture was washed with water (5 mL), dried over Na_2SO_4, filtered and solvents removed under reduced pressure. Crystallisation from CH_2Cl_2 to Et_2O afforded **357** (342 mg, 0.44 mmol, 73%) as dark red crystals.

$C_{29}H_{30}F_6IrNOP_2$ (M_W = 776.72 g/mol):
^{1}H-NMR (500 MHz, CD_2Cl_2) δ 8.08 (dd, *J* = 7.9, 4.0 Hz, 1H), 7.61 (t, *J* = 7.6 Hz, 1H), 7.56 (t, *J* = 7.6 Hz, 1H), 7.50 (dd, *J* = 8.2, 6.2 Hz, 2H), 7.42 (ddt, *J* = 18.9, 11.7, 5.2 Hz, 9H), 5.18 (dt, *J* = 4.8, 2.6 Hz, 2H), 4.56 (t, *J* = 9.9 Hz, 2H), 4.16 (t, *J* = 10.0 Hz, 2H), 3.09 – 3.01 (m, 2H), 2.33 – 2.24 (m, 2H), 2.20 (ddd, *J* = 15.7, 11.3, 5.6 Hz, 2H), 2.08 – 1.98 (m, 2H), 1.88 (dd, *J* = 14.2, 6.8 Hz, 2H); **^{13}C{^{1}H}-NMR** (126 MHz, CD_2Cl_2) δ 165.87, 165.81, 134.88, 134.79, 134.03, 133.98, 133.57, 133.51, 133.49, 132.53, 132.51, 132.42, 132.40, 130.02, 129.65, 129.62, 129.60, 129.53, 129.49, 127.15, 126.70, 96.18, 96.09, 69.46, 63.99, 55.28, 32.49, 32.46, 30.19, 30.18; **^{31}P{^{1}H}-NMR** (202 MHz, CD_2Cl_2) δ 16.00 , -145.68 (sept, $^1J_{P,F}$ = 714 Hz).

(η^4-1,5-cyclooctadiene)-{2-(2-(diphenylphosphino)phenyl)-4,5-dihydrooxazole}-iridium(I)-chloride (358)

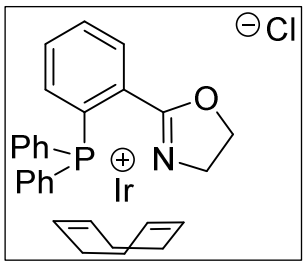

By general method, 2-(2-(diphenylphosphanyl)phenyl)-4,5-dihydrooxazole (200 mg, 0.6 mmol, 2.0 eq.), $[Ir(COD)Cl]_2$ (203 mg, 0.3 mmol, 1.0 eq.) were dissolved in CH_2Cl_2 (5 mL). **358** was isolated as a brown amorphous solid (366 mg, 0.549 mmol, 91%).

$C_{29}H_{30}ClIrNOP$ (M_W = 667.21 g/mol):
^{31}P{^{1}H}-NMR (202 MHz, CD_2Cl2) δ 9.45.

[{2-(2-(diphenylphosphino)phenyl)-4,5-dihydrooxazole}-iridium(III)-((*S*)-N-benzylidene-1-phenylethanamine)(hydrido)(chloride)] (356)

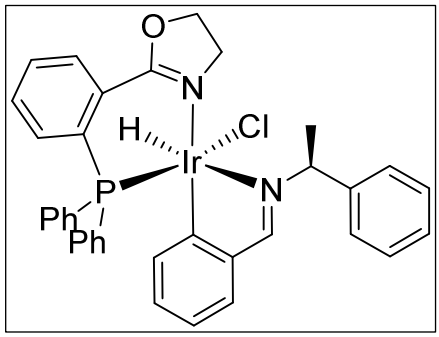

General method:
To an over-dried argon-purged 8 mL vial equipped with a magnetic stirrer and a septum was added **336** (75 mg, 0.1124 mmol, 1.0 eq.) and **352** (47 mg, 0.2248 mmol, 2.0 eq.). The vial was evacuated and purged with hydrogen. Anhydrous THF (2 mL) was added and the reaction mixture stirred at room temperature for two hours. Solvents were evaporated by a stream of nitrogen and the crude was suspended in EtOAc and subjected to elution chromatography (SiO_2, EtOAc) to afford an oil. Trituration with *n*-pentane gave a yellow amorphous solid which was dried *in vacuo* affording **356** (3 mg, 3.8 μmol, 3.4%).

$C_{36}H_{33}ClIrN_2OP$ (M_W = 768.31 g/mol):
^{1}H-NMR (500 MHz, CH_2Cl_2) δ -18.70 (dd, *J* = 21.4, 2.6 Hz, 1H).

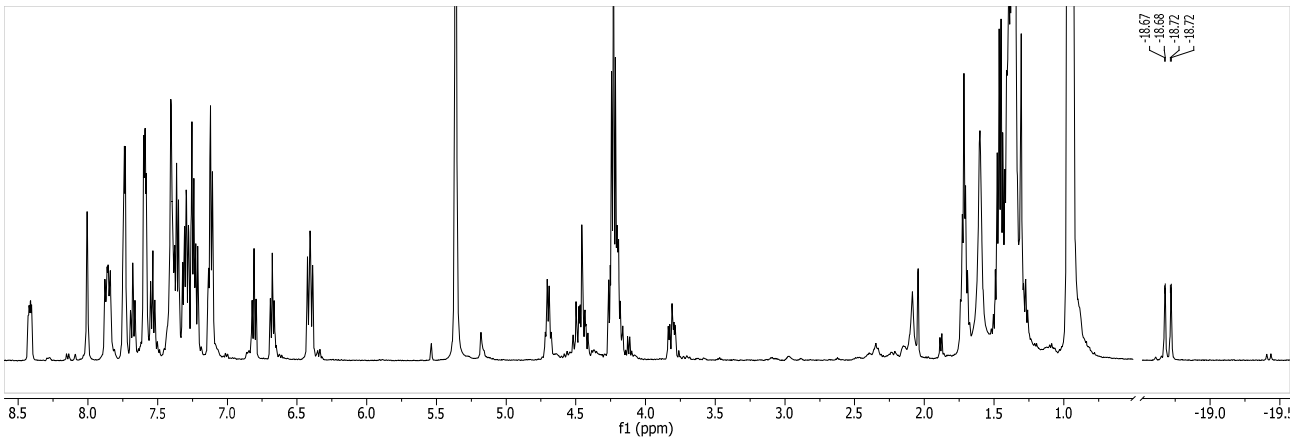

[{2-(2-(diphenylphosphino)phenyl)-4,5-dihydrooxazole}-iridium(III)-((*S*)-1-phenyl-*N*-(1-phenylethylidene)ethanamine)(hydrido)(chloride)] (359)

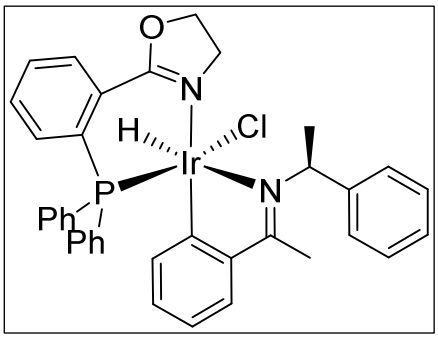

By general method, **336** (75 mg, 0.05 mmol, 1.0 eq.) and **353** (22.3 mg, 0.1 mmol, 2.0 eq.) were reacted to afford **359** (33 mg, 0.042 mmol, 83%) as a yellow solid.

$C_{37}H_{35}ClIrN_2OP$ (M_W = 782.34 g/mol):
^{1}H-NMR (500 MHz, CD_2Cl_2) δ -18.25 (d, *J* = 22.7 Hz, 1H), -19.47 (d, *J* = 21.7 Hz, 1H); **^{31}P{^{1}H}-NMR** (202 MHz, CD_2Cl_2) δ 5.25 (d, *J* = 20.2 Hz), 3.50 (d, *J* = 19.8 Hz); **MS** (EI, 70 eV): 745.2 (49.6%); **MS** (MALDI): 780.2253 ([M-H]$^+$). 746.2364 ([M-Cl]$^+$);
MS (ESI): *m/z* (%) = 747.13 (100, [M-Cl]$^+$).

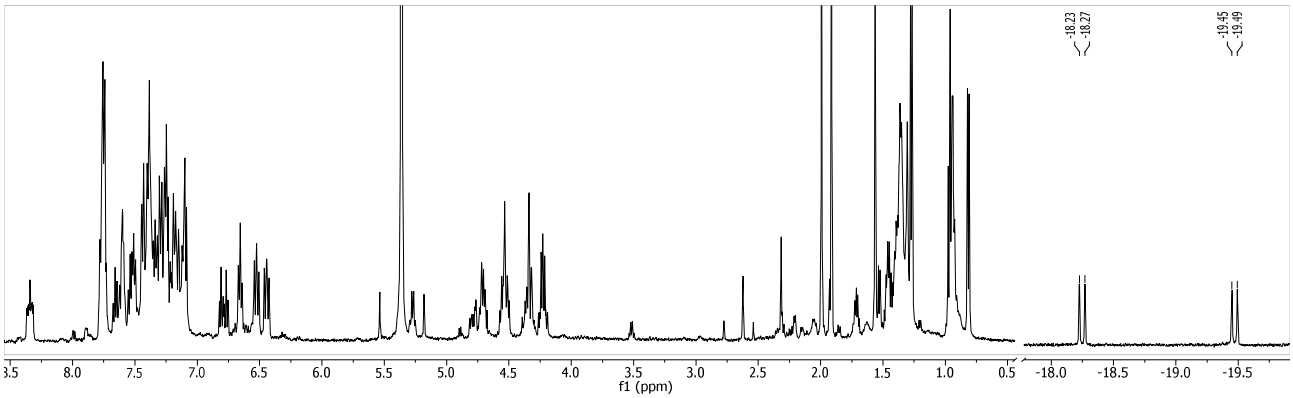

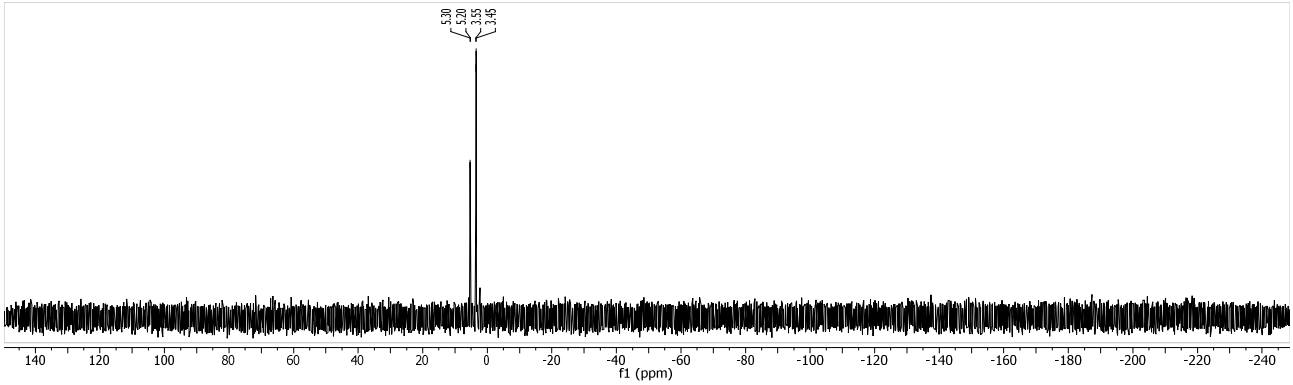

[[{2-(2-(diphenylphosphino)phenyl)-4,5-dihydrooxazole}-iridium(III)-((*S*)-1-phenyl-*N*-(1-phenylethylidene)ethanamine)(H)(CH_2Cl_2)]-tetrakis(3,5-bis(trifluoromethyl)phenyl)borate (360)

In the glove box, **359** (5 mg, 6.3 μmol, 1.0 eq.) and $NaBAr_F$ (6 mg, 6.8 μmol, 1.08 eq.) were added to a young's NMR tube and dissolved in CD_2Cl_2 (0.4 mL) at room temperature.The mixture was shaken until it turned homogenous and NMR spectra of **360** were recorded.

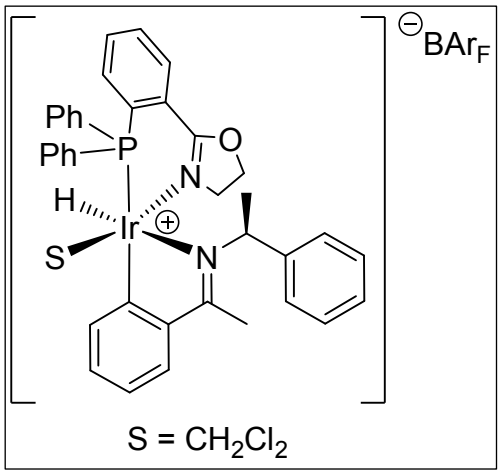

$C_{70}H_{49}BCl_2F_{24}IrN_2OP$ (1694.23 g/mol):
^{1}H-NMR (500 MHz, CD_2Cl_2) δ 8.23 – 8.17 (m, 1H), 7.87 (dd, *J* = 12.1, 7.7 Hz, 2H), 7.77 (dt, *J* = 5.1, 2.3 Hz, 13H), 7.75 – 7.69 (m, 2H), 7.67 (dd, *J* = 8.4, 6.4 Hz, 1H), 7.61 (s, 6H), 7.56 (ddt, *J* = 10.5, 7.8, 3.8 Hz, 4H), 7.43 (d, *J* = 7.8 Hz, 1H), 7.35 – 7.27 (m, 2H), 7.04 (t, *J* = 7.6 Hz, 1H), 6.96 (t, *J* = 7.5 Hz, 1H), 6.62 (t, *J* = 7.6 Hz, 1H), 6.42 (d, *J* = 8.1 Hz, 1H), 5.35 – 5.29 (m, 1H), 4.14 – 4.03 (m, 1H), 3.97 (dt, *J* = 10.8, 8.6 Hz, 1H), 3.01 (ddd, *J* = 13.6, 11.0, 8.6 Hz, 1H), 2.77 (s, 3H), 1.76 (d, *J* = 6.6 Hz, 3H), 1.47 (dt, *J* = 13.6, 10.3 Hz, 1H), -16.85 (d, *J* = 14.6 Hz, 1H); **^{31}P{^{1}H}-NMR** (202 MHz, CD_2Cl_2) δ 10.28 (d, *J* = 5.7 Hz).

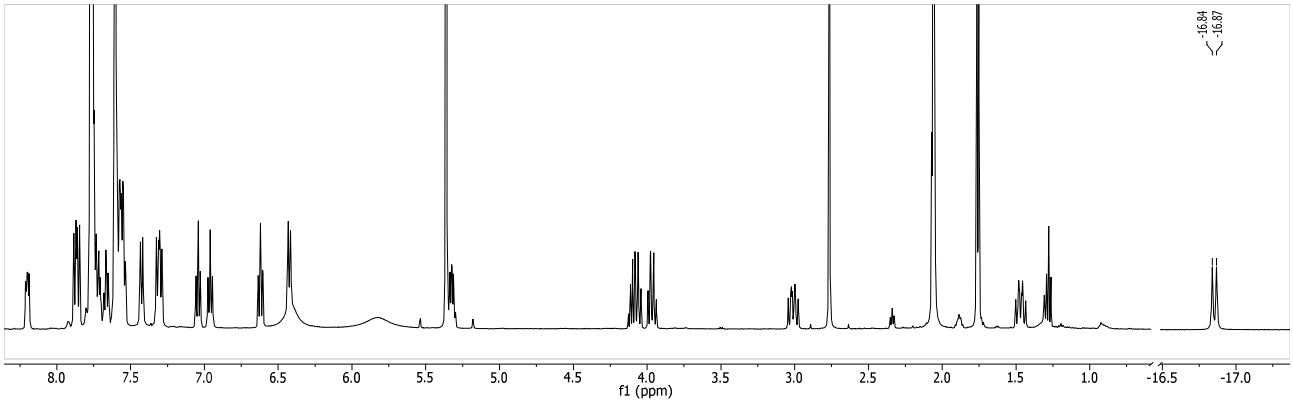

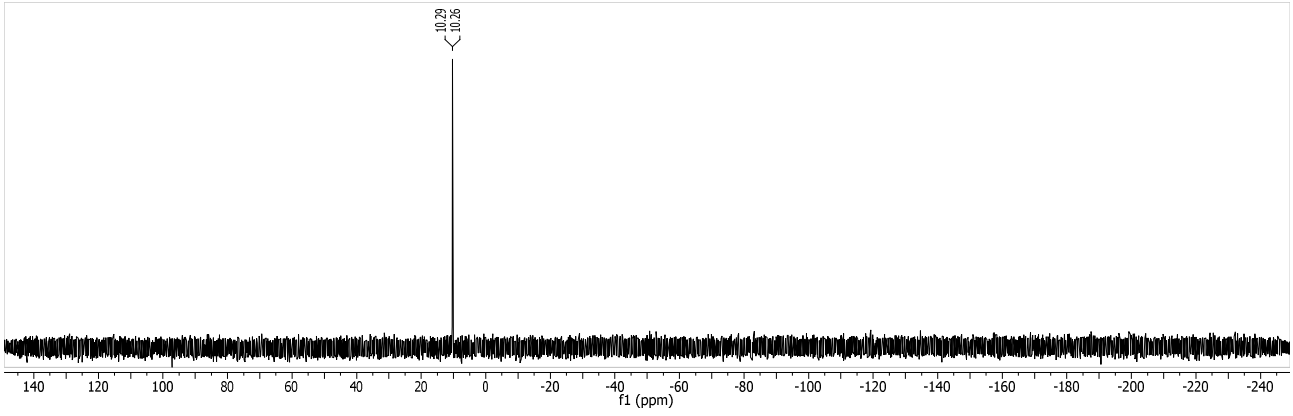

[{2-(2-(diphenylphosphino)phenyl)-4,5-dihydrooxazole}-iridium(III)-((*R*)-*N*-benzylidene-1-phenylpropan-1-amine)(hydrido)(chloride)] (364)

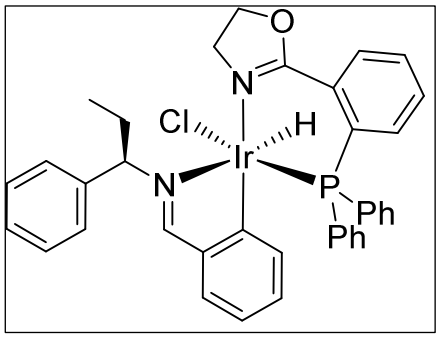

By general method, **336** (75 mg, 0.05 mmol, 1.0 eq.) and **362** (33.47 mg, 0.15 mmol, 3.0 eq.) were reacted to afford **364** (3.5 mg, 4.5 μmol, 9%) as a yellow solid.

$C_{37}H_{35}ClIrN_2OP$ (MW = 782.34 g/mol):
^{1}H-NMR (600 MHz, CD_2Cl_2) δ 8.39 (ddd, *J* = 8.2, 4.0, 1.3 Hz, 1H), 7.95 (t, *J* = 2.0 Hz, 1H), 7.79 (ddt, *J* = 12.0, 6.0, 1.8 Hz, 2H), 7.66 – 7.62 (m, 1H), 7.51 – 7.48 (m, 1H), 7.44 – 7.18 (m), 7.16 (dd, *J* = 7.4, 1.5 Hz, 1H), 7.12 – 7.10 (m, 2H), 7.07 (td, *J* = 7.7, 2.4 Hz, 2H), 7.05 (d, *J* = 7.5 Hz, 1H), 6.74 (td, *J* = 7.4, 1.2 Hz, 1H), 6.60 (td, *J* = 7.4, 1.5 Hz, 1H), 6.39 – 6.33 (m, 2H), 4.29 (ddd, *J* = 9.6, 6.3, 3.4 Hz, 1H), 3.95 – 3.89 (m, 1H), 3.61 (d, *J* = 13.2 Hz, 1H), 3.54 – 3.50 (m, 1H), 1.77 – 1.69 (m, 1H), 1.62 (dp, *J* = 13.5, 7.5 Hz, 1H), 0.80 (t, *J* = 7.4 Hz, 3H), 0.52 (t, *J* = 7.3 Hz, 3H), -18.87 (dd, *J* = 21.4, 2.6 Hz, 1H); **MS** (ESI): *m/z* (%) = 747.03 (72.84, $[M\text{-}Cl]^+$), 745.01 (100, $[M\text{-}H\text{-}Cl]^+$).

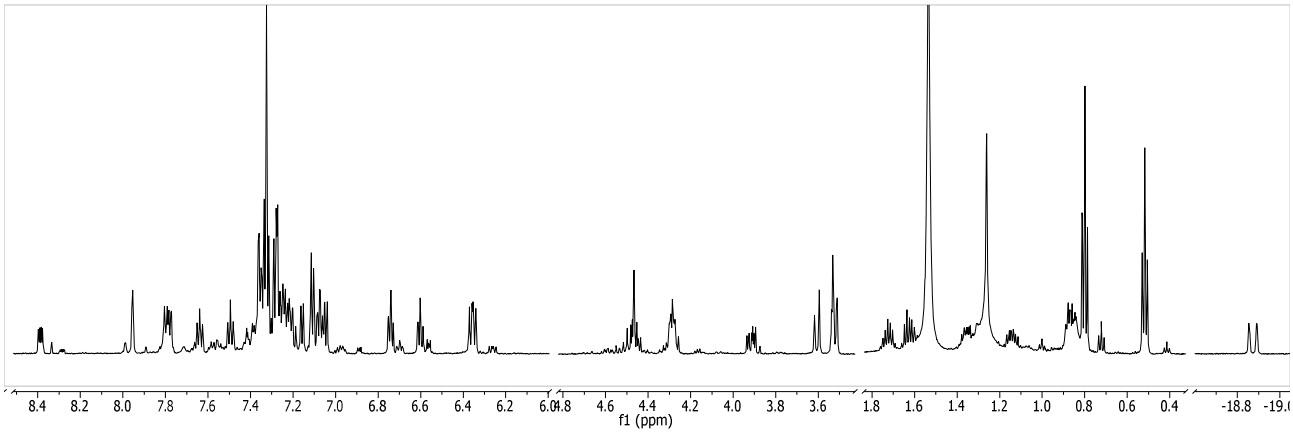

[{2-(2-(diphenylphosphino)phenyl)-4,5-dihydrooxazole}-iridium(III)-((*R*)-1-phenyl-*N*-(1-phenylethylidene)propan-1-amine)(hydrido)(chloride)] (365)

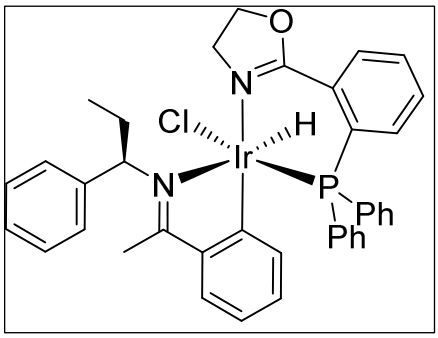

By general method, **336** (50 mg, 0.033 mmol, 1.0 eq.) and **363** (23.7 mg, 0.1 mmol, 3.0 eq.) were reacted to afford **365** (22 mg, 0.028 mmol, 83%) as a yellow solid.

$C_{38}H_{37}ClIrN_2OP$ (M_W = 796.37 g/mol):
^{1}H-NMR (500 MHz, CD_2Cl_2) δ 8.24 (dd, *J* = 8.0, 4.1 Hz, 1H), 7.82 – 7.69 (m, 3H), 7.57 – 6.98 (m), 6.65 (t, *J* = 7.4 Hz, 1H), 6.53 (t, *J* = 7.3 Hz, 1H), 6.36 (dd, *J* = 10.6, 7.7 Hz, 2H), 4.82 (dt, *J* = 15.4, 10.7 Hz, 1H), 4.63 (ddd, *J* = 15.9, 10.6, 7.5 Hz, 1H), 4.56 – 4.44 (m, 1H), 4.31 (q, *J* = 10.0 Hz, 1H), 3.78 (d, *J* = 11.1 Hz, 1H), 1.73 (s, 3H), 0.84 – 0.76 (m, 2H), 0.48 (t, *J* = 7.3 Hz, 3H), -19.86 (d, *J* = 20.9 Hz, 1H); **^{31}P{^{1}H}-NMR** (202 MHz, CD_2Cl2) δ 6.67 (s); **MS** (ESI): *m/z* (%) = 761.34 (80.56, $[M\text{-}Cl]^+$), 759.32 (100, $[M\text{-}H\text{-}Cl]^+$).

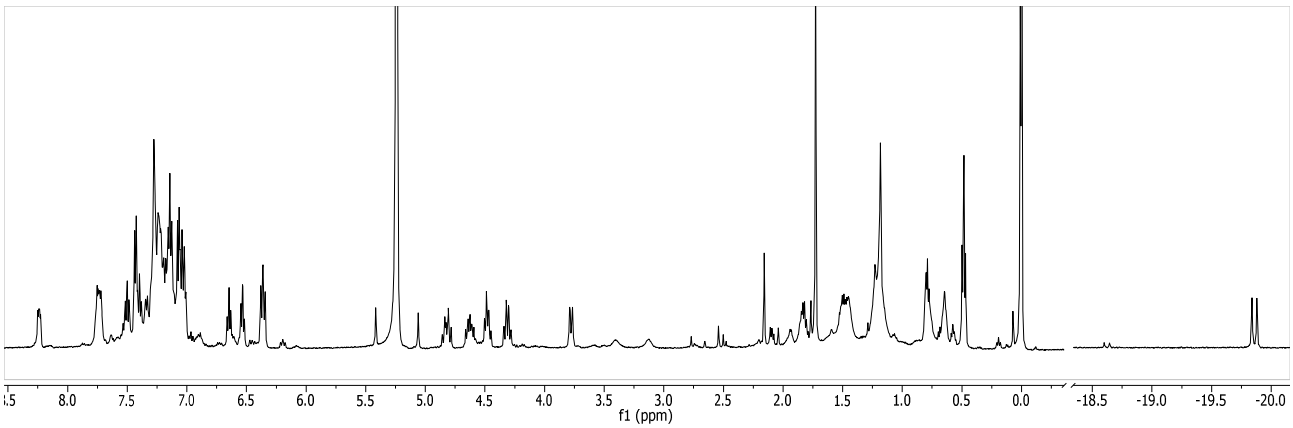

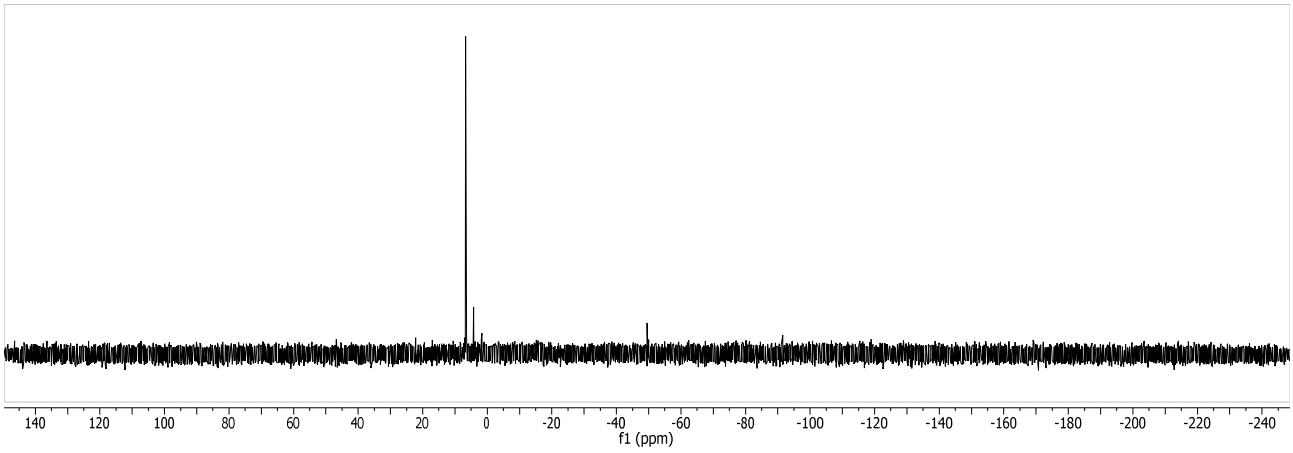

[{2-(2-(diphenylphosphino)phenyl)-4,5-dihydrooxazole}-iridium(III)-((*R*)-*N*-benzylidene-1-(naphthalen-1-yl)ethanamine)(hydrido)(chloride)] (376)

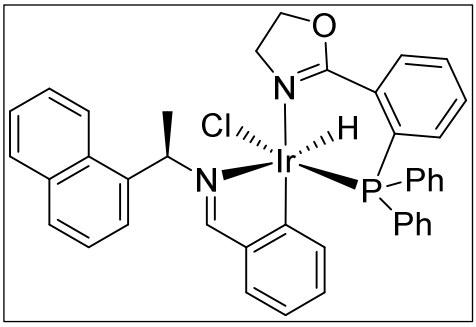

By general method, **336** (25 mg, 0.0167 mmol, 1.0 eq.) and **372** (10.8 mg, 0.042 mmol, 3.0 eq.) were reacted to afford **376** as a yellow solid. No yield was determined.

$C_{40}H_{35}ClIrN_2OP$ (M_W = 818.37 g/mol):
^{1}H-NMR (400 MHz, CD_2Cl_2) δ 8.24 (dd, *J* = 7.9, 4.2 Hz, 1H), 8.04 (t, *J* = 2.0 Hz, 1H), 7.95 – 7.06 (m, 20H), 6.81 (t, *J* = 7.5 Hz, 1H), 6.68 (td, *J* = 7.4, 1.5 Hz, 1H), 6.43 (dd, *J* = 10.6, 7.8 Hz, 2H), 5.47 (q, *J* = 6.9 Hz, 1H), 4.19 (dt, *J* = 15.2, 10.9 Hz, 1H), 3.98 (dt, *J* = 11.2, 7.4 Hz, 1H), 3.06 (ddd, *J* = 15.1, 10.8, 6.9 Hz, 1H), 2.76 (td, *J* = 10.7, 8.0 Hz, 1H), 1.06 (d, *J* = 6.8 Hz, 3H), -18.70 (dd, *J* = 21.0, 2.6 Hz, 1H); **^{31}P{^{1}H}-NMR** (162 MHz, CD_2Cl_2) δ 6.05 (s); **MS** (ESI): *m/z* (%) = 783.16 (100, $[M\text{-}Cl]^+$).

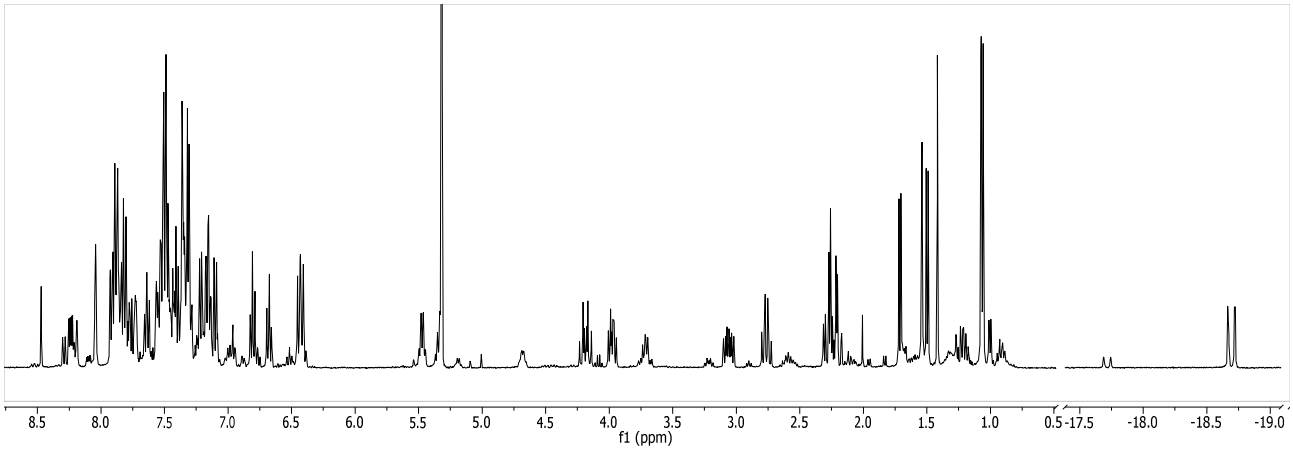

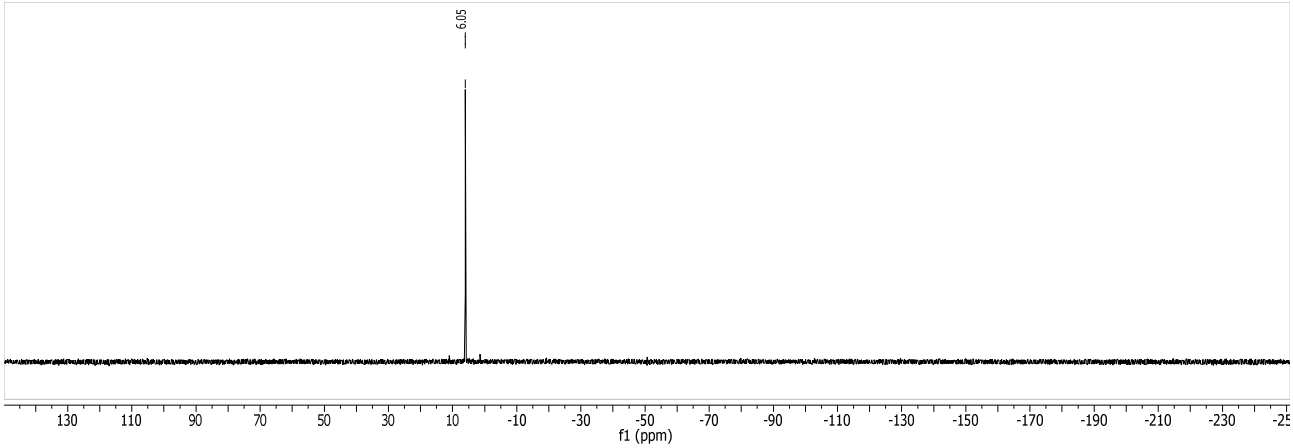

[{(*S*)-2-(2-(diphenylphosphino)phenyl)-4-isopropyl-4,5-dihydrooxazole}-iridium(III)-(*N*-(2-(*tert*-butyl)-3,4-dihydronaphthalen-1(2H)-ylidene)aniline)(hydrido)(chloride)] (384)

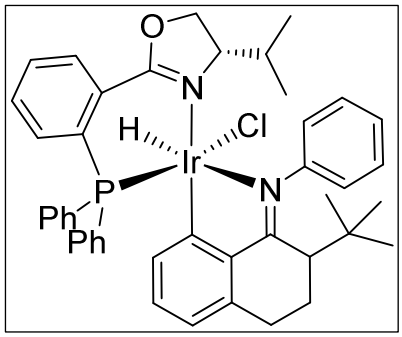

By general method, **86** (125 mg, 0.081 mmol, 1.0 eq.) and **383** (67 mg, 0.244 mmol, 3.0 eq.) were reacted to afford **384** (25.2 mg, 0.0287 mmol, 35%) as a yellow solid.

$C_{44}H_{47}ClIrN_2OP$ (M_W = 878.51 g/mol):
^{1}H-NMR (500 MHz, CD_2Cl_2) δ -18.40 (d, *J* = 19.9 Hz), -23.13 (d, *J* = 16.2 Hz); **MS** (ESI): *m/z* (%) = 877.17 (100, $[M-H]^+$).

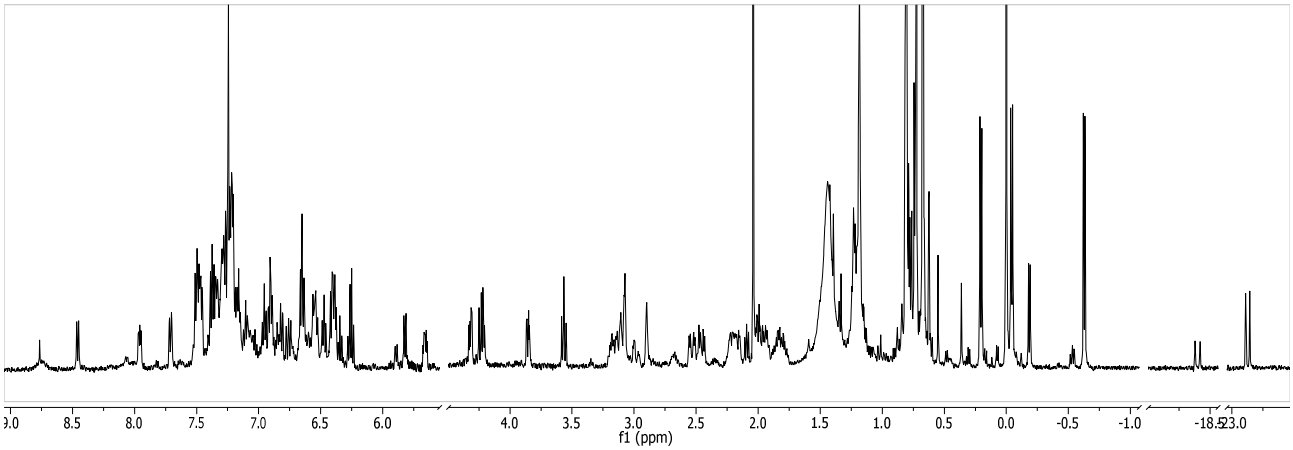

[{(*S*)-2-(2-(diphenylphosphino)phenyl)-4-isopropyl-4,5-dihydrooxazole}-iridium(III)-(*N*-(1-(naphthalen-2-yl)ethylidene)aniline)(hydrido)(chloride)] ([Ir(PHOX)(80)(H)(Cl)]

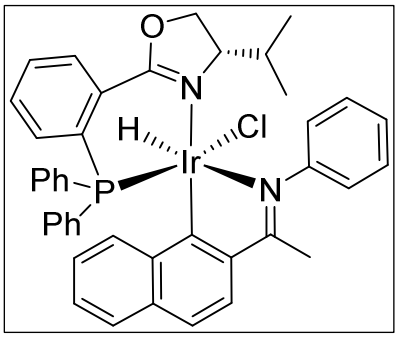

By general method, **86** (50 mg, 0.0325 mmol, 1.0 eq.) and **80** (24 mg, 0.0976 mmol, 3.0 eq.) were reacted to afford **[Ir(PHOX)(80)(H)(Cl)]** as a yellow solid. No yield was determined.

$C_{42}H_{39}ClIrN_2OP$ (M_W = 846.43 g/mol):

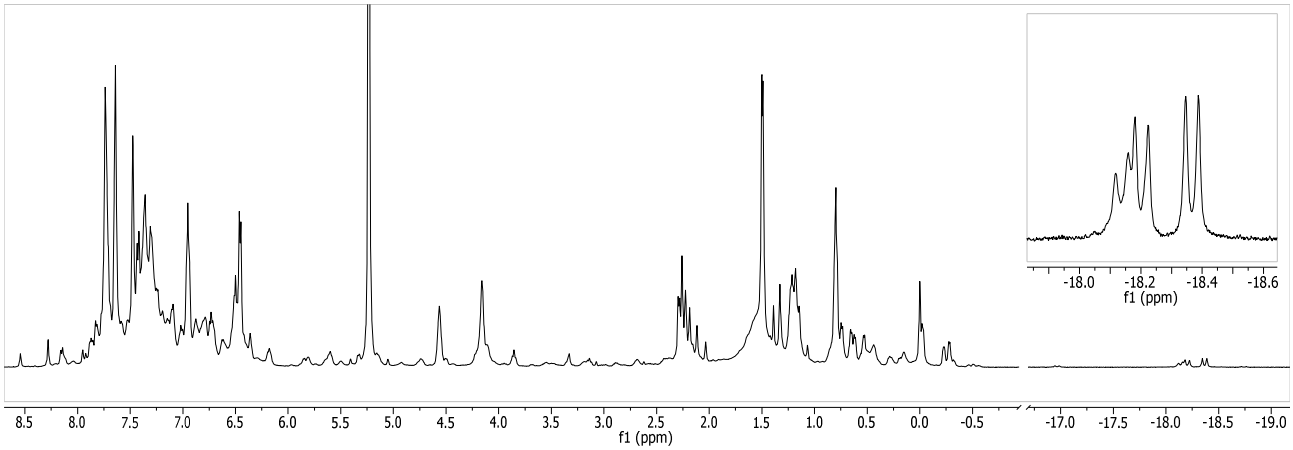

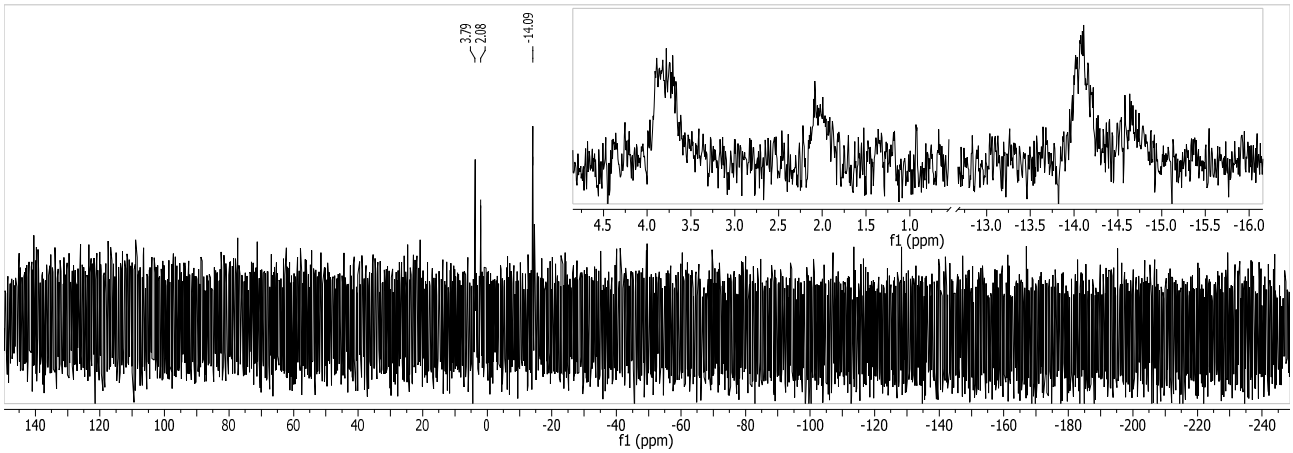

[{(*S*)-2-(2-(diphenylphosphino)phenyl)-4-isopropyl-4,5-dihydrooxazole}-iridium(III)-(*N*-(1-(4-methoxyphenyl)ethylidene)aniline)(hydrido)(chloride)] ([Ir(PHOX)(322)(H)(Cl)]

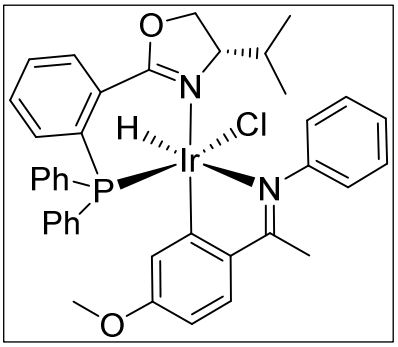

By general method, **86** (50 mg, 0.0325 mmol, 1.0 eq.) and **322** (22 mg, 0.0976 mmol, 3.0 eq.) were reacted to afford **([Ir(PHOX)(322)(H)(Cl)]** as a yellow solid. No yield was determined.

$C_{39}H_{39}ClIrN_2O_2P$ (M_W = 826.39 g/mol):

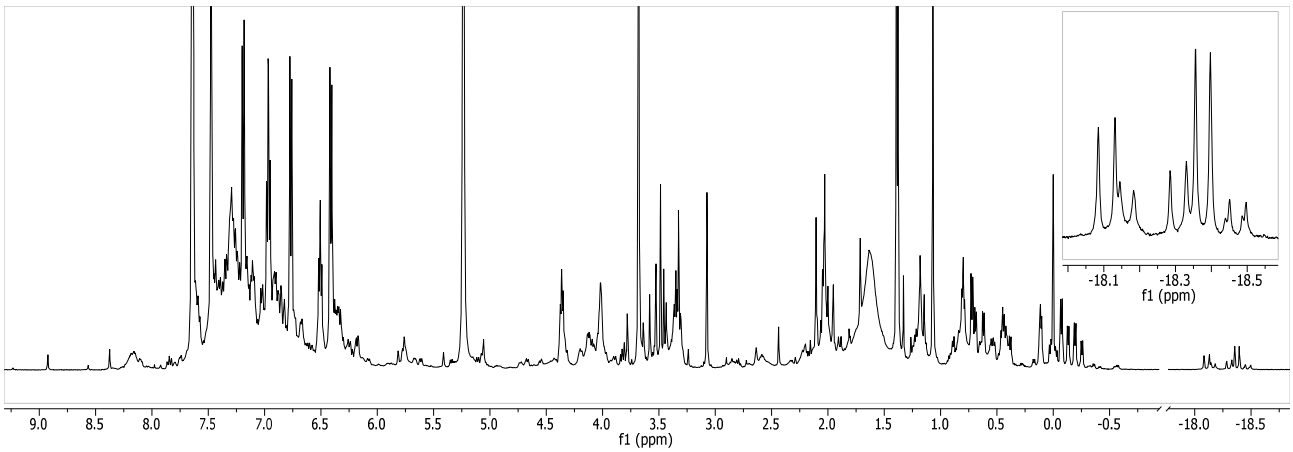

[{2-(2-(diphenylphosphino)phenyl)-4,5-dihydrooxazole}-iridium(III)-((3a*S*,8a*R*)-2-phenyl-8,8a-dihydro-3aH-indeno[1,2-d]oxazole)(hydrido)(chloride)] (373)

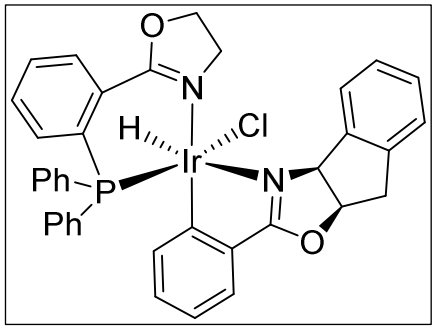

By general method, **336** (25 mg, 0.0167 mmol, 1.0 eq.) and **367** (9.8 mg, 0.042 mmol, 2.5 eq.) were reacted to afford **373** (14 mg, 0.0176 mmol, >99%) as a yellow solid. ^{19}F-NMR displayed residual BAr_F.

$C_{37}H_{31}ClIrN_2O_2P$ (M_W = 794.31 g/mol):
^{1}H-NMR (400 MHz, CD_2Cl_2) δ -19.13 (d, *J* = 21.6 Hz), -19.36 (d, *J* = 18.7 Hz), -19.51 (d, *J* = 16.0 Hz), -22.81 (d, *J* = 24.3 Hz); **^{31}P{^{1}H}-NMR** (162 MHz, CD_2Cl_2) δ 12.93 (s), 6.24 (d, *J* = 4.9 Hz), 6.04 (m), 4.61 (m); **MS** (ESI): *m/z* (%) = 759.18 (100, $[M-Cl]^+$).

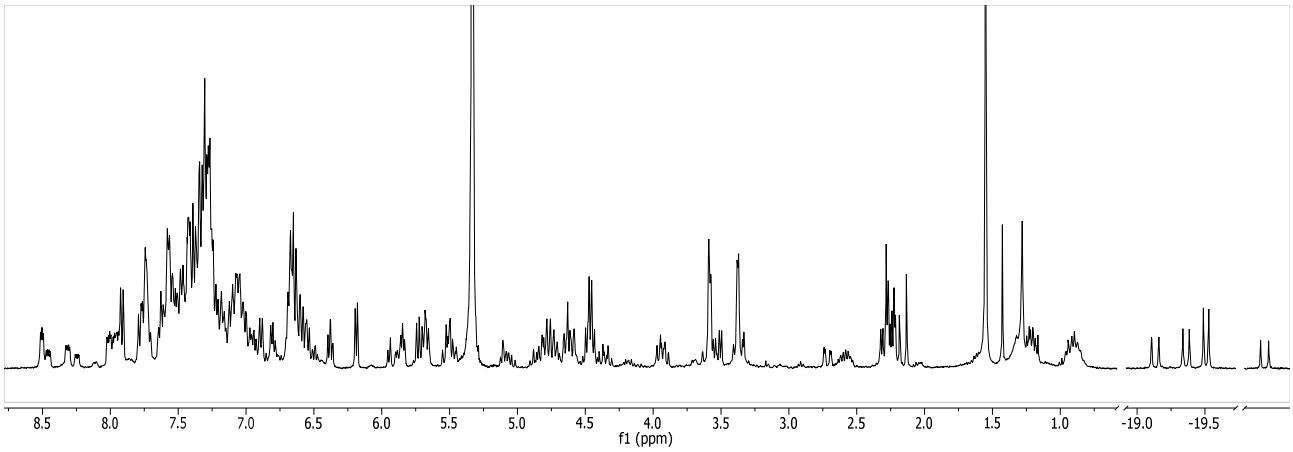

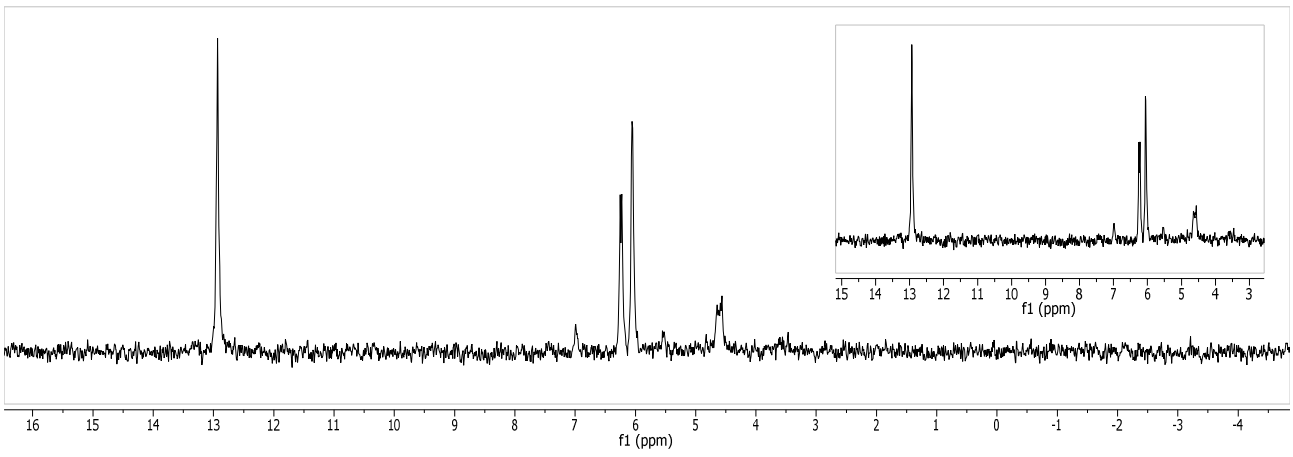

[{2-(2-(diphenylphosphino)phenyl)-4,5-dihydrooxazole}-iridium(III)-((*S*)-*N*-(2,6-dimethylbenzylidene)-1-phenylpropan-1-amine)(hydrido)(chloride)] (377)

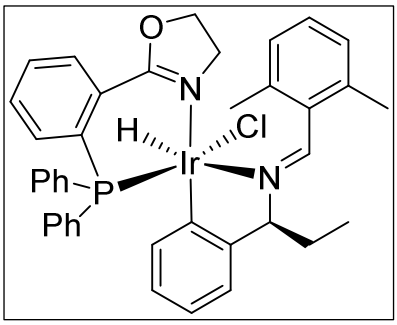

By general method, **336** (25 mg, 0.0167 mmol, 1.0 eq.) and **371** (12.6 mg, 0.05 mmol, 3.0 eq.) were reacted to afford **377** as a yellow solid. No yield was determined.

$C_{39}H_{39}ClIrN_2OP$ (M_W = 810.39 g/mol):
^{1}H-NMR (500 MHz, CD_2Cl_2) δ -19.70 (d, *J* = 17.0 Hz), -19.77 (d, *J* = 17.5 Hz), -21.85 (d, *J* = 18.1 Hz).

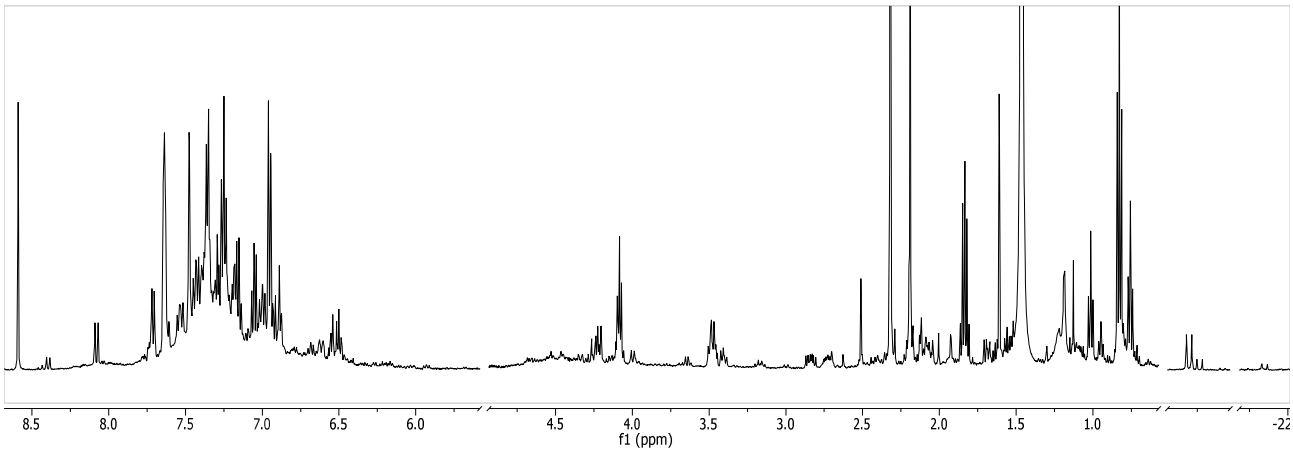

[{(*S*)-2-(2-((dicyclohexylphosphino)oxy)propan-2-yl)-4-isopropyl-4,5-dihydrooxazole}-iridium(III)-(*N*-(1-phenylethylidene)aniline)(hydrido)(chloride)] (391)

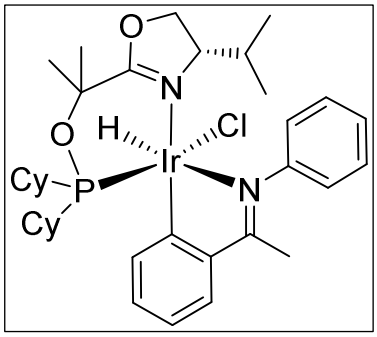

By general method **87** (50 mg, 0.03 mmol, 1.0 eq.) and **59** (13 mg, 0.06 mmol, 2.0 eq.) afforded **391** (18 mg, 0.03 mmol, 76%) as a yellow solid. X-Ray quality crystals were obtained by redissolving the precipitate in CH_2Cl_2 and layering with *n*-pentane. After evaporation of solvents an oily residue was observed which solidified into a crystalline material in the course of a few weeks.

$C_{35}H_{51}ClIrN_2O_2P$ (790.45 g/mol):
^{1}H-NMR (500 MHz, CD_2Cl_2) δ 7.72 (s, 1H), 7.68 – 7.61 (m, 1H), 7.56 – 7.49 (m, 1H), 7.36 (s, 2H), 7.17 (t, J = 7.4 Hz, 1H), 6.94 (dd, J = 8.3, 4.4 Hz, 2H), 6.90 (s, 1H), 5.13 (d, J = 9.3 Hz, 1H), 4.28 (dd, J = 8.7, 3.1 Hz, 1H), 3.83 (t, J = 9.1 Hz, 1H), 2.90 – 2.69 (m, 1H), 2.42 (s, 3H), 2.32 (d, J = 7.7 Hz, 1H), 2.16 (d, J = 12.1 Hz, 1H), 1.91 – 1.45 (m, 10H), 1.35 – 1.18 (m, 6H), 1.15 (s, 6H), 0.90 (d, J = 7.1 Hz, 3H), 0.69 (d, J = 6.9 Hz, 3H), -19.50 (d, J = 24.3 Hz, 1H); **^{31}P{^{1}H}-NMR** (202 MHz, CD_2Cl_2) δ 101.41 (d, J = 21.9 Hz); **X-Ray**: Crystal data for **391**: formula $C_{22.77}Cl_{2.12}Ir_{0.75}N_{1.50}O_{1.50}P_{0.75}$, M = 561.22, F(000) = 4227.800, ? ?, size ? · ? · ? mm^3, triclinic, space group P 1 , Z = 16, a = 20.3432(8) Å, b = 20.3463(8) Å, c = 32.2232(19) Å, α = 91.006(3)°, β = 99.548(3)°, γ = 119.941(2)°, V = 11318.5(10) Å^3, $D_{calc.}$ = 1.317 Mg · m^{-3}. The crystal was measured on a Unknown diffractometer at 193K using graphite-monochromated Mo K_α-radiation with λ = 0.71073 Å, Θ_{max} = 26.434°. Minimal/maximal transmission 1.0000/1.0000, μ = 3.804 mm^{-1}. The USER DEFINED DATA COLLECTION suite has been used for datacollection and integration. From a total of 149545 reflections, 87895 were independent (merging r = 0.049). From these, 52759 were considered as observed (I>2.0σ(I)) and were used to refine 1886 parameters. The structure was solved by Other methods using the program Superflip. Least-squares refinement against F was carried out on all non-hydrogen atoms using the program CRYSTALS. R = 0.1539 (observed data), wR = 0.2405 (all data), GOF = 0.5291. Minimal/maximal residual electron density = -8.07/14.87 e Å^{-3}. Chebychev polynomial weights were used to complete the refinement. Plots were produced using CAMERON.

[{(*S*)-2-(2-(diphenylphosphino)phenyl)-4-isopropyl-4,5-dihydrooxazole}-iridium(III)-(*N*-(1-phenylethylidene)aniline)(hydrido)(chloride)] (325)

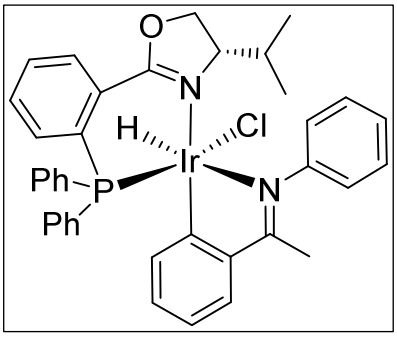

By general method **86** (100 mg, 0.065 mmol, 1.0 eq.) and **59** (25.3 mg, 0.13 mmol, 2.0 eq.) afforded **325** (24 mg, 0.03 mmol, 46%) as a yellow solid.

$C_{38}H_{37}ClIrN_2OP$ (796.36 g/mol):

^{1}H-NMR (400 MHz, CD_2Cl_2) δ 7.70 – 7.61 (m, 2H), 7.59 (d, *J* = 7.5 Hz, 1H), 7.55 – 7.49 (m, 1H), 7.47 (d, *J* = 7.4 Hz, 1H), 7.36 (m, 6H), 7.12 (t, *J* = 7.2 Hz, 1H), 7.05 (t, *J* = 7.4 Hz, 1H), 6.96 (td, *J* = 8.0, 2.4 Hz, 2H), 6.86 – 6.80 (m, 1H), 6.72 (m, 2H), 6.62 (t, *J* = 7.1 Hz, 1H), 6.49 (dd, *J* = 11.3, 7.8 Hz, 2H), 5.88 (d, *J* = 7.2 Hz, 1H), 5.26 (ddd, *J* = 10.0, 4.2, 3.1 Hz, 1H), 4.22 (dd, *J* = 8.8, 4.5 Hz, 1H), 4.02 – 3.94 (m, 1H), 2.76 – 2.66 (m, 1H), 2.28 (s, 3H), 0.81 (d, *J* = 7.1 Hz, 3H), -0.03 (d, *J* = 6.8 Hz, 3H), -18.21 (d, *J* = 20.7 Hz, 1H); **^{13}C{^{1}H}-NMR** (126 MHz, CD_2Cl_2) δ 180.57, 159.73, 148.50, 148.28, 141.70, 134.04, 133.95, 132.80, 132.72, 132.67, 132.65, 131.57, 131.51, 131.44, 131.03, 130.91, 130.89, 130.77, 130.75, 130.59, 130.00, 129.75, 128.97, 128.54, 128.37, 128.28, 127.75, 127.66, 124.99, 123.28, 121.47, 120.04, 72.82, 70.52, 67.53, 49.46, 28.94, 27.12, 19.05, 17.80, 12.76; **^{31}P{^{1}H}-NMR** (162 MHz, CD_2Cl_2) δ 2.63 (d, *J* = 14.5 Hz); **EA**: calc.: C, 57.31; H, 4.68; N, 3.52; found: C, 54.95; H, 4.90; N, 3.10

[{(*S*)-2-(2-(diphenylphosphino)phenyl)-4-isopropyl-4,5-dihydrooxazole}-iridium(III)-(*N*-(1-phenylethylidene)aniline)(hydrido)(tetrahydrofuran)])-tetrakis(3,5-bis(trifluoro-methyl)phenyl)borate (308)

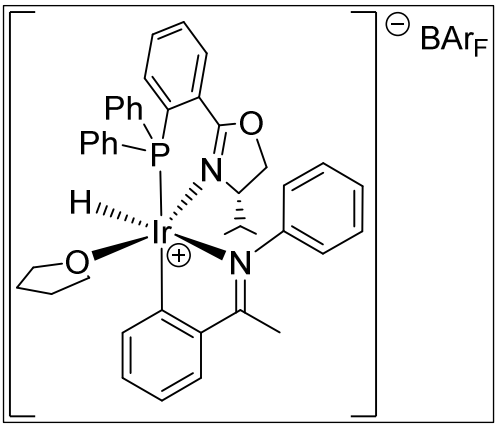

In the glove box, **325** (10 mg, 0.0126 mmol, 1.0 eq.) and $NaBAr_F$ (11.1 mg, 0.0126 mmol, 1.0 eq.) were added to a young's NMR tube and dissolved in THF-d_8 at room temperature.The mixture was shaken until it turned homogenous and NMR spectra were recorded.

$C_{74}H_{57}BF_{24}IrN_2O_2P$ (M_W = 1696.34 g/mol):
^{1}H-NMR (500 MHz, THF) δ 7.68 (s, 8H), 7.59 – 7.50 (m, 3H), 7.46 (s, 4H), 7.44 (d, *J* = 2.9 Hz, 1H), 7.35 – 7.28 (m, 3H), 7.24 (d, *J* = 18.7 Hz, 4H), 7.19 (d, *J* = 7.9 Hz, 1H), 6.98 (t, *J* = 7.4 Hz, 1H), 6.92 (t, *J* = 7.4 Hz, 1H), 6.83 (t, *J* = 7.1 Hz, 2H), 6.81 – 6.76 (m, 1H), 6.64 (d, *J* = 7.3 Hz, 1H), 6.52 (t, *J* = 7.4 Hz, 1H), 6.41 (t, *J* = 9.0 Hz, 3H), 5.83 (d, *J* = 7.2 Hz, 1H), 5.30 – 5.17 (m, 1H), 4.16 (dd, *J* = 8.6, 4.5 Hz, 1H), 3.87 (t, *J* = 9.4 Hz, 1H), 2.72 – 2.63 (m, 1H), 2.14 (s, 3H), 0.68 (d, *J* = 7.1 Hz, 3H), -0.09 (d, *J* = 6.9 Hz, 3H), -18.30 (d, *J* = 20.7 Hz, 1H); **^{31}P{^{1}H}-NMR** (202 MHz, THF) δ 0.80 (d, *J* = 19.8 Hz).

[{(*S*)-4-(*tert*-butyl)-2-(2-(diphenylphosphino)phenyl)-4,5-dihydrooxazole}-iridium(III)-(*N*-(1-phenylethylidene)aniline)(hydrido)(chloride)] (337)

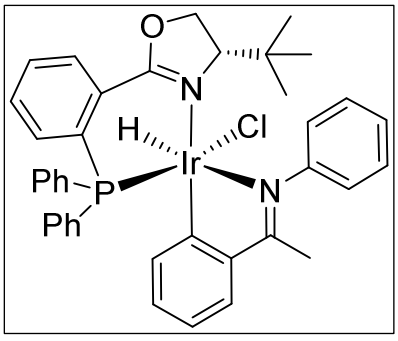

By general method **388** (50.4 mg, 0.325 mmol, 1.0 eq.) and **59** (12.6 mg, 0.065 mmol, 2.0 eq.) afforded **337** (20.7 mg, 0.0255 mmol, 78%) as a yellow solid.

$C_{39}H_{39}ClIrN_2OP$ (M_W = 810.39 g/mol):
^{1}H-NMR (400 MHz, CD_2Cl_2) δ 7.58 – 7.46 (m, 4H), 7.36 – 7.23 (m, 8H), 7.07 – 6.99 (m, 2H), 6.85 (td, *J* = 7.7, 2.4 Hz, 2H), 6.73 – 6.67 (m, 1H), 6.67 – 6.61 (m, 2H), 6.50 (td, *J* = 7.4, 1.5 Hz, 1H), 6.40 (ddt, *J* = 11.7, 6.7, 1.4 Hz, 2H), 5.76 – 5.66 (m, 1H), 5.21 (dd, *J* = 9.0, 2.6 Hz, 1H), 4.29

(dd, *J* = 9.0, 2.7 Hz, 1H), 3.81 (t, *J* = 9.0 Hz, 1H), 2.15 (s, 3H), 0.61 (s, 9H), -18.62 (d, *J* = 22.1 Hz, 1H); **^{13}C{^{1}H}-NMR** (126 MHz, CD_2Cl_2) δ 180.46, 163.33, 163.30, 148.84, 147.75, 141.94, 134.78, 134.25, 133.78, 133.69, 132.97, 132.89, 132.55, 132.53, 132.19, 132.13, 131.88, 131.82, 131.16, 131.04, 130.85, 130.83, 130.79, 130.74, 130.73, 130.60, 130.15, 130.12, 130.07, 129.74, 129.72, 128.89, 128.84, 128.79, 128.37, 128.28, 127.69, 127.61, 125.09, 122.99, 122.06, 120.00, 72.82, 71.95, 70.31, 49.46, 35.32, 30.08, 27.12, 26.28, 17.95; **^{31}P{^{1}H}-NMR** (162 MHz, CD_2Cl_2) δ 3.00 (dt, *J* = 8.9, 4.3 Hz).

[{(*S*)-2-(2-(diphenylphosphino)phenyl)-4-isopropyl-4,5-dihydrooxazole}-iridium(III)-(2,6-dimethyl-*N*-(1-phenylethylidene)aniline)(hydrido)(chloride)] (389)

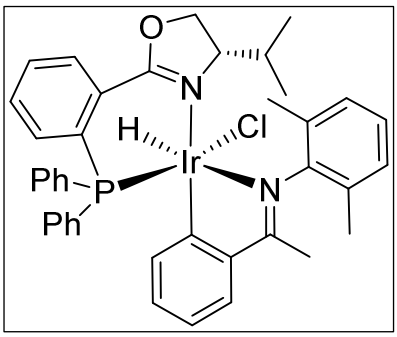

By general method **86** (100 mg, 0.065 mmol, 1.0 eq.) and **340** (29 mg, 0.13 mmol, 2.0 eq.) afforded **389** (62 mg, 0.075 mmol, >99%) as a yellow solid. Trituration with *n*-pentane gave 25 mg (0.03 mmol, 46%) of pure material.

$C_{40}H_{41}ClIrN_2OP$ (824.41 g/mol):
^{1}H-NMR (500 MHz, CD_2Cl_2) δ 7.68 (dd, *J* = 7.7, 1.4 Hz, 13H), 7.63 (d, *J* = 7.5 Hz, 12H), 7.57 – 7.30 (m, 517H), 7.30 – 7.25 (m, 20H), 7.21 (d, *J* = 7.6 Hz, 39H), 7.14 (t, *J* = 7.4 Hz, 40H), 7.11 (s, 19H), 7.09 (d, *J* = 7.4 Hz, 120H), 7.06 (d, *J* = 7.3 Hz, 12H), 7.02 (qd, *J* = 7.8, 1.8 Hz, 35H), 6.94 (t, *J* = 7.7 Hz, 90H), 6.90 (dd, *J* = 7.3, 1.3 Hz, 11H), 6.81 (d, *J* = 7.5 Hz, 11H), 6.77 (t, *J* = 7.3 Hz, 39H), 6.67 – 6.61 (m, 25H), 6.59 – 6.56 (m, 7H), 6.56 – 6.52 (m, 33H), 6.36 (td, *J* = 7.5, 1.4 Hz, 28H), 6.25 (d, *J* = 7.5 Hz, 9H), 5.30 (ddd, *J* = 10.0, 4.3, 2.7 Hz, 9H), 4.28 (dd, *J* = 8.8, 4.2 Hz, 10H), 4.16 (t, *J* = 9.3 Hz, 10H), 4.02 (dd, *J* = 8.8, 2.5 Hz, 29H), 3.67 (t, *J* = 8.8 Hz, 30H), 3.20 (s, 36H), 2.66 (s, 86H), 2.58 (s, 8H), 2.55 (s, 29H), 2.38 (dt, *J* = 8.8, 2.6 Hz, 31H), 2.31 (s, 31H), 2.28 (s, 8H), 2.23 (s, 86H), 2.17 (s, 10H), 2.09 (s, 190H), 2.08 (s, 87H), 2.04 (s, 372H), 1.69 (pd, *J* = 7.0, 2.5 Hz, 31H), 1.57 (s, 18H), 1.29 (s, 31H), 1.20 (s, 122H), 0.77 (d, *J* = 7.1 Hz, 32H), 0.56 (d, *J* = 7.1 Hz, 7H), 0.39 (d, *J* = 7.0 Hz, 90H), -0.25 (d, *J* = 6.9 Hz, 30H), -0.34 (d, *J* = 7.0 Hz, 8H), -0.48 (d, *J* = 6.7 Hz, 90H), -19.34 (d, *J* = 23.1 Hz, 9H), -22.44 (d, *J* = 27.7 Hz, 1H), -22.52 (d, *J* = 15.6 Hz, 30H); **^{31}P{^{1}H}-NMR** (202 MHz,CD_2Cl_2) δ 4.16 (d, *J* = 14.3 Hz), -0.34 (dd, *J* = 18.1, 4.6 Hz), -3.65 (d, *J* = 25.5 Hz); **EA**: calc.: C, 58.28; H, 5.01, N, 3.40; found: C, 64.18; H, 5.74, N, 4.32; **HRMS**: calculated: 789.2586 $[M\text{-}Cl]^+$, found: 789.2595.

[{(S)-4-(*tert*-butyl)-2-(2-(diphenylphosphino)phenyl)-4,5-dihydrooxazole}-iridium(III)-(2,6-dimethyl-*N*-(1-phenylethylidene)aniline)(hydrido)(chloride)] (390)

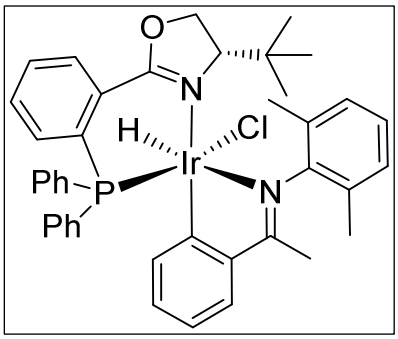

By general method **388** (50.4 mg, 0.325 mmol, 1.0 eq.) and **340** (14.5 mg, 0.065 mmol, 2.0 eq.) afforded **390** (11.9 mg, 0.0142 mmol, 43%) as a yellow solid.

$C_{41}H_{43}ClIrN_2OP$ (M_W = 838.45 g/mol):
^{1}H-NMR (500 MHz, CD_2Cl_2) δ 8.15 (ddd, *J* = 7.7, 3.9, 1.3 Hz, 2H), 7.64 (dd, *J* = 7.7, 1.4 Hz, 1H), 7.57 – 7.29 (m, 31H), 7.29 – 7.25 (m, 2H), 7.20 – 7.14 (m, 5H), 7.13 – 7.09 (m, 4H), 7.03 (td, *J* = 7.9, 2.3 Hz, 3H), 6.98 – 6.93 (m, 2H), 6.91 – 6.82 (m, 6H), 6.76 (t, *J* = 7.4 Hz, 3H), 6.69 – 6.63 (m, 2H), 6.60 – 6.55 (m, 3H), 6.35 (td, *J* = 7.6, 1.6 Hz, 3H), 5.28 (dd, *J* = 8.8, 2.4 Hz, 1H), 4.41 (dd, *J* = 8.9, 2.4 Hz, 1H), 4.19 (dd, *J* = 9.0, 1.8 Hz, 2H), 4.09 (d, *J* = 8.9 Hz, 1H), 3.76 – 3.70 (m, 2H), 2.68 (s, 7H), 2.55 (s, 4H), 2.26 (d, *J* = 11.5 Hz, 10H), 0.61 (s, 11H), 0.22 (s, 21H), -19.75 (d, *J* = 24.8 Hz, 1H), -22.74 (d, *J* = 16.8 Hz, 2H); **^{13}C{^{1}H}-NMR** (126 MHz, CD_2Cl_2) δ 183.66, 181.13, 166.85, 149.38, 148.64, 147.78, 146.42, 142.03, 140.31, 140.28, 135.71, 135.63, 135.30, 135.28, 133.67, 133.59, 133.30, 133.01, 132.96, 132.93, 132.90, 132.59, 132.51, 132.36, 132.33, 132.28, 132.25, 131.89, 131.77, 131.71, 131.67, 131.59, 131.38, 131.06, 131.00, 130.87, 130.85, 130.80, 130.78, 130.71, 130.69, 130.63, 130.60, 130.41, 130.15, 129.46, 129.37, 129.15, 128.89, 128.79, 128.61, 128.46, 128.31, 128.25, 128.16, 127.73, 127.65, 126.83, 125.01, 120.33, 119.88, 100.37, 73.38, 72.82, 72.76, 70.11, 69.41, 49.46, 35.34, 34.76, 30.08, 27.12, 25.92, 25.58, 21.85, 21.06, 19.17, 18.21, 18.08, 17.07, 17.04; **^{31}P{^{1}H}-NMR** (162 MHz, CD_2Cl_2) δ 3.89 (s), -0.03 (d, *J* = 9.2 Hz).

[{(*S*)-2-(2-(diphenylphosphino)phenyl)-4-isopropyl-4,5-dihydrooxazole}-iridium(III)-(d_{10}-*N*-(1-phenylethylidene)aniline)(hydrido)(hydrido)(chloride)] (d_{10}-325)

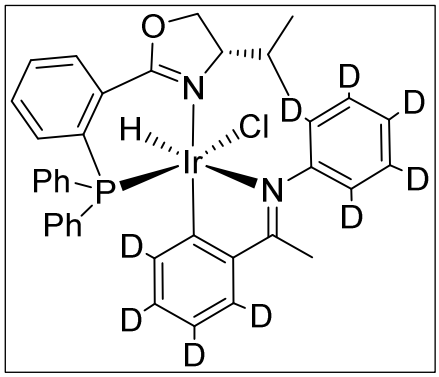

By general method **86** (50 mg, 0.0325 mmol, 1.0 eq.) and **d_{10}-59** (12.1 mg, 0.065 mmol, 2.0 eq.) afforded **d_{10}-325** (4.7 mg, 0.0058 mmol, 18%) as a yellow solid.

$C_{38}H_{28}D_9ClIrN_2OP$ (M_W = 805.42 g/mol):
^{1}H-NMR (500 MHz, CD_2Cl_2) δ 7.68 (ddt, *J* = 12.1, 6.3, 1.8 Hz, 2H), 7.54 (tdd, *J* = 4.2, 3.3, 1.3 Hz, 1H), 7.45 – 7.35 (m, 5H), 7.15 (tt, *J* = 7.2, 1.5 Hz, 1H), 6.99 (td, *J* = 7.9, 2.5 Hz, 2H), 6.90 – 6.82 (m, 1H), 6.53 (ddd, *J* = 11.6, 8.0, 1.4 Hz, 2H), 5.29 (ddd, *J* = 10.3, 4.7, 3.1 Hz, 1H), 4.26 (dd, *J* = 8.7, 4.5 Hz, 1H), 4.01 (ddd, *J* = 10.5, 8.7, 2.0 Hz, 1H), 2.74 (dqd, *J* = 10.0, 7.0, 2.9 Hz, 1H), 2.31 (s, 2H), 0.85 (d, *J* = 7.2 Hz, 3H), 0.00 (d, *J* = 6.9 Hz, 3H); **^{31}P{^{1}H}-NMR** (162 MHz, CD_2Cl_2) δ 2.76 , 2.64 (d, *J* = 14.4 Hz).

[{(*S*)-2-(2-(diphenylphosphino)phenyl)-4-isopropyl-4,5-dihydrooxazole}-iridium(III)-(*N*-(1-(3,5-dimethylphenyl)ethylidene)aniline)(hydrido)(chloride)] (514)

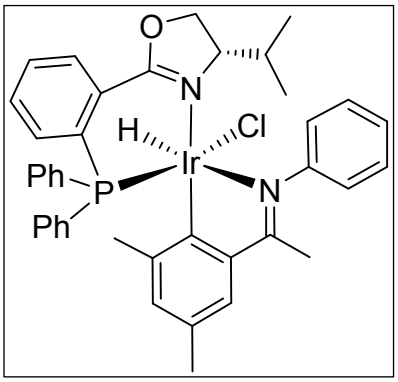

By general method **86** (50 mg, 0.0325 mmol, 1.0 eq.) and **512** (15 mg, 0.065 mmol, 2.0 eq.) afforded **514** as a yellow solid. No yield was determined.

$C_{40}H_{41}ClIrN_2OP$ (M_W = 824.42 g/mol)
^{1}H-NMR (400 MHz, CD_2Cl_2) δ 7.85 – 7.69 (m, 2H), 7.59 – 7.45 (m, 1H), 7.36 – 7.30 (m, 1H), 7.25 (dddd, *J* = 13.7, 10.8, 7.6, 1.5 Hz, 5H), 7.02 (td, *J* = 7.4, 1.6 Hz, 1H), 6.98 – 6.92 (m, 2H), 6.92 – 6.86 (m, 2H), 6.82 (td, *J* = 7.8, 2.5 Hz, 2H), 6.63 (td, *J* = 7.6, 1.5 Hz, 1H), 6.45 (s, 1H), 6.43 – 6.38 (m, 2H), 5.79 – 5.72 (m, 1H), 5.26 (ddt, *J* = 6.7, 3.8, 1.9 Hz, 1H), 4.13 (dd, *J* = 8.7, 4.3 Hz, 1H), 3.88 (dd, *J* = 10.1, 8.7 Hz, 1H), 2.70 (pd, *J* = 6.9, 2.7 Hz, 1H), 2.16 (s, 3H), 2.11 (s, 3H), 2.07 (s, 3H), 0.79 (d, *J* = 5.5 Hz, 4H), 0.01 (d, *J* = 6.8 Hz, 3H), -17.80 (d, *J* = 19.7 Hz, 1H); **^{31}P{^{1}H}-NMR** (162 MHz, CD_2Cl_2) δ 4.28 (d, *J* = 11.8 Hz).

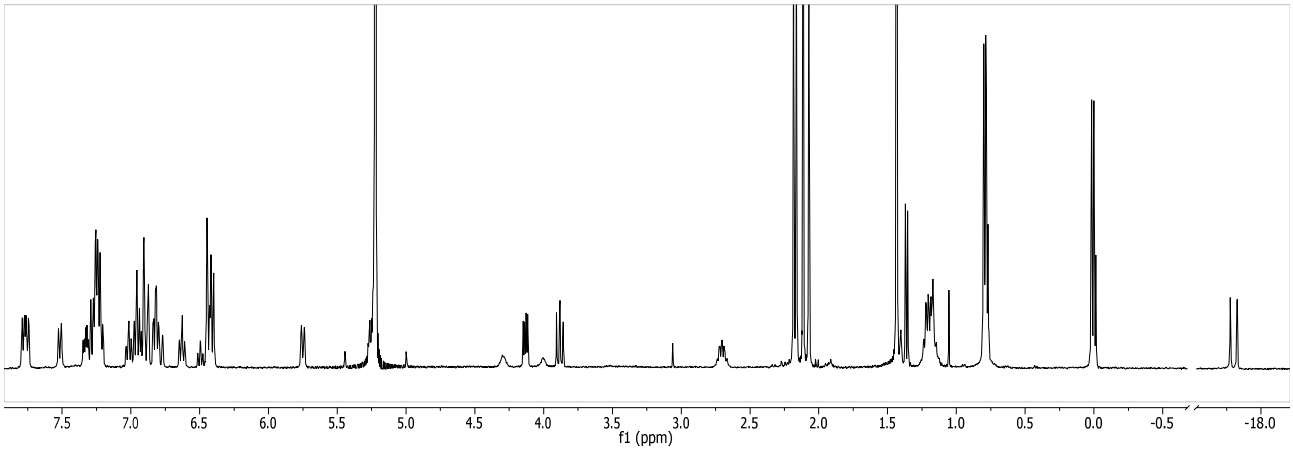

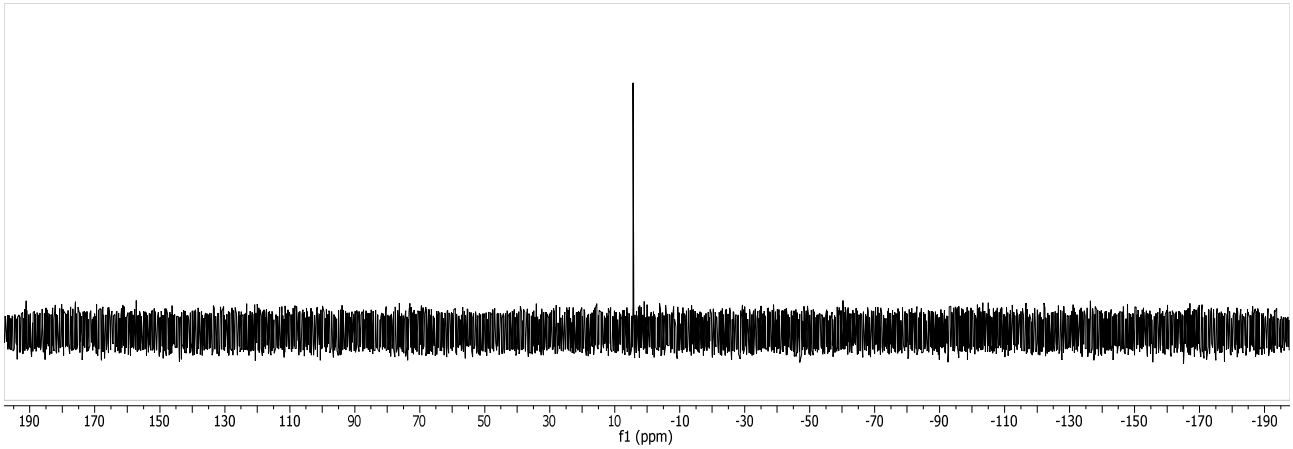

[{(*S*)-2-(2-((dicyclohexylphosphino)oxy)propan-2-yl)-4-isopropyl-4,5-dihydrooxazole}-iridium(III)-(*N*-(1-(3,5-dimethylphenyl)ethylidene)aniline)(hydrido)(chloride)] (515)

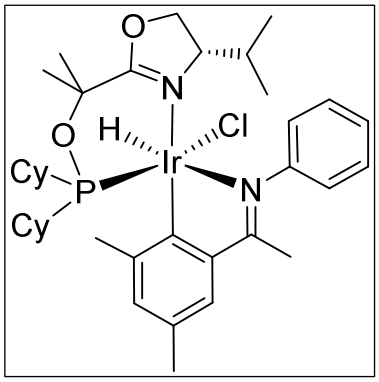

By general method **87** (50 mg, 0.0325 mmol, 1.0 eq.) and **512** (15 mg, 0.065 mmol, 2.0 eq.) afforded **515** as a yellow solid. No yield was determined.

$C_{37}H_{55}ClIrN_2O_2P$ (M_W = 818.50 g/mol):
^{1}H-NMR (400 MHz, CD_2Cl_2) δ 7.64 (s, 1H), 7.50 (d, *J* = 1.6 Hz, 1H), 7.47 (s, 0H), 7.26 (td, *J* = 8.1, 4.1 Hz, 3H), 7.16 (d, *J* = 1.8 Hz, 1H), 7.13 (d, *J* = 2.0 Hz, 0H), 7.08 (tt, *J* = 7.4, 1.4 Hz, 1H), 7.04 (s, 0H), 7.01 – 6.93 (m, 1H), 6.88 (s, 1H), 6.85 – 6.81 (m, 1H), 6.78 (s, 1H), 6.70 – 6.64 (m, 1H), 6.51 (t, *J* = 7.3 Hz, 0H), 6.45 – 6.39 (m, 1H), 5.06 (dt, *J* = 9.3, 3.0 Hz, 1H), 4.31 (p, *J* = 6.5 Hz, 1H), 4.17 (dd, *J* = 8.7, 3.2 Hz, 1H), 4.02 (q, *J* = 5.8, 4.9 Hz, 0H), 3.70 (t, *J* = 9.0 Hz, 1H), 2.99 – 2.86 (m, 1H), 2.77 (pd, *J* = 7.0, 2.8 Hz, 1H), 2.39 (s, 3H), 2.33 (s, 3H), 2.29 (s, 2H), 2.19 (d, *J* = 1.4 Hz, 5H), 2.09 (s, 1H), 2.05 – 1.91 (m, 1H), 1.83 (dddt, *J* = 16.6, 13.3, 7.1, 2.9 Hz, 2H), 1.31 (s, 4H), 0.82 (d, *J* = 7.1 Hz, 3H), 0.77 (s, 3H), 0.61 (d, *J* = 6.9 Hz, 4H), -18.86 (d, *J* = 22.5 Hz, 1H); **^{31}P{^{1}H}-NMR** (162 MHz, CD_2Cl_2) δ 103.61 (d, *J* = 17.1 Hz).

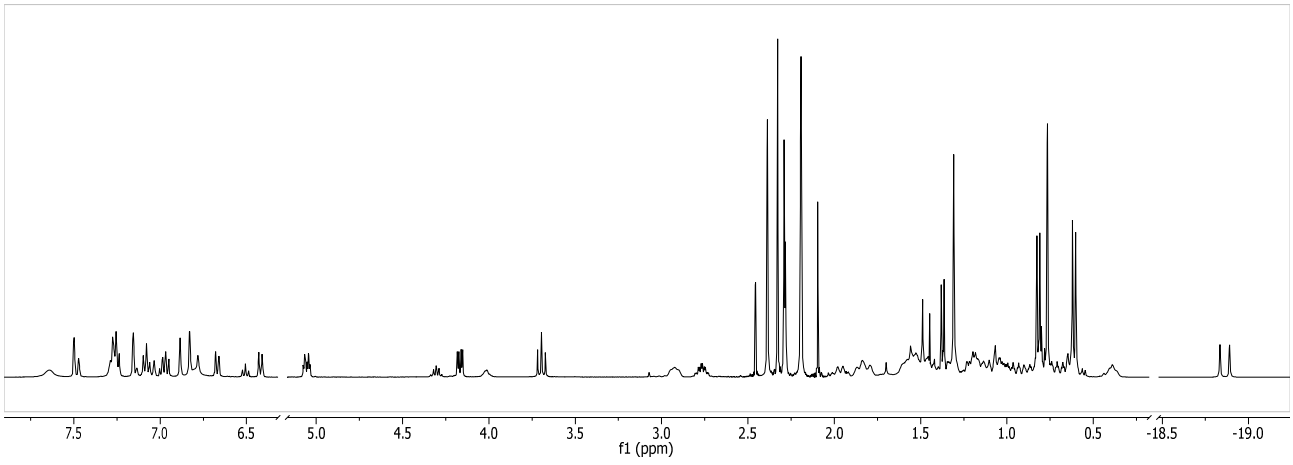

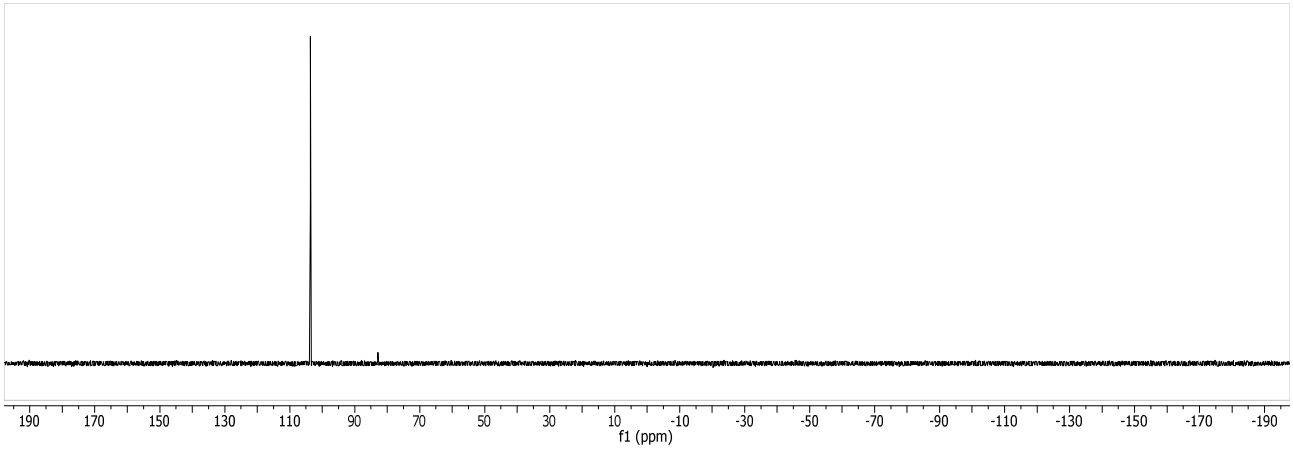

[{(*S*)-2-(2-(diphenylphosphino)phenyl)-4-isopropyl-4,5-dihydrooxazole}-iridium(III)-(*N*-(1-(3,5-diisopropylphenyl)ethylidene)aniline)(hydrido)(chloride)] (527)

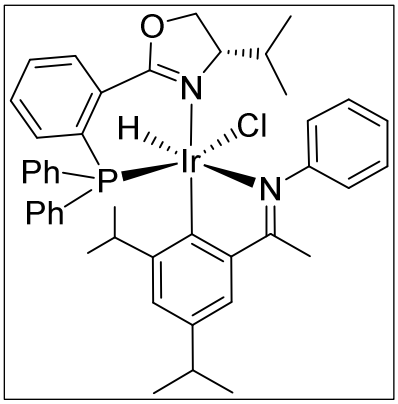

By general method **87** (50 mg, 0.0325 mmol, 1.0 eq.) and **522** (15 mg, 0.065 mmol, 2.0 eq.) afforded **527** (5.1 mg, 0.0058 mmol, 18%) as a yellow solid.

$C_{44}H_{49}ClIrN_2OP$ (M_W = 880.53 g/mol):
^{1}H-NMR (500 MHz, CD_2Cl_2) δ 7.85 (ddt, *J* = 9.8, 5.7, 2.1 Hz, 2H), 7.72 – 7.68 (m, 1H), 7.53 (ddd, *J* = 7.8, 3.9, 1.5 Hz, 1H), 7.42 (d, *J* = 7.5 Hz, 1H), 7.41 – 7.35 (m, 5H), 7.13 – 7.06 (m, 7H), 7.01 (t, *J* = 1.8 Hz, 1H), 6.92 (td, *J* = 7.9, 2.5 Hz, 2H), 6.80 (td, *J* = 7.8, 1.7 Hz, 1H), 6.66 (s, 1H), 6.65 – 6.62 (m, 1H), 6.57 (d, *J* = 8.1 Hz, 2H), 6.49 (dd, *J* = 11.4, 7.7 Hz, 2H), 5.91 (dt, *J* = 7.7, 1.5 Hz, 1H), 5.40 (ddd, *J* = 10.1, 4.2, 2.6 Hz, 1H), 4.49 (q, *J* = 6.7 Hz, 1H), 4.27 (dd, *J* = 8.7, 4.2 Hz, 1H), 4.12 (q, *J* = 7.1 Hz, 2H), 3.97 (dd, *J* = 10.0, 8.6 Hz, 1H), 3.85 – 3.74 (m, 1H), 2.94 – 2.75 (m, 3H), 2.23 (s, 3H), 1.34 (dd, *J* = 6.9, 3.6 Hz, 3H), 1.28 – 1.24 (m, 18H), 0.94 (d, *J* = 7.1 Hz, 3H), 0.77 (d, *J* = 6.9 Hz, 3H), 0.20 (d, *J* = 6.9 Hz, 3H), -17.60 (d, *J* = 19.6 Hz, 1H); **^{31}P{^{1}H}-NMR** (162 MHz, CD_2Cl_2) δ 3.80 (d, *J* = 12.0 Hz).

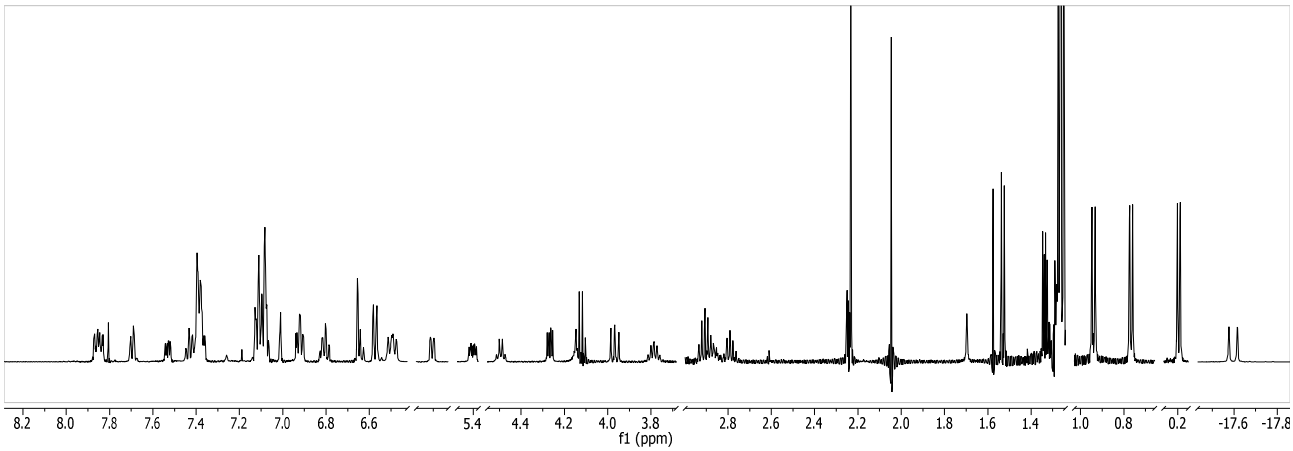

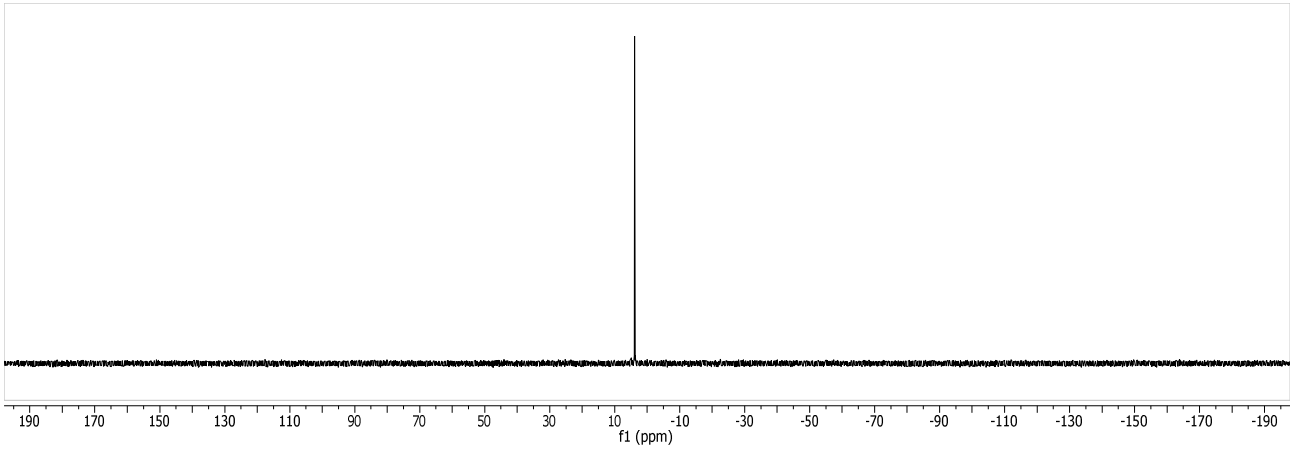

[{(*S*)-2-(2-(diphenylphosphino)phenyl)-4-isopropyl-4,5-dihydrooxazole}-iridium(III)-((*E*)-4-phenylbut-3-en-2-one)(hydrido)(chloride)] (387)

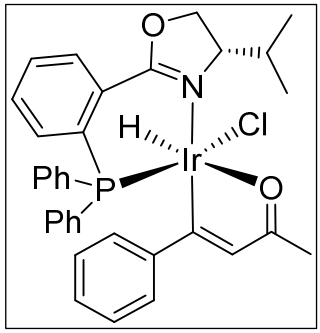

By general method **87** (50 mg, 0.0325 mmol, 1.0 eq.) and **386** (14.4 mg, 0.065 mmol, 2.0 eq.) afforded **387** as a yellow solid. No yield was determined.

$C_{34}H_{34}ClIrNO_2P$ (M_W = 747.29 g/mol):
^{1}H-NMR (400 MHz, CD_2Cl_2) δ 7.57 – 7.24 (m, 12H), 7.21 – 7.16 (m, 3H), 7.13 (t, *J* = 7.2 Hz, 1H), 6.97 (ddd, *J* = 9.5, 7.3, 1.7 Hz, 1H), 6.86 – 6.79 (m, 2H), 6.77 (s, 1H), 5.50 (ddd, *J* = 10.1, 4.6, 2.9 Hz, 1H), 4.34 (dd, *J* = 8.7, 4.6 Hz, 1H), 4.19 (dd, *J* = 10.2, 8.7 Hz, 1H), 2.80 (ddq, *J* = 9.9, 7.0, 3.5, 2.9 Hz, 1H), 2.27 (s, 3H), 0.95 (d, *J* = 7.0 Hz, 3H), -0.01 (d, *J* = 6.8 Hz, 3H), -17.93 (d, *J* = 19.4 Hz, 1H); **^{13}C{^{1}H}-NMR** (126 MHz, CD_2Cl_2) δ 180.46, 159.96, 151.22, 148.69, 148.15, 142.64, 134.14, 133.81, 133.72, 133.35, 133.27, 132.72, 132.70, 131.48, 131.42, 130.81, 130.79, 130.76, 130.40, 130.37, 129.55, 128.77, 128.68, 128.38, 128.21, 128.13, 128.10, 127.93, 127.84, 127.08, 126.99, 126.12, 124.39, 117.03, 113.38, 70.15, 67.63, 48.25, 39.24, 32.82, 20.89; **^{31}P{^{1}H}-NMR** (162 MHz, CD_2Cl_2) δ -0.02 (d, *J* = 5.2 Hz).

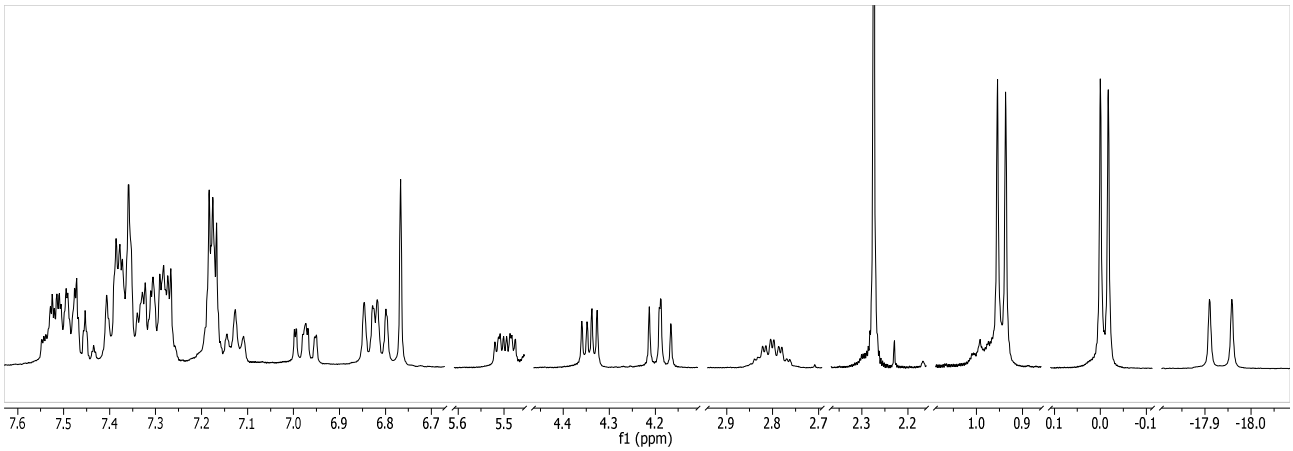

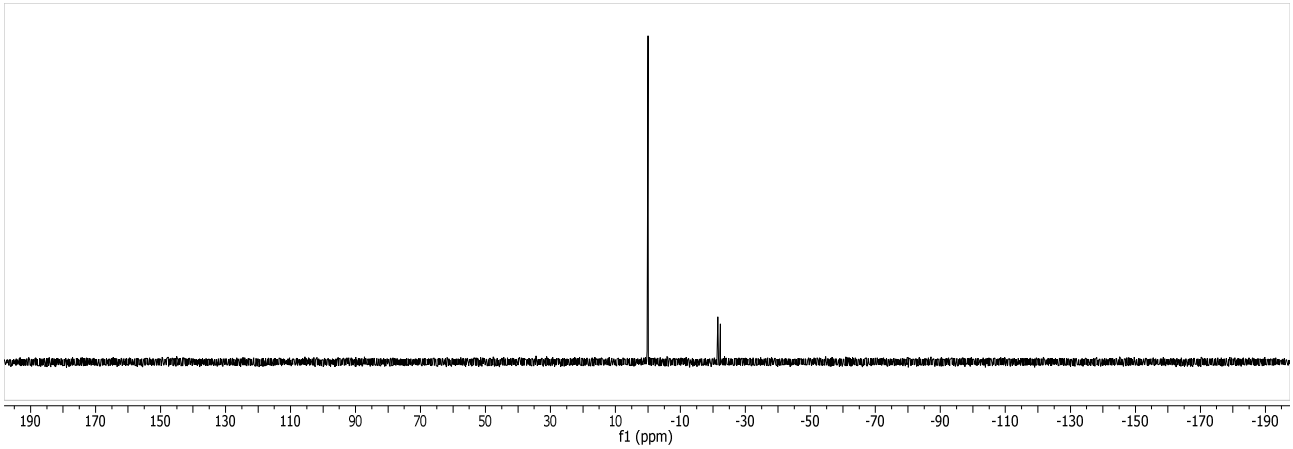

[{2-(2-(diphenylphosphino)phenyl)-4,5-dihydrooxazole}-iridium(III)-(1-isopropyl-4,4-dimethyl-3-phenyl-1,4-dihydroisoquinoline)(hydrido)(chloride)] (393)

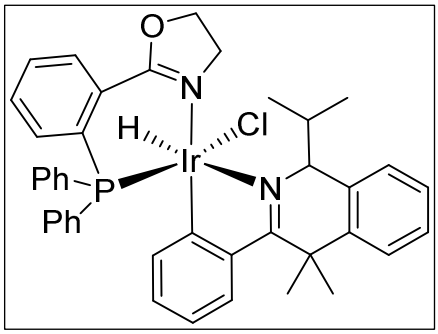

By general method, **336** (25 mg, 0.0167 mmol, 1.0 eq.) and (*R*)-**392** (5 mg, 0.018 mmol, 1.1 eq.) were reacted to afford **393** as a yellow solid. No yield was determined.

$C_{41}H_{41}ClIrN_2OP$ (M_W = 836.43 g/mol):
^{1}H-NMR (500 MHz, CD_2Cl_2) δ 7.99 – 7.92 (m, 3H), 7.88 – 7.84 (m, 1H), 7.67 – 7.63 (m, 1H), 7.58 (q, *J* = 6.7, 6.3 Hz, 2H), 7.54 – 7.47 (m, 4H), 7.41 – 7.37 (m, 1H), 7.34 – 7.30 (m, 1H), 7.29 – 7.23 (m, 3H), 7.21 (dd, *J* = 7.8, 1.6 Hz, 1H), 7.08 – 6.99 (m, 2H), 6.92 (dt, *J* = 8.1, 1.7 Hz, 1H), 6.69 (t, *J* = 7.6 Hz, 1H), 6.55 (t, *J* = 2.4 Hz, 1H), 6.28 (t, *J* = 7.5 Hz, 1H), 4.54 – 4.45 (m, 1H), 4.38 (dt, *J* = 10.9, 8.0 Hz, 1H), 4.20 (dt, *J* = 11.1, 8.7 Hz, 1H), 3.56 (ddd, *J* = 13.5, 10.9, 8.0 Hz, 1H), 3.24 (ddq, *J* = 12.5, 8.6, 5.3, 4.2 Hz, 1H), 2.19 (s, 3H), 1.93 (s, 3H), 1.17 (d, *J* = 7.1 Hz, 3H), 0.94 – 0.83 (m, 3H), 0.46 (d, *J* = 6.9 Hz, 3H), -19.13 (d, *J* = 15.4 Hz, 1H); **^{31}P{^{1}H}-NMR** (202 MHz, CD_2Cl_2) δ 13.76 (d, *J* = 13.2 Hz).

[{2-(2-(diphenylphosphino)phenyl)-4,5-dihydrooxazole}-iridium(III)-((*R*)-2-isopropyl-6-phenyl-2,3,4,5-tetrahydropyridine)(hydrido)(chloride)] (396)

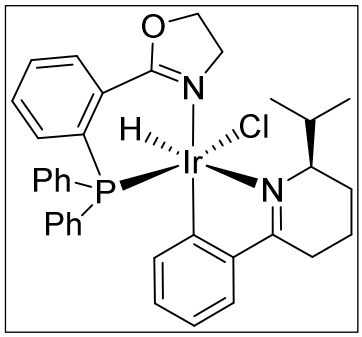

By general method, **336** (50 mg, 0.0335 mmol, 1.0 eq.) and (*R*)-**394** (7 mg, 0.035 mmol, 1.1 eq.) were reacted to afford **396** as a yellow solid. No yield was determined.

$C_{35}H_{37}ClIrN_2OP$ (M_W = 760.33 g/mol):
^{1}H-NMR (400 MHz, CD_2Cl_2) δ -19.62 (d, *J* = 15.4 Hz, 1H); **^{31}P{^{1}H}-NMR** (162 MHz, CD_2Cl_2) δ -3.05 (s) .

[{η^5-pentamethylcyclopentadienyl}-iridium(III)-((*R*)-2-isopropyl-6-phenyl-2,3,4,5-tetrahydropyridine)(chloride)] (397)[160]

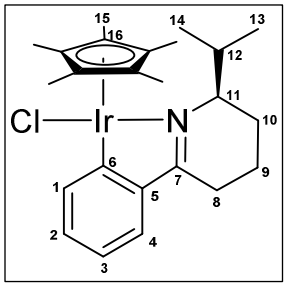

In a 10 mL flame-dried and argon-purged Schlenk vial were placed **279** (14 mg, 0.0175 mmol, 0.5 eq), (*R*)-**394** (7 mg, 0.035 mmol, 1.1 eq.) and NaOAc (7.2 mg, 0.0875 mmol, 2.5 eq.). Anhydrous CH_2Cl_2 (2.5 mL) was added and the reaction mixture was stirred at 23 °C for 18 hours. The reaction mixture was filtered over a pad of Cellite and a clear orange solution was obtained. After removal of solvents under reduced pressure, crystallisation of **397** (10 mg, 0.0173 mmol, 99%) from $CHCl_3$ to *n*-pentane failed.

$C_{25}H_{36}ClIrN$ (M_W = 578.24 g/mol):
^{1}H-NMR (500 MHz, CD_2Cl_2) δ 7.70 (ddd, *J* = 7.6, 1.2, 0.5 Hz, 1H), 7.43 (dd, *J* = 7.7, 1.4 Hz, 1H), 7.18 (td, *J* = 7.4, 1.4 Hz, 1H), 7.00 (ddd, *J* = 7.7, 7.2, 1.2 Hz, 1H), 3.96 (tdt, *J* = 6.6, 3.3, 1.5 Hz, 1H, H12), 3.13 (dtt, *J* = 17.9, 5.6, 1.5 Hz, 1H, H8), 3.06 (ddp, *J* = 10.5, 6.9, 3.7 Hz, 1H, H12), 2.88 (dddd, *J* = 18.0, 7.9, 5.8, 1.7 Hz, 1H, H8), 2.03 (m, 1H, H9), 1.94 (m, 1H, H10), 1.91 (m, 1H, H10), 1.69 (m, 1H, H9), 1.65 (s, 15H, H15), 1.13 (d, *J* = 7.1 Hz, 3H, H13), 0.75 (d, *J* = 6.6 Hz, 3H, H14).

[{η^5-pentamethylcyclopentadienyl}-iridium(III)-((*R*)-2-isopropyl-6-phenyl-2,3,4,5-tetrahydropyridine)(acetonitrile)]hexafluorophosphate (398)[160]

In a 10 mL flame-dried and argon-purged Schlenk vial were placed **397** (10 mg, 0.0175 mmol, 1.0 eq) and KPF_6 (13 mg, 0.053 mmol, 3.0 eq.). Anhydrous $MeCN/CH_2Cl_2$ (1:1, 1 mL) was added and the reaction mixture was stirred at 23 °C for 18 hours. The reaction mixture was filtered over a pad of Cellite and a clear orange solution was obtained. After removal of solvents under reduced pressure, crystallisation to afford **398** from $CHCl_3$ to *n*-pentane failed. During recrystallisation the product decomposed.

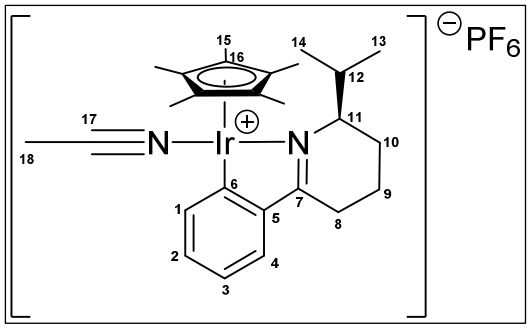

$C_{27}H_{39}F_6IrN_2P$ (M_W = 728.80 g/mol):
^{1}H-NMR (400 MHz, CD_2Cl_2) δ 7.62 (dd, *J* = 7.6, 1.2 Hz, 1H, H4), 7.41 (dd, *J* = 7.7, 1.4 Hz, 1H, H1), 7.19 (td, *J* = 7.4, 1.4 Hz, 1H, H3), 7.07 (td, *J* = 7.5, 1.2 Hz, 1H, H2), 3.70 (dq, *J* = 7.8, 3.3, 2.6 Hz, 1H, H11), 3.14 – 3.03 (m, 1H), 2.76 (dddd, *J* = 18.4, 9.6, 5.7, 2.1 Hz, 1H), 2.65 – 2.58 (m, 1H), 2.30 (s, 3H, H18), 1.59 (s, 15H, H15), 1.09 (d, *J* = 7.0 Hz, 3H, H13), 0.58 (d, *J* = 6.7 Hz, 3H, H14).

[{2-(2-(diphenylphosphino)phenyl)-4,5-dihydrooxazole}-iridium(III)-((*S*)-4-Methyl-2-phenyl-4H-benzo[e][1,3]oxazine)(hydrido)(chloride)] (401)

By general method **336** (25 mg, 0.017 mmol, 1.0 eq.) and (*S*)-**399** (3 mg, 0.013 mmol, 0.8 eq.) afforded 6 mg (0.008 mmol, 59%) of **401** as a yellow solid.

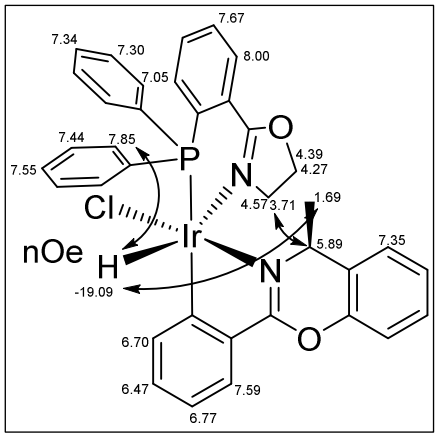

$C_{36}H_{31}ClIrN_2O_2P$ (782.29 g/mol):
^{1}H-NMR (400 MHz, CD_2Cl_2) δ 7.89 (dd, *J* = 7.7, 3.2 Hz, 1H), 7.73 (dd, *J* = 11.4, 7.3 Hz, 2H), 7.57 – 7.08 (m, 21H), 6.93 (dd, *J* = 11.1, 6.9 Hz, 2H), 6.66 (t, *J* = 7.4 Hz, 1H), 6.59 (d, *J* = 7.9 Hz, 1H), 6.38 – 6.30 (m, 1H), 5.77 (dd, *J* = 12.4, 5.9 Hz, 1H), 4.52 – 4.39 (m, 2H), 4.29 (ddd, *J* = 16.4, 12.9, 10.0 Hz, 2H), 4.17 (dt, *J* = 17.7, 8.9 Hz, 1H), 3.60 (ddd, *J* = 13.6, 11.1, 8.5 Hz, 2H), 1.58 (d, *J* = 6.6 Hz, 3H), -19.09 (d, *J* = 15.9 Hz, 1H); **^{31}P{^{1}H}-NMR** (162 MHz, CD_2Cl_2) δ 12.44 (s_{br}).

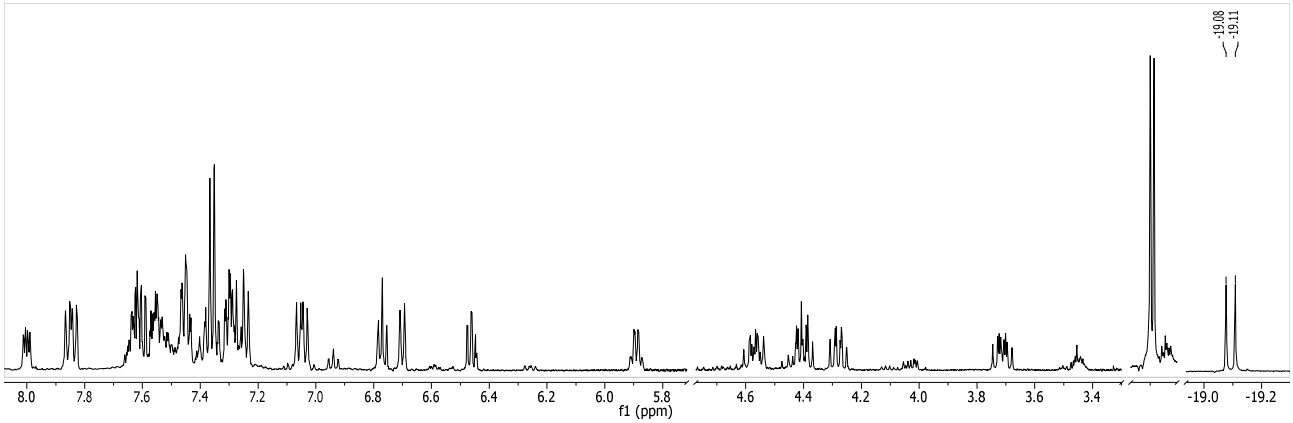

[{2-(2-(diphenylphosphino)phenyl)-4,5-dihydrooxazole}-iridium(III)-((*S*)-4-Isopropyl-2-phenyl-4H-benzo[e][1,3]oxazine)(hydrido)(chloride)] (402)

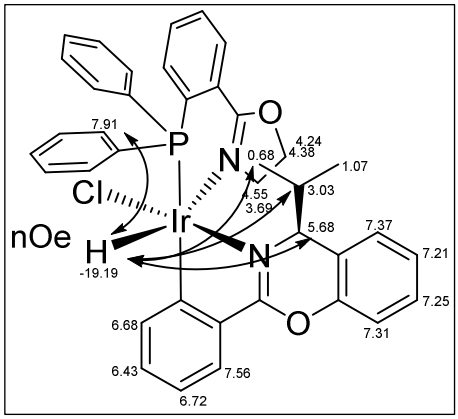

By general method **336** (25 mg, 0.017 mmol, 1.0 eq.) and (*S*)-**395** (10.5 mg, 0.042 mmol, 2.5 eq.) afforded 10.4 mg (0.013 mmol, 75%) of **402** as a yellow solid.

$C_{38}H_{35}ClIrN_2O_2P$ (810.34 g/mol):
^{1}H-NMR (400 MHz, CD_2Cl_2) δ 7.88 (dd, *J* = 6.9, 3.5 Hz, 1H), 7.75 (dd, *J* = 11.4, 7.4 Hz, 2H), 7.55 – 7.38 (m, 5H), 7.34 (td, *J* = 7.6, 2.0 Hz, 2H), 7.31 – 7.25 (m, 1H), 7.25 – 7.09 (m, 5H), 6.98 – 6.86 (m, 2H), 6.64 (t, *J* = 7.3 Hz, 1H), 6.59 (d, *J* = 7.9 Hz, 1H), 6.34 (td, *J* = 7.7, 1.6 Hz, 1H), 5.59 – 5.51 (m, 1H), 4.44 (ddd, *J* = 13.6, 10.9, 9.4 Hz, 1H), 4.31 – 4.22 (m, 1H), 4.14 (dt, *J* = 10.9, 9.0 Hz, 1H), 3.57 (ddd, *J* = 13.6, 11.1, 8.3 Hz, 1H), 2.96 – 2.84 (m, 1H), 0.94 (d, *J* = 7.1 Hz, 3H), 0.56 (d, *J* = 6.9 Hz, 3H), -19.19 (d, *J* = 15.9 Hz, 1H); **^{31}P{^{1}H}-NMR** (162 MHz, CD_2Cl_2) δ 12.49 (s).

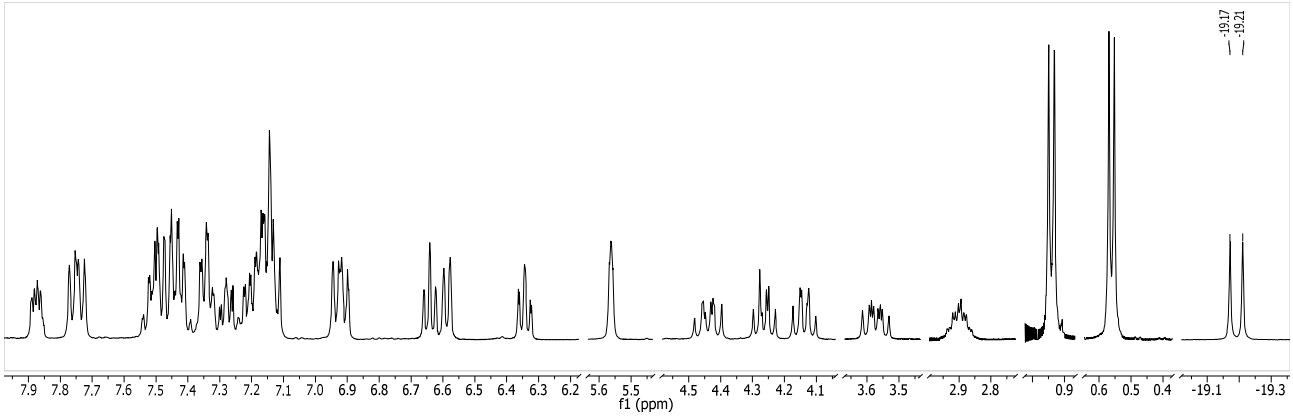

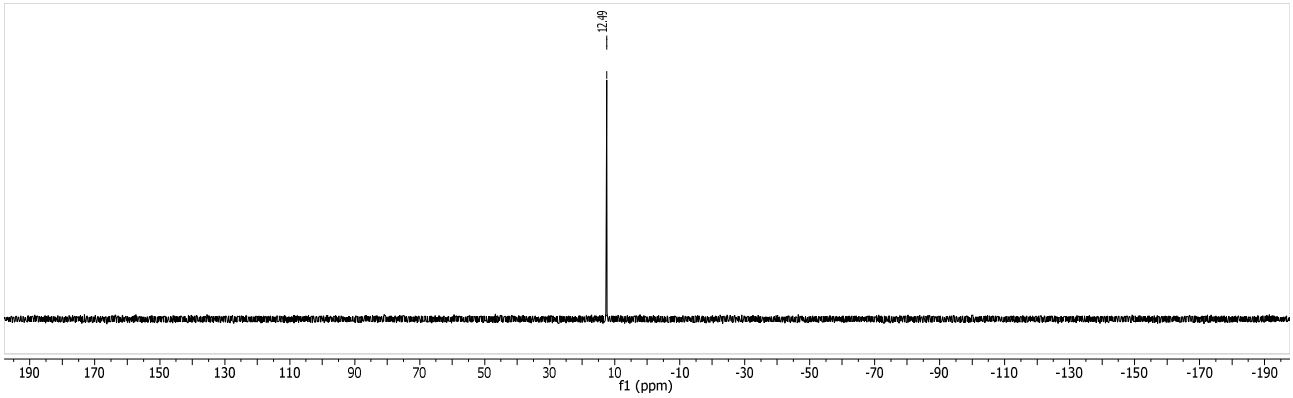

[{2-(2-(diphenylphosphino)phenyl)-4,5-dihydrooxazole}-iridium(III)-((*S*)-4-*tert*-butyl-2-phenyl-4H-benzo[e][1,3]oxazine)(hydrido)(chloride)] (403)

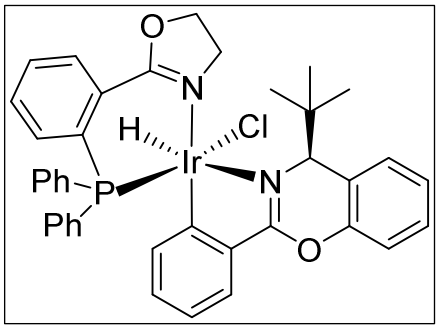

By general method **336** (50 mg, 0.0334 mmol, 1.0 eq.) and (*S*)-**400** (17.2 mg, 0.067 mmol, 2.0 eq.) afforded 15.1 mg (0.018 mmol, 55%) of **403** as a yellow solid.

$C_{39}H_{37}ClIrN_2O_2P$ (824.37 g/mol):
^{1}H-NMR (500 MHz, CD_2Cl_2) δ 7.80 (dd, *J* = 11.6, 7.6 Hz, 2H), 7.73 (dd, *J* = 8.0, 3.7 Hz, 1H), 7.55 – 7.33 (m, 8H), 7.33 – 7.10 (m, 8H), 6.94 (dd, *J* = 11.2, 7.5 Hz, 2H), 6.63 (dd, *J* = 8.1, 5.3 Hz, 2H), 6.33 (t, *J* = 7.5 Hz, 1H), 5.75 (d, *J* = 2.5 Hz, 1H), 4.27 (ddd, *J* = 13.8, 11.0, 8.7 Hz, 1H), 4.17 – 4.06 (m, 1H), 3.96 (dt, *J* = 11.1, 8.5 Hz, 1H), 3.03 (ddd, *J* = 13.7, 10.9, 8.6 Hz, 1H), 1.01 (s, 9H), -19.44 (d, *J* = 16.7 Hz, 1H); **^{31}P{1H}-NMR** (202 MHz, CD_2Cl_2) δ 12.41 (d, *J* = 10.9 Hz).

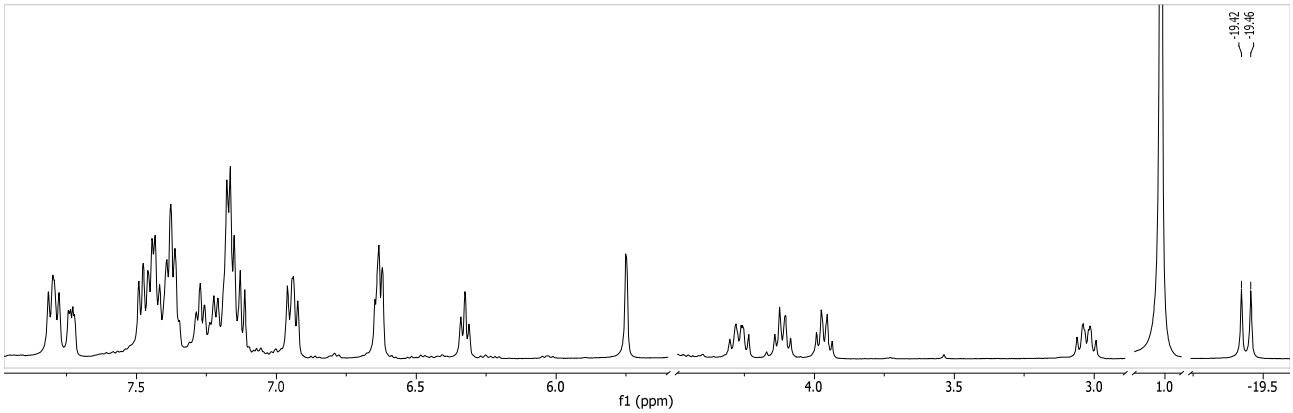

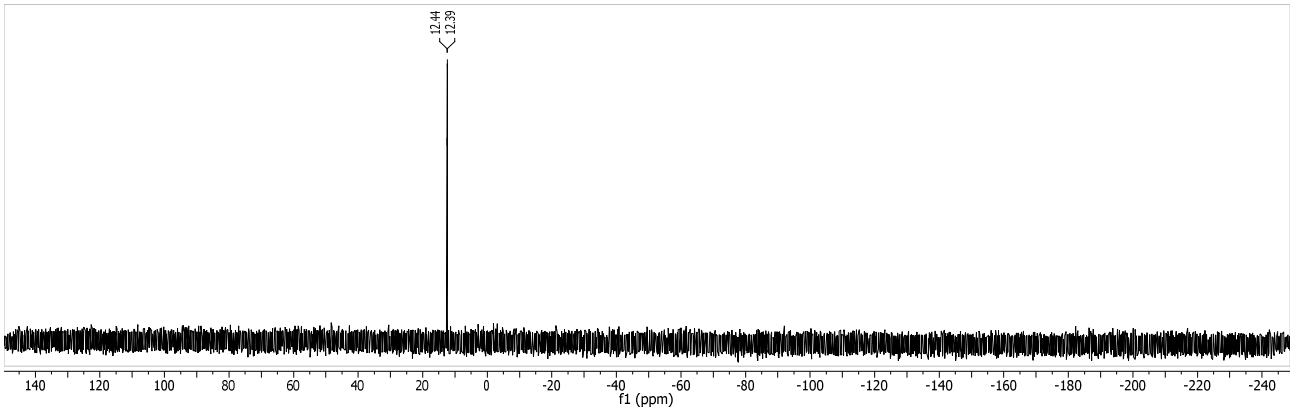

[{η^5-pentamethylcyclopentadienyl}-iridium(III)-((*S*)-4-isopropyl-2-phenyl-4H-benzo[e][1,3]oxazine)(chloride)] (404)

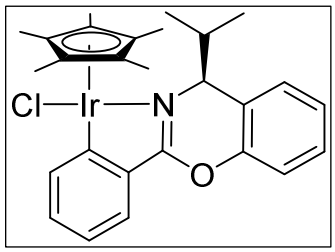

In a 10 mL flame-dried and argon-purged Schlenk vial were placed **279** (22.3 mg, 0.028 mmol, 0.5 eq), (*S*)-**395** (14.7 mg, 0.059 mmol, 2.02 eq.) and NaOAc (4 mg, 0.048 mmol, 2.4 eq.). Anhydrous CH_2Cl_2 (2.5 mL) was added and the reaction mixture was stirred at 23 °C for 18 hours. The reaction mixture was filtered over a pad of Cellite and a clear orange solution was obtained. After removal of solvents under reduced pressure, crystallisation of **404** from $CHCl_3$ to *n*-pentane afforded orange crystals suitable for X-Ray crystal structure analysis.

$C_{28}H_{34}ClIrNO$ (M_W = 628.25 g/mol):
^{1}H-NMR (400 MHz, $CDCl_3$) δ 7.76 (d, *J* = 7.4 Hz, 1H), 7.64 (dd, *J* = 7.7, 1.4 Hz, 1H), 7.36 (td, *J* = 8.0, 1.6 Hz, 1H), 7.28 – 7.24 (m, 1H), 7.24 – 7.20 (m, 1H), 7.18 (dd, *J* = 8.1, 1.2 Hz, 1H), 7.11 (dd, *J* = 7.6, 1.6 Hz, 1H), 7.03 (td, *J* = 7.6, 1.1 Hz, 1H), 4.76 (d, *J* = 3.0 Hz, 1H), 3.06 (pd, *J* = 6.9, 3.1 Hz, 1H), 1.71 (s, 15H), 1.04 (d, *J* = 7.2 Hz, 3H), 0.61 (d, *J* = 6.6 Hz, 3H); **^{13}C{^{1}H}-NMR** (101 MHz, $CDCl_3$) δ 170.09, 162.97, 149.34, 137.01, 134.52, 132.45, 128.86, 126.99, 126.80, 124.93, 121.69, 119.33, 115.96, 87.90, 66.42, 31.89, 19.84, 15.70, 9.62, 9.21; **X-Ray**: formula $C_{27}H_{31}Cl$ Ir NO, M = 613.22, F(000) = 1208, orange needle, size 0.030 · 0.040 · 0.210 mm^3, monoclinic, space group P 2_1, Z = 4, a = 9.1793(7) Å, b = 14.6017(12) Å, c = 18.2189(15) Å, α = 90°, β = 99.183(5)°, γ = 90°, V = 2410.6(3) Å^3, $D_{calc.}$ = 1.690 Mg · m^{-3}. The crystal was measured on a Bruker Kappa Apex2 diffractometer at 123K using graphite-monochromated Mo K_α-radiation with λ = 0.71073 Å, Θ_{max} = 30.033°. Minimal/maximal transmission 0.80/0.84, μ = 5.668 mm^{-1}. The Apex2 suite has been used for datacollection and integration. From a total of 52809 reflections, 14034 were independent (merging r = 0.083). From these, 10430 were considered as observed (I>2.0σ(I)) and were used to refine 560 parameters. The structure was solved by direct methods using the program SIR92. Least-squares refinement against F was carried out on all non-hydrogen atoms using the program CRYSTALS. R = 0.0422 (observed data), wR = 0.0549 (all data), GOF = 1.0993. Minimal/maximal residual electron density = -1.82/2.70 e Å^{-3}. Chebychev polynomial weights were used to complete the refinement. Plots were produced using CAMERON.

[{η^5-pentamethylcyclopentadienyl}-iridium(III)-((*R*)-N-benzylidene-1-(naphthalen-1-yl)ethanamine)(chloride)] (379)

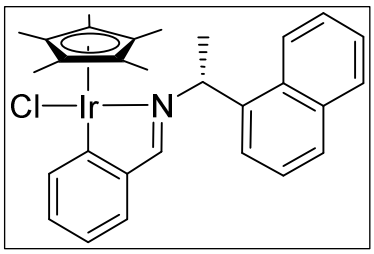

In a 10 mL flame-dried and argon-purged Schlenk vial were placed **279** (32 mg, 0.04 mmol, 0.5 eq), **370** (20.7 mg, 0.08 mmol, 2.02 eq.) and NaOAc (16.4 mg, 0.2 mmol, 5.0 eq.). Anhydrous CH_2Cl_2 (2.5 mL) was added and the reaction mixture was stirred at 23 °C for 18 hours. The reaction mixture was filtered over a pad of Cellite and a clear orange solution was obtained. After removal of solvents under reduced pressure, crystallisation of **379** from $CHCl_3$ to *n*-pentane afforded orange crystals suitable for X-Ray crystal structure analysis.

$C_{30}H_{34}ClIrN$ (M_W = 636.28 g/mol):
^{1}H-NMR (400 MHz, $CDCl_3$) δ 7.99 (s, 1H), 7.94 (dd, *J* = 8.1, 1.1 Hz, 1H), 7.90 (d, *J* = 8.1 Hz, 2H), 7.77 (d, *J* = 7.6 Hz, 1H), 7.57 (d, *J* = 6.7 Hz, 1H), 7.55 – 7.44 (m, 3H), 7.31 (dd, *J* = 7.5, 1.1 Hz, 1H), 7.15 (td, *J* = 7.5, 1.4 Hz, 1H), 6.90 (td, *J* = 7.4, 0.9 Hz, 1H), 6.04 (q, *J* = 7.0 Hz, 1H), 2.08 (d, *J* = 7.0 Hz, 3H), 1.73 (s, 15H); **^{13}C{^{1}H}-NMR** (101 MHz, $CDCl_3$) δ 174.36, 167.72, 147.08, 136.21, 134.83, 134.20, 131.63, 131.26, 129.33, 129.15, 128.82, 126.69, 126.02, 125.63, 125.49, 123.77, 121.88, 89.39, 65.42, 21.80, 9.53; **X-Ray**: formula $C_{29}H_{31}Cl_1Ir_1N_1$, M = 621.24, F(000) = 1224, orange plate, size 0.030 · 0.110 · 0.240 mm^3, orthorhombic, space group P 2_1 2_1 2_1, Z = 4, a = 8.6842(10) Å, b = 13.0346(14) Å, c = 21.364(2) Å, α = 90°, β = 90°, γ = 90°, V = 2418.3(5) Å^3, $D_{calc.}$ = 1.706 Mg · m^{-3}. The crystal was measured on a Bruker Kappa Apex2 diffractometer at 123K using graphite-monochromated Mo K_α-radiation with λ = 0.71073 Å, Θ_{max} = 45.392°. Minimal/maximal transmission 0.54/0.84, μ = 5.649 mm^{-1}. The Apex2 suite has been used for datacollection and integration. From a total of 147574 reflections, 20281 were independent (merging r = 0.044). From these, 18362 were considered as observed (I>2.0σ(I)) and were used to refine 290 parameters.

The structure was solved by Other methods using the program Superflip. Least-squares refinement against F was carried out on all non-hydrogen atoms using the program CRYSTALS. R = 0.0167 (observed data), wR = 0.0186 (all data), GOF = 1.0872. Minimal/maximal residual electron density = -1.95/1.74 e $Å^{-3}$. Chebychev polynomial weights were used to complete the refinement. Plots were produced using CAMERON.

Hydrogenations

All hydrogenation reactions were carried out in anhydrous crown-cap dichloromethane, which was used without further purification.

Procedure for the hydrogenation at elevated pressure: Imine (0.1 mmol), catalyst (2 μmol), addtive (2 μmol), and a stir bar were added to an oven-dried glass vial that had been placed in an autoclave (60 mL) and purged with argon for 5 min. Anhydrous CH_2Cl_2 (1 mL) was added by syringe under a stream of argon and the autoclave was closed. For reactions at low temperature the autoclave was immersed in a cooling bath for 60 min before starting the reaction. The autoclave was pressurized with hydrogen gas, hydrogen was released and the autoclave pressurized again. It was then placed on a stirring plate for the time indicated. After pressure release the solvent was evaporated under a stream of nitrogen.

Procedure for the hydrogenation at atmospheric pressure:
Same procedure as above, but the vials were placed in a flask equipped with 24/40 joint which was closed with a rubber septum. The flask was evacuated and purged with hydrogen gas via H_2-filled balloon (Dräger 1.5 L) three times. The solvent (1 mL) was added via syringe and the flask placed on a stirring plate for the time indicated.

The residue was suspended in pentane/ether (5:1) and filtered through a short elution plug (cotton bottom, 40x5 mm silica gel). The crude filtrate was analysed by GC for conversion before being purified by flash chromatography (SiO_2, pentane/ether 20:1, 15x2 cm) and analysed by HPLC on a chiral stationary phase for determination of the enantiomeric excess.

Derivatization for the determination of enantiomeric excess:
N-(1-cyclohexylethyl)propan-2-amine was dissolved in CH_2Cl_2 (1 mL) before acetic anhydride and triethylamine (4 drops each) were added. The solution was stirred for 30 minutes at room temperature and solvents evaporated by a stream of nitrogen. The residue was suspended in pentane/ether (5:1) and filtered through a CHROMAPHIL HPLC filter prior to GC analysis.
N-benzyl-1-cyclohexylethanamine and *N*-(1-cyclohexylethyl)cyclohexanamine was dissolved in CH_2Cl_2 (1 mL) before 1-naphtoyl chloride and triethylamine (4 drops each) were added. The solution was stirred for 30 minutes at room temperature. The product was purified by flash chromatography prior to HPLC analysis.

Assignment of the absolute configuration:

The absolute configuration of (*R*)-(-)-*N*-(1-cyclohexylethyl)aniline**,** (*R*)-(-)-*N*-(3-methylbutan-2-yl)aniline**,** (*S*)-(+)-*N*-(octan-2-yl)aniline and (*R*)-(-)-*N*-(3,3-dimethylbutan-2-yl)aniline was determined by comparison of optical rotation as well as the chiral staionary phase GC or HPLC data obtained after conducting a Buchwald-Hartwig amination.[161]

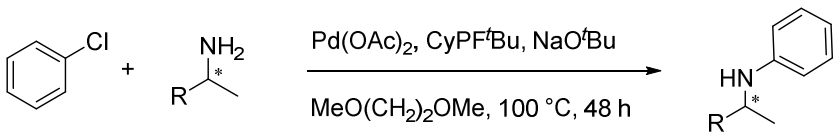

The absolute configuration of (*R*)-N-benzyl-1-cyclohexylethanamine, (*R*)-N-(1-cyclohexylethyl)butan-1-amine, (*R*)-*N*-(1-cyclohexylethyl)propan-2-amine and (*R*)-*N*-(1-cyclohexylethyl)cyclohexanamine was determined by comparison of the optical rotation and the chiral staionary phase GC or HPLC data obtained after condensation of (*R*)-cyclohexylethylamine with the corresonding aldehyde and subsequent reduction with $NaBH_4$ or $LiAlH_4$.

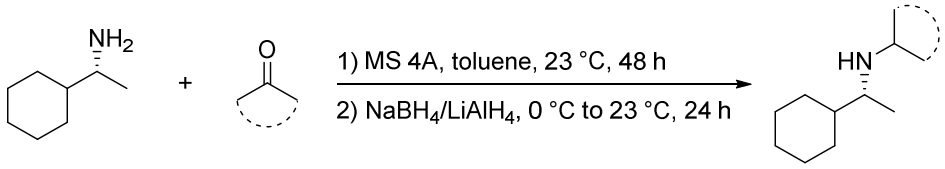

_N_-(1-phenylethyl)aniline (60)[30]

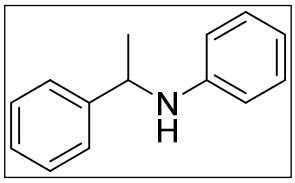

$C_{14}H_{15}N$ (M_W = 197.28 g/mol):
GC (Machary-Nagel Optima-5-Amin (0.50 µm x 0.25 µm x 30 m), 60 kPa He, 150 °C min, 7°C/min, 250 °C/10 min): t_R = 12.8 min; **HPLC** (Daicel Chiracel OD-H (2.6 x 250 mm), *n*-heptane/iso-propanol 99:1, 0.5 mL/min, 20 °C, 210 nm): t_R = 24.6 min (*S*), t_R = 33.0 min (*R*).

_N_-(1-(4-methoxyphenyl)ethyl)aniline (323)[[Schnider, 1997 #1]]

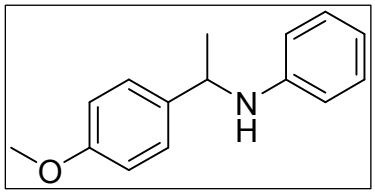

$C_{15}H_{17}NO$ (M_W = 227.31 g/mol):
GC (Machary-Nagel Optima-5-Amin (0.50 µm x 0.25 µm x 30 m), 60 kPa He, 150 °C min, 7°C/min, 250 °C/10 min): t_R = 19.6 min.

(*R*)-(-)-*N*-(1-cyclohexylethyl)aniline (97)[148]

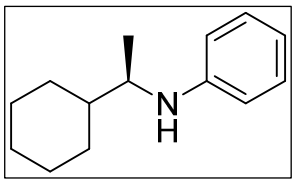

$C_{14}H_{21}N$ (M_W = 203.32 g/mol):
^{1}H-NMR (400 MHz, $CDCl_3$) δ 7.19 – 7.10 (m, 2H), 6.64 (t, *J* = 7.3 Hz, 1H), 6.57 (d, *J* = 7.7 Hz, 2H), 3.48 (s, 1H), 3.39 – 3.25 (m, 1H), 1.88 – 1.61 (m, 5H), 1.51 – 1.39 (m, 1H), 1.32 – 1.15 (m, 3H), 1.12 (d, *J* = 6.5 Hz, 3H), 1.10 – 0.99 (m, 2H); **^{13}C{^{1}H}-NMR** (101 MHz, $CDCl_3$) δ 148.10, 129.40, 116.63, 113.07, 53.10, 43.10, 29.93, 28.54, 26.79, 26.63, 26.49, 17.55; **GC** (Machary-Nagel Optima-5-Amin (0.50 µm x 0.25 µm x 30 m), 60 kPa H_2, 100 °C/2 min, 10°C/min, 250 °C/10 min): t_R = 19.6 min; **GC-MS**: (Rtx-5MS, 100.2/10.270/10): t_R = 15.7 min, *m/z* = 203 ($[M]^+$), 120; **HPLC** (Daicel Chiracel OJ-H, *n*-heptane/iso-propanol 99:1, 0.5 mL/min, 25 °C, 247/297 nm): t_R = 21.0 min ((*R*)-(-)), t_R = 24.0 min ((*S*)-(+)); **Optical Rotation**: $[\alpha]_D^{20}$ = - 19.0 (c 1.0 in $CHCl_3$, 0.75% EtOH).

(*R*)-(-)-*N*-(3-methylbutan-2-yl)aniline (513)[141]

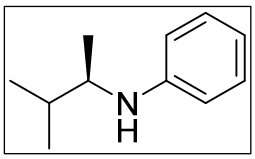

$C_{11}H_{17}N$ (M_W = 163.26 g/mol):
^{1}H-NMR (400 MHz, $CDCl_3$) δ 7.16 (t, *J* = 7.9 Hz, 2H), 6.65 (t, *J* = 7.3 Hz, 1H), 6.58 (d, *J* = 7.8 Hz, 2H), 3.48 (s, 1H), 3.42 – 3.27 (m, 1H), 1.93 – 1.77 (m, 1H), 1.10 (d, *J* = 6.4 Hz, 3H), 0.98 (d, *J* = 6.9 Hz, 3H), 0.92 (d, *J* = 6.8 Hz, 3H); **^{13}C{^{1}H}-NMR** (101 MHz, $CDCl_3$) δ 147.98, 129.41, 116.75, 113.18, 53.55, 32.35, 19.34, 17.65, 16.71; **GC-MS** (EI, 70 eV, PhMeSi, 80.2/10.270/10): tR = 10.4 min, *m/z* = 163 ($[M]^+$), 120 ($[M-(C(CH_3)_3)]^+$); **GC** (Machary-Nagel Optima-5-Amin (0.50 µm x 0.25 µm x 30 m), 60 kPa H_2, 100 °C/2 min, 10°C/min, 250 °C/7 min): t_R = 13.3 min; **HPLC** (Daicel Chiracel OJ, *n*-heptane/iso-propanol 100:0, 0.5 mL/min, 25 °C, 247/297 nm): t_R = 31.2 min ((*R*)-(-)), t_R = 36.1 min ((*S*)-(+)); **Optical Rotation**: $[\alpha]_D^{20}$ = - 49.4 (c 1.0 in $CHCl_3$, 0.75% EtOH).

(-)-*N*-(4-methylpentan-2-yl)aniline (119)[162]

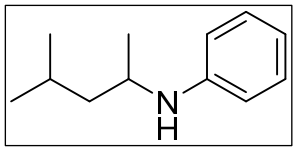

$C_{12}H_{19}N$ (M_W = 177.29 g/mol):
^{1}H-NMR (400 MHz, $CDCl_3$) δ 7.16 (t, *J* = 7.9 Hz, 2H), 6.66 (t, *J* = 7.3 Hz, 1H), 6.58 (d, *J* = 7.8 Hz, 2H), 3.60 – 3.47 (m, 1H), 3.36 (s, 1H), 1.84 – 1.68 (m, 1H), 1.48 (dt, *J* = 14.0, 7.1 Hz, 1H), 1.26 (dt, *J* = 13.7, 6.9 Hz, 1H), 1.16 (d, *J* = 6.2 Hz, 3H), 0.95 (d, *J* = 6.6 Hz, 3H), 0.91 (d, *J* = 6.6 Hz, 3H); **^{13}C{^{1}H}-NMR** (101 MHz, $CDCl_3$) δ 147.85, 129.42,

116.86, 113.15, 47.07, 46.58, 25.23, 23.10, 22.72, 21.21; **GC-MS**: (Rtx-5MS, 100.2/10.270/10): t_R = 9.8 min, *m/z* = 177 ($[M]^+$), 162, 120; **GC** (Machary-Nagel Optima-5-Amin (0.50 µm x 0.25 µm x 30 m), 60 kPa H_2, 100 °C/2 min, 10°C/min, 250 °C/7 min): t_R = 14.4 min; **HPLC** (Daicel Chiracel OJ-H, *n*-heptane/iso-propanol 99:1, 0.5 mL/min, 25 °C, 247/297 nm): t_R = 19.6 min (+), t_R = 22.5 min (-); **Optical Rotation**: $[a]_D^{20}$ = - 24.6 (c 1.10 in $CHCl_3$ 0.75% EtOH), 69% *ee*.

_N_-(1-phenylpropan-2-yl)aniline (82)[148]

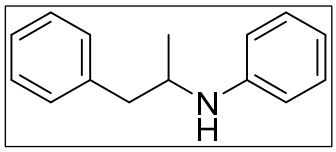

$C_{15}H_{17}N$ (M_W = 211.30 g/mol):
^{1}H-NMR (400 MHz, $CDCl_3$) δ 7.30 (m, 2H, CH_{Ar}), 7.20 (m, 5H, CH_{Ar}), 6.69 (t, *J* = 7.3 Hz, 1H, CH_{Ar}CH_{Ar}CH_{Ar}C$_{Ar}$-N), 6.63 (dd, *J* = 8.5, 0.9 Hz, 2H, CH_{Ar}C$_{Ar}$-N)), 3.77 (qdd (m), 1H, C*H*NH), 3.53 (s_{br}, 1H, N*H*), 2.95 (dd, *J* = 13.4, 4.7 Hz, 1H, CH_2Ph), 2.70 (dd, *J* = 13.4, 7.3 Hz, 1H, CH_2Ph), 1.16 (d, *J* = 6.4 Hz, 3H, CH_3CHNH); **^{13}C{^{1}H}-NMR** (101 MHz, $CDCl_3$) δ 147.37, 138.69, 129.66, 129.51, 128.47, 126.42, 117.32, 113.50, 49.49, 42.46, 20.35; **GC-MS**: (Rtx-5MS, 100.2/10.270/10): t_R = 17.3 min, *m/z* = 211 ($[M]^+$), 120, 103, 91; **GC** (Machary-Nagel Optima-5-Amin (0.50 µm x 0.25 µm x 30 m), 60 kPa H_2, 100 °C/2 min, 10°C/min, 250 °C/7 min): t_R = 21.1 min; **HPLC** (Daicel Chiracel OJ-H, *n*-heptane/iso-propanol 97:3, 0.5 mL/min, 25 °C, 208/243 nm): t_R = 21.2 min (+), t_R = 23.2 min (-); **Optical Rotation**: $[a]_D^{20}$ = +1.3 (c 0.65 in $CHCl_3$ 0.75% EtOH), 72% *ee*.

(-)-_N_-(pentan-2-yl)aniline (67)[162]

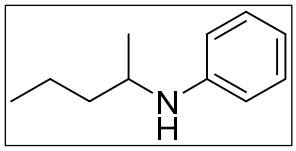

$C_{11}H_{17}N$ (M_W = 163.26 g/mol):
^{1}H-NMR (400 MHz, $CDCl_3$) δ 7.21 - 7.11 (m, 2H), 6.69 - 6.63 (m, 1H), 6.61 - 6.55 (m, 2H), 3.48 (dq, J = 21.1, 5.9 Hz, H), 3.42 (s, 1H), 1.60 - 1.51 (m, 1H), 1.48 - 1.36 (m, 3H), 1.18 (d, *J* = 6.3 Hz, 3H), 0.94 (ddd, *J* = 7.1, 4.1, 3.2 Hz, 3H);
^{13}C{^{1}H}-NMR (101 MHz, $CDCl_3$) δ 147.87 (*C*$_{Ar}$-N), 129.41 (*C*H$_{Ar}$CH$_{Ar}$C$_{Ar}$-N), 116.86 (*C*H$_{Ar}$CH$_{Ar}$CH$_{Ar}$C$_{Ar}$-N), 113.18 (*C*H$_{Ar}$C$_{Ar}$-N), 48.30 (*C*HNH), 39.60 (*C*H$_2$CHNH), 20.92 (*C*H$_2$CH$_2$CHNH), 19.47 (*C*H$_3$CHNH), 14.27 (*C*H$_3$CH$_2$); **GC-MS** (EI, 70 eV, PhMeSi, 100.2/10.270/10): t_R = 7.9 min, *m/z* = 163 ($[M]^+$), 148, 132, 120; **GC** (Machary-Nagel Optima-5-Amin (0.50 µm x 0.25 µm x 30 m), 60 kPa H_2, 100 °C/2 min, 10°C/min, 250 °C/7 min): t_R = 13.6 min; **HPLC** (Daicel Chiracel OJ-H, *n*-heptane/iso-propanol 99:1, 0.5 mL/min, 25 °C, 247/297 nm): t_R = 19.1 min (+), t_R = 21.6 min (-);
Optical Rotation: $[a]_D^{20}$ = -14.5 (c 2.565 in $CHCl_3$ 0.75% EtOH), 40% *ee*.

_N_-(6-methylhept-5-en-2-yl)aniline (543)[42]

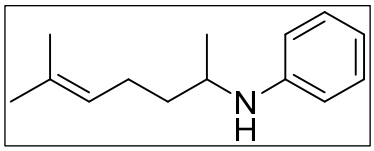

$C_{14}H_{21}N$ (M_W = 203.32 g/mol):
^{1}H-NMR (400 MHz, $CDCl_3$) δ 7.16 (t, *J* = 7.7 Hz, 2H, CH_{Ar}CH$_{Ar}$C$_{Ar}$-N), 6.66 (t, *J* = 7.3 Hz, 1H, CH_{Ar}CH$_{Ar}$CH$_{Ar}$C$_{Ar}$-N), 6.57 (d, *J* = 7.9 Hz, 2H, CH_{Ar}C$_{Ar}$-N), 5.13 (t, *J* = 7.3 Hz, 1H, (CH$_3$)$_2$C=C*H*CH$_2$), 3.47 (qd, *J* = 12.8, 6.4 Hz, 1H, C*H*NH), 3.42 (s_{br}, 1H, N*H*), 2.09 (dd, *J* = 14.7, 7.5 Hz, 2H, (CH$_3$)$_2$C=CHCH_2CH$_2$), 1.70 (s, 3H, (CH_3)$_2$C=CH), 1.60 (m, 1H, CH$_2$CH_2CHNH), 1.59 (s, 3H, (CH_3)$_2$C=CH), 1.48 (dt, *J* = 13.9, 7.1 Hz, 1H, CH$_2$CH_2CHNH), 1.19 (d, *J* = 6.2 Hz, 3H, CH_3CHNH); **^{13}C{^{1}H}-NMR** (101 MHz, $CDCl_3$) δ 147.86 (*C*$_{Ar}$-N), 132.14 ((CH$_3$)$_2$*C*=CH), 129.39 (*C*H$_{Ar}$CH$_{Ar}$C$_{Ar}$-N), 124.14 ((CH$_3$)$_2$C=*C*H), 116.91 (*C*H$_{Ar}$CH$_{Ar}$CH$_{Ar}$C$_{Ar}$-N), 113.25 (*C*H$_{Ar}$C$_{Ar}$-N), 48.23 (*C*HNH), 37.34 (*C*H$_2$CHNH), 25.86 ((*C*H$_3$)$_2$C=CH), 24.87 (C=CH*C*H$_2$), 20.93 (*C*H$_3$CHNH), 17.82 ((*C*H$_3$)$_2$C=CH); **GC-MS**: (Rtx-5MS, 100.2/10.270/10): t_R = 14.2 min, *m/z* = 203 ($[M]^+$), 188, 160, 1446, 133, 120; **GC** (Machary-Nagel Optima-5-Amin (0.50 µm x 0.25 µm x 30 m), 60 kPa H_2, 100 °C/2 min, 10°C/min, 250 °C/7 min): t_R = 17.9 min; **HPLC** (Daicel Chiracel OJ-H, *n*-heptane/iso-propanol 99:1, 0.5 mL/min, 25 °C, 247/297 nm): t_R = 16.1 min (+), t_R = 18.6 min (-); **Optical Rotation**: $[a]_D^{20}$ = -0.8 (c 1.0 in $CHCl_3$ 0.75% EtOH), 50% *ee*.

(*S*)-(+)-*N*-(octan-2-yl)aniline (335)[163]

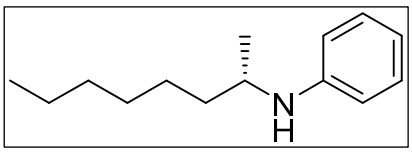

$C_{14}H_{23}N$ (M_W = 205.34 g/mol):
^{1}H-NMR (400 MHz, $CDCl_3$) δ 7.19 – 7.13 (m, 2H), 6.68 – 6.63 (m, 1H), 6.60 – 6.55 (m, 2H), 3.46 (dt, *J* = 12.6, 6.2 Hz, 1H), 3.43 – 3.37 (m, 1H), 1.62 – 1.52 (m, 1H), 1.47 – 1.34 (m, 3H), 1.34 – 1.24 (m, 6H), 1.17 (d, *J* = 6.2 Hz, 3H), 0.92 – 0.85 (m, 3H); **^{13}C{^{1}H}-NMR** (101 MHz, $CDCl_3$) δ 147.85, 129.40, 116.85, 113.19, 48.59, 37.38, 32.00, 29.52, 26.29, 22.78, 20.93, 14.25; **GC-MS**: (Rtx-5MS, 100.2/10.270/10): t_R = 14.2 min, *m/z* = 205 ($[M]^+$), 190, 132, 120; **GC** (Machary-Nagel Optima-5-Amin (0.50 µm x 0.25 µm x 30 m), 60 kPa H_2, 100 °C/2 min, 10°C/min, 250 °C/7 min): t_R = 18.07 min; **HPLC** (Daicel Chiracel OB-H, *n*-heptane/iso-propanol 99:1, 0.5 mL/min, 40 °C, 247/297 nm): t_R = 9.97 min ((*R*)-(-)), t_R = 10.71 min ((*S*)-(+)); **Optical Rotation**: $[\alpha]_D^{20}$ = +14.8 (c 1.0 in $CHCl_3$, 0.75% EtOH).

(-)-*N*-(1-cyclopentylethyl)aniline (539)

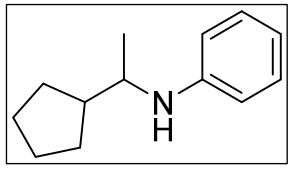

$C_{13}H_{19}N$ (M_W = 189.30 g/mol):
^{1}H-NMR (400 MHz, $CDCl_3$) δ 7.15 (t, *J* = 7.9 Hz, 2H), 6.64 (t, *J* = 7.3 Hz, 1H), 6.58 (d, *J* = 7.7 Hz, 2H), 3.47 (s, 1H), 3.32 (s, 1H), 1.92 (dq, *J* = 16.3, 8.0 Hz, 1H), 1.86 – 1.70 (m, 2H), 1.69 – 1.48 (m, 4H), 1.37 – 1.23 (m, 2H), 1.16 (d, *J* = 6.2 Hz, 3H); **^{13}C{^{1}H}-NMR** (101 MHz, $CDCl_3$) δ 148.10, 129.39, 116.73, 113.14, 53.07, 46.80, 29.91, 29.62, 25.84, 25.65, 19.49; **IR** (neat, ATR) ν/cm^{-1} = 3401 (w_{br}), 3050 (w), 3017 (w), 2950 (m), 2864 (m), 1600 (s), 1502 (s), 1450 (w), 1426 (w), 1318 (m), 1250 (w), 1178 (w), 1144 (m), 1074 (w), 993 (w), 745 (s), 692 (m); **GC-MS**: (Rtx-5MS, 100.2/10.270/10): t_R = 13.8 min, *m/z* = 189 ($[M]^+$), 120; **GC** (Machary-Nagel Optima-5-Amin (0.50 µm x 0.25 µm x 30 m), 60 kPa H_2, 100 °C/2 min, 10°C/min, 250 °C/7 min): t_R = 17.8 min; **HPLC** (Daicel Chiracel OJ-H, *n*-heptane/iso-propanol 99:1, 0.5 mL/min, 25 °C, 247/297 nm): t_R = 23.1 min (+), t_R = 26.1 min (-): **EA**: calc. C, 82.48; H, 10.12; N, 7.40; found: C, 82.19; H, 9.95; N, 7.58; **Optical Rotation**: $[\alpha]_D^{20}$ = - 0.5 (c 0.05 in $CHCl_3$ 0.75% EtOH), 76% *ee*.

(*R*)-(-)-*N*-(3,3-dimethylbutan-2-yl)aniline (98)[148]

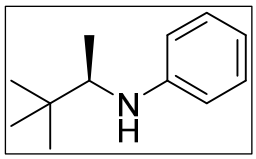

$C_{12}H_{19}N$ (M_W = 177.29 g/mol):
^{1}H-NMR (400 MHz, $CDCl_3$) δ 7.15 (t, *J* = 7.9 Hz, 2H, CH_{Ar}CH_{Ar}C$_{Ar}$-N), 6.63 (t, *J* = 7.4 Hz, 1H, CH_{Ar}CH_{Ar}CH_{Ar}C$_{Ar}$-N), 6.59 (d, *J* = 8.5 Hz, 2H, CH_{Ar}C$_{Ar}$-N), 3.39 (s_{br}, 1H, NH), 3.24 (q, *J* = 6.5 Hz, 1H, CH_3C*H*), 1.09 (d, *J* = 6.4 Hz, 3H, CH_3CHNH), 0.96 (s, 9H, C(CH_3)$_3$); **^{13}C{^{1}H}-NMR** (101 MHz, $CDCl_3$) δ 148.63 (*C*$_{Ar}$-N), 129.40 (*C*H$_{Ar}$CH$_{Ar}$C$_{Ar}$-N), 116.65 (*C*H$_{Ar}$CH$_{Ar}$CH$_{Ar}$C$_{Ar}$-N), 113.13 (*C*H$_{Ar}$C$_{Ar}$-N), 57.32 (*C*HNH), 34.92 (*C*(CH$_3$)$_3$), 26.68 (C(*C*H$_3$)$_3$), 15.98 (*C*H$_3$CHNH); **GC-MS**: (Rtx-5MS, 100.2/10.270/10): t_R = 9.3 min, *m/z* = 177 ($[M]^+$), 120; **GC** (Machary-Nagel Optima-5-Amin (0.50 µm x 0.25 µm x 30 m), 60 kPa H_2, 100 °C/2 min, 10°C/min, 250 °C/10 min): t_R = 14.1 min; **HPLC** (Daicel Chiracel OJ-H, *n*-heptane/iso-propanol 99:1, 0.5 mL/min, 25 °C, 247/297 nm): t_R = 15.1 min ((*R*)-(-)), t_R = 18.4 min ((*S*)-(+)); **Optical Rotation**: $[\alpha]_D^{20}$ = - 65.6 (c 1.0 in $CHCl_3$, 0.75% EtOH).

(*R*)-*N*-benzyl-1-cyclohexylethanamine (84)[62]

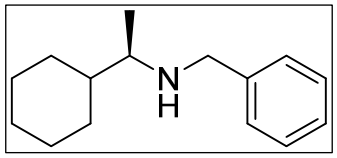

$C_{15}H_{23}N$ (M_W = 217.35 g/mol):
^{1}H-NMR (400 MHz, $CDCl_3$) δ 7.35 – 7.28 (m, 4H), 7.26 – 7.21 (m, 1H), 3.84 (d, J = 13.1 Hz, 1H), 3.71 (d, J = 13.1 Hz, 1H), 2.50 (p, J = 6.3 Hz, 1H), 1.80 – 1.62 (m, 5H), 1.36 (tdt, J = 11.5, 5.6, 3.1 Hz, 1H), 1.30 – 1.19 (m, 2H), 1.19 – 1.10 (m, 2H), 1.03 (m, 2H), 1.03 (d, J = 6.5 Hz, 3H); **GC** (Machary-Nagel Optima-5-Amin (0.50 µm x 0.25 µm x 30 m), 60 kPa H_2, 100 °C/2 min, 10°C/min, 250 °C/7 min): t_R = 20.0 min; **GC-MS**: (Rtx-5MS, 100.2/10.270/10): t_R = 16.2 min, *m/z* = 202 ($[M\text{-}CH_3]^+$), 134 ($[M\text{-}C_6H_{11}]^+$), 91; **HPLC** (Daicel Chiracel OD-H, *n*-heptane/iso-propanol 95:5, 0.8 mL/min, 25 °C, 225/287 nm): t_R = 15.9 min ((*R*)-1-naphtamide), t_R = 19.9 min ((*S*)-1-naphtamide); **Optical Rotation**: $[\alpha]_D^{20}$ = - 23.7° (c 1.0 in $CHCl_3$ 0.75% EtOH)

(*R*)-*N*-(1-cyclohexylethyl)butan-1-amine (553)

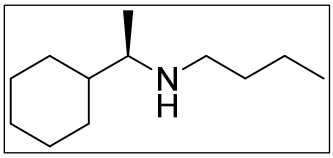

$C_{12}H_{25}N$ (M_W = 183.33 g/mol):
^{1}H-NMR (400 MHz, $CDCl_3$) δ 2.63 (dt, J = 13.9, 7.3 Hz, 1H), 2.50 (dt, J = 11.3, 7.2 Hz, 1H), 2.42 (p, J = 6.2 Hz, 1H), 1.75 (dt, J = 12.4, 3.4 Hz, 2H), 1.71 – 1.61 (m, 3H), 1.45 (p, J = 7.1 Hz, 2H), 1.34 (h, J = 7.5 Hz, 3H), 1.27 – 0.98 (m, 5H), 0.97 (d, J = 6.6 Hz, 3H), 0.91 (t, J = 7.1 Hz, 3H), 0.81 (s, 1H, NH); **^{13}C{^{1}H}-NMR** (101 MHz, $CDCl_3$) δ 58.03, 47.54, 43.06, 32.79, 30.18, 28.10, 26.96, 26.85, 26.69, 20.76, 16.98, 14.19; **IR** (neat, ATR) ν/cm^{-1} = 2956 (m), 2920 (s), 2851 (s), 2809 (w), 1463 (w), 1447 (m), 1370 (m), 1154 (w), 1124 (w), 890 (w), 834 (w); **GC** (Machary-Nagel Optima-5-Amin (0.50 µm x 0.25 µm x 30 m), 60 kPa H_2, 100 °C/2 min, 10°C/min, 250 °C/7 min): t_R = 13.7 min; **GC-MS**: (Rtx-5MS, 100.2/10.270/10): t_R = 9.0 min, *m/z* = 168 ([M-CH_3]$^+$), 140, 100 ([M-C_6H_{11}]$^+$); **GC** (MEGA Diethyl-terbutylsilyl-b-086 (0.25 µm x 0.25 mm x 25 m), 60 kPa H_2, 90 °C/10 min, 1°C/min to 120°C, 10°C/min to 180°C, 10 min): t_R = 21.7 min (*S*), t_R = 22.1 min (*R*); **HRMS:** calc. 183.1987, found: 184.2062 (M+H); **Optical Rotation**: $[\alpha]_D^{20}$ = - 12.2° (c 1.0 in $CHCl_3$ 0.75% EtOH)

(*R*)-*N*-(1-cyclohexylethyl)propan-2-amine (555)

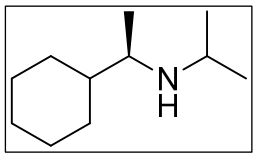

$C_{11}H_{23}N$ (M_W = 169.31 g/mol):
^{1}H-NMR (500 MHz, $CDCl_3$) δ 2.84 (hept, *J* = 6.3 Hz, 1H), 2.48 (p, *J* = 6.3 Hz, 1H), 1.73 (dt, *J* = 11.8, 3.5 Hz, 2H), 1.64 (q, *J* = 11.4 Hz, 3H), 1.28 (tq, *J* = 11.3, 3.4 Hz, 1H), 1.20 (dddd, J = 15.9, 9.7, 5.1, 3.3 Hz, 2H), 1.16 – 1.08 (m, 1H), 1.02 (d, *J* = 6.3 Hz, 3H), 0.99 (d, *J* = 6.2 Hz, 3H), 0.97 (m, 1H), 0.96 (m, H), 0.94 (d, J = 6.5 Hz, 3H), 0.63 (s, 1H, NH); **^{13}C{^{1}H}-NMR** (101 MHz, $CDCl_3$) δ 54.64, 45.69, 43.23, 30.33, 27.93, 26.97, 26.86, 26.67, 23.99, 23.27, 17.54; **GC-MS**: (Rtx-5MS, 100.2/10.270/10): t_R = 6.1 min, *m/z* = 154 ([M-CH_3]$^+$), 86; **GC** (Machary-Nagel Optima-5-Amin (0.50 µm x 0.25 µm x 30 m), 60 kPa H_2, 100 °C/2 min, 10°C/min, 250 °C/7 min): t_R = 11.1 min; **GC** (MEGA Diethyl-*tert*-butylsilyl-β-086 (0.25 µm x 0.25 mm x 25 m), 60 kPa H_2, 100 °C/2 min, 1 °C/min to 135°C, 10°C/min to 180 °C, 10 min): t_R = 32.1 min ((*R*)-acetamide), t_R = 32.4 min ((*S*)-acetamide); **IR** (neat, ATR) ν/cm^{-1} = 2959 (m), 2921 (s), 2851 (s), 1465 (m), 1448 (m), 1377 (m), 1336 (w), 1168 (m), 1134 (w), 890 (w), 834 (w), 713 (m); **HRMS:** calc. 169.1830, found: 170.1901 (M+H); **Optical Rotation**: $[\alpha]_D^{20}$ = - 13.6 (c 1.0 in $CHCl_3$ 0.75% EtOH).

(*R*)-*N*-(1-cyclohexylethyl)cyclohexanamine (557)

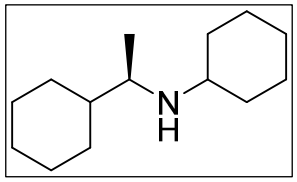

$C_{14}H_{27}N$ (M_W = 209.37 g/mol):
^{1}H-NMR (500 MHz, $CDCl_3$) δ 2.59 – 2.49 (m, 1H), 2.49 – 2.38 (m, 1H), 1.83 (t, *J* = 14.5 Hz, 2H), 1.77 – 1.55 (m, 8H), 1.33 – 0.96 (m, 11H), 0.95 (d, *J* = 6.5 Hz, 3H), 0.66 (s, 1H); **^{13}C{^{1}H}-NMR** (101 MHz, $CDCl_3$) δ 54.23, 54.09, 43.36, 34.79, 34.05, 30.32, 28.10, 26.96, 26.84, 26.67, 26.40, 25.51, 25.35, 17.85; **GC-MS** (Rtx-5MS, 50.2/30.250/5): t_R = 8.2 min, *m/z* = 209 ([M]$^+$), 194, 166, 127, 126, 44; **GC** (Machary-Nagel Optima-5-Amin (0.50 µm x 0.25 µm x 30 m), 60 kPa H_2, 100 °C/2 min, 10 °C/min, 250 °C/7 min): t_R = 17.6 min; **HPLC** (Daicel Chiracel OD-H, *n*-heptane/iso-propanol 97:3, 0.5 mL/min, 40 °C, 225/284 nm): t_R = 19.2 min ((*S*)-1-naphtamide), t_R = 21.3 min ((*R*)-1-naphtamide); **IR** (neat, ATR) ν/cm^{-1} = 2919 (s), 2848 (s), 1463 (m), 1447 (m), 1371 (m), 1155 (w), 1115 (w), 888 (w), 843 (w); **HRMS:** calc. 209.2143, found: 210.2217 (M+H); **Optical Rotation**: $[\alpha]_D^{20}$ = - 17.3 (c 1.0 in $CHCl_3$ 0.75% EtOH).

2-methylpyrrolidine[164]

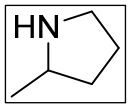

$C_5H_{11}N$ (M_W = 85.15 g/mol):
GC (Machary-Nagel Optima-5-Amin (0.50 µm x 0.25 µm x 30 m), 60 kPa H_2, 100 °C/2 min, 10 °C/min, 250 °C/7 min): t_R = 10.9 min (*N*-acetamide); **GC-MS**: (Rtx-5MS, 100.2/10.270/10): t_R = 7.3 min (*N*-acetamide), *m/z* = 127 ([M]$^+$), 112, 99, 94, 70.

2-cyclohexylpyrrolidine (570)[165]

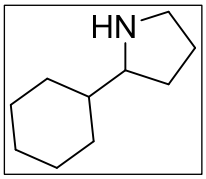

$C_{10}H_{19}N$ (M_W = 153.26 g/mol):
GC (Machary-Nagel Optima-5-Amin (0.50 µm x 0.25 µm x 30 m), 60 kPa H_2, 100 °C/2 min, 10 °C/min, 250 °C/7 min): t_R = 16.3 min (*N*-trifluoroacetamide)[166]; **GC** (MEGA Diethyl-*tert*-butylsilyl-β-086 (0.25 µm x 0.25 mm x 25 m), 60 kPa H_2, 115 °C/20 min, 10 °C/min to 180 °C, 10 min): t_R = 15.4 (*N*-trifluoroacetamide), t_R = 16.2 (*N*-trifluoroacetamide).

2-benzylpyrrolidine[167]

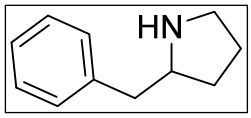

$C_{11}H_{15}N$ (M_W = 161.24 g/mol):
GC (Machary-Nagel Optima-5-Amin (0.50 µm x 0.25 µm x 30 m), 60 kPa H_2, 100 °C/2 min, 10 °C/min, 250 °C/7 min): t_R = 21.6 min (*N*-acetamide); **GC-MS**: (Rtx-5MS, 100.2/10.270/10): t_R = 17.4 min (*N*-acetamide), *m/z* = 203 ($[M]^+$), 112, 91, 70.

2-phenylpyrrolidine (573)[137]

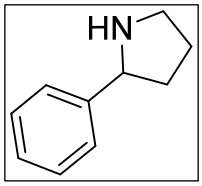

$C_{10}H_{13}N$ (M_W = 147.22 g/mol):
GC (Machary-Nagel Optima-5-Amin (0.50 µm x 0.25 µm x 30 m), 60 kPa H_2, 100 °C/2 min, 10 °C/min, 250 °C/7 min): t_R = 19.7 min (*N*-acetamide); **GC-MS**: (Rtx-5MS, 100.2/10.270/10): t_R = 15.9 min (*N*-acetamide), *m/z* = 189 ($[M]^+$), 161, 146, 130, 119, 104; **GC** (MEGA Diethyl-*tert*-butylsilyl-β-086 (0.25 µm x 0.25 mm x 25 m), 60 kPa H_2, 100 °C/2 min, 1 °C/min to 150°C, 10 °C/min to 180 °C, 10 min): t_R = 46.8 min (*N*-acetamide), t_R = 49.7 min (*N*-acetamide).

2-methylpiperidine (571)[168],[169]

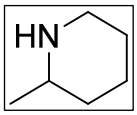

$C_6H_{13}N$ (M_W = 99.17 g/mol):
GC (Machary-Nagel Optima-5-Amin (0.50 µm x 0.25 µm x 30 m), 60 kPa H_2, 100 °C/2 min, 10 °C/min, 250 °C/7 min): t_R = 12.4 min (*N*-acetamide); **GC** (CP-Chiralsil-Dex CB (0.25 µm x 0.25 mm x 25 m), 60 kPa H_2, 100 °C/5 min, 3 °C/min to 155 °C, 5 min. 10 °C/min to 180 °C, 10 min): t_R = 13.4 min ((*R*)-*N*-acetamide), t_R = 13.9 min ((*S*)-*N*-acetamide).

2-butylpiperidine[170]

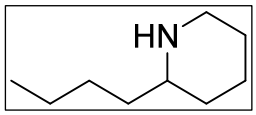

$C_9H_{19}N$ (M_W = 141.25 g/mol):
GC (Machary-Nagel Optima-5-Amin (0.50 µm x 0.25 µm x 30 m), 60 kPa H2, 100 °C/2 min, 10°C/min, 250 °C/7 min): tR = 16.5 min (A42-acetamide); **GC-MS**: (Rtx-5MS, 100.2/10.270/10): tR = 7.9 min (A42-acetamide), m/z = 183 ($[M]^+$), 468, 140, 126, 84.

2-phenylpiperidine (572)[171]

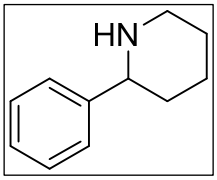

$C_{11}H_{15}N$ (M_W = 161.24 g/mol):
GC (Machary-Nagel Optima-5-Amin (0.50 µm x 0.25 µm x 30 m), 60 kPa H_2, 100 °C/2 min, 10 °C/min, 250 °C/7 min): t_R = 21.4 min (*N*-acetamide); **GC-MS**: (Rtx-5MS, 100.2/10.270/10): t_R = 17.5 min (*N*-acetamide), m/z = 203 ($[M]^+$), 174, 160, 145, 132, 104, 84, 77; **HPLC** (Daicel Chiracel OJ-H, *n*-heptane/iso-propanol 95:5, 0.5 mL/min, 25 °C, 210/254 nm): t_R = 25.1 min (*N*-acetamide), t_R = 33.7 min (*N*-acetamide).

Quinolines

2-(2-Bromophenyl)-1-phenylpropan-1-one (432)[104]

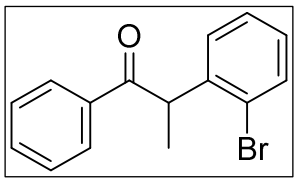

A oven-dried 50 mL Schlenk vial was evacuated and purged with Argon three times before it was transferred to the glove box. $Pd_2(dba)_3$ (58 mg, 0.063 mmol, 0.005 eq.), [(^{t}Bu)$_3$PH][BF_4] (92 mg, 0.32 mmol, 0.025 eq.) and NaO^{t}Bu (1.6 g, 16.56 mmol, 1.3 eq.) were added. Outside the glove box the reaction mixture was suspended in dry 1,4-dioxane (12.7 mL) before 1-bromo-2-iodobenzene **431** (3.6 g, 12.74 mmol, 1.0 eq.) and propiophenone **426** (2.05 g, 15.28 mmol, 1.2 eq.) were added via syringe. The reaction mixture was placed in an oil bath (90 °C) and heated for 14 hours. After cooling to room temperature, the reaction mixture was diluted with Et_2O (50 mL), washed with water (100 mL) and the organic components extracted with Et_2O (3x100 mL). After washing with brine (100 mL) the organic layer was dried over Na_2SO_4, filtered and solvents removed under reduced pressure. The residue was subjected to flash chromatography (SiO_2, n-hexane/Et_2O 25:1 to 10:1 gradient, 17x3.5 cm, 20 mL fractions) to afford **432** (1.28 g, 6.52 mmol, 70%) as a colourless oil.

$C_{15}H_{13}BrO$ (M_W = 289.17 g/mol):
m.p.: 56.5 °C; **^{1}H-NMR** (400 MHz, $CDCl_3$) δ 7.95 – 7.91 (m, 1H), 7.60 (d, *J* = 8.0 Hz, 1H), 7.48 (t, *J* = 7.4 Hz, 1H), 7.39 (t, *J* = 7.6 Hz, 1H), 7.19 (t, *J* = 8.0 Hz, 1H), 7.12 (dd, *J* = 7.8, 1.8 Hz, 1H), 7.06 (td, *J* = 7.6, 1.8 Hz, 1H), 5.11 (q, *J* = 6.8 Hz, 1H), 1.48 (d, *J* = 6.8 Hz, 2H); **GC-MS**: (Optima-5-Amine, 80.2/10.270/10): t_R = 18.2 min, *m/z* = 209 ([M-Br]$^+$), 105.

2-(2-Bromophenyl)-2-methyl-1-phenylpropan-1-one (433)

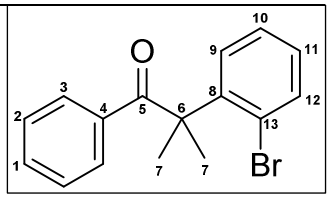

An oven-dried 50 mL three necked round-bottom flask was evacuated and purged with Argon three times before being charged with KO^{t}Bu (6.2 g, 55.3 mmol, 4.0 eq.), 18-crown-6 ether (364 mg, 1.38 mmol, 0.1 eq.) and suspended in dry THF (120 mL). The reaction mixture was cooled to 0 °C by the aid of a water/ice bath. Subsequently **432** (4.0 g, 13.83 mmol, 1.0 eq.) was dissolved in dry THF (30 mL) and cooled to 0 °C. Methyliodide (7.85 g, 55.3 mmol, 4.0 eq.) was added thereto and the resultant mixture transferred to the reaction mixture. The ice bath was removed and the resultant suspension stirred for one hour while warming to room temperature. A colour change from from clear yellow to milky white is observed. After TLC control (SiO_2, pentane/EtOAc 10:1) the suspension was filtered, the filter cake rinsed with ethyl acetate (150 mL) and solvents removed under reduced pressure. The residue was subjected to flash chromatography (SiO_2, *n*-hexane/EtOAc 20:1, 18x4.5 cm, 20 mL fractions) to afford **433** (790 mg, 2.6 mmol, 19%) as a colourless solid. Furthermore, **436** (3.02 g, 10 mmol, 72%) was isolated.

$C_{16}H_{15}BrO$ (MW = 303.19 g/mol):
m.p.: 92 °C; **^{1}H-NMR** (500 MHz, $CDCl_3$) δ 7.58 (d, *J* = 7.8 Hz, 1H, H9), 7.55 (d, *J* = 8.0 Hz, 2H, H3), 7.35 (m, 2H, H10, H12), 7.28 (t, *J* = 7.4 Hz, 1H, H1), 7.12 (t, *J* = 7.5 Hz, 2H, H2), 7.04 (t, *J* = 7.6 Hz, 1H, H11), 1.66 (s, 6H, H7); **^{13}C{^{1}H}-NMR** (126 MHz, $CDCl_3$) δ 202.66 (C5), 145.45 (C8), 136.06 (C4), 134.96 (C12), 132.08 (C1), 129.33 (C3), 128.62 (C11), 128.29 (C10), 127.96 (C2), 126.95 (C9), 123.90 (C13), 52.89 (C6), 27.53 (C7); **IR** (neat, ATR) ν/cm^{-1} = 3059 (w), 2979 (w), 2934 (w), 2907 (w), 1673 (s), 1596 (w), 1577 (w), 1464 (m), 1446 (m), 1425 (m), 1383 (m), 1362 (w), 1238 (s), 1163 (m), 1140 (m), 1022 (s), 969 (s), 909 (m), 898 (m); **MS** (EI, 70 eV): 223.1 (9.6%, [M]$^+$), 170.9 (7.5%), 168.9 (7.9%), 105 (100%); **EA**: calc. C, 63.38; H, 4.99; found: C, 62.99; H, 5.08.

(*Z*)-1-Bromo-2-(1-methoxy-1-phenylprop-1-en-2-yl)benzene (436)

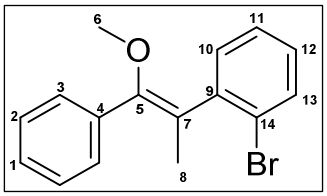

$C_{16}H_{15}BrO$ (MW = 303.19 g/mol):
^{1}H-NMR (500 MHz, $CDCl_3$) δ 7.49 (d, *J* = 7.8 Hz, 1H, H13), 7.1343 (m, 2H, H3), 7.139 (m, 2H, H2), 7.12 (m, 1H, H1), 7.06 (t, *J* = 7.4 Hz, 1H, H11), 6.98 (m, 1H, H12), 6.95 (d, *J* = 7.5 Hz, 1H, H10), 3.47 (s, 3H, H6), 2.12 (s, 3H, H8); **^{13}C{^{1}H}-NMR** (126 MHz, $CDCl_3$) δ 152.22 (C5), 143.07 (C9), 134.85 (C4), 132.68 (C13), 131.83 (C10),

129.24 (C2), 128.07 (C12), 127.79 (C3), 127.68 (C1), 127.39 (C11), 124.49 (C14), 121.09 (C7), 57.68 (C6), 17.64 (C8); **GC-MS**: (Optima-5-Amine, 100.2/10.270/10): t_R = 15.0 min, *m/z* = 302 ([M-1]$^+$), 223, 208; **IR** (neat, ATR) ν/cm^{-1} = 3054 (w), 2989 (w), 2932 (w), 2829 (w), 1649 (w), 1599 (w), 1557 (w), 1490 (m), 1466 (m), 1426 (m), 1312 (w), 1257 (m), 1237 (s), 1189 (w), 1125 (s), 1083 (s), 1024 (s), 962 (m), 919 (w).

(*Z*)-1-Bromo-2-(1-bromo-1-phenylprop-1-en-2-yl)benzene (437)

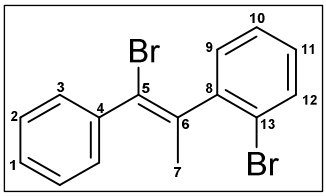

$C_{15}H_{12}Br_2$ (MW = 352.07 g/mol):
^{1}H-NMR (500 MHz, $CDCl_3$) δ 7.37 (dd, *J* = 7.0, 0.9 Hz, 1H, H13), 7.13 (dd, *J* = 8.0, 1.5 Hz, 2H, H3), 7.01 (m, 2H, H2), 6.98 (m, 1H, H1), 6.96 (td, *J* = 7.5, 1.2 Hz, 1H, H10), 6.90 (dd, *J* = 7.8, 1.7 Hz, 1H, H11), 6.85 (dd, *J* = 7.5, 1.6 Hz, 1H, H9), 2.24 (s, 3H, H7); **^{13}C{^{1}H}-NMR** (126 MHz, $CDCl_3$) δ 142.75 (C8), 140.51 (C4), 138.46 (C6), 132.77 (C12), 130.77 (C9), 129.21 (C3), 128.62 (C11), 127.88 (C1), 127.78 (C2), 127.30 (C10), 123.02 (C5), 122.71 (C13), 25.58 (C7); **GC-MS**: (Optima-5-Amine, 100.2/10.270/10): t_R = 16.4 min, *m/z* = 352 ([M]$^+$), 271, 192, 165; **IR** (neat, ATR) ν/cm^{-1} = 3053 (w), 2909 (w), 2845 (w), 1596 (w), 1586 (w), 1577 (w), 1559 (w), 1486 (w), 1467 (m), 1441 (w), 1432 (w), 1369 (w), 1278 (w), 1216 (w), 1025 (m), 1010 (m), 907 (m), 875 (m), 746 (s).

2-((*E*)-((4-Methoxyphenyl)imino)methyl)-3,4,4-trimethyl-1-phenyl-1,2,3,4 tetrahydronaphthalen-1-ol (444)

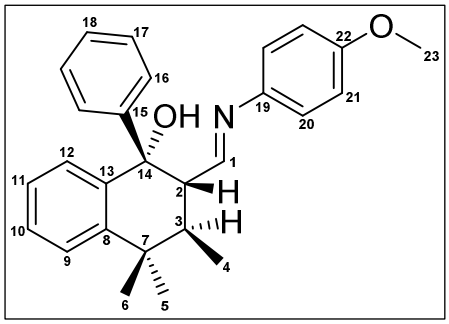

In a flame-dried and argon-purged 25 mL two-necked round-bottomed flask was placed **433** (92 mg, 0.32 mmol, 1.0 eq.) and dissolved in anhydrous THF (3 mL). The reaction mixture was cooled to -78 °C by the aid of a dry ice/acetone bath and *n*-BuLi (0.24 mL, 1.6 M, 0.38 mmol, 1.2 eq.) was added. It was stirred for 30 minutes at -78 °C. Subsequently, **443** (66.5 mg, 0.47 mmol, 1.4 eq) was added dropwise. The reaction mixture was stirred at -78 °C for 30 minutes before being allowed to warm to room temperature while stirring overnight. It was quenched with water (2 mL), extracted with CH_2Cl_2 (3x50 mL), washed with brine (20 mL), dried over Na_2SO_4, filtered and solvents removed under reduced pressure. The residue was purified by flash chromatography (SiO_2, CH_2Cl_2/TBME 6:1, 15x2.5 cm, 10 mL frctns) to afford **444** (59 mg, 0.148 mmol, 46%) as a white amorphous solid.

$C_{27}H_{29}NO_2$ (MW = 399.53 g/mol):
^{1}H-NMR (600 MHz, $CDCl_3$) δ 7.44 (dd, *J* = 8.6, 1.3 Hz, 1H, H9), 7.29 (m, 2H, H10&H12), 7.25 (m, 2H, H17), 7.22 (m, 1H, H18), 7.20 (m, 1H, H1), 7.15 (td, *J* = 7.4, 1.3 Hz, 1H, H11), 7.11 (m, 2H, H16), 6.92 (d, *J* = 8.8 Hz, 2H, H20), 6.82 (d, *J* = 8.8 Hz, 2H, H21), 4.06 (s, 1H, OH), 3.81 (s, 3H, H23), 3.02 (dd, *J* = 12.6, 7.4 Hz, 1H, H2), 2.24 (dq, *J* = 13.4, 6.8 Hz, 1H, H3), 1.50 (s, 3H, H5), 1.25 (s, 3H, H6), 0.92 (d, *J* = 6.8 Hz, 3H, H4); **^{13}C{^{1}H}-NMR** (126 MHz, $CDCl_3$) δ 165.76 (C1), 158.10 (C22), 145.36 (C8), 145.10 (C13), 144.16 (C19), 141.40 (C15), 128.51 (C16), 128.14 (C10/C12), 127.80 (C10/C12), 127.52 (C17), 127.07 (C18), 126.62 (C11), 126.45 (C9), 122.35 (C20), 114.29 (C21), 77.01 (C14), 55.60 (C23), 54.93 (C2), 37.83 (C7), 36.82 (C3), 28.87 (C5), 26.09 (C6), 14.34 (C4); **GC-MS**: (Optima-5-Amine, 100.2/10.270/25): t_R = 28.7 min, *m/z* = 380 ([M-19]$^+$), 366 ([M-33]$^+$), 243; **MS** (EI, 70 eV): 399.3 (17.6%, [M]$^+$), 380.2 (20.6%), 366.2 (16.5%), 212.1 (100%); **IR** (neat, ATR) ν/cm^{-1} = 3185 (w_{br}), 3061 (w), 3029 (w), 2941 (w), 2827 (w), 1650 (m), 1609 (w), 1582 (w), 1503 (s), 1488 (m), 1464 (m), 1447 (m), 1440 (m), 1364 (m), 1296 (w), 1244 (s), 1214 (m), 1204 (m), 1177 (m), 1166 (m), 1036 (s), 1010 (m), 830 (m), 820 (s); **HPLC** (Daicel Chiracel OD-H, *n*-heptane/iso-propanol 98:2, 0.5 mL/min, 20 °C, 210/260 nm): t_R = 13.1 min (enantiomer 1), t_R = 18.4 min (enantiomer 2).

_N_-(1-(2-Bromophenyl)ethylidene)-1-phenylmethanamine (445)[172]

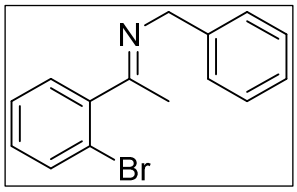

A 25mL oven-dried two-neck round-bottom flask equipped with a stirrer, reflux condenser and a stopper was evacuated and purged with Argon gas three times. Freshly activated 4Å mol sieves were added under an argon counterflow. The stopper was replaced with a septum and 1-(2-bromophenyl)ethanone (1.0 g, 5 mmol, 1.0 eq.), benzylamine (535 mg, 5 mmol, 1.0 eq.) were added and dissolved in dry CH_2Cl_2 (7 mL). The reaction mixture was stirred three days until GC-MS analysis indicated completion. The mixture was filtered, the filter cake washed with CH_2Cl_2 (20 mL) and solvents removed under reduced pressure. Kugelrohr distillation (150 °C, 0.08 mbar) afforded **445** (517 mg, 1.8 mmol, 36%) as a colourless oil.

$C_{15}H_{14}BrN$ (M_W = 288.18 g/mol):
E/Z isomers 2:1, signals overlaying: *E*-isomer: **^{1}H-NMR** (400 MHz, $CDCl_3$) δ 7.63 (dd, *J* = 8.0, 1.1 Hz, 1H), 7.44 – 7.15 (m, 7H), 7.07 (dd, *J* = 7.6, 1.7 Hz, 1H), 4.34 (dd, *J* = 15.0, 1.8 Hz, 1H, C*H*$_2$), 4.18 (d, *J* = 14.9 Hz, 1H, C*H*$_2$), 2.35 (t, *J* = 1.3 Hz, 3H, C*H*$_3$),; *Z*-isomer: **^{1}H-NMR** (400 MHz, $CDCl_3$) δ 7.63 (dd, *J* = 8.0, 1.1 Hz, 1H), 7.55 (d, *J* = 8.0 Hz, 1H), 7.44 – 7.15 (m, 8H), 4.71 (m, 2H, C*H*$_2$), 2.32 (d, *J* = 1.0 Hz, 3H, C*H*$_3$); **GC-MS**: (Optima-5-Amine, 100.2/10.270/10): t_R = 15.3 min, *m/z* = 287 ([M-1]$^+$), 208, 91.

1-(2-Bromophenyl)ethanone *O*-benzyl oxime[110]

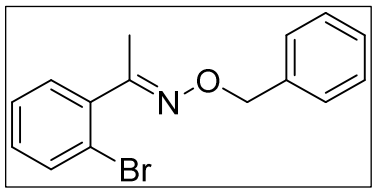

A 250 mL round bottom flask was equipped with a stirrer and charged with 1-(2-bromophenyl)ethanone (2.95 g, 14.33 mmol, 1.0 eq.), *O*-benzylhydroxylamine hydrochloride (2.6 g, 16.32 mmol, 1.1 eq.) and NaOAc (1.34 g, 16.32 mmol, 1.1 eq.). The resultant mixture was dissolved in ethanol (15 mL) and water (7.5 mL) and heated to 90 °C for 1 hour. After cooling to room temperature, diluted HCl (1.0 M, 60 mL) was added and the organic components extracted with EtOAc (100 mL). After washing with diluted HCl (1.0 M, 60 mL), diluted NaOH (1.0 M, 60 mL) and water (50 mL) the organic layer was dried over anhydrous $MgSO_4$ and filtered. Solvents were removed under reduced pressure to afford 1-(2-bromophenyl)ethanone *O*-benzyl oxime (3.9 g, 12.8 mmol, 86%) as a white solid.

$C_{15}H_{14}BrNO$ (M_W = 304.18 g/mol):
E/Z isomers, signals overlaying: **^{1}H-NMR** (400 MHz, Chloroform-*d*) δ 7.58 (ddd, *J* = 7.9, 6.6, 1.2 Hz, 1H), 7.44 – 7.40 (m, 2H), 7.37 (tt, *J* = 8.1, 1.7 Hz, 2H), 7.34 – 7.28 (m, 4H), 7.28 – 7.23 (m, 2H), 7.20 (dddd, *J* = 8.1, 7.3, 5.1, 1.9 Hz, 1H), 7.07 (dd, *J* = 7.6, 1.7 Hz, 0H), 5.24 (s, 2H), 5.07 (s, 1H), 2.26 (s, 3H), 2.16 (s, 1H); *E*-isomer: **^{13}C{^{1}H}-NMR** (101 MHz, $CDCl_3$) δ 157.69, 139.03, 138.06, 133.23, 130.43, 130.12, 128.49, 128.29, 128.12, 127.52, 121.98, 76.23, 17.01; *Z*-isomer: **^{13}C{^{1}H}-NMR** (101 MHz, $CDCl_3$) δ 155.00, 138.37, 138.13, 132.76, 129.68, 128.14, 127.88, 127.86, 127.59, 127.44, 119.94, 75.79, 21.34.

1-(2-Bromophenyl)ethanamine[110]

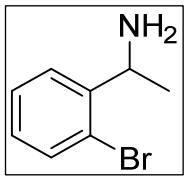

An oven-dried 100 mL 3-necked round-bottom flask was evacuated and purged with Argon three times before being charged with 1-(2-bromophenyl)ethanone *O*-benzyl oxime (3.9 g, 12.8 mmol, 1.0 eq.) and dissolved in dry THF (21 mL). Borane dimethyl sulfide complex (2.05 g, 27 mmol, 2.1 eq.) was added dropwise over the course of 30 minutes. The reaction mixture was stirred for 17 hours at room temperature. GC-MS analysis indicated complete conversion. The reaction was quenched by the dropwise addition of HCl (4.0 M, 13.5 mL) and neutralized by addition of NaOH (10% w/w, 35 mL). The organic layer was decanted and solvents removed under reduced pressure to afford 1-(2-bromophenyl)ethanamine (1.64 g, 8.2 mmol, 64%) as a colourless oil.

$C_8H_{10}BrN$ (M_W = 200.08 g/mol):
^{1}H-NMR (400 MHz, $CDCl_3$) δ 7.52 (m, 2H), 7.32 (t, J = 7.6 Hz, 1H), 7.09 (t, J = 7.7 Hz, 1H), 4.50 (q, J = 6.6 Hz, 1H), 1.56 (s, 3H), 1.38 (d, J = 6.6 Hz, 3H); **^{13}C{^{1}H}-NMR** (101 MHz, $CDCl_3$) δ 146.32, 133.01, 128.35, 127.96, 126.64, 123.26, 50.14, 23.92; **GC-MS**: (Optima-5-Amine, 100.2/10.270/10): t_R = 8.5 min, *m/z* = 184 ([M-CH_3]$^+$), 157, 108.

---

tert-Butyl (1-(2-bromophenyl)ethyl)carbamate (448)

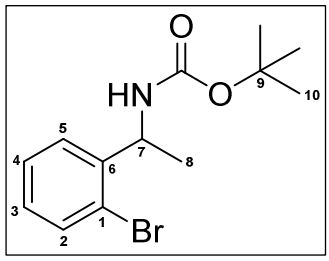

In a 50 mL round-bottom flask was placed 1-(2-bromophenyl)ethanamine (500 mg, 2.5 mmol, 1.0 eq.) and dissolved in a water/THF mixture (1:1, 15 mL). After cooling to 0 °C, $NaHCO_3$ (630 mg, 7.5 mmol, 3.0 eq.) and di-tert-butyl dicarbonate (654 mg, 3 mmol, 1.2 eq.) were added. The reaction mixture was stirred at 0 °C for 30 minutes before the cooling bath was removed and stirring continued at room temperature overnight. GC-MS analysis indicated full conversion. The reaction mixture was transferred to a separation funnel and organic components extracted with Et_2O (2x100 mL). The combined organic layers were dried over Na_2SO_4, filtered and solvents removed under reduced pressure. The residue was subjected to flash chromatography (SiO_2, pentane/EtOAc (4:1), 16x3.5 cm, 20 mL fractions) to afford **448** (600 mg, 2 mmol, 80%) as a white solid.

$C_{13}H_{18}BrNO_2$ (M_W = 300.19 g/mol):
m.p.: 97 °C; **^{1}H-NMR** (500 MHz, $CDCl_3$) δ 7.52 (d, *J* = 7.9 Hz, 1H, H2), 7.33 (d, *J* = 7.8 Hz, 1H, H5), 7.28 (t, *J* = 7.5 Hz, 1H, H4), 7.09 (td, *J* = 7.5, 1.9 Hz, 1H, H3), 5.11 (m, 1H, H7), 4.99 (s, 1H, NH), 1.44 (s_{br}, 9H, H10), 1.42 (m_{br}, 3H, H8); **^{13}C{^{1}H}-NMR** (125 MHz, $CDCl_3$) δ C=O not detected, 143.26 (C6), 133.35 (C2), 128.57 (C3), 127.83 (C4), 126.52 (C5), 122.73 (C1), 50.34 (C7), 28.49 (C10), 27.54 (C9), 21.86 (C8); **IR** (neat, ATR) ν/cm^{-1} = 3438 (w_{br}), 3337 (w_{br}), 3059 (w), 2981 (m), 2927 (m), 2854 (w), 1676 (m), 1663 (m), 1519 (m), 1444 (s), 1363 (s), 1301 (m), 1245 (s), 1233 (m), 1118 (m), 1104 (m), 1064 (s), 1000 (m), 971 (m), 753 (s); **GC-MS**: (Optima-5-Amine, 100.2/10.270/10): t_R = 14.2 min, *m/z* = 230, 210, 184, 164; **EA**: calc.: C, 52.01; H, 6.04; N, 4.67; found: C, 53.55; H, 6.25; N, 5.04.

***N*-(1-(2-Bromophenyl)ethyl)-4-methylbenzenesulfonamide (447)**

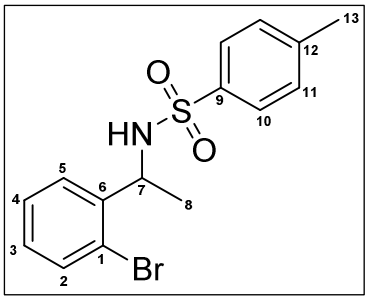

In a 50 mL round-bottom flask was placed 1-(2-bromophenyl)ethanamine (500 mg, 2.5 mmol, 1.0 eq.), 4-methylbenzene-1-sulfonyl chloride (491 mg, 2.575 mmol, 1.03 eq.) and K_2CO_3 (1.1 g, 8 mmol, 4.0 eq.). The reaction mixture was dissolved in a water/Et_2O mixture (1:1, 7 mL) and vigorously stirred at room temperature for 2 hours. TLC analysis (SiO_2, pentane/EtOAc 2:1) indicated complete consumption of starting material. The organic components were extracted with dichlormethane (3x 20 mL) and the combined organic layers dried over anhydrous $MgSO_4$. After filtration and solvent removal under reduced the residue was subjected to flash chromatography (SiO_2, pentane/EtOAc (2 :1), 15x3.5 cm, 20 mL fractions) to afford **447** (512 mg, 1.45 mmol, 58%) as a white solid.

$C_{15}H_{16}BrNO_2S$ (M_W = 354.26 g/mol):
m.p.: 120 °C; **^{1}H-NMR** (400 MHz, $CDCl_3$) δ 7.63 (d, *J* = 8.3 Hz, 2H, H10), 7.37 (dd, *J* = 8.0, 1.1 Hz, 1H, H2), 7.22 (dd, *J* = 7.8, 1.6 Hz, 1H, H5), 7.13 (m, 3H, H4, H11), 6.99 (td, *J* = 7.9, 1.7 Hz, 1H, H3), 5.50 (d, *J* = 7.3 Hz, 1H, N*H*), 4.87 (m, 1H, H7), 2.35 (s, 3H, H13), 1.39 (d, *J* = 6.9 Hz, 3H, H8); **^{13}C{^{1}H}-NMR** (101 MHz, $CDCl_3$) δ 143.32 (C6), 141.30 (C9), 137.12 (C12), 132.97 (C2), 129.49 (C11), 128.71 (CH_{Ar}), 127.88 (CH_{Ar}), 127.83 (CH_{Ar}), 127.26 (C10), 122.08 (C1), 53.21 (C7), 23.09 (C13), 21.58 (C8); **IR** (neat, ATR) ν/cm^{-1} = 3432 (w_{br}), 3337 (w_{br}), 3058 (w), 2981 (w), 2926 (m), 2854 (w), 1663 (m), 1463 (m), 1444 (m), 1363 (m), 1257 (m), 1246 (m), 1231 (m), 1076 (m), 1064 (s), 1052 (s), 1031 (m), 1001 (m), 971 (m), 823 (m), 756 (s); **EA**: calc.: C, 50.86; H, 4.55; N, 3.95; found: C, 51.31; H, 4.68; N, 4.23.

(1-(2-Bromophenyl)ethoxy)(_tert_-butyl)dimethylsilane (419)[100]

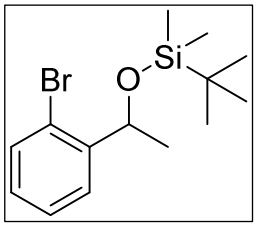

In a 25 mL round-bottom flask was placed imidazole (1.02 g, 15.0 mmol, 3.0 eq.) and **425** (804 mg, 6.0 mmol, 1.2 eq.). The flask was evacuated and purged with argon three times before **424** (1.0 g, 5.0 mmol, 1.0 eq.) was added and the resultant mixture dissolved in dry DMF (5 mL). The reaction mixture was stirred overnight. TLC control (SiO_2, *n*-pentane/EtOAc 5:1) indicated complete consumption of starting material. DMF was removed by aid of a second cooling trap under high vacuum and the residue was

suspended in *n*-pentane/EtOAc (5:1) and subjected to flash chromatography (SiO_2, 12x3.5 cm, 20 mL fractions) to afford **419** (1.6 g, 5 mmol, 99%) as a colourless oil.

$C_{14}H_{23}BrOSi$ (M_W = 315.32 g/mol):
^{1}H-NMR (400 MHz, $CDCl_3$) δ 7.61 (dd, *J* = 7.8, 1.4 Hz, 1H), 7.46 (dd, *J* = 8.0, 0.7 Hz, 1H), 7.31 (t, *J* = 7.5 Hz, 1H), 7.08 (td, *J* = 7.9, 1.6 Hz, 1H), 5.16 (q, *J* = 6.2 Hz, 1H), 1.38 (d, *J* = 6.2 Hz, 3H), 0.90 (s, 10H), 0.06 (s, 3H), -0.03 (s, 3H); **^{13}C{^{1}H}-NMR** (101 MHz, $CDCl_3$) δ 146.04, 132.31, 128.33, 127.71, 127.55, 120.89, 70.02, 26.01, 25.70, 18.37, -4.75, -4.81; **GC-MS**: (Optima-5-Amine, 100.2/7.270/10): t_R = 14.1 min, *m/z* = 301 ([M-CH_3]$^+$).

2-(2-(1-((*tert*-Butyldimethylsilyl)oxy)ethyl)phenyl)-1-phenylpropan-1-one (428)

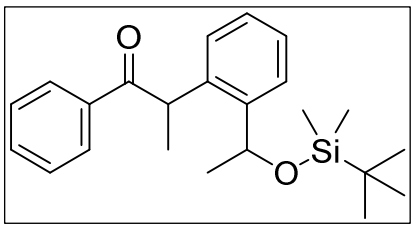

A oven-dried 25 mL Schlenk tube was evacuated and purged with argon three times and transferred to the glove box. $Pd(dba)_2$ (60 mg, 0.1 mmol, 0.05 eq.), D^{t}BuPF (60 mg, 0.125 mmol, 0.06 eq.) and NaO^{t}Bu (310 mg, 3.33 mmo, 1.6 eq.) were added and the vial brought out of the glove box to add **419** (656 mg, 2.08 mmol, 1.0 eq.) and **426** (300 mg, 2.5 mmol, 1.2 eq.). The reaction mixture was then suspended in dry 1,4-dioxane (5 mL), sealed and heated to 90 °C for 24 hours. The reaction was allowed to cool to room temperature, quenched with water and organic components extracted with *tert*-butylmethylether (3 x 25 mL). Solvents were reduced under reduced pressure and the sticky brown residue was subjected to flash chromatography (SiO_2, 19x3 cm, cyclohexane/Et_2O 20:1, 20 mL fractions) to afford **428** (652.4 mg, 1.77 mmol, 85%) as a colourless oil.

$C_{23}H_{32}O_2Si$ (M_W = 368.58 g/mol):
mixture of 2 diastereomers and 2 rotamers overlaying:^{1}**H-NMR** (500 MHz, $CDCl_3$) δ 7.86 (d, *J* = 7.5 Hz, 1H), 7.83 (d, *J* = 7.5 Hz, 1H), 7.60 (d, *J* = 7.7 Hz, 1H), 7.57 (d, *J* = 7.8 Hz, 1H), 7.47 (t, *J* = 7.4 Hz, 1H), 7.36 (t, *J* = 7.7 Hz, 2H), 7.31 (q, *J* = 7.9 Hz, 1H), 7.23 (t, *J* = 7.0 Hz, 1H), 7.14 (dd, *J* = 17.6, 7.7 Hz, 1H), 7.04 (d, *J* = 7.6 Hz, 1H), 5.32 (q, *J* = 6.2 Hz, 1H), 5.21 (q, *J* = 6.3 Hz, 1H), 4.92 – 4.83 (m, 1H), 1.55 (d, *J* = 5.3 Hz, 2H), 1.52 (d, *J* = 6.8 Hz, 2H), 1.48 (d, *J* = 6.3 Hz, 1H), 1.45 (d, *J* = 6.3 Hz, 2H), 1.41 (d, *J* = 6.4 Hz, 1H), 0.89 (d, *J* = 6.3 Hz, 5H), 0.08 (s, 1H), 0.06 (s, 1H), 0.05 (s, 1H), -0.03 (s, 2H), -0.06 (s, 1H); **GC-MS**: (Optima-5-Amine, 100.2/10.270/10): t_R = 19.8 min, *m/z* = 353 ([M-CH_3]$^+$), 311 ([M-C_4H_9]$^+$), 219.

2-(2-(1-((*tert*-butyldimethylsilyl)oxy)ethyl)phenyl)-2-methyl-1-phenylpropan-1-one (427)

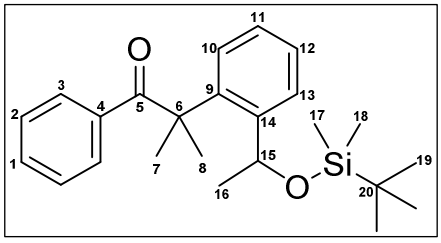

A oven-dried 50 mL Schlenk vial was evacuated and purged with Argon three times before it was transferred to the glove box. $Pd(dba)_2$ (132 mg, 0.32 mmol, 0.1 eq.), [(^{t}Bu)$_3$PH][BF_4] (202 mg, 0.7 mmol, 0.22 eq.) and NaO^{t}Bu (487 mg, 5.07 mmol, 1.6 eq.) were added. Outside the glove box the reaction mixture was suspended in dry 1,4-dioxane (3 mL) before **419** (1.0 g, 3.17 mmol, 1.0 eq.) and **418** (564 mg, 3.81 mmol, 1.2 eq.) were added via syringe. The reaction mixture was placed in an oil bath (100 °C) and heated for 2 days. After cooling to room temperature, the reaction mixture was transferred to a separating funnel, the Schlenk vial rinsed with Et_2O (10 mL) and the reaction quenched with water (20 mL). The organic components were extracted with Et_2O (3x20 mL) and the combined organic layers dried over anhydrous $MgSO_4$. After filtration and solvent removal under reduced pressure the residue was subjected to flash chromatography (SiO_2, cyclohexane/Et_2O 50:1, 19x5.5 cm, 20 mL fractions) to afford **427** (522 mg, 1.36 mmol, 43%) as a white solid.

$C_{24}H_{34}O_2Si$ (M_W = 382.61 g/mol):
^{1}H-NMR (500 MHz, $CDCl_3$) δ 7.62 (m, 1H, H13), 7.59 (m, 2H, H3), 7.56 (m, 1H, H10), 7.39 (m, 1H, H1), 7.36 (m, 1H, H11), 7.35 (m, 1H, H12), 7.21 (t, *J* = 7.6 Hz, 2H, H2), 4.99 (q, *J* = 6.0 Hz, 1H, H15), 1.63 (s, 3H, H7), 1.60 (s, 3H, H8), 0.93 (d, *J* = 6.0 Hz, 3H, H16), 0.72 (s, 9H, H19), 0.00 (s, 3H, H17), -0.27 (s, 3H, H18); **^{13}C{^{1}H}-NMR** (126 MHz, $CDCl_3$) δ 204.25 (C5), 146.32 (C14), 140.19 (C9), 136.08 (C4), 132.35

(C1), 129.99 (C3), 128.75 (C13), 128.25 (C2), 127.80 (C11), 127.61 (C12), 66.03 (C15), 51.71 (C6), 29.27 (C8), 28.91 (C7), 27.39 (C16), 25.80(C19), 17.96 (C20), -3.98 (C18), -4.77 (C17); **GC-MS**: (Optima-5-Amine, 100.2/10.270/10): t_R = 19.8 min, *m/z* = 367 ($[M\text{-}CH_3]^+$), 325 ($[M\text{-}C_4H_9]^+$), 233, 205; **IR** (neat, ATR) ν/cm^{-1} = 2955 (w), 2926 (w), 2845 (w), 1663 (s), 1462 (m), 1444 (m), 1256 (m), 1246 (m), 1102 (s), 1075 (s), 1052 (m), 1020 (m), 1007 (m), 957 (s), 823 (s); **EA**: calc.: C, 75.34; H, 8.96; found: C, 75.04; H, 8.99; **HRMS**: calculated: 405.2220 $[M+Na]^+$, found: 405.2225.

1,4,4-trimethyl-3-phenylisochroman-3-ol (435)

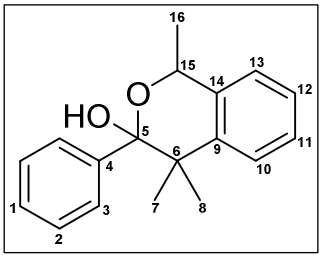

An oven-dried and Argon-purged 25 mL 2-neck round-bottom flask was charged with **427** (572 mg, 1.495 mmol, 1.0 eq.) and dissolved in dry THF (5 mL). Then TBAF (430 mg, 1.65 mmol, 1.1 eq.) was added and the resultant reaction mixture heated to 50 °C for 2 hours. TLC control (SiO_2, pentane/EtOAc 10:1) indicated complete consumption of starting material. The reaction mixture was allowed to cool to room temperature and transferred to a separation funnel. Water (5 mL) was added and organic components were extracted with CH_2Cl_2 (3x10 mL). After drying over $MgSO_4$, filtration, removal of solvents under reduced pressure the residue was subjected to flash chromatography (SiO_2, pentane/Et_2O 4:1, 17x3.5 cm, 20 mL fractions) to afford **435** (347 mg, 1.295 mmol, 86%) as a white crystalline solid.

$C_{18}H_{20}O_2$ (M_W = 268.35 g/mol):
m.p.: 115 °C; **^{1}H-NMR** (500 MHz, $CDCl_3$) δ 7.70 (m, 2H, H3), 7.40 (m, 1H, H10), 7.38 (m, 2H, H2), 7.35 (m, 1H, H1), 7.25 (m, 1H, H11), 7.23 (m, 1H, H12), 7.13 (m, 1H, H13), 5.26 (q, *J* = 6.6 Hz, 1H, H15), 2.68 (s, 1H, OH), 1.67 (d, *J* = 6.6 Hz, 3H, H16), 1.36 (s, 3H, H7), 1.09 (s, 3H, H8); **^{13}C{^{1}H}-NMR** (126 MHz, $CDCl_3$) δ 141.89 (C4), 141.78 (C9), 137.26 (C14), 128.09 (C1), 128.06 (C3), 127.36 (C2), 126.89 (C11), 125.92 (C12), 125.68 (C10), 124.19 (C13), 100.50 (C5), 68.30 (C15), 41.53 (C6), 30.70 (C8), 23.04 (C16), 22.19 (C7); **IR** (neat, ATR) ν/cm^{-1} = 3439 (w_{br}), 3057 (w), 2981 (w), 2926 (w), 2853 (w), 1663 (w), 1491 (w), 1463 (w), 1444 (w), 1361 (w), 1257 (w), 1230 (m), 1102 (w), 1081 (w), 1052 (w), 970 (m), 833 (w); **EA**: calc.: C, 80.56; H, 7.51; found: C, 80.20; H, 7.57.

[{di-η^5-cyclopentadienyl}(dimethyl)titanocene][116]
''Petasis reagent''

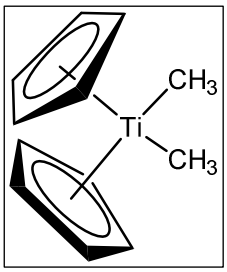

A 100 mL oven-dried three-neck round bottom flask was charged with a stirrer, dropping funnel, claisen adapter, thermometer and a septum before being charged with [{di-η^5-cyclopentadienyl}(dichloro)titanocene] (4.15 g, 16.7 mmol, 1.0 eq.) and suspended in dry toluene (50 mL). The reaction mixture was cooled to 0 °C and methyl magnesium chloride (3.0 M, 12.6 mL, 37.8 mmol, 2.25 eq.) was added dropwise not allowing the reaction mixture to warm up more than 8 °C. After addition stirring was continued for 1 hour at 0 °C. Another 250 mL three-necked round-bottom flask was equipped with a thermometer, septum and a gas inlet, evacuated and purged with argon three times. NH_4Cl (700 mg, 13 mmol, 0.78 eq.), dissolved in water (11.7 mL), was added and cooled to 0 °C. The titanocene solution was transferred slowly *via* cannula not allowing the reaction mixture to warm up to more than 5 °C. The titanocene flask was rinsed with dry toluene (3 mL). A 250 mL separation funnel was charged with the quenched reaction mixture, the aeqeous layer separated and the organic layer washed with cold water (3x10 mL), brine (3x10 mL) sequentually. The organic layer was then dried over anhydrous Na_2SO_4, filtered and the solvents carefully removed under reduced pressure to afford the *Petasis reagent* as a 15.4 % *w/w* solution in toluene.

^{1}H-NMR (400 MHz, $CDCl_3$) δ 6.06 (s, 10H), -0.15 (s, 6H).

---

tert-Butyldimethyl(1-(2-(2-methyl-3-phenylbut-3-en-2-yl)phenyl)ethoxy)silane (449)

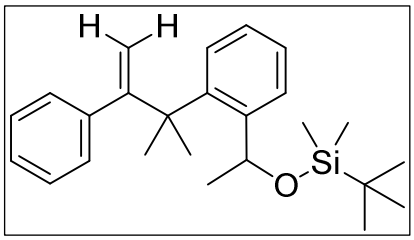

A 25 mL Schlenk vial equipped with a magnetic stirrer was oven-dried, evacuated and purged with Argon three times before being charged with **427** (300 mg, 0.784 mmol, 1.0 eq.) and dissolved in dry toluene (2 mL). Subsequently *Petasis reagent* (408 mg, 1.96 mmol, 2.5 eq.) was added and the Schlenk tube wrapped up in alumina foil. It was then placed in a oil bath and heated to 70 °C for 41 hours. After cooling to room temperature, the crude reaction mixture was subjected to elution chromatography (SiO_2, EtOAc) to afford a orange solution. After removal of solvent under reduced pressure the residue was purified by flash chromatography (SiO_2, cyclohexane/Et_2O 10:1, 17x2.5 cm, 20 mL fractions) to afford **449** (115 mg, 0.302 mmol, 39%) as an orange oil. *The product could not be obtained in a pure fashion and therefore the crude was directly used in the deprotection step. The silyl protection group readily comes off in $CDCl_3$.*

$C_{25}H_{36}OSi$ (M_W = 380.64 g/mol):
^{1}H-NMR (500 MHz, $CDCl_3$) δ 7.70 (d, *J* = 7.8 Hz, 1H), 7.33 – 7.28 (m, 1H), 7.24 (d, *J* = 7.8 Hz, 1H), 7.19 – 7.15 (m, 2H), 7.12 (t, *J* = 7.4 Hz, 2H), 6.87 (d, *J* = 7.3 Hz, 2H), 5.72 (q, *J* = 6.0 Hz, 1H), 5.27 (s, 1H), 5.14 (s, 1H), 1.52 (s, 3H), 1.51 (s, 3H), 1.36 (d, *J* = 5.9 Hz, 3H), 0.86 (s, 9H), 0.09 (s, 3H), -0.10 (s, 3H); **^{13}C{^{1}H}-NMR** (126 MHz, $CDCl_3$) δ 158.22, 146.89, 142.59, 141.93, 128.87, 128.45, 127.51, 126.98, 126.89, 126.80, 126.10, 113.92, 66.50, 44.56, 31.09, 30.86, 27.44, 25.96, 18.09, -3.67, -4.13; **GC-MS**: (Optima-5-Amine, 100.2/10.270/10): t_R = 18.6 min, *m/z* = 365 ($[M-CH_3]^+$), 323 ($[M-C_4H_9]^+$), 305, 205; **IR** (neat, ATR) ν/cm^{-1} = 3435 (w_{br}), 3059 (w), 2955 (m), 2927 (m), 2854 (m), 1663 (m), 1490 (w), 1462 (m), 1444 (m), 1386 (w), 1363 (m), 1251 (m), 1102 (m), 1075 (s), 957 (m), 831 (m); **HRMS**: calculated: 403.2428 $[M+Na]^+$, found: 403.2430.

1-(2-(2-Methyl-3-phenylbut-3-en-2-yl)phenyl)ethanol (451)

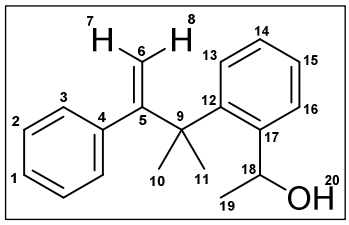

An oven-dried 25 mL 2-necked round-bottomed flask was evacuated and purged with Argon three times before being charged with **449** (250 mg, 0.657 mmol, 1.0 eq.) and dissolved in dry THF (10 mL). TBAF (430 mg, 1.642 mmol, 2.5 eq.) was added and instantly the reaction mixture turned black. The reaction mixture was heated to 50 °C for 20 hours until TLC analysis (SiO_2, pentane/Et_2O 10:1) indicated complete consumption of starting material. Purification by elution chromatography (SiO_2, 5x2 cm, cyclohexane/Et_2O 20:1, then 1:1) afforded **451** (88 mg, 0.33 mmol, 50%) as an orange-brown oil.

$C_{19}H_{22}O$ (M_W = 266.38 g/mol):
^{1}H-NMR (400 MHz, $CDCl_3$, d/ppm): 7.57 (dd, ^3J = 7.7 Hz, ^4J = 1.6 Hz, 1H, H16), 7.40 (dd, ^3J = 7.8 Hz, ^4J = 1.4 Hz, 1H, H13), 7.30 (td, ^3J = 7.4 Hz, ^4J = 1.4 Hz, 1H, H14), 7.26-7.21 (m, 1H, H15), 7.21-7.17 (m, 3H, H1, H2), 7.11-7.06 (m, 2H, H3), 5.53 (q, ^3J = 6.3 Hz, 1H, H18), 5.18 (d, ^2J = 1.2 Hz, 1H, H7), 5.15 (d, ^2J = 1.2 Hz, 1H, H8), 1.67 (s, 3H, H10/H11), 1.51 (s, 3H, H10/H11), 1.44 (d, ^3J = 6.3 Hz, 3H, H19). **^{13}C{^{1}H}-NMR** (126 MHz, $CDCl_3$) δ 158.3, 146.6, 143.6, 142.5, 129.0, 128.8, 128.5, 128.4, 126.9, 126.3, 126.3, 114.0, 63.9, 44.2, 31.6, 30.8, 25.3; **GC-MS**: (Optima-5-Amine, 100.2/10.270/10): t_R = 15.8 min, *m/z* = 250 ($[M-OH]^+$), 145 ($[M-C_8H_9O]^+$), 129 ($[M-C_9H_{12}O]^+$); **IR** (neat, ATR) ν/cm^{-1} = 3360 (w_{br}), 3058 (w), 2969 (w), 2925 (w), 2851 (w), 1489 (w), 1448 (w), 1381 (w), 1364 (w), 1067 (m), 1001 (w), 904 (w); **HRMS**: calculated: 289.1563 $[M+Na]^+$, found: 289.1566.

1-(2-methyl-3-phenylbut-3-en-2-yl)-2-vinylbenzene (452)

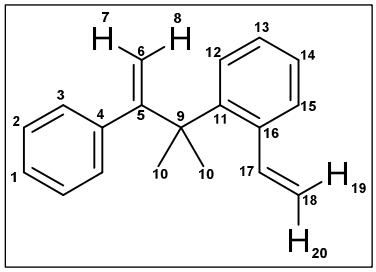

A 10 mL Schlenk tube equipped with a stirring bar under argon atmosphere was charged with **451** (20 mg, 75.1 µmol, 1.0 eq), Boc_2NH (65.2 mg, 0.300 mmol, 4.0 eq), PPh_3 (78.8 mg, 0.300 mmol, 4.0 eq) and CH_2Cl_2 (1.1 mL). The mixture was cooled to 0 °C, diisopropyl azodicarboxylate (74 µL, 0.375 mmol, 5.0 eq) was added. After stirring overnight and warming to

room temperature, 1 M HCl (2 mL) was added. The mixture was poured on saturated aqueous $NaHCO_3$ (10 mL) and extracted with CH_2Cl_2 (3x20 mL). The combined oragnic layers were dried over Na_2SO_4 and the solvent was removed under reduced pressure. Flash chromatography (SiO_2, 18 cm x 2.5 cm, cyclohexane/Et_2O 2:1) gave **452**. No yield was determined.

$C_{19}H_{20}$ (M_W = 248.37 g/mol):
^{1}H-NMR (500 MHz, $CDCl_3$) δ 7.56 (dd, *J* = 10.9 Hz, 17.3 Hz, 1H, H17), 7.45 (dd, *J* = 7.2 Hz, ^4J = 2.0 Hz, 1H, H15), 7.29 (dd, *J* = 7.3 Hz, ^4J = 1.6 Hz, 1H, H12), 7.24-7.19 (m, 3H, H1, H2), 7.15-7.11 (m, 2H, H13, H14), 6.91 (dd, *J* = 7.9 Hz, ^4J = 1.2 Hz, 2H, H3), 5.51 (dd, *J* = 17.3 Hz, ^2J = 1.6 Hz, 1H, H19), 5.28 (d, ^2J = 1.2 Hz, 1H, H7), 5.19 (dd, *J* = 10.9 Hz, ^2J = 1.6 Hz, 1H, H20), 5.12 (d, ^2J = 1.2 Hz, 1H, H8), 1.54 (s, 6H, H10); **^{13}C{^{1}H}-NMR** (126 MHz, $CDCl_3$) δ 157.3 (C5), 144.2 (C11), 142.8 (C4), 138.5 (C16), 138.2 (C17), 128.8 (C3), 128.2 (C15), 127.8 (C13), 127.4 (C2), 126.8 (C14), 126.7 (C1), 126.6 (C12), 114.6 (C18), 114.3 (C6), 44.8 (C9), 30.2 (C10); **IR** (neat, ATR) ν/cm^{-1} = 2985 (w), 2929 (w), 1771 (s), 1683 (w), 1469 (w), 1456 (w), 1378 (w), 1232 (ss), 1183 (m), 1093 (s), 893 (m).

2-(2-bromophenyl)-2-methyl-1,3-dioxane (446)

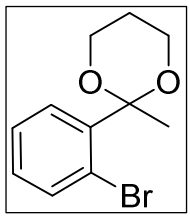

An ovendried two-necked round bottomed flask, equipped with a magnetic stirrer and a septum, was evacuated and purged with Argon three times before being charged with $ZrCl_4$ (37.7 mg, 0.1 mmol, 0.02 eq.). Dry CH_2Cl_2 (15 mL), 1-(2-bromophenyl)ethanone (1.0 g, 5 mmol, 1.0 eq.), propane-1,3-diol (761 mg, 10 mmol, 2.0 eq.) and triethoxymethane (741 mg, 5 mmol, 1.0 eq.) were added and the reaction mixture stirred at room temperature for 18 hours. Again triethoxymethane (446 mg, 3 mmol, 0.6 eq.) was added an stirring continued for 24 hours at room temperature. GC-MS analysis indicated ~65% consumption of starting material. The reaction mixture was quenched with NaOH (10% w/w, 25 mL) and organic components extracted with CH_2Cl_2 (3x40 mL). After washing with water (2x15 mL) the organic layer was dried over anhydrous $MgSO_4$, filtered and solvents removed under reduced pressure. Purification by Kugelrohr distillation (75 °C, 0.08 mbar) afforded **446** (437 mg, 1.7 mmol, 34 %) as a viscous colourless oil.

$C_{11}H_{13}BrO_2$ (M_W = 257.12 g/mol):
^{1}H-NMR (400 MHz, $CDCl_3$) δ 7.64 (d, *J* = 8.0 Hz, 1H), 7.62 – 7.57 (m, 1H), 7.35 (t, *J* = 7.6 Hz, 1H), 7.15 (t, *J* = 7.6 Hz, 1H), 3.90 (dd, *J* = 11.5, 4.7 Hz, 2H), 3.78 – 3.68 (m, 2H), 2.25 – 2.10 (m, 1H), 1.59 (s, 3H), 1.28 (d, *J* = 13.2 Hz, 1H); **GC-MS**: (Optima-5-Amine, 100.2/10.270/10): t_R = 11.8 min, *m/z* = 243, 183, 157, 101.

2-methyl-1-phenyl-2-(2-vinylphenyl)propan-1-one (454)

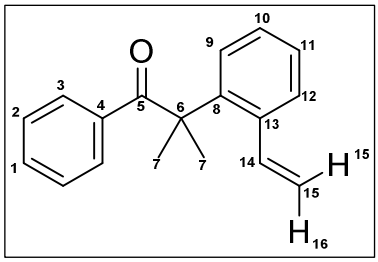

A 50 mL Schlenk vial was charged with a magnetic stirrer, evacuated and flame-dried with a bunsen burner before being purged with Argon three times. It was then transferred to the glove box where $Pd(dba)_2$ (92 mg, 0.16 mmol, 0.1 eq.), [(^{t}Bu)$_3$PH][BF_4] (102 mg, 0.352 mmol, 0.22 eq.) and NaO^tBu (246 mg, 2.56 mmol, 1.6 eq.) were added. Outside the glove box the reaction mixture was suspended in dry 1,4-dioxane (8 mL) before **418** (282 mg, 1.91 mmol, 1.2 eq.) and **453** (292 mg, 1.6 mmol, 1.0 eq.) were added via syringe. The reaction mixture was heated to 100 °C for 3 days. After cooling to room temperature, the reaction mixture was diluted with Et_2O (30 mL), washed with water (20 mL), and the aequeous layer was extracted with Et_2O (20 mL). The combined organic layers were dried over Na_2SO_4, filtered and solvents removed under reduced pressure. The residue was subjected to flash chromatography (SiO_2, cyclohexane/Et_2O 50:1, 20x3.5 cm, 20 mL fractions) to afford **454** (305 mg, 1.22 mmol, 76 %) as a yellow oil.

$C_{18}H_{18}O$ (M_W= 250.33 g/mol):
^{1}H-NMR (500 MHz, $CDCl_3$) δ 7.62 (d, *J* = 8.2 Hz, 1H, H9), 7.59 (d, *J* = 7.5 Hz, 2H, H3), 7.42 (t, *J* = 7.6 Hz, 1H, H10), 7.37 (m, 1H, H12), 7.36 (m, 1H, H1), 7.30 (d, *J* = 7.5 Hz, 1H, H11), 7.19 (t, *J* = 7.8 Hz, 2H, H2), 6.79 (dd, *J* = 16.9 Hz, 10.9 Hz, 1H, H14), 5.30 (dd, *J* = 16.9 Hz, ^2J = 1.0 Hz, 1H, H15), 5.10 (dd, *J* = 10.9 Hz, ^2J = 1.0 Hz, 1H, H16), 1.66 (s, 6H, H7); **^{13}C{^{1}H}-NMR** (125 MHz, $CDCl_3$) δ 204.32 (C5), 142.83 (C8),

137.87 (C13), 135.97 (C4), 135.37 (C14), 132.12 (C1), 129.59 (C3), 128.64 (C10), 128.22 (C12), 128.01 (C2), 127.41 (C11), 117.51 (C15), 28.31 (C7); **GC-MS** (EI, 70 eV, PhMeSi, 100.2/10.270/10): t_R = 18.6 min, *m/z* = 250 ($[M]^+$); **IR** (neat, ATR) ν/cm^{-1} = 3087 (w), 3059 (w), 3023 (w), 2974 (m), 2932 (w), 2867 (w), 1673 (s), 1596 (w), 1466 (w), 1446 (w), 1384 (w), 1240 (m), 1164 (w), 1117 (w), 969 (m), 917 (w); **HRMS**: calculated: 273.1250 $[M+Na]^+$, found: 273.1250; **EA**: calc.: C, 86.36; H, 7.25; found: C, 86.23; H, 7.53.

2-(2-methyl-1-oxo-1-phenylpropan-2-yl)benzaldehyde (455)

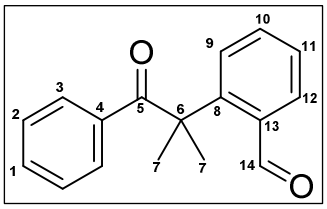

A 25 mL three necked round-bottomed flask was charged with **454** (200 mg, 0.8 mmol, 1.0 eq.) and dissolved in CH_2Cl_2/methanol (5:1, 8 mL). After cooling to -78 °C, ozone was bubbled through until the solution became dark blue. Stirring was continued for 5 minutes before oxygen, and then argon were bubbled through until the solution became clear again. TLC control (SiO_2, pentane/EtOAc 20:1) indicated complete consumption of starting material. Triphenylphosphine (1.0 g, 4 mmol, 5.0 eq.) was added and the reaction mixture allowed to warm up while stirring overnight. After removal of solvents under reduced pressure the residue was subjected to flash chromatography (SiO_2, cyclohexane/Et_2O 10:1 gradient to 5:1, 18.5x3 cm, 20 mL fractions) to afford **455** (179 mg, 0.71 mmol, 89%) as a white powder.

$C_{17}H_{16}O_2$ (M_W = 252.31 g/mol):
m.p.: 124 °C; **^{1}H-NMR** (400 MHz, $CDCl_3$) δ 9.91 (s, 1H, H14), 7.78 (m, 1H, H10), 7.76 (m, 1H, H9), 7.71 (td, *J* = 7.5, 1.5 Hz, 1H, H12), 7.53 (dt, *J* = 8.6, 1.6 Hz, 2H, H3), 7.46 (td, *J* = 7.5, 1.0 Hz, 1H, H11), 7.32 (m, 1H, H1), 7.18 (m, 2H, H1), 1.77 (s, 6H, H7); **^{13}C{^{1}H}-NMR** (101 MHz, $CDCl_3$) δ 203.03 (C5), 191.79 (C14), 148.06 (C8), 135.91 (C4), 134.82 (C12), 134.18 (C13), 133.35 (C10), 131.99 (C1), 129.77 (C3), 128.02 (C2), 127.53 (C11), 126.18 (C9), 51.42 (C6), 29.34 (C7); **GC-MS**: (Optima-5-Amine, 100.2/10.270/10): t_R = 17.4 min, *m/z* = 252, 147, 129, 105; **IR** (neat, ATR) ν/cm^{-1} = 3058 (w), 2974 (w), 2928 (w), 2835 (w), 2741 (m), 1700 (s), 1677 (s), 1595 (m), 1570 (m), 1469 (m), 1443 (m), 1381 (m), 1359 (m), 1296 (m), 1246 (m), 1236 (m), 1190 (m), 1166 (m), 971 (m); **HRMS**: calculated: 275.1043 $[M+Na]^+$, found: 275.1043; **EA**: calc.: C, 80.93; H, 6.39; found: C, 80.25; H, 6.47.

2-(2-(((4-methoxyphenyl)imino)methyl)phenyl)-2-methyl-1-phenylpropan-1-one (456)

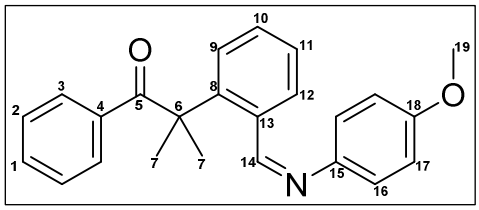

An oven-dried 50 mL Schlenk tube was charged with 4Å mol sieves and purged with Argon three times before being charged with **455** (450 mg, 1.78 mmol, 1.0 eq.) and **118** (241.6 mg, 1.96 mmol, 1.1 eq.). Dry toluene (10 mL) was added and the reaction mixture stirred at room temperature for 24 hours. Solvents were removed under reduced pressure and the residue was dried under high vacuum to afford **456** as a sticky orange solid. Crude NMR analysis indicated >95% conversion to the aldimine which was directly used in the next step without purification.

$C_{24}H_{23}NO_2$ (MW = 357.44 g/mol):
^{1}H-NMR (500 MHz, $CDCl_3$) δ 8.59 (s, 1H, H14), 8.09 (d, *J* = 7.7 Hz, 1H, H12), 7.71 (d, *J* = 7.9 Hz, 1H, H9), 7.57 (dd, *J* = 11.5, 7.9 Hz, 3H, H10, H3), 7.38 (m, 1H, H11), 7.32 (m, 1H, H1), 7.17 (t, *J* = 7.8 Hz, 2H, H2), 7.07 (d, *J* = 8.8 Hz, 2H, H16), 6.90 (d, *J* = 8.8 Hz, 2H, H17), 3.82 (s, 3H, H19), 1.77 (s, 6H, H7); **^{13}C{^{1}H}-NMR** (126 MHz, $CDCl_3$) δ 204,39 (C5), 158.55 (C18), 156.19 (C14), 145.60 (C8), 144.49 (C15), 135.43 (C4), 135.14 (C13), 132.45 (C1), 131.45 (C10), 129.80 (C3), 129.18 (C12), 128.23 (C2), 127.56 (C11), 125.22 (C9), 122.53 (C16), 114.51 (C17), 55.59 (C19), 51.68 (C6), 29.35 (C7); **GC-MS**: (Optima-5-Amine, 100.2/10.270/20): t_R = 31.0 min, *m/z* = 357 ($[M]^+$), 252, 129, 105.

2-(2-(1-((4-methoxyphenyl)amino)-2-methylpropyl)phenyl)-2-methyl-1-phenylpropan-1-one (459)

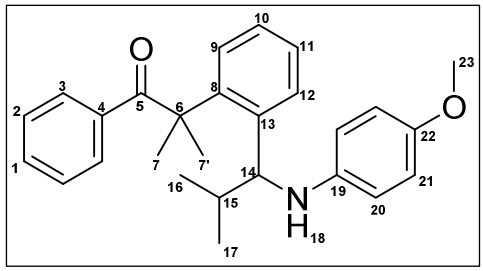

A crude reaction mixture of **456** (~1.78 mmol, 1.0 eq.) was dissolved in dry THF (20 mL) and transferred to a 100 mL oven-dried round-bottomed flask purged with argon. After cooling to 0 °C, isopropyl magnesium chloride (2.05 mmol, 1.2 eq.) was added dropwise and the reaction mixture stirred at 0 °C for 15 minutes before being allowed to warm up to room temperature while stirring overnight. After cooling to 0 °C the reaction was quenched with $NaHCO_3$ (10 mL) and organic components were extracted with Et_2O (3x25 mL). The combined organic layers were washed with brine (20 mL), dried over Na_2SO_4, filtered and solvents removed under reduced pressure. The residue was subjected to flash chromatography (SiO_2, cyclohexane/EtOAc 8:1, 16x3 cm, 20 mL fractions) to afford **459** (420 mg, 1.05 mmol, 58%) as a red-brownish solid. Purification by semipreparative HPLC yields a white solid which rapidly degrades to a sticky yellow solid upon exposure to air. Spectral data dies not agree with the crude isolated material prior to HPLC separation.

$C_{27}H_{31}NO_2$ (M_W = 401.54 g/mol):
^{1}H-NMR (500 MHz, $CDCl_3$) δ 7.67 (dd, *J* = 7.8, 1.6 Hz, 1H, H9), 7.55 (dd, *J* = 8.3, 1.0 Hz, 2H, H3), 7.47 (dd, *J* = 7.5, 1.9 Hz, 1H, H12), 7.39 (td, *J* = 7.5, 1.9 Hz, 1H, H10), 7.35 (td, *J* = 7.3, 1.6 Hz, 1H, H11), 7.32 (tt, *J* = 7.4, 1.3 Hz, 1H, H1), 7.14 (dd, *J* = 8.4, 7.2 Hz, 2H, H2), 6.64 (m, 2H, H20), 6.40 (m, 2H, H21), 4.41 (d, *J* = 7.2 Hz, 1H, H14), 3.72 (s, 3H, H23), 3.24 (s_{br}, 1H, NH), 1.92 (dq, *J* = 12.8, 6.4, 6.0 Hz, 1H, H15), 1.71 (s, 3H, H7), 1.57 (s, 3H, H7‘), 0.89 (d, *J* = 6.7 Hz, 3H, H16), 0.49 (d, *J* = 6.8 Hz, 3H, H17); **^{13}C{^{1}H}-NMR** (101 MHz, $CDCl_3$) δ 203.57 (C5), 151.62 (C22), 143.38 (C13), 142.42 (C8), 142.17 (C19), 135.90 (C4), 132.19 (C1), 130.07 (C3), 127.95 (C2), 127.89 (C12), 127.77 (C11), 127.70 (C10), 126.12 (C9), 114.59 (C21), 114.56 (C20), 58.21 (C14), 55.86 (C23), 52.06 (C6), 36.53 (C15), 29.60 (C7), 29.35 (C7‘), 20.53 (C17), 19.20 (C16); **IR** (neat, ATR) ν/cm^{-1} = 3061 (w), 3025 (w), 2964 (w), 2928 (w), 2905 (w), 2854 (w), 2830 (w), 1601 (w), 1580 (w), 1502 (s), 1463 (m), 1450 (m), 1385 (m), 1361 (m), 1279 (m), 1232 (s), 1194 (w), 1174 (m), 1146 (m), 1039 (s), 822 (s), 763 (s); **GC-MS**: (Optima-5-Amine, 100.2/10.270/20): t_R = 27.5 min, *m/z* = 382 ([M]$^+$), 248, 197; **HPLC** (semipreparative : Daicel Chiracel OD, *n*-heptane/iso-propanol 90:10, 6.0 mL/min, 20 °C, 265 nm): t_R = 21.0 min (+), t_R = 25.0 min (-); **Optical Rotation**: $[a]_D^{20}$ = -246 (c 1.0 in $CHCl_3$ 0.75% EtOH).

2-(2-(1-((4-methoxyphenyl)amino)-2,2-dimethylpropyl)phenyl)-2-methyl-1-phenylpropan-1-one (460)

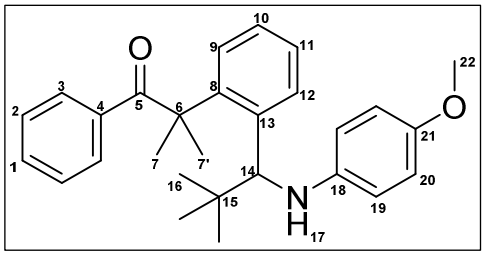

An oven-dried 10 mL Schlenk tube was purged with Argon three times before being charged with **455** (150 mg, 0.595 mmol, 1.0 eq.) and **118** (80.5 mg, 0.655 mmol, 1.1 eq.). Dry toluene (3 mL) was added and the reaction mixture stirred at room temperature for 24 hours. Solvents were removed under reduced pressure and the residue dried under high vacuum before being suspended in dry THF (3 mL). The reaction mixture was cooled to 0 °C and *tert*-butyl magnesium chloride (0.9 mmol, 1.5 eq.) was added. An instant colourchange from towards yellow-orange was observed. The reaction mixture was allowed to warm to room temperature while stirring for 22 hours. The reaction was quenched with $NaHCO_3$ (2 mL) and organic components extracted with Et_2O (3x10 mL) before the combined organic layers were dried over anhydrous $MgSO_4$, filtered and solvents removed under reduced pressure.The residue was subjected to flash chromatography (SiO_2, cyclohexane/EtOAc 20:1 gradient to 5:1, 18x4 cm, 25 mL fractions) to afford **460** (61 mg, 0.15 mmol, 25%) as a off-white yellowish solid.

$C_{28}H_{33}NO_2$ (M_W = 415.57 g/mol):
^{1}H-NMR (400 MHz, $CDCl_3$) δ 7.62 (dd, *J* = 7.5, 1.9 Hz, 2H, H11), 7.56 (d, *J* = 7.5 Hz, 2H, H3), 7.50 (dd, *J* = 7.3, 2.1 Hz, 1H, H12), 7.34 (m, 1H, H10), 7.33 (m, 1H, H9), 7.30 (dd, *J* = 7.4, 1.1 Hz, 1H, H1), 7.11 (dd, *J* = 8.4, 7.3 Hz, 2H, H2), 6.71 (ddd, *J* = 9.0, 3.6, 2.2 Hz, 2H, H20), 6.60 (dt, *J* = 8.9, 3.5, 2.2 Hz, 2H, H19), 4.73 (s, 1H, H14), 3.74 (s, 3H, H22), 3.41 (s_{br}, 1H, NH), 1.74 (s, 3H, H7), 1.53 (s, 3H, H7’), 0.80 (s, 9H, H16); **^{13}C{^{1}H}-NMR** (101 MHz, $CDCl_3$) δ 203.98 (C5), 151.57 (C21), 143.52 (C13), 142.33 (C8), 142.32

(C18), 136.06 (C4), 132.12 (C1), 130.23 (C3), 128.11 (C12), 127.88 (C2), 127.68 (C10), 127.25 (C9), 126.64 (C11), 114.93 (C19), 114.64 (C20), 59.60 (C14), 55.86 (C22), 52.40 (C6), 38.75 (C15), 29.89 (C7), 29.81 (C7'), 29.16 (C16); **IR** (neat, ATR) ν/cm^{-1} = 3061 (w), 3024 (w), 2962 (w), 2929 (m), 2905 (m), 2865 (w), 2855 (w), 2830 (w), 1668 (m), 1597 (w), 1577 (w), 1503 (s), 1465 (m), 1449 (m), 1385 (m), 1362 (m), 1232 (s), 1175 (m), 1038 (m); **MS** (EI, 70 eV): 223.1 (9.6%, $[M]^+$). 415.1 (2.3%), 359.2 (26.6%), 358.2 (100%); **GC-MS**: (Optima-5-Amine, 100.2/10.270/20): t_R = 26.2 min, *m/z* = 382 ($[M\text{-}CH_3]^+$), 340, 325, 217; **HRMS**: calculated: 416.2584 $[M+H]^+$; found: 416.2585.

1-isopropyl-4,4-dimethyl-3-phenyl-1,4-dihydroisoquinoline (392)

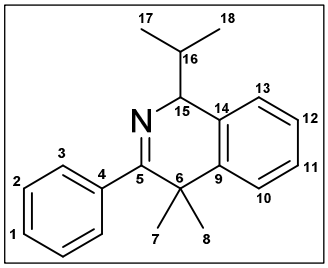

A 25 mL round-bottomed flask was charged with **459** (100 mg, 0.25 mmol, 1.0 eq.) and dissolved in methanol/water (6:1, 17.5 mL) before being cooled to 0 °C. Cerium ammonium nitrate (1.37 g, 2.5 mmol, 10 eq.) was added and the resultant suspension stirred 24 hours where again cerium ammonium nitrate (1 g, 1.8 mmol, 7.3 eq.) was added and stirring continued for another 20 hours. The reaction mixture as then diluted with water (10 mL) and CH_2Cl_2 (10 mL) and transferred to a separation funnel. The aeqeuous layer was basified with NaOH (1M, 10 mL) and organic components extracted with EtOAc (3x30 mL). The combined organic layers were washed with brine (25 mL and dried over anhydrous $MgSO_4$, filtered and and solvents removed under reduced pressure. The residue was subjected to flash chromatography (SiO_2, cyclohexane/EtOAc 4:1, 18x2 cm, 7 mL fractions) to afford **392** (15.5 mg, 0.056 mmol, 22%) as a clear oil.

$C_{20}H_{23}N$ (MW = 277.40 g/mol):
^{1}H-NMR (500 MHz, $CDCl_3$) δ 7.40 (m, 1H, H10), 7.39 (m, 2H, H2), 7.36 (m, 2H, H3), 7.29 (m, 1H, H11), 7.27 (m, 1H, H1), 7.25 (m, 1H, H12), 7.23 (m, 1H, H13), 4.84 (d, *J* = 4.4 Hz, 1H, H15), 2.31 (heptd, *J* = 6.8, 4.6 Hz, 1H, H16), 1.52 (s, 3H, H7), 1.47 (s, 3H, H8), 1.23 (d, *J* = 6.8 Hz, 3H, H18), 0.84 (d, *J* = 6.8 Hz, 3H, H17); **^{13}C{^{1}H}-NMR** (101 MHz, $CDCl_3$) δ 174.00 (C5), 141.92 (C4), 141.20 (C9), 134.75 (C14), 128.20 (C3), 127.91 (C2), 127.61 (C13), 126.92 (C11), 126.04 (C1), 125.73 (C12), 125.08 (C10), 65.39 (C15), 38.01 (C6), 35.87 (C16), 29.92 (C7), 29.53 (C8), 21.07 (C18), 17.56 (C17); **GC-MS**: (Optima-5-Amine, 100.2/10.270/20): t_R = 17.7 min, *m/z* = 277 ($[M]^+$), 262, 234, 174, 159; **HPLC** (Daicel Chiracel OD-H, *n*-heptane/iso-propanol 99:1, 0.5 mL/min, 25 °C, 206/238 nm): t_R = 9.2 min (-), t_R = 11.2 min (+); **IR** (neat, ATR) ν/cm^{-1} = 2974 (w), 2925 (m), 2851 (w), 2742 (w), 1700 (s), 1677 (s), 1595 (m), 1569 (s), 1443 (m), 1381 (m), 1359 (m), 1297 (m), 1246 (m), 1236 (m), 1190 (m), 1166 (m), 1077 (w), 971 (s), 903 (m); **HRMS**: calculated: 278.1903 $[M+H]^+$; found: 278.1903; **Optical Rotation**: $[a]_D^{20}$ = -15.6 (c 0.035 in $CHCl_3$ 0.75% EtOH); **Optical Rotation**: $[a]_D^{20}$ = +12.2 (c 0.035 in $CHCl_3$ 0.75% EtOH).

Benzoxazines

2-(1-aminoethyl)phenol (490)[173]

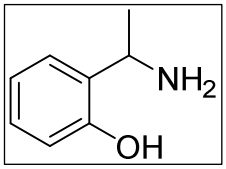

In a 500 mL three-neck round bottom flask equipped with a magnetic stirrer and a reflux condenser was inserted 2-methoxybenzonitrile **488** (4.50 g, 33.8 mmol, 1.0 eq), CuBr (98.0 mg, 0.683 mmol, 0.02 eq) and dissolved in dry THF (75 mL). A solution of MeMgCl in THF (3M, 21.4 mL, 4.81 g MeMgCl, 64.3 mmol, 1.9 eq) was added and the resultant mixture heated to reflux for 16 hours. A short reaction control via TLC depicted all the starting material had not been consumed and therefore again a solution of MeMgCl in THF (3M, 5.00 mL, 1.12 g, 15.0 mmol, 0.4 eq; total 5.93 g MeMgCl) was added and refluxing continued for further 5 hours. Afterwards the reaction mixture was allowed to cool to room temperature. A mechanical stirrer, a ammonia condensation vessel and washing bottles were mounted and the mixture cooled to -78 °C. Subsequently ammonia (approx. 200 mL) was condensed into the reaction mixture. Lithium (1.19 g, 169 mmol, 5.0 eq) was added in small pieces until the reaction mixture turned blue. The cooling bath was removed and the reaction mixture was allowed to warm up overnight while stirring and evaporating all ammonia. *tert*-Butylmethylether (MTBE) was added to the mixture, cooled to 0 °C and titrated with concentrated HCl to pH 8. The organic layer was separated, the aeqeuous layer salted out and extracted with MTBE (3 x 100 mL). The combined organic layers were washed with brine (100 mL), 0.5 M HCl (3 x 150 mL) and the acidic aeqeuous phase extracted with MTBE (3 x 50 mL). The acidic aeqeuous

layer was set to pH 11 with 10% NaOH (10%), salted out and extracted with MTBE (3 x 50 mL). The combined organic layers were dried over $MgSO_4$, solvents removed under reduced pressure and the residue was purified via distillation (60-65 °C at 0.08 mbar). **490** was obtained as a greenish oil (1.03 g, 7.5 mmol, 22%). The product contained 1-(2-Methoxyphenyl)ethanamine **489** as an impurity (0.265 g, 1.8 mmol, 4%).

$C_8H_{11}NO$ (137.18 g/mol):
b.p.: 65°C (0.08 mbar); **^{1}H-NMR** (400 MHz, $CDCl_3$) δ 7.15 (td, ^3J = 7.9 Hz, ^4J = 1.7 Hz, 1H, CH_{Ar}CH$_{Ar}$C$_{Ar}$CH(NH$_2$)); 6.97 (dd, ^3J = 7.5 Hz, ^4J = 1.5 Hz, 1H, CH_{Ar}C$_{Ar}$(OH)); 6.84 (dd, ^3J = 8.1 Hz, ^4J = 0.9 Hz, 1H, CH_{Ar}C$_{Ar}$CH(NH$_2$)); 6.78 (td, ^3J = 7.4 Hz, ^4J = 1.1 Hz, 1H, CH_{Ar}CH$_{Ar}$C$_{Ar}$(OH)); 4.33 (q, J = 6.6 Hz, 1H, CH(NH$_2$)(CH$_3$)); 3.85 (s, 2H, NH_2); 1.48 (d, J = 6.7 Hz, 3H, CH_3); **^{13}C{^{1}H}-NMR** (126 MHz, $CDCl_3$) δ 157.76 (C_{Ar}(OH), 128.59 (C_{Ar}CH); 128.23 (CH$_{Ar}$); 127.31 (CH$_{Ar}$); 119.13 (CH$_{Ar}$); 117.35 (CH$_{Ar}$); 51.87 (CH(NH$_2$)(CH$_3$)); 24.01 (CH$_3$).

***N*-(1-(2-hydroxyphenyl)ethyl)benzamide (495)**

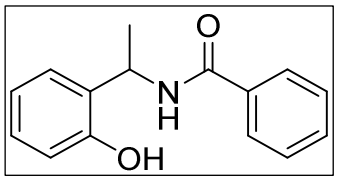

In a 25 mL two-neck round bottom flash equipped with a magnetic stirrer and a septum was placed crude **490** (1.295 g, 9.3 mmol, 1.24 eq), dissolved in CH_2Cl_2 (10 mL) and cooled to 0 °C. Benzoylchloride (1.05 g, 7.50 mmol, 1.0 eq) and triethylamine (0.833 g, 8.25 mmol, 1.1 eq) were added via syringe pump over a period of 5 minutes. After another 10 minutes the cooling bath was removed and the reaction mixture allowed to warm to room temperature while stirring overnight. Solvents were removed at the rotavap and the crude was purified *via* elution chromatography (7 cm x 4 cm, SiO_2, EtOAc) to give **495** as a yellow oil. The product contained *N*-(1-(2-Methoxy-phenyl)ethyl)benzamide as an impurity of about 25%. Thus, the crude product was transferred to an 25 mL oven-dried argon-purged two-neck round bottom flask, dissolved in 5 mL CH_2Cl_2 and cooled to -78 °C. A solution of BBr_3 (1M in CH_2Cl_2) was added dropwise via syringe and the resultant mixture stirred for 15 minutes. The cooling bath was removed and reaction mixture allowed warming up to room temperature overnight. 10% NaOH (10 mL) were added dropwise and the resultant mixture stirred for 10 minutes. Layers were separated and the aeqeous layer was acidified with 1M HCl (25 mL), set to pH 8 via addition of saturated $NaHCO_3$ solution and extracted with CH_2Cl_2 (2 x 25 mL). The combined organic layers were dried over $MgSO_4$, solvents removed under reduced pressure and **495** obtained as a yellow oil (1.54 g, 6.4 mmol, 85%). Enantiomers were separated by semipreparative HPLC. **495** was dissolved in a mixture of heptane/2-propanol (9:1) to a concentration of 0.3g mL^{-1}. Daicel Chiralcel OD (2 cm x 25 cm), *n*-hexane : 2-propanol (90:10), 6 mL min^{-1}, 40 °C, 0.25 mL injection volume, t_R = 41.0 min (*S*)-(+), t_R = 49.0 min (*R*)-(-).

$C_{15}H_{15}NO_2$ (241.29 g/mol):
m.p.: 131-133 °C; **^{1}H-NMR** (500 MHz, $CDCl_3$) δ 9.23 (s, 1H, C$_{Ar}$(OH)), 7.75 (m, 2H, CH_{Ar}C$_{Ar}$C=O), 7.51 (m, 1H, CH_{Ar}CH$_{Ar}$CH$_{Ar}$C$_{Ar}$C=O), 7.43 (m, 2H, CH_{Ar}CH$_{Ar}$C$_{Ar}$C=O), 7.28 (dd, ^3J = 7.7, ^4J = 1.7 Hz, 1H, CH_{Ar}C$_{Ar}$CHNH), 7.20 (ddd, ^3J = 8.1, 7.3, ^4J = 1.7 Hz, 1H, CH_{Ar}CH$_{Ar}$C$_{Ar}$(OH)), 6.97 (dd, ^3J = 8.1, ^4J = 1.3 Hz, 1H, CH_{Ar}C$_{Ar}$(OH)), 6.90 (td, ^3J = 7.5, ^4J = 1.3 Hz, 1H, CH_{Ar}CH$_{Ar}$C$_{Ar}$CHNH), 6.53 (d, ^3J = 8.5 Hz, 1H, NH), 5.51 (dq, ^3J = 8.6, 7.1 Hz, 1H, CHNH), 1.73 (d, ^3J = 7.0 Hz, 3H, CH_3); **^{13}C{^{1}H}-NMR** (101 MHz, $CDCl_3$) δ 168.73 (C=O); 155.47 (C_{Ar}(OH)); 133.12 (C_{Ar}C=O); 132.31 (CH$_{Ar}$CH$_{Ar}$CH$_{Ar}$C$_{Ar}$C=O); 129.48 (CH$_{Ar}$CH$_{Ar}$C$_{Ar}$(OH)); 128.82 (CH$_{Ar}$CH$_{Ar}$C$_{Ar}$C=O); 128.57 (C_{Ar}CHNH); 127.26 (CH$_{Ar}$C$_{Ar}$C=O); 125.91 (CH$_{Ar}$C$_{Ar}$CHNH); 120.39 (CH$_{Ar}$CH$_{Ar}$C$_{Ar}$CHNH); 118.60 (CH$_{Ar}$C$_{Ar}$(OH)); 43.64 (CHNH); 19.79 (CH$_3$); **IR** (neat, ATR) ν/cm^{-1} = 3350 (m), 3065 (w), 2932 (w), 2733 (w), 2677 (w), 2620 (w), 1623 (m), 1602 (m), 1568 (w), 1538 (s), 1488 (s), 1409 (m), 1349 (m), 1277 (m), 1232 (s), 1188 (m), 1132 (m), 1102 (m), 1019 (m), 928 (w), 872 (w), 838 (m), 765 (s), 705 (s), 696 (s); **MS** (EI, 70 eV): 241.1 (45.8%, [M]$^+$). 226.1 (11%, [M-CH$_3$]$^+$); **HRMS**: calculated: 241.1098 [M]$^+$; found: 241.1102; **EA**: calculated: C: 74.67, H: 6.27, N: 5.81; found: C: 74.39, H: 6.45, N: 5.67; **Optical Rotation** (*R*)-isomer: $[a]_D^{20}$ = -26.5 (c 0.75 in $CHCl_3$, 0.75% EtOH); **Optical Rotation** (*S*)-isomer: $[a]_D^{20}$ = +24.8 (c 0.75 in $CHCl_3$, 0.75% EtOH).

4-Methyl-2-phenyl-4H-benzo[e][1,3]oxazine (399)

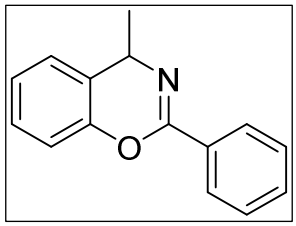

In a 10 mL 2-neck round bottom flask was placed (*R*)-**495** (61.3 mg, 0.254 mmol, 1.0 eq.), dissolved in CH_2Cl_2 (2 mL) and cooled to -40 °C. $POCl_3$ (0.63 mL of a 0.4M solution, 0.254 mmol, 1.0 eq.) was added and the reaction mixture stirred for 30 minutes. Then pyridine (125 uL, 120 mg, 1.524 mmol, 6.0 eq) was added and stirring continued for 15 minutes. Afterwards the cooling bath was removed and the mixture allowed to warm to room temperature while stirring overnight. Reaction was quenched with 1M NaOH (2.5 mL), extracted with diethylether (2 x 5 mL) and solvents removed under reduced pressure. Purification *via* flash chromatography (SiO_2, 18 x 2.5 cm, 7 mL frctns, cyclohexane/EtOAc 10:1, frctns 12-14) gave (*R*)-**399** as a clear oil (1.3 mg, 0.0058 mmol, 2%). With the identical procedure, (*S*)-**495** (58.9 mg, 0.244 mmol, 1.0 eq.) gave (*S*)-**399** (3.3 mg, 0.015 mmol, 6%) as a clear oil.

$C_{15}H_{13}NO$ (223.27 g/mol):
^{1}H-NMR (400 MHz, $CDCl_3$) δ 8.10 (m, 2H, CH_{Ar}C$_{Ar}$C=N), 7.47 (m, 3H, CH_{Ar}CH$_{Ar}$C$_{Ar}$C=N and CH_{Ar}CH$_{Ar}$CH$_{Ar}$C$_{Ar}$C=N), 7.23 (m, 1H, CH_{Ar}CH$_{Ar}$C$_{Ar}$-O), 7.14 (m, 2H, CH_{Ar}C$_{Ar}$CH(CH$_3$)N and CH_{Ar}CH$_{Ar}$C$_{Ar}$CH(CH$_3$)N), 7.04 (d, *J* = 8.0 Hz, 1H, CH_{Ar}C$_{Ar}$-O), 4.83 (q, *J* = 6.9 Hz, 1H, C*H*(CH$_3$)N), 1.58 (d, *J* = 6.9 Hz, 3H, CH(C*H*$_3$)N); **^{13}C{^{1}H}-NMR** (101 MHz, $CDCl_3$) δ 151.72 (O-*C*=N), 148.97 (*C*$_{Ar}$-O), 132.55 (*C*$_{Ar}$C=N), 131.05 (*C*H$_{Ar}$CH$_{Ar}$CH$_{Ar}$C$_{Ar}$C=N), 128.36 (*C*H$_{Ar}$CH$_{Ar}$C$_{Ar}$C=N), 128.04 (*C*H$_{Ar}$CH$_{Ar}$C$_{Ar}$-O), 127.55 (*C*H$_{Ar}$C$_{Ar}$C=N), 126.12 (*C*H$_{Ar}$C$_{Ar}$CH(CH$_3$)N), 124.89 (*C*H$_{Ar}$CH$_{Ar}$C$_{Ar}$CH(CH$_3$)N), 115.62 (*C*H$_{Ar}$C$_{Ar}$-O), 50.16 (*C*H(CH$_3$)N), 25.51 (*C*H$_3$); **IR** (neat, ATR) ν/cm^{-1} = 3059 (w), 2964 (m), 2925 (m), 2854 (w), 1670 (s), 1585 (w), 1488 (m), 1462 (w), 1449 (m), 1347 (m), 1289 (w), 1248 (m), 1226 (s), 1198 (m), 1112 (m), 1055 (m), 1023 (m); **HRMS**: calculated: 223.0992 [M]$^+$; found: 223.0986; **Optical Rotation** (*R*)-isomer: $[a]_D^{20}$ = -8.6 (c 0.13 in $CHCl_3$, 0.75% EtOH); **Optical Rotation** (*S*)-isomer: $[a]_D^{20}$ = +10.3 (c 0.165 in $CHCl_3$, 0.75% EtOH).

1-(2-methoxyphenyl)-2-methylpropan-1-amine (479)[130]

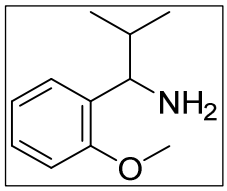

In a 500 mL three-neck round bottom flask equipped with a magnetic stirrer and a reflux condenser was inserted **488** (4.50 g, 33.8 mmol, 1.0 eq), CuBr (98.0 mg, 0.683 mmol, 0.02 eq) and dissolved in dry THF (75 mL). A solution of isopropyl magnesium chloride in THF (2 M, 32 mL, 6.61 g ^{i}PrMgCl, 64.27 mmol, 1.9 eq) was added and the resultant mixture heated to reflux for 16 hours. Afterwards the reaction mixture was allowed to cool to room temperature. A mechanical stirrer, an ammonia condensation vessel and washing bottles were mounted and the mixture cooled to -78 °C. Subsequently ammonia (approx. 200 mL) was condensed into the reaction mixture. Lithium (735 mg, 105 mmol, 3.1 eq) was added in small pieces until the reaction mixture turned blue. The cooling bath was removed and the reaction mixture was allowed to warm up overnight while stirring and evaporating all ammonia. *Tert*-butylmethylether (MTBE) was added to the mixture, cooled to 0 °C and titrated with concentrated HCl to pH 8. The organic layer was separated and the aequeous layer salted out and extracted with MTBE (3 x 100 mL). The combined organic layers were washed with brine (100 mL), 0.5 M HCl (3 x 150 mL) and the acidic aequeous phase extracted with MTBE (3 x 50 mL). The acidic aequeous layer was set to pH 11 with 10% NaOH (10%), salted out and extracted with MTBE (3 x 50 mL). The combined organic layers were dried over anhydrous $MgSO_4$, solvents removed at the rotavap and the residue was purified *via* distillation (63 °C at 0.08 mbar) to afford **479** (5.21 g, 29 mmol, 86%) as a yellow oil.

$C_{11}H_{17}NO$ (179.26 g/mol):
b.p.: 65 °C at 0.08 mbar; **^{1}H-NMR** (400 MHz, $CDCl_3$) δ 7.24 (m, 1H, CH_{Ar}C$_{Ar}$CH(NH$_2$)), 7.19 (m, 1H, CH_{Ar}CH$_{Ar}$C$_{Ar}$CH(NH$_2$)), 6.93 (t, *J* = 7.5, 1H, CH_{Ar}CH$_{Ar}$C$_{Ar}$(OCH$_3$)), 6.85 (d, *J* = 8.2 Hz, 1H, CH_{Ar}C$_{Ar}$(OCH$_3$)), 3.88 (d, *J* = 7.6 Hz, 1H, C*H*(NH$_2$)), 3.82 (s, 3H, OC*H*$_3$), 1.97 (m, 1H, C*H*(CH$_3$)$_2$), 1.50 (s, 2H, N*H*$_2$), 0.99 (d, *J* = 6.7 Hz, 3H, CH(C*H*$_3$)$_2$), 0.79 (d, *J* = 6.8 Hz, 3H, CH(C*H*$_3$)$_2$).

_N_-(1-(2-hydroxyphenyl)-2-methylpropyl)benzamide (497)

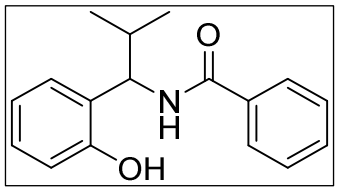

In a 25 mL round-bottom flask was placed **479** (1.0 g, 5.59 mmol, 1.0 eq.) and cooled to 0 °C. Benzoyl chloride (782 mg, 5.59 mmol, 1.0 eq.) and triethylamine (621 mg, 6.15 mmol, 1.1 eq.) were added dropwise and the reaction mixture was stirred at room temperature for 24 hours. Elution chromatography (SiO_2, EtOAc) and removal of solvents under reduced pressure afforded *N*-(1-(2-methoxyphenyl)-2-methylpropyl)benzamide (1.52 g, 5.36 mmol, 96 %) which was dissolved in dry dichloromethane (12 mL) and cooled to -78 °C. Boron tribromide (1.0 M in CH_2Cl_2, 16.1 mmol, 3.0 eq.) was added dropwise, the cooling bath removed and the reaction mixture allowed warming up to room temperature while stirring overnight. It was then cooled to 0 °C and quenched by addition NaOH (10% w/w, 30 mL). After seizure of gas evolution layers were separated and the aeqeous layer acidified with concentrated HCl (8 mL). It was then basified to pH of 8 by addition of $NaHCO_3$ (150 mL) and extracted with CH_2Cl_2 (2 x 25 mL). The combined organic layers were dried over anhydrous $MgSO_4$, filtered and solvents removed under reduced pressure. The residue was dried *in vacuo* to afford **497** (1.2 g, 4.46 mmol, 83 %) as a white solid. Enantiomers were separated via semipreparative HPLC (Daicel Chiralcel AD (2 cm x 25 cm), *n*-hexane : 2-propanol (90:10), 6 mL min^{-1}, 25 °C, 0.4 mL injection volume, t_R = 43.0 min (+), t_R = 52.0 min (-), **497** was dissolved in a mixture of heptane/2-propanol (9:1) to a concentration of 0.3g mL^{-1}.

$C_{17}H_{19}NO_2$ (269.34 g/mol):
m.p.: 138 °C; **^{1}H-NMR** (500 MHz, $CDCl_3$) δ 8.56 (s, 1H, O*H*), 7.75 (m, 2H, C$H_{Ar}C_{Ar}$C=O), 7.48 (m, 1H, CH_{Ar}CH_{Ar}C$H_{Ar}C_{Ar}$C=O), 7.39 (m, 2H, CH_{Ar}C$H_{Ar}C_{Ar}$C=O), 7.17 (dd, J = 7.6, 1.6 Hz, 1H, C$H_{Ar}C_{Ar}$CHNH), 7.14 (m, 1H, CH_{Ar}C$H_{Ar}C_{Ar}$(OH)), 7.02 (d, *J* = 9.1 Hz, 1H, NH), 6.94 (dd, *J* = 8.1, 1.2 Hz, 1H, C$H_{Ar}C_{Ar}$(OH)), 6.87 (td, *J* = 7.5, 1.2 Hz, 1H, CH_{Ar}C$H_{Ar}C_{Ar}$CHNH), 4.91 (dd, *J* = 10.3, 9.1 Hz, 1H, C*H*NH), 2.43 (dhept, *J* = 10.3, 6.6 Hz, 1H, C*H*$(CH_3)_2$), 1.18 (d, *J* = 6.6 Hz, 3H, CH_3), 0.87 (d, *J* = 6.6 Hz, 3H, CH_3); **^{13}C{^{1}H}-NMR** (101 MHz, $CDCl_3$) δ 168.46 (*C*=O), 155.22 (C_{Ar}(OH)), 133.87 (C_{Ar}C=O), 131.96 (*C*H_{Ar}CH_{Ar}C$H_{Ar}C_{Ar}$C=O), 128.85 (*C*H_{Ar}C$H_{Ar}C_{Ar}$(OH)), 128.75 (*C*H_{Ar}C$H_{Ar}C_{Ar}$C=O), 128.14 (*C*$H_{Ar}C_{Ar}$CHNH), 127.44 (C_{Ar}CHNH), 127.19 (*C*$H_{Ar}C_{Ar}$C=O), 120.54 (*C*H_{Ar}C$H_{Ar}C_{Ar}$CHNH), 118.02 (*C*$H_{Ar}C_{Ar}$(OH)), 56.86 (*C*HNH), 31.32 (*C*H$(CH_3)_2$), 20.61 (*C*H_3), 20.51 (*C*H_3); **IR** (neat, ATR) ν/cm^{-1} = 3401 (m), 3155 (w), 3103 (w), 3076 (w), 2955 (w), 2870 (w), 1633 (s), 1603 (s), 1576 (m), 1487 (m), 1453 (s), 1380 (m), 1311 (m), 1259 (m), 1252 (m), 1188 (m), 1130 (m), 1116 (s), 1104 (w), 1040 (m), 930 (m), 857 (m), 756 (s), 704 (s), 685 (s); **MS** (EI, 70 eV): 269.1 (3.4%, $[M]^+$). 226.1 (49%, $[M\text{-}C_3H_7]^+$); **HRMS**: calculated: 269.1411 $[M]^+$; found: 269.1413; **EA**: calculated: C, 75.81; H, 7.11; N, 5.20; found: C, 74.60 H, 7.13; N, 5.13; **Optical Rotation** (*R*)-isomer: $[\alpha]_D^{20}$ = -24.3 (c 0.75 in $CHCl_3$, 0.75% EtOH); **Optical Rotation** (*S*)-isomer: $[\alpha]_D^{20}$ = +25.7 (c 0.75 in $CHCl_3$, 0.75% EtOH).

4-Isopropyl-2-phenyl-4H-benzo[e][1,3]oxazine (398)

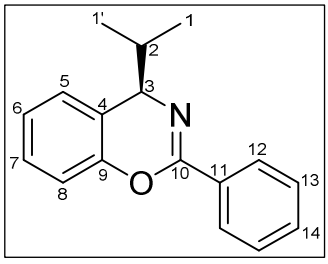

In a 10 mL Schlenk vial was placed (*R*)-**497** (100 mg, 0.37 mmol, 1.0 eq.) and dissolved in CH_2Cl_2 (1 mL). The solution was cooled to -40 °C with the aid of a cryostat. Then a solution of $POCl_3$ (0.4 M in CH_2Cl_2, 1 mL, 0.4 mmol, 1.08 eq.) was added dropwise. The reaction mixture was stirred at -40 °C for 2 hours. Pyridine (176 mg, 2.23 mmol, 6.0 eq.) was added dropwise and stirring continued for one hour. The cryostat was removed and the reaction mixture allowed warming to room temperature while stirring overnight. It was then cooled to 0 °C and quenched with NaOH solution (1 M, 5 mL, 5 mmol). After ether extraction (3 x 25 mL) the combined organic layers were dried over $MgSO_4$, filtered and solvents removed under reduced pressure. The residue was purified by flash chromatography to afford (*R*)-**398** (39 mg, 0.155 mmol, 42%) as an off-white oil. Identical to the procedure above, (*S*)-**497** (538 mg, 2.0 mmol, 1.0 eq.) , a solution of $POCl_3$ (306 mg, 2.0 mmol, 1.0 eq.) and pyridine (949 mg, 12 mmol, 6.0 eq.) gave (*S*)-**398** (114 mg, 0.45 mmol, 23%) as a clear oil.

$C_{17}H_{17}NO$ (251.32 g/mol):
^{1}H-NMR (400 MHz, $CDCl_3$) δ 8.10 (m, 2H, H12), 7.46 (m, 3H, H13 and H14), 7.25 (td, *J* = 7.7, 1.8 Hz, 1H, H7), 7.14 (td, *J* = 7.4, 1.2 Hz, 1H, H6), 7.09 (dd, *J* = 7.5, 1.7 Hz, 1H, H5), 7.04 (dd, *J* = 8.1, 1.0 Hz, 1H, H8), 4.67 (d, *J* = 3.9 Hz, 1H, H3), 2.14 (m, 1H, H2), 1.09 (d, *J* = 6.8 Hz, 3H, H1), 0.86 (d, *J* = 6.8 Hz, 3H, H1'');

$^{13}C\{^1H\}$-NMR (101 MHz, $CDCl_3$) δ 152.10 (C10), 149.90 (C9), 132.53 (C11), 131.04 (C14), 128.36 (C13), 127.96 (C7), 127.62 (C12), 126.80 (C5), 124.56 (C6), 122.50 (C4), 115.39 (C8), 60.06 (C3), 36.56 (C2), 18.93 (C1), 17.20 (C1'); **IR** (neat, ATR) ν/cm^{-1} = 3066 (w), 3044 (w), 2959 (m), 2928 (w), 2871 (w), 1675 (s), 1586 (w), 1486 (m), 1458 (m), 1355 (m), 1291 (m), 1243 (m), 1224 (s), 1194 (m), 1063 (m), 1028 (w); **HRMS**: calculated: 251.1305 $[M]^+$; found: 251.1308; **EA**: calc. C, 81.24; H, 6.82; N, 5.57; O, 6.37; found: C, 80.91; H, 7.48; N, 5.20; **Optical Rotation** (*R*)-isomer: $[a]_D^{20}$ = -44.4 (c 1.65 in $CHCl_3$, 0.75% EtOH); **Optical Rotation** (*S*)-isomer: $[a]_D^{20}$ = +20.4 (c 0.75 in $CHCl_3$, 0.75% EtOH).

***N*-(2-methoxybenzylidene)-1-phenylmethanamine (492)[128]**

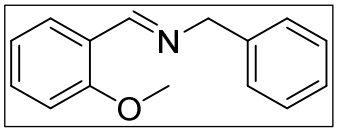

A 50 mL two-necked round-bottom flask equipped with a stirring bar and a Schlenk bridge was set under argon atmosphere and charged with 4 Å molecular sieves (4.00 g). Benzylamine (8.0 mL, 73.4 mmol, 1.0 eq) was added and dissolved in CH_2Cl_2 (19 mL). To the stirred mixture was added a solution of 2-methoxybenzaldehyde **491** (10.0 g, 73.4 mmol, 1.0 eq) in CH_2Cl_2 (4.3 mL) and stirring continued for three hours.The reaction mixture was filtered through a pad of celite and the solvent was removed under reduced pressure. Distillation (0.09-0.10 mbar, 136-138 °C) of the filtrate gave **492** (14.5 g, 64.4 mmol, 88%) as a colourless oil.

$C_{15}H_{15}NO$ (225.29 g/mol):
b.p.: 136-138 °C at 0.09-0.10 mbar; **^{1}H-NMR** (400 MHz, $CDCl_3$) δ 8.85 (s, 1H, C*H*=N), 8.01 (dd, ^3J = 7.7 Hz, ^4J = 1.6 Hz, 1H, CH_{Ar}C$_{Ar}$CH=N), 7.39 (m, 1H, CH_{Ar}CH$_{Ar}$C$_{Ar}$(OCH$_3$)), 7.33 (m, 4H, CH_{Ar}CH$_2$ and CH_{Ar}CH$_{Ar}$CH$_2$), 7.24 (m, 1H, CH_{Ar}CH$_{Ar}$CH$_{Ar}$CH$_2$), 6.98 (t, ^3J = 7.5 Hz, 1H, CH_{Ar}C$_{Ar}$(OCH$_3$)), 6.92 (d, *J* = 8.3 Hz, 1H, CH_{Ar}CH$_{Ar}$C$_{Ar}$CH=N), 4.82 (s, 2H, CH_2), 3.88 (s, 3H, OCH_3); **GC-MS** (EI, 70 eV, PhMeSi, 100.2/10.270/10): t_R = 16.9 min, *m/z* = 224 ($[M-H]^+$).

***N*-benzyl-1-(2-methoxyphenyl)-2,2-dimethylpropan-1-amine (493)[128]**

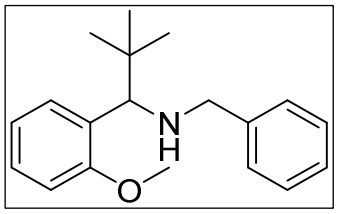

A 250 mL two-necked round-bottom flask equipped with a stirring bar and a Schlenk bridge was set under argon atmosphere and charged with *tert*-BuLi (22 mL of a 1.7 M solution in pentane, 37.8 mmol, 1.7 eq). The solution was cooled to -30 °C and via a cooling trap the solvent was removed *in vacuo*. The resulting colourless solid was cooled to -78 °C and THF (22 mL) was added slowly resulting in a yellow suspension. Afterwards a solution of **492** (5.00 g, 22.2 mmol, 1.0 eq) in THF (11 mL) was added over a period of two hours using a syringe pump and causing the mixture to turn purple. After three hours h the mixture was allowed to warm to 0 °C and stirring was continued overnight. A saturated aqueous solution of NH_4Cl (11 mL) was added and the mixture turned yellow. Layers were separated, the aqueous layer was extracted with Et_2O (2 x 20 mL), the combined organic layers were dried over Na_2SO_4 and solvent was removed under reduced pressure. Distillation (0.06-0.08 mbar, 131-142 °C) of the residue gave **493** (4.82 g, 17.0 mmol, 77%) as a yellow oil.

$C_{19}H_{25}NO$ (283.41 g/mol):
b.p.: 131-142 °C at 0.06-0.08 mbar; **^{1}H-NMR** (400 MHz, $CDCl_3$) δ 7.45 (d, *J* = 7.3 Hz, 1H, CH_{Ar}C$_{Ar}$CHNH), 7.18 (m, 4H, CH_{Ar}C$_{Ar}$CH$_2$ and CH_{Ar}CH$_{Ar}$C$_{Ar}$CH$_2$), 7.21 (m, 2H, CH_{Ar}CH$_{Ar}$C$_{Ar}$CHNH and CH_{Ar}CH$_{Ar}$CH$_{Ar}$C$_{Ar}$CH$_2$), 6.97 (t, *J* = 7.2 Hz, 1H, CH_{Ar}CH$_{Ar}$C$_{Ar}$(OCH$_3$)), 6.87 (d, *J* = 8.1 Hz, 1H, CH_{Ar}C$_{Ar}$(OCH$_3$)), 4.06 (s, 1H, C*H*NH), 3.77 (s, 3H, OCH_3), 3.55 (d, *J* = 13.2 Hz, 1H, CH_2), 3.39 (d, *J* = 13.2 Hz, 1H, CH_2), 0.89 (s, 9H, C(CH_3)$_3$).

1-(2-methoxyphenyl)-2,2-dimethylpropan-1-amine (494)[128]

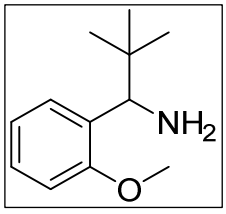

A 50 mL round-bottom flask equipped with a stirring bar and an argon tube was charged with Pd/C (Degussa type 101 NE/W, 0.343 g), **493** (4.82 g, 17.0 mmol, 1.0 eq) and EtOH (15 mL). The mixture was degassed performing three "freeze-pump-thaw" cycles purging with hydrogen each time. Afterwards the mixture was heated to 60 °C and stirred for 26 hours under ambient hydrogen pressure. After cooling to room temperature the mixture

was filtered through a pad of celite and the solvent was removed under reduced pressure. Distillation (0.06-0.08 mbar, 82-85 °C) of the residue gave **494** (2.93 g, 15.2 mmol, 89%). Enantiomers were separated by recrystallisation. A 25 mL round-bottom flask equipped with a stirring bar and a reflux condenser was charged with **494** (2.93 g, 15.2 mmol, 1.0 eq), (*S*)-mandelic acid **498** (2.31 g, 15.2 mmol, 1.0 eq) and AcOEt (4.5 mL). The mixture was heated to reflux until all the solid was dissolved and the stirring bar was removed from the hot solution. After 22 hours the mother liquor was decanted and the remaining crystals were washed with Et_2O and *n*-pentane and dried *in vacuo*. Afterwards the obtained (*R*,*S*)-salt was recrystallized twice as follows. A 50 mL round-bottom flask with a stirring bar was charged with the (*R*,*S*)-salt (1.95 g, 5.64 mmol), AcOEt (14.5 mL) and EtOH (1.16 mL). The mixture was heated until all salt dissolved and the stirring bar was removed. After 40 hours the mother liquor was decanted and the precipitated crystals were washed with Et_2O and *n*-pentane and dried in vacuo. A diastereomeric excess >96% was detected by ^{1}H-NMR. The enantiomerically enriched (*R*,*S*)-salt (0.980 g, 2.84 mmol) was put into a separating funnel and 10% aqueous NaOH (10 mL) was added. Extraction of this mixture with AcOEt (3 x 25 mL), drying over Na_2SO_4 and evaporation of the solvent gave (*R*)-**494** (0.544 g, 2.81 mmol, 37%) as a colourless oil. The mother liquors from the preceeding recrystallisations were combined in a separating funnel, diluted with TBME (40 mL) and washed with 10% aqueous NaOH (2 x 20 mL). The combined aqeuos layers were extracted with TBME (3 x 40 mL). The combined organic layers were dried over Na_2SO_4 and evaporation of the solvent gave already partially enantiomerically enriched (*S*)-**494** (2.37 g, 12.3 mmol). A 50 mL round-bottom flask was charged with partially enantiomerically enriched (*S*)-**494**, (*R*)-mandelic acid **498** (1.86 g, 12.3 mmol), AcOEt (26.3 mL) and EtOH (0.7 mL) and the mixture was heated until all solid dissolved. After 20 hours the mother liquor was decanted and the crystals were washed with Et_2O and *n*-pentane. This recrystallisation procedure was repeated once. A diastereomeric excess >96% was detected by ^{1}H-NMR. The free amine was obtained from the (*S*,*R*)-salt (0.727 g, 2.11 mmol) by addition of 10% aqueous NaOH and subsequent extraction with AcOEt as described above to afford (*S*)-**494** (0.381 g, 1.97 mmol, 26%) as a colourless oil.

$C_{12}H_{19}NO$ (193.29 g/mol):
b.p.: 82-85 °C at 0.06-0.08 mbar; **^{1}H-NMR** (500 MHz, $CDCl_3$) δ 7.34 (m_{br}, 1H, CH_{Ar}C$_{Ar}$CHNH$_2$), 7.19 (t, *J* = 7.8 Hz, 1H, CH_{Ar}CH$_{Ar}$C$_{Ar}$CHNH$_2$), 6.93 (t, *J* = 7.4 Hz, 1H, CH_{Ar}CH$_{Ar}$C$_{Ar}$(OCH$_3$)), 6.84 (d, *J* = 8.2 Hz, 1H, CH_{Ar}C$_{Ar}$(OCH$_3$)), 4.26 (s, 1H, C*H*NH$_2$), 3.79 (s, 3H, OCH_3), 1.52 (s_{br}, 2H, NH_2), 0.91 (s, 9H, C(CH$_3$)$_3$); **GC-MS** (EI, 70 eV, PhMeSi, 100.2/10.270/10): t_R = 10.3 min, *m/z* = 136 ([M-(C(CH$_3$)$_3$)]$^+$).
Optical Rotation (*R*)-isomer: $[\alpha]_D^{20}$ = +37.0 (c 2.02 in EtOH); **Optical Rotation** (*S*)-isomer: $[\alpha]_D^{20}$ = -37.1 (c 2.02 in EtOH).

(*R*)-(-)-2-(1-amino-2,2-dimethylpropyl)phenol (499)[128]

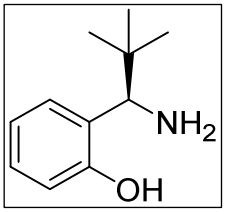

In a 25 mL two-necked round-bottom flask equipped with a stirring bar and a Schlenk bridge (*R*)-**494** (0.537 g, 2.78 mmol, 1.0 eq) was dissolved in CH_2Cl_2 (4.7 mL) and cooled to -78 °C. BBr_3 (7.5 mL of a 1 M solution in CH_2Cl_2) was added dropwise and the mixture was stirred overnight. The reaction mixture was poured on a saturated aqueous solution of $NaHCO_3$ (20 mL) and ice. Additional $NaHCO_3$ solution was added until a pH at 9 was observed. Phase separation, extraction with CH_2Cl_2 (3 x 30 mL), drying over Na_2SO_4 and evaporation of the solvent gave crude (*R*)-**499** (511 mg, 2.78 mmol, 99%) as a brown solid.

$C_{11}H_{17}NO$ (179.26 g/mol):
^{1}H-NMR (250 MHz, $CDCl_3$) δ 7.14 (t, *J* = 7.3 Hz, 1H, CH_{Ar}CH$_{Ar}$C$_{Ar}$CH(NH$_2$)), 6.90 (d, *J* = 7.1 Hz, 1H, CH_{Ar}C$_{Ar}$CH(NH$_2$)), 6.81 (d, *J* = 8.0 Hz, 1H, CH_{Ar}C$_{Ar}$(OH)), 6.74 (t, *J* = 7.2 Hz, 1H, CH_{Ar}CH$_{Ar}$C$_{Ar}$(OH)), 3.87 (s, 1H, C*H*(NH$_2$)), 0.96 (s, 9H, C(CH_3)$_3$); **Optical Rotation** (*R*)-isomer: $[\alpha]_D^{20}$ = -37.6 (c 2.06 in $CDCl_3$, 0.75% EtOH).

(*R*)-(-)-*N*-(1-(2-hydroxyphenyl)-2,2-dimethylpropyl)benzamide (500)[127]

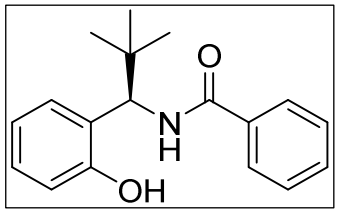

In a 25 mL two-necked round-bottom flask equipped with a stirring bar and a Schlenk bridge a solution of crude (*R*)-**499** (0.470 g, 2.62 mmol, 1.0 eq) in CH_2Cl_2 (7.5 mL) was cooled to 0 °C and benzoyl chloride (0.33 mL, 2,88 mmol, 1.1 eq) and triethylamine (0.44 mL, 3.15 mmol, 1.2 eq) were added.

The cooling bath was removed after 5 min. and the mixture was stirred at room temperature for 18 hours. Elution of the reaction mixture with AcOEt through a short silica gel column gave (*R*)-**500** (435 mg, 1.54 mmol, 59%) as a grey solid.

$C_{18}H_{21}NO_2$ (283.36 g/mol):
m.p.: 151-152 °C; **^{1}H-NMR** (400 MHz, $CDCl_3$) δ 8.23 (d, *J* = 7.2 Hz, 1H, N*H*), 7.80 (d, *J* = 6.9 Hz, 2H, CH_{Ar}C$_{Ar}$C=O), 7.52 (t, *J* = 7.7 Hz, 1H, CH_{Ar}CH$_{Ar}$CH$_{Ar}$C$_{Ar}$C=O), 7.40 (t, *J* = 7.7 Hz, 2H, CH_{Ar}CH$_{Ar}$C$_{Ar}$C=O), 7.13 (t, *J* = 7.3 Hz, 1H, CH_{Ar}CH$_{Ar}$C$_{Ar}$(OH)), 6.89 (t, *J* = 7.5 Hz, 1H, CH_{Ar}CH$_{Ar}$C$_{Ar}$CHNH), 6.78 (d, *J* = 8.1 Hz, 1H, CH_{Ar}C$_{Ar}$(OH)), 5.25 (d, *J* = 9.9 Hz, 1H, C*H*NH), 1.06 (s, 9H, C(CH_3)$_3$); **IR** (neat, ATR) ν/cm^{-1} = 3395 (m), 3236 (w), 3185 (w), 2961 (m), 2866 (w), 1639 (s), 1625 (s), 1600 (m), 1531 (s), 1487 (m), 1453 (s), 1356 (m), 1245 (m), 1208 (m), 1174 (m), 1110 (m), 1063 (m), 1024 (m), 838 (m), 751 (s), 704 (s), 691 (s); **MS** (EI, 70 eV): 283.1 (1.4%, $[M]^+$). 226.1 (100%, $[M\text{-}C_4H_9]^+$); **Optical Rotation** (*R*)-isomer: $[\alpha]_D^{20}$ = -114.0 (c 3.26 in EtOH).

(*R*)-(-)-4-(*tert*-butyl)-2-phenyl-4H-benzo[e][1,3]oxazine (400)[127]

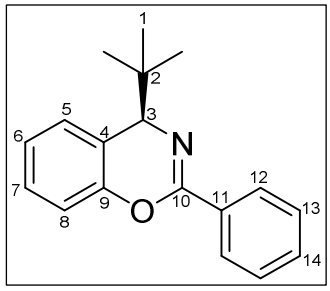

In a 10 mL Schlenk vial was placed (*R*)-**500** (75 mg, 0.265 mmol, 1.0 eq.) and dissolved in CH_2Cl_2 (2.6 mL). The solution was cooled to -40 °C with the aid of a cryostat. Then a solution of $POCl_3$ (40 mg, 0.265 mmol, 1.0 eq.) was added dropwise. The reaction mixture was stirred at -40 °C for 30 minutes. Pyridine (126 mg, 1.59 mmol, 6.0 eq.) was added dropwise and stirring continued for one hour. The cryostat was removed and the reaction mixture allowed to warm to room temperature while stirring overnight. It was then cooled to 0 °C and quenched with NaOH solution (1 M, 5 mL, 5 mmol). After ether extraction (3 x 25 mL) the combined organic layers were dried over $MgSO_4$, filtered and solvents removed under reduced pressure. The residue was purified by flash chromatography (SiO_2, cyclohexane/EtOAc 20:1, 20x2 cm, 7 mL fractions) to afford (*R*)-**500** (20 mg, 0.073 mmol, 28%) as a clear oil.

$C_{18}H_{19}NO$ (265.35 g/mol):
^{1}H-NMR (400 MHz, $CDCl_3$) δ 8.13 (m, 2H, H12), 7.50 (m, 1H, H14) 7.47 (m, 2H, H13), 7.30 (m, 1H, H7), 7.16 (m, 1H, H6), 7.13 (m, 1H, H5), 7.08 (d, *J* = 7.9 Hz, 1H, H8), 4.46 (s, 1H, H3), 0.99 (s, 9H, H1); **^{13}C{^{1}H}-NMR** (101 MHz, $CDCl_3$) δ 152.32 (C10), 150.39 (C9), 132.37 (C11), 131.12 (C14), 128.68 (C5), 128.40 (C13), 128.02 (C7), 127.79 (C12), 123.96 (C6), 121.61 (C4), 115.50 (C8), 64.71 (C3), 38.88 (C2), 26.18 C(1); **IR** (neat, ATR) ν/cm^{-1} = 3058 (w), 3032 (w), 2950 (m), 2930 (w), 2905 (m), 1667 (s), 1583 (w), 1494 (m), 1486 (m), 1477 (m), 1458 (m), 1449 (m), 1391 (w), 1363 (m), 1348 (s), 1287 (w), 1244 (s), 1221 (s), 1193 (s), 1177 (m), 1091 (s), 1066 (s), 1023 (m); **HRMS**: calculated: 265.1462 $[M]^+$; found: 265.1464; **Optical Rotation** (*R*)-isomer: $[\alpha]_D^{20}$ = -11.0 (c 1.1 in $CHCl_3$, 0.75% EtOH).

Tetrahydropyridines

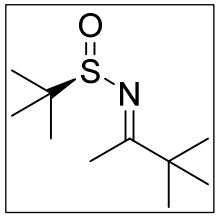

(*R*)-*N*-(3,3-dimethylbutan-2-ylidene)-2-methylpropane-2-sulfinamide (474)[124]

A 50 mL Schlenk tube was equipped with a magnetic stirrer and evacuated. It was then dried with a bunsen burner, allowed to cool to room temperature and purged with argon three times. It was then charged with $Ti(OEt)_4$ (1.86 g, 8.25 mmol, 2.0 eq.) and dissolved in dry THF (16.5 mL). 3,3-dimethylbutan-2-one **473** (413 mg, 4.125 mmol, 1.0 eq.) and (*R*)-2-methylpropane-2-sulfinamide **468** (500 mg, 4.125 mmol, 1.0 eq.) were added and the reaction mixture heated to 70 °C for 24 hours. After cooling to room temperature, the reaction mixture was poured into brine (17 mL) and the resultant suspension filtered over Cellite. The filter cake was washed with EtOAc (20 mL) and the aeqeous layer decanted. The organic layer was washed with brine (20 mL) and the combined aequous layers extracted with EtOAc (20 mL). The combined organic layers were dried over Na_2SO_4, filtered and solvents removed under reduced pressure. The residue was subjected to flash chromatography (SiO_2, cyclohexane/Et_2O 1:1, 18x3 cm, 20 mL fractions) to afford (*R*)-**465** (313 mg, 1.54 mmol, 37%) as a clear oil.

$C_{10}H_{21}NOS$ (M_W = 203.34 g/mol):

^{1}H-NMR (500 MHz, $CDCl_3$) δ 2.31 (s, 3H), 1.23 (s, 9H), 1.16 (s, 9H); **Optical Rotation**: $[a]_D^{20}$ = -188 (c 1.0 in $CHCl_3$, 0.75% EtOH; Lit:[174] -192, c 1.0 in CH_2Cl_2).

(*R*)-2-methyl-*N*-(3-methylbutan-2-ylidene)propane-2-sulfinamide (465)[124]

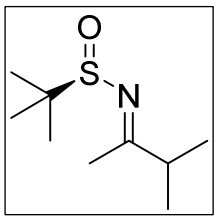

A 50 mL Schlenk tube was equipped with a magnetic stirrer and evacuated. It was then dried with a bunsen burner, allowed to cool to room temperature and purged with argon three times. It was then charged with $Ti(OEt)_4$ (1.86 g, 8.25 mmol, 2.0 eq.) and dissolved in dry THF (16.5 mL). 3-methylbutan-2-one **467** (355 mg, 4.125 mmol, 1.0 eq.) and (*R*)-2-methylpropane-2-sulfinamide **468** (500 mg, 4.125 mmol, 1.0 eq.) were added and the reaction mixture heated to 70 °C for 24 hours. After cooling to room temperature, the reaction mixture was poured into brine (17 mL) and the resultant suspension filtered over Cellite. The filter cake was washed with EtOAc (20 mL) and the aequeous layer decanted. The organic layer was washed with brine (20 mL) and the combined aequous layers extracted with EtOAc (20 mL). The combined organic layers were dried over Na_2SO_4, filtered and solvents removed under reduced pressure. The residue was subjected to flash chromatography (SiO_2, cyclohexane/Et_2O 1:1, 18x3 cm, 20 mL fractions) to afford (*R*)-**465** (700 mg, 3.7 mmol, 89%) as a clear oil.

$C_9H_{19}NOS$ (M_W = 189.32 g/mol):
^{1}H-NMR (400 MHz, $CDCl_3$) δ 2.64 – 2.49 (m, 1H), 2.31 (s, 3H), 1.23 (s, 9H), 1.13 (d, *J* = 6.8 Hz, 5H), 1.12 (d, *J* = 6.8 Hz, 1H); **^{13}C{^{1}H}-NMR** (125 MHz, $CDCl_3$) δ 189.34, 56.56, 41.45, 22.31, 21.21, 19.92, 19.69; **Optical Rotation**: $[a]_D^{20}$ = -185 (c 1.0 in $CHCl_3$, 0.75% EtOH; Lit:[175] -185.7, c 1.0 in $CHCl_3$).

1-phenylprop-2-en-1-one (466)

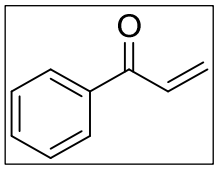

Variant A:[125]
A 250 mL round-bottom flask equipped with a reflux condenser and a magnetic stirrer was charged with acetophenone **117** (6 g, 50 mmol, 1.0 eq.), *para*-formaldehyde **475** (3 g, 100 mmol, 2.0 eq.) and dissolved in THF (100 mL). Diisopropylammonium 2,2,2-trifluoroacetate (10.75 g, 50 mmol, 1.0 eq.) was added and the reaction mixture heated to reflux for 2 hours. After cooling to room temperature, again paraformaldehyde **475** (3 g, 100 mmol, 2.0 eq.) was added and the reaction mixture heated to reflux while stirring overnight. After cooling to room temperature, volatiles were removed under reduced pressure and the residue was dissolved in Et_2O (50 mL). It was then washed with HCl (1.0 M, 25 mL), NaOH (1.0 M, 25 mL) and brine (25 mL) before being dried over Na_2SO_4, filtered and solvents removed under reduced pressure. The residue was subjected flash chromatography (SiO_2, cyclohexane/EtOAc 20:1 gradient to 8:1, 23x6 cm, 50 mL fractions) to afford **466** (3.02 g, 22.88 mmol, 45%) as a clear oil.

Variant B:[126]
An oven-dried 250 mL three-necked round-bottom flask was equipped ith a magnetic stirrer and purged with argon three times. It was then charged with 3-chloro-1-phenylpropan-1-one **476** (2.5 g, 14.83 mmol, 1.0 eq.) and dissolved in CH_2Cl_2 (33 mL). Triethylamine (3.6 g, 35.57 mmol, 2.4 eq.) was added dropwise via syringe over a time course of 5 minutes. The reaction mixture was stirred at room temperature for 18 hours before being quenched with HCl (4.0 M, 3x 150 mL), washed with water (150 mL), $NaHCO_3$ (150 mL) and brine (150 mL). The organic layer was dried over Na_2SO_4, filtered and solvents removed under reduced pressure. The residue was purified by distillation (35 °C, 0.06 mbar) to afford **466** (1.39 g, 10.48 mmol, 70%) as a clear oil. It was directly dissolved in dry THF (10.5 mL) and stored as 1.0 M solution in the freezer.

C_9H_8O (M_W = 132.16 g/mol):
^{1}H-NMR (400 MHz, $CDCl_3$) δ 7.95 (dt, *J* = 8.5, 1.7 Hz, 1H), 7.62 – 7.54 (m, 1H), 7.53 – 7.44 (m, 1H), 7.16 (dd, *J* = 17.1, 10.6 Hz, 1H), 6.44 (dd, *J* = 17.1, 1.7 Hz, 1H), 5.94 (dd, *J* = 10.6, 1.7 Hz, 1H); **^{13}C{^{1}H}-NMR** (125 MHz, $CDCl_3$) δ 191.19, 137.39, 133.12, 132.50, 130.34, 128.83, 128.77, 128.75.

(*S*)-2-methyl-*N*-(2-methyl-7-oxo-7-phenylheptan-3-ylidene)propane-2-sulfinamide (464)

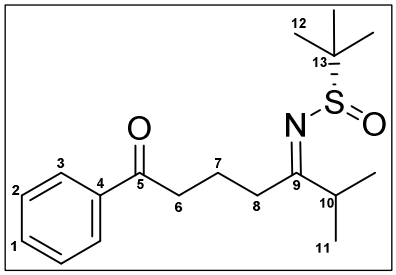

A 50 mL Schlenk tube was equipped with a magnetic stirrer and evacuated before being flame-dried with a bunsen burner. After purging with Argon three times, it was charged with dry THF (5.3 mL), diisopropylamine (352 mg, 3.49 mmol, 1.2 eq.) and cooled to -10 °C. *n*-butyl lithium (1.6 M, 3.2 mmol, 1.1 eq.) was added dropwise and the reaction mixture stirred for 20 minutes. It was then cooled to -78 °C and (*S*)-**465** (550 mg, 2.91 mmol, 1.0 eq.) was added. The reaction mixture was stirred for 30 minutes. Zinc bromide (786 mg, 3.49 mmol, 1.2 eq.) was added and stirring continued at -78° C for 45 minutes. A solution of **466** (1.0 M in THF, 3.78 mmol, 1.3 eq.) was colled to -78° C and added dropwise via cannula to the reaction mixture. Stirring was continued at -78 °C for 6 hours. The reaction was quenched with a THF/acetic acid mixture (4:1) at -78°C until the pH reached ~6. It was diluted with EtOAc (30 mL) and washed with brine (3x20 mL). The organic layer was dried over Na_2SO_4, dissolved in dry toluene (20 mL) and volatiles removed under reduced pressure (procedure repeated twice). The residue was subjected to flash chromatography (SiO_2, cyclohexane/EtOAc 4:1, 18x6 cm, 20 mL fractions) to afford (*R*)-**464** (502 mg, 1.575 mmol, 54 %) as a clear oil. It was further purified by sempreparative HPLC. Flash chromatography was hampered by co-elution of sideproducts.

$C_{18}H_{27}NO_2S$ (M_W = 321.48 g/mol):
^{1}H-NMR (500 MHz, $CDCl_3$) δ 7.95 (m, 2H, H3), 7.56 (t, *J* = 7.4 Hz, 1H, H1), 7.46 (t, *J* = 7.7 Hz, 2H, H2), 3.08 (t, *J* = 7.0 Hz, 2H, H6), 2.87 (td, *J* = 11.4, 5.3 Hz, 1H, H8), 2.74 (m, 1H, H8'), 2.70 (m, 1H, H10), 2.06 (m, 2H, H7), 1.24 (s, 9H, H12), 1.13 (m, 6H, H11); **^{13}C{^{1}H}-NMR** (125 MHz, $CDCl_3$) δ 199.40 (C5), 191.05 (C9), 136.75 (C4), 133.07 (C1), 128.55 (C2), 127.99 (C3), 56.29 (C13), 39.04 (C10), 38.12 (C6), 34.19 (C8), 22.17 (C12), 21.89 (C7), 20.37 (C11); **HPLC** (Silica, *n*-hexane/iso-propanol 98:2, 6.0 mL/min, 25 °C, 207/240 nm): t_R = 93.0 min; **HRMS**: calculated: 322.1835 $[M+H]^+$; found: 322.1829; **IR** (neat, ATR) ν/cm^{-1} = 2963 (m), 2928 (w), 2903 (w), 2869 (w), 1705 (w), 1684 (s), 1619 (m), 1598 (m), 1580 (w), 1448 (m), 1362 (m), 1259 (w), 1208 (m), 1180 (m), 1068 (s), 825 (m), 755 (m); **Optical rotation**: $[\alpha]_D^{20}$ = -74.0 (c = 2.17 in $CHCl_3$ with 0.75% EtOH)

(*S*)-*N*-((3*R*)-7-hydroxy-2-methyl-7-phenylheptan-3-yl)-2-methylpropane-2-sulfinamide (477)

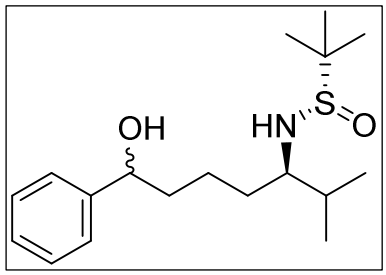

An oven-dried 10 mL two-necked round-bottom flask was equipped with a magnetic stirrer and a septum before being charged with (*S*)-**464** (166 mg, 0.517 mmol, 1.0 eq.), dissolved in dry THF (3 mL) and cooled to -50 °C. *L*-Selectride (1.0 M, 2.6 mmol, 5 eq.) was added dropwise and the reaction mixture stirred at -50 °C overnight. It was then warmed to 0 °C and quenched by slowly adding methanol (2 mL). After warming to room temperature while stirring the reaction mixture was diluted with Et_2O (10 mL) and washed with brine (2x25 mL). Organic components were extracted with EtOAc (2x25 mL) and the combined organic layers were dried over anhydrous $MgSO_4$, filtered and solvents removed under reduced pressure. The residue was subjected to flash chromatography (SiO_2, cyclohex/EtOAc 3:1 gradient to 1:1, 21.5x3.5 cm, 20 mL fractions) to afford (*S*)-**477** (226 mg, 0.695 mmol, 44 %) as a mixture of diastereomers.

$C_{18}H_{31}NO_2S$ (M_W = 325.51 g/mol):
mixture of diastereomers, partially superimposed:**^{1}H-NMR** (400 MHz, $CDCl_3$) δ 7.39 – 7.35 (m, 4H), 7.35 – 7.32 (m, 4H), 7.26 – 7.21 (m, 2H), 4.78 (dd, *J* = 7.7, 4.8 Hz, 1H), 4.66 (dd, *J* = 9.1, 3.6 Hz, 1H), 3.10 – 3.01 (m, 2H), 2.93 (d, *J* = 7.9 Hz, 1H), 2.89 (d, *J* = 7.6 Hz, 1H), 1.89 – 1.45 (m, 14H), 1.24 (s, 9H), 1.23 (s, 9H), 0.89 (d, *J* = 6.8 Hz, 3H), 0.88 (d, *J* = 6.7 Hz, 3H), 0.86 (d, *J* = 6.8 Hz, 3H), 0.84 (d, *J* = 6.9 Hz, 3H); **^{13}C{^{1}H}-NMR** (101 MHz, $CDCl_3$) δ 145.75, 145.17, 128.42, 128.38, 127.21, 127.19, 125.91, 125.83, 74.00, 73.20, 62.17, 61.47, 56.39, 56.36, 38.82, 38.48, 33.00, 32.66, 32.59, 32.40, 23.05, 22.99, 22.86, 22.33, 20.67, 19.39, 17.66, 17.23; **IR** (neat, ATR) ν/cm^{-1} = 3325 (mbr), 3062 (w), 3027 (w), 2959 (m), 2928 (m), 2870 (m), 2455 (m), 1388 (w), 1364 (m), 1043 (s), 953 (w), 820 (m), 760 (m), 701 (s); **HRMS**: calculated:

348.1968 $[M+Na]^+$; found: 348.1968; **HPLC** (Daicel Chiracel IC, *n*-heptane/iso-propanol 90:10, 0.5 mL/min, 25 °C, 209/258 nm): t_R = 24.47 min, t_R = 30.21, t_R = 38.50.

(*S*)-2-methyl-*N*-((*R*)-2-methyl-7-oxo-7-phenylheptan-3-yl)propane-2-sulfinamide (463)

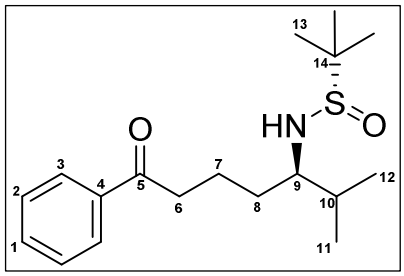

A 25 mL round-bottom flask was equipped with a magnetic stirrer, charged with (*S*)-**477** (266 mg, 0.695 mmol, 1.0 eq.) and dissolved in CH_2Cl_2 (2.5 mL, saturated with water). Dess-Martin-Periodane (593 mg, 1.4 mmol, 2.0 eq.) was added in one portion and the reaction mixture stirred for 2 hours at room temperature. The reaction mixture was diluted with CH_2Cl_2 (1.5 mL, saturated with water) being added over the course of 15 minutes before $Na_2S_2O_3$ (2.2 g, 6 mmol, 8.7 eq.) dissolved in sat. $NaHCO_3$ solution was added. The resulting suspension was stirred vigorously until both phases became clear. The organic components were extracted with Et_2O (2x10 mL) and the combined organic layers washed with $NaHCO_3$ (2x10 mL), brine (2x10 mL), dried over anhydrous $MgSO_4$, filtered and solvents removed under reduced pressure. The residue was purified by flash chromatography (SiO_2, cyclohexane/EtOAc 1:1, 15x4 cm, 20 mL fractions) to afford (*S*)-**463** (169 mg, 0.523 mmol, 75%) as a sticky yellow solid. Diastereomeric excess was determind to >97:3 by ^{1}H-NMR.

$C_{18}H_{29}NO_2S$ (MW = 323.49 g/mol):
^{1}H-NMR (400 MHz, $CDCl_3$) δ 7.95 (d, *J* = 7.1 Hz, 1H, H3), 7.54 (t, *J* = 7.4 Hz, 1H, H1), 7.45 (t, *J* = 7.8 Hz, 2H, H2), 3.16 (d, *J* = 7.2 Hz, 1H, NH), 3.10 (td, *J* = 7.2, 3.5 Hz, 1H, H9), 3.02 (td, *J* = 6.9, 2.2 Hz, 2H, H6), 1.94 (m, 1H, H7), 1.78 (m, 2H, H7‘), 1.65 (ddt, *J* = 13.9, 11.0, 5.6 Hz, 1H, H8), 1.55 (dddd, *J* = 13.8, 10.7, 7.7, 4.6 Hz, 1H, H8‘), 1.24 (s, 9H, H13), 0.89 (d, *J* = 6.8 Hz, 3H, H11), 0.86 (d, *J* = 6.8 Hz, 3H, H12); **^{13}C{^{1}H}-NMR** (101 MHz, $CDCl_3$) δ 200.16 (C5), 137.13 (C4), 133.11 (C1), 128.71 (C2), 128.15 (C3), 61.90 (C9), 56.23 (C14), 38.10 (C6), 32.97 (C8), 32.09 (C10), 23.03 (C13), 20.40 (C7), 19.26 (C11), 17.13 (C12); **IR** (neat, ATR) ν/cm^{-1} = 3544 (w), 2974 (w), 2958 (w), 2928 (w), 2869 (w), 1700 (m), 1680 (s), 1595 (m), 1570 (m), 1469 (m), 1443 (m), 1407 (w), 1381 (m), 1359 (m), 1247 (m), 1231 (m), 1190 (m), 1166 (m), 1039 (m), 972 (m); **MS** (FAB, NBA): 324.2 (100%); **HRMS**: calculated: 324.1992 $[M+H]^+$; found: 324.1995; **EA**: calc.: C, 66.83; H, 9.04; N, 4.33; found: C, 65.17; H, 8.94; N, 4.48; **Optical rotation**: $[\alpha]_D^{20}$ = -44.6 (c = 0.7 in $CHCl_3$ with 0.75% EtOH); **HPLC** (Silica, *n*-hexane/iso-propanol 90:10, 8.0 mL/min, 25 °C, 207/240 nm): t_R = 20.8 min.

(*R*)-2-isopropyl-6-phenyl-2,3,4,5-tetrahydropyridine (392)

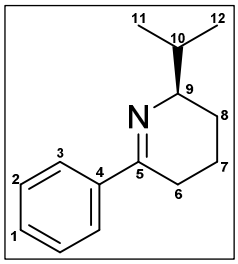

In a 25 mL round-bottom flask was placed (*R*)-**463** (24.8 mg, 0.077 mmol, 1.0 eq.) and dissolved in methanol (2.5 mL). HCl (4.0 M in 1,4-dioxane, 0.77 mmol, 10 eq.) was added and the reaction mixture stirred for two hours at room temperature. The reaction was quenched by adding NaOH (1.0 M, 2 mL) and organic components were extracted with CH_2Cl_2 (3x5 mL). The combined organic layers were dried over anhydrous $MgSO_4$, filtered and solvents removed under reduced pressure. The residue was dried *in vacuo* to afford (*R*)-**392** which was used directly without further purification.

$C_{14}H_{19}N$ (M_W = 201.31 g/mol):
^{1}H-NMR (500 MHz, CD_2Cl_2) δ 7.82 (m, 2H, H3), 7.36 (m, 3H, H1, H2), 3.28 (dddd, *J* = 10.2, 7.8, 3.5, 2.2 Hz, 1H, H9), 2.69 (ddtd, *J* = 18.0, 6.0, 2.3, 1.2 Hz, 1H, H6), 2.43 (dddd, *J* = 17.9, 10.6, 6.9, 3.4 Hz, 1H, H6’), 1.96 (dtdd, *J* = 10.3, 7.8, 5.3, 2.8 Hz, 1H, H7), 1.87 (pd, *J* = 6.9, 5.7 Hz, 1H, H10), 1.77 (dtdd, *J* = 13.8, 4.3, 3.5, 1.2 Hz, 1H, H8), 1.67 (tddd, *J* = 13.0, 10.9, 6.3, 3.6 Hz, 1H, H7’), 1.23 (tdd, *J* = 12.7, 10.6, 3.5 Hz, 1H, H8’), 1.04 (d, *J* = 6.8 Hz, 3H, H12), 1.00 (d, *J* = 6.8 Hz, 3H, H11); **^{13}C{^{1}H}-NMR** (125 MHz, CD_2Cl_2) δ 164.01 (C5), 140.82 (C4), 129.55 (C1), 128.35 (C2), 126.36 (C3), 64.15 (C9), 34.71 (C10), 27.08 (C6), 24.35 (C8), 20.19 (C7), 19.22 (C11), 19.16 (C12); **GC-MS**: (Optima-5-Amine, 100.2/10.270/10): t_R = 8.0 min, m/z = 201 ($[M]^+$), 186, 158, 104; **HRMS**: calculated: 202.1590 $[M+H]^+$; found: 202.1589; **IR** (neat, ATR) ν/cm^{-1} = 01 (w), 3057 (w), 3024 (w), 2953 (m), 2934 (m), 2868 (m), 1695 (w), 1635 (m), 1577 (w), 1491 (w), 1467 (w), 1445 (m), 1380 (w), 1362 (m), 1340 (w), 1261 (m), 1203 (w), 1177 (w), 1162 (w), 1126

(w), 1104 (w), 1086 (w), 1061 (w), 1030 (w), 1017 (w), 1005 (w), 753 (m), 692 (s); **HPLC** (Daicel Chiracel OD-H, *n*-heptane/iso-propanol 99:1, 0.5 mL/min, 20 °C, 208/243 nm): t_R = 8.0 min (*R*), t_R = 8.6 min (*S*); **Optical rotation**: $[\alpha]_D^{20}$ = +72.6 (c = 0.42 $CHCl_3$ with 0.75% EtOH);

Phosphoric acids

(*R*)-2,2'-dimethoxy-1,1'-binaphthalene (502)[135]

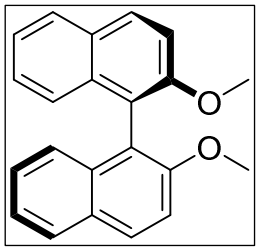

A 250 mL round-bottomed flask was equipped with a magnetic stirrer, charged with (*R*)-[1,1'-binaphthalene]-2,2'-diol **501** (5 g, 17.5 mmol, 1.0 eq.) and dissolved in acetone (70 mL). K_2CO_3 (9.76 g, 70.67 mmol, 4.0 eq.) was added, the flask equipped with a reflux condenser and then heated to reflux to effect dissolution. Methyliodide (15 g, 106 mmol, 6.0 eq.) was added via syringe in two portions and stirring continued while heating to reflux for 24 hours. Solvents were removed under reduced pressure and the residue suspended in water (100 mL) and stirred for 8 hours at room temperature. The suspension was filtered, the filter cake washed with water (100 mL) and dried in vacuo to afford (*R*)-**502** (5.43 g, 17.29 mmol, 98 %) as a white solid.

$C_{22}H_{18}O_2$ (M_W = 314.38 g/mol):
m.p.: 238 °C; **^{1}H-NMR** (400 MHz, $CDCl_3$) δ: 7.98 (d, *J* = 9.0 Hz, 2H), 7.87 (d, *J* = 8.1 Hz, 2H), 7.46 (d, *J* = 9.0 Hz, 2H), 7.31 (ddd, *J* = 8.1 Hz, 6.7 Hz, 1.2 Hz, 2H), 7.21 (ddd, *J* = 8.1 Hz, 6.7 Hz, 1.3 Hz, 2H), 7.10 (d, *J* = 8.5 Hz, 2H), 3.77 (s, 6H, 7); **^{13}C{^{1}H}-NMR** (101 MHz, $CDCl_3$) δ 155.10, 134.14, 129.53, 129.35, 128.05, 126.43, 125.39, 123.64, 119.72, 114.38, 57.04; **Optical rotation**: $[\alpha]_D^{20}$ = +55.8 (c = 1.0 $CHCl_3$ with 0.75% EtOH); lit. +57.5 (c = 1.0 in $CHCl_3$)[176]

(*R*)-3,3'-diiodo-2,2'-dimethoxy-1,1'-binaphthalene (503)[133]

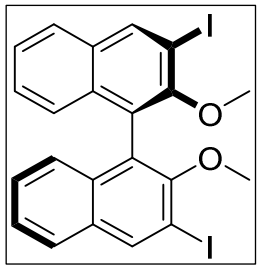

An oven-dried 100 mL three-necked round-bottom flask was evacuated and purged with Argon three times before being charged with TMEDA (1.16 g, 10 mmol, 1.4 eq.) and dissolved in dry Et_2O (30 mL). *n*-Butyl lithium (1.6 M, 18 mmol, 2.5 eq.) was added dropwise and the reaction mixture stirred for 20 minutes. (*R*)-**502** (2.26 g, 7.2 mmol, 1.0 eq.) was added in one portion and the solution stirred at room temperature overnight. It was then cooled to -78 °C and iodine (1.0 M in THF, 4.55 g, 18 mmol, 2.5 eq.) was added slowly. Stirring at -78 °C was continued for 1 hour until the reaction mixture was warmed to room temperature and stirred for another 12 hours. The reaction was quenched by puring into an ice/water mixture (60 mL) and stirred for 4 hours. The organic layer was decanted and organic components extracted with Et_2O/THF (1:1, 3x5 mL). The combined organic layers were washed with Na_2SO_3 (3x10 mL), then water (10 mL) and dried over Na_2SO_4. Filtration and removal of volatiles under reduced pressure followed by flash chromatography (SiO_2, cyclohexane/Et_2O 20:1, 15x4 cm, 20 mL fractions) afforded an off-white solid. It was further purified by recrystallisation from CH_2Cl_2 to afford (*R*)-**503** (2.82 g, 4.98 mmol, 69 %) as a white solid.

$C_{22}H_{16}I_2O_2$ (M_W = 566.17 g/mol):
m.p.: 196-197 °C; lit. 194-195 °C[177]; **^{1}H-NMR** (400 MHz, $CDCl_3$) δ 8.53 (s, 2H), 7.79 (d, *J* = 8.2 Hz, 2H), 7.41 (t, *J* = 7.5 Hz, 2H), 7.30 – 7.22 (m, 2H), 7.07 (d, *J* = 8.5 Hz, 2H), 3.41 (d, *J* = 5.6 Hz, 3H); **^{13}C{^{1}H}-NMR** (101 MHz, $CDCl_3$) δ 154.60, 140.02, 133.97, 132.30, 127.22, 127.10, 125.90, 125.79, 125.50, 92.50, 61.27; **Optical rotation**: $[\alpha]_D^{20}$ = -26.4 (c 1.0 in $CHCl_3$ with 0.75% EtOH); lit. -30 (c = 1.0 in $CHCl_3$[178]

(*R*)-3,3'-dimesityl-[1,1'-binaphthalene]-2,2'-diol (507)[133]

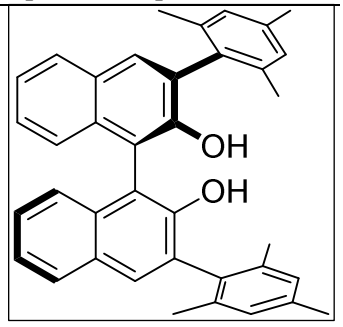

A 50 mL Schlenk tube was equipped with a magnetic stirrer and evacuated before being flame-dried with a bunsen burner. After cooling to room temperature it was purged with Argon three times and charged with (*R*)-**503** (200 mg, 0.353 mmol, 1.0 eq.) and $Ni(acac)_2$ (9.1 mg, 0.035 mmol, 0.1 eq.). It was then dissolved in dry benzene (1.75 mL) and stirred at room temperature for 20 minutes. Mesityl magnesium bromide (1.0 M in Et_2O, 1.41 mmol, 4.0 eq.) was added dropwise and the reaction mixture stirred at room temperature for 30 minutes before being heated to reflux overnight. After cooling to room temperature the reaction mixture was quenched with HCl (1.0 M, 2.12 mmol, 6.0 eq.) and stirred at room temperature for 1 hour. Et_2O (10 mL) was added and the organic layer separated. After being dried over anhydrous MgSO4, filtered the solution was subjected to elution chromatography (SiO_2, Et_2O). The filter cake was washed with Et_2O (20 mL) and solvents removed under reduced pressure. The residue was dried in vacuo before being transferred to a 25 mL Schlenk tube with CH_2Cl_2 (1.5 mL). The solution was cooled to -10 °C and boron tribromide (1.0 M in CH_2Cl_2, 2.12 mmol, 6.0 eq.) was added dropwise. The cooling bath was removed and the reaction was allowed to warm to room temperature while stirring overnight. After quenching with water (3 mL) the organic components were extracted with CH_2Cl_2 (3x6 mL) and the combined organic layers were dried over Na_2SO_4, filtered and solvents removed under reduced pressure. The residue was subjected to flash chromatography (SiO_2, cyclohexane/CH_2Cl_2 6:1 gradient to 2:1, 20x4 cm, 25 mL fractions) to afford (*R*)-**507** (96 mg, 0.184 mmol, 52 %) as a yellow solid.

$C_{38}H_{34}O_2$ (M_W = 522.68 g/mol):
m.p.: 179 °C; **^{1}H-NMR** (400 MHz, $CDCl_3$) δ 7.87 (d, *J* = 7.9 Hz, 2H), 7.74 (s, 2H), 7.41 – 7.35 (m, 2H), 7.34 – 7.29 (m, 2H), 7.24 (d, *J* = 8.9 Hz, 2H), 7.01 (s, 4H), 4.99 (s, 2H), 2.34 (s, 6H), 2.15 (s, 6H), 2.07 (s, 6H); **^{13}C{^{1}H}-NMR** (101 MHz, $CDCl_3$) δ 150.14, 137.90, 137.29, 137.22, 133.56, 133.05, 130.81, 129.59, 129.58, 128.66, 128.58, 128.39, 126.95, 124.69, 123.99, 113.07, 21.30, 20.68, 20.59; **Optical rotation**: $[a]_D^{20}$ = +34.2 (c = 1.0 in $CHCl_3$ with 0.75 % EtOH); Lit. +72.3 (c = 0.97 in $CHCl_3$)[179]

(*R*)-3,3'-bis(2,4,6-triisopropylphenyl)-[1,1'-binaphthalene]-2,2'-diol (511)[134]

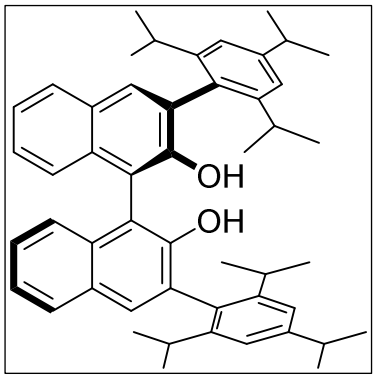

A 10 mL Schlenk tube was equipped with a magnetic stirrer, evacuated and flame-dried with a Bunsen burner. After cooling to room temperature it was purged with argon three times before being charged with 2-bromo-1,3,5-triisopropylbenzene (200 mg, 0.706 mmol, 2.0 eq.) and dissolved in dry THF (0.5 mL). It was then cooled to -78 °C and *n*-butyllithium (1.6 M, 0.724 mmol, 2.05 eq.) were added. The reaction mixture was stirred for 20 minutes before zinc bromide (1.0 M in THF, 0.942 mmol, 2.67 eq.) was added. The reaction mixture was warmed to room temperature and volatile components removed in vacuo. (*R*)-**503** (200 mg, 0.353 mmol, 1.0 eq.) and (^{t}Bu$_3$P)$_2$Pd **509** (1.78 mg, 0.0035 mmol, 0.01 eq.) were added. The reaction mixture was dissolved in dry THF (2 mL) and storred at room temperature for 2 hours before being heated to reflux overnight. After cooling to room temperature, the reaction was quenched by addition of HCl, diluted with Et_2O and the organic layer dried over anhydrous $MgSO_4$. After filtration and elution chromatography (SiO_2, Et_2O) the residue was dried *in vacuo*. It was then redissolved in CH_2Cl_2 (1.5 mL), transferred to a 25 mL Schlenk tube, cooled to -10 °C and boron tribromide (1.0 M in CH_2Cl_2, 2.12 mmol, 6.0 eq.) was added. The reaction mixture was allowed to warm to room temperature while stirring overnight. It was then quenched with water (3 mL) at 0 °C and organic components were extracted with CH_2Cl_2 (2x6 mL). The combined organic layers were dried over Na_2SO_4, filtered and solvents removed under reduced pressure. The residue was subjected to flash chromatography (SiO_2, cyclohexane/CH_2Cl_2 5:1, 18x2.5 cm, 12 mL fractions) to afford (*R*)-**511** (123 mg, 0.178 mmol, 50 %) as a white solid.

$C_{50}H_{58}O_2$ (M_W = 690.99 g/mol):
m.p.: >290 °C (decomposition); **^{1}H-NMR** (400 MHz, $CDCl_3$) δ 7.86 (d, *J* = 7.9 Hz, 2H), 7.76 (s, 2H), 7.41 – 7.35 (m, 2H), 7.31 (dt, *J* = 15.7, 5.1 Hz, 4H), 7.13 (d, *J* = 6.3 Hz, 4H), 4.91 (s, 2H), 2.96 (dt, *J* = 13.8, 6.9

Hz, 2H), 2.85 (dt, *J* = 13.8, 6.9 Hz, 2H), 2.69 (dt, *J* = 13.8, 6.9 Hz, 2H), 1.31 (d, *J* = 6.9 Hz, 12H), 1.20 (d, *J* = 6.8 Hz, 6H), 1.11 (d, *J* = 6.9 Hz, 6H), 1.09 (d, *J* = 6.9 Hz, 6H), 1.03 (d, *J* = 6.9 Hz, 6H); **$^{13}C\{^1H\}$-NMR** (101 MHz, $CDCl_3$) δ 150.77, 149.26, 147.92, 147.87, 133.59, 130.79, 130.50, 129.24, 129.18, 128.37, 126.76, 124.66, 123.90, 121.37, 121.31, 113.22, 34.49, 31.03, 30.99, 24.46, 24.43, 24.22, 24.15, 24.07, 23.87; **Optical rotation**: $[\alpha]_D^{20}$ = +52.3 (c = 1.0 in $CHCl_3$ with 0.75% EtOH); lit. +88-89 (c = 3.0 in THF)[180]

(*R*)-3,3-(dimesityl)-[1,1'-binaphthalene]-2,2'-phosphoric acid (408)[179]

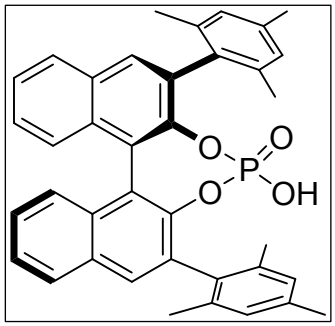

A 25 mL two-necked round bottom flask was equipped with a reflux condenser, a magnetic stirrer and a stopper. It was then evacuated and flame-dried with a bunsen burner. After cooling to room temperature it was purged with argon three times and charged with (*R*)-**507** (375 mg, 0.72 mmol, 1.0 eq.). Dry pyridine (3 mL) and phosphor oxychloride (336 mg, 2.15 mmol, 3.0 eq.) were added and the reaction mixture heated to reflux for 14 hours. After cooling to room temperature water (2 mL) was added and refluxing continued for 3 hours. After cooling to room temperature, CH_2Cl_2 (6 mL) was added and the reaction mixture washed with HCl (1.0 M, 3x6 mL). The organic layer was dried over anhydrous $MgSO_4$. After filtration and removal of solvents under reduced pressure, the residue was recrystallized from acetonitrile to afford (*R*)-**408** (102 mg, 0.177 mmol, 25 %) as white crystals.

$C_{38}H_{33}O_4P$ (M_W = 584.64 g/mol):
m.p.: 156 °C; lit. 224-230 °C (decomposition)[179]; **^{1}H-NMR** (400 MHz, CD_2Cl_2) δ 7.93 (d, *J* = 8.2 Hz, 2H), 7.76 (s, 2H), 7.53 – 7.47 (m, 2H), 7.36 (d, *J* = 8.0 Hz, 2H), 7.33 – 7.27 (m, 2H), 6.80 (s, 2H), 6.73 (s, 2H), 2.09 (s, 6H), 2.01 (s, 6H), 1.94 (s, 6H); **$^{31}P\{^1H\}$-NMR** (162 MHz, CD_2Cl_2) δ 4.16; **Optical rotation**: $[\alpha]_D^{20}$ = -89.1 (c = 1.0 in $CHCl_3$ with 0.75% EtOH); lit. : -93.1 (c = 1.08 in $CHCl_3$)[179]

(*R*)-3,3-bis(2,4,6-triisopropylphenyl)-[1,1'-binaphthalene]-2,2'-phosphoric acid (407)[135]
(*R*-TRIP)

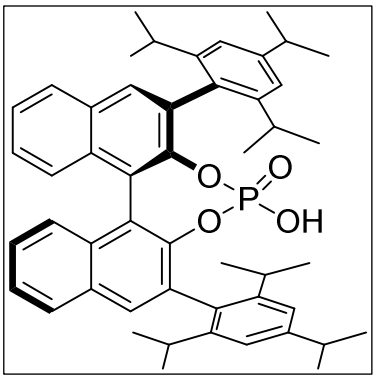

A 25 mL two-necked round bottom flask was equipped with a reflux condenser, a magnetic stirrer and a stopper. It was then evacuated and flame-dried with a bunsen burner. After cooling to room temperature it was purged with Argon three times and charged with (*R*)-**511** (250 mg, 0.36 mmol, 1.0 eq.). Dry pyridine (2 mL) and phosphor oxychloride (166 mg, 1.09 mmol, 3.0 eq.) were added and the reaction mixture heated to reflux for 14 hours. After cooling to room temperature water (2 mL) was added and refluxing continued for 3 hours. After cooling to room temperature, CH_2Cl_2 (6 mL) was added and the reaction mixture washed with HCl (1.0 M, 3x6 mL). The organic layer was dried over anhydrous $MgSO_4$. After filtration and removal of solvents under reduced pressure, the residue was recrystallized from acetonitrile to afford (*R*)-**407** (148 mg, 0.197 mmol, 55 %) as white crystals.

$C_{50}H_{57}O_4P$ (M_W = 752.96 g/mol):
m.p.: >290 °C (decomposition); **^{1}H-NMR** (400 MHz, CD_2Cl_2) δ 7.90 (d, *J* = 8.2 Hz, 2H), 7.79 (s, 2H), 7.49 (dd, *J* = 10.8, 4.0 Hz, 2H), 7.34 – 7.27 (m, 2H), 7.24 (d, *J* = 8.3 Hz, 2H), 6.97 (d, *J* = 1.6 Hz, 4H), 2.85 (dt, *J* = 13.8, 6.9 Hz, 2H), 2.56 (tt, *J* = 13.4, 6.8 Hz, 4H), 1.22 (dd, *J* = 6.9, 3.8 Hz, 12H), 1.07 (d, *J* = 6.8 Hz, 6H), 0.98 (d, *J* = 6.8 Hz, 6H), 0.89 (d, *J* = 6.8 Hz, 6H), 0.81 (d, *J* = 6.7 Hz, 6H); **$^{31}P\{^1H\}$-NMR** (162 MHz, CD_2Cl_2) δ 2.56; **Optical rotation**: $[\alpha]_D^{20}$ = -60.2 (c = 1.0 in $CHCl_3$ with 0.75% EtOH); lit. -59.6 (c = 1.06 in $CHCl_3$)[181]

Imine precursors and ligands

1-Cyclopentylethanone[182]

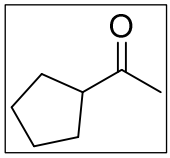

Into a 25 mL two-necked round-bottom flask was placed a magnetic stirrer, the flask was closed with a stopper, and dried with a Bunsen burner while evacuating. After cooling to room temperature, the flask was purged with argon three times and cyclopentanoic acid (1 g, 8.85 mmol, 1.0 eq.) was added and dissolved in dry diethylether (8 mL). The reaction mixture was cooled to -78 °C with the aid of a dry ice / acetone bath and a solution of MeLi (1.6 M, 12.5 mL, 20.11 mmol, 2.3 eq.) was added dropwise via syringe over a period of 15 minutes. The reaction was allowed to warm to room temperature while stirring overnight. After quenching with saturated NH_4Cl solution (8 mL) the mixture turned clear and layers were separated. The organic layer was washed with water (10 mL= and the aeqeuous layer washed with ether (10 mL). The combined organic phases were dried over $MgSO_4$, filtered and solvents removed under reduced pressure to afford 0.5 g (4.4 mmol, 50%) of 1-cyclopentylethanone as a clear oil.

$C_7H_{12}O$ (112.17 g/mol):

^{1}H-NMR (400 MHz, $CDCl_3$) δ 2.94 – 2.78 (m, 1H, C*H*), 2.16 (s, 3H, CH_3), 1.88 – 1.45 (m, 10H, CH_2); **^{13}C{^{1}H}-NMR** (101 MHz, $CDCl_3$) δ 211.44 (*C*=O), 52.40 (*C*H), 28.95 (CH_2CH_2CH), 28.86 (CH_2CH_2CH), 26.10 (CH_3); **GC-MS:** (Rtx-5MS, 100.2/10.270/10): t_R = 3.3 min, *m/z* = 113 ($[M+1]^+$).

4-Bromo-2,6-diisopropylaniline (517)[183]

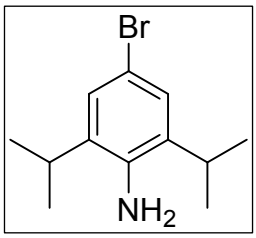

In a 500 mL round-bottom flask was placed 2,6-diisopropylaniline **516** (6 mL, technical, ~90%, ~30 mmol) and dissolved in CH_2Cl_2 (250 mL). Tetrabutylammonium tribromide (15.4 g, 32 mmol) was added in one go. The reaction was stirred for 30 minutes before the solvent was removed under reduced pressure. The residue was redissolved in diethyl ether (250 mL), washed with NaOH (0.5 M, 150 mL), water (2 x 150 mL), dried over $MgSO_4$, filtered and solvents removed under reduced pressure to afford 7.6 g (29.7 mmol, 98%) of **517** as a yellow oil.

$C_{12}H_{18}BrN$ (256.18 g/mol):
^{1}H-NMR (400 MHz, $CDCl_3$) δ 7.11 (s, 2H, CH_{Ar}), 3.70 (s, 2H, NH_2), 2.95 – 2.81 (m, 2H, C*H*(CH_3)$_2$), 1.25 (d, *J* = 6.8 Hz, 12H, CH_3).

1-Bromo-3,5-diisopropylbenzene (518)[183]

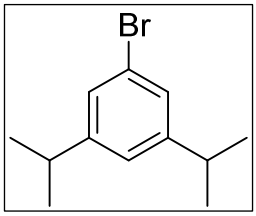

In a 500 mL round-bottom flask was placed **517** (7.6 g, 29.7 mmol, 1.0 eq.) and suspended in HCl (2 M, 70 mL). The reaction mixture was cooled to -5 °C and sodium nitrite (5.12 g, 74 mmol, 1.05 eq) was added portionwise. After addition the reaction was stirred for 30 minutes before H_3PO_4 (50% in water, 35 mL, 300 mmol, 4.0 eq.) was added. The mixture was stirred at 4 °C overnight. Ether (100 mL) was added and layers were separated. The aeqeuous layer was washed with ether (2 x 100 mL) and the combined organic layers were dried over $MgSO_4$, filtered and solvents removed under reduced pressure. Purification by distillation (115 °C, 0.15 mbar) afforded 4.0 g (16.6 mmol, 56%) of **518** as a yellow oil.

$C_{12}H_{17}Br$ (241.17 g/mol):
b.p.: 115°C at 0.1 torr; **^{1}H-NMR** (400 MHz, $CDCl_3$) δ 7.18 (d, *J* = 1.5 Hz, 2H, CH_{Ar}CBrCH_{Ar}), 6.98 (s, 1H, CH_{Ar}), 2.92 – 2.77 (m, 2H, C*H*(CH_3)$_2$), 1.23 (d, *J* = 6.9 Hz, 12H, CH_3).

3,5-Di-isopropylbenzaldehyde (519)[183]

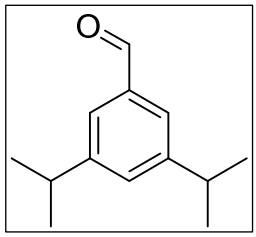

In a 100 mL three-necked round-bottom flask equipped with a magnetic stirrer, argon inlet, a thermometer and a stopper was placed **518** (4.0 g, 16.6 mmol, 1.0 eq.) and cooled to -78 °C with the aid of a dry ice / acetone bath. *n*-BuLi (1.6 M, 18.26 mmol, 1.1 eq.) was added dropwise via syringe and the resultant suspension was stirred for 20 minutes at -78 °C. Then DMF (1.33 g, 18.26 mmol, 1.1 eq.) was added dropwise via syringe, the mixture stirred for 10 minutes being allowed to warm to -10 °C. The reaction was quenched with water (12 mL) at -10 °C and the mixture warmed to room temperature. Layers were separated and the aequeuous layer washed with ether (100 mL). Organic layers were combined and solvents removed under reduced pressure. The residue was purified by flash chromatography (SiO_2, 18 x 4.5 cm, cyclohexane/EtOAc 20:1) to afford 2.05 g (10.77 mmol, 65%) of **519** as a clear oil.

$C_{13}H_{18}O$ (190.28 g/mol):
R_f (SiO_2, *n*-pentane/AcOEt 10:1, UV, $Ce(SO_4)_2$) = 0.63; **^{1}H-NMR** (400 MHz, $CDCl_3$) δ 9.99 (s, 1H, C*H*O), 7.57 (d, *J* = 1.7 Hz, 2H, CH_{Ar}CHOCH_{Ar}), 7.35 (s, 1H, CH_{Ar}), 3.04 – 2.90 (m, 2H, C*H*$(CH_3)_2$), 1.29 (dd, *J* = 6.9, 1.8 Hz, 12H, CH_3).

1-(3,5-Di-isopropylphenyl)ethanol (520)

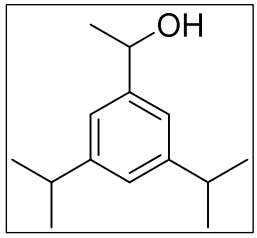

In a 100 mL three-necked round-bottom flask equipped with a magnetic stirrer, argon inlet and a stopper was placed **519** (2.05 g, 10.77 mmol, 1.0 eq.) and dissolved in dry diethyl ether (40 mL). The solution was cooled to 0 °C and MeMgBr (3.0 M, 16.2 mmol, 1.5 eq.) was added dropwise via syringe. The reaction mixture was stirred at 0 °C for 15 minutes before being allowed to warm to room temperature and stirred for 2 hours. The mixture was cooled to 0 °C again and quenched with sat. NH_4Cl (40 mL) and water (20 mL). After warming to room temperature, layers were separated and the aq. layer was extracted with EtOAc (3 x 60 mL). The combined organic layers were dried over $MgSO_4$, filtered and solvents removed under reduced pressure. The residue was purified via flash chromatography (SiO_2, 15 x 3 cm, cyclohexane/EtOAc 5:1) to afford 1.89 g (9.16 mmol, 85%) of **520** as an orange viscous oil.

$C_{14}H_{22}O$ (206.32 g/mol):
^{1}H-NMR (400 MHz, $CDCl_3$) δ 7.06 (d, *J* = 1.6 Hz, 2H, CH_{Ar}), 7.01 (d, *J* = 1.6 Hz, 1H, CH_{Ar}), 4.87 (qd, *J* = 6.4, 3.6 Hz, 1H, C*H*(OH)), 2.90 (hept, *J* = 6.9 Hz, 2H, C*H*$(CH_3)_2$), 1.51 (d, *J* = 6.4 Hz, 3H, CH_3CHOH), 1.26 (d, *J* = 6.9 Hz, 12H, CH(C$H_3)_2$); **^{13}C{^{1}H}-NMR** (101 MHz, $CDCl_3$) δ 149.30 (*C*CH$(CH_3)_2$), 145.89 (*C*CH(OH)), 124.12 (*C*H_{Ar}CCH$(CH_3)_2$), 121.10 (*C*H_{Ar}CCH$(CH_3)_2$CCH(OH)), 70.98 (*C*H(OH)), 34.40 (*C*H$(CH_3)_2$), 25.22 (C=O*C*H_3), 24.24 (CH(*C*$H_3)_2$); **IR** (neat, ATR) ν/cm^{-1} = 3340 (m_{br}), 2961 (s), 2929 (m), 2887 (m), 2868 (m), 1603 (w), 1467 (m), 1459 (m), 1450 (m), 1382 (w), 1363 (m), 1176 (w), 1112 (w), 1073 (w), 1020 (w), 873 (w), 716 (m); **GC-MS**: (Rtx-5MS, 100.2/10.270/10): t_R = 11.8 min, *m/z* = 206 ([M]$^+$).

1-(3,5-Di-isopropylphenyl)ethanone (521)[184]

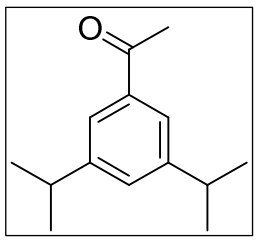

In a 100 mL round-bottom flask was placed **520** (1.0 g, 4.5 mmol, 1.0 eq.) and dissolved in CH_2Cl_2 (50 mL). Dess-Martin Periodane (2.7 g, 6.37 mmol, 1.4 eq.) was added in one portion and the resultant mixture stirred for one hour at room temperature. The reaction mixture was poured into a solution of pentane/EtOAc (4:1, 80 mL) and a white precipitate was formed. The suspension was filtered over a frit (SiO_2) and a yellow solution was obtained. The fritt was rinsed with more pentane/EtOAc (4:1, 100 mL) and solvents were removed under reduced pressure. The residue was purified by flash chromatography (SiO_2, 18 x 3 cm, cyclohexane/EtOAc 20:1) to afford 1.0 g (4.31 mmol, 96%) of **521** as an orange oil.

$C_{14}H_{20}O$ (204.31 g/mol):
^{1}H-NMR (400 MHz, $CDCl_3$) δ 7.64 (d, *J* = 1.7 Hz, 2H, CH_{Ar}), 7.29 (t, *J* = 1.6 Hz, 1H, CH_{Ar}), 3.03 – 2.86 (m, 2H, C*H*$(CH_3)_2$), 2.60 (s, 3H, CH_3C=O), 1.28 (d, *J* = 6.9 Hz, 12H, CH(C$H_3)_2$); **^{13}C{^{1}H}-NMR** (101 MHz,

$CDCl_3$) δ 198.83 (*C*=O), 149.46 (*C*CH(CH_3)$_2$), 137.59 (*C*C=O), 129.93 (C*H*$_{Ar}$), 124.07 (2 C*H*$_{Ar}$), 34.32 (*C*H(CH_3)$_2$), 26.92 (C=O*C*H$_3$), 24.12 (CH(*C*H$_3$)$_2$).

1-(3,5-Di-*tert*-butylphenyl)ethanol (524)[185]

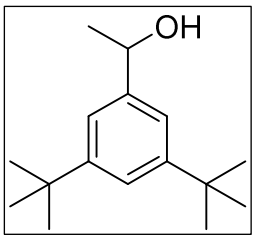

In a 100 mL three-necked round-bottom flask equipped with a magnetic stirrer, argon inlet and a stopper was placed 3,5-di-*tert*-butylbenzaldehyde **523** (1.0 g, 4.5 mmol, 1.0 eq.) and dissolved in dry diethyl ether (18 mL). The solution was cooled to 0 °C and MeMgBr (3.0 M, 6.82 mmol, 1.5 eq.) was added dropwise via syringe. The reaction mixture was stirred at 0 °C for 15 minutes before being allowed to warm to room temperature and stirred for 2 hours. The mixture was cooled to 0°C again and quenched with sat. NH_4Cl (40 mL) and water (20 mL). After warming to room temperature, layers were separated and the aq. layer was extracted with EtOAc (3 x 60 mL). The combined organic layers were dried over $MgSO_4$, filtered and solvents removed under reduced pressure to afford 1.05 g (4.47 mmol, 96%) of **524** as a white solid.

$C_{16}H_{26}O$ (234.38 g/mol):
^{1}H-NMR (400 MHz, $CDCl_3$) δ 7.36 (t, *J* = 1.8 Hz, 1H, C*H*$_{Ar}$), 7.23 (d, *J* = 1.7 Hz, 2H, C*H*$_{Ar}$), 4.90 (q, *J* = 6.4 H, 1H, C*H*OH), 1.77 (s$_{br}$, 1H, O*H*), 1.52 (d, *J* = 6.5 Hz, 3H, C*H*$_3$), 1.34 (s, 18H, C(C*H*$_3$)$_3$).

1-(3,5-Di-*tert*-butylphenyl)ethanone (525)[186]

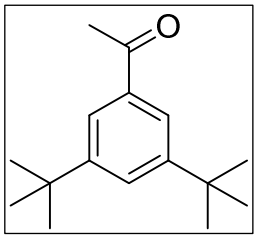

In a 100 mL round-bottom flask was placed **524** (1.05 g, 4.47 mmol, 1.0 eq.) and dissolved in CH_2Cl_2 (50 mL). Dess-Martin Periodane (2.5 g, 5.9 mmol, 1.32 eq.) was added in one portion and the resultant mixture stirred for one hour at room temperature. The reaction mixture was poured into a solution of pentane/EtOAc (4:1, 80 mL) and a white precipitate was formed. The suspension was filtered over a fritt (SiO_2) and a yellow solution was obtained. The fritt was rinsed with more pentane/EtOAc (4:1, 100 mL) and solvents were removed under reduced pressure. The residue was purified by flash chromatography (SiO_2, 18 x 3 cm, cyclohexane/EtOAc 20:1) to afford 1.0 g (4.31 mmol, 96%) of **525** as a clear oil.

$C_{16}H_{24}O$ (232.36 g/mol):
^{1}H-NMR (400 MHz, $CDCl_3$) δ 7.81 (d, *J* = 1.8 Hz, 2H, C*H*$_{Ar}$), 7.65 (t, *J* = 1.8 Hz, 1H, C*H*$_{Ar}$), 2.62 (s, 3H, C=OC*H*$_3$), 1.36 (s, 18H, C(C*H*$_3$)$_3$); **^{13}C{^{1}H}-NMR** (101 MHz, $CDCl_3$) δ 199.04 (*C*=O), 151.36 (*C*$_{Ar}$C(CH$_3$)$_3$), 137.04 (*C*$_{Ar}$C=O), 127.50 (1 *C*H$_{Ar}$), 122.66 (2 *C*H$_{Ar}$), 35.13 (*C*(CH$_3$)$_3$), 31.54 (C(*C*H$_3$)$_3$), 27.07 (C=O*C*H$_3$).

1-(trimethylsilyl)piperidin-2-one (559)[155]

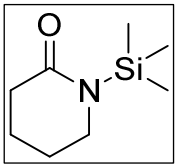

A three-necked 500 ml round-bottom flask equipped with an overhead stirrer, thermometer and a septum, was dried with a bunsen burner while evacuating. After cooling to room temperature, the flask was purged with argon three times and charged with Δ-valerolactam **558** (10 g, 100 mmol, 1.0 eq.) in anhydrous toluene (100 mL). Triethylamine (12.75 g, 0.126 mol, 1.25 eq.) and TMSCl (12.06 g, 0.11 mol, 1.1 eq.) were added via syringe. The mixture was heated to 50 °C for 6 hours while stirring vigorously. Afterwards it was cooled to 0 °C, diluted with hexane/ether (1:1, 100 mL) and filtered through cellite. The filtrate was concentrated under reduced pressure and the residue was distilled (80 °C, 0.4 mbar) to afford 11.64 g (68 mmol, 68%) of **559** as a colourless oil.

$C_8H_{17}NOSi$ (M_W = 171.31 g/mol):
^{1}H-NMR (400 MHz, CDCl3) δ 3.20 (t, *J* = 5.8 Hz, 2H), 2.36 (t, *J* = 6.7 Hz, 2H), 1.78 (p, *J* = 6.5 Hz, 2H), 1.71 (tq, *J* = 8.9, 5.3, 4.3 Hz, 2H), 0.27 (s, 9H); **^{13}C{^{1}H}-NMR** (126 MHz, $CDCl_3$) δ 177.29, 44.27, 32.73, 23.46, 20.99, -0.09.

***tert*-Butyl 2-oxopiperidine-1-carboxylate (561)**[187]

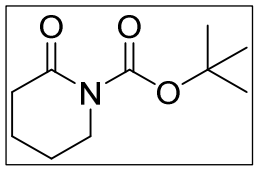

To a stirred solution of **558** (5 g, 50 mmol, 1.0 eq.) in anhydrous THF (100 mL) at -78ºC was added dropwise *n*-BuLi (50 mmol, 31.25 mL, 1.6M, 1.0 eq.). The mixture was allowed to stir at -78 ºC for one h before a solution of di-*tert*-butyldicarbonate (10.9 g, 11.5 mL, 50 mmol, 1.0 eq.) in THF (25 mL) was added dropwise. The reaction was allowed to stir for another two hours and then warmed to room temperature. Saturated NH_4Cl solution (50 mL) and water (25 mL) were added and the organic layer was separated. The aqueous phase was extracted with Et_2O (3 x 50 mL). The combined organic phases were dried over $MgSO_4$ and solvents removed under reduced pressure. The residue was purified by flash chromatography (SiO_2, 15x4 cm, 5:1 ethyl acetate/pentane) to afford **561** (7.12 g, 3.6 mmol, 71%) as a clear oil.

$C_{10}H_{17}NO_3$ (M_W = 199.25 g/mol):
^{1}H-NMR (400 MHz, $CDCl_3$) δ 3.70 – 3.60 (m, 2H), 2.51 (td, *J* = 6.7, 5.5, 2.9 Hz, 2H), 1.87 – 1.75 (m, 4H), 1.53 (s, 9H); **^{13}C{^{1}H}-NMR** (101 MHz, $CDCl_3$) δ 171.44, 152.87, 82.95, 46.42, 35.01, 28.14, 22.91, 20.63.

***tert*-Butyl (5-oxononyl)carbamate (564)**[187]

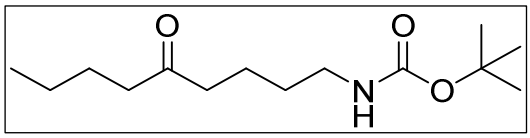

To a solution of **561** (2 g, 10 mmol, 1.0 eq.) in anhydrous THF (40 mL), cooled to -78 °C, was added *n*-BuMgCl (7.14 mL, 12 mmol, 1.2 eq. 20% wt) dropwise and stirred for a total of 90 minutes. The reaction mixture was allowed to warm to room temperature and then quenched with HCl (2M) until a pH of 1-3 was observed. The aqueous layer was washed with CH_2Cl_2 (3x50 mL) and the combined organic layers were dried over $MgSO_4$, filtered and solvents removed under reduced pressure. The product was purified via flash chromatography (SiO_2, 18x3 cm, 4:1 cyclohexane/ethyl acetate) to afford **564** (0.86 g, 3.34 mmol, 33%) as a viscous colourless oil.

$C_{14}H_{27}NO_3$ (M_W = 257.37 g/mol):
^{1}H-NMR (400 MHz, $CDCl_3$) δ 3.56 (t, *J* = 6.7 Hz, 2H), 2.46 – 2.35 (m, 4H), 1.59 – 1.54 (m, 4H), 1.50 (s, 9H), 1.29 (dt, *J* = 14.8, 7.5 Hz, 2H), 0.90 (t, *J* = 7.3 Hz, 3H); **^{13}C{1H}-NMR** (101 MHz, $CDCl_3$) δ 211.12, 152.82, 82.30, 46.15, 42.67, 42.42, 28.70, 28.22, 26.11, 22.50, 21.10, 13.99.

***tert*-Butyl (5-oxo-5-phenylpentyl)carbamate (562)**[187]

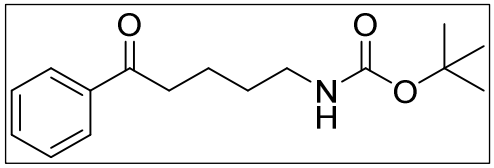

To a solution of **561** (2 g, 10 mmol, 1.0 eq.) in anhydrous THF (40 mL), cooled to -78 °C, was added PhMgBr (4.6 mL, 12 mmol, 1.2 eq. 2.6M) dropwise and the reaction mixture stirred for 90 minutes. It was allowed to warm to room temperature before being quenched with HCl (2M) until pH of 1-3 was observed. The aqueous layer was washed with CH_2Cl_2 (3x50 mL) and the combined organic layers were dried over $MgSO_4$, filtered and solvents removed under reduced pressure. The product was purified via recrystallisation from CH_2Cl_2 layered with *n*-pentane to afford **562** (1.25 g, 4.5 mmol, 45%) as white needles.

$C_{16}H_{23}NO_3$ (M_W = 277.36 g/mol):
m.p.: 89 °C; **^{1}H-NMR** (400 MHz, $CDCl_3$) δ 7.96 (d, *J* = 7.8 Hz, 2H), 7.56 (t, *J* = 7.4 Hz, 1H), 7.46 (t, *J* = 7.6 Hz, 2H), 4.60 (s, 1H, NH), 3.17 (d, *J* = 5.8 Hz, 2H), 3.00 (t, *J* = 7.2 Hz, 2H), 1.78 (dt, *J* = 15.1, 7.2 Hz, 2H), 1.58 (p, *J* = 7.1 Hz, 2H), 1.44 (s, 9H); **^{13}C{^{1}H}-NMR** (101 MHz, $CDCl_3$) δ 200.12, 156.12, 137.01, 133.12, 128.69, 128.13, 79.24, 40.34, 38.09, 29.76, 28.53, 21.35.

(3a*S*,8a*R*)-2-phenyl-8,8a-dihydro-3aH-indeno[1,2-d]oxazole (367)[188]

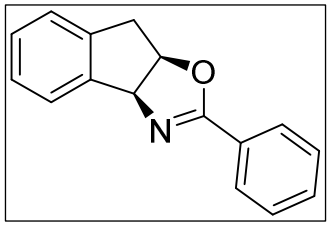

An oven-dried 50 two-neck round-bottomed flask was charged with (1*S*,2*R*)-1-amino-2,3-dihydro-1H-inden-2-ol (447 mg, 3 mmol, 1.0 eq.), 4Å mol sieves (4.5 g) and dissolved in dry CH_2Cl_2 (20 mL). Subsequently freshly distilled benzaldehyde (310 mg, 3 mmol, 1.0 eq.) and the reaction mixture was stirred at room temperature for 14 hours. TLC control (SiO_2, CH_2Cl_2/EtOAc 10:1) indicated complete consumption of starting material. Afterwards, *N*-bromosuccinimide (534 mg, 3 mmol, 1.0 eq.) was added and stirring continued for another four hours. The reaction was quenched by pouring the reaction mixture over saturated $NaHCO_3$. The organic layer was washed with water, dried over anhydrous $MgSO_4$, filtered and solvents removed under reduced pressure. The residue was subjected to flash chromatography (SiO_2, cyclohexane/*tert*-butylmethylether 1 :1, 12.5x3.5 cm, 20 mL fractions) to afford **367** (390 mg, 1.66 mmol, 55%) as a white solid.

$C_{16}H_{13}NO$ (M_W = 235.28 g/mol):
m.p.: 123 °C; **^{1}H-NMR** (400 MHz, $CDCl_3$) δ 7.92 (dd, *J* = 5.3, 3.3 Hz, 2H), 7.62 – 7.54 (m, 1H), 7.43 (ddd, *J* = 6.4, 3.8, 1.3 Hz, 1H), 7.41 – 7.33 (m, 2H), 7.31 – 7.23 (m, 3H), 5.74 (d, *J* = 7.9 Hz, 1H), 5.53 – 5.44 (m, 1H), 3.51 (dd, *J* = 17.9, 6.8 Hz, 1H), 3.37 (d, *J* = 17.8 Hz, 1H); **^{13}C{^{1}H}-NMR** (101 MHz, $CDCl_3$) δ 164.12, 142.18, 139.88, 131.40, 128.59, 128.48, 128.36, 128.01, 127.61, 125.76, 125.42, 83.29, 39.97.

(*S*)-4-benzyl-2-(*tert*-butyl)-4,5-dihydrooxazole (369)[188]

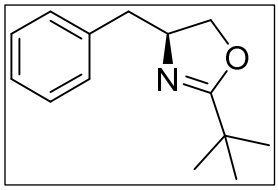

An oven-dried 50 two-neck round-bottomed flask was charged (*S*)-2-amino-3-phenylpropan-1-ol (500 mg, 3.3 mmol, 1.0 eq.), 4Å mol sieves (4.5 g) and dissolved in dry CH_2Cl_2 (20 mL). Subsequently freshly distilled pivalaldehyde (284 mg, 3.3 mmol, 1.0 eq.) and the reaction mixture was stirred at room temperature for 14 hours. TLC control (SiO_2, CH_2Cl_2/EtOAc 10:1) indicated complete consumption of starting material. Afterwards, *N*-bromosuccinimide (588 mg, 3.3 mmol, 1.0 eq.) was added and stirring continued for another four hours. The reaction was quenched by pouring the reaction mixture over saturated $NaHCO_3$. The organic layer was washed with water, dried over anhydrous $MgSO_4$, filtered and solvents removed under reduced pressure. The residue was subjected to flash chromatography (SiO_2, cyclohexane/*tert*-butylmethylether/triethylamine 9:1:0.1, 18x3.5 cm, 20 mL fractions) to afford (*S*)-**369** (140 mg, 0.65 mmol, 20%) as a clear oil.

$C_{14}H_{19}NO$ (M_W = 217.31 g/mol):
^{1}H-NMR (400 MHz, $CDCl_3$) δ 7.29 (t, *J* = 7.3 Hz, 2H), 7.20 (dd, *J* = 10.4, 6.6 Hz, 3H), 4.35 (dtd, *J* = 8.9, 6.9, 4.5 Hz, 1H), 4.11 (t, *J* = 8.9 Hz, 1H), 3.96 (dd, *J* = 8.4, 6.9 Hz, 1H), 3.09 (dd, *J* = 13.7, 4.4 Hz, 1H), 2.64 (dd, *J* = 13.6, 8.6 Hz, 1H), 1.19 (s, 9H).

((3,4-dihydronaphthalen-1-yl)oxy)trimethylsilane (381)[93]

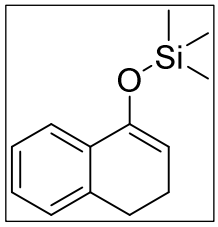

A 250 mL Schlenk tube was charged with LiCl (580 mg, 13.68 mmol, 2.0 eq.) and evacuated while being heated out with a bunsen burner. After cooling to room temperature and three Argon purge cycles it was charged mesityl magnesium bromide (6.84 mmol, 1.0 eq.) and dissolved in 1,4-dioxane (10 mL) and tetrahydrofuran (60 mL). The resultant suspension was stirred for 15 minutes before it was cooled to 0 °C. Trimethylsilylchloride (742 mg, 6.84 mmol, 1.0 eq.) was added and stirring was continued for 5 minutes before 3,4-dihydronaphthalen-1(2H)-one **380** (1.0 g, 6.84 mmol, 1.0 eq.), dissolved in dry THF (15 mL), was added via syringe pump over the course of 35 minutes. The reaction mixture was stirred overnight at 0 °C before being quenched with $NaHCO_3$ (50 mL) at 0 °C. After warming up to room temperature, the organic components were extracted with tertbutylmethylether (3x50 mL), dried over anhydrous $MgSO_4$, filtered and solvent removed under reduced pressure. The residue was subjected to flash chromatography (SiO_2, 15x4.5 cm, cyclohexane/Et_2O 50:1, 20 mL fractions) to afford **381** (1.2 g, 5.5 mmol, 88%) as a colourless oil.

$C_{13}H_{18}OSi$ (M_W = 218.37 g/mol):

^{1}H-NMR (400 MHz, $CDCl_3$) δ 7.42 (d, *J* = 7.1 Hz, 1H), 7.20 (t, *J* = 7.5 Hz, 1H), 7.16 (td, *J* = 7.4, 1.5 Hz, 1H), 7.11 (d, *J* = 6.6 Hz, 1H), 5.20 (t, *J* = 4.6 Hz, 1H), 2.77 (t, *J* = 8.0 Hz, 2H), 2.36 – 2.30 (m, 2H), 0.27 (s, 10H); **^{13}C{^{1}H}-NMR** (101 MHz, $CDCl_3$) δ 148.18, 137.20, 133.66, 127.41, 127.08, 126.30, 121.95, 105.4, 28.30, 22.30, 0.35.

2-(*tert*-butyl)-3,4-dihydronaphthalen-1(2H)-one (382)[93]

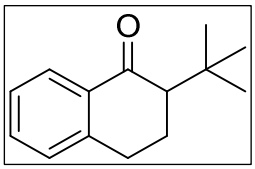

A flame-dried 50 mL two-necked round bottom flask was purged with argon three times before being charged with **381** (1.18 g, 5.4 mmol, 1.0 eq.) and 2-chloro-2-methylpropane (521 mg, 5.63 mmol, 1.04 eq.). The reactants were dissolved in dry CH_2Cl_2 (10 mL) and the reaction mixture cooled to -40 °C. In another flask was placed $TiCl_4$ (1.025 g, 5.4 mmol, 1.0 eq.) and dissolved in dry CH_2Cl_2 (15 mL) and cooled to -40 °C. It was then transferred to the reaction mixture via cannula over the course of 5 minutes. Stirring was continued at -40 °C for 2 hours. TLC analysis (SiO_2, pentane/Et_2O 10:1) indicated complete consumption of starting material. The cold solution was then poured on ice/water (80 mL) and extracted with CH_2Cl_2 (3x50 mL). The organic layer was washed with $NaHCO_3$ (10% *w*/*w*, 50 mL). The combined aequeous layers were re-extracted with CH_2Cl_2 (15 mL) and the combined organic layers then dried over anhydrous $MgSO_4$, filtered and solvents removed under reduced pressure. The residue was purified by distillation (150 °C, 0.08 torr), where small amounts of tetralone were observed. The product was further purified by flash chromatography (SiO_2, pentane/Et_2O 20:1, 10x3 cm, 20 mL fractions) to afford **382** (369 mg, 1.82 mmol, 34 %) as a clear oil.

$C_{14}H_{18}O$ (MW = 202.29 g/mol):
^{1}H-NMR (400 MHz, $CDCl_3$) δ 7.95 (dd, *J* = 7.8, 1.1 Hz, 1H), 7.43 (td, *J* = 7.5, 1.4 Hz, 1H), 7.29 (d, *J* = 7.5 Hz, 1H), 7.20 (d, *J* = 7.6 Hz, 1H), 3.06 – 2.90 (m, 2H), 2.36 – 2.25 (m, 2H), 1.94 (dddd, *J* = 14.3, 12.9, 10.4, 5.5 Hz, 1H), 1.11 (s, 9H); **^{13}C{^{1}H}-NMR** (400 MHz, $CDCl_3$) δ 200.31, 143.55, 134.72, 132.78, 128.42, 127.30, 126.59, 56.87, 33.34, 29.64, 28.50, 25.48.

2-(2-(diphenylphosphino)phenyl)-4,4-dimethyl-4,5-dihydrooxazole[98]

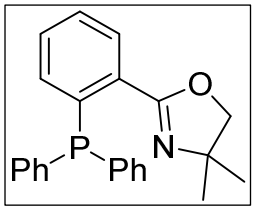

A 250 mL three-necked round-bottom flask was equipped with a magnetic stirrer and evacuated before being flame-dried with a bunsen burner. After cooling to room temperature it was purged with argon three times, charged with 4,4-dimethyl-2-phenyl-4,5-dihydrooxazole (1.0 g, 5.7 mmol, 1.0 eq.) and dissolved in dry pentane (45 mL). TMEDA (730 mg, 6.27 mmol, 1.1 eq.) was added and the solution was degassed by three freeze-pump-thaw cycles. It was then cooled to -78 °C and *n*-butyllithium (1.4 M, 6.27 mmol, 1.1 eq.) was added dropwise and the reaction stirred at -78 °C for 10 minutes. It was then warmed up to 0 °C and stirred for 10 minutes before chlorodiphenylphosphine (1.63 g, 7.41 mmol, 1.3 eq.) was added, the solution stirred for another 10 minutes at 0 °C before being allowed to warm to room temperature while stirring overnight. The volatiles were removed under reduced pressure and the residual semi-solid subjected to flash chromatography (SiO_2, Et_2O/pentane 9:1, 16x5.5 cm, 20 mL fractions) to afford as a sticky oil/solid. It was further purified by dissolving in a minimal amount of ethanol and heated to reflux to effect crystallisation which afforded 2-(2-(diphenylphosphino)phenyl)-4,4-dimethyl-4,5-dihydrooxazole (1.0 g, 2.8 mmol, 49 %) as white crystals.

$C_{23}H_{22}NOP$ (M_W = 359.40 g/mol):
m.p.: 103 °C; **^{1}H-NMR** (400 MHz, $CDCl_3$) δ 7.85 (ddd, *J* = 7.5, 3.5, 1.5 Hz, 1H), 7.38 – 7.30 (m, 10H), 7.30 – 7.24 (m, 2H), 6.81 (ddd, *J* = 7.7, 4.5, 1.0 Hz, 1H), 3.73 (s, 2H), 1.05 (s, 6H); **^{31}P{^{1}H}-NMR** (162 MHz, $CDCl_3$) δ -7.54.

2-(2-(diphenylphosphino)phenyl)-4,5-dihydrooxazole[98]

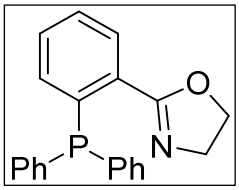

A 250 mL three-necked round-bottom flask was equipped with a magnetic stirrer and evacuated before being flame-dried with a bunsen burner. After cooling to room temperature it was purged with argon three times, charged with 2-phenyl-4,5-

dihydrooxazole (1.0 g, 6.8 mmol, 1.0 eq.) and dissolved in dry pentane (50 mL). TMEDA (864 mg, 7.48 mmol, 1.1 eq.) was added and the solution was degassed by three freeze-pump-thaw cycles. It was then cooled to -78 °C and *n*-butyllithium (1.4 M, 7.48 mmol, 1.1 eq.) was added dropwise and the reaction stirred at -78 °C for 10 minutes. It was then warmed up to 0 °C and stirred for 10 minutes before chlorodiphenylphosphine (1.94 g, 8.84 mmol, 1.3 eq.) was added, the solution stirred for another 10 minutes at 0 °C before being allowed to warm to room temperature while stirring overnight. The volatiles were removed under reduced pressure and the residual semi-solid subjected to flash chromatography (SiO_2, Et_2O/pentane 9:1, 16x5.5 cm, 20 mL fractions) to afford as a sticky oil/solid. It was further purified by dissolving in a minimal amount of ethanol and heated to reflux to effect crystallisation which afforded 2-(2-(diphenylphosphino)phenyl)-4,5-dihydrooxazole (1.4 g, 4.4 mmol, 65 %) as white crystals.

$C_{21}H_{18}NOP$ (M_W = 331.35 g/mol):

m.p.: 107 °C; **^{1}H-NMR** (400 MHz, $CDCl_3$) δ 7.85 (ddd, *J* = 7.5, 3.5, 1.3 Hz, 1H), 7.39 – 7.28 (m, 12H), 6.89 (ddd, *J* = 7.8, 4.3, 1.0 Hz, 1H), 4.08 (t, *J* = 9.4 Hz, 2H), 3.78 (t, *J* = 9.4 Hz, 2H); **^{31}P{^{1}H}-NMR** (162 MHz, $CDCl_3$) δ -4.46.

(*S*)-Valinol[189]

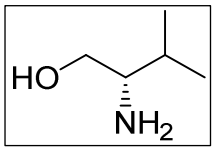

A 500 mL three-neck round bottom flask was equipped with a magnetic stirrer, a reflux condenser, a thermometer and a dropping funnel. It was then evacuated and flame-dried with a bunsen burner before being purged with Argon three times. It was then charged with (*S*)-valine (10 g, 85.4 mmol, 1.0 eq.) and dissolved in dry THF (200 mL). The reaction mixture was cooled to 4 °C in a water/ice bath and $NaBH_4$ (7.75 g, 205 mmol, 2.4 eq.) were added in one portion. To the dropping funnel was added iodine (21.67 g, 85.4 mmol, 1.0 eq.) and dissolved in dry THF (50 mL) before being added dropwise to the reaction mixture. The cooling bath was removed and the reaction mixture heated to reflux for 18 hours. After cooling to 0 °C with an ice bath it was quenched by adding methanol (100 mL) dropwise and stirred for one hour while warming to room temperature. The solvents were then removed under reduced pressure and the residual semisolid was dissolved in KOH (20% w/w, 150 mL). The mixture was stirred for 5 hours before the organic components were extracted with CH_2Cl_2 (6x150 mL), dried over Na_2SO_4, filtered and solvents removed under reduced pressure. Purification by distillation (60 °C, 0.1 mbar) afforded (*S*)-valinol (7.35 g, 71.25 mmol, 83 %) as a clear oil.

$C_5H_{13}NO$ (M_W = 103.16 g/mol):
^{1}H-NMR (500 MHz, $CDCl_3$) δ 4.39 – 4.30 (m, 1H), 4.09 (t, *J* = 8.0 Hz, 1H), 3.94 (ddd, *J* = 9.6, 7.6, 6.1 Hz, 1H), 3.21 (s, 1H), 1.76 (dq, *J* = 13.3, 6.7 Hz, 1H), 0.95 (d, *J* = 6.8 Hz, 3H), 0.88 (d, *J* = 6.8 Hz, 3H); **Optical rotation**: $[a]_D^{20}$ = -17 (c = 1.0 in $CHCl_3$ with 0.75% EtOH); lit. $[a]_D^{26}$ = -23.2 (c = 3.7 in $CHCl_3$)[190]

(*S*)-2-(4-isopropyl-4,5-dihydrooxazol-2-yl)propan-2-ol[191]

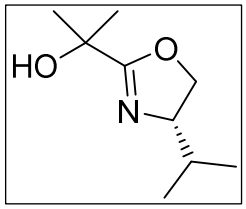

A 50 mL two-necked round bottom flask was equipped with a reflux condenser and a septum and purged with Argon three times. It was then charged with (*S*)-valinol (3 g, 29 mmol, 1.05 eq.) and 2-hydroxy-2-methylpropanoic acid (2.88 g, 27.7 mmol, 1.0 eq.) and dissolved in mesitylene (25 mL). The reaction mixture was heated to reflux for 2.5 days before being cooled to room temperature. The crude reaction mixture was subjected to elution chromatography (SiO_2, cyclohexane) to remove the solvent before the crude product was washed down with EtOAc. After removal of solvents under reduced pressure, the residue was subjected to flash chromatography (SiO_2, cyclohexane/EtOAc 1:1, 13x4 cm, 20 mL fractions) to afford (*S*)-2-(4-isopropyl-4,5-dihydrooxazol-2-yl)propan-2-ol (411 mg, 2.4 mmol, 9 %) as a clear oil.

$C_9H_{17}NO_2$ (M_W = 171.24 g/mol):
^{1}H-NMR (500 MHz, $CDCl_3$) δ 4.35 (t, *J* = 9.1 Hz, 1H), 4.09 (t, *J* = 8.0 Hz, 1H), 3.98 – 3.89 (m, 1H), 3.24 (s, 1H), 1.81 – 1.69 (m, 1H), 1.44 (s, 6H), 0.95 (d, *J* = 6.8 Hz, 3H), 0.88 (d, *J* = 6.8 Hz, 3H); **Optical rotation**: $[a]_D^{20}$ = -78 (c = 1.0 in $CHCl_3$ with 0.75% EtOH); lit. -78.5 (c = 1.07 in $CHCl_3$)[191]

***N*-(triphenylphosphoranylidene)aniline**[192]

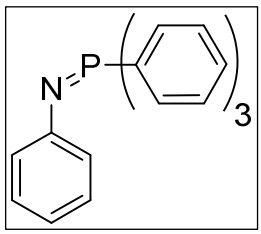

Aniline (6 mL, 6.3 mmol, 1.0 eq.) was suspended in water (50 mL) in a 250 mL round-bottomed flask and cooled to 0 °C. $NaNO_2$ (5.45 g, 7.9 mmol, 1.25 eq.) was added and HCl (37% *w*/*w*, 20 mL) was added *via* dropping funnel. The reaction mixture was stirred for one hour until a dark blue colour was observed. NaN_3 (5.5 g, 8.46 mmol, 1.34 eq.) was added in one portion and the reaction stirred for another two hours. PPh_3 (18 g, 6.86 mmol, 1.09 eq.) was added portionwise at 0 °C and then the reaction mixture was allowed to warm up to 23 °C while stirring overnight. After dilution with Et_2O (50 mL), the heterogeneous mixture was rinsed through a silica plug (4 cm, 6 cm ø) and rinsed with Et_2O (100 mL) to give an orange clear solution. The organic phase was decanted, dried over Na_2SO_4 and solvents removed under reduced pressure. The residue was resuspended in *n*-hexane to remove any soluble components before the residual solids were purified by recrystallisation from MeOH. Upon trituration of the saturated MeOH solution, *N*-(triphenylphosphoranylidene)aniline (8.16 g, 2.5 mmol, 40%) was obtained as an amorphous orange solid, which was dried *in vacuo* and stored under an atmosphere of argon in the freezer.

$C_{24}H_{20}NP$ (M_W = 353.40 g/mol):
^{1}H-NMR (400 MHz, $CDCl_3$) δ 7.82 – 7.73 (m, 6H), 7.56 – 7.49 (m, 3H), 7.49 – 7.41 (m, 6H), 7.03 (t, *J* = 7.6 Hz, 2H), 6.87 – 6.80 (m, 2H), 6.68 (dd, *J* = 10.6, 3.8 Hz, 1H); **^{13}C{^{1}H}-NMR** (101 MHz, $CDCl_3$) δ 151.22 (d, *J* = 3 Hz), 132.73 (d, *J* = 10 Hz), 131.73 (d, J = 2 Hz), 128.74, 128.70 (d, *J* = 1 Hz), 128.62, 123.64 (d, *J* = 18 Hz), 117.41; **^{31}P{^{1}H}-NMR** (162 MHz, $CDCl_3$) δ 3.53.

List of Abbreviations

α	alpha
Å	Ångstrom
Ac	Acetyl
Alk	Alkyl
aq.	Aequeous
ATR	attenuated total reflection (IR)
Ar	Aryl
BAr_F	Tetrakis[3,5-bis(trifluoromethyl)phenyl]borate
BINAP	2,2'-Bis(diphenylphosphino)-1,1'-binaphtyl
Bn	Benzyl
br	broad
b.p.	boiling point
Bu	Butyl
°C	Degrees Centigrade
c	concentration
calc.	calculated
cat.	Catalyzed
COD	Cyclooctadiene
conv.	conversion
Cp	Cyclopentadienyl
Cp*	Pentamethylcyclopentadienyl
Cy	Cyclohexyl
d	days
DCM	Dichloromethane
dec.	decomposed
DIOP	*O*-Isopropylidene-2,3-dihyroxy-1,4-bis(diphenylphosphino)butane
DMF	Dimethylformamide
DMSO	Dimethylsulfoxide
D^tBPF	Di-*tert*-butyl-phosphinoferrocene
EA	Elemental Analysis
ee	enantiomeric excess
EI (MS)	Electronic ionisation
eq.	equivalents
ESI (MS)	Electronic Spray Ionisation
Et	Ethyl
EtOAc	Ethyl Acetate
FAB (MS)	Fast Atom Bombardement
FTIR	Fourier Transformation Infrared Spectroscopy
GC	Gas Chromatography
h	hour
HMBC	Heteronuclear Multiple Bond Coherence
HMQC	Heteronuclear Multiple Quantum Coherence
HPLC	High Performance Liquid Chromatography
Hz	Hertz
IR	Infrared Spectroscopy
^{i}Pr	isopropyl
J	Coupling constant
K	Kelvin
L	Ligand
LDA	Lithium diisopropyl amine

L-DOPA	L-3,4-Dihydroxyphenylalanine
M	Molarity in solution
m	*meta*
MALDI	Matrix Assisted Laser Desorption Ionization
Me	Methyl
MeOH	Methanol
min	minutes
mL	milliliters
m.p.	melting point
MS	Mass Spectroscopy
MTBE	Methyl *tert*-butyl ether
m/*z*	mass to charge ratio
n.d.	not determined
n-BuLi	1-butyl lithium
NMR	Nuclear Magnetic Resonance
NOE	Nuclear Overhause Effect
n-Pr	1-propyl
o	*ortho*
o-Tol	*ortho*-Tolyl
p	*para*
Pd/C	Palladium on charcoal
Ph	Phenyl
PHOX	Phosphineoxazoline
ppm	parts per million
rac.	racemic
RT	Room Temperature
sat.	saturated
^{t}Bu	*tert*-butyl
T	Temperature
TBAF	tetrabutylammonium fluoride
t-BuLi	*tert*-butyl lithium
TBDMS	*tert*-butyl dimethylsilyl
TFAA	Trifluoroacetic anhydride
THF	Tetrahydrofuran
TLC	Thin Layer Chromatography
TMS	Trimethylsilyl
t_R	retention time
Ts	Tosyl
υ	wave number in cm^{-1}

Summary

The mechanistic studies on iridium catalysed imine hydrogenation commenced by *Dr. Fabiola Barrios* were continued towards the development of an efficient hydrogenation protocol for purely aliphatic imines. Chapter 2 summarizes the previous results where new iridium(III) complexes, formed under the reaction conditions, were observed and characterized.

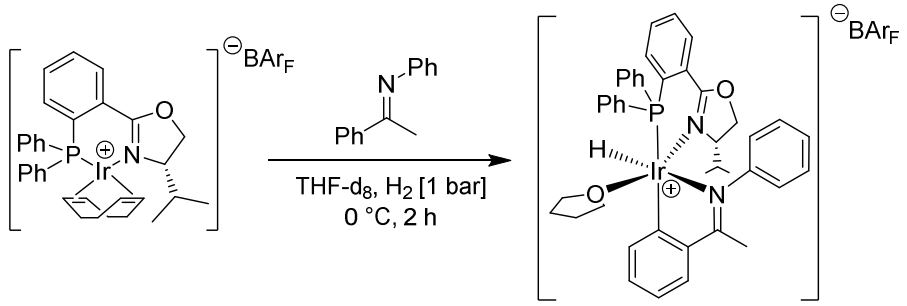

These iridacycles bear a cyclometalated imine and were used as catalysts, showing virtually identical enantioselectivity and similar conversion as the iridium(I) complexes initially used as catalysts for imine and olefin hydrogenation. Furthermore, these *in situ* formed iridacycles demonstrated superior reactivity in the hydrogenation of dialkyl imines compared to their corresponding iridium(I) complexes.

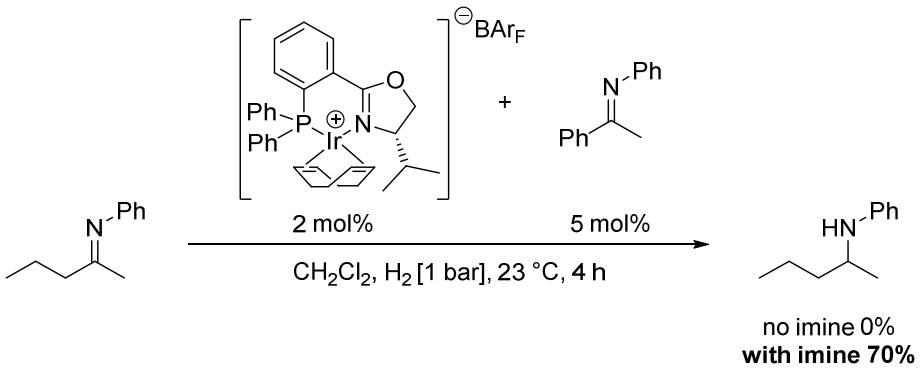

In-depth understanding of the reaction course was obtained with extended mechanistic investigations outlined in chapter 3. Cyclometalation of a chiral imine to an achiral iridium complex generated a chiral catalyst was formed. The structure of the cyclometalated imine was demonstrated to influence the enantioselectivity of the catalyst as well as to be involved in the enantiodiscriminating step of the hydrogenation. Furthermore, the iridacycle remained stable throughout the reaction as no dissociation of the cyclometalated imine was observed.

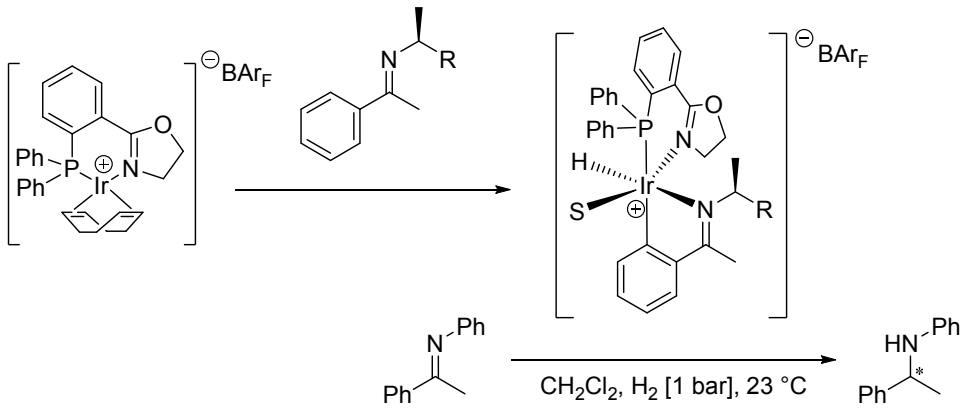

While acyclic chiral imines as cyclometalating ligands gave only low *ee*'s, cyclic ligand structures with a C-N double bond such as benzoxazines gave consistently higher *ee*'s.

The iridacycles were investigated in further detail by two-dimensional NMR studies and their preparation was improved by counterion metathesis. Deuterium labelling experiments depicted addition of hydrogen along the C-N double bond. Nevertheless, multiple isomerisation and scrambling processes were detected as well. Imine-enamine tautomerism occurs under hydrogenation conditions but hydrogenation proceeding *via* the enamine tautomer was excluded with imine substrates preventing tautomerism. Chiral phosphoric acids were evaluated as additives but resulted in low reactivity as well as imine hydrolysis.

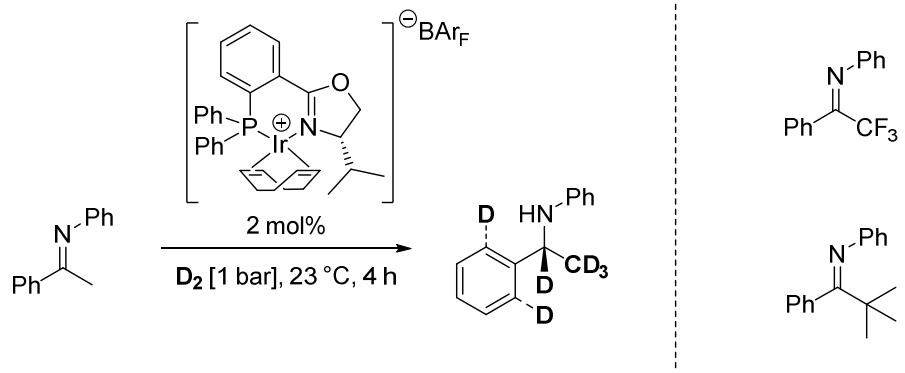

Chapter 4 summarizes the synthetic efforts for the synthesis of the different ligands with a C-N double bond employed in cyclometalation. Three different ligand scaffolds were prepared.

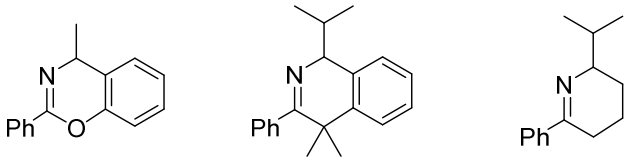

Chapter 5 presents the optimisation studies for an efficient asymmetric hydrogenation protocol for purely aliphatic imines. Identification of the optimal imine additive used as a cyclometalating ligand led to the sterically demanding 2,6-dimethyl aniline derived imine. Furthermore, hydrogenations could be conducted at –5 °C achieving full conversion and improving enantioselectivity up to 92%. Cyclic aliphatic imines could also be hydrogenated with these iridacycles, but required elevated reaction temperatures as well as hydrogen pressures to achieve turnover and displayed low conversions and enantioselectivities.

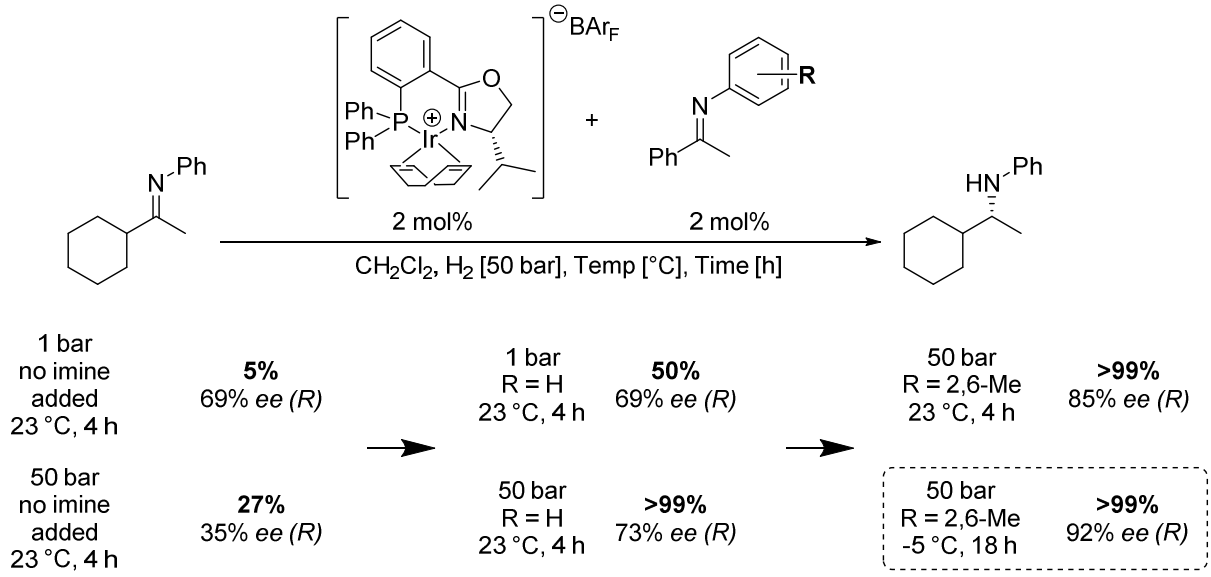

These studies concluded that iridium-catalysed imine hydrogenation is commenced by cyclometalation of the imine substrate to form an active iridium(III) catalyst prior to hydrogenation. If the imine substrate subjected to hydrogenation cannot undergo cyclometalation, low conversions and enantioselectivities as well as competitive hydrolysis are observed, as other catalytically active complexes are formed in solution. Therefore, acetophenone-derived imines can be used as additives to improve both reactivity and enantioselectivity of iridium catalysts for the hydrogenation of dialkyl imines generating a superior catalyst *in situ*. A postulated catalytic cycle is presented and includes both the possibility of an Ir^{III}/Ir^{V} cycle as well as a constant oxidation state of Ir^{III}.

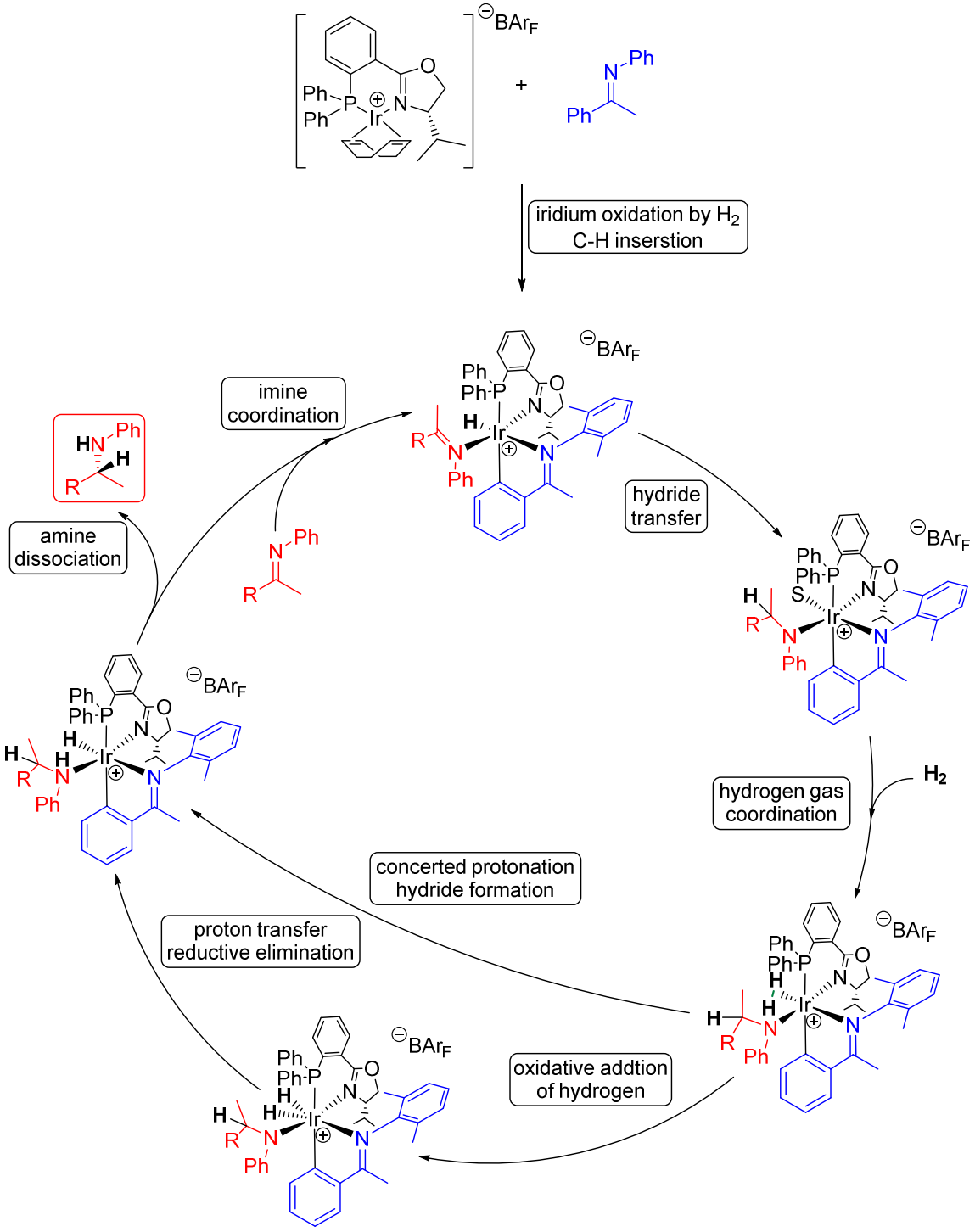

References

[1] R. S. Shallenberger, *Taste Chemistry*, Springer, **1994**.
[2] J. P. Rasor, E. Voss, *Applied Catalysis A: General* **2001**, *221*, 145-158.
[3] H. U. Blaser, F. Spindler, M. Studer, *Applied Catalysis A: General* **2001**, *221*, 119-143.
[4] W. S. Knowles, M. J. Sabacky, B. D. Vineyard, *J. Chem. Soc., Chem. Commun.* **1972**, *0*, 10-11.
[5] W. S. Knowles, *Acc. Chem. Res.* **1983**, *16*, 106-112.
[6] S. Akutagawa, *Applied Catalysis A: General* **1995**, *128*, 171-207.
[7] H.-U. Blaser, H.-P. Buser, K. Coers, R. Hanreich, H.-P. Jalett, E. Jelsch, B. Pugin, H.-D. Schneider, F. Spindler, A. Wegmann, *Chimia* **1999**, *53*, 275-280.
[8] K. Satoh, M. Inenaga, K. Kanai, *Tetrahedron: Asymmetry* **1998**, *9*, 2657-2662.
[9] R. Imwinkelried, *Chimia* **1997**, *51*, 300-302.
[10] T. Gizur, E. Fogassy, J. Bálint, G. Egri, J. Törley, Á. Demeter, I. Greiner, *Chirality* **2008**, *20*, 790-795.
[11] Z. Ye, R. Lan, W. Yang, L. Yao, X. Yu, *J. Int. Med. Res.* **2008**, *36*, 244-252.
[12] D. Y. Curtin, E. J. Grubbs, C. G. McCarty, *J. Am. Chem. Soc.* **1966**, *88*, 2775-2786.
[13] A. Reiker, H. Kessler, *Tetrahedron* **1967**, *23*, 3723-3732.
[14] R. A. Clark, D. C. Parker, *J. Am. Chem. Soc.* **1971**, *93*, 7257-7261.
[15] W. B. Jennings, D. R. Boyd, *J. Am. Chem. Soc.* **1972**, *94*, 7187-7188.
[16] H. Ahlbrecht, S. Fischer, *Tetrahedron* **1973**, *29*, 659-664.
[17] J. Bjorgo, D. R. Boyd, C. G. Watson, W. B. Jennings, *J. Chem. Soc., Perkin Trans. 2* **1974**, *0*, 757-762.
[18] G. Ball, W. R. Cullen, M. D. Fryzuk, W. J. Henderson, B. R. James, K. S. MacFarlane, *Inorg. Chem.* **1994**, *33*, 1464-1468.
[19] N. Langlois, T.-P. Dang, H. B. Kagan, *Tetrahedron Lett.* **1973**, *14*, 4865-4868.
[20] I. Ojima, T. Kogure, Y. Nagai, *Tetrahedron Lett.* **1973**, *14*, 2475-2478.
[21] I. Jardine, F. J. McQuillin, *Journal of the Chemical Society D: Chemical Communications* **1970**, *0*, 626a-626a.
[22] A. Levi, G. Modena, G. Scorrano, *J. Chem. Soc., Chem. Commun.* **1975**, *0*, 6-7.
[23] J. Bakos, I. Tóth, B. Heil, L. Markó, *J. Organomet. Chem.* **1985**, *279*, 23-29.
[24] J. Bakos, I. Tóth, B. Heil, G. Szalontai, L. Párkányi, V. Fülöp, *J. Organomet. Chem.* **1989**, *370*, 263-276.
[25] F. Spindler, B. Pugin, H.-U. Blaser, *Angew. Chem. Int. Ed. Engl.* **1990**, *29*, 558-559.
[26] Y. N. C. Chan, D. Meyer, J. A. Osborn, *J. Chem. Soc., Chem. Commun.* **1990**, *0*, 869-871.
[27] Y. Ng Cheong Chan, J. A. Osborn, *J. Am. Chem. Soc.* **1990**, *112*, 9400-9401.
[28] C. A. Willoughby, S. L. Buchwald, *J. Am. Chem. Soc.* **1992**, *114*, 7562-7564.
[29] N. Uematsu, A. Fujii, S. Hashiguchi, T. Ikariya, R. Noyori, *J. Am. Chem. Soc.* **1996**, *118*, 4916-4917.
[30] P. Schnider, G. Koch, R. Prétôt, G. Wang, F. M. Bohnen, C. Krüger, A. Pfaltz, *Chem. Eur. J.* **1997**, *3*, 887-892.
[31] A. Baeza, A. Pfaltz, *Chem. Eur. J.* **2010**, *16*, 4003-4009.
[32] D. Xiao, X. Zhang, *Angew. Chem. Int. Ed.* **2001**, *40*, 3425-3428.
[33] G. Hou, F. Gosselin, W. Li, J. C. McWilliams, Y. Sun, M. Weisel, P. D. O'Shea, C.-y. Chen, I. W. Davies, X. Zhang, *J. Am. Chem. Soc.* **2009**, *131*, 9882-9883.
[34] A. Trifonova, J. S. Diesen, C. J. Chapman, P. G. Andersson, *Org. Lett.* **2004**, *6*, 3825-3827.
[35] A. Trifonova, J. S. Diesen, P. G. Andersson, *Chem. Eur. J.* **2006**, *12*, 2318-2328.
[36] C. Moessner, C. Bolm, *Angew. Chem. Int. Ed.* **2005**, *44*, 7564-7567.
[37] T. Imamoto, N. Iwadate, K. Yoshida, *Org. Lett.* **2006**, *8*, 2289-2292.
[38] S.-F. Zhu, J.-B. Xie, Y.-Z. Zhang, S. Li, Q.-L. Zhou, *J. Am. Chem. Soc.* **2006**, *128*, 12886-12891.
[39] M. N. Cheemala, P. Knochel, *Org. Lett.* **2007**, *9*, 3089-3092.
[40] N. a. Mršić, A. J. Minnaard, B. L. Feringa, J. G. d. Vries, *J. Am. Chem. Soc.* **2009**, *131*, 8358-8359.
[41] C. Li, C. Wang, B. Villa-Marcos, J. Xiao, *J. Am. Chem. Soc.* **2008**, *130*, 14450-14451.

[42] C. Li, B. Villa-Marcos, J. Xiao, *J. Am. Chem. Soc.* **2009**, *131*, 6967-6969.
[43] C. Wang, A. Pettman, J. Bacsa, J. Xiao, *Angew. Chem. Int. Ed.* **2010**, *49*, 7548-7552.
[44] S. Zhou, S. Fleischer, K. Junge, S. Das, D. Addis, M. Beller, *Angew. Chem. Int. Ed.* **2010**, *49*, 8121-8125.
[45] S. Zhou, S. Fleischer, K. Junge, M. Beller, *Angew. Chem. Int. Ed.* **2011**, *50*, 5120-5124.
[46] A. V. Malkov, K. Vranková, S. Stončius, P. Kočovský, *J. Org. Chem.* **2009**, *74*, 5839-5849.
[47] S. Itsuno, Y. Sakurai, K. Ito, A. Hirao, S. Nakahama, *Bull. Chem. Soc. Jpn.* **1987**, *60*, 395-396.
[48] K. D. Sugi, T. Nagata, T. Yamada, T. Mukaiyama, *Chem. Lett.* **1997**, *26*, 493-494.
[49] M. Rueping, E. Sugiono, C. Azap, T. Theissmann, M. Bolte, *Org. Lett.* **2005**, *7*, 3781-3783.
[50] S. Hoffmann, A. M. Seayad, B. List, *Angew. Chem. Int. Ed.* **2005**, *44*, 7424-7427.
[51] C. Zhu, T. Akiyama, *Org. Lett.* **2009**, *11*, 4180-4183.
[52] X.-Y. Liu, C.-M. Che, *Org. Lett.* **2009**, *11*, 4204-4207.
[53] R. Dorta, D. Broggini, R. Kissner, A. Togni, *Chem. Eur. J.* **2004**, *10*, 4546-4555.
[54] R. H. Crabtree, H. Felkin, T. Khan, G. E. Morris, *J. Organomet. Chem.* **1978**, *144*, C15-C17.
[55] R. H. Crabtree, H. Felkin, T. Fillebeen-Khan, G. E. Morris, *J. Organomet. Chem.* **1979**, *168*, 183-195.
[56] B. F. M. Kimmich, E. Somsook, C. R. Landis, *J. Am. Chem. Soc.* **1998**, *120*, 10115-10125.
[57] C. Mazet, S. P. Smidt, M. Meuwly, A. Pfaltz, *J. Am. Chem. Soc.* **2004**, *126*, 14176-14181.
[58] R. H. Crabtree, R. J. Uriarte, *Inorg. Chem.* **1983**, *22*, 4152-4154.
[59] A. C. Cooper, W. E. Streib, O. Eisenstein, K. G. Caulton, *J. Am. Chem. Soc.* **1997**, *119*, 9069-9070.
[60] A. A. H. Van der Zeijden, G. Van Koten, R. Luijk, R. A. Nordemann, A. L. Spek, *Organometallics* **1988**, *7*, 1549-1556.
[61] M. D. Fryzuk, P. A. MacNeil, S. J. Rettig, *J. Am. Chem. Soc.* **1987**, *109*, 2803-2812.
[62] C. A. Willoughby, S. L. Buchwald, *J. Am. Chem. Soc.* **1994**, *116*, 8952-8965.
[63] C. A. Willoughby, S. L. Buchwald, *J. Am. Chem. Soc.* **1994**, *116*, 11703-11714.
[64] P. Marcazzan, C. Abu-Gnim, K. N. Seneviratne, B. R. James, *Inorg. Chem.* **2004**, *43*, 4820-4824.
[65] R. Dorta, D. Broggini, R. Stoop, H. Rüegger, F. Spindler, A. Togni, *Chem. Eur. J.* **2004**, *10*, 267-278.
[66] Y. Shvo, D. Czarkie, Y. Rahamim, D. F. Chodosh, *J. Am. Chem. Soc.* **1986**, *108*, 7400-7402.
[67] N. Menashe, Y. Shvo, *Organometallics* **1991**, *10*, 3885-3891.
[68] N. Menashe, E. Salant, Y. Shvo, *J. Organomet. Chem.* **1996**, *514*, 97-102.
[69] G. Csjernyik, A. H. Éll, L. Fadini, B. Pugin, J.-E. Bäckvall, *J. Org. Chem.* **2002**, *67*, 1657-1662.
[70] C. P. Casey, T. B. Clark, I. A. Guzei, *J. Am. Chem. Soc.* **2007**, *129*, 11821-11827.
[71] A. Comas-Vives, G. Ujaque, A. Lledós, *Organometallics* **2008**, *27*, 4854-4863.
[72] M. Martín, E. Sola, S. Tejero, J. L. Andrés, L. A. Oro, *Chem. Eur. J.* **2006**, *12*, 4043-4056.
[73] P. Marcazzan, B. O. Patrick, B. R. James, *Russ. Chem. Bull.* **2003**, *52*, 2715-2721.
[74] F. Torres, E. Sola, M. Martín, C. Ochs, G. Picazo, J. A. López, F. J. Lahoz, L. A. Oro, *Organometallics* **2001**, *20*, 2716-2724.
[75] E. Sola, V. I. Bakhmutov, F. Torres, A. Elduque, J. A. López, F. J. Lahoz, H. Werner, L. A. Oro, *Organometallics* **1998**, *17*, 683-696.
[76] V. R. Landaeta, B. K. Muñoz, M. Peruzzini, V. Herrera, C. Bianchini, R. A. Sánchez-Delgado, *Organometallics* **2005**, *25*, 403-409.
[77] K. H. Hopmann, A. Bayer, *Organometallics* **2011**, *30*, 2483-2497.
[78] M. Martín, E. Sola, S. Tejero, J. A. López, L. A. Oro, *Chem. Eur. J.* **2006**, *12*, 4057-4068.
[79] J. F. Van Baar, K. Vrieze, D. J. Stufkens, *J. Organomet. Chem.* **1975**, *85*, 249-263.
[80] J. F. van Baar, K. Vrieze, D. J. Stufkens, *J. Organomet. Chem.* **1974**, *81*, 247-259.
[81] F. Lorenzini, P. Marcazzan, B. O. Patrick, B. R. James, *Can. J. Chem.* **2008**, *86*, 253-260.
[82] P. Marcazzan, B. James, *React. Kinet. Catal. Lett.* **2009**, *98*, 193-204.
[83] K. Gruet, E. Clot, O. Eisenstein, D. H. Lee, B. Patel, A. Macchioni, R. H. Crabtree, *New J. Chem.* **2003**, *27*, 80-87.

[84] M. Gomez, J. Granell, M. Martinez, *Journal of the Chemical Society, Dalton Transactions* **1998**, *0*, 37-44.
[85] L. Barloy, J.-T. Issenhuth, M. G. Weaver, N. Pannetier, C. Sirlin, M. Pfeffer, *Organometallics* **2011**, *30*, 1168-1174.
[86] L. Li, W. W. Brennessel, W. D. Jones, *Organometallics* **2009**, *28*, 3492-3500.
[87] K. Tani, J.-i. Onouchi, T. Yamagata, Y. Kataoka, *Chem. Lett.* **1995**, *24*, 955-956.
[88] G. Zhu, X. Zhang, *Tetrahedron: Asymmetry* **1998**, *9*, 2415-2418.
[89] H. Adams, N. A. Bailey, T. N. Briggs, J. A. McCleverty, H. M. Colquhoun, D. J. Williams, *Journal of the Chemical Society, Dalton Transactions* **1986**, *0*, 813-819.
[90] H. Yamada, T. Kawate, A. Nishida, M. Nakagawa, *J. Org. Chem.* **1999**, *64*, 8821-8828.
[91] K. Funabiki, N. Honma, W. Hashimoto, M. Matsui, *Org. Lett.* **2003**, *5*, 2059-2061.
[92] S. P. Smidt, A. Pfaltz, E. Martínez-Viviente, P. S. Pregosin, A. Albinati, *Organometallics* **2003**, *22*, 1000-1009.
[93] W. J. Kerr, A. J. B. Watson, D. Hayes, *Org. Biomol. Chem.* **2008**, *6*, 1238-1243.
[94] M. T. Reetz, W. F. Maier, I. Chatziiosifidis, A. Giannis, H. Heimbach, U. Löwe, *Chem. Ber.* **1980**, *113*, 3741-3757.
[95] S. T. Madrahimov, D. Markovic, J. F. Hartwig, *J. Am. Chem. Soc.* **2009**, *131*, 7228-7229.
[96] M. Viciano, E. Mas-Marzá, M. Poyatos, M. Sanaú, R. H. Crabtree, E. Peris, *Angew. Chem.* **2005**, *117*, 448-451.
[97] R. I. Storer, D. E. Carrera, Y. Ni, D. W. C. MacMillan, *J. Am. Chem. Soc.* **2005**, *128*, 84-86.
[98] B. Wüstenberg, A. Pfaltz, *Adv. Synth. Catal.* **2008**, *350*, 174-178.
[99] M. Butters, J. N. Harvey, J. Jover, A. J. J. Lennox, G. C. Lloyd-Jones, P. M. Murray, *Angew. Chem. Int. Ed.* **2010**, *49*, 5156-5160.
[100] T. I. Richardson, P. L. Ornstein, K. Briner, M. J. Fisher, R. T. Backer, C. K. Biggers, M. P. Clay, P. J. Emmerson, L. W. Hertel, H. M. Hsiung, S. Husain, S. D. Kahl, J. A. Lee, T. D. Lindstrom, M. J. Martinelli, J. P. Mayer, J. T. Mullaney, T. P. O'Brien, J. M. Pawlak, K. D. Revell, J. Shah, J. M. Zgombick, R. J. Herr, A. Melekhov, P. B. Sampson, C.-H. R. King, *J. Med. Chem.* **2004**, *47*, 744-755.
[101] M. Kawatsura, J. F. Hartwig, *J. Am. Chem. Soc.* **1999**, *121*, 1473-1478.
[102] D. A. Culkin, J. F. Hartwig, *Acc. Chem. Res.* **2003**, *36*, 234-245.
[103] M. Palucki, S. L. Buchwald, *J. Am. Chem. Soc.* **1997**, *119*, 11108-11109.
[104] M. C. Willis, D. Taylor, A. T. Gillmore, *Org. Lett.* **2004**, *6*, 4755-4757.
[105] G. Brenchley, M. Fedouloff, E. Merifield, M. Wills, *Tetrahedron: Asymmetry* **1996**, *7*, 2809-2812.
[106] M. Waibel, M. De Angelis, F. Stossi, K. J. Kieser, K. E. Carlson, B. S. Katzenellenbogen, J. A. Katzenellenbogen, *Eur. J. Med. Chem.* **2009**, *44*, 3412-3424.
[107] M. E. Jung, M. A. Lyster, *J. Org. Chem.* **1977**, *42*, 3761-3764.
[108] M. E. Jung, M. A. Lyster, *Org. Synth.* **1988**, *59*.
[109] J. M. M. Verkade, L. J. C. van Hemert, P. J. L. M. Quaedflieg, P. L. Alsters, F. L. van Delft, F. P. J. T. Rutjes, *Tetrahedron Lett.* **2006**, *47*, 8109-8113.
[110] L. M. Klingensmith, K. A. Nadeau, G. A. Moniz, *Tetrahedron Lett.* **2007**, *48*, 4589-4593.
[111] H. Firouzabadi, N. Iranpoor, B. Karimi, *Synlett* **1999**, *1999*, 321-323.
[112] R. Gopinath, S. J. Haque, B. K. Patel, *J. Org. Chem.* **2002**, *67*, 5842-5845.
[113] A. Thurkauf, A. E. Jacobson, K. C. Riee, *Synthesis* **1988**, *1988*, 233-234.
[114] M. H. Ali, M. Goretti Gomes, *Synthesis* **2005**, *2005*, 1326-1332.
[115] T.-H. Yan, C.-C. Tsai, C.-T. Chien, C.-C. Cho, P.-C. Huang, *Org. Lett.* **2004**, *6*, 4961-4963.
[116] J. F. Payack, D. L. Hughes, D. Cai, I. F. Cottrell, T. R. Verhoeven, *Org. Synth.* **2004**, *Coll. Vol. 10*.
[117] A. Vailaya, T. Wang, Y. Chen, M. Huffman, *J. Pharm. Biomed. Anal.* **2001**, *25*, 577-588.
[118] N. A. Petasis, E. I. Bzowej, *J. Am. Chem. Soc.* **1990**, *112*, 6392-6394.
[119] N. A. Petasis, S.-P. Lu, *Tetrahedron Lett.* **1995**, *36*, 2393-2396.
[120] M. L. Edwards, D. M. Stemerick, J. R. McCarthy, *Tetrahedron Lett.* **1990**, *31*, 3417-3420.

[121] N. Morita, N. Krause, *Eur. J. Org. Chem.* **2006**, *2006*, 4634-4641.
[122] W. Sun, J. C. Pelletier, *Tetrahedron Lett.* **2007**, *48*, 7745-7746.
[123] K. M. Miller, W.-S. Huang, T. F. Jamison, *J. Am. Chem. Soc.* **2003**, *125*, 3442-3443.
[124] H. M. Peltier, J. A. Ellman, *J. Org. Chem.* **2005**, *70*, 7342-7345.
[125] A. Bugarin, K. D. Jones, B. T. Connell, *Chem. Commun. (Cambridge, U. K.)* **2010**, *46*, 1715-1717.
[126] H.-Y. Jang, R. R. Huddleston, M. J. Krische, *J. Am. Chem. Soc.* **2002**, *124*, 15156-15157.
[127] E. P. Kündig, P. Meier, *Helv. Chim. Acta* **1999**, *82*, 1360-1370.
[128] G. Bernardinelli, D. Fernandez, R. Gosmini, P. Meier, A. Ripa, P. Schüpfer, B. Treptow, E. P. Kündig, *Chirality* **2000**, *12*, 529-539.
[129] G. H. Bernardinelli, E. P. Kündig, P. Meier, A. Pfaltz, K. Radkowski, N. Zimmermann, M. Neuburger-Zehnder, *Helv. Chim. Acta* **2001**, *84*, 3233-3246.
[130] F. J. Weiberth, S. S. Hall, *J. Org. Chem.* **1986**, *51*, 5338-5341.
[131] U. Azzena, T. Denurra, G. Melloni, E. Fenude, G. Rassu, *J. Org. Chem.* **1992**, *57*, 1444-1448.
[132] S. A. Weissman, D. Zewge, *Tetrahedron* **2005**, *61*, 7833-7863.
[133] W. C. P. Tsang, R. R. Schrock, A. H. Hoveyda, *Organometallics* **2001**, *20*, 5658-5669.
[134] D. V. Gribkov, K. C. Hultzsch, F. Hampel, *Chem. Eur. J.* **2003**, *9*, 4796-4810.
[135] M. Klussmann, L. Ratjen, S. Hoffmann, V. Wakchaure, R. Goddard, B. List, *Synlett* **2010**, *2010*, 2189-2192.
[136] J.-H. Xie, S.-F. Zhu, Q.-L. Zhou, *Chem. Rev.* **2010**, *111*, 1713-1760.
[137] M. Chang, W. Li, G. Hou, X. Zhang, *Adv. Synth. Catal.* **2010**, *352*, 3121-3125.
[138] J. Barluenga, M. A. Fernández, F. Aznar, C. Valdés, *Chem. Eur. J.* **2004**, *10*, 494-507.
[139] X.-Y. Liu, P. Ding, J.-S. Huang, C.-M. Che, *Org. Lett.* **2007**, *9*, 2645-2648.
[140] D. Pei, Z. Wang, S. Wei, Y. Zhang, J. Sun, *Org. Lett.* **2006**, *8*, 5913-5915.
[141] J. S. M. Samec, J.-E. Bäckvall, *Chem. Eur. J.* **2002**, *8*, 2955-2961.
[142] M. C. Hansen, S. L. Buchwald, *Org. Lett.* **2000**, *2*, 713-715.
[143] Z. Wang, M. Cheng, P. Wu, S. Wei, J. Sun, *Org. Lett.* **2006**, *8*, 3045-3048.
[144] Z. Han, Z. Wang, X. Zhang, K. Ding, *Angew. Chem. Int. Ed.* **2009**, *48*, 5345-5349.
[145] C. R. Venkat Reddy, S. Urgaonkar, J. G. Verkade, *Org. Lett.* **2005**, *7*, 4427-4430.
[146] L. L. Anderson, J. Arnold, R. G. Bergman, *Org. Lett.* **2004**, *6*, 2519-2522.
[147] C. G. Hartung, A. Tillack, H. Trauthwein, M. Beller, *J. Org. Chem.* **2001**, *66*, 6339-6343.
[148] A. H. Vetter, A. Berkessel, *Synthesis* **1995**, *1995*, 419-422.
[149] F. Chen, Z. Ding, Y. He, J. Qin, T. Wang, Q.-H. Fan, *Tetrahedron* **2012**, *68*, 5248-5257.
[150] S. R. Landor, O. O. Sonola, A. R. Tatchell, *Bull. Chem. Soc. Jpn.* **1984**, *57*, 1658-1661.
[151] N. V. Kirij, L. A. Babadzhanova, V. N. Movchun, Y. L. Yagupolskii, W. Tyrra, D. Naumann, H. T. M. Fischer, H. Scherer, *J. Fluorine Chem.* **2008**, *129*, 14-21.
[152] V. Pace, L. Castoldi, P. Hoyos, J. V. Sinisterra, M. Pregnolato, J. M. Sánchez-Montero, *Tetrahedron* **2011**, *67*, 2670-2675.
[153] G. B. Shinde, N. C. Niphade, S. P. Deshmukh, R. B. Toche, V. T. Mathad, *Org. Process Res. Dev.* **2011**, *15*, 455-461.
[154] E. Rogalska, C. Belzecki, *J. Org. Chem.* **1984**, *49*, 1397-1402.
[155] D. H. Hua, S. W. Miao, S. N. Bharathi, T. Katsuhira, A. A. Bravo, *J. Org. Chem.* **1990**, *55*, 3682-3684.
[156] C. A. Zezza, M. B. Smith, B. A. Ross, A. Arhin, P. L. E. Cronin, *J. Org. Chem.* **1984**, *49*, 4397-4399.
[157] F. Chen, Z. Ding, J. Qin, T. Wang, Y. He, Q.-H. Fan, *Org. Lett.* **2011**, *13*, 4348-4351.
[158] A. Lightfoot, P. Schnider, A. Pfaltz, *Angew. Chem. Int. Ed.* **1998**, *37*, 2897-2899.
[159] M. G. Schrems, **2009**.
[160] D. L. Davies, O. Al-Duaij, J. Fawcett, K. Singh, *Organometallics* **2010**, *29*, 1413-1420.
[161] Q. Shen, S. Shekhar, J. P. Stambuli, J. F. Hartwig, *Angew. Chem. Int. Ed.* **2005**, *44*, 1371-1375.
[162] L. Rubio-Pérez, F. J. Pérez-Flores, P. Sharma, L. Velasco, A. Cabrera, *Org. Lett.* **2008**, *11*, 265-268.

[163] P. Yin, T.-P. Loh, *Org. Lett.* **2009**, *11*, 3791-3793.
[164] T. Taniguchi, D. Yonei, M. Sasaki, O. Tamura, H. Ishibashi, *Tetrahedron* **2008**, *64*, 2634-2641.
[165] M. Yus, T. Soler, F. Foubelo, *J. Org. Chem.* **2001**, *66*, 6207-6208.
[166] A. Wrobleski, J. Aubé, *J. Org. Chem.* **2001**, *66*, 886-889.
[167] W. Zeng, S. R. Chemler, *J. Am. Chem. Soc.* **2007**, *129*, 12948-12949.
[168] A. G. Al-Sehemi, R. S. Atkinson, J. Fawcett, *J. Chem. Soc., Perkin Trans. 1* **2002**, *0*, 257-274.
[169] A. N. Parvulescu, P. A. Jacobs, D. E. De Vos, *Adv. Synth. Catal.* **2008**, *350*, 113-121.
[170] C. Ludwig, L. G. Wistrand, *Acta Chem. Scand.* **1990**, *44*, 707-710.
[171] H. Prokopcová, S. D. Bergman, K. Aelvoet, V. Smout, W. Herrebout, B. Van der Veken, L. Meerpoel, B. U. W. Maes, *Chem. Eur. J.* **2010**, *16*, 13063-13067.
[172] P. Vachal, E. N. Jacobsen, *Org. Lett.* **2000**, *2*, 867-870.
[173] E. P. Kündig, C. Botuha, G. Lemercier, P. Romanens, L. Saudan, S. Thibault, *Helv. Chim. Acta* **2004**, *87*, 561-579.
[174] Ó. Pablo, D. Guijarro, G. Kovács, A. Lledós, G. Ujaque, M. Yus, *Chem. Eur. J.* **2012**, *18*, 1969-1983.
[175] G. Liu, D. A. Cogan, T. D. Owens, T. P. Tang, J. A. Ellman, *J. Org. Chem.* **1999**, *64*, 1278-1284.
[176] M. Periasamy, M. Nagaraju, N. Kishorebabu, *Synthesis* **2007**, *2007*, 3821-3826.
[177] A. Kickova, J. Donovalova, P. Kasak, M. Putala, *New J. Chem.* **2010**, *34*, 1109-1115.
[178] L. Gobbi, P. Seiler, F. o. Diederich, V. Gramlich, *Helv. Chim. Acta* **2000**, *83*, 1711-1723.
[179] M. Yamanaka, J. Itoh, K. Fuchibe, T. Akiyama, *J. Am. Chem. Soc.* **2007**, *129*, 6756-6764.
[180] S. S. Zhu, D. R. Cefalo, D. S. La, J. Y. Jamieson, W. M. Davis, A. H. Hoveyda, R. R. Schrock, *J. Am. Chem. Soc.* **1999**, *121*, 8251-8259.
[181] T. Akiyama, (Ed.: L. Toagosei Co.), **2004**.
[182] M. Hanack, K. A. Fuchs, C. J. Collins, *J. Am. Chem. Soc.* **1983**, *105*, 4008-4017.
[183] V. Diemer, H. Chaumeil, A. Defoin, A. Fort, A. Boeglin, C. Carré, *Eur. J. Org. Chem.* **2006**, *2006*, 2727-2738.
[184] N. Yoneda, T. Fukuhara, Y. Takahashi, A. Suzuki, *Chem. Lett.* **1979**, *8*, 1003-1006.
[185] D. C. Ebner, J. T. Bagdanoff, E. M. Ferreira, R. M. McFadden, D. D. Caspi, R. M. Trend, B. M. Stoltz, *Chem. Eur. J.* **2009**, *15*, 12978-12992.
[186] L. Zhang, A. M. Nadzan, R. A. Heyman, D. L. Love, D. E. Mais, G. Croston, W. W. Lamph, M. F. Boehm, *J. Med. Chem.* **1996**, *39*, 2659-2663.
[187] G. D. Williams, R. A. Pike, C. E. Wade, M. Wills, *Org. Lett.* **2003**, *5*, 4227-4230.
[188] K. Schwekendiek, F. Glorius, *Synthesis* **2006**, *2006*, 2996-3002.
[189] D. A. Evans, G. S. Peterson, J. S. Johnson, D. M. Barnes, K. R. Campos, K. A. Woerpel, *J. Org. Chem.* **1998**, *63*, 4541-4544.
[190] D. Benoit, E. Coulbeck, J. Eames, M. Motevalli, *Tetrahedron: Asymmetry* **2008**, *19*, 1068-1077.
[191] D. K. Heldmann, D. Seebach, *Helv. Chim. Acta* **1999**, *82*, 1096-1110.
[192] S. R. Stauffer, J. Sun, B. S. Katzenellenbogen, J. A. Katzenellenbogen, *Bioorg. Med. Chem.* **2000**, *8*, 1293-1316.

Curriculum Vitae

Date of Birth:	16.09.1984
Nationality:	Swiss
Hometown:	Baden AG

Education

Mar 09 – Mar 13	**Ph.D.** Synthetic Organic Chemistry, Laboratory of Prof. Andreas Pfaltz, University of Basel: "*Synthetic and Mechanistic studies of iridium catalysed imine hydrogenation*"
Jan 09	**M. Sc.** in Chemistry, University of Basel
Jul 08 – Dec 08	Master thesis, Laboratory of Prof. Guy Lloyd-Jones, University of Bristol: "*Counterion and conformational structure studies in Pd-allyl complexes coordinated to the Trost Modular Ligand by 2D-NOESY- and EXSY-NMR*"
Jul 08	**B. Sc.** in Chemistry, University of Basel
Oct 04 – Jan 09	Chemistry studies, University of Basel
Jul 04	**Matura MAR**, Kantonsschule Baden

Scholarships and Awards

2012	**SCNAT/SCS Travel Award**
2006-2009	**Federal Stipend** by the State of Argovia

Teaching Experience

Sep 10 - Nov 10	Supervision of M.Sc. Student: Robin Wehlauch, Research Project: „Synthesis of New Ligands as Additives for Asymmetric Imine Hydrogenation"
Sep 09 – Dec 10	Laboratory Teaching Assistant Supervision of laboratory courses, exercises and presentations of chemistry student in basic and advanced organic chemistry

Scientific Publications

"*Discovery of an Iridacycle Catalyst with Improved Reactivity and Enantioselectivity in the Hydrogenation of Dialkyl Ketimines*", Y. Schramm, F. Barrios-Landeros, A. Pfaltz, *Chemical Science*, **2013**, *4*, 2760–2766.

"*Pharmacological characterization of novel designer cathinones in vitro*", L. D. Simmler, T. A. Buser, M. Donzelli, Y. Schramm, L.-H. Dieu, J. Huwyler, S. Chaboz, M. C. Hoener, M. E. Liechti, *British Journal of Pharmacology*, **2013**, *168*, 458–470.

"*Structure-Based Rationale for Selectivity in the Asymmetric Allylic Alkylation of Cycloalkenyl Esters Employing the Trost 'Standard Ligand' (TSL): Isolation, Analysis and Alkylation of the Monomeric form of the Cationic* η^3*-Cyclohexenyl Complex* $[(\eta^3\text{-}c\text{-}C_6H_9)Pd(TSL)]^+$", C. P. Butts, E. Filali, G. C. Lloyd-Jones, P.-O. Norrby, D. A. Sale, Y. Schramm, *Journal of the American Chemical Society*, **2009**, *131*, 9945–9957.

Oral Presentations and Poster Communications

Asymmetric Hydrogenation of Aliphatic Imines, Fall Meeting of the Swiss Chemical Society, ETH Zurich (CH), September **2012**

Mechanistic Investigations of Iridium-Catalysed Imine Hydrogenation, International Symposium of Homogenous Catalysis (ISHC), Toulouse (F), July **2012**

Intermediates in Iridium-Catalyzed Imine Hydrogenation, 5th CARLA Winter School, BASF Heidelberg (GER), March **2012**

Intermediates in Iridium-Catalyzed Imine Hydrogenation, Symposium of Modern Catalysis for Sustainable Chemistry, Syngenta Stein (CH), October **2011**

Intermediates in Iridium-Catalyzed Imine Hydrogenation, Fall Meeting of the Swiss Chemical Society, EPFL Lausanne (CH), September **2011**

Intermediates in Iridium-Catalyzed Imine Hydrogenation, OMCOS 16, Shanghai (CN), July **2011**

Mechanistic Studies of Iridium-PHOX catalysed Imine Hydrogenation, Fall Meeting of the Swiss Chemical Society, ETH Zurich (CH), September **2010**

Mechanistic Studies of Iridium-PHOX catalysed Imine Hydrogenation, 30th Regio Symposium of the Cross-Border University Study Programs of the Universities of Basel (CH), Freiburg i. Br. (GER) and Mulhouse (F), Mittelwihr (F), September **2010**

Mechanistic Studies of Iridium-PHOX catalysed Imine Hydrogenation, 3rd EuCheMS Chemistry Congress, Nürnberg (GER), August **2010**

During my education at the University of Basel, I attended lectures given by:

W. P. Meier, H. Wennemers, K. M. Fromm, B. Giese, U. Séquin, M. Oehme, P. C. Hauser, D. Häussinger, H.-J. Wirz, G. Palivan, E. C. Constable, M. Schwarz, E. Stulz, C. E. Housecroft, J. P. Maier, M. Meuwly, A. Pfaltz, W. Bonrath, H. Wegner, M. Mayor, K. Gademann, W.-D. Woggon, T. Ward, C. Schönenberger, H. Walser, T. Briellmann, F. E. Dussy.

Eidesstattliche Erklärung

Ich erkläre, dass ich die Dissertation „*Synthetic and Mechanistic Investigations of Iridium-Catalysed Imine Hydrogenation*“ mit der darin angegebenen Hilfe verfasst und bei keiner anderen Universität und keiner anderen Fakultät der Universität Basel eingereicht habe.

Basel, den 10. März 2013

York Schramm